FRACTIONATION AND SEPARATION BY CONTINUOUS LIQUID-LIQUID CHROMATOGRAPHY

A Thesis submitted

by

A. N. Williams, B.Sc.,

to the Faculty of Engineering,

University of Aston in Birmingham

for the Degree of Doctor of Philosophy

4 OCT 1976

197436

543.544WIL

Department of Chemical Engineering

University of Aston in Birmingham

April 1976

SUMMARY

Reviews are given of chromatographic theory with particular reference to gel permeation chromatography. The various process schemes that have been proposed for preparative and production scale chromatography have been discussed.

A laboratory scale unit was made available in which a solute rich liquid system is made to move counter-current to a liquid held in the pores of a solid porous support. Polymeric fractionation of dextran is achieved on the basis of molecular size. The counter-current movement is obtained by moving an annular bundle of 44 interconnected tubes (28.5 cm x 0.8 cm) about fixed liquid input and output ports. Cam operated spring loaded valves ensure the unidirectional flow of liquid counter-current to the direction of rotation of the bundle. The operation of the equipment is dependent on the reliability of a moving face seal. Mechanical difficulties were encountered with the moving face seal, which reduced the amount of experimental work that could be performed using the equipment.

Experimental studies have been carried out in which the continuous chromatographic process has been applied to the fractionation of dextran. Dextran with a weight average molecular weight of 32,000 and a molecular weight distribution of about 2000 to 300,000 was used. The effect of increasing the feed concentration from 0.5% w/v to 20.8% w/v at a nominal feed rate of 0.5 cm^3 min^{-1} has been investigated. A concentration dependent partition coefficient was shown to influence the process.

Throughputs of up to 1.14 g hr^{-1} have been achieved. The equipment has successfully been used to fractionate dextran to give a molecular weight distribution comparable with that produced by ethanol precipitation. The eluent and chromatographic packing used were distilled water and Spherosil XOB075 (200 μm-400 μm).

Attempts have been made to elucidate the influences of process operating parameters using a synthetic binary mixture, dyed bovine serum albumin and dyed pepsin. A decrease in the surface tension of the sealed fluid was shown to adversely affect the operation of the mechanical seal.

A computer simulation of the process has been developed. This enabled the key parameters affecting the process to be theoretically determined.

ACKNOWLEDGEMENTS

The Author is indebted to the following:

Professor G. V. Jeffreys and the Department of Chemical Engineering for making available the facilities for research.

Professor P. E. Barker and Dr. B. W. Hatt, who supervised the work, for their advice and encouragement.

Fisons Ltd. for their financial support.

F. J. Ellison, a fellow research worker, for many thought provoking discussions on both practical and theoretical aspects of the research topic.

Mr. M. F. Lea for the construction of the electronic equipment.

Mr. N. Roberts, Mr. R. G. Evans and other members of the departmental technical staff who provided technical assistance.

Miss Eileen Broughton of "The Secretary Byrds" for her diligence in typing this thesis.

The Science Research Council for the provision of a scholarship.

CONTENTS

	Page
SUMMARY	
ACKNOWLEDGEMENTS	
1. INTRODUCTION	1
2. CONTINUOUS CHROMATOGRAPHY	7
2.1 Concepts and Terminology	7
2.1.1 The Basic Process	7
2.1.2 The Theories of Chromatography	11
2.1.2.1 The Plate Theory	13
2.1.2.2 The Rate Theory	16
2.2 Continuous Chromatographic Process Schemes	18
2.2.1 The Co-current Process	19
2.2.2 The Continuous Systems	20
2.2.2.1 Cross-current Flow Processes	20
2.2.2.2 Counter-current Flow Processes	23
2.2.2.2.1 Moving-Bed Systems	25
2.2.2.2.2 Moving-Column Systems	29
3. THE DESIGN AND CONSTRUCTION OF THE CONTINUOUS CHROMATOGRAPHIC MACHINE	
3.1 General Operating Principle	37
3.2 The CCR1 Machine	39
3.2.1 Overall Description	39
3.2.2 Detailed Design and Construction	40
3.2.2.1 The Mechanical Seal	40
3.2.2.2 The Tube Bundle	45
3.2.2.3 The Valves and Connecting Blocks	48
3.2.2.4 The Drive Mechanism	48
3.2.2.5 Measurement and Control of Fluid Flow	52

Contents (Continued)

		Page
	3.2.3 The Packing Procedure	53
	3.2.4 General Operating Procedure	54
3.3	Preliminary Trials	55
3.4	Analysis of the Sealing Problem	62
	3.4.1 Introduction	62
	3.4.2 Analysis of the Moving Seal	66
	3.4.3 Conclusion	72
3.5	Modifications to the CCR1 Machine	72
	3.5.1 Design Changes and Trials	74
	3.5.2 The Addition of the Liquid Lock and Further Trials	82
	3.5.3 Conclusions	86
	3.5.3.1 The Effect of Fluid Physical Properties	86
4.	LITERATURE REVIEW OF GEL PERMEATION CHROMATOGRAPHY	
4.1	Chromatographic Methods	89
4.2	The Theory of Gel Permeation Chromatography	91
	4.2.1 General Principles	92
	4.2.2 The Mechanisms	96
	4.2.3 The Significance of Dispersion Phenomena in G.P.C.	103
	4.2.4 The Operating Parameters Influencing Efficiency in G.P.C.	114
4.3	Practical Gel Permeation Chromatography	121
	4.3.1 Packings	121
	4.3.2 Practical Aspects	123
	4.3.2.1 Column Calibration	128

Contents (Continued)

Page

4.3.2.2 The Correction of G.P.C. Chromatograms for Dispersion 131

4.3.2.3 The Effects of Sample Quantity and Volume 136

4.4 Applications of Gel Permeation Chromatography 136

5. THE THEORY AND PRACTICE OF GEL PERMEATION CHROMATOGRAPHY IN A MOVING COLUMN CHROMATOGRAPH

5.1 The Ideal Case 138

5.2 The Practical Case 147

5.2.1 The Effect of a Finite Feed Flowrate 147

5.2.2 The Effect of a Finite Component Concentrations 150

5.2.3 The Effect of a Finite Separation Length 153

5.2.4 The Effect of a Discontinuous Mode of Operation 154

5.2.4.1 The Influence of a Discontinuous Mode of Operation on Polymer Fractionation 155

6. THE FRACTIONATION OF DEXTRAN BY GEL PERMEATION CHROMATOGRAPHY

6.1 Introduction 162

6.1.1 Industrial Background 162

6.1.2 Research Objectives 164

6.2 Methods and Materials 164

6.2.1 The Packing 164

6.2.2 The Eluent and Associated Equipment 165

6.2.3 The Analytical System 167

6.2.3.1 The AutoAnalyser System 167

6.2.3.2 Analytical Columns and Column Calibration 171

6.2.3.3 Procedure for Analysing Samples 174

Contents (Continued)

		Page
	6.2.4 Data Treatment	175
	6.2.5 Experimental Errors	177
6.3	Selection of Analytical Conditions	178
	6.3.1 Column Dimensions and Packing Particle Size	179
	6.3.2 Analytical Column Flowrates	184
6.4	Operation of the Continuous Chromatograph	188
	6.4.1 Introduction	188
	6.4.2 Preliminary Experiments	189
	6.4.3 Dextran Fractionation Results	194
	6.4.4 Conclusions	244
7.	STUDIES ON THE CONTINUOUS SEPARATION OF A BINARY MIXTURE	
7.1	Introduction	249
7.2	The Choice of Binary Components	250
7.3	The Analysis of the Dyed Proteins	253
7.4	The Development of the Experimental Methods	253
	7.4.1 The Dyeing Technique	253
	7.4.2 The Choice of Eluent	260
	7.4.3 Preliminary Continuous Chromatograph Experiments	266
	7.4.4 Data Treatment	271
	7.4.5 Experimental Errors	272
7.5	Binary Separation Studies	275
	7.5.1 Experimental Results	275
	7.5.2 Discussion	296
8.	COMPUTER SIMULATION STUDIES	
8.1	Simulation of the Continuous Chromatograph used in this Study	302

Contents (Continued)

		Page
	8.1.1 Theoretical Basis	303
	8.1.2 Simulation of the Counter-Current Movement of the Packing	307
	8.1.3 Program Layout	308
8.2	Results	317
8.3	Discussion and Conclusion	318
	8.3.1 The Effect of the Number of Equilibrium Stages, N	318
	8.3.2 Simulation of the Binary Experiments	324
	8.3.3 The Effect of Increasing the Feed Concentration	330
	8.3.4 The Effect of Changing the Tube Bundle Speed	330
	8.3.5 Accuracy of the Simulation	337
9.	CONCLUSIONS AND RECOMMENDATIONS FOR FUTURE WORK	
	APPENDICES	344
	NOMENCLATURE	398
	REFERENCES	404

CHAPTER 1

INTRODUCTION

The fundamental need for separation processes is epitomized by Treybal's comment that: "a substantial number of the unit operations of chemical engineering are concerned with the problems of changing the composition of solutions and mixtures through methods not necessarily involving chemical reactions. Usually these operations are directed toward separating a substance into its component parts". In all the developed processes, separation is achieved by components differing in their physical properties. These processes can be divided into two categories. Firstly the techniques of mechanical separation such as the filtration of solids from a suspension in a liquid, the screening of a solid into fractions of different particle size or the separation, according to density, of particles of a ground solid. Secondly there are those processes involving a change in the composition of a solution. These processes form the mass transfer operations.

The applications of these operations in the chemical and process industries are numerous. There is rarely a chemical process that does not require a mass transfer operation in one form or another for the preliminary purification of raw materials or the final separation of products from by-products. Included in this type of process are the classical separation processes of distillation and liquid-liquid extraction. However in addition to these and other commonly used mass transfer operations there are several comparatively new processes such as zone refining, electroldialysis, ultrafiltration and electrophoresis. These operations are used relatively infrequently although they are rapidly increasing in importance.

The increasing demand for pure chemicals has not only promoted the use of newer separation methods but has also stimulated research into developing novel processes. One such process is chromatography. Following the successful demonstration of elution gas/liquid chromatography by James and Martin[2] the technique has become firmly established as a powerful method for the resolution of chemical mixtures on a small scale.

Chromatography involves the partitioning of differing solutes, by a variety of means which are discussed in Section 4.1, between a mobile and a stationary phase. The degree to which a solute is retarded by the stationary phase governs the rate at which it progresses through a chromatographic column. Hence, if a mixture is injected into a stream of mobile phase, which can be either a gas or a liquid, passing through a column packed with a suitable stationary phase the constituent components will be eluted from the column at different times and therefore separated.

The potential of chromatography was soon realised and the problems of improving throughput and scale-up tackled by several researchers. Though its development as an analytical technique was meteoric, many problems have impeded its development as a large scale unit operation. Despite this the direct scale up of the analytical technique has taken place.

The restrictions imposed on throughput by this mode of operation have, however, limited its development. Consequently, because of the advantages of continuous operation, a number of novel designs for both cross and counter current continuous chromatography have been proposed. The designs for cross-current operation have subsequently not proved practical on a large scale.

Counter-current continuous chromatography has actively been developed by Barker and co-workers[3-9] who have successfully demonstrated its viability with the separation of a wide range of volatile organic compounds. More recently the equipments developed and used by Barker et al.[3-9] have been applied to gel permeation chromatography (G.P.C.), a form of liquid-liquid chromatography.

Continuous chromatography has many possible industrial applications when G.P.C. is the type of chromatography employed. Unlike other forms of chromatography G.P.C. relies on the differences in molecular size to govern the partitioning of solutes in solution between a liquid mobile phase and a liquid contained within the pores of a porous material. The liquid in both phases is the same and it is the variation in pore sizes and molecular sizes which determine the degree to which individual solute molecules permeate the stationary phase. Separation and fractionation therefore occur on the basis of molecular size rather than by solubility or boiling point.

The terms separation and fractionation are often used interchangeably but in this thesis they are used to distinguish between (i) chemical systems where the components have identical chemical properties and only differ in molecular size, for example the fractionation of polymers; and (ii) chemical systems where the components differ in both chemical and physical properties, for example the separation of glucose and soluble starch.

Gel permeation chromatography has applications in the separation of such chemicals as enzymes, proteins, isomers and pharmaceutical products. It is currently used in a batch mode of operation to commercially produce insulin in Sweden[10]. Since separation is on the basis of molecular size it can also be used to fractionate polymeric materials such as dextran, a polyglucose extensively used as a blood plasma substitute and in preparations for the treatment of anaemia. This particular possible application prompted Fisons (Pharmaceuticals) Ltd. to financially support an investigation into the feasibility of using continuous G.P.C. to improve the molecular weight distribution of commercially produced dextran. Experimental work carried out as part of this research formed an integral part of this investigation. A fellow researcher, F. J. Ellison, was also involved in this study, but was concerned with developing equipment suitable for large scale studies.

The development of continuous liquid-liquid chromatography has gone through a number of stages, illustrated in Figure 1.1. In common with other development projects research has continued on a conditional basis until the first "accept" point (Figure 1.1). An important feature in the development of continuous G.P.C. was that once the initial idea had been successfully demonstrated two parallel lines of development were undertaken. These were large scale applications of the process with a view to its development as an industrial separation technique and more important from the point of view of this thesis was its small scale development.

Information from a small scale study of a process is useful in a number of ways. It provides data on equipment performance and

FIGURE 1.1 The Development of Continuous Liquid-Liquid Chromatography

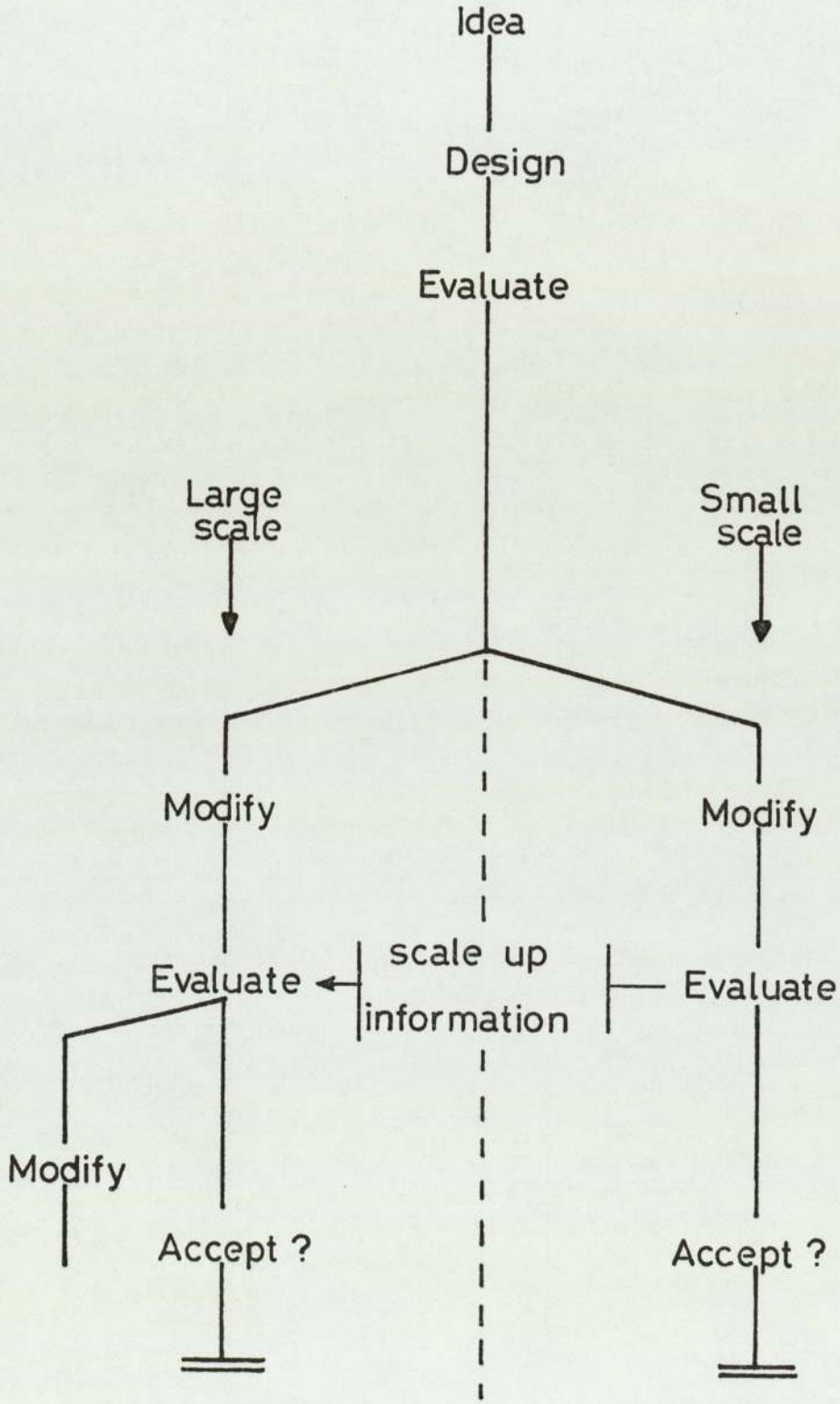

design and also gives scale up information on the influence of operating parameters for larger scale studies. These factors were of particular importance in chromatography because of the high cost of chromatographic media. In addition, a small scale piece of equipment is useful to assess the potential of possible systems for study on a large scale.

The success of a prototype continuous chromatographic unit used by Hatt[11] prompted Rank Hovis McDougall (Research) Ltd. to commission the design and construction of a unit similar in design to the prototype but which theoretically eliminated the mechanically weak features. This equipment was the main piece of apparatus used in the research program, one aspect of which was to investigate the operation of this new chromatographic machine.

Experimental studies were to be undertaken to provide information on the feasibility of using this type of fractionation technique to improve polymer molecular weight distributions. In addition to this the influence of the operating parameters was to be investigated so as to provide information for a study of the fractionation, on a large scale, of dextran by continuous G.P.C.

The complexities of quantitatively analysing a mass transfer process using polymeric materials are well known. Therefore, using a suitable binary system, experimental studies were to be carried out in an attempt to understand the basic process.

From the experimental studies a model of the process was to be attempted. In common with other mass transfer processes an equilibrium stage model could be adopted to enable a more detailed study.

CHAPTER 2

CONTINUOUS CHROMATOGRAPHY

The literature survey has been divided into two parts. The first part is discussed in this chapter and deals with the basic concepts and terminology used in chromatography and the way it has been applied as a technique for the continuous separation of chemicals. Particular attention is paid to the different modes of continuous chromatographic operation together with practical details where available. The second part of the literature survey, given in Chapter 4, is devoted to one aspect of liquid-liquid chromatography, namely "Gel Permeation Chromatography" (G.P.C.). The theory behind this type of chromatography and the practical problems associated with its application are reviewed and discussed.

2.1 CONCEPTS AND TERMINOLOGY

The basic theory of chromatography is given in the following subsection to provide an introduction to the subject area. More specific details are given in a number of general texts[12-14].

2.1.1 The Basic Process

Regardless of the particular type of chromatography, an essential feature of the process is the flow of an inert fluid carrier, termed the "mobile phase", which contains a mixture of solutes to be separated through a column packed with a finely divided particulate solid, called the "stationary phase". The solutes are retarded by the stationary phase to varying degrees depending on their individual affinities for the stationary phase.

As a result of this preferential retardation, solute bands move at a fraction, R, of the mobile phase velocity. Giddings[12] has defined R, at infinite dilution, in four ways.

(i) The relative solute band migration rate.

(ii) The probability that a solute molecule is in the mobile phase.

(iii) The limiting fraction of time a molecule spends in the mobile phase.

(iv) The fraction of molecules in the solute band in the mobile phase at equilibrium.

From these definitions it can be seen that the migration of a solute band is governed by equilibrium parameters. However, since the nature of fluid dynamic dispersion[15] and mass transfer processes operating in porous media cause spreading of the solute band, the precise value of R only applies to the band centre; i.e. equilibrium between the solute in the stationary and mobile phase only occurs at the point of maximum concentration in the migrating solute band.

Figure 2.1 shows a typical chromatogram obtained when two components, 1 and 2, are fully resolved by the chromatographic process. The retention time of individual components contain a contribution from the extra column apparatus, the injection and detection system, the sum of which is designated the "dead time", t_D. Retention times can be related to volumes through the mobile phase flow rate. Hence the elution volume, V_e, of a component can be

FIGURE 2.1 An Example of an Analytical Chromatogram

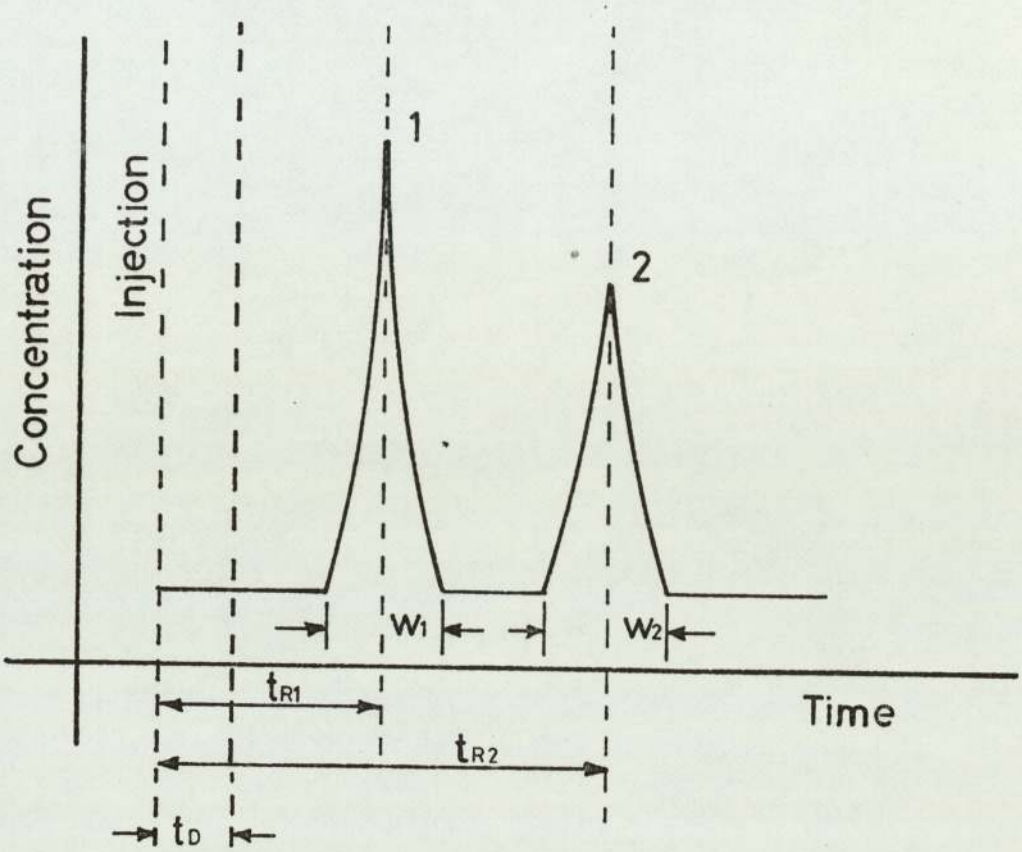

t_D = Dead time

t_R = Elution time

w = Peak width at the base

calculated from,

$$V_e = t'_R . Q \qquad 2.1$$

where:

Q = volumetric flow rate (elution rate)

t'_R = "adjusted" retention time.

Since a component can only progress through a chromatographic column whilst in the mobile phase, its "partition" or "distribution" coefficient, K, determines the rate at which it moves. A component's partition coefficient is defined as the equilibrium ratio of the component concentration in the stationary phase to the concentration in the mobile phase.

$$\text{Therefore } K = \frac{C_s}{C_m} \qquad 2.2$$

C_m = solute mobile phase concentration.

C_s = solute stationary phase concentration.

The partition coefficient can also be expressed in terms of measured volumes,

$$K = \frac{V_e - V_o}{V_i} \qquad 2.3$$

where: V_e = solute elution volume

V_o = column void volume, equivalent to the elution volume of an unretarded component

V_i = stationary phase volume.

From the definition of the retention factor, R, given by Giddings[12], K may also be expressed as,

$$K = \frac{1 - R}{R} \qquad 2.4$$

The partition coefficient is therefore a measure of the affinity of a solute for the mobile phase and it is independent of the column on which it is measured. The ratio of the partition coefficients between the two different solutes, namely the "separation factor", defines the ease with which the solutes can be separated.

$$S = \frac{K_2}{K_1} \qquad 2.5$$

S = Separation factor.

By convention $K_2 > K_1$. The nearer the separation factor is to unity the more difficult the separation becomes.

2.1.2 The Theories of Chromatography

Van Deemter et al.[16], by making use of the following assumptions, established that chromatography has four forms.

(i) The equilibrium concentration in the two phases are proportional - a linear partition isotherm operates ("linear chromatography").

(ii) Longitudinal diffusion and processes such as a non-uniform velocity profile that cause spreading of a solute band are assumed to be small. Mass transfer is infinitely fast, equilibrium between the two phases immediate and the exchange process is thermodynamically reversible ("ideal chromatography").

The forms that chromatography can take are as follows:

(i) Linear - ideal.

(ii) Non-linear - ideal.

(iii) Linear - non ideal.

(iv) Non-linear - non ideal.

The first of these, linear - ideal chromatography, is the simplest case and assumes that the retardation of a solute depends on the product of the partition coefficient and the ratio of the mobile and stationary phases present in one unit volume. It further assumes that the shape of the solute band remains unaltered and that different solutes behave independently[17].

In non-linear ideal chromatography the effects of a non-linear isotherm are appreciable but since mass transfer is assumed to be fast, diffusional effects are neglected. In contrast solute interaction can affect individual solute partition coefficients which has restricted a rigorous treatment of this type of chromatography.

Linear - non ideal chromatography involves the assumption of a linear isotherm. Consequently the shape of a solute band remains symmetrical but broadens due to the slowness of solute transfer between the two phases.

The last form of chromatography, non-linear non ideal is the most general case. The solute bands are both diffuse and assymetric. Klinkenberg and Sjenitzer[18] have proposed kinetic based theories for this type of chromatography and the mathematics involved become very complex.

In common with other mass transfer processes there are two basic theories which can be used to interpret their operation, the plate theory and the rate theory. Martin and Synge[19] were the first to realise the similarities between the chromatographic elution technique and the processes occuring in distillation columns and, therefore, adopted the plate theory, which treats the chromatographic column in terms of idealised discontinuous flow model. The second theory, the rate theory, treats the column as a continuum and takes into account the various kinetic phenomena governing mass transfer between the two phases. These phenomena contribute to the broadening of a solute band as it passes through a chromatographic column.

2.1.2.1 <u>The Plate Theory</u>

The plate theory is the simplest theory and utilises the following assumptions[20].

(i) The chromatographic column is conceived as consisting of volume elements, or plates.

(ii) The partitioning of the solute between the mobile and stationary phases, on each plate, is assumed to be fast and therefore equilibrium is established instantaneously.

(iii) The partition coefficient of a solute is independent of concentration and hence constant throughout the column; i.e. linear isotherm is assumed.

(iv) Solute diffusion in the axial direction is confined to individual plates, and is therefore neglected.

(v) The mobile phase flow is discontinuous, consisting of a stepwise addition of volumes of mobile phase, each equal to the free volume of a plate.

The effect of this stagewise operation on a single solute band, in the ideal case, is to spread the band into a Gaussian distribution curve. The degree of spreading of a solute band is quantified by the second moment, or variance, of the curve. A parameter used to characterise the efficiency of chromatographic columns is the plate height, H, the height equivalent to a theoretical plate (H.E.T.P.). The term H is defined by,

$$H = \frac{d\sigma_z^2}{dz} = \frac{\sigma^2(L)}{L} \qquad 2.6$$

where σ_Z^2 and Z are the length based second moment and the distance along a column of length, L. Equation 2.6 is the rate of increase of the second moment per unit length of column.

Height equivalent to a theoretical plate is an empirical quantity which can be calculated from;

$$H = \frac{L.W^2}{16(t'_R)^2} = \frac{L}{N} \qquad 2.7$$

where:

L = total column length

H = H.E.T.P.

N = number of theoretical plates

$$= 16 \left(\frac{t'_R}{W}\right)^2 \qquad 2.8$$

An alternative form of the above equation is

$$N = \frac{t_R}{\sigma_t} \qquad 2.9$$

W = peak base width

$= 2\sigma_t$

σ_t = time based peak standard deviation.

An important feature of Equation 2.6 is that, by making use of one of the rules of statistics, if there are several processes which contribute to the peak spreading, and assuming the

processes are independent of each other, then the variance of the peak will be the total sum of the variances associated with each process. The plate height due to individual effects can then be expressed as,

$$H = \frac{\Sigma\ \sigma^2(L)i}{L}$$ which is an alternative form of

Equation 2.6.

The plate concept is a misnomer when applied to differential packed columns, but serves as a useful means of determining the influence of mobile phase velocity, packing particle size, solubility phenomena and column packing uniformity on the efficiency of the process.

In an attempt to reduce the simplicity of the plate theory Glueckauf[21] who, by reducing the plate volumes to infinitely small dimensions, developed a continuous plate theory. From this theory it was shown that the shape of the eluting solute curve was of the Poisson type. Van Deemter et al.[16] have subsequently shown that providing the total number of plates in the column is large (> 100) the elution curve could be approximated by a Gaussian distribution curve.

2.1.2.2 The Rate Theory

Rate theories, in principle, take into account the various kinetic phenomena influencing the spreading of a solute band. A number of equations both empirical and theoretical have been proposed. Chapter 4 discusses in detail those expressions that have been developed and applied to gel permeation chromatography. It is therefore not proposed at this stage to give comprehensive details of these equations.

Van Deemter et al.[16] developed a theory accounting for the contribution to plate height of longitudinal diffusion in the mobile phase, eddy diffusion resulting from the inhomogeneity of the packing and finally a finite rate of mass transfer. The equation developed was as follows;

$$H = A + \frac{B}{U} + C'_m.U + C'_s.U \qquad 2.10$$

where:

A = eddy diffusion term

B = longitudinal mobile phase diffusion term

U = the interstitial mobile phase velocity

C'_m and C'_s = the resistances to mass transfer in the mobile and stationary phase respectively.

Implicit in Equation 2.10 is the assumption that the individual contributions to plate height, H, are independent. However it is recognised that this is not the case, a point which Giddings[12] takes into account in his "coupling theory", where, in a more realistic manner the resistance to mass transfer in the mobile phase and the eddy diffusion term are not independent but coupled. The simplified form of the equation is;

$$H = \frac{B}{U} + C'_s.U + \frac{1}{1/A + 1/C'_m.U} \qquad 2.11$$

The terms have the same meaning as those given above.

In addition to the coupling theory Giddings[12] also developed a more rigorous procedure, "the generalised non-equilibrium theory". This theory is concerned only with the effects of the various mass transfer terms which frequently (particularly at high mobile phase flow rates) contribute the most to the plate height[20]. The theory deals independently with the mass transfer processes in a variety of systems, each having different characteristics. A quantitative treatment of the theory is given in the text by Giddings[12]. Grushka et al.[20] have qualitatively described the theory and comment that the difficulty in applying it is the intractability of the mathematics used to describe such phenomena as mobile phase mass transfer.

2.2 CONTINUOUS CHROMATOGRAPHIC PROCESS SCHEMES

Chromatography with its unique separating power and near univeral applicability could become a useful preparative and production scale separations technique. The major drawback to achieving a greater degree of application is the limitation on throughput. Many researchers have concentrated on the scale-up problem[232] and have devised a variety of mechanical devices aimed at improving throughput in the chromatographic process. These devices fall into two categories.

(i) Batch or co-current systems.

(ii) Continuous systems.

2.2.1 The Co-Current Process

In the co-current process direct scale-up of the conventional analytical system has been attempted. The problems associated with scaling up batch systems with particular reference to gas-liquid chromatography are discussed in an excellent review by Deeble[8]. Ellison[22] has carried out a similar review, particular attention was paid to the factors influencing the scale-up of the liquid-liquid chromatographic process. Essentially, scaling-up the analytical process has involved the use of larger diameter packed beds, some of which have incorporated baffling systems[23-25] to promote radial mixing and reduce longitudinal dispersion. Column utilisation and therefore throughput is increased by introducing a "repeated injection" technique. Batch samples are injected at as frequent an interval as the total on-column width of the preceding sample permits without extensive overlap.

The literature provides a number of references to the large scale application of liquid-liquid chromatography. Pharmacia Ltd. (Upsalla, Sweden) commercially produce a piece of process equipment, "The Sephamatic Gel Filter", which has been used for the industrial separation of large and small molecular weight biological components from milk and whey; it has also been applied to the purification of proteins and enzymes[26,27]. Samuelsson et al.[28] have reported using three 20 cm diameter columns to produce protein enriched milk. Skim milk feedrates up to 1000 cm^3 min^{-1} were reported in this study. Columns, 30 cm in diameter, have been used by Janson[10] to separate rape seed proteins and to purify insulin. The latter is now commercially produced by Vitrum A.B. (Stockholm, Sweden) using a battery of six 45 cm internal diameter by 15 cm deep columns packed

with Sephadex G-50 fine[10]. In all the examples quoted above, the equipment operates in the repeated batch mode. Conder[29] has published a review discussing the criteria that can be applied in the selection of large columns for repeated batch chromatography over more conventional separation techniques.

2.2.2 The Continuous Systems

The inherent advantages of the continuous mode of operation over batch operation have been well established. Consequently, since the introduction of continuous chromatography in 1956[60] several mechanical devices have been put forward whereby continuous operation is achieved, these can conveniently be put into two classes;

(i) cross current flow processes

(ii) counter-current flow processes

and are now discussed in detail.

2.2.2.1 Cross-Current Flow Processes

Cross-current flow processes involve the movement of the chromatographic bed laterally to the movement, within the bed, of the mobile phase. The chromatographic bed can be arranged as a circular array of parallel tubes, a single annular cylinder (Figure 2.2a) or as an annular disc (Figure 2.2b). Rotation of the annulus about its centre while the mobile phase flows in the axial or radial direction results in each component describing a helical path (see Figure 2.2a)

FIGURE 2.2 Cross-current Flow Schemes

a) Helical flow

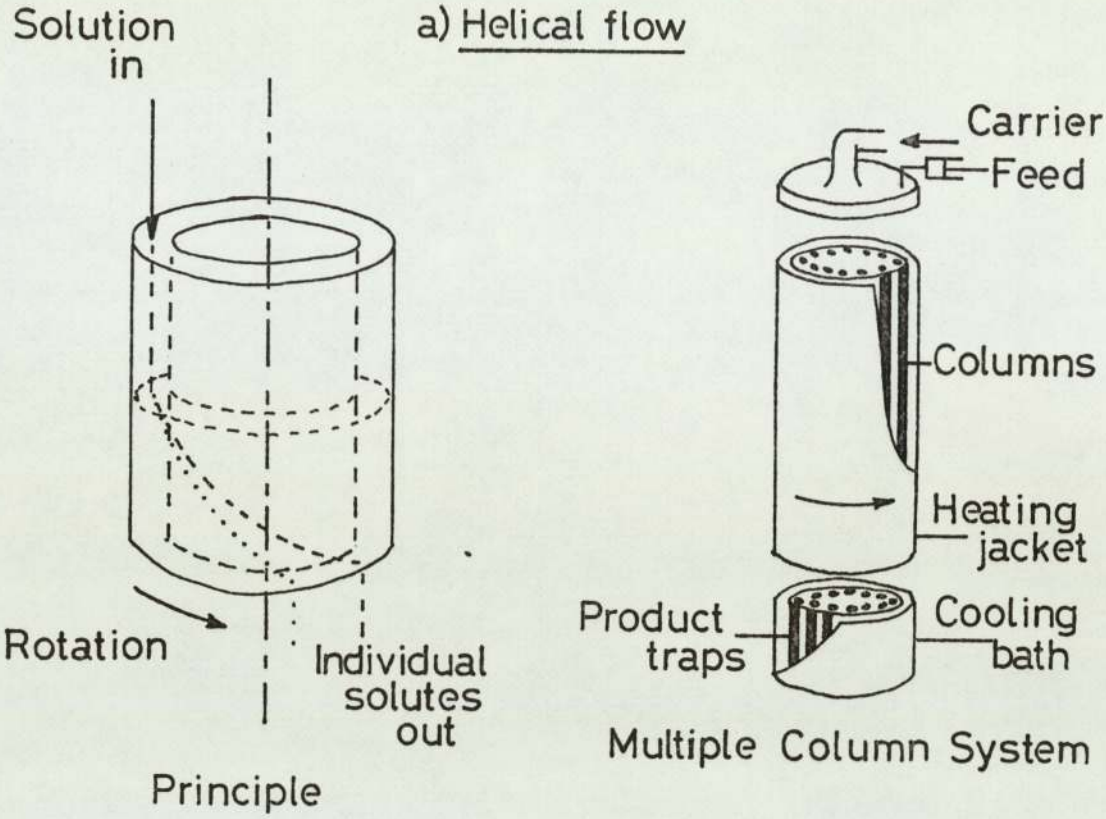

b) Radial flow

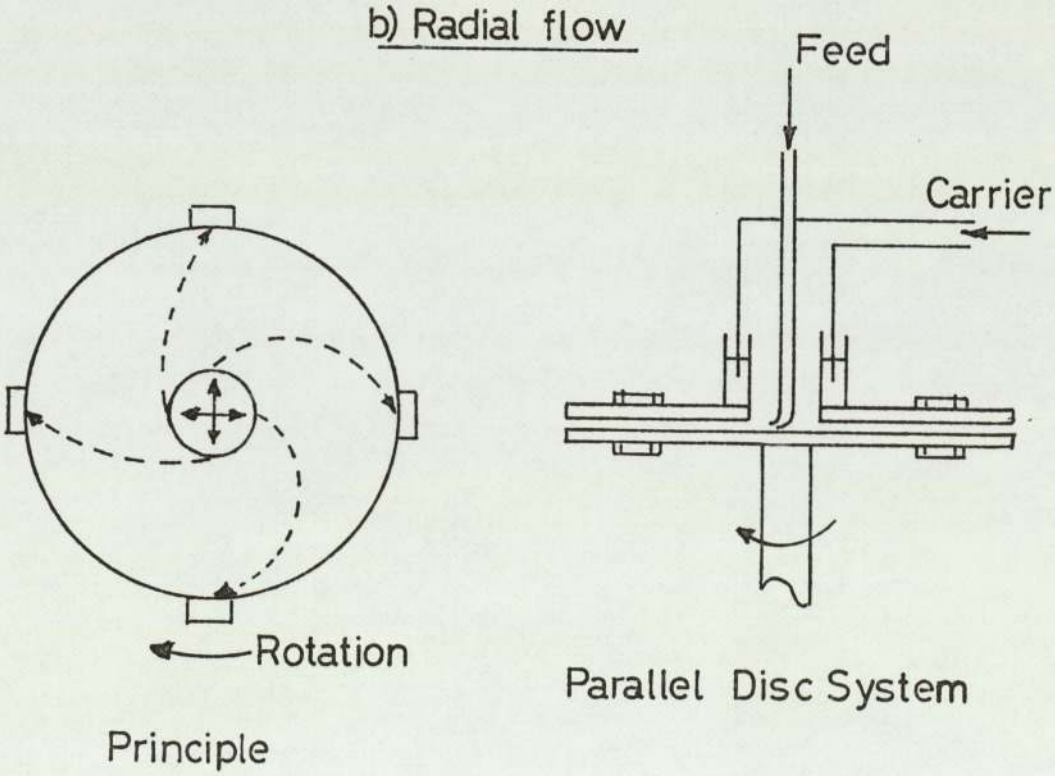

from the point of entry to each individual component exit port. Martin[30] in 1949 proposed a scheme based on this principle and also provided a theoretical analysis of its operation.

In a theoretical appraisal of a cylindrical rotating cross-flow bed system Giddings[31] concluded that this scheme was capable of better resolution and throughput than a conventional column of similar packed cross-section. Dinelli et al.[32-35] constructed a unit based on this principle which consisted of 100 columns, 0.6 cm diameter and 1.2 metres long, arranged to form an annulus of parallel columns, each column operating as a batch column. This arrangement was used to successfully separate cyclohexane and benzene at experimental feed rates up to 200 cm^3 hr^{-1}. Svenson[36,37] has described a circular array of parallel columns as well as an annular packed bed. Both were capable of continuous operation and the separation of liquid mixtures.

Fox et al.[38-40] and Dunhill and Lilly[41] have reported using small scale axial flow annular columns for liquid-liquid systems. Both groups of authors employed gel permeation chromatography and in the case of the former the equipment was used to separate skim milk proteins and to purify cow heart myoglobin on Sephadex G75. The application of axial flow annular systems has a restricted scale-up potential due to mechanical problems, cost and the problems of achieving a uniform packing density.

Mosier[42] has patented a chromatographic unit based on the rotating annular principle. In this case the feed travels from the centre of an annular packing, Fig. 2.2b, and moves horizontally rather than vertically. Sussman [43] constructed a practical system

similar in principle to that proposed by Mosier[42] (see Fig. 2.2d). Called a continuous surface chromatograph this system utilises two parallel annular discs. Separation occurs between a stationary phase coated on to surfaces between 50 μm and 150 μm apart. The primary application of this system is in the continuous monitoring and multi-component analysis of gases[44].

Tuthill[45,46] conceived a cross-flow chromatographic process in 1970 termed a "chromatographic slab", Figure 2.3. The operating principle is similar to the parametric pumping process proposed by Wilhelm and co-workers[47], in that it achieves a high degree of separation by the phased cycling of mobile phase flow and temperature within a packed bed.

In conclusion it is interesting to note that neither of the units constructed on the cross-flow principle have been used to exploit its major theoretical advantage, the ability to continuously resolve a multi-component mixture in a one-stage operation. Deeble[8] has noted there are both mechanical and physical disadvantages in the large scale application of some of the devices proposed.

2.2.2.2 Counter-Current Flow Processes

Continuous processing has long been established as the preferred means of operating mass transfer processes in the chemical industry, mainly because there are both throughput and economic advantages over the equivalent batch process. The restrictions imposed by the cross-current mode of operation have resulted in the development of counter-current flow processes. Many attempts have been made to increase throughput over the more conventional co-current flow systems.

FIGURE 2.3 Chromatographic Slab

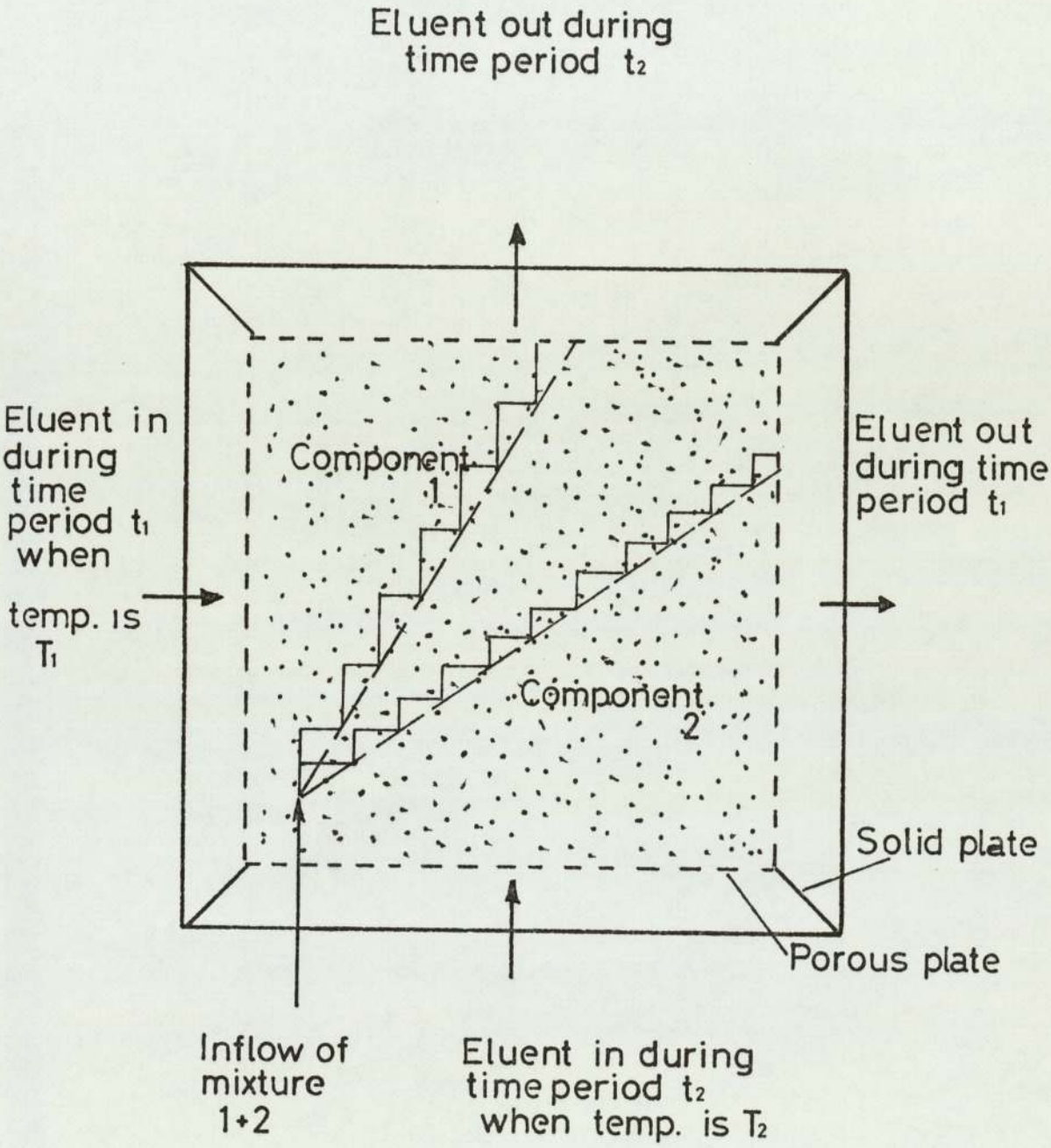

In counter-current flow systems the stationary phase is moved in the opposing direction to that of the mobile phase by a variety of means. Unlike the co-current systems greater use is made of the available mass transfer area to affect separation. Higher throughputs should therefore in principle be achieved. Figure 2.4 represents an idealised concentration profile for a binary mixture separated by the counter-current flow process. It shows that the entire column length can be used to improve resolution and as a result solute overloading, by co-current standards, is possible.

The majority of the development work to date on counter-current chromatography has been restricted to the field of gas-liquid chromatography. Only comparatively recently has the work been extended to include liquid-liquid chromatographic systems. Initially the major disadvantage was the availability[38] of suitable packing materials. Recent advances in the development of chromatographic packings have, to a great extent removed this restriction.

The development of mechanical systems based on the principle of counter-current chromatography can be divided into the following stages.

(i) Moving bed.

(ii) Moving columns.

2.2.2.2.1 Moving Bed Systems

Nearly thirty years ago the Union Oil Company, California developed the "Hypersorption Process"[48]. This process used an activated carbon adsorbent flowing continuously downward through a stream of

FIGURE 2.4 Binary Mixture Concentration Profile

Counter-current flow process

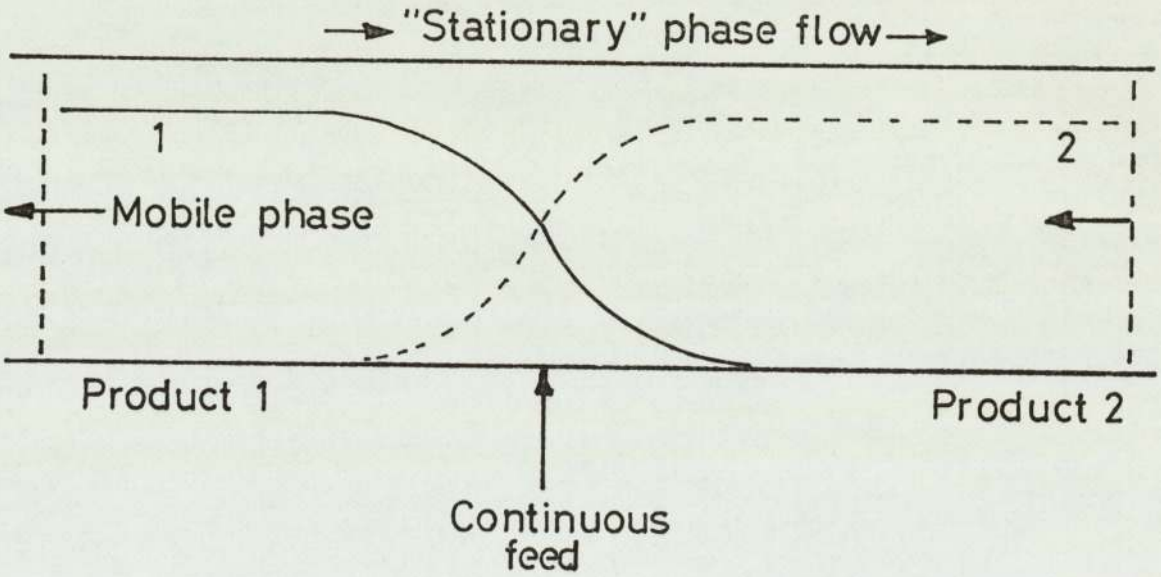

Component 1 = least retarded component

Component 2 = more retarded component

($K_2 > K_1$)

light hydrocarbons in a vertical column. Primarily used commercially to recover ethylene it has subsequently proved uneconomic[44] since the development of low temperature distillation. Despite the failure of this system the literature contains many references to moving bed chromatographic systems.

A typical example of the equipment developed is that by Barker and co-workers[3-7], a simplified illustration of which is given in Figure 2.5. A vertical column which may be glass or metal with a reported diameter of 2.5 cm is fed with a suitable chromatographic medium from a hopper A, the flow of the packing is controlled by a variable orifice B at the column base and removed by a table C. The column is vibrated to ensure a continuous steady stream of solids and dry gas enters at the base of the column D. The liquid or gas feed mixture is introduced at a point, G, between the product offtake ports E and F. Details of the gas-liquid chromatographic separations carried out using this equipment are given in the literature[3-7]. Schultz[49], Scott[50] and Fitch[51,52] have used variations on the equipment described above for gas-liquid chromatographic studies.

Bradley and Tiley[53] have reported using a moving bed system where liquid (dinonylphthalate) flows downwards through a packed column. This variation is analogous to two solvent counter-current liquid-liquid extraction. Buhl and Yeagle[54] have described a system where the packed bed is moved by a helical screw. A moving bed unit with a 15 cm diameter column has been patented and successfully applied by the Phillips Petroleum Company[55].

FIGURE 2.5 Moving-bed Apparatus for Counter-current Chromatography

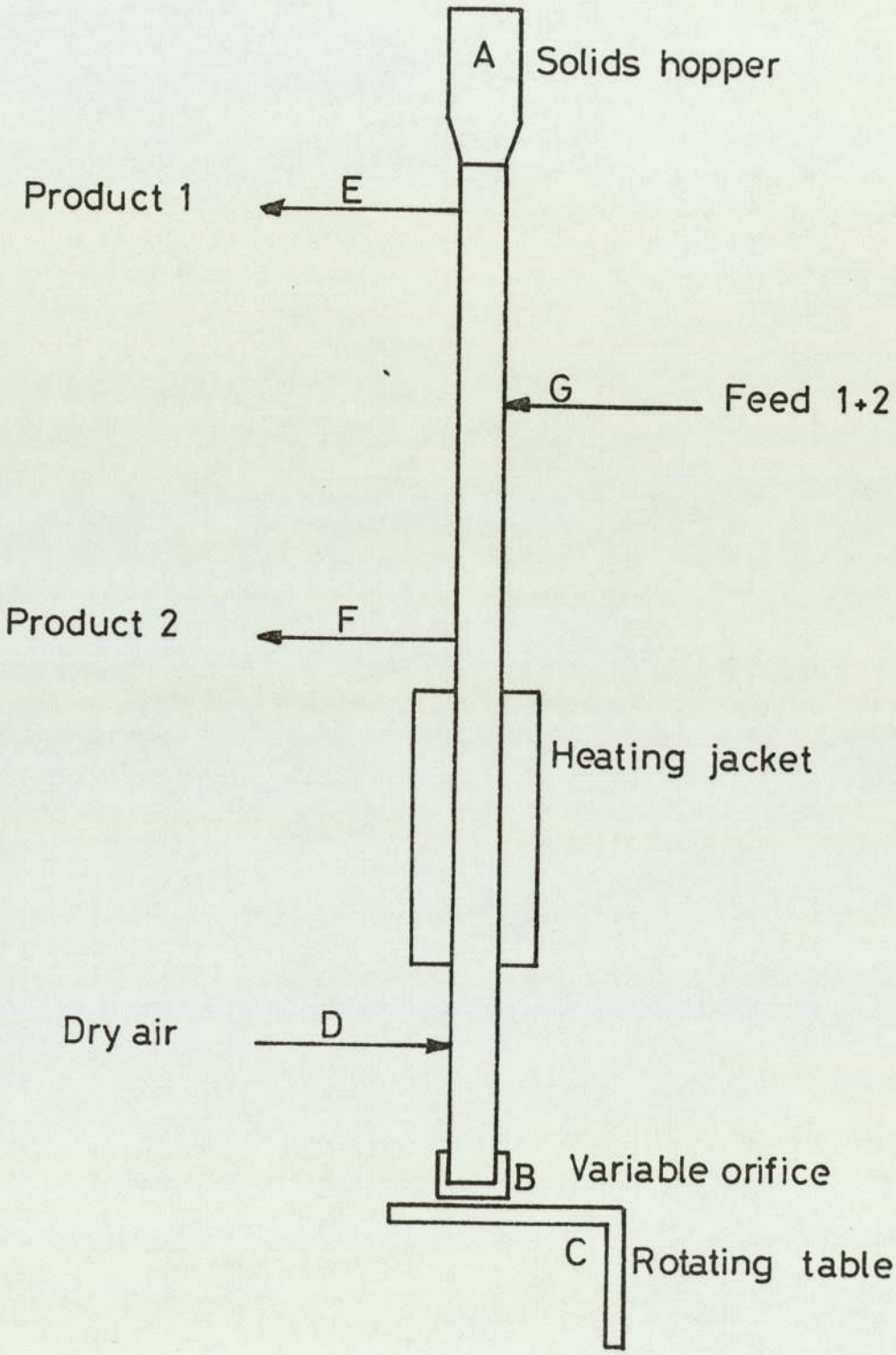

Moving bed chromatographic systems suffer from the following disadvantages:

(i) Problems with solids handling.

(ii) Inefficient column operation due to back mixing and low uneven packed densities.

(iii) Attrition and elutriation of the chromatographic packing.

(iv) Mobile phase velocities are limited to values below the minimum fluidising velocity of the packing.

Attempts to obviate these problems have concentrated on moving packed columns of equal lengths past fixed input and output ports, both by physically moving the columns and by simulating movement.

2.2.2.2.2 Moving-Column Systems

Moving column systems usually incorporate packed tubes arranged in circular form. The counter-current movement of the mobile phase and stationary phases has been achieved by employing one of the following methods:

(i) Mechanically moving the columns with fixed input and output ports.

(ii) Moving input and output ports with fixed columns.

(iii) Simulating the movement of the columns by sequencing the operation of fixed input and output ports on individual columns.

Designs based on the first of these have been proposed by Pichler and Schultz[56], Luft[57], Glasser[58], Gulf Research and Development[59] and Barker[60,61]. Figure 2.6 schematically represents the flow arrangement for these systems. The first four of these, Figures 2.6(a), (b), suggested that the relative port positions and mobile phase flow rates be selected such that the direction of flow was correctly maintained by balancing pressure drops. Barker[62] removed this restriction on the system by proposing that a mobile phase lock be installed between the two product outlets, Figure 2.6c. This arrangement ensured that the mobile phase travels in one direction only and, in addition, makes a greater column length available for separation.

Barker and Huntington[7] constructed a unit based on this principle (Figure 2.7). It consisted of eight equal square cross section chambers, 3.8 cm square, linked end to end by external values to form a toroid, 1.5 metres in diameter. The mobile phase lock was provided byclosing pairs of these values. Each chamber contained helical copper tubing through which heating or cooling fluids could be passed.

To permit the flow of the mobile phase into and out of the toroid, 80 self-sealing valves (face valves) were equally spaced over the chamber face, each mobile phase passage being closed by a self sealing valve. These face valves were automatically operated by cams in the port zones, thus connecting the port with the interior of the toroid. Sealing is achieved on the face of the chamber by means of 'O' rings that covered at least three of the face-value holes at anytime under each port. The 'O' rings are sealed against the face by

FIGURE 2·6 Circular Column for Counter-current Flow Processes

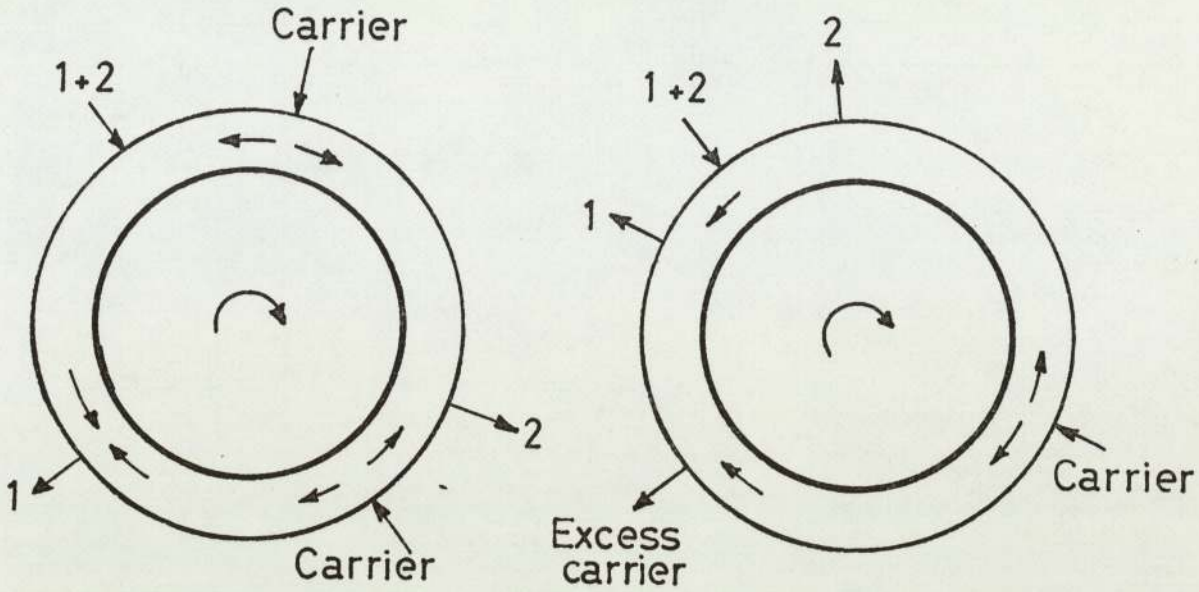

a) Pichler(56), Glasser(58) b) Luft(57)

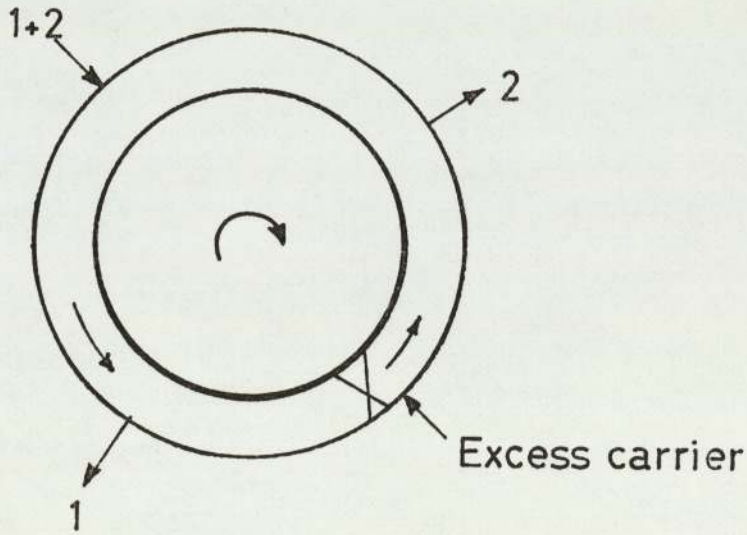

c) Barker(60,61)

FIGURE 2.7 Circular Moving Column Chromatograph

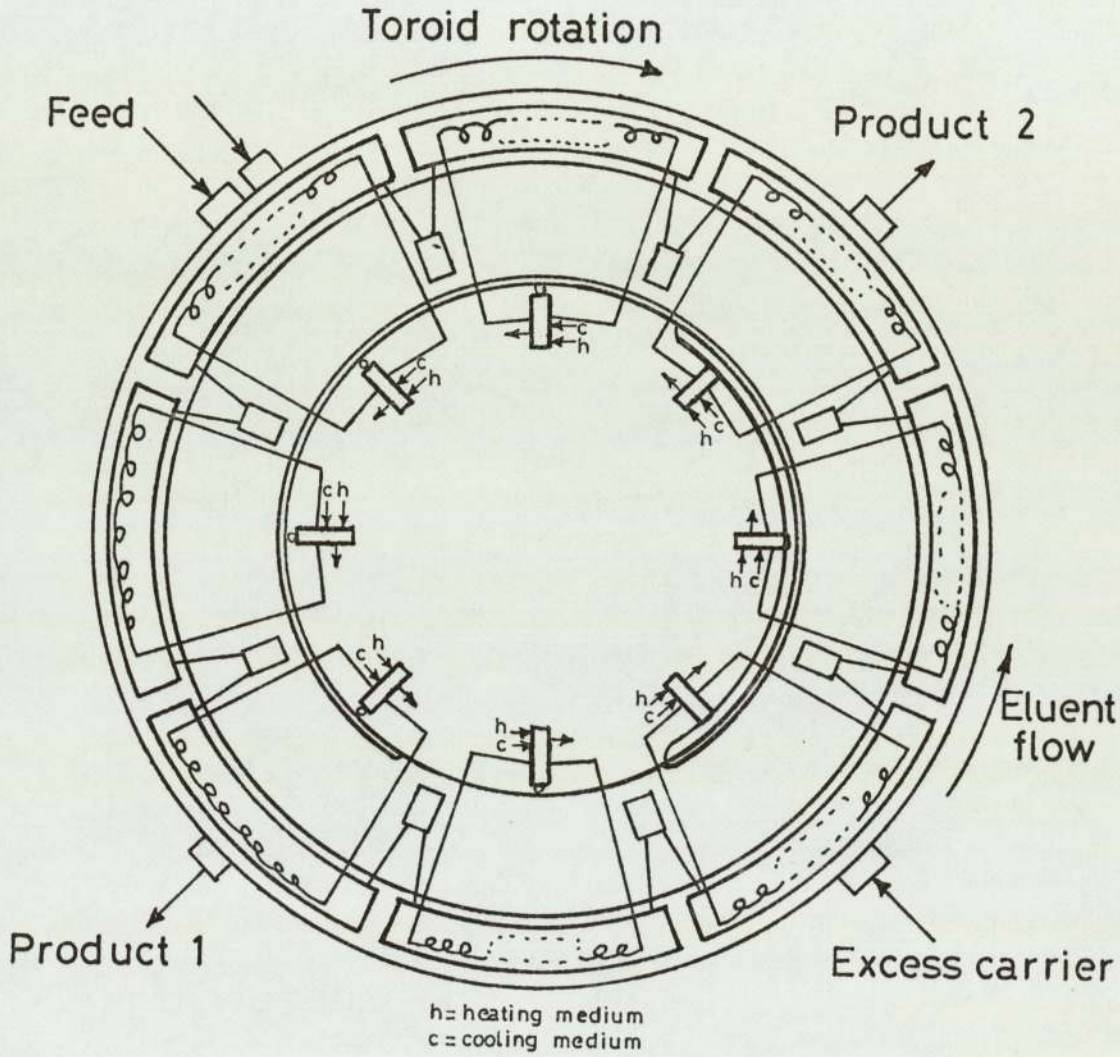

means of spring loaded plates. A chain drive mechanism rotated the toroid at between 1 and 10 revolutions per hour. This equipment was successfully used to separate azeotropic andclose boiling mixtures at feedrates up to 450 cm^3 hr^{-1}.

Hatt[11] applied the equipment used by Huntington[63] to liquid-liquid chromatographic separations. Using an ion exchange resin as the stationary phased and distilled, deionised water as the mobile phase Hatt[11] successfully separated a mixture of D-glucose and soluble starch at feedrates up to 2.4 g hr^{-1}.

Scaling up the toroidal chromatograph was not thought practical because of the large and cumbersome nature of the machine. Barker[64], in collaboration with Universal Fisher Group Ltd., overcame the problem of obtaining a greater separating power in a smaller volume by forming a cylindircal nest of 44 stainless steel tubes, 2.5 cm in diameter and 22.8 cm long. These tubes were linked alternatively at the top and bottom to give a closed loop, Figure 2.8. The columns were held between two stainless steel annular rings. Poppet valves in the bottom controlled the transfer of mobile phase between the columns. As the tube bundle was rotated a fixed cam depressed at least two of the valves in the bottom ring to provide the necessary lock and also to maintain unidirectional mobile phase flow.

Two sets of evenly spaced holes were drilled in the upper face of the top ring. One set provided access to the columns for the feed and the other for excess mobile phase inlet and product outlet. As the columns rotated under four fixed positions parts, cams operated poppet valves and permitted flow to and from the tube bundle. Spring loaded "Graphlon" seals were held against the top face of the upper ring

FIGURE 2.8 Compact Circular Moving- Column Chromatograph

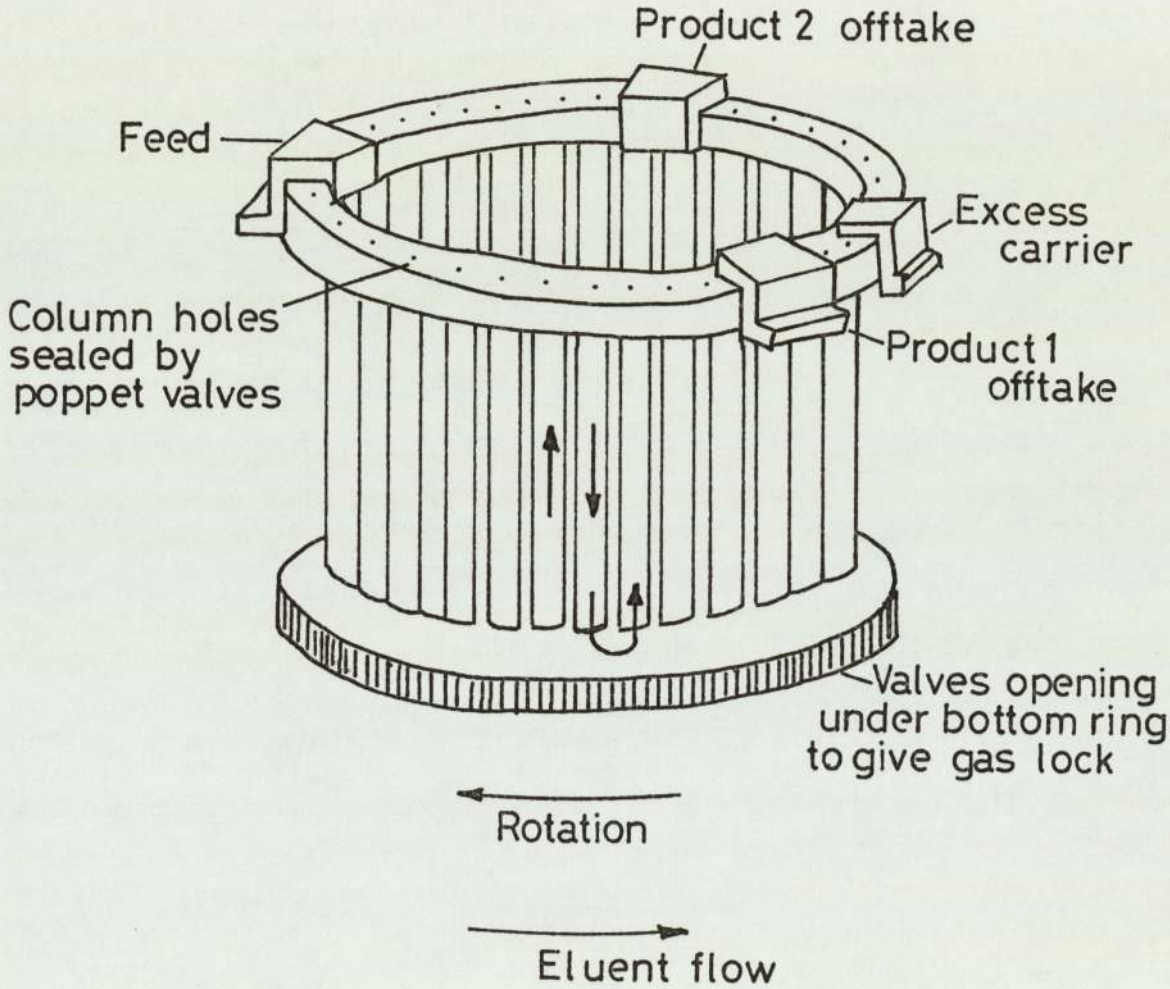

to prevent leakage from the ports when the valves were open. The complete unit was housed in an electrically heated thermostatically controlled oven operating to 200°C.

Barker and co-workers[7,65] have published experimental performance data demonstrating the improved separating power of this system over the 1.5 metre toroidal chromatograph. Feeds of 97% pure cyclopentane and 99% pure cyclohexane were used at throughputs up to 154 cm^3 hr^{-1}, with product purities exceeding 99.99%. Several other examples are quoted in the literature[65,66].

The operating experience gained with the compact circular chromatograph established that the poppet valves were unreliable under conditions of stress, temperature and corrosive chemicals. A bench scale version of the tubular chromatograph was constructed in which the reliance on poppet values was to a great extent removed. This unit consisted of 44 stainless steel tubes, 0.8 cm internal diameter arranged, in an annular form between two stainless steel rings, to form a circular tube bundle. An essential feature of this systems was a moving mechanical seal one part of which was a static annular ring containing the input and output ports, the other sealing face was the top of the tube bundle.

Barker et al.[61] and Hatt[11] applied this equipment to the liquid-liquid chromatographic separation of D-glucose and soluble starch. The possibility of applying the equipment to fractionate polymers was also demonstrated[11]. Two equipments have been built by Szepesy et al.[67] and Unidev Ltd.[68], both are in principle similar to that used by Barker et al.[61]. The modified Unidev equipment is currently commercially marketed by a subsiduary of Unilever Ltd., Precision

Engineering Products (Suffolk) Ltd. The equipment developed by Szepesyet al.[67] has been applied to the separation of fatty acid methyl esters at feedrates of 5 cm^3 hr^{-1}. The unit consists of eight interconnected columns, 50 cm long and 1 cm in diameter, arranged in a circular manner around a centrally mounted programmed disc, which is mechanically rotated at preset time intervals.

The reliance of the above systems on the successful operation of moving mechanical seals impose severe limitations on their large scale application. Barker and Deeble[69] effectively removed this limitation with the development of a chromatographic unit in which the counter-current movement of the two phases was simulated using solenoid valves. Successful separation of a chlorinated hydrocarbon mixture at feedrates up to 1000 cm^3 hr^{-1} have been recorded using this equipment[70]. Ellison[22] has constructed a unit based on the same operating principle and has applied it to pilot plant scale liquid-liquid chromatographic studies.

From an industrial point of view the development of equipment suitable for scale up is of paramount importance. However, in view of the high cost of chromatographic media the importance of reliable laboratory scale equipment is particular relevant, since such equipment enables the assessment of both packings and suitable systems for study to be economically undertaken.

CHAPTER 3

The Design and Construction of the Continuous Chromatographic Machine

Prompted by the earler work of Barker and co-workers[61] on liquid-liquid chromatography, Rank Hovis Macdougall (Research) Limited commisioned the design and construction of a new chromatographic machine, the design of which was based on the earlier prototype used by Hatt[11]. The new machine was built and designed by the Shirley Institute, Manchester, and was specifically designed to avoid the mechanical problems encountered with the prototype[11,61].

In designing the machine particular attention had been paid to those parts of the prototype that were regarded as

a) mechanically unsatisfactory, and

b) had in some way proved to be unreliable.

In particular, the tube cage forming the moving bed section of the machine needed strengthening and the valves at the base of the tube cage needed redesigning. The rapidly escalating cost and the shortage of time prevented the complete redesign of the whole unit. As a result, some of the areas which had caused operational difficulties with the prototype were not completely redesigned in the new machine. Details of those parts common to both machines are given in the following text.

The new chromatographic machine formed the essential part of the equipment needed for the projected experimental fractionation and separation studies.

3.1 GENERAL OPERATING PRINCIPLE

Figure 3.1a schematically represents the distribution of two components within the system a short time after the introduction of feed to the system. Carrier fluid (the mobile

FIGURE 3.1 Diagram of Continuous Chromatograph Operating Principle

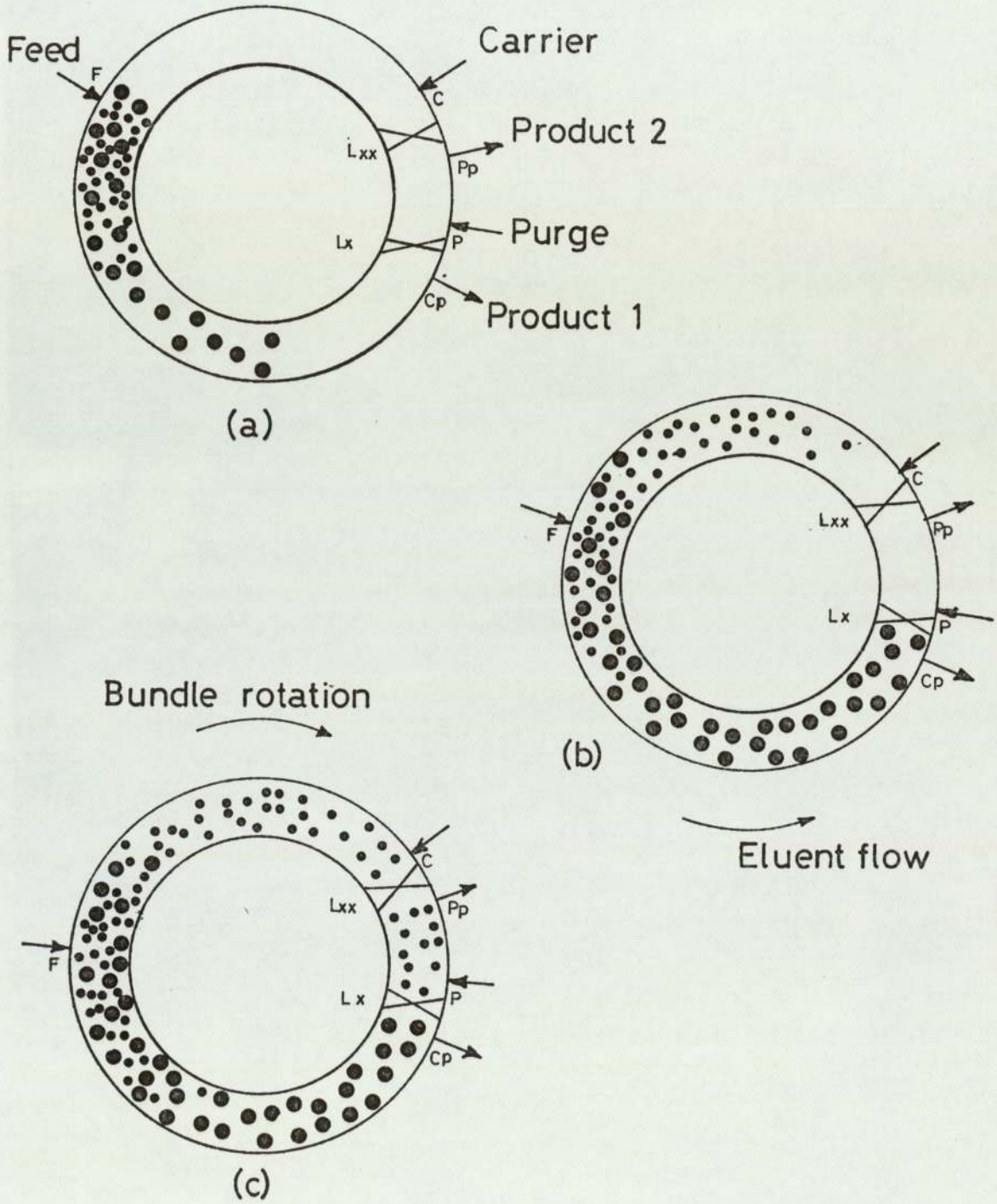

phase) enters at point C and flows through and around the packing. The component which prefers the mobile phase, component 1, preferentially moves towards the Product 1 offtake port Cp. A section of the system is isolated by locks Lx and Lxx, and forms the purge section. An independent fluid stream enters the purge section at port P and exits via port Pp.

In Figure 3.1b the columns have been rotated past the fixed port functions in a counter-current manner to the direction of fluid flow. Component 2, which prefers the stationary phase, moves with the columns. Consequently component 2 moves in a direction opposing that of the carrier fluid, while component moves towards Product 1 offtake port Cp with the carrier fluid.

Figure 3.1c represents the fully established operating condition of the system. The isolated section, now containing component 2, is purged to give Product 2 and thereby clean the packing ready to receive the advancing component 1, at present issuing from Cp. It can be seen that the counter-current movement of the carrier (mobile phase) and the packing has been simulated by moving the packed columns counter-current to the mobile phase, port fixed input and output ports.

3.2 THE CHROMATOGRAPHIC MACHINE

3.2.1 Overall Description

Figure 3.1 shows the necessary moving and stationary functions of the chromatographic machine. The stationary functions are; the feed inlet, carrier inlet and outlet, purge inlet, and outlet ports and two liquid locks, and the moving function is the packed bundle of columns. The ports are set in a stainless steel ring which acts as a backing plate to a ring of graphlon

(graphite/P.T.F.E. composite) (ring A, Figure 3.2 and Plate1). Twelve pneumatically operated rams act on the metal ring and firmly press the graphlon (Plate 2) on to the stainless steel top of the tube bundle (Plate 3). The bundle consists of forty-four (44) tubes contained between two stainless steel rings (Figure 3.2, rings B and C) which in turn are fixed on the inside by a mild steel cylinder. The tubes were open at both ends of the bundle. At the lower end, ring C, alternate pairs of tubes were connected by either a connecting block or a cam-operated spring loaded valve, these valves provided the necessary liquid locks. At the top of the tube bundle pairs of tubes were connected to one another by an elliptical trough, machined into ring B (Figure 3.2). The tubes were thus connected to form a continuous zig-zag path for fluid flow. The outer edge of ring C (Figure 3.2) was machined to form gear teeth (210) which meshed with a drive from a variable speed servo controlled electric motor. The complete machine was contained in an oven (Plate 4) so that experimental studies could be carried out at different temperatures, although in fact the oven was not used as such in any of the present work.

3.2.2 Detailed Design and Construction

3.2.2.1 The Mechanical Seal

The mechanical seal consists of a static and a moving section. The moving section of the seal was the top face of the tube bundle and the static section was the metal backing ring and the graphlon ring. Figures 3.3 and 3.4 are scaled diagrams of the

FIGURE 3·2 Diagram of Continuous Chromatograph

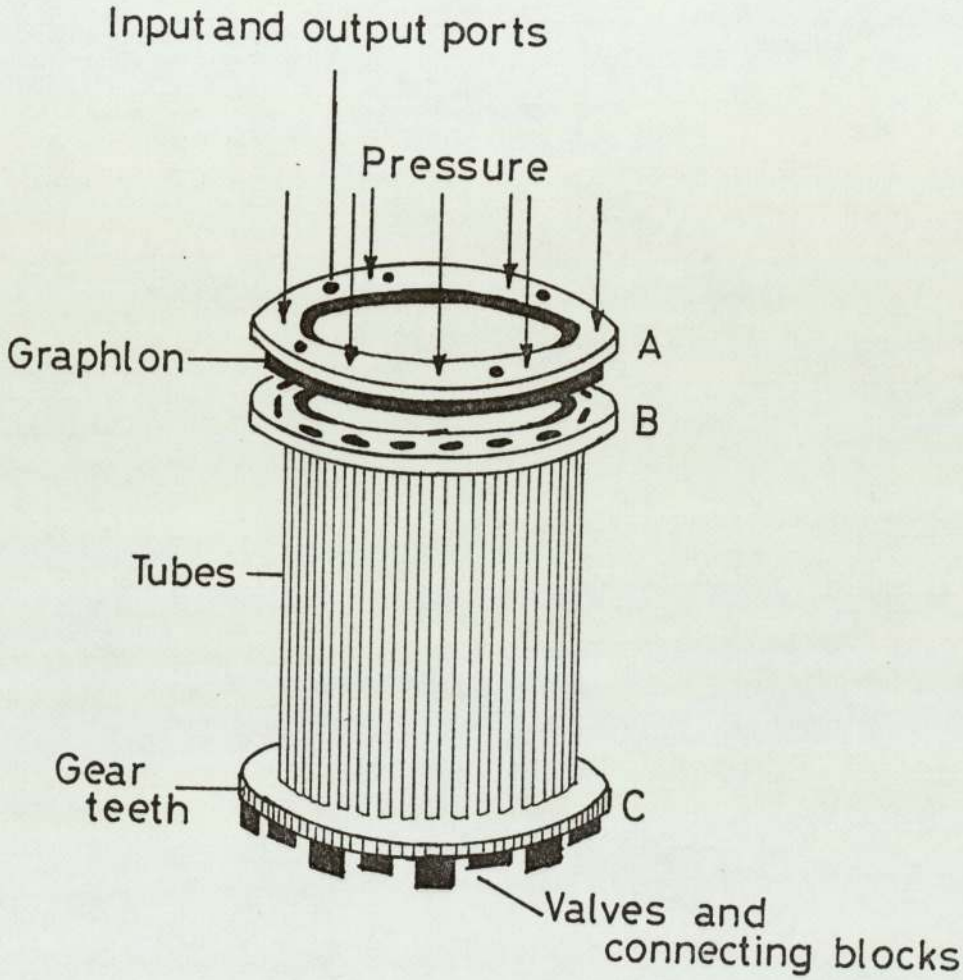

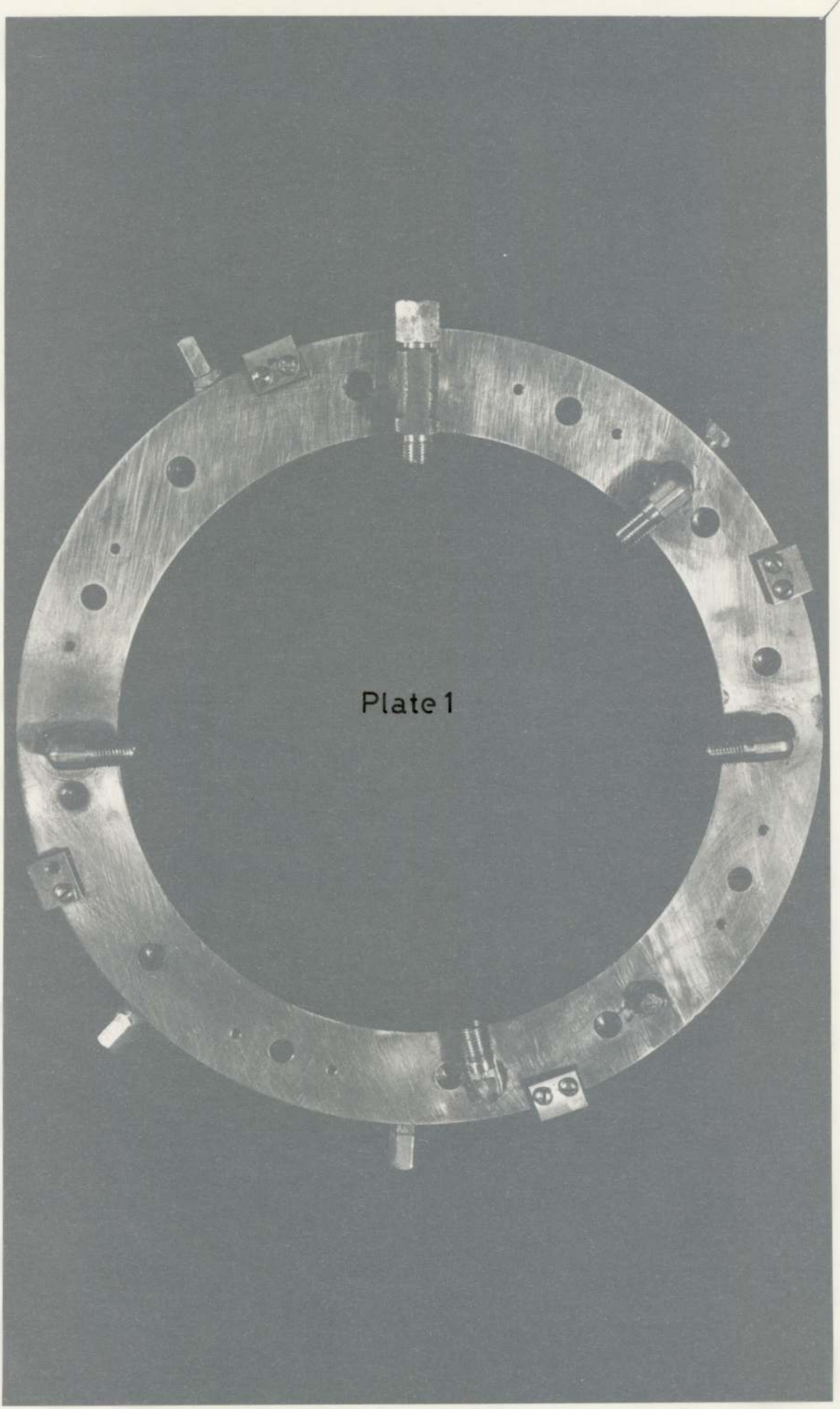

Plate 1

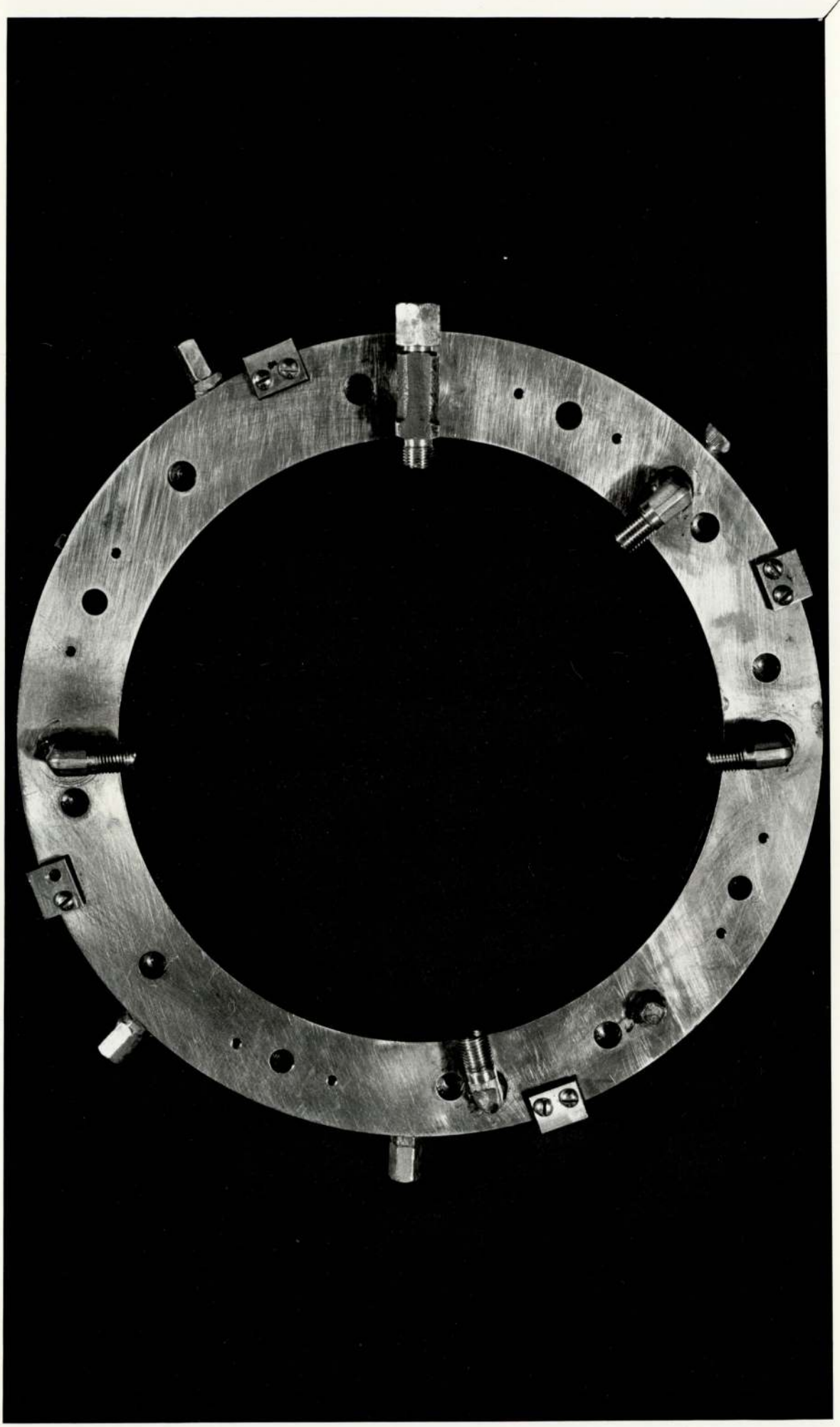

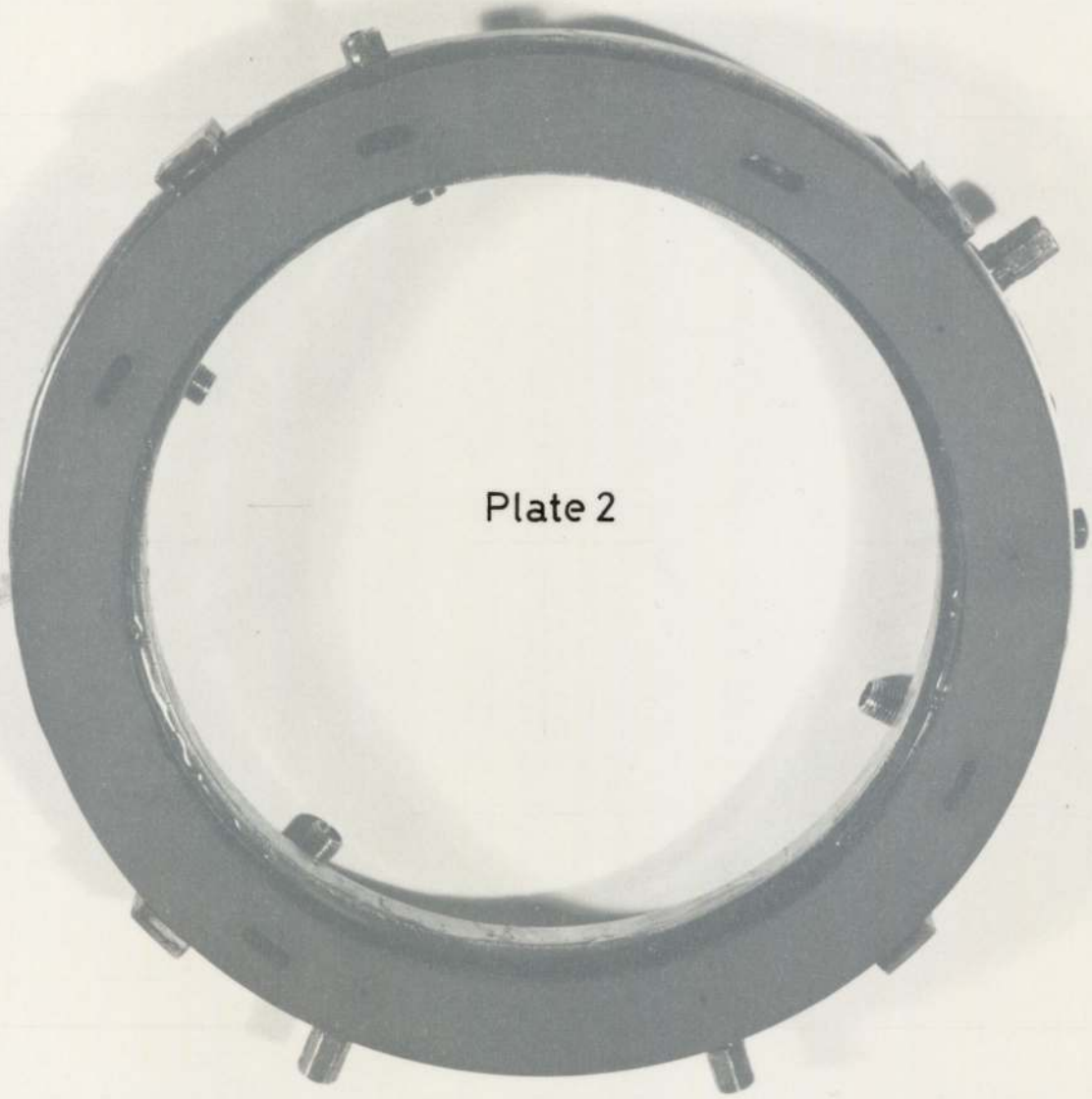

Plate 2

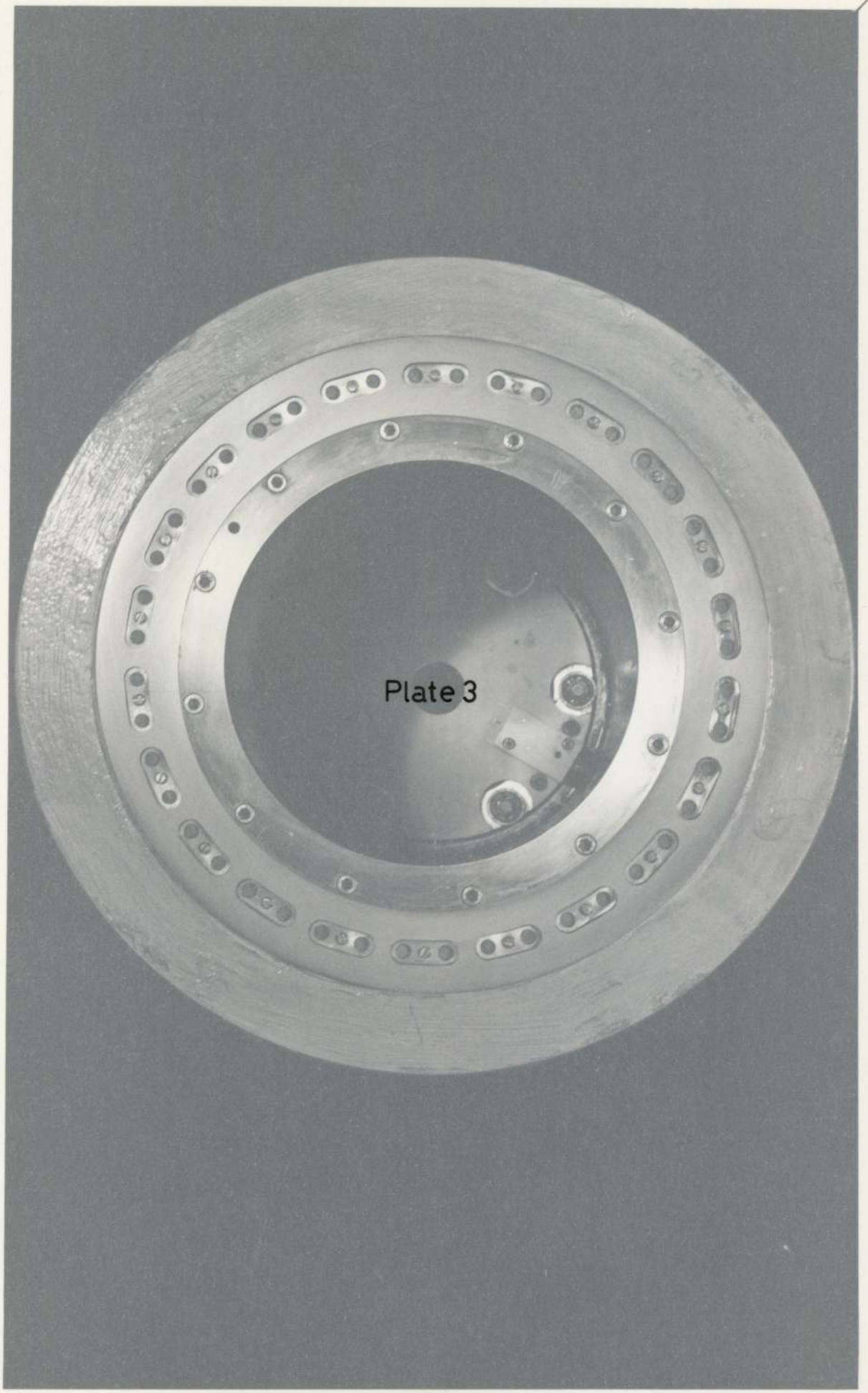
Plate 3

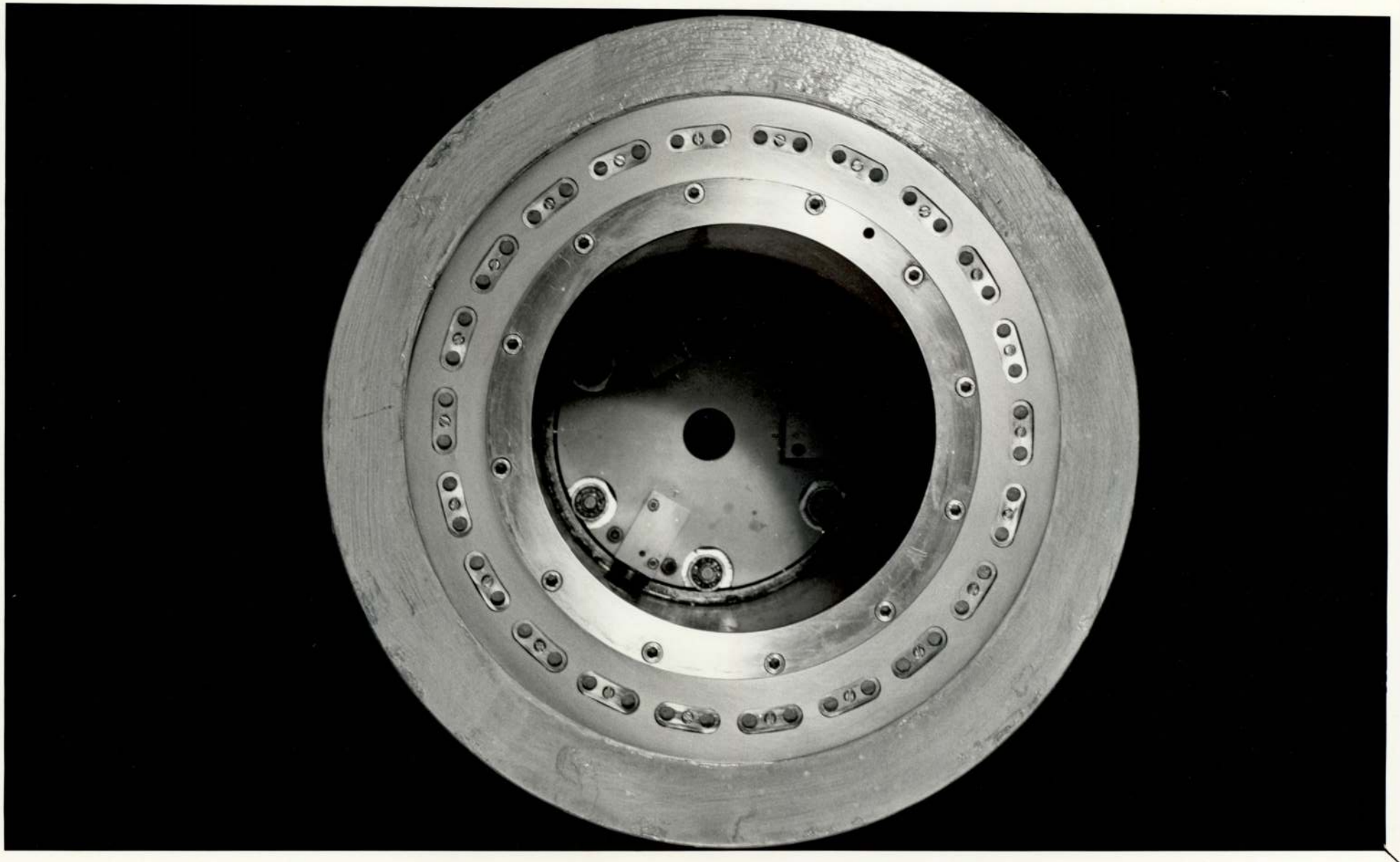

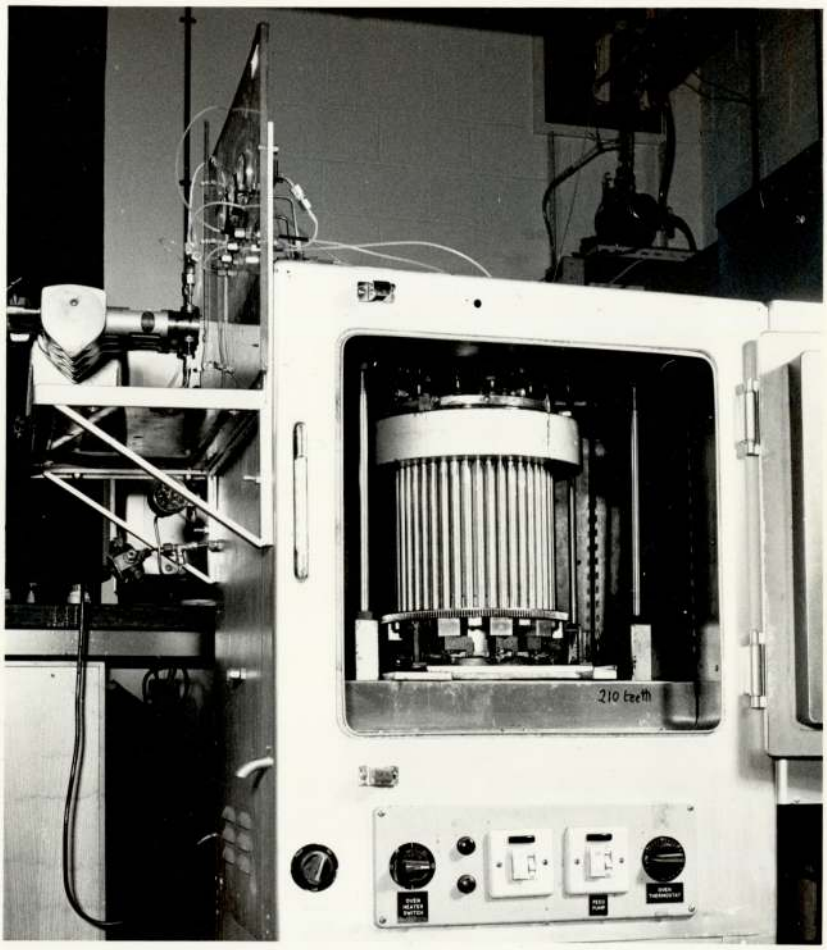

Plate4 The Continuous Chromatographic Machine

FIGURE 3·3 Diagram of Static Part of Seal

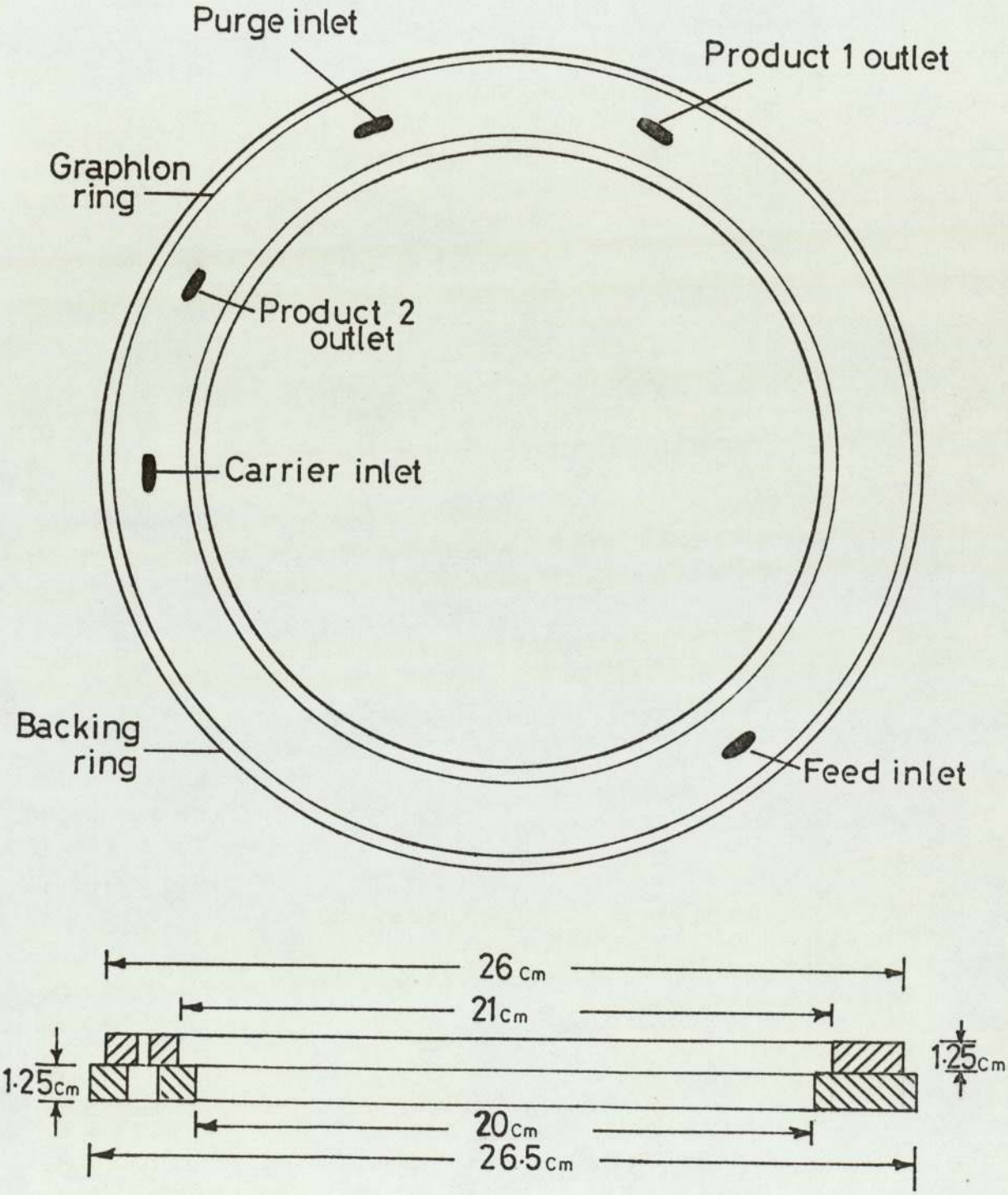

FIGURE 3·4 Diagram of Moving Part of Seal

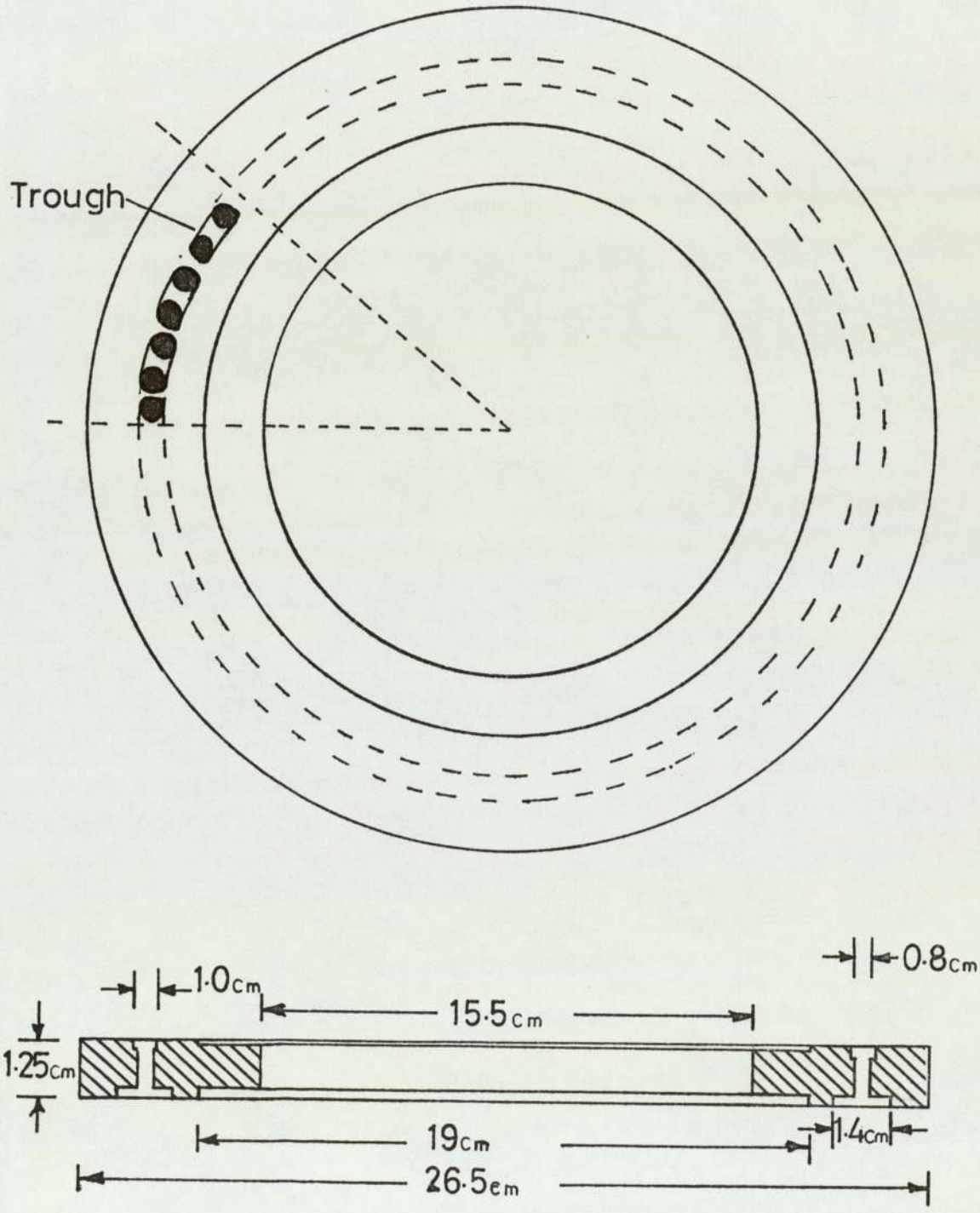

FIGURE 3.5 Vertical Section Through Tube Bundle

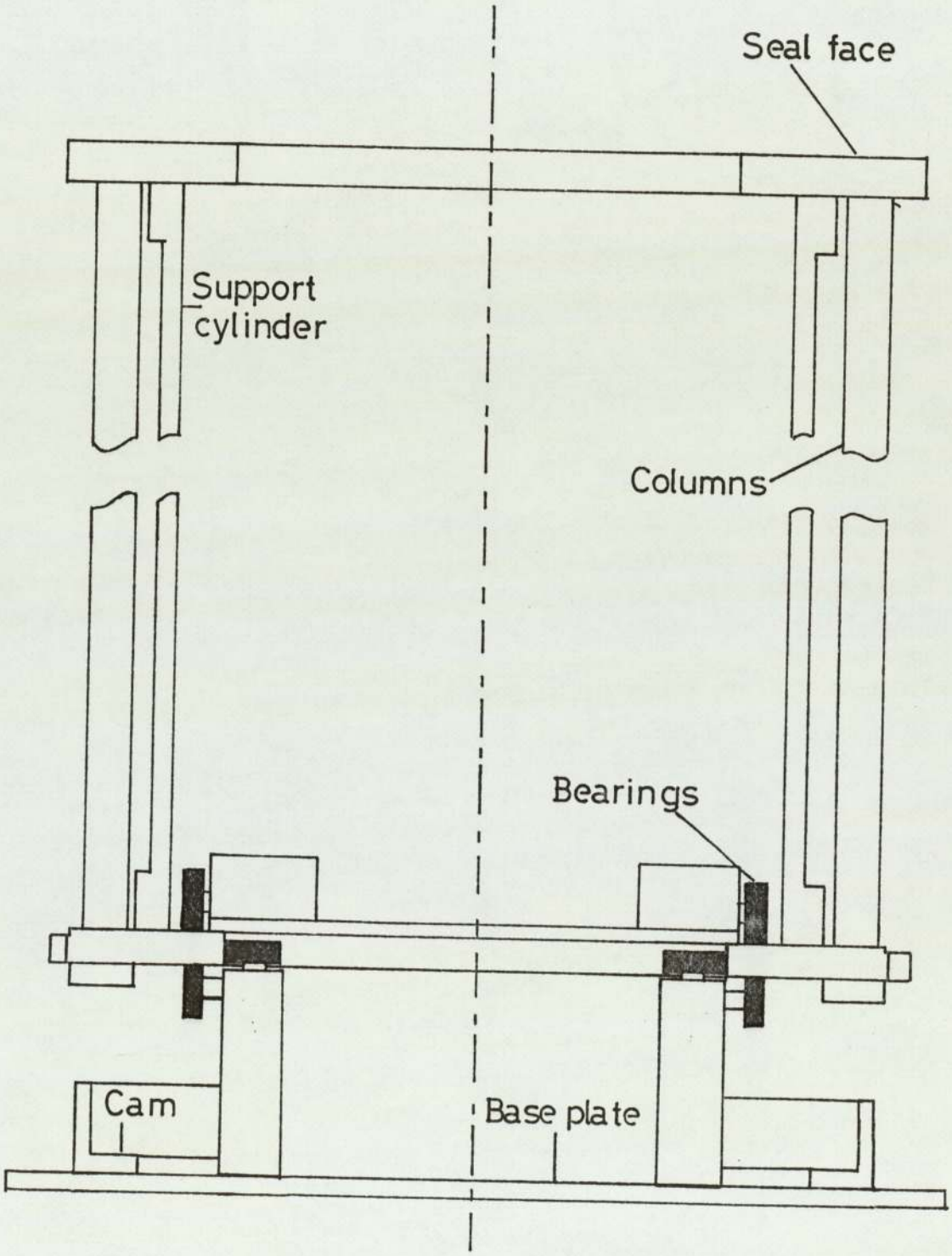

faces forming the seal. The graphlon ring was originally held firmly to the steel backing ring by four equi-spaced screws attached by brackets to the outer edge of the backing ring. This meant that one face of the graphlon and one face of the backing ring were in pressure contact and formed a static seal. The backing ring was fixed to four of the twelve pneumatic rams set in the roof of the oven. These rams were activated by compressed air from a cylinder and applied pressure at equidistant points around the backing ring. By adjusting the cylinder pressure regulator the pressure in the rams could be varied from 0-1000 kN/m^2 (0-160 p.s.i.g.).

The basic seal design and the method of applying pressure to the sealing faces was common to the equipment used in the research and the prototype employed by Barker and co-workers[11,61].

3.2.2.2 The Tube Bundle

Figure 3.5 shows a vertical section through the tube bundle. It can be seen how the two annular stainless steel (type EN58J) rings (26.5 cm O.D., 16.5 cm I.D. and 1.25 cm thick), supported at their inside by a mild steel cylinder (28 cm in length), act as retaining members for the 44 equispaced stainless tubes (0.8 cm I.D. and 28.6 cm long). A detailed diagram of a tube and how it is held between the two metal rings is given in Figure 3.6. The packing was held in the tubes by a stainless steel sintered disc, at the base of each tube, and by a gauze and backing plate, screwed into an elliptical trough cut into the top ring (Figure 3.7). The complete tube assembly was mounted on six equispaced ball races

FIGURE 3.6 Diagram Showing Method of Retaining Columns

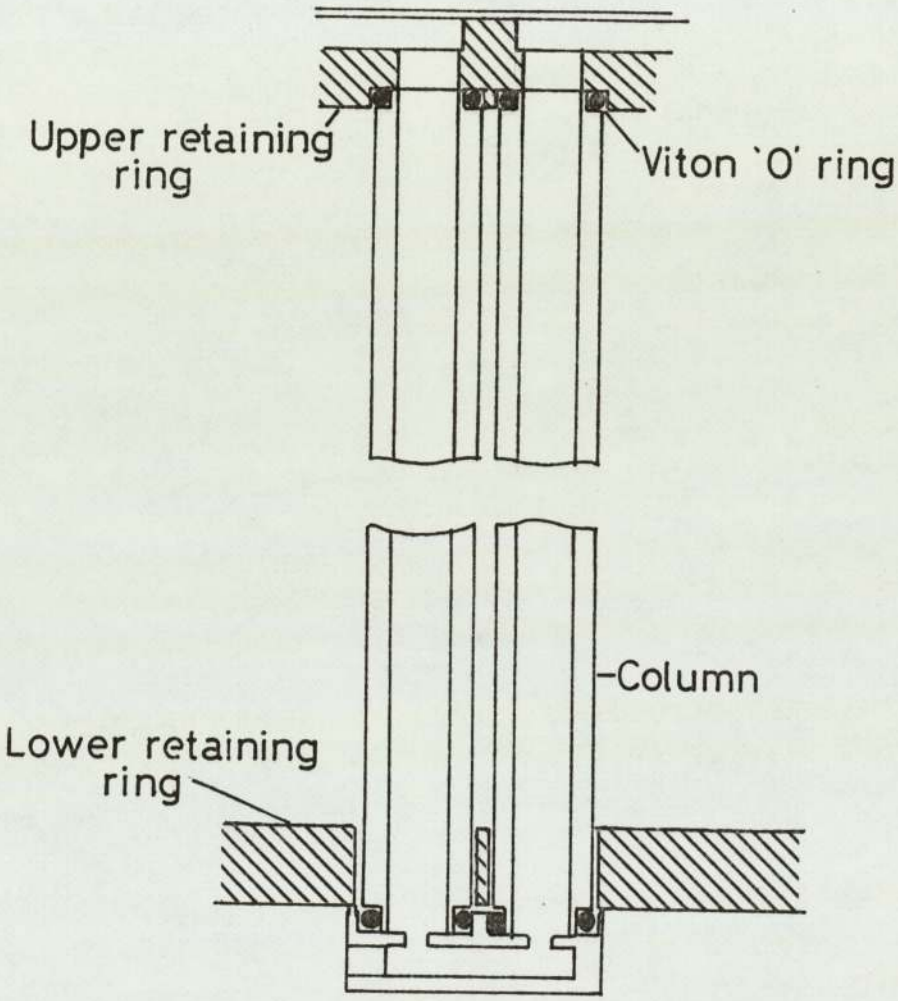

FIGURE 3.7 Diagram of Trough, Gauze and Backing plate

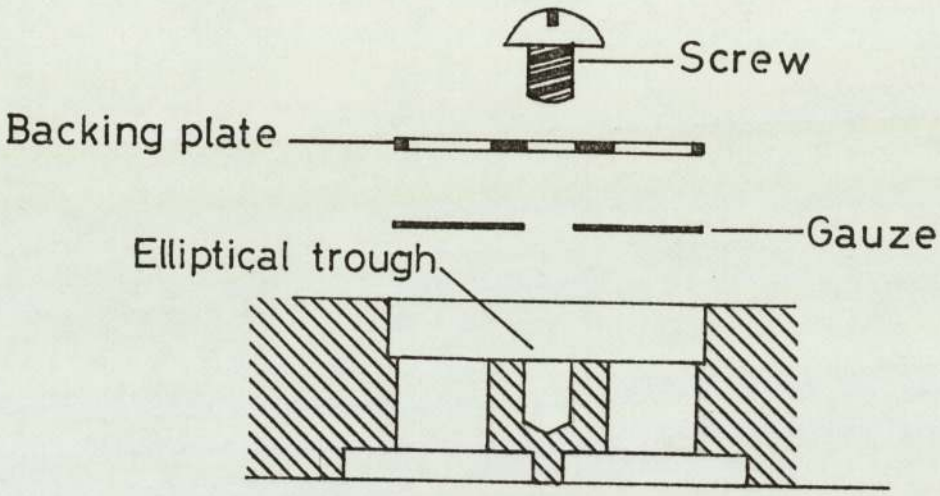

fixed into the side of a cylindrical aluminium pedestal (Figure 3.8). This pedestal was mounted on a base plate, which in turn was located in the oven by two metal pegs. Additional bearings fixed to the top of the pedestal effectively prevented any unwanted horizontal and vertical movement of the tube bundle.

3.2.2.3 The Valves and Connecting Blocks

The connecting blocks (Figure 3.9) were made from hexagonally shaped blocks of stainless steel into which a 'U'-shaped hole had been drilled. Eleven such blocks connected alternate pairs of tubes. The remaining eleven pairs of tubes were connected by cam-operated spring loaded valves (Figure 3.10). The cam operating these valves was permanently attached to the base plate of the tube bundle.

3.2.2.4 The Drive Mechanism

A variable speed servo controlled electric motor was mounted beneath the main body of the oven. A drive shaft from the motor extended through the oven floor at the end of which fixed a small toothed gear wheel. The wheel meshed with the toothed edge of the lower ring of the tube bundle, thus enabling the 1/4 H.P. motor to rotate it. The servo control mechanism was fixed to the side of the oven. This mechanism was specifically designed to ensure a constant bundle rotation speed and, when required, accurate temperature control.

FIGURE 3·8 Diagram of Pedestal and Bearings

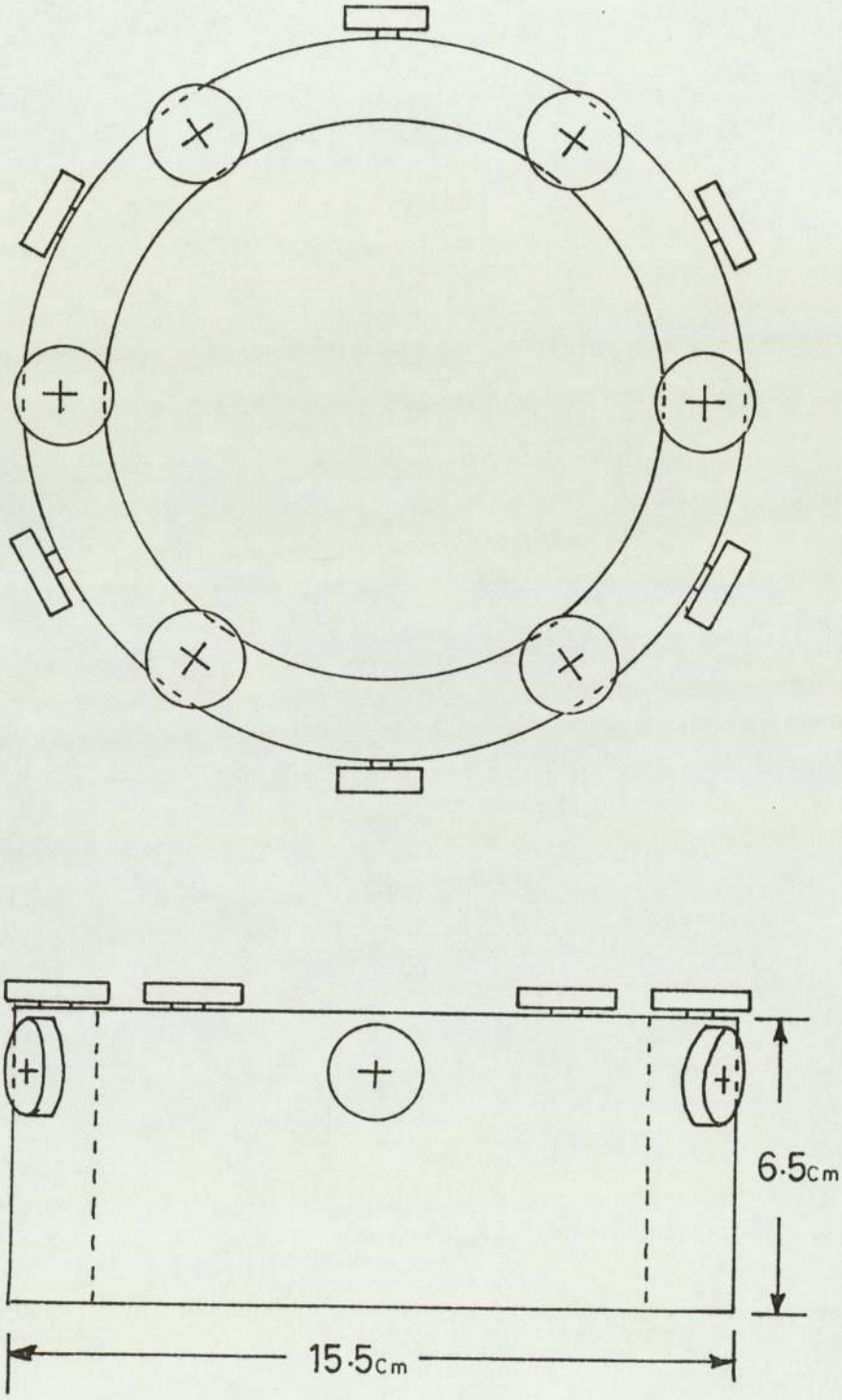

FIGURE 3·9 Tube Connecting Block

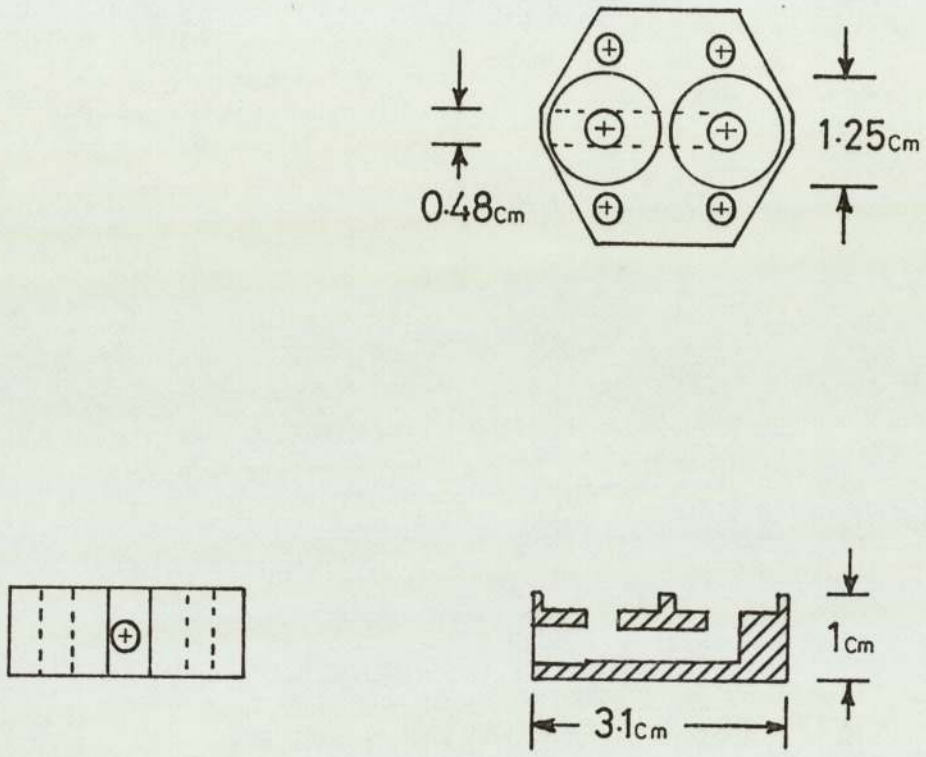

FIGURE 3.10 Cam-operated Spring Loaded Valve

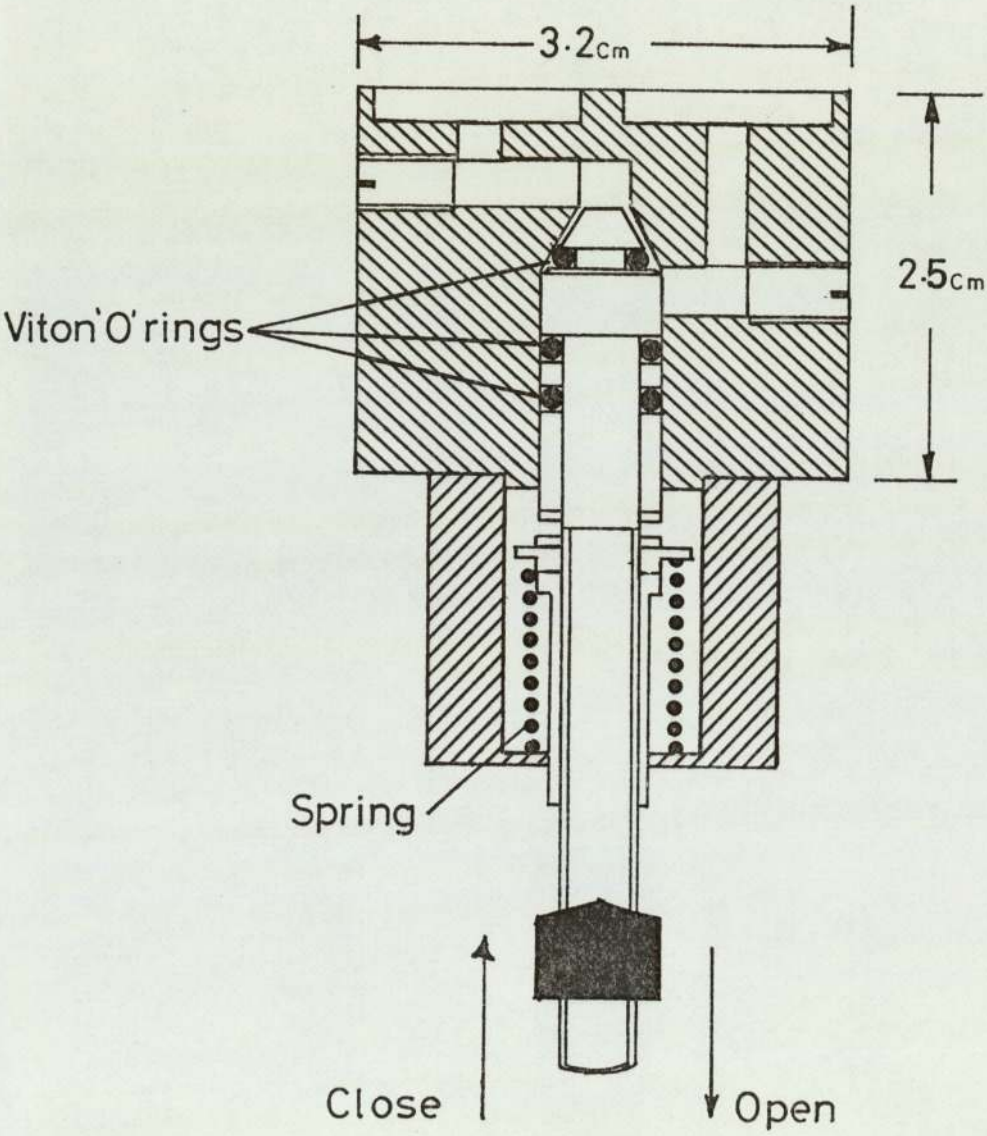

3.2.2.5 Measurement and Control of Fluid Flow

Calibrated burettes on the input lines were used to measure the liquid input rates to the machine. Output rates were measured by accurately weighing the liquid output from each product line over a known time period. By measuring the time taken for a known fraction, usually one-tenth of the gear teeth on the lower ring, to pass a fixed point an accurate determination of the bundle speed could be made.

All the input lines were fitted with replaceable sintered glass filters and calibrated pressure guages. When required, liquid deaerators were also used. The object of employing deaerators was to prevent dissolved gases coming out of solution, particularly on the packing in the tube bundle. Three positive displacement pumps (Metering Pumps Ltd.), were used head sizes 1, 2 and 3 respectively. All the pumps were carefully maintained so that they delivered constant flow rates over long periods. As a consequence of this regular maintenance the two larger pump heads, 2 (0-150 $cm^3\ hr^{-1}$) and 3 (0-340 $cm^3\ hr^{-1}$), gave very few problems throughout the course of the research. However, the pump that delivered the smallest delivery rate, head size 1 (0-11 $cm^3\ hr^{-1}$), proved to be very susceptible to;

(i) any change in the pumped fluid viscosity,

(ii) the presence of minute amounts of air in the pump plunger chamber, and

(iii) the effect of very slight damage to the seats on the non-return valves.

Initially this pump proved to be very unreliable. However a maintenance technique was developed (Appendix 1) which ensured the consistent running of the pump. Accurate delivery rates from this pump were particularly important since it was used to pump the feed. Feed flow rates employed during the research work were of the order of 0.05 cm^3 min^{-1} to 0.1 cm^3 min^{-1}. The pump head size1 was found to be best suited for this range of flow rates. One of the operating requirements of the positive displacement type of pump is that there should be a positive pressure on the pump inlet side. Provision was made for this in the design of the feed and eluent reservoirs by placing them at least 60-100 cm above the level of the pumps.

To enable the products to be sampled regularly a fraction collector, of novel design, was designed and built in the Departments workshops. Commercially available alternatives were unsuitable because they were either too expensive or not practically suitable. Further details of the fraction collector are given in Appendix 1. Subsequently Pharmacia Ltd. have marketed a machine which works on identical principles.

3.2.3 The Packing Procedure

For reasons that will be discussed in Chapter 6, the chromatographic packing used in this research was Spherosil(Porasil) XOB075 (200-400 μm). The total volume of the tube bundle occupied by the packing was calculated as 635 cm^3. The bundle was first bodily removed from the oven and all the packing retaining gauzes removed. The Spherosil beads, which had been deaerated by

evacuating under distilled water, were added as an aqueous slurry to the water filled bundle. An adapted polythene wash-bottle proved a very convenient dispenser for the slurry of beads. Each tube was then continuously manually tapped until a stabilised packed bed was obtained. Where necessary the tubes were topped up with packing and the tapping procedure repeated. When all the tubes were full the retaining gauzes were replaced and the excess packing very carefully removed from the sealing face. The tube bundle was then replaced in the oven, the top plate lowered on to the bundle and pressurised by introducing compressed air into the rams. Water was pumped through it for several hours whilst the bundle rotated so that each tube passed through the region of highest pressure. The levels of packing in the tubes were checked and the procedure repeated until all tubes were fully packed.

3.2.4 General Operating Procedure

A formal operating procedure was established as follows. A general check and servicing of the various functions of the unit was performed. The pumps were checked and if necessary cleaned and maintained, as were the filters and pressure gauges. Special attention was paid to the moving mechanical seal as the success of the experimental programme depended on its satisfactory operation. Section 3.4 is devoted to a detailed account of the problems associated with the mechanical seal and the measures taken to solve them. A series of liquid mass balances were performed and a mass loss of less than 5% was regarded as satisfactory.

The flow rates required for the experiment were then set and experimentally checked. If required the bundle rotation speed was altered and measured. Finally, the machine was allowed to stabilise at the set conditions for at least 24 hours. The feed reservoir was then hastily connected to the feed pump, which had previously been pumping water, and the run started. The flow rates and pressure drops were measured at regular intervals. Mass balances were performed to provide information on the performance of the mechanical seal. The product outlet lines were linked either with the analytical unit and/or the fraction collector, or allowed to go to waste. When the fraction collector was not used, samples of the two product streams were manually taken at regular intervals during the experiment.

In some experiments attempts were made to determine the component concentrations within the tube bundle. This information was obtained by stopping the flow of eluent and feed to the bundle and allowing each tube pair to pass through the section. The contents of each tube pair were then purged, collected and analysed. The purging time was a function of the bundle speed; each tube was purged for a time equivalent to one "switch time", T. The "switch time" was equal to $^{1}/_{22}$ nd of the complete cycle time.

3.3 PRELIMINARY TRIALS

During the work with the prototype machine it had been established how important it was that the two faces forming the seal were kept clean and flat. In addition, it was also

found that the seal faces required a running-in period before a suitable seal was obtained. In an attempt to avoid long running-in times, the motor, normally used to drive the tube bundle, was replaced by a faster one (1-2 r.p.h. compared to about 0.125 r.p.h.). The faces forming the seal were then cleaned and the machine assembled. A pressure of 276 kN/m^2 (40 p.s.i.g.) was applied to the rams pressurising the top plate on to the tube bundle. The bundle was then rotated for 3-4 weeks during which time the seal faces were regularly inspected. The face formed by the metal ring of the tube bundle altered very little in its physical appearance. However, the graphlon face had a high degree of shine on its outer edge. On increasing the pressure in the rams to 1000 kN/m^2 (160 p.s.i.g.) the polished area increased until it covered the whole of the seal face. It was assumed that the seal was now in a suitable condition to be pressure tested. Distilled water was pumped into the unpacked machine and an artificial back pressure applied to the liquid outlet. During this test there was visible evidence of liquid leakage at the inside surface of the moving seal and also from the static seal formed by the graphlon and its metal backing ring. Leakage was particularly noticeable in the region by the four locating screws which held the graphlon to the backing ring. At the end of a four week running-in period there was no evidence of any improvement in the seal. Investigations were then undertaken to determine the exact shape of the sealing faces, how they mated, and, if possible, their degree of flatness.

A Taylor-Hobson Tallylin 4 (Metrology Lab., Department of Production Engineering, University of Aston) was initially used. Unfortunately, this instrument could only traverse over a small section (10 cms) of the sealing face. Therefore no information could be gained as to whether the faces were truly flat and parallel with respect to each other. An instrument capable of determining flatness over a 26.5 cm diameter circle was a Taylor-Hobson Tallylin 20. Enquiries were made and it was established that such an instrument was available at the Royal Radar Research Establishment (R.R.R.E., Malvern). Permission was obtained for its use and the sections forming the seal removed from the oven and transported to Malvern.

Measurements were taken of both surfaces of the graphlon ring, the mating surface of the backing ring and finally the top face of the tube bundle. Figure 3.11 and 3.12 are typical examples of the traces obtained during these investigations. The horizontal axis on these diagrams is distance in centimetres and the vertical axis is a measure of the difference in height from a fixed reference point. The traces of the faces forming the moving seal (Figure 3.11) clearly shows the near compatability of their shapes. In contrast, the faces forming the static seal (Figure 3.12) are both concave in shape, and therefore would not mate correctly. The traces show that the two highest areas of both surfaces were in intimate contact and therefore it is probable that as the sealing pressure was increased the graphlon deformed bringing the remainder of the sealing surface into contact. This would explain why it was that as the pressure was increased the degree of shine extended over the whole surface.

FIGURE 3·11 Moving Seal Tallylin Traces

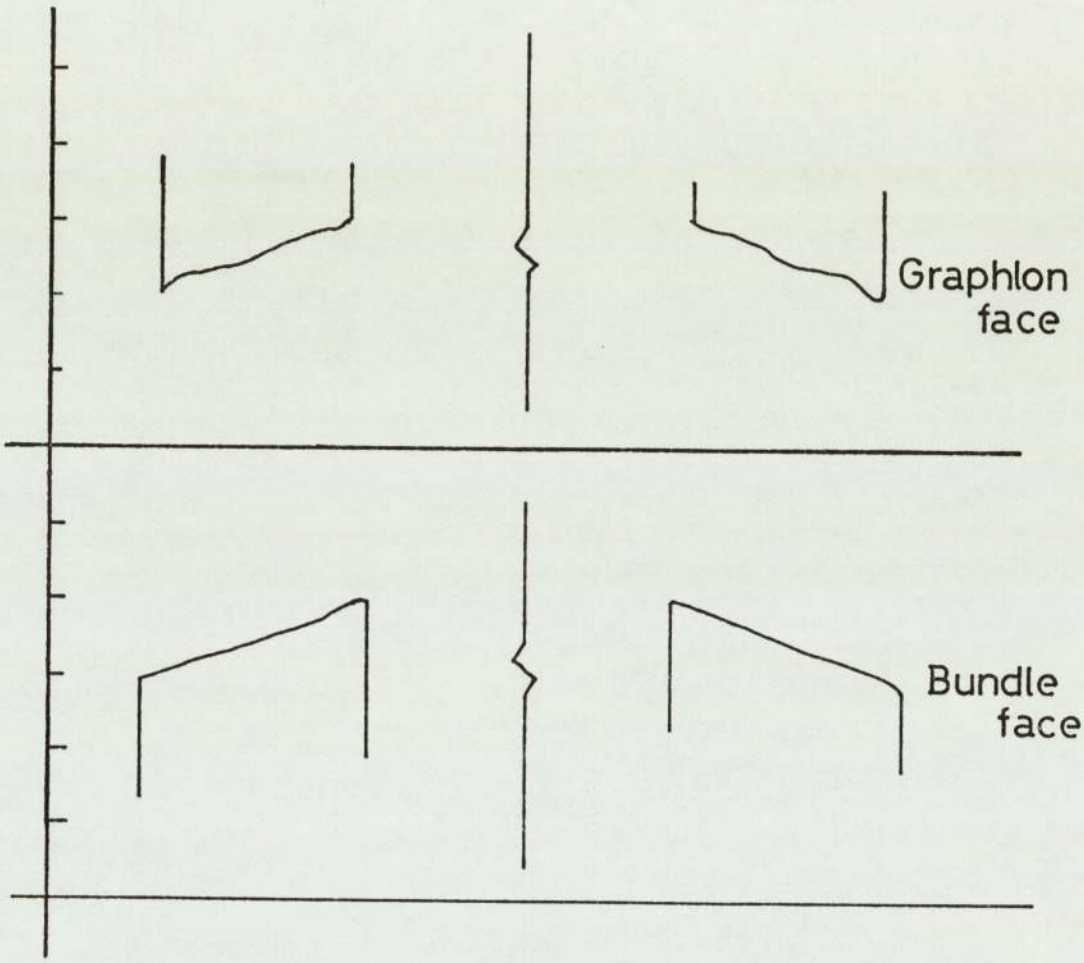

Magnification: horizontal x 1 (Cm)
vertical x 2000
Scale : 1division = 10μm

FIGURE 3.12 Static Seal Tallylin Traces

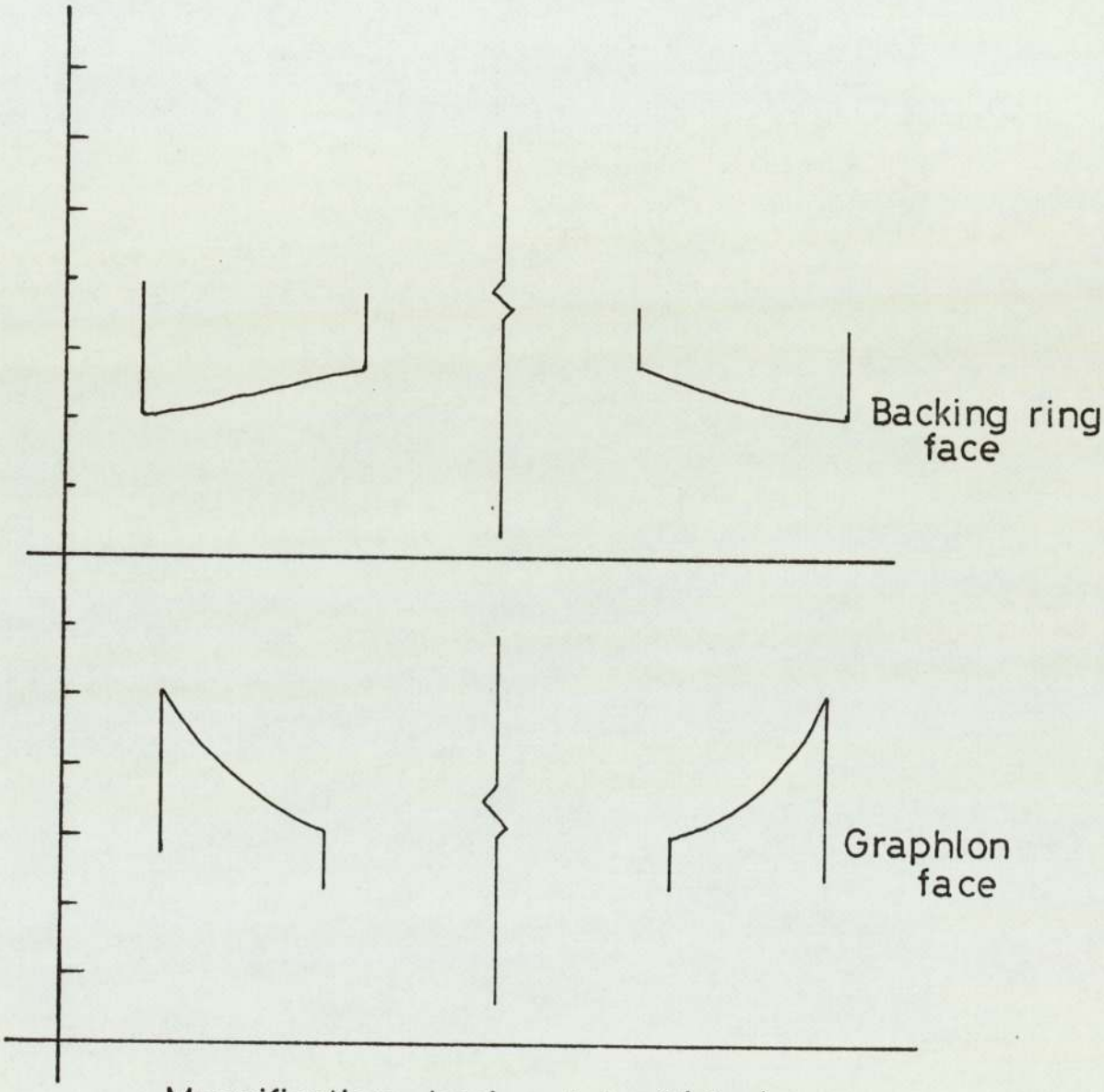

Magnification: horizontal x1(Cm)
vertical x2000
Scale : 1division = 10μm

Before reassembling the machine the two faces forming the static seal were manually ground. This was carried out on a piece of plate glass using a mixture of ethylene glycol and fine carborundum. The two faces were then firmly fixed together with a silicone rubber. Silicone rubber was initially used because it was thought the elastic properties of the rubber would prevent the transmission of distortions from the backing ring to the graphlon. Care was taken to ensure that the liquid paths through the graphlon remained clear. The faster electric motor was then replaced with the original one and finally the tube bundle packed with Porasil D (150-200 μm, 75-100 mesh). The packed bundle was then replaced in the oven, the rams pressurised and water pumped through it. This was an attempt to improve the seal by running the machine under real operating conditions. Over an extended running-in period of several weeks further attempts to improve the seal were made by:

a) increasing the oven temperature

b) grinding the seal faces in 'in situ'

with fine carborundum and grease but unfortunately all to no avail. In fact the leakage at this stage was measured as being 65% at a back pressure of 68.9 kN/m^2 (10 p.s.i.g.). The seal faces were then separated and examined. Both faces showed a high degree of scratching and roughness. It was therefore decided to have both faces professionally lapped. This was undertaken by Payne International Products Ltd. (Slough) who attempted to get the faces flat to within 1-3 lightbands (1 μm or 11.5×10^{-6} inches)[73]. This degree of flatness defines the maximum variation in the flatness across a surface.

After lapping, the machine was reassembled and water pumped through the bundle. The leakage was measured, and found to be 30% at 68.9 kN/m^2 (10 p.s.i.g.). Increasing the gas pressure in the rams from 561 kN/m^2 to 827 kN/m^2 (80-120 p.s.i.g.) reduced the leakage to 11%. Periodic examination of the graphlon seal face indicated that the silicone rubber was having an adverse effect on the faces bedding-in properly. Consequently the silicone rubber was replaced with Araldite. As a result, the leakage fell to less than 10% at 68.9 - 103 kN/m^2 (10-15 p.s.i.g.). A further increase in the pneumatic pressure to 1000 kN/m^2 (160 p.s.i.g.) and a reduction in the liquid flow rate through the bundle reduced the liquid leakage to less than 5%. The main disadvantage of having to reduce the liquid rate was that it severely limited the operating range of the machine. This problem was partially solved by repacking the bundle with a packing of larger average particle diameter. The packing chosen was Spherosil XOB075 (200 μm - 400 μm) equivalent to Porasil C. A number of experimental runs were then performed, the details of which will be discussed later. Regular mass balance carried out during the runs showed that there was a gradual increase in the leakage rate until reached a level of 30%. Further experimental work at this level of leakage was considered futile.

The continual failure of the mechanical seal led the author to assume that there were some basic design faults in the seal. Consequently, it was decided to investigate the problem in further detail in the hope that a solution, leading to the satisfactory operation of the seal, could be found.

Dr. C. Hooke (Mechanical Engineering Department, University of Birmingham), Mr. Ellis (Mechanical Engineering Department, University of Aston) assisted in the analysis of the sealing problem. In conjunction with Mr. Ellis, Messrs. Bush and Adamson (1974 final year undergraduates) were given a project on the subject.

3.4 ANALYSIS OF THE SEALING PROBLEM

3.4.1 Introduction

The successful operation of a mechanical face seal is dependent on the maintenance of adequate boundary film lubrication between the seal faces. This prevents excessive galling (rubbing) and wear[71]. In turn, the finite film separating the seal faces presents a path for the potential introduction of the sealed medium, be it liquid or gas, between the seal faces with the attendant possibility of leakage.

The elimination of boundary film conditionswould theoretically provide an ultimate mating of the seal faces, thus providing an absolute barrier to the introduction of the sealed medium. Research into the operating parameters required led to the development of face seals operating on a self-generating graphitic film without the necessity for any boundary fluid lubrication. Seals employing this principle should provide positive liquid and gas sealing.

In fact for this reason the original designers of the seal, employed in the continuous chromatograph chose Graphlon (a graphite/P.T.F.E. composite) as one of the materials of construction for the seal faces.

However, one point which may not have been considered was the fact that a back pressure would develop when liquid is pumped into the machine. This back pressure would promote the separation of the faces and the formation of a liquid film between them.

Since the formation and presence of an adequate homogeneous boundary film was obviously an important factor in the successful operation of the chromatographic machine. An appreciation of the importance of lubrication and the occurrence of wear is required in analysing the boundary film separation of seal faces.

The Boundary Film[71]

When sealing surfaces are in intimate contact under dynamic conditions of load and speed, their elastic molecular bonds oppose easy shearing of the surface layer and produce such undesirable features as adhesion, galling and ploughing with subsequent seal failure. The purpose of lubrication is to interpose a material possessing low shear strength between the surfaces to alleviate the above condition, and to also provide sufficient film strength to maintain separation of the surfaces under load. The separation of the faces may not be absolute; boundary lubrication has been described[71] as a film which varies in thickness and therefore provides varying degrees of face separation.

The separation of the face provides a finite orifice for flow of the pressurised fluid between the faces. Leakage will always exist as a result of this, although it may not be easily visible due to its low rate and surface evaporation. In many applications the presence of the working fluid between the seal faces not only does not harm the faces but actually provides the necessary

lubrication. On the other hand, the presence of liquid film lubrication in some seal applications may be undesirable. The latter case is particularly important in the chromatographic machine, were the presence of a liquid boundary film could result in product contamination.

In practice there are certain important mechanical and operating characteristics which act against the maintenance of a lubricating boundary film between mechanical seal faces. These are most notably the inability to maintain flatness, whilst in operation, and the inability to mechanically maintain exact intimate tracking and parallel presentation of the seal faces.

Seal Design Factors[72]

There are five fundamental factors which must be given serious consideration on the design of any mechanical seal. They are:-

i) The provision of two optically flat surfaces which will run in rubbing contact with each other.

Face seals are normally lapped flat to within a maximum of 3 lightbands variation[73] between high and low points. Usual methods of checking flatness involve optical interferometry and/or the use of surface measuring equipment. The text by Galyer and Shotbolt[74] gives a good description of the theory and practice behind these two techniques.

ii) The components forming the seal should be designed such that the parallel presentation of the lapped surfaces is not affected by distortions due to mechanical, thermal or hydraulic effects.

The latter is one of the most important factors influencing mechanical seal design. Far more important than the actual flatness of the seal faces is the problem of maintaining the parallel presentation of the faces. Under thermal, hydraulic and mechanical influences the seal distorts. This distortion leads to the breakdown and eventual destruction of the lubricating film between the faces. Under normal running conditions allowances must be made for the influence of wear. With self-lubricating materials the majority of wear occurs during the early graphite film generation period. When a seal is first run-in the tolerances allowed in lapping the surfaces cause a degree of out-of-parallel presentation, but this error is soon corrected as the faces bed themselves in.

iii) The mountings for the seat and face of a seal must prevent distortion.

If the two lapped surfaces are not mounted accurately, so that rotation does not maintain parallel presentation, then a very considerable movement outside the range of lapped tolerances can result, which will cause seal failure. Extreme care must be taken to avoid the introduction of distortions into either face due to the clamping forces applied by securing bolts.

iv) The face and seat should be designed so that they are not subjected to excessive hydraulic pressure.

The most critical factor here is the design of the component made from the softer material. Materials that have elastic properties tend to distort readily in cross-section when a load is applied. This can lead to the breakdown of the lubricating film, because of uneven wear, which results in face separation.

v) Provision should be made for the adequate dissipation of heat generated by friction between the seal faces.

At high rotation speeds, high temperatures can be generated which result in expansion stresses and increased wear rates. This factor is not so relevant to the chromatographic machine because of the very low rotation speeds used.

For a mechanical seal to function correctly the above specifications must be satisfied. Basically the requirement is that the two optically flat plates which run in rubbing contact to form the seal must be free from distortion and run in parallel. Bearing the various factors in mind, the fact that the mechanical seal, used in the chromatograph, was subject to breakdown and failure indicates that the necessary requirements were not met. It is therefore probable that distortion on one or both seal faces were causing the seal to fail. The extremely slow running speeds of the seal (0.1-0.2 r.p.h.) and the presence of continuously flowing cold water eliminate the possibility of any thermally induced distortion effects. This then left mechanical and hydraulic effects as the sources of distortion in the chromatographic machine.

3.4.2 Analysis of the Moving Seal

The approach to the analysis of the seal problem was as follows, discussions were initially held with Dr. Hooke (Mechanical Engineering Department, University of Birmingham) particular attention was paid to the identification and solution

of the problem of the breakdown and subsequent failure of the mechanical seal. Reference has been made to the reports produced by Hooke[75], Adamson[76] and Bush[77] in the following text.

Identification of the Problem

Hooke[75], analysed the loading of the graphlon ring, and the reaction of the supporting cylinder, attached to the stainless steel face, and established that the effective reaction of these two forces was in such a position that, unless the seal faces bedded in, sealing would be impossible. A copy of the calculations involved is included in Appendix 2.

For the seal to be effective the reaction must act in the middle of the seal. In fact the reaction was calculated to be acting at the inner edge of the seal faces. Hooke[75] also paid attention to the effect of circumferential pressure variations. The fluid pressure in a typical run was expected to vary from a maximum of 241 kN/m^2 (35 p.s.i.g.) to zero between ports P and Cp (Figure 3.22). This pressure acted at a radius opposing the clamping load. At the maximum value of the sealed pressure the reaction point, described above, would move further inwards and cause localised separation of the seal faces.

It was concluded from Hooke's[75] report that distortions of the seal faces were causing local separation of the seal faces at the point of highest sealed pressure, Port P Figure 3.22. Wear might have reduced this but was unlikely to eliminate it. The only effective solution would be to significantly reduce the distortion.

Sources of Distortion

Under normal operating conditions there are considerable distortions present in the chromatographic machine. There is the force due to the loading of the seat against the face by the pneumatic rams, and to the friction between the stainless and the graphlon ring. The rotation of the bundle must overcome these forces by the drive torque introduced into the bundle at its base. This torque is transmitted to the seal via the central support cylinder of the bundle. The bearings on which the bundle is mounted should remove any component of the drive torque which is tending to force the bundle away from the drive (Figure 3.13). If this is not so, as it is in the chromatographic machine, then the effects of this component force is to try and tilt the bundle, thus causing an additional force to act on the seal.

Consider the static forces acting within the machine. The top face of the seal is pressed on to the bundle face by 12 rams. The graphlon, now sandwiched between two metal surfaces, is under load and due to its elasticity will deform in cross-section. This deformation should be uniform if the parallel tracking of the seal faces is to be maintained. However, because of the circumferential variation in the sealed pressure the deformation in the graphlon will not be uniform. In particular, in the section of the seal above the liquid lock there is a large change in pressure over a small area. The change in pressure in this area will cause stressing and the formation of a bending moment which could result in localised face separation.

FIGURE 3·13 Forces Induced by Drive Gear

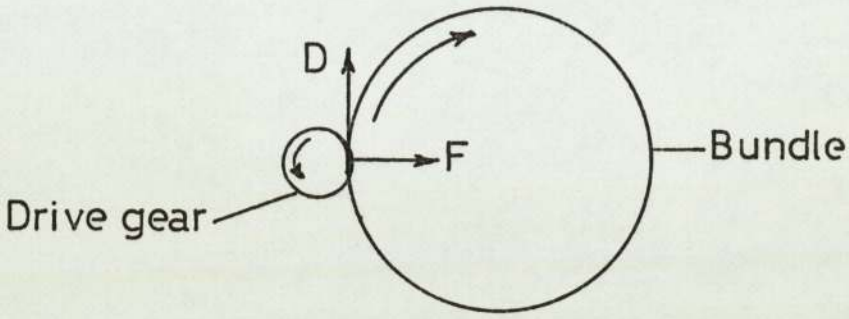

D = Driving force
F = Reaction caused by drive

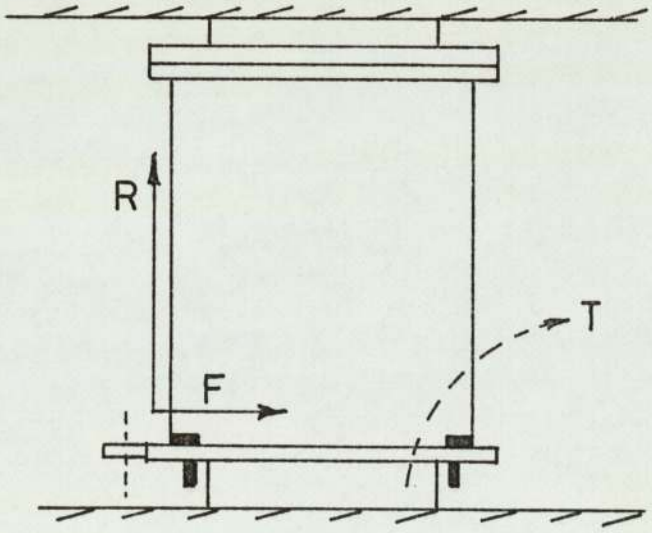

R = Reaction due to the bearings
T = Resultant tilting force

The force of the load applied by the graphlon ring on the bundle face and the hydraulic force within the packed tubes will cause the bundle top plate to have a reactive moment about the central support cylinder. This moment will result in the downward deflections of the outer edge of the bundle top face with the resultant destruction of any lubricating film between the seal faces. Providing the seal is loaded uniformily the deflection will be uniform and the elastic properties of the graphlon will allow it to deform with the metal ring and, after a short running-in period, the seal faces will bed themselves in. But the load is not even, and it is probable that the top face of the tube bundle will adopt some form of wave pattern. This wave in one of the seal faces will cause uneven wear and the eventual breakdown and failure of the seal.

Any forces that were not taken out or reduced by distortion would be transmitted, through the bundle, to the bearings. This combined with the tilting force induced by the drive mechanism could cause uneven loading on the bearings and the possibility of their failure.

Experimental Studies

In conjunction with Bush[77] and Adamson[76] a full size model of the sealing rings was constructed. The model consisted of a graphlon ring with metal backing plate, a mild steel ring was used in place of the stainless steel one, and a considerably stiffer simulated support was used at the ring's innder edge to eliminate support deflections (Figure 3.14).

FIGURE 3·14 Sectioned Diagram of Model used for Compression Test

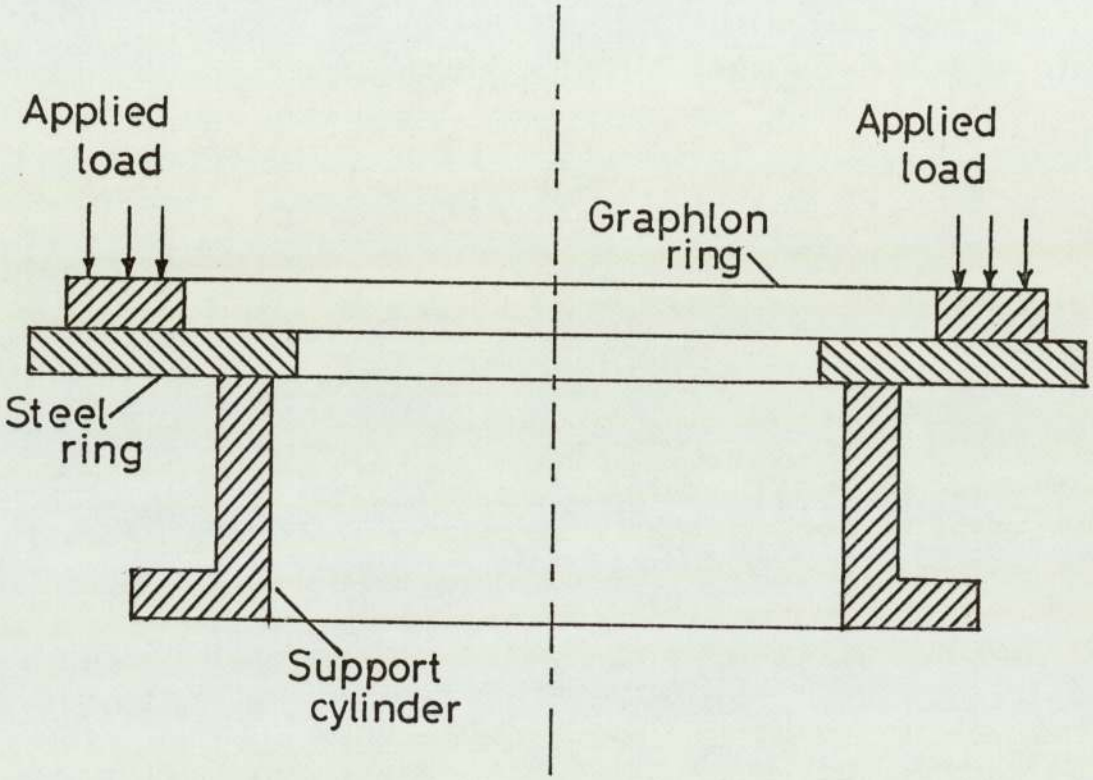

The model was tested on a compression testing machine and subjected to loads up to 5 kN. The deflection of the lower ring was measured with a clock guage at the inside, the centre and the outside edge. Graphs of deflection versus load were plotted for the 3 sections examined. Figure 3.15 is a typical example of the graphs obtained. The conclusion drawn from these experiments was that the top face of the bundle would under conditions of load deflect in a cantilever fashion about the central support cylinder.

3.4.3 Conclusion

The conclusions drawn from the analysis of the structure of the chromatographic machine are:

i) The prime cause of the seal failure were the distortions introduced into the seal by various static and dynamic forces. These distortions resulted in localised face separation and subsequent seal failure.

ii) The drive mechanism and the bearings on the chromatographic machine were positioned too far from the forces they were supposed to overcome.

3.5 MODIFICATIONS TO THE CCRI MACHINE

To eliminate all the structural weaknesses of the chromatograph would involve its complete redesign. This was both practically and economically impossible. The modifications made were therefore a balance between the need to get the machine operating satisfactorily and economic considerations.

FIGURE 3.15 Graph of Deflection versus Applied Load

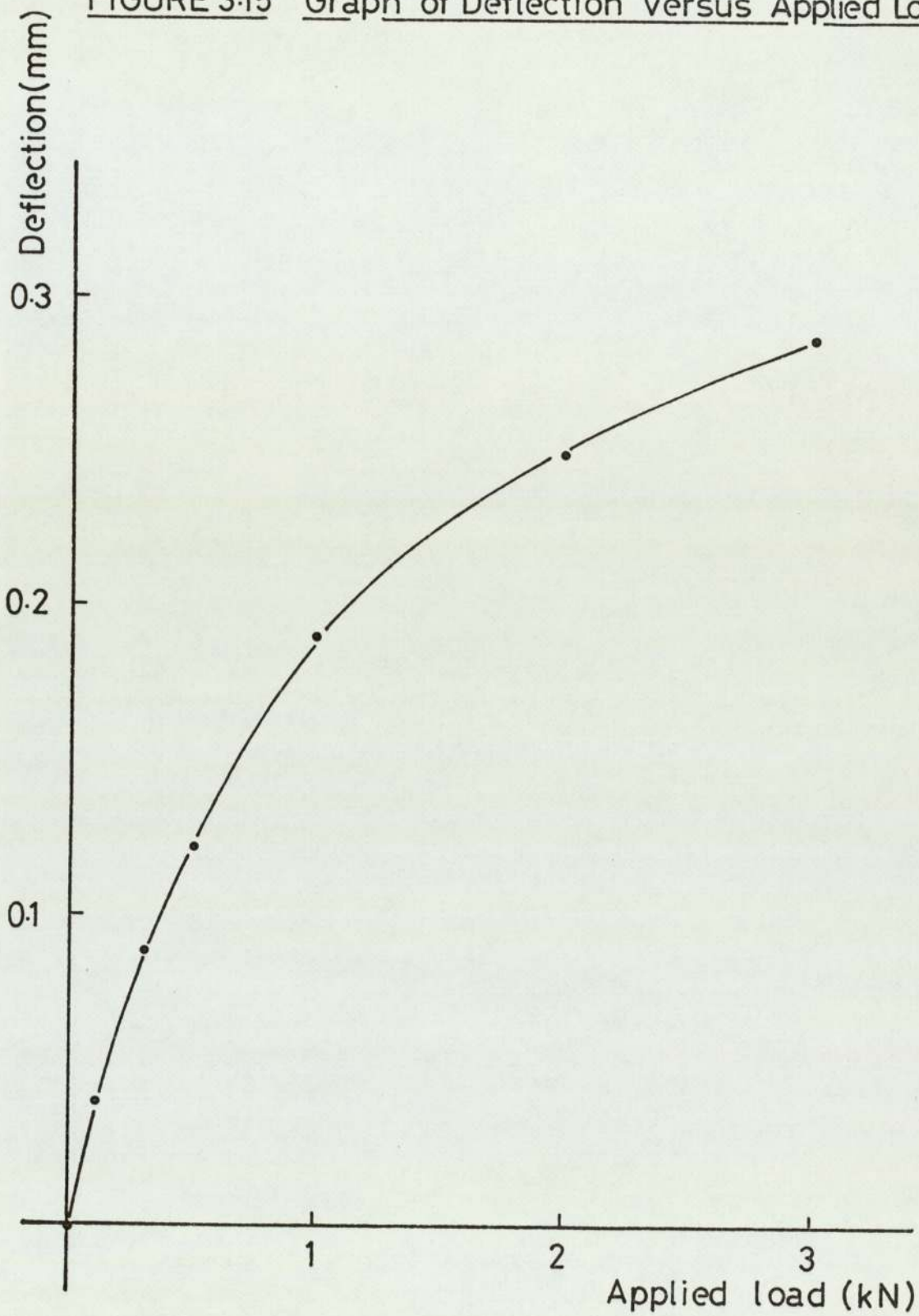

3.5.1 Design Changes and Trials

The design of the chromatographic machine was such that no major alterations could be made without a complete redesign of either the machine housing, the oven, or the majority of the tube bundle. Attention was therefore concentrated on the measures that could reasonably be taken to improve the structure of the seal faces and thus reduce their distortion when under load.

Shortage of space in the oven and the positioning of the pneumatic rams precluded any alterations to the stationary section of the seal. The promising solution was to strengthen the top face of the bundle in order to unify any distortion, and thus allow the softer more elastic graphlon to bed in more easily.

It was finally suggested that a large metal ring (32 cm. O.D., 24.5 cm I.D. and 6.4 cm thick) be attached to the outer edge of the tube bundle top face. The object of metal ring was to reduce the bending of the seal face at its outer edge. Figure 3.16 schematically represents the effect of the metal ring on the distortion of the sealing face. Considerable thought had to be given to the method of attaching the ring. Any form of welding or heat treatment was unsuitable because of the possibility of inducing thermal stresses into the sealing face. It was finally decided to attach the ring with a cyanoacrylate adhesive, commercially available as 'Loctite' (Douglas Kane Group Ltd.). This particular adhesive is extensively used in the engineering industry where the joining of metals by thermal techniques has to be avoided. The stiffening ring was made of EN 8 rust proof steel. The use of stainless steel would have been

FIGURE 3·16 Diagram Showing the Effects of Strengthening Seal Face

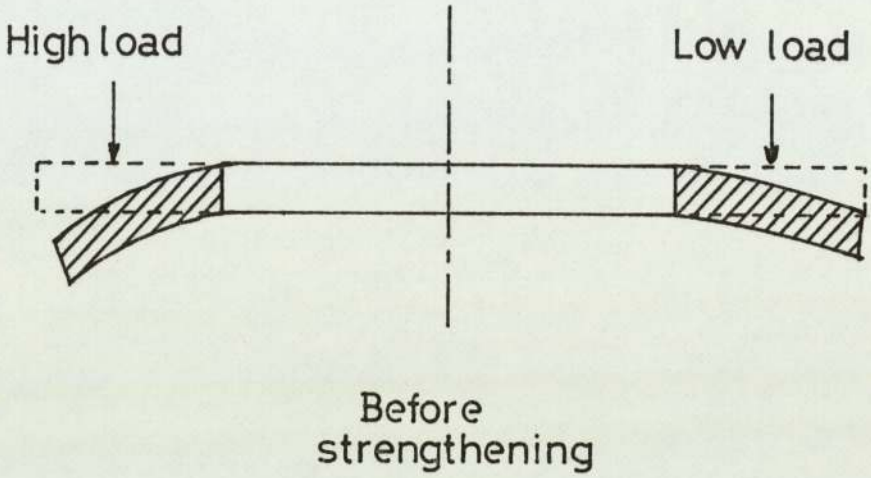

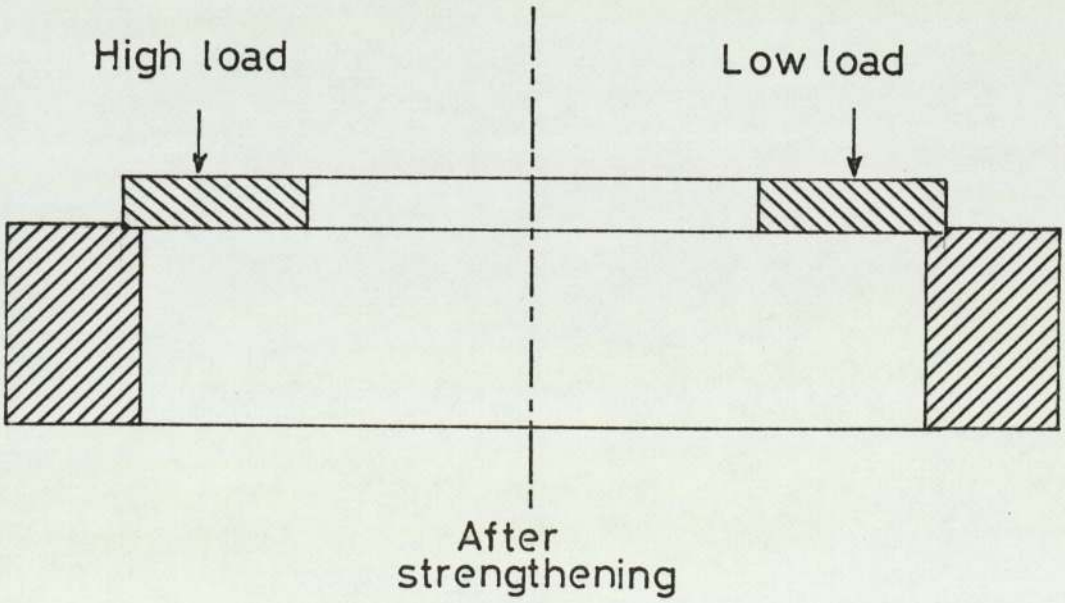

preferable but the cost was prohibitive. Figure 3.17 gives a scaled diagram of the bundle top face with the stiffening ring attached.

Whilst the stiffening ring was being made and attached to the tube bundle face the opportunity was taken to check and, where necessary, replace the bearings on which the tube cage was mounted. In addition, all the 'O' rings at the top and bottom of the packed tubes and in the spring loaded valves were replaced. The tube bundle was then completely reassembled and the surfaces of the faces forming the seal examined using a Taylor Hobson Tallyrond and the Taylor Hobson Tallylin 20 at Malvern (Figures 3.18 and 3.19). Both faces were then lapped flat by Precisionlap Ltd. (Camberley, Surrey), and the faces re-examined (Figures 3.20 and 3.21). As a result of lapping the metal face proved to be flat to within 1 lightband (11.5×10^{-6} inches, 1 micron). The same degree of flatness could not be obtained on the graphlon face but this was not considered a serious disadvantage because it was hoped the graphlon would bed in.

On reassembling the complete chromatographic machine in the oven and pumping water through the bundle it seen became apparent that the addition of the stiffening ring was successful. Over a six week period the machine operated with a leakage consistently below 2% at a back pressure of up to 138 kN/m^2 (20 p.s.i.g.). Details of the experimental runs performed over this period are discussed in Chapter 6.

At this stage in the research it was necessary to move the chromatographic machine to a new building. Though every

FIGURE 3.17 Seal Face plus Stiffening Ring

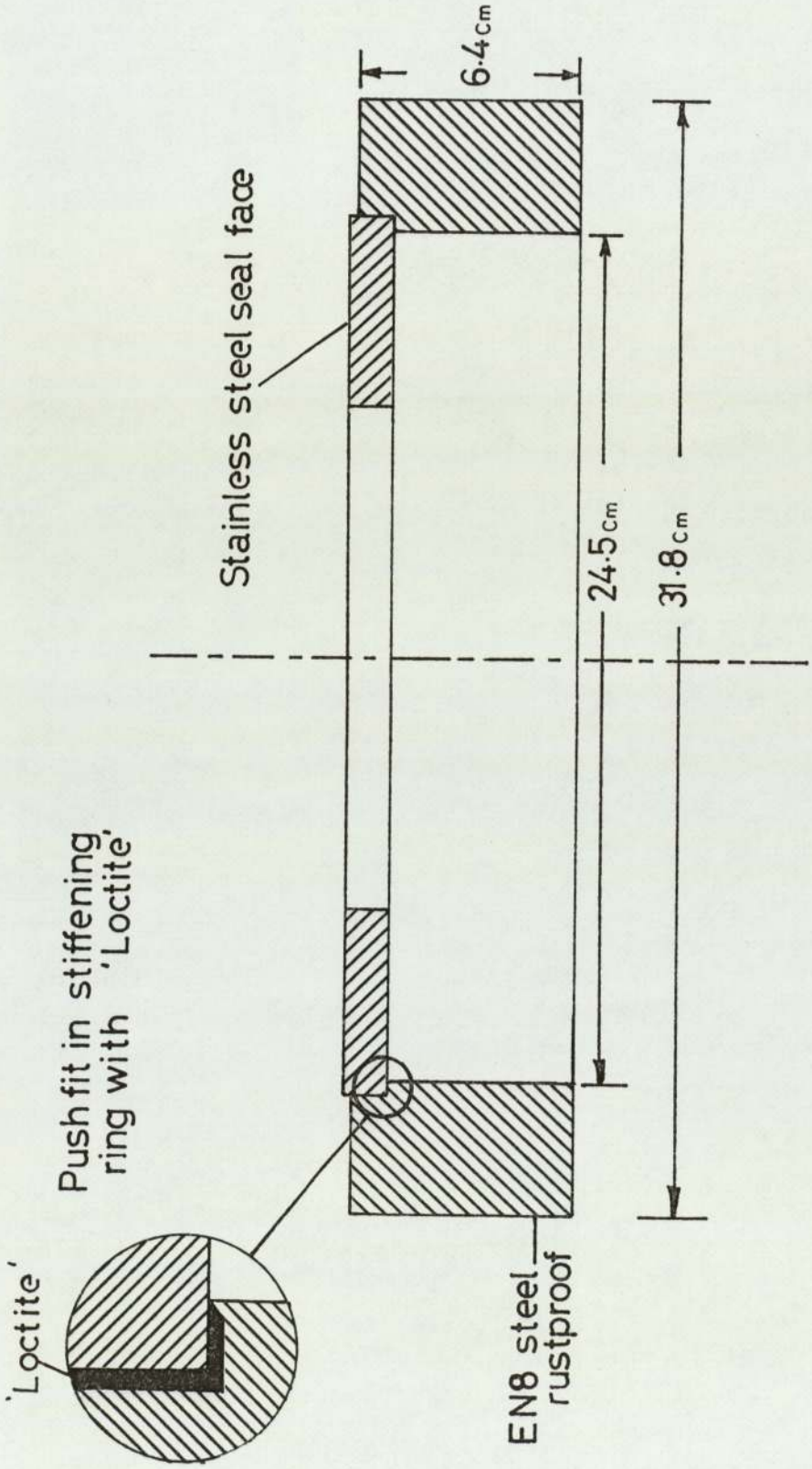

FIGURE 3·18 Surface Finish of Graphlon Face Before Lapping

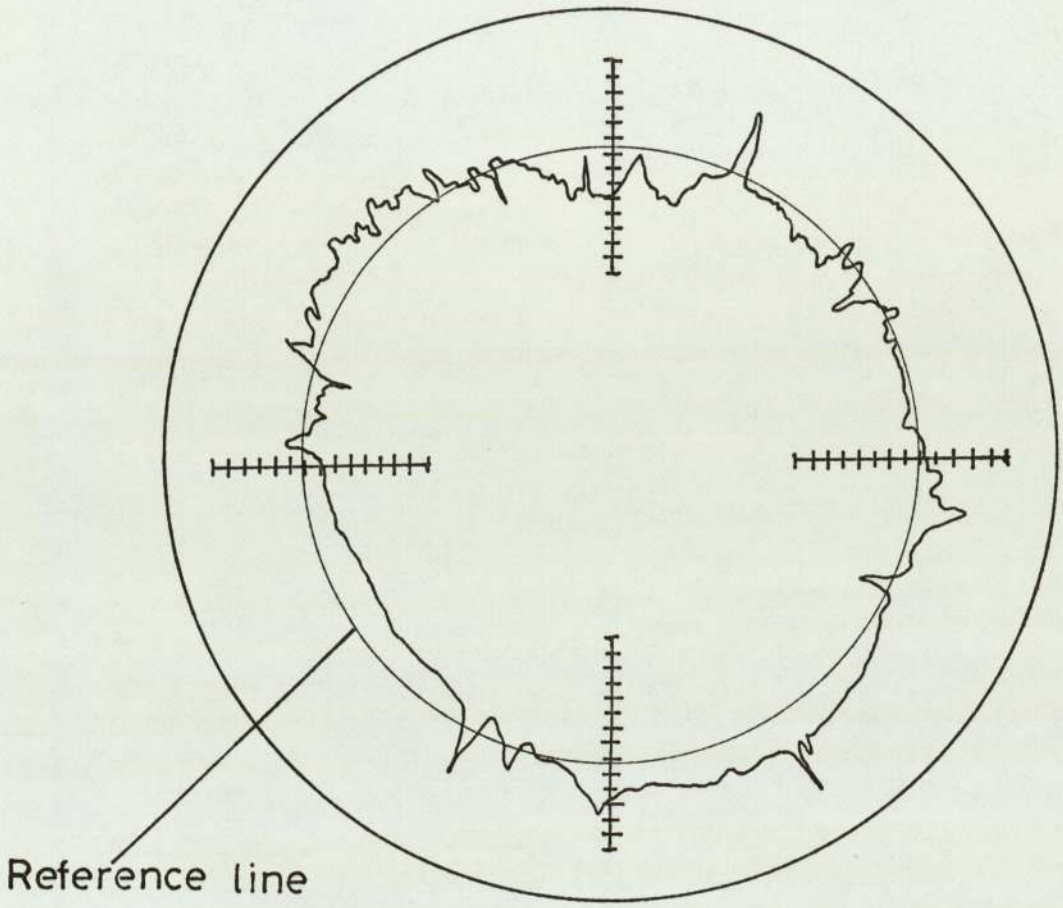

Magnification = x 2000
Scale : 1 division = 1·3 μm

FIGURE 3·19 Surface Finish of Stainless Steel Seal Face Before Lapping

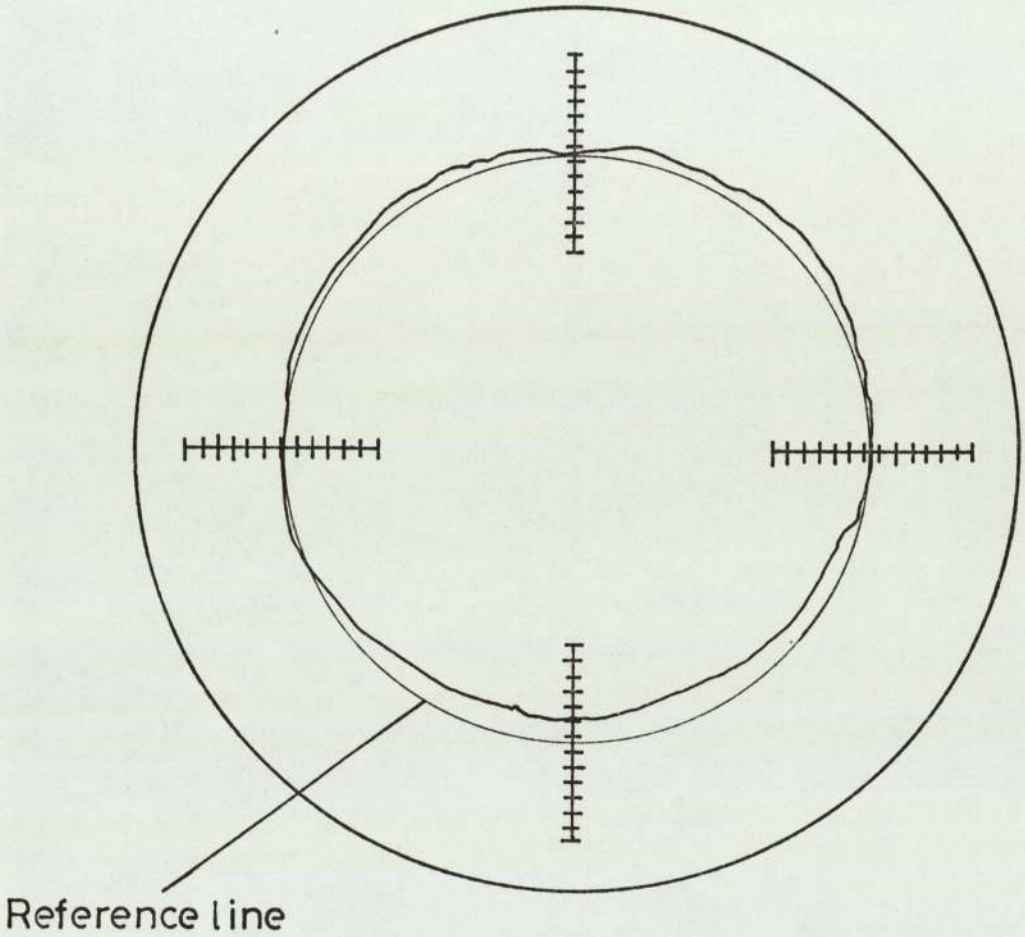

Magnification = x 1000
Scale: 1division = 2·6μm

FIGURE 3·20 Surface Finish of Graphlon Seal Face after Lapping

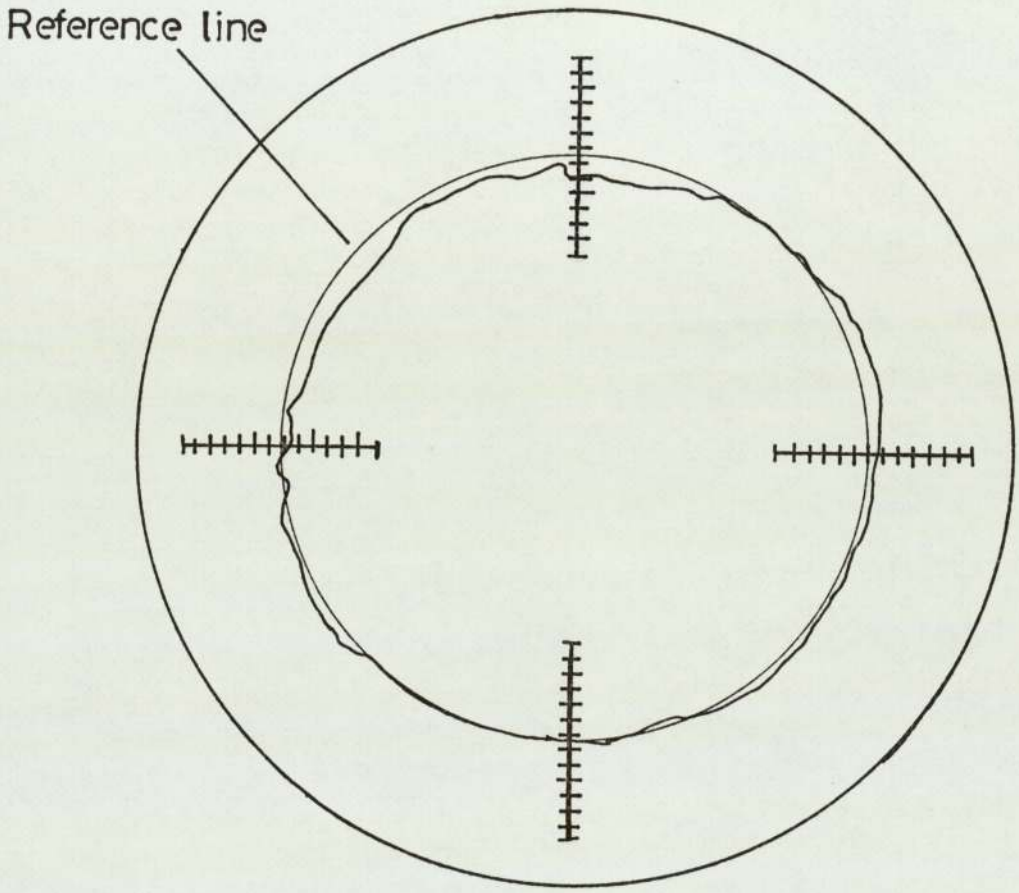

Magnication = x 400
Scale: 1 division = 6·5 μ m

FIGURE 3·21 Surface Finish of Stainless Steel Seal Face after Lapping

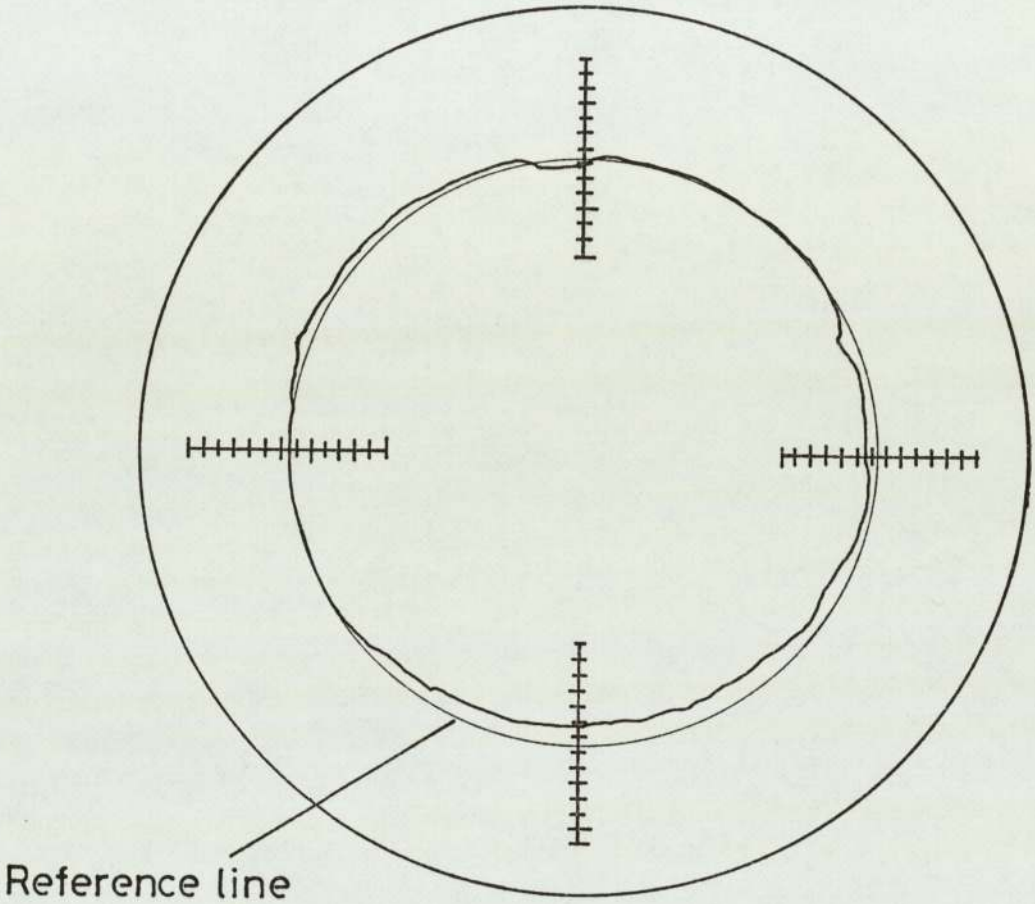

Magnification = x10000
Scale: 1division = 0·26μm

precaution was taken to avoid any damage, particularly to the two sealing faces, mass balances revealed that, as a result of the move, the leakage had risen to over 20%. On inspecting the tube bundle it was found that one of the ball races supporting the bundle was damaged. This was replaced and the leakage soon dropped to less than 2%. The experimental programme was then resumed.

Unfortunately, over the following two weeks the leakage gradually increased to just under 40%. This increase in leakage was assumed to be caused by two factors, firstly the failure of the bearing may have affected the parallel presentation of the faces and caused uneven wear or excess localised distortion. Secondly the temperature in the laboratory was several degrees lower than the normal ambient temperature of 22°C. This decrease was due to a lack of heating and may have caused some thermal distortion due to the differences in the coefficient of thermal expansion between stainless and EN 8 steel. Both faces were therefore relapped.

Prior to relapping a second liquid lock was built into the machine. This modification made the operation of the machine more analogous to the chromatographic equipment designed by Barker and Deeble[69]. The second liquid lock also reduced the effects of localised high pressure drops around the liquid locks.

3.5.2 The Addition of the Second Liquid Lock and Further Trials

To date the machine had operated with only one liquid lock (Figure 3.22). Liquid carrier entering at point P was used to purge the packing of the component preferentially travelling with it.

FIGURE 3·22 Continuous Chromatograph with a Single Liquid Lock

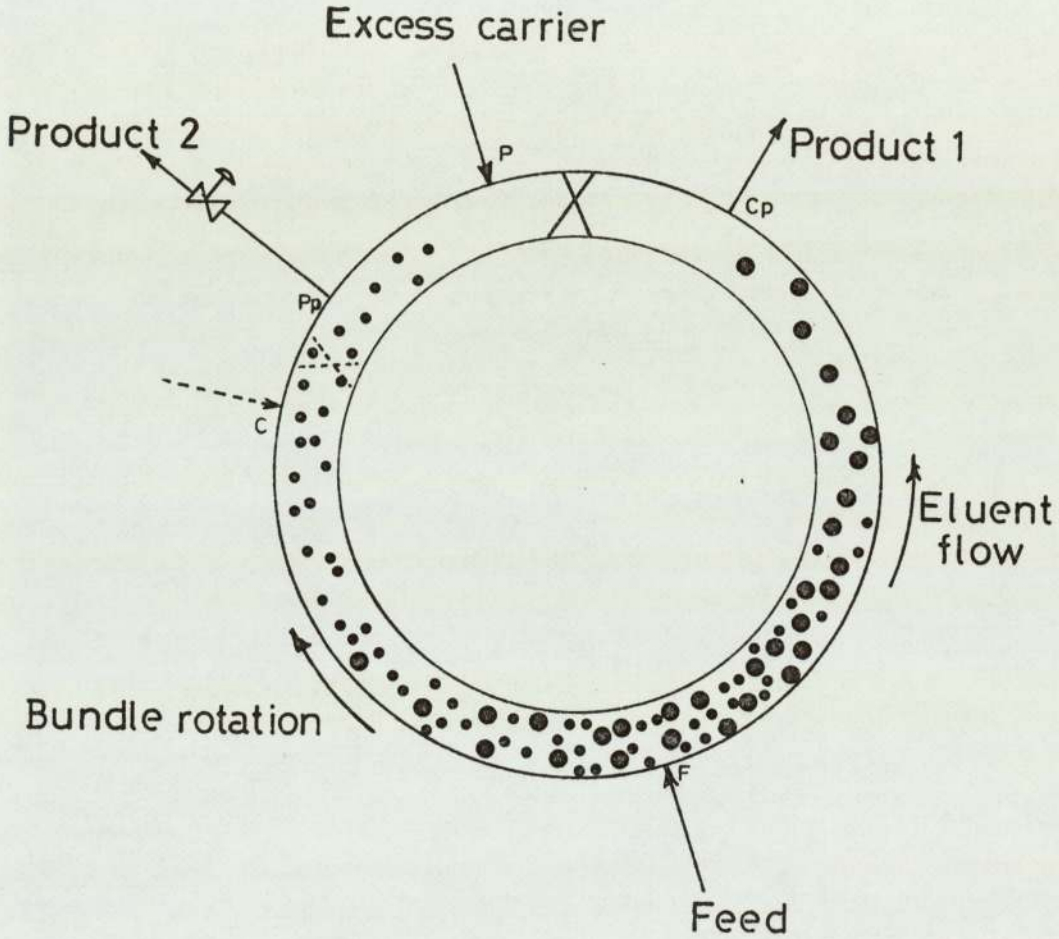

A portion of the carrier, plus product, was metered out at point Pp by a metering pump operating against an artificial back pressure. The remainder of the carrier flowed through and around the packing and carried the second product to offtake port Cp. This was the mode of operation employed in the prototype chromatograph used by Hatt[11,61]. By installing the second lock immediately after port Pp and an additional liquid input port, point C, the machine operated as described in Section 3.1. The advantages of this mode of operation were:

i) It was consistent with more modern forms of continuous chromatographic equipment not employing moving seals[8,69].

ii) Any distortions in the top face of the seal due to large localised pressure drops were reduced.

iii) Lower operating pressures meant a greater range of possible operating conditions.

Practically the lock was installed by removing the base plate of the bundle and machining a second notch in the cam which operated the spring loaded valves, Figure 3.23.

The chromatographic machine could now be split into specific sections. Of the 22 pairs of packed tubes two sets of three pairs were isolated in the liquid locks at any one time. A further four pairs formed the purge section and finally the remaining twelve pairs were available to be used for fractionation. The twelve pairs forming the fractionation section of the bundle were divided by the feed port into two sets of six pairs.

After relapping and a running-in period, the leakage fell to less than 2%. The machine was now in such a condition that the

FIGURE 3·23 Diagram of Cam and the Notches that Operate the Valves

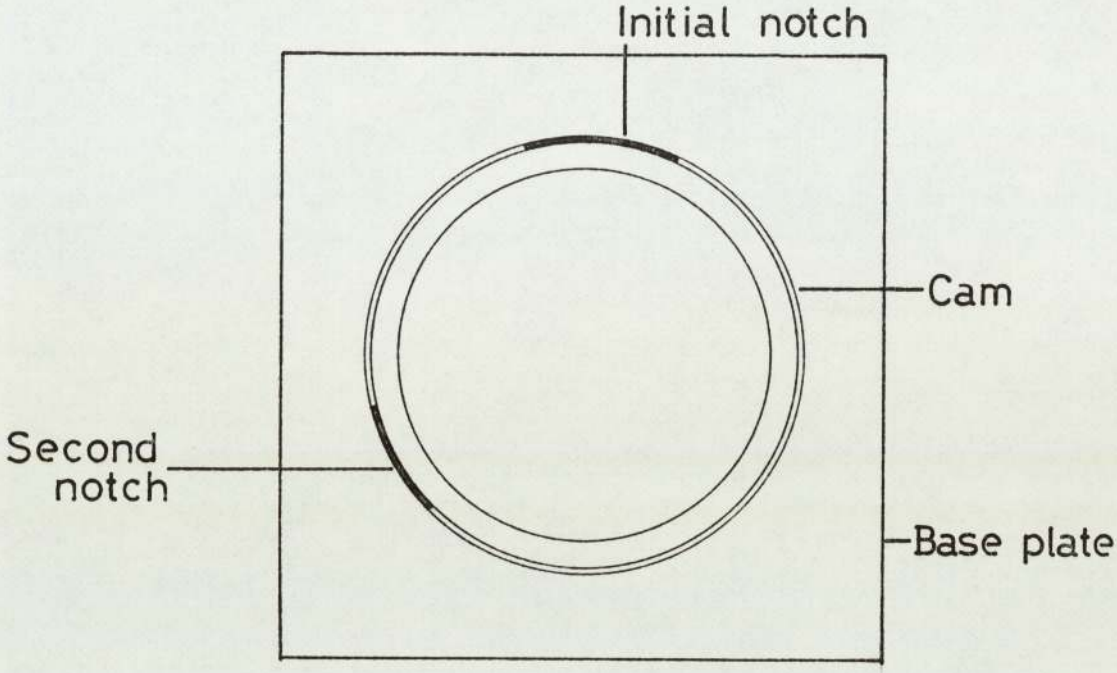

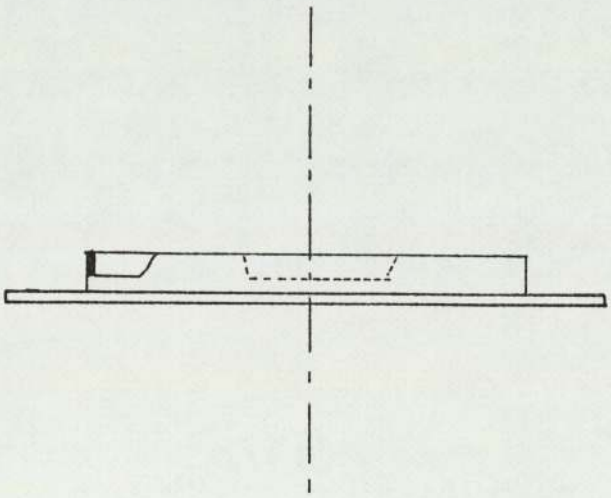

experimental programme could recommence. During the course of this programme further information about the mechanical limitations and the practical difficulties of operating the chromatographic machine became known. These are discussed in the following section (3.5.3).

3.5.3 Conclusions

The conclusions drawn from the practical operation of the machine can be split into two areas. Firstly those that arose as a result of the mechanics of the machine and secondly those that became known due to the effects of liquid physical properties used in the machine.

3.5.3.1 Mechanical Limitations

One of the first conclusions was that there was a practical limit on the back pressure that the seal could withstand before it broke down. This was found by trial and error to be 138-172 kN/m^2 (20-25 p.s.i.g.). Increasing the pneumatic pressure on the rams would have increased this but rather than run the risk of seal breakdown due to increased distortion in the static portion of the seal, it was thought best to keep the pressure constant. A gas pressure of 689 kN/m^2 (100 p.s.i.g.) was found to be best. As a consequence of the restricted back pressure the maximum flow rate through the machine was limited. The bearings supporting the tube cage gradually wore out and on a number of occasions failed. On each occasion the free rotation of the bundle was restricted and it is probable that the seal was adversely affected.

A most noticeable feature observed during the running of the machine was the build-up of flecks of graphlon in between the seal faces. This was particularly pronounced during the separation studies using proteins. Invariably when flecks of graphlon had built up the seal failed. Careful cleaning of the faces with water and acetone was sufficient to restore satisfactory operating conditions for a limited period. As has been discussed the use of self-lubricating materials, such as graphlon, in mechanical seals results in the formation of a thin boundary film. This film is supposed to substitute for the formation of a liquid lubricating film. However the eluent, feed and product fluids are pumped through the two sealing faces. This combined with the hydraulic pressure acting against the sealing pressure at the eluent input promotes the formation of a liquid lubricating film. The situation therefore exists where the liquid film dominates in those areas of high liquid pressure and the graphlon film dominates in those areas of lowest pressure. As the bundle moved, the graphlon film would tend to move from low to high pressure areas with the resultant destruction of the graphlon film. The graphlon would then be washed off the sealing faces, build-up and cause seal failure. A contributory factor may also have been the noticeable degree of non-homogeneity in the graphlon's macrostructure. Such lack of homogeneity may have affected the formation of a uniform boundary film.

3.5.3.1 The Effects of Fluid Physical Properties

Throughout the experimental programme, the physical properties of the fluids in use had a significant effect on the operation of the chromatographic machine. Increasing the viscosity had the obvious effect of increasing the pressure drop.

At these conditions the maximum flow rate had to be reduced, further restricting the operating range.

The maintenance of a satisfactory seal depended on the formation of the lubricating film between the seal faces. Fluids whose surface tension was significantly lower than water effectively prevented the formation of a stable liquid lubricating film. The result was breakdown of the liquid film and leakage from the seal. Breakdown of the seal due to reduced surface tensions occurred during the experimental studies with proteins. The surfactant properties of the proteins caused increased wetting of the seal faces which prevented the formation of a lubricating film. A rigorous procedure had to be developed before any experimental programme with proteins could be attempted. This will be discussed in Chapter 7.

CHAPTER 4

Literature Review of Gel Permeation Chromatography

4.1 CHROMATOGRAPHIC METHODS

The initial conception of chromatography as a means of separation cannot be dated exactly. The early literature has been summarised by Weil and Williams[78]. However, the first worker to use chromatography in the modern sense on an extensive scale, and to realise its potentialities was the Russian botanist, M. Tswett[79]. He published his first paper on the subject in 1903 and published the first book on chromatographic methods in 1910. Since then its development has been meteoric to such a degree that many hundreds of papers are published on many aspects of the subject each year. The majority of these papers are concerned with chromatography as an analytical technique. Hence after a basic introduction to the background of chromatography this survey will necessarily be restricted to one particular type of chromatography, its development, theory and application - as a separation technique.

Martin[80] defined chromatography as "the uniform percolation of a fluid through a column of more or less finely divided substances, which selectively retards, by whatever means, certain components of the fluid". This definition is of course very wide. It includes mixtures of gases as well as liquid solutions, and explicitly avoids any description of the mechanism responsible for the selective retardation. There are now several different chromatographic techniques which embody Martin's[80] original definition. These are commonly classified into three groups:

1) Adsorption chromatography
2) Ion exchange chromatography
3) Partition chromatography.

The first of these, adsorption chromatography, is historically the oldest. Adsorption chromatography essentially involves the following components, the solute, the adsorbent and the solvent (the mobile phase). This technique involves the preferential adsorption of one of the solutes on to the stationary phase (the adsorbent). Deitz[81] reviews more than 100 materials that have been used as adsorbents.

The development of new stationary phases in the period 1940-1945 resulted in ion exchange and partition chromatography. The former is described as the transfer of ions from the solvent to a stationary phase which contains covalently bound ionic groups and the subsequent transfer of ions, already present in the stationary phase, to the solvent. The latter, partition chromatography encompasses the following chromatographic methods:

(i) Gas-liquid.

(ii) Liquid-liquid.

a. Different solvents - Partition chromatography.

b. The same solvent - Gel permeation chromatography.

Gas-liquid chromatography is the form of partition chromatography, developed by James and Martin[2], in which the mobile phase, an inert gas, carries the mixture to be fractionated through a packed column. The components of the mixture, in a vapour state, partition between a liquid phase, coated on to a solid support, and the inert mobile phase. How each component partition between the two phases depends on their respective solubilities in the liquid phase. Another form of partition chromatography is liquid-liquid chromatography. Developed by Martin and Synge[20] liquid-liquid chromatography relies on the partitioning of solutes

between the two liquid phases. Where the two liquid phases differ the technique is commonly referred to as partition chromatography.

An alternative form of liquid-liquid chromatography exists where the liquid phases are identical and the separation is brought about by making use of the varying ability of molecules of differing sizes to penetrate suitable porous stationary phases. This form of chromatography is known by a variety of names; "gel chromatography", "gel filtration", "exclusion chromatography", "molecular sieve chromatography""restricted diffusion chromatography" and "gel permeation chromatography". It is this type of chromatography to which this literature review is restricted and for the purposes of this review the commonly used name Gel Permeation Chromatography (G.P.C.) is used, but without any conviction that it is the ideal term. Reservation about its use will be discussed in Section 4.2.1.

4.2 THE THEORY OF GEL PERMEATION CHROMATOGRAPY

Historically gel permeation chromatography has been attributed to the work of Porath and Flodin (1959)[82] and Moore (1964)[83]. The former demonstrated that columns of gel particles of cross-linked dextran could be used to successfully separate substances of large or intermediate molecular weight. They adopted the name gel filtration considering it more important to emphasize a description of the chromatographic medium rather than the mechanism. Despite the undoubted contribution of Porath and Flodin[82] and Moore[83] to the upsurge of gel permeation chromatography as an accepted fractionation method, earlier publications by Lathe and Ruthven[84], Lindquist and Storgårds[85] and others[86-89]

also made significant contributions, without their realisation, to the development of the technique. A more detailed account of its historical development has been given by Altgelt and Moore[90].

Gel permeation chromatography is a fractionation method in which molecules in solution are separated on porous media. It is unique in three ways: (i) it separates molecules by their size; (ii) the larger molecules elute before the smaller ones; and (iii) the separation takes place in a limited volume which is smaller than the total column volume. As in other chromatographic methods, a mobile phase capable of mass exchange is made to move through a stationary phase. The mobile phase is a liquid that readily dissolves the components to be separated. The stationary phase constitutes a porous material whose pore sizes are of similar dimensions to those of the molecules to be separated. Reviews of G.P.C. have been published by Altgelt and Moore[90], Lambert[91], Andrews[92], Cooper[93], Boyer[94], Cantow et al.[95], Heitz and Kern[96], Bly[97], Heitz[98], Fischer[99], Kelley and Billmeyer[100] and books on the subject have been published by Determann[13] and Altgelt and Segal[14].

4.2.1 General Principle

It is generally accepted that the separation in G.P.C. is based on the difference in available pore volume between molecules of differing sizes. A column of total volume, V_t, is packed with a G.P.C. packing immersed in solvent. In general chromatographic terms the solvent contained in the internal pore volume, V_i, is the stationary phase, and the solvent in the interstitial volume, V_o,

is the mobile phase. Each particle of the packing contains pores of various sizes into which molecules that are small enough, can diffuse more or less freely. The largest molecules are only able to diffuse into the relatively few pores that are large enough; smaller molecules can enter the larger pores in addition to the smaller pore sizes. Consequently, the available pore volume decreases with increasing molecular size. Thus, when a sample containing a distribution of molecular sizes is loaded on to a G.P.C. column and allowed to pass through it, the largest molecules will exit from the column in the smallest volume, and the smallest in the largest volume. Molecules whose sizes lie in between the smallest and the largest will exit at volumes in between those for the smallest and largest molecules. Figure 4.1 gives an idealised picture of gel permeation chromatography.

The basic equation defining the operation of G.P.C. column is given by[101,102]

$$V_e = V_o + K_D V_i$$

V_e = elution volume

= elution time x liquid flow rate

K_D = the fraction of the total pore volume V_i that is available to the molecule

The term K_D is defined as the distribution or partition coefficient. The accessible pore volume $V_{i.acc.}$ is given by $K_D.V_i$, and the partition coefficient is therefore given by:

$$K_D = \frac{V_{i.acc.}}{V_i} = \frac{V_e - V_o}{V_i} \qquad 4.2$$

From equation 4.1 it can be seen that the distribution coefficient has two limiting values, zero and one[114]. When the partition

FIGURE 4.1 Idealised Illustration of Gel Permeation Chromatography

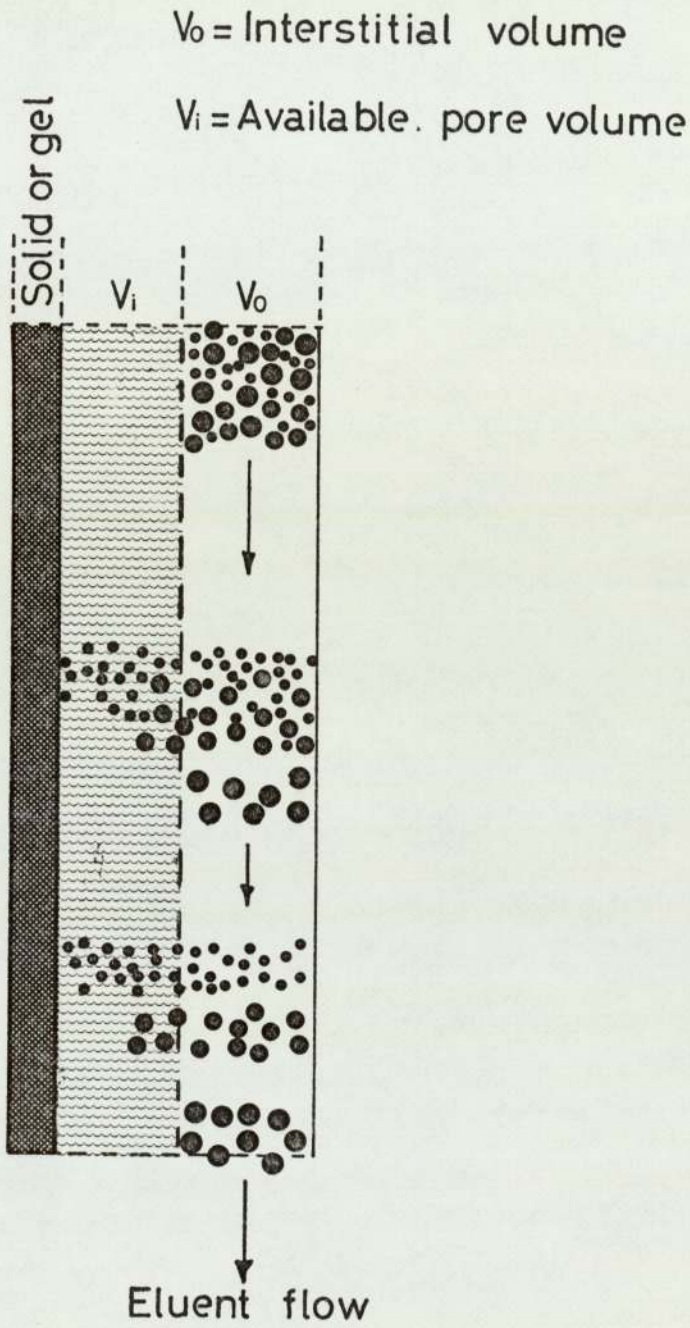

- Totally excluded ($K_D = 0$), $V_e = V_o$
- Partially included ($0 < K_D < 1$), $V_e = V_o + K_D.V_i$
- Totally included ($K_D = 1$), $V_e = V_o + V_i$

coefficient K_D equals zero, the elution volume of a molecule is equal to the interstitial volume of the column. When this occurs the molecule, by virtue of its size, is unable to penetrate the porous volume of the packing and exits from the column at what is defined as the totally excluded volume of the column. At the other extreme a small molecule whose partition coefficient is equal to unity will ideally exist from the column at an elution volume corresponding to the interstitial volume plus the total accessible pore volume. The molecule has been able to penetrate all the available pore volume and is said to exit at the totally included volume of the column. Theoretically, provided there is no interaction between the solute and packing and neglecting dispersion effects, all the molecules should exit from a G.P.C. column at volumes between its totally excluded and totally included volumes.

Each of the various names attributed to G.P.C. implies that the mechanism is known. For example, the name gel filtration[82] suggests that the separation mechanism relies on some form of filtration mechanism, where the largest molecules are preferentially retained in the column. This is in conflict with the fact that the largest molecules exit from a G.P.C. column before the smallest. Alternatively the name gel permeation, which is commonly used implies the need for a gel. However it is well know that the support matrix need not be gelatinous for the process to occur, for example, the aerogel[174] class of packings. Each of the other names given to this form of chromatography by a variety of research workers[103-106] gives an indication about the possible mechanisms governing the G.P.C. process.

4.2.2 The Mechanisms

Extensive literature[13,103-130] on the mechanisms involved in gel permeation chromatography agree that there are three major explanations: (i) restricted diffusion, (ii) steric exclusion and (iii) the loss of conformational entropy of a macromolecule near a surface. A paper by Casassa[131] discusses some of the theories and in particular concentrates on their interrelations and elucidates some apparent differences between the theories.

The restricted diffusion theory, originally proposed by Ackers and Steere[106], is of hydrodynamic origin[130], and arises from the increased frictional drag on a solute molecule. The increase in frictional drag is as a result of the proximity of the pore walls which cause a decrease in the solute diffusion rates. Frictional effects increase with increasing molecular size which result in the larger molecules preferentially remaining in the mobile phase. The restricted diffusion theory has been discounted on the grounds that if the G.P.C. mechanism were diffusion controlled, the elution volume would be dependent on the mobile phase flow rate. Yau and Malone[111] however, did produce experimental evidence in support of a dependence of the elution volume on the mobile phase flow rate. The results of these authors was reanalysed by Van Kreveld and Van Den Hoed[139] who, by applying their criteria for determining the elution volume, the position of the first statistical moment, were able to show no dependence of elution volume on elution rate. Yau and co-workers[122-124,126] have subsequently produced experimental evidence that demonstrates that the gel permeation process relies primarily on the extent to which solute molecules permeate the packing.

Conclusions drawn by Ackers[103] about the validity of the restricted diffusion model were based on a comparison of statically measured partition coefficients with those determined by gel permeation chromatography. A significant deviation was observed particularly on highly swollen gels such as Sephadex G200. For these cases an equation relating the partition coefficient to the Stokes radius of a diffusing molecule was developed. This equation, based on an original equation developed by Renkin [132], takes the following form:

$$K_D = (1 - \frac{a}{R'})^2 \{1 - 2.104 (\frac{a}{R'}) + 2.09 (\frac{a}{R'})^3 - 0.95 (\frac{a}{R'})^5\} \quad 4.3$$

The term a is defined as the Stokes radius of a molecule diffusing through a membrane containing cylindrical channel of radius R'. Experimentally Ackers[103], in his studies with Sephadex G200 found no flow rate dependence of the elution volume in the flow rate range 4.8 - 19.3 ml/cm^2/hr (1.1 cm I.D. column). Ackers explained this contradiction of his theory by making the assumption that a liquid surrounding each bed restricted solute diffusion. The thickness of the film varying inversely with flow rate. The existence of such a boundary film would reduce the flow rate dependence of elution volume but would enhance tailing. Little or no tailing is observed in G.P.C. except when there is some specific interaction between solute and packing.

Altgelt[109], with reference to the model proposed by Ackers[103], points out that the pores of gels are not uniform but

vary in width as well as in general shape. The author adds that the model yielded excellent agreement with the partition coefficient measurement of proteins.

Steric exclusion, another mechanism proposed for G.P.C. was used as early as 1956 by Lathe and Ruthven[84] to interpret the exclusion of solute molecules from starch granules. Since then the steric exclusion concept has been developed by several authors[101,105, 113,133-135]. The basis of the theory is that due to the structure of the porous particles and the distribution of pore sizes, chromatographed solute molecules are excluded from a part of the porous volume. The size of the excluded volume increasing with the molecular size of the solute. In attempts to elucidate the theory various research workers have assigned the gel a structure and then attempted to correlate the exclusion of various molecules from the structure with experimental data. Porath[113] derived a theoretical formula relating the partition coefficient to the Stokes radius which takes the form given below,

$$K_D = K_1' \{ 1 - K_2' \frac{M^{\frac{1}{2}}}{(R_s - \alpha)} \}^3 \qquad 4.4$$

where

R_s = solvent regain for the gel (gm/gm)

α = the part of R_s that is not available to any solute

K_1' and K_2' are proportionality constant.

An assumption of this model is that the pores in a cross-linked dextran gel particle are conical in shape. Squire[133] extended Porath's[113]

treatment to include cones, cylinders and crevices. The more sophisticated treatment of Squire[133] yielded an equation for the elution volume of the form,

$$V_e = V_o \{1 + g (1 - \frac{M^{1/3}}{M_{ex}^{1/3}})\}^3 \qquad 4.5$$

The term M_{ex} is the molecular weight of the smallest molecule that is completely excluded from the gel. M_{ex} and the geometrical constant g are evaluated from experimental data. Both relationships have been shown[133,135] to hold for both globular proteins and dextran fractions on cross-linked dextran gels. Gelotte and Porath[136] have subsequently pointed out that of these models (Equations 4.4 and 4.5) neither was developed to represent a true physical picture of Sephadex gels, for which they were proposed. These gels consist of highly cross-linked polymer chains rather than of rigid tight walls surrounding geometrically simple openings.

Laurent and Killander[101] proposed a more realistic model by assuming that the gel particle, in their case Sephadex, consisted of straight long rigid randomly distributed rods. From an expression derived by Ogston[137], who calculated the available volume for a spherical particle in such a system, they derived the following formula for the partition coefficient,

$$K_{av} = \exp (- \pi L' (R'' + r)^2) \qquad 4.6$$

where,

L' = concentration of rods cm cm^{-3} of gel

R'' = radius of spherical solute molecule

r = radius of the rods

K_{av} = distribution factor

$$K_{av} = (V_e - V_o)/(V_t - V_o)$$

$$= K_D \cdot \frac{V_i}{V_i + V_{am}}$$

V_{am} = Volume of gel matrix.

With an assumed radius r, 7Å, of a dextran chain and carefully chosen values of L, Laurent and Killander[107] were able to show good agreement between their theoretical and experimental results, and also with published data.

In contrast to modelling the shape of the pore of the support matrix, with the general assumptions of a simple spherically shaped molecule, Casassa[118] has developed a rigorous treatment of the equilibrium distribution of flexible polymer chains in a variety of simple pore shapes. The three pore shapes treated are for spherical, cylindrical and slab shaped pores. Casassa[118] defines the conformations of polymer chains by random flight statistics and describes the distribution of a polymer between the mobile and stationary phases as being governed by the loss of conformational entropy attendant in the transfer of a polymer chain from the outside to the limited space within a pore. Van Kreveld and Van Den Hoed[129] state that the "steric exclusion" theory and the "loss of conformational entropy" theory can

be shown to lead to similar results. Giddings et al.[107] have explained the similarities between the two theories in the following way. Molecules are unable to penetrate pores that are theoretically large enough due to partial exclusion. This partial exclusion is due to configurational entropy phenomena. Which means that a macromolecule in close proximity of a solid medium, in this case the packing, is not free to rotate. The significance of these restrictions on rotation are that certain molecular configurations are impossible to achieve[118]. The restrictions are due to constraints imposed by the nearby surfaces. The loss of entropy resulting from these constraints, and thus partial exclusion from parts of the pore, are magnified in porous media because of the large surface area.

In addition to the main theories already described a number of others have been proposed. Beau et al.[138] have developed a theory for predicting elution volumes which incorporates both a pore size distribution function and the thermodynamic theory proposed by Casassa[118]. Verhoff and Sylvester[128] questioned the theory that the elution volume of a macromolecular species in gel chromatography, is under ordinary conditions, determined primarily by the equilibrium partitioning of the species between the mobile phase and the stationary phase. These authors proposed that gel permeation should be renamed "hydrodynamic fractionation" on the basis that separation is achieved by liquid flow through the support matrix. Casassa[118] has shown that this theory differs from a similar one derived by Di Marzio and Guttman[112,115] only because of certain approximations, and that with these removed both theories become indistinguishable. In this publication Casassa[118] shows that the hydrodynamic theories agree with an equilibrium model. The significance of an equilibrium model is discussed later.

Experimental evidence[14] against the capillary flow models have shown that both styrene and polystyrene elute near the void volume of a column packed with smooth glass beads. The velocity profile in the interstitial spaces of the beads does not provide sufficient separation capability.

It is not clear which of the proposed mechanisms dominates the gel permeation process. Haller[139] has shown that both the restricted diffusion theory and the exclusion theory operate and that the dominating mechanism is related to the ratio of the solute size to pore size. The ranges of the ratio of solute size to pore diameter in which one or other of the mechanisms dominates, and how large and important is the transition range, is as yet uncertain. However, central to much chromatographic work is the assumption that the rate of movement of a solute zone through a chromatographic medium is a function of equilibrium parameters[107,131]. The implication of the equilibrium assumption in relation to general chromatographic theory is comprehensively dealt with by Giddings[12] in his now standard text "Dynamics of Chromatography".

With particular reference to G.P.C., Giddings[107] has stated that the evidence that the chromatographic process is an equilibrium phenomenon is very strong. The arguments favouring the equilibrium concept are: (i) partition coefficients obtained by chromatographic means are generally in excellent agreement with those obtained by static methods; (ii) elution volumes are usually independent of flowrate; and (iii) on fundamental theoretical grounds, a large deviation from equilibrium is incompatible with the narrow peaks obtained from efficient chromatographic systems. The influence of transport

properties has been assumed to enter only when considering peak dispersion. Excessive peak dispersion is regarded[107] as a sign of non-equilibrium.

4.2.3 Dispersion Phenomena in Gel Permeation Chromatography

The efficiency of the chromatographic process is dependent on the nature and extent of the mechanisms causing dispersion in packed beds. As a consequence of these processes, not all molecules of the same solute species elute at the same time. This leads to a spread of elution times about a mean, and the degree of spreading determines the column efficiency. It is therefore a prerequisite of successful column design that the various factors influencing dispersion and how they have been theoretically quantified be understood.

The parameter extensively used to evaluate the separating efficiency of chromatographic columns in the "height equivalent to a theoretical plate" (H.E.T.P., H). The significance of H.E.T.P. in terms of general chromatographic theory is discussed in Section 2.2. Theoretically it has been expressed by equations of the form,

$$H = \frac{2D}{U} + \text{(a mass transfer contribution)} \qquad 4.7$$

where, D is an overall dispersion number and U is the average linear flow velocity. Van Deemter[16], with the assumption that the dispersion number was composed of a longitudinal molecular diffusion term and an eddy diffusion term and that the mass transfer contribution was a linear function of flow rate, showed that

$$H = A + \frac{B}{U} + CU \qquad 4.8$$

where,

A = eddy diffusion term

B = mobile phase term

C = mass transfer term

Van Deemters[16] approach did not correlate well with experimental results and Giddings[12,140-142] in an attempt to explain these deviations between theory and experiment developed his "coupling theory". In this theory, the eddy diffusivity is coupled in a non-additive manner with the mobile phase resistance to non-equilibrium mass transfer. In a general form the coupling theory equation can be written as,

$$H = \left(\frac{B}{U}\right) + C''_s.U + \sum \frac{1}{(1/A'_i) + (1/C_{mi}.U)} \qquad 4.9$$

Giddings and Mallik[153] applied the above equation specifically to the theory of dispersion in G.P.C., defining the parameters A'_i, B, C''_s and C_{mi} in the context of the G.P.C. process. Due to the resistance to diffusion posed by the packing, the diffusion coefficient for the solute in the mobile phase, D_m, differs from that in the stationary phase, D_s. The implication of this reduction in mobile phase diffusivity has recently been investigated by Cotton, Satterfield and Lai[130]. Giddings and Mallik[143] have defined an obstruction factor, γ_s, for the gel as the ratio of the stationary and mobile phase diffusivities, D_s/D_m. A factor, R''_c was defined

by the ratio of the solute zone velocity to the mobile phase velocity, their proposed equation has the following form

$$H = \frac{4}{3}\ \frac{D_m}{R''_c.U} + \frac{1}{20}\ R''_c(1-R''_c)\ \frac{d^2p.U}{D_m} + \sum \frac{1}{(1/2\lambda idp) + (D_m/W_i d_p^2 U)} \qquad 4.10$$

where,

λ_i and W_i are geometric factors

d_p = particle diameter

In terms of two dimensionless parameters, the reduced plate height, h, and the reduced velocity, v, Equation 4.10 becomes,

$$h = \frac{4}{3R} \cdot \frac{1}{v} + \frac{1}{20}\ R''_c(1-R''_c)v + \sum \frac{1}{(1/2\lambda_i) + (1/W_i v)} \qquad 4.11$$

h and v are defined by

$$h = \frac{H}{d_p} \quad \text{and} \quad v = \frac{dp.v}{D_m} \qquad 4.12$$

The reduced velocity is analogous to a Peclet number based on molecular diffusivity, and is the product of the Reynolds number and the Schmidt number.

Sie and Rijnders[144] extended Van Deemter's theory by incorporating an additional term to account for the velocity profile effects, induced by a non-uniform velocity profile. Non-uniform velocity profiles result from particle size segregation and variations in packed density. Such factors cause a greater void

fraction at the column walls and therefore flowing fluid encounters less resistance, hence the fluid velocity near the wall is greater than that at the centre of the packed column. Velocity profile effects have been incorporated into the equation for H.E.T.P. by making use of the longitudinal dispersion number, D. The longitudinal dispersion number has been defined by Taylor[145] and Aris[146] in an equation of the form given below.

$$D = \phi D_m + \lambda U d_p + h' R_c^2 U^2 / \bar{D}_r \qquad 4.13$$

h' = velocity profile constant

ϕ = tortuosity factor

R_c = column radius

λ = eddy-diffusion proportionality constant

d_p = particle diameter

D_m = mobile phase diffusivity

$\bar{D}_r$ = average radial diffusivity.

The disadvantage of using an expression of the form given in Equation 4.13 is that its utility is highly dependent on the evaluation of the radial diffusivity, $\bar{D}_r$, and the velocity profile constant, h'. Several research workers[144,147,148] have shown that radial diffusivity is governed by radial concentration gradients, which come about as a result of molecular-diffusion and eddy diffusion processes. These in turn are dependent on the velocity variations within a column. Researchers[149] have, however, developed

an equation for the average radial diffusivity,

$$\overline{D}_r = \phi D_m + d_p U \qquad 4.14$$

Substitution of Equation 4.14 into 4.13 gives:

$$D = \phi D_m + \lambda U d_p + h' R_c^2 U^2 / (\phi D_m + \lambda d_p U) \qquad 4.15$$

Neglecting mass transfer effects, the equation for the plate height, H, becomes:

$$H = 2[(\phi D_m/U) + \lambda d_p] + 2h' R_c^2 / [(\phi D_m/U + \lambda d_p] \qquad 4.16$$

Equation 4.16 describes mobile phase dispersion with a velocity profile model. The denominator of the second term in Equation 4.16 represents a coupling of the eddy and molecular diffusivities, similar to that proposed by Giddings[12], Equation 4.9.

It can be seen from Equation 4.16 that for a given particle diameter the contribution to the plate height from the velocity profile term increases with the square of the column radius. Kelley and Billmeyer[14] have shown that this is not the case, since the last term can be written as,

$$\frac{2h' R_c^2}{(\phi D_m/U) + \lambda . d_p} = \frac{h' \delta^2 d_p^2}{2[(\phi D_m/U) + \lambda . d_p]} \qquad 4.17$$

With reference to work by Johnson these authors state that, for a constant particle size, d_p, the contribution to the plate height from velocity profile effects varies linearly with the dispersion parameter, $h'\delta^2$, which has been shown[14] to be nearly constant above aspect ratios of forty. The equation for the plate height, neglecting mass transfer effects, can therefore be written as

$$H = 2[(\phi D_m/U) + \lambda d_p] + \frac{h'.\delta^2.d_p^2}{2[(\phi D_m/U) + \lambda d_p]} \qquad 4.18$$

Equation 4.18 only describes the contribution to the plate height from the mobile phase dispersion phenomena. Kelley and Billmeyer[149,150] experimentally quantified the effect of the permeation process on the plate height. They showed that the contribution to H.E.T.P. from the mass transfer effects associated with permeation is a linear function of the liquid flow rate. Kelley and Billmeyer[150] were then able to express an overall equation for plate height in gel permeation chromatography.

$$H = 2[(\phi D_m/U) + \lambda.d_p] + \frac{h'.\delta^2.d_p^2}{2[(\phi D_m/U) + \lambda.d_p]} + CU \qquad 4.19$$

The relative importance of the terms in Equation 4.19 is schematically represented in Figure 4.2.

FIGURE 4.2 Relative Contributions to Plate Height with a Velocity-Profile Model (14)

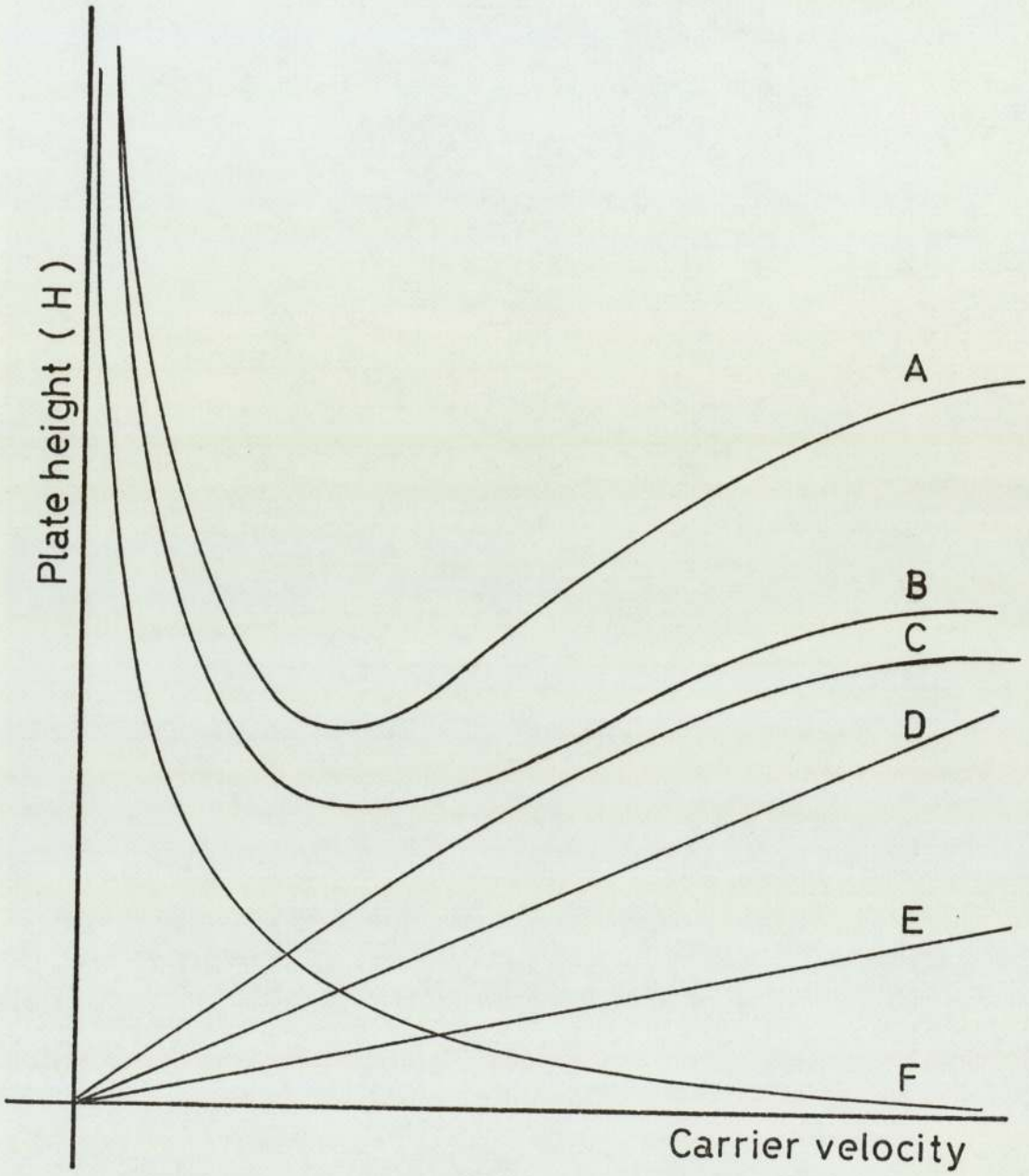

A - Overall H

B - All mobile phase

C - Velocity profile

D - Mass transfer

E - Eddy diffusion

F - Molecular diffusion

In addition to the equations for H.E.T.P. described above, other researchers have contributed to the theoretical prediction of plate height. Huber[151,152] expressed the plate height as the sum of the individual contributions. These include mixing which arises from diffusion and convection in the mobile phase and contributions from mass transfer effects in the mobile and stationary phase. The equation developed by Huber, partly theoretical and partly empirical, expressed the plate height by,

$$H = H_{md.} + H_{mc.} + H_{em.} + H_{es.} \qquad 4.20$$

where,

H_{md} = mixing due to mobile phase

$= (2\ \varepsilon_m/\gamma_m)\ (D_{ia}/U)$

H_{mc} = mixing due to stationary phase

$= 2\ \lambda_1 d_p/(1 + \lambda_2\ (D_{ia}/Ud_p)^{\frac{1}{2}}$

H_{em} = mass transfer effect in mobile phase

$$= \frac{1}{5.7}\ \left\{ \frac{\varepsilon_a - \varepsilon_m + K_i.\varepsilon_\beta}{\varepsilon_a + K_i.\varepsilon_\beta} \right\}^2 \frac{\varepsilon_m^{1/2}.d_p^{3/2}.\ v_a^{1/6}.U_{ia}^{2/3}}{(1-\varepsilon_m).D_{ia}^{1/2}}$$

H_{es} = mass transfer effects in stationary phase

$$= \frac{1}{30}\ \left\{ \frac{\varepsilon_a - \varepsilon_m + K_i.\varepsilon_\beta}{(\varepsilon_a + K_i.\varepsilon_\beta)^2} \right\}\left\{ \frac{\varepsilon_m\ (1-\varepsilon_m)\ \gamma'_s}{\varepsilon_s} \right\}\left\{ \frac{d_p^2.U}{D_{is}} \right\}$$

ε_m = interstitial volume fraction

ε_s = internal pore volume occupied by stationary phase

ε_a = volume fraction occupied by the moving phase

ε_β = volume fraction occupied by the stationary phase

λ_1 and λ_2 = geometric factors

γ_m and γ_s' = tortuosity factors

K_i = partition coefficient

= ratio of equilibrium concentration in stationary phase and mobile phase

v_α = kinematic viscosity of the mobile phase

D_{ia} = diffusion coefficient in the mobile phase

D_{is} = diffusion coefficient in the stationary phase

Kelley and Billmeyer[14] commented that the qualitative behaviour of equation developed by Huber[151,152] is very similar to those proposed Giddings[12,14,143] and Kelley and Billmeyer[14,149,150].

Hendrickson[153] proposed that peak dispersion obeys an equation of the form.

$$\overline{W}_b^2 = \overline{W}_m^2 + \overline{W}_a^2 + \overline{W}_i^2 + \overline{W}_d^2 + \overline{W}_s^2 \qquad 4.21$$

$\overline{W}_b$ = base width of chromatogram

$\overline{W}_m$ = contribution from molecular size distribution

$\overline{W}_a$ = contribution from the apparatus

$\overline{W}_i$ = contribution from the interstitial volume within the column

$\overline{W}_d$ = contribution from the diffusion spreading due to the hold up of molecules in the pores

$\overline{W}_s$ = contribution from sorption effects.

Vink[154], like Van Deemter[16], adopted an approach based on a diffusion model and produced an equation of the form

$$S' = \frac{2D_1}{Lv} + \frac{2D_2(1-W_1)}{Lv\ W_1} + \frac{2K'}{L} + \frac{v\ V_2^2\ W_1(1-W_1)}{LD_2} + \frac{\mu_2^o.v}{V_e^2} \qquad 4.22$$

where,

L = length of column

D_1, D_2 = diffusion coefficients in the mobile and gel phase respectively

v = mobile phase velocity

W_1, W_2 = mass fraction of solute in the mobile and stationary phase respectively

K' = eddy diffusion coefficient

V_2 = volume per unit of interphase area of stationary phase

V_e = elution volume

$\mu_2 v$ = variance with respect to the efflux volume

Vink[154] defined the term S' as the reduced dispersion which, like plate height, should be as small as possible for efficient columns. By comparing Equations 4.22 with the one produced from the dynamic theory by Giddings and Mallik[143], Equation 4.10, Vink[154] was able to show that both these equations were essentially identical despite their different origins.

Kubin[155], like Vink[154], used a diffusion model and developed an equation for plate height which took into account, in an elementary way, the complicated geometry of the porous packing.

$$H = \frac{2D_p}{W'} + \frac{W'^2}{15} \cdot \frac{R_o}{D} \cdot \frac{A'(1-\rho^3)}{[1+A'K(1-\rho^3)]^2} \cdot [1-G(\rho)] \qquad 4.23$$

D_p = longitudinal dispersion coefficient

W' = linear velocity of the solvent flow

R_o = diameter of spherical particle

D = diffusion coefficient in the particle

A' = $\frac{(1-\alpha)}{\alpha}$ where α is the fractional free cross section of the column

K = equilibrium partition coefficient

$$G(\rho) = \rho^3 . \frac{4 + 4\rho + 5\rho^2}{1+\rho+\rho^2}$$

ρ = dimensionless parameter characterising maximum depth of penetration

$= \frac{R_d}{R_o}$

R_d = diameter of impermeable core in particle

Several other theories have been developed to determine plate height, their similarities, differences and theoretical basis have recently been discussed by Grushka, Snyder and Knox[20].

The variety and number of equations defining plate height provide a guide to the factors influencing the efficient design of G.P.C. columns. The majority of equations divide the contributions to the overall plate height into two main sections, the mobile phase

dispersion effects and the mass transfer effects. Mobile phase dispersion effects include molecular diffusion, eddy diffusion (convective diffusion) and non-equilibrium effects associated with velocity variations due to packing geometry. Other dispersion mechanisms such as boundary-layer phenomena, convective mass transfer resulting from density gradients, viscous effects and dispersion induced by stagnant regions have been discussed by Kelley and Billmeyer[14] and Biesenberger and Ouano[239].

4.2.4 The Operating Parameters Influencing Column Efficiency in Gel Permeation Chromatography

The parameters that influence G.P.C. efficiency are:

1. Diffusivity and flow rate.
2. Aspect ratio and particle size distribution.
3. Packing type.
4. Temperature, solute concentration and viscosity.

Diffusivity and flow rate

Axial dispersion of molecules passing through a chromatographic column is governed by molecular diffusion, eddy diffusion and velocity profile effects. Sie and Rijnders[144] have shown that, due to increased stream splitting, the magnitudes of eddy diffusion and molecular diffusivities are often of the same magnitude in liquid chromatography. Molecular diffusion dominates at very low flow rates and eddy diffusion dominates at high flow rates. It has experimentally been demonstrated[149] that the effect of molecular diffusivity on the resulting peak dispersion is a function of flow rate,

expressed in terms of Reynolds number. The results obtained showed that in the range of Reynolds numbers studied, 0.01 to 10 Re,based on particle size, the dispersion, as measured by plate height, of low diffusivity (high Schmidt number) solutes was independent of flow rate. Solutes with high diffusivities (low Schmidt number) exhibited a decrease in dispersion with decreasing flow rate. At higher Reynolds numbers the difference in dispersion between high and low diffusivity solutes became appreciably less. Huber[152] noted a similar effect. The theoretical prediction of the dependence of dispersion on diffusivity is given by the various models for the plate height.

Horne, Knox and McLaren[156] noted that in the flow region where molecular diffusion dominates dispersion and that where turbulence, eddy diffusion, dominates, a major factor contributing to dispersion is the slow rate at which transcolumn equilibrium is achieved. In support of this, Kelley and Billmeyer[149] found that a major source of dispersion was the velocity profile term in their equation for plate height, Equation 4.19, which contains radial diffusivity in the denominator. This term becomes particularly important with solutes of high molecular weight which have low molecular diffusivities. Low diffusivities result in decreased radial diffusion and increased dispersion due to velocity profile effects and lack of equilibrium[14].

The Aspect Ratio and Particle Size Distribution Effects

The aspect ratio, defined as the column diameter divided by the particle diameter, is important in determining the magnitude of wall, velocity profile and transcolumn non-equilibrium effects[157].

In practice the influence of the aspect ratio is investigated by either altering the particle diameter at constant column diameter or by changing the column diameter for a given packing. Both techniques have their limitations because of the problems of obtaining consistent packing uniformity. Experimentally, dispersion is very dependent upon the packing technique used.

The effect of particle size and its distribution on the efficiency of G.P.C. columns is not clear. Kelley and Billmeyer[149] reported a major study on peak dispersions of polymeric materials and small molecules flowing through columns packed with spherical non-porous glass beads. They developed a theoretical model, Equation 4.18, that predicted increased efficiency (i.e. decreased dispersion) with decreasing particle size, all other variables being held constant. They experimentally verified this, but could not find a significant effect due to particle size distribution. In earlier publications, De Vries and co-workers[138,158,159], using benzene as the test solute and Porasil as the packing, concluded that large particle sizes and narrow distributions produce the most efficient columns. The observed decrease in dispersion at higher particle sizes is difficult to explain in view of the theories of peak dispersion that have been proposed by Kelley and Billmeyer[150], Flodin[160] and Knox[156,161]. Kelley and Billmeyer[14] have put this discrepancy down to a variation in the pore geometry with particle size, difference in packing techniques, combined with the possibility of agglomeration of the finer particles during packing.

Cooper and Kiss[162], in a carefully planned experimental study, reanalysed the results of De Vries and co-workers[158,159] using

plate height instead of the reduced plate height and showed that these results, in general, agreed with theory. These workers compared the different methods of determining column efficiency and also compared two different packing techniques. Resolution, R_L, and resolution index[162,163], RI, were compared with the height equivalent to a theoretical plate, H, in a study involving o-dichlorobenzene, n-hexane and two polystyrene samples with mean molecular weights of 411,000 and 200,000 respectively, as the different solutes. The solutes were chromatographed on Bioglass 1000. The authors' conclusions did not help to clarify the position of particle size and particle size distribution effects on column efficiency in gel permeation chromatography. In general they concluded that the use of plate height for small, monodisperse solutes does not predict the efficiency of G.P.C. columns for larger molecular weights, particularly polymeric solutes. In these cases it was found best to use plate height, resolution and resolution index to examine column performance in the polymer molecular weight range. Le Page et al.[158] have noted that the plate height is strongly dependent on the diffusion coefficient of the solute, which is of particular importance in the separation of polymers.

With regard to particle size, the conclusions of Cooper and Kiss[162] contradicted the theory that decreased dispersion accompanied a decrease in particle size. Sliemens[164] examined factors affecting the efficiency of G.P.C. columns packed with porous silica, Porasil. Column efficiency, as evaluated by plate height, was shown to increase with increasing aspect ratio, achieved by decreasing particle size.

Packing Structure

The type of packing used in G.P.C. columns can influence their performance. Column efficiency related to the difference in pore structure[150] indicates that pore geometry is an important factor in G.P.C. column efficiency. A deep interconnected pore structure should lead to reduced efficiency[14]. Kelley and Billmeyer[150] discuss in detail the difference in pore structure between Styragel and Porasil. Porasil has been established[138,165] as having a structure consisting of a three dimensional network of interconnected pores, with a narrow pore size distribution, the pore heading to large interconnected cavities. Styragel, on the other hand, is reported[150] to have a broad pore size distribution without the many gross irregularities found with the Porasil bead.

A molecule entering a pore in Porasil is able to diffuse more easily towards the centre of the bead than in Styragel. Such an effect promotes increased dispersion over that due to mobile phase effects. Thus, in columns packed with porous glass, dispersion is primarily controlled by mass transfer effects, while in columns packed with Styragel dispersion is controlled by mobile phase effects occurring outside the gel[150]. This demonstrates the importance of understanding both the origin of mobile phase dispersion and the influence of pore structure on dispersion if column efficiency is to be maximised.

Temperature Solute Concentration and Viscosity

Temperature does not appear directly in any of the equations that have been developed for plate height, but it is

obviously crucial to the equilibrium relationship and speed of mass transfer. Operation of G.P.C. columns at elevated temperature reduces liquid viscosity and increases the rate at which trans-column equilibrium is established. This reduces mobile phase dispersion effects, particularly for high molecular weight solutes.

Papers describing the effect of temperature have been published by Little et al.[166] and Barker et al.[167]. Little and co-workers[166] concluded that, at elevated temperatures, the size of a molecule increases and, as a result, a greater proportion of molecules are excluded from the pores with a subsequent reduction in elution time. Increased temperature results in increased resolution and decreased peak dispersion, which is represented by a reduction in peak width[11].

Unlike gas-liquid chromatography there is very little information quantifying the effects of concentration in gel permeation chromatography. Concentration effects arise from the presence of solute molecules in the mobile phase influencing the partitioning of molecules between the mobile and stationary phases. Hellsing[168] investigated the effect of solvents containing dextran, polyethyleneglycol, polyvinylalcohol, or Ficol (a synthetic polysucrose) on the elution of human serum albumin on Sephadex G200. The elution volume increased with increasing polymer concentration in the solvent. The increase in elution volume was attributed to the polymeric mobile phase acting as a secondary chromatographic medium. Adding polymeric material to the mobile phase gives it similar exclusion properties to the stationary support matrix. Hellsing[168] hypothesised that the use of polymeric mobile phases could improve resolution.

Altgelt[14], whilst investigating the influence of high sample loads in G.P.C., noticed that under certain conditions good separations were achieved with loads ten times greater than those normally applied to G.P.C. columns. In an attempt to explain this phenomena Altgelt named this additional separation mechanism "secondary exclusion". Molecules diffuse in and out of the pores on the support matrix. The diffusion rate in the gel and the mobile phase is governed by molecular size and also by the ratio of the molecular size to the pore size[169]. If a concentrated solution of small and large molecules are loaded on to a G.P.C. packing the small ones will rapidly diffuse into the available pores. The larger ones, since they diffuse more slowly, will find more pores occupied. The probability of them diffusing into an occupied pore will be reduced depending on the reduction of available pore size[14] and the motion of the smaller molecule in the pore. If the smaller molecule is moving away from the oncoming larger molecule it will have no effect. If it is moving toward it or lateral to it, it will obstruct the other molecule. In the case of obstruction the larger molecule will move on until it finds an unobstructed pore. Thus, larger molecules are effectively excluded from pores they would otherwise have been accessible to. This is called secondary exclusion.

An alternative explanation could be made of the secondary exclusion proposed by Altgelt[14] by applying the concepts developed by Hellsing[168]. Where, instead of the smaller molecules excluding the larger ones from pores, the larger molecules act as a secondary gel permeation medium and exclude the smaller molecules from moving

freely between the mobile and stationary phase. Alternatively the most suitable explanation would be a combination of both theories, the dominating theory being dependent on the distribution of molecular weights in the two phases. Hatt[11] has postulated qualitatively an explanation to this effect.

Ouano[170] has discussed the overloading phenomena in conventional batch gel permeation chromatography. Various investigators[171-173] have attributed the overloading effect to several causes: fingering effect[171], concentration dependence of the solute molecular size[172] and non-equilibrium partition of the solute between the mobile and stationary phase[173].

4.3 PRACTICAL GEL PERMEATION CHROMATOGRAPHY

4.3.1 Packings

Reviews of G.P.C. packings have been given by Epton and Holliday[174], Lambert[91] and Dark and Limpert[175]. Epton and Holloway[174] in a comprehensive review categorise the packings into three groups, xerogels, aerogels and xerogel-aerogel hybrids. Each group having particular advantages and specific applications.

Xerogels[174], formed when a substance undergoes the process of restricted dissolution, a true gel in the classical sense, were the first type of packing to be applied to gel permeation chromatography[81,83]. Typical xerogels consist of a solution of linear macromolecules whose movement, relative to one another, is restricted either by chemical or physical interaction. It can therefore be described as partly solvent and partly a three dimensional network of saturated polymer chains. Typical examples are cross-linked dextran and cross-linked

polyacrylamide. Diffusion of various solutes may occur within the gel just as in the case of normal fluids. Gelation is by definition a process of restricted dissolution, and a given polymer will only form a xerogel in a limited number of solvents in which the individual polymer chains are soluble. Removal of solvent from the xerogel causes the solvated polymer matrix to collapse.

The aerogels[174], not gels in the strict sense, are those classes of packings which consist of rigid, performed matrices containing pores into which a solvent has been introduced. Typical examples are porous silica[159] and porous glass[176]. In contrast to the xerogels, aerogels do not depend on the constrained dissolution of the matrix which consequently does not collapse or change in porosity on the removal of the liquid component, solvent. The formation of an aerogel by the solid matrix is therefore independent of the solvent used.

Xerogel-aerogel hybrids[174] have structural features common to both xerogels and aerogels. The polymer matrix from which they are derived may be a semi-rigid structure which undergoes minimal dissolution on constituting the gel. Cross-linked polystyrene produced by a macro-reticular polymerisation technique, is an example. Macro-reticular chromatographic media[174] are prepared by the copolymerisation of monomers in a solvent which the polymer chains are sparingly soluble. The process used in producing this type of packing results in a polymer matrix with large pore sizes and which is very resistant to compressive stress.

Tables 4.1-4.3 summarise the commercially available gel permeation packings.

4.3.2 Practical Aspects

Gel permeation chromatography is normally employed both as an analytical method and as a preparative technique. The experimental arrangement commonly used for analytical work is essentially that given in Figure 4.3. The equipment consists of a solvent reservoir, a degassing device, a sample inlet, a packed column, a detector, a recorder and a solvent flow monitoring device. In practice a sample of the mixture to be analysed is loaded on to the top of the packed column and eluent pumped through it, pumps are carefully chosen to ensure constant flowrates. In aqueous systems peristatic pumps may be used, but piston pumps are commonly used in the case of organic solvents.

Eluent, which has passed through the column, is monitored by a detector that responds to the different solutes in the sample as they emerge at different times, from the column. The various methods of detection have been reviewed by Conlon[177]. No detector is universally accepted as being suitable for all G.P.C. applications; often it is necessary to select one or more methods depending on the problems. Differential refractometers[178] have proved particularly suitable being sensitive, non destructive, non-specific and easy to operate.

Flow through spectrophotometric detectors utilising ultraviolet[179], visible fluorescence and infrared absorption[180] may be used for solutes with suitable absorption bands. Other detectors include those based on heat of adsorption[181], flame ionisation[182],

Table 4.1 Xerogel Packings

Chemical Nature	Operating solvents	U.K. Supplier	Trade Name	Fractionation range or exclusion limit	Special Features
Cross-linked polyac lamide	Aqueous	Bio-Rad Laboratories	Bio-Gel P2-P300	200-2,500 10,000-400,000	Fractionation range refers to peptides and proteins
Cross-linked dextran	Aqueous Dimethyl-formamide Dimethyl-sulphoxide	Pharmacia Fine ChemicalsA.B., (London)	Sephadex G10-G200	-700,5000-800,000	"
Cross-linked hydroxypropyl ether	Polar organic	Pharmacia Fine Chemicals A.B. (London)	Sephadex LH20	-5000	Exclusion limit is solvent dependent
Cross-linked polyacryloyl-morpholine	Aqueous Polar organic excluding simple alcohols	Koch-Light Laboratories	Enzacryl Gel K1 K2	0-10,000 (3,000) 0-100,000 (10,000)	Fractionation range refers to polyethylene glycol in water or chloroform. Figures in parenthesis refer to polystyrene in chloroform
Cross-linked polystyrene	Organic	Bio-Rad Laboratories	Bio-Beed SX1-SX12	600-14,000 -400	Fractionation range refers to polystyrene in tetrahydrofuran
Cross-linked polystyrene	Organic	Waters Associates Ltd.	Poragel A	Not known	Stable up to 150°C
"	Organics and Aqueous	"	Poragel P	Not known	Cross-linking agent had various functional groups attached

Table 4.2 Aerogel Packings

Chemical Nature	Operating solvents	U.K. Supplier	Trade Name	Fractionation range or exclusion limit	Special Features
Porous silica	Aqueous and organics	Waters Associates Ltd.	Porasil A-F	60,000-2,000,000	Exclusion limits are for polystyrene in organic solvents, stable at high temp. Unstable in solvent with pH > 8
"	"	"	Durapak	400,000	Porasil C with organic coating
"	"	Andermamix Co. Ltd.	Merckogel SI	Not known	-
Porous glass	"	Bio-Rad Laboratories	Bio-Glass 200-2500	30,00-30,000 800,000-9,000,000	Fractionation range refers to polystyrene in toluene
"	"	Corning Glass Works	CPG10-75 -CPG10-2000	300-28,000 120,000-1,200,000	Fractionation range refers to dextrans in water
"	"	Waters Associates Ltd.	Corasil	Not known	Glass beads with porous surface
Spherical siliceous particle with porous surface	"	DuPont(U.K.) Ltd.	C.S.P. beads	Not known	A liquid coating can be impregnated on the beads

Table 4.3 Xerogel Aerogel Packings

Chemical Nature	Operating solvents	U.K. Supplier	Trade Name	Fractionation range or exclusion limit	Special Features
Agarose gel	Aqueous	Bio-Rad Laboratories	Bio-Gel A-05→A-150	10,000-500,000 1,000,000-150,000,000	Fractionation range refers to dextrans in water
"	"	Litex	Gelarose 2%-10%	-	Percentage refer to % agarose in gel
"	"	Seravac Laboratories	Sag(Ago-Gel) 10-2	10,000-250,000 500,000-150,000,000	Fractionation range refers to peptides and proteins in water
"	"	Pharmacia Fine Chemicals A.B.	Sepharose[R] 2B-6B	40,000,000 4,000,000	Exclusion limits are for proteins in water
Macro-reticular cross-linked polystyrene	Non-polar organics	Waters Associates Ltd.	Styragel 39720-39731	1,600 - 400,000,000	Exclusion limits are appropriate figures for polystyrenes
Sulphonated macro-reticular cross-linked polystyrene	Aqueous	"	Aquapak	100,000	
Cross-linked polyvinyl acetate	Polar organics	Andermamix Co. Ltd.	Merck-O-Gel OR-750,- OR-1,000,000	750 - 1,000,000	Exclusion limits for polystyrene

FIGURE 4.3 Line Diagram for Analytical Gel Permeation Chromatography

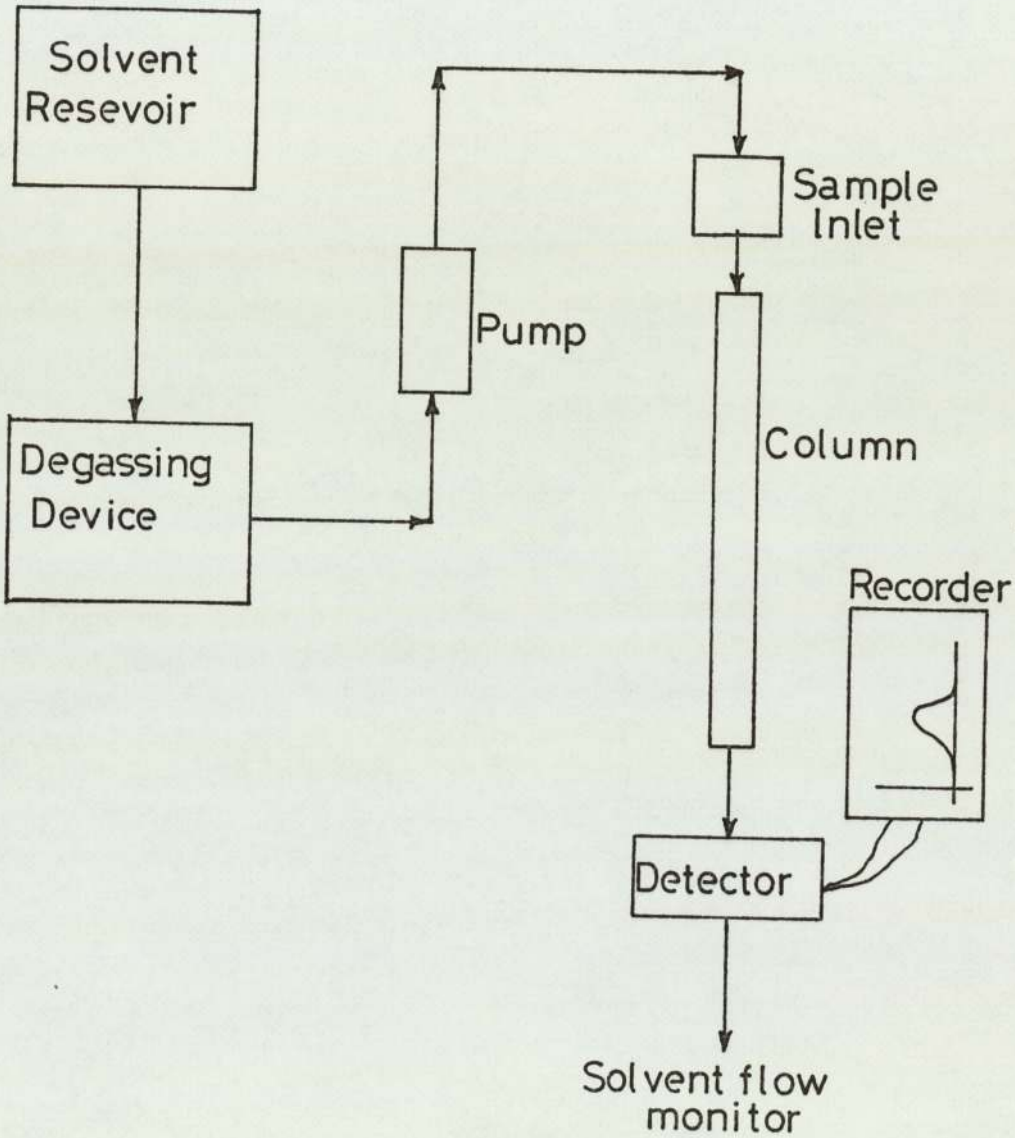

polarographic and radioactivity measurement. Some of these have been described by Perry[183].

Gel permeation chromatography is not an absolute technique, calibration of the columns is required before information about analysed samples can be determined. Calibration is done with standard solutes whose physical properties are known and whose G.P.C. behaviour matches that of the solutes under investigation. Further details of the problems associated with column calibration are discussed in the following subsection.

4.3.2.1 Column Calibration

Gel permeation chromatography permits the separation of mixtures of solutes having different molecular dimensions, but it is not an absolute method and G.P.C. columns require calibration. Practically this can be achieved by using a series of reference solutes belonging to a homologous series. In this way the characteristic sigma-shaped curve, as shown in Figure 4.4, is obtained. The calibration curve relates the logarithm of molecular weight to the elution volume, V_e, or to a function of the elution volume. For monodisperse reference solutes, for example proteins, the elution volume is characterised by the peak maximum. In the case of polymeric solutes the position of the peak maximum cannot, with the possible exception of very narrow molecular weight distributions, be directly related to any particular average molecular weight.

The commonly used average molecular weights are given below[184].

FIGURE 4·4 G.P.C. Calibration Curve

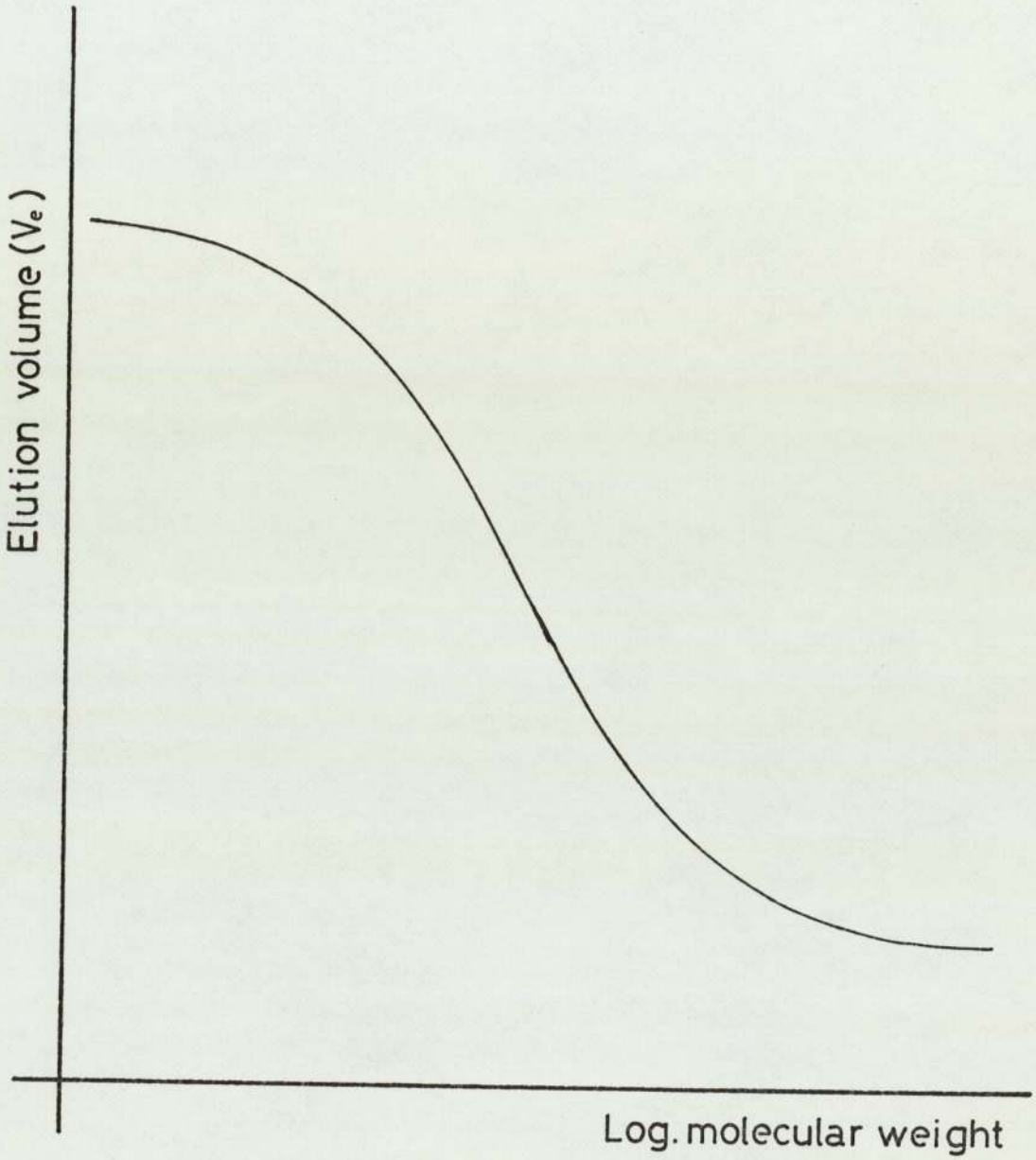

(i) Number average, $\overline{M}_n$.

$$\overline{M}_n = \frac{\Sigma\, n_i M_i}{\Sigma\, n_i} \qquad 4.24$$

(ii) Weight average, $\overline{M}_w$.

$$\overline{M}_w = \frac{\Sigma\, n_i M_i^2}{\Sigma\, n_i M_i} \qquad 4.25$$

(iii) Viscosity average, $\overline{M}_v$

$$\overline{M}_v = \left\{ \frac{\Sigma\, n_i M_i^{1-\alpha}}{\Sigma\, n_i M_i} \right\}^{1/\alpha} \qquad 4.26$$

The term α is the Mark Houwink constant of the sample.

The choice of which average molecular weight to apply can be dependent on the method of analysis used. Number average molecular weight is used when colligative methods such as end group analysis are employed. Weight average molecular weight is usually determined by light scattering or by a method which involves an estimate of solute weight or concentration. For heterogeneous samples $\overline{M}_w$ is always greater than $\overline{M}_n$. The ratio of $\overline{M}_w$ and $\overline{M}_n$ defines the heterogeneity of a polymer sample, the nearer the ratio is to unity the narrower the sample distribution. The final formula (Equation 4.26) describes the average obtained from viscosity measurements. This average becomes equal to $\overline{M}_w$ if α equals unity. In general the value of $\overline{M}_v$ lies in between $\overline{M}_w$ and $\overline{M}_n$.

Van Kreveld and Van Den Hoed[129] advocate, on theoretical grounds[185,186], the use of the first statistical moment of a peak to

calculate the elution volume representing the weight average molecular weight, $\overline{M}_W$. These authors note that for assymetric peaks the median of the elution curve of a polymer sample serves as a satisfactory approximation. The median and the first moment can be determined more accurately than the peak maximum, especially with flat and broad chromatograms.

Calibration curves are not valid if the material under investigation is structurally different from the reference solutes used to calibrate the column. This is because of the following factors[11]; (i), the relationship between molecular weight and molecular size varies for different molecular species; (ii), different types of molecules are likely to be hydrated to different extents and thus have different sizes in solution for the same molecular weight, (iii), different types of molecules of the same molecular weight adopt different conformations in solution.

Considerable effort has been expended in the search for a "universal" parameter of the solute molecule which governs its elution volume. Details of the various techniques used to find a "universal calibration" parameter have been discussed by Heitz[98], Cooper[93] and Coll[14].

4.3.2.2 The Correction of Gel Permeation Chromatograms for Dispersion

A sample of a monomeric solute loaded on to a gel permeation volumn exits as a curve of finite width, as shown in Figure 4.5, the elution volume depending on the molecular size of the solute. The area of the peak is proportional to the weight in the original sample and the width is dependent on the various dispersion mechanisms operating both within and without the column. When a polymeric sample

FIGURE 4.5 Chromatogram for a Monomeric Solute

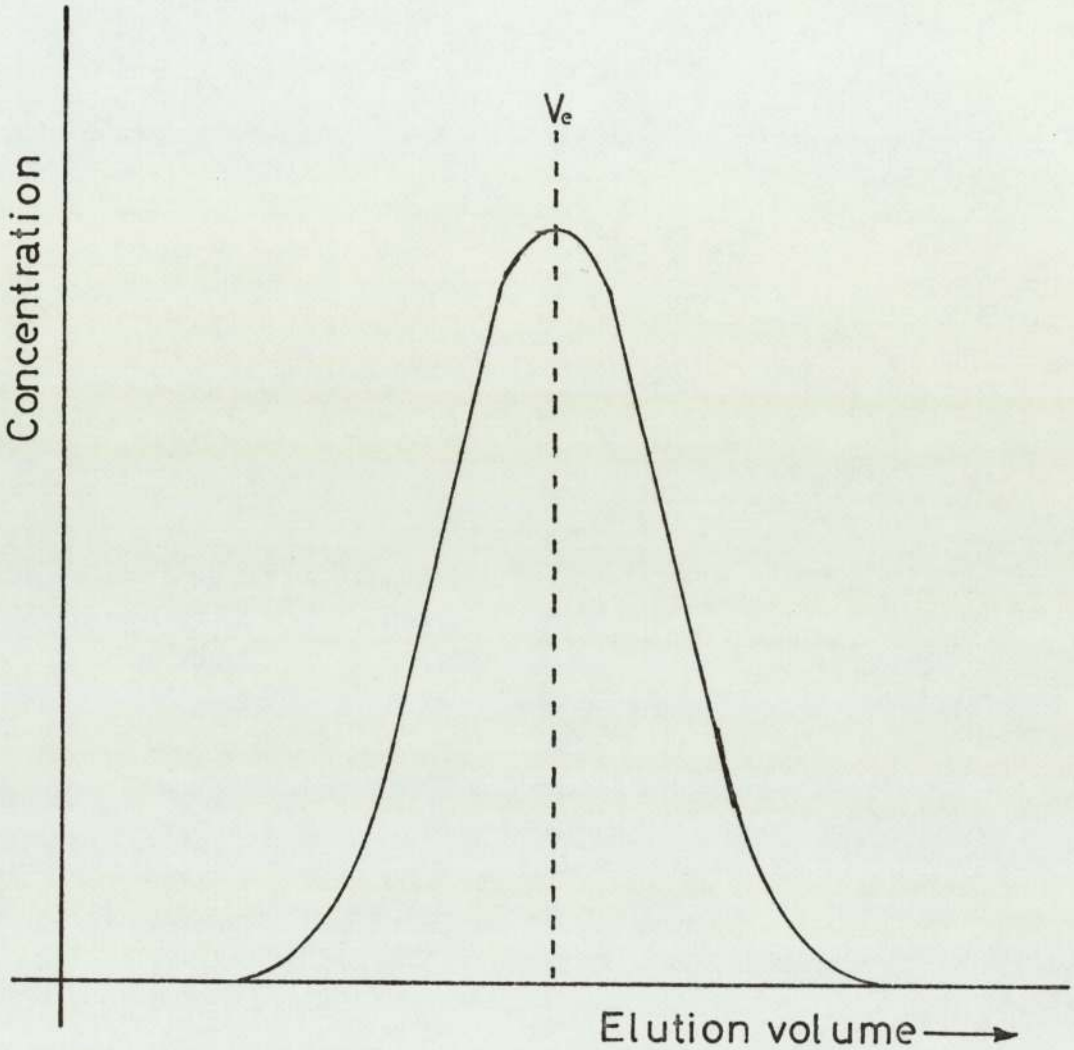

is analysed the resulting chromatogram is a composite curve of the elution curves of all its components. The total area of the curve is proportional to the amount of each component, but the height does not accurately represent the relative amounts of each component at the corresponding elution volume. This is because the height at specific elution volume is influenced by the degree of spreading undergone by itself and the neighbouring components, and in fact represents the sum of heights of several components, see Figure 4.6. As a result of the various dispersion processes operating in a column a proportion of a polymer sample can elute, depending on the molecular size range, at volumes outside the totally excluded or totally included volumes of the column. Thus the spreading of a sample on an analytical column results in an imperfect analysis. There are, however, a number of methods of correcting the chromatogram when precise molecular weight distributions are required. These methods are by no means infallible.

The basis of the first method is mathematical and, in essence, relies on the solution of the integral given below.

$$f(v) = \int_a^b w(y).g(v-y)dy \qquad 4.27$$

First suggested by Tung[187], this integral, which has the form of the convolution integral, relates the experimental chromatogram, f(v), the true chromatogram, w(y), and the function describing spreading, g(v). V and y are elution volumes and the terms a and b are the initial and final elution volumes respectively. The problem

FIGURE 4.6 Chromatogram for a Polymer

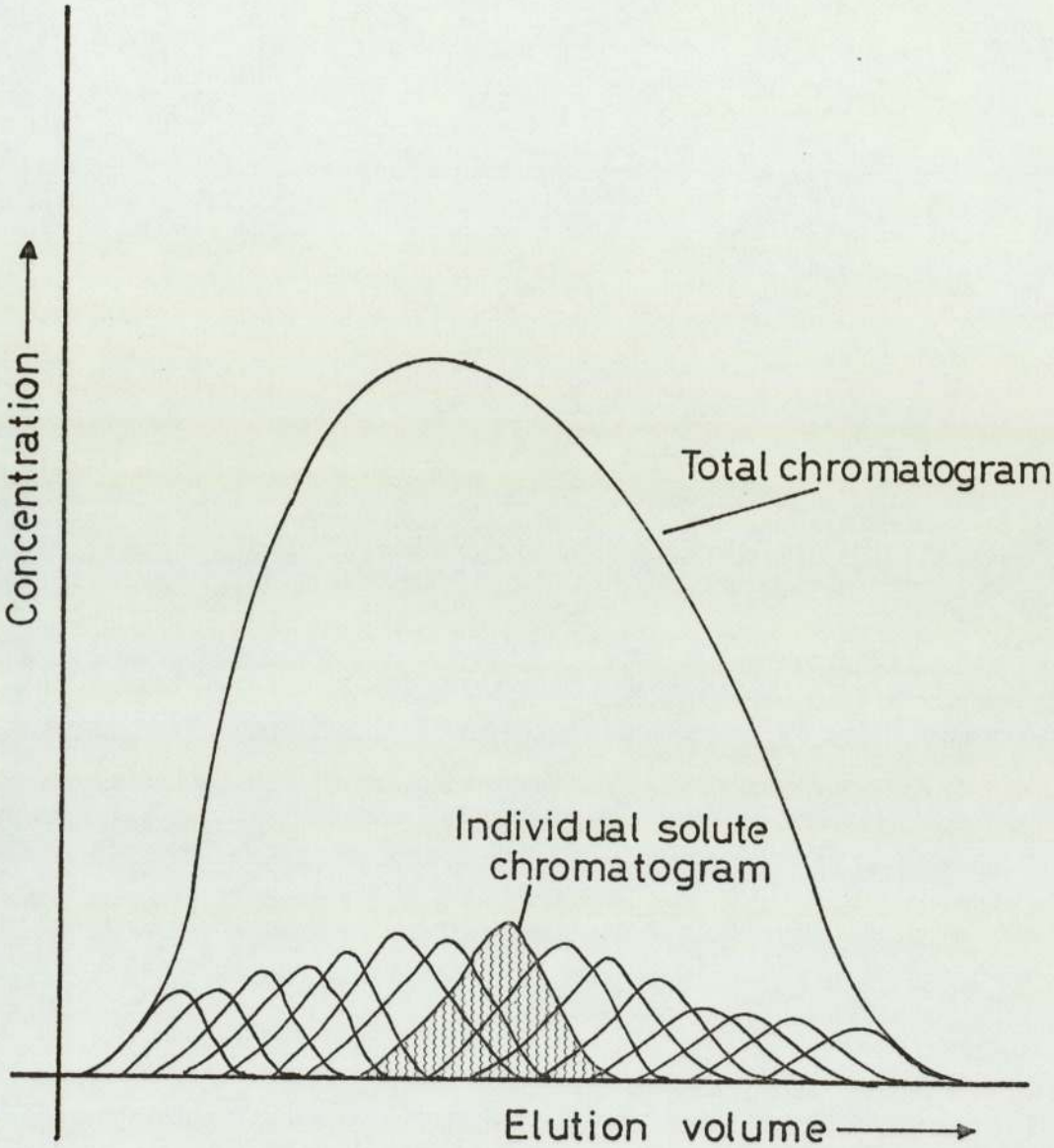

to be solved therefore, is knowing the function f(v) of the chromatogram, and by determining g(v), determine w(y).

Several research workers have produced solutions to Equation 4.27. Early solutions by Tung[187], Smith[188], Hess and Kratz[189] and Picket, Cantow and Johnson[190] produced artificial oscillations in the corrected chromatograms. Pierce and Armonas[191] and Aldhouse and Stanford[192] obtained solutions that proved inaccurate when the spreading correction was large. Vink[193] has also proposed a solution. Improved techniques of solving Equation 4.27 were developed by Provder and Rosen[194,195], Hamialec and Balke[196], Tung[197-200], Vladimiroff[201], Chang and Huang[202-203] and Hamialec and Ray[204]. Duerksen[205] has compared several of these methods. The conclusions drawn were that most of the solutions exhibit inconsistent oscillations in the corrected molecular weight distributions. These oscillations are caused by instrumental noise in the uncorrected chromatogram and in the limited accuracy to which trace heights can be read off, rather than by the mathematical techniques involved. Data smoothing techniques[202,203] have been used to treat the raw chromatogram which circumvent the problems of induced oscillation.

De Vries[206] has proposed an alternative technique to applying mathematical correction procedures. Essentially, by carefully choosing particle size, column diameter, packing technique and sample loading and detection procedures the spreading can be reduced to an acceptable level.

4.3.2.3 Effects of Sample Quantity and Volume

In analytical G.P.C. systems the sample volume injected can significantly effect the elution volume, V_e, and the peak width, W. Altgelt[109] noted that for a sample volume, V_s, the elution volume would be greater by $^1/_2\ V_s$ than the elution volume, Ve_o, of an infinitely small sample.

$$Ve = Ve_o + {}^1/_2\ Vs \qquad 4.28$$

Normally the effect of sample size is small but practically the sample size should be kept as small as possible, at least less than 1% of the total bed volume ($^{Vt}/_{100}$), so as to reduce its effect on peak width. Van Deemter[16] has calculated the effect of sample size on peak width.

Of more importance than the sample size are the sample concentration, density and viscosity. The significance of concentration has already been discussed in Section 4.2.4. Density and viscosity effects will influence peak dispersion. Samples of high viscosity, especially polymer solutions, must be diluted to a viscosity comparable with that of the eluting solvent, this prevents serious distortion of the chromatogram.

4.4 APPLICATIONS OF GEL PERMEATION CHROMATOGRAPHY

The many applications of gel permeation chromatography have been extensively reviewed by Determan[13] and in the comprehensive bibliography published by Pharmacia A.B. (Uppsala, Sweden). The latter

is restricted to the applications of Sephadex.

Although extensively used as an analytical technique for the determination of the average molecular weight of almost all soluble polymers, its potential as a preparative tool will undoubtedly increase. Some possible applications are listed below.

(i) The isolation of enzymes.

(ii) The separation of hormones, viruses and oligonucleotides.

(iii) Preparation and separation of serum and plasma proteins.

(iv) The fractionation of carbohydrates.

CHAPTER 5

The Theory and Practice of Gel Permeation Chromatography in a Moving Column Chromatograph

5.1 THE IDEAL CASE

The process of separation and fractionation by continuous gel permeation chromatography is dependent on the fact that molecules of differing sizes distribute themselves to varying degrees between a liquid mobile phase and a liquid in the pores of a suitable packing, the stationary or liquid phase. Since gel permeation chromatography involves the use of two chemically identical liquid phases the terms mobile phase and liquid phase have been used respectively in the following text to distinguish between the interstitial liquid and the liquid within the pores of the packing.

In continuous chromatography the packing moves in the opposing direction to that of the mobile phase. The "stationary", or liquid phase is made to move counter-current to the mobile phase. By careful control of the operating conditions different components fed into the chromatograph can be made to move in opposing directions with respect to the stationary feed point. What factors influence the direction a component moves can best be explained by adopting a similar approach, to that used by Barker et al.[60,207], Huntington[208] and Deeble[8] to explain the significance of component partition coefficients in continuous gas-liquid chromatography.

Feed containing two components 1 and 2 enters the chromatograph at the feed point F (figure 5.1a). It is required that component 1 leaves, as product 1, with the mobile phase (or eluent) from port M and that component 2 leaves as the purged product, product 2, with the purge fluid from port P. The partition coefficients of the components at infinite dilution are K_1^∞ and K_2^∞, and L_m and L_s are the mobile and liquid phase flow rates relative

FIGURE 5.1 Continuous Liquid-Liquid Chromatography - The Ideal Case

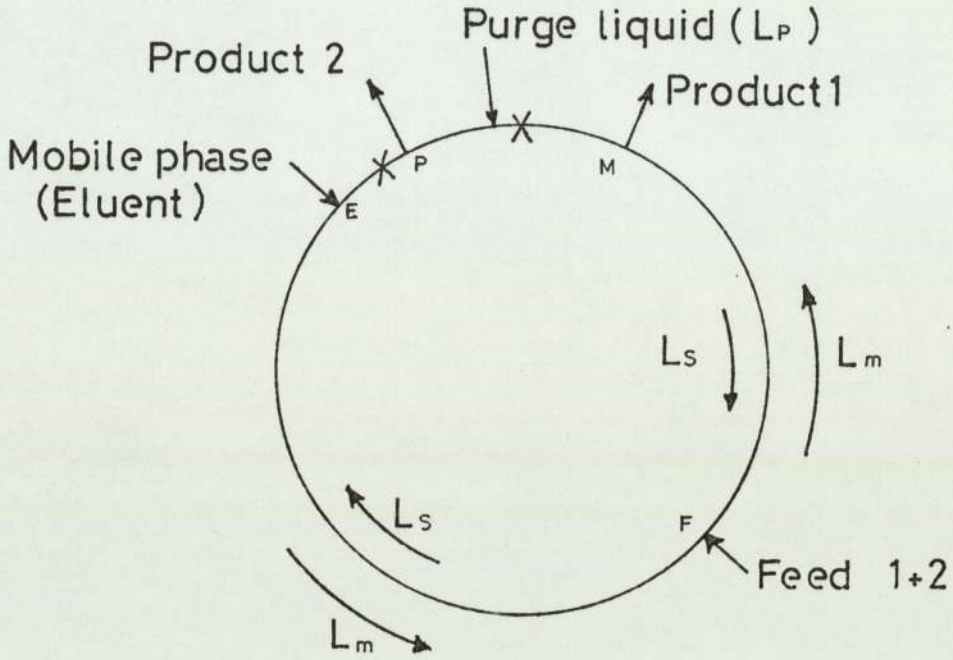

(a)

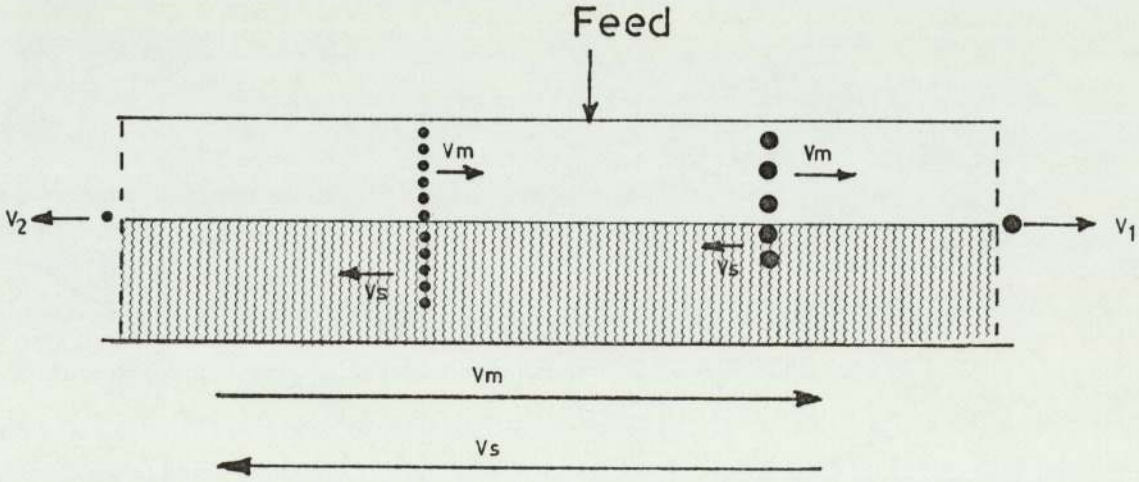

(b)

to the feed point. The feed is assumed, in this simple model, to enter at a negligible volumetric flow rate.

A material balance or component 1 about the feed point gives:

$$F_1 = L_m Y_1 + L_s X_1 \qquad 5.1$$

where

F_1 = mass rate of component 1 input at the feed point

X_1 = concentration of component 1 in the liquid phase

Y_1 = concentration of component 1 in the mobile phase.

The conditions for the movement of component 1 with the mobile phase is therefore that

$$L_m Y_1 > L_s X_1 \qquad 5.2$$

therefore

$$\frac{L_m}{L_s} > \frac{X_1}{Y_1} \qquad 5.3$$

Since

$$K_1^{\infty} = \frac{X_1}{Y_1} \qquad 5.4$$

therefore

$$\frac{L_m}{L_s} > K_1^{\infty} \qquad 5.5$$

Similarly for the movement of component 2 with the liquid phase

$$\frac{L_m}{L_s} < K_2^\infty \qquad 5.6$$

Combining 5.5 and 5.6 we can obtain the theoretical limits of mobile and liquid phase flow rates for the separation of components 1 and 2 in this simplified model.

$$K_1^\infty < \frac{L_m}{L_s} < K_2^\infty \qquad 5.7$$

Let L_m/L_s define the "cut" partition coefficient, K_c, effected by the machine under these operating conditions. Then the inequality above becomes

$$K_1^\infty < K_c < K_2^\infty \qquad 5.8$$

By the same process it can be shown that component 2 will be purged from the isolated section if,

$$K_2^\infty < \frac{L_p}{L_s} \qquad 5.9$$

where L_p = the purge flow rate.

For the sake of simplicity a binary mixture has had to be used to develop Equations 5.8 and 5.9. However, they do not only apply to two component systems. In a N component system, and a column of infinite length, all components with partition coefficients less

than K_c will travel in the same direction as the mobile phase, and those with partition coefficients greater than K_c will preferentially be transported in the liquid phase. Therefore to resolve an N component mixture into individual components, in a high state of purity, either N-1 chromatographs would be needed or N-1 separations would have to be carried out using one chromatograph.

Equations 5.8 and 5.9 provide a basis for the selection of the theoretical operating conditions.

From a practical point of view, Hatt[11] developed an equation that can be used to determine the "cut" partition coefficient, K_c, to which the flow conditions of the continuous chromatograph corresponded. The equation related experimental data from an analytical column and the flow conditions of the chromatographic machine to the partition coefficient of the "cut". The form the equation takes is,

$$K_c = \frac{\text{R.F. (excl)}}{\text{R.F. (incl)} - \text{R.F. (excl)}} \cdot \left\{\frac{R_D}{A_o r_2} - 1\right\} \qquad 5.10$$

where

R.F. (excl) = retention factor of a totally excluded molecule

R.F. (incl) = retention factor of totally included component

R_D = mobile phase output rate, measured at port M_p (Figure 5.1a) ($cm^3 min^{-1}$)

r_2 = rate of movement of total tube length

= total bundle length/time for one complete cycle of the tube bundle ($cm\ min^{-1}$)

A_o = available tube cross sectional area for fluid flow (cm^2) in the chromatograph

= $A^* \times$ R.F. (excl)

$A'' =$ tube cross-sectional area (cm^2)

The terms R_D, A_o, r_2 and A'' are all related to the chromatographic machine.

Retention factor = component elution volume/total bed volume

The retention factors of the totally excluded and totally included components are experimentally determined on an analytical column packed with the same packing as that used in the tube bundle.

$$\frac{\text{R.F. (excl)}}{\text{R.F. (incl)} - \text{R.F. (excl)}} = \frac{V_o}{V_i} \qquad 5.11$$

V_o = column interstitial volume (cm^3)

V_i = column pore volume (cm^3)

For a unit length of column V_o/V_i can be written as A_o/A_i. The area A_i is defined as the column cross-sectional area equivalent to the pores of the packing. The term V_o/V_i is the inverse of the packing capacity factor[14], which is analogous to the phase ratio in liquid-liquid extraction. Equation 5.10 therefore becomes,

$$K_c = \frac{A_o}{A_i} \left\{ \frac{R_D}{A_o r_2} - 1 \right\} \qquad 5.12$$

$$= \frac{R_D - A_o r_2}{A_i r_2} \qquad 5.13$$

Hatt[11] noted that,

$R_d - A_o r_2$ = the mobile phase flow rate, L_m ($cm^3 min^{-1}$)

and that

$A_i r_2$ = the liquid phase flow rate, L_s ($cm^3 min^{-1}$).

Equation 5.13 provides a practical basis on which the selection of theoretical operating conditions can be made.

At this stage it is convenient to introduce the idea of component resultant velocities. The "cut" partition coefficient, K_c, is defined by the operating conditions of the chromatograph and corresponds to the partition coefficient of a theoretically stationary component.

From $K_c = \frac{L_m}{L_s}$ and converting the mobile and liquid phase flow rates to velocities we obtain

$$K_c = \frac{v_m}{v_s} \cdot \frac{A_o}{A_i} \qquad 5.4$$

$$= \frac{v_m}{v_s . P} \qquad 5.15$$

where

v_m = mobile phase velocity (cm min^{-1})

v_s = r_2, already defined (Equation 5.10)

P = Capacity factor[14]

= $A_i/A_o = V_i/V_o$

For a stationary component, by definition, its resultant velocity, v_c, must be zero . Therefore, from Equation 5.15

$$v_c = v_m - v_s . K_c . P = 0 \qquad 5.16$$

Components travelling preferentially either with the mobile phase or the liquid phase must therefore have positive and negative resultant velocities respectively. All resultant velocities are with respect to the feed point. If this principle is applied to a binary

mixture, containing components 1 and 2, which enters the idealised chromatographic machine at the feed point F (Figure 5.1a). Then the two components will move at different resultant velocities, v_1 and v_2 (Figure 5.1b).

$$v_1 = v_m - v_s K_1^{\infty} P \qquad 5.17$$

$$v_m > v_s K_1^{\infty} P \quad \therefore \quad v_1 \text{ +ve}$$

$$v_2 = v_m - v_s K_2^{\infty} P \qquad 5.18$$

$$v_m < v_s K_2^{\infty} P \quad \therefore \quad v_2 \text{ -ve}$$

The velocities v_1 and v_2 are positive and negative respectively as a result of the inequality $K_1^{\infty} < K_c < K_2^{\infty}$ and, by definition the resultant velocity of a component corresponding to a partition coefficient must be zero (Equation 5.16).

By the very nature of the partitioning process at any instant in time there will be a proportion of both components in each of the two phases. Thus, a proportion of component 1, which preferentially moves with the mobile phase, will move with the liquid phase. The same will apply to the movement of component 2 with the mobile phase, instead of preferentially with the liquid phase. A consequence of this movement is the spreading of the two components through the machine (Figure 5.2a). The degree of spreading is influenced by the difference in the partition coefficients of the feed components and the operating conditions of the machine.

FIGURE 5.2 Concentration Profiles

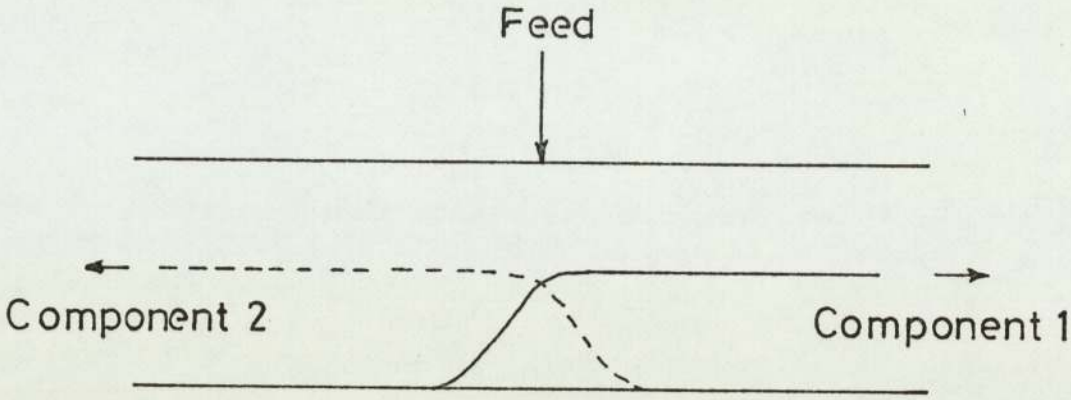

(a)

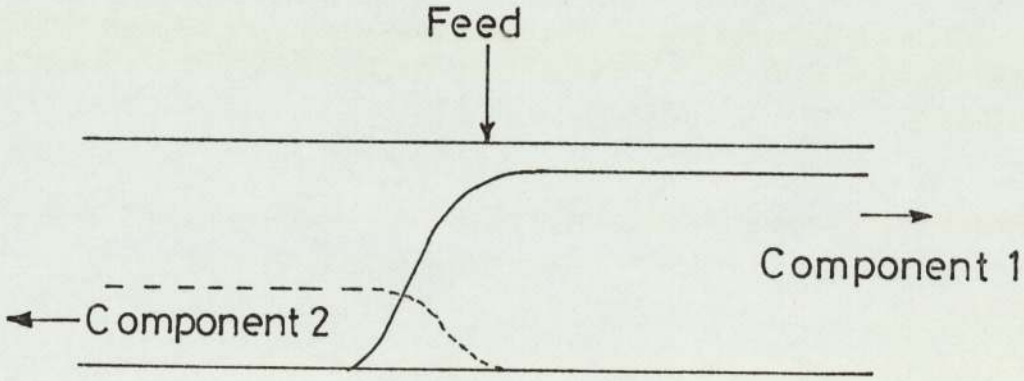

(b)

For example, if the operating conditions are set so that the "cut" effected is near to the partition coefficient of component 1 then this component will, as a result, move more slowly because of a decrease in its resultant velocity. This decrease will cause an increase in the concentration of component 1 and an increase in the spreading of this component through the chromatograph (Figure 5.2b).

5.2 THE PRACTICAL CASE

In reality, the separation processes occurring within the chromatograph are not simple, nor is the mechanical arrangement of the system. A number of factors influence the limits of the machine operating conditions. For a binary mixture these limits have, theoretically, been defined by Equations 5.8 and 5.9. The factors that will influence separation are,

(i) a finite feed flow rate

(ii) a finite component concentration

(iii) a limited separation length

(iv) a discontinuous mode of operation.

Each of these factors and their effects on the operation of the chromatograph is now qualitatively considered.

5.2.1 The Effect of a Finite Feed flow rate

In developing the inequality given in Equation 5.8 the assumption of a negligible feed flow rate was made, whereas, in practice this is not the case. The feed, entering in a finite volume, has the effect of changing the operating conditions of the machine at, and beyond, the feed point. The separating length has, as a result, been divided into two parts, the prefeed section and

the post feed sections (Figure 5.3a). Hence two sets of operating conditions will exist. The difference between the two is dependent on the magnitude of the feed flow rate.

Using an approach similar to that adopted to develop Equation 5.8, the theoretical limits on operating conditions for the separation of a two component system in each section can be developed.

(i) For the port feed section:

$$K_1^\infty < \frac{L'_m}{L_s} < K_2^\infty \qquad 5.19$$

L'_m = mobile phase flow rate in port feed section

(ii) For the prefeed section.

$$K_1^\infty < \frac{L_m}{L_s} < K_2^\infty \qquad 5.20$$

Equation 5.20 is identical to 5.8.

Combining the inequalities given above the limits on operating condition become

$$K_1^\infty < \frac{L_m}{L_s} < \frac{L'_m}{L_s} < K_2^\infty \qquad 5.21$$

$$L'_m = L_m + F_e \qquad 5.22$$

F_e = feed flow rate ($cm^3\ min^{-1}$)

FIGURE 5.3 Continuous Liquid-Liquid Chromatography - The Practical Case

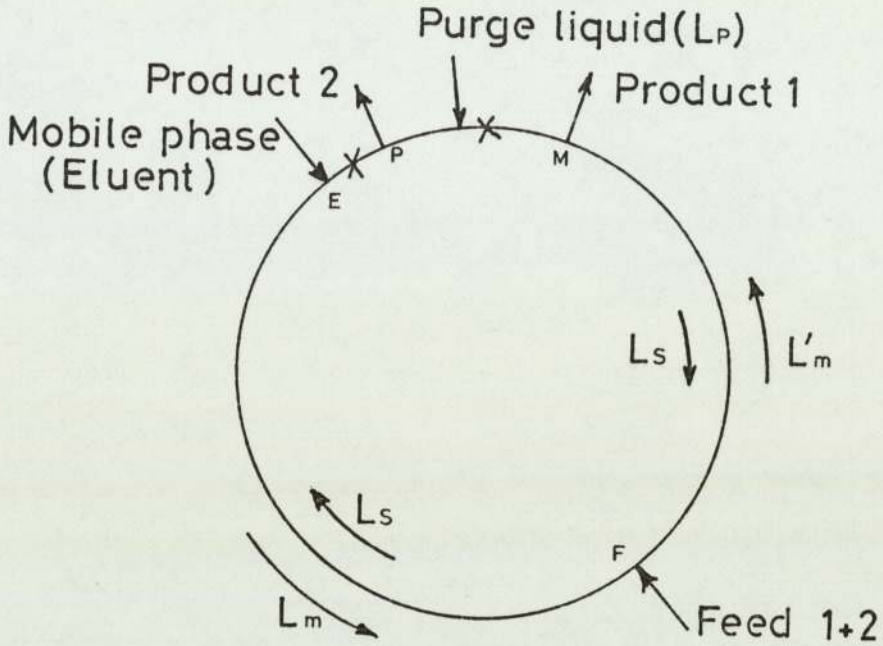

(a)

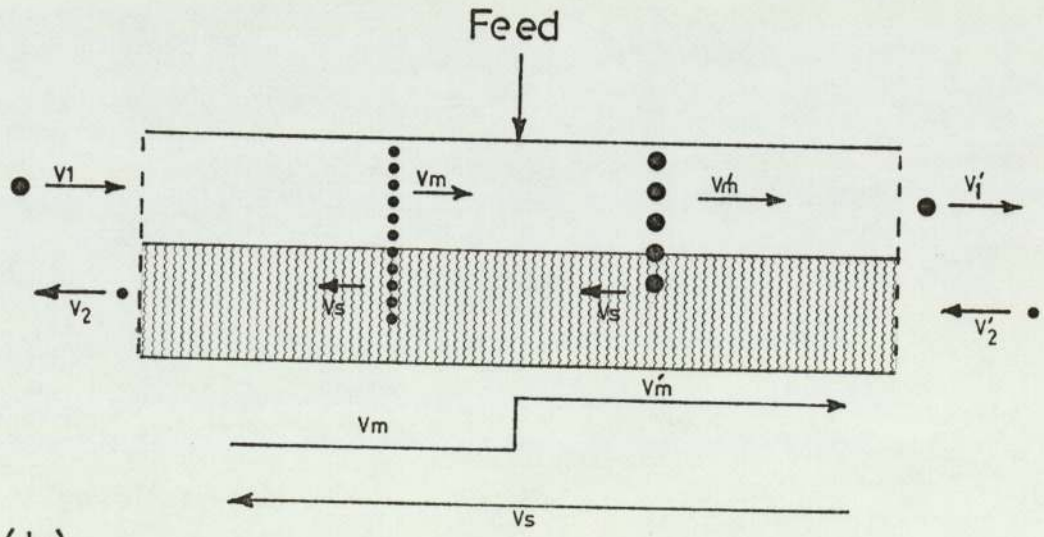

(b)

Equation 5.21 implies that there is a limit to the maximum feed volumetric flow rate if separation of a two component mixture is to be achieved.

The change in mobile phase flow rate results in a corresponding change in the resultant velocities of components entering with the feed. With reference to the binary example, component 2, which preferentially moves with the liquid phase in the prefeed section, will have this preference reduced in the post feed section. In fact component 2 will travel faster, with respect to the mobile phase, in the post feed section and consequently this component will spread further into the port feed section. Conversely component 1 when it enters the prefeed section will have its preference for the mobile phase decreased and hence it will spread further into the prefeed section as a result of an effective increase in its velocity with respect to the liquid phase.

Any decrease in the resultant velocity of a component, irrespective of the direction a component travels, will cause an increase in its residence time per unit of available liquid volume. Since the process is essentially continuous, such an increase will cause an increase in the component concentration.

5.2.2 The Effect of a Finite Component Concentration

Equation 5.21 uses partition coefficients measured at infinite dilution, which limits its practical use. The basic form of the equation is correct, but qualitative allowances can be made to take into account the influence of a finite component concentration on the machine operating limits.

In gel permeation chromatography component partition coefficients have been shown to be affected by concentration[167,168,172,209]. The precise effect is as yet uncertain. Both Hatt[11] and Ellison[22] have experimentally observed a change in the chromatographic behaviour of polymer molecules at increased concentrations. Hatt[11] concluded, that during fractionation, a species having a particular molecular weight will be affected both by molecules of a greater and lesser molecular weights. Molecules of smaller molecular weights permeate the liquid phase to a greater extent and have the effect of excluding other larger molecules. In contrast larger molecules preferring the mobile phase exert a similar effect on the smaller ones causing them to be included to a greater extent. Thus, the larger molecules remain in the mobile phase and therefore travel faster, whilst the smaller ones are retarded and therefore travel slower. The combined effect is to alter the partition coefficients of individual molecular species. Whether concentration effects increase or decrease partition coefficients will therefore be dependent on the concentration and molecular weights of those components present. A change in partition coefficient, β_i, of component i when being fractionated in the presence of a finite concentration of molecules having a range of molecular weights could be defined by,

$$\beta_i = f\{(C_i.M_{wi})\ i = 1,N\} \qquad 5.23$$

where

C_i = concentration of component i

M_{wi} = molecular weight of component i

N = number of components.

The sign and magnitude of β_i will be dependent on the overall effect of the other molecules on component i. Partition coefficients at a finite concentration can therefore be expressed as,

$$K = K^{\infty} + \beta \qquad 5.24$$

Equation 5.21 can then be rewritten as:

$$(K_1^{\infty} + \beta_1) < \frac{L_m}{L_s} < \frac{L'_m}{L_s} < (K_2^{\infty} + \beta_2) \qquad 5.25$$

or

$$K_1 < \frac{L_m}{L_s} < \frac{L'_m}{L_s} < K_2 \qquad 5.26$$

The terms K_1 and K_2 are the partition coefficients of components 1 and 2 at a finite concentration and β_1 and β_2 the changes in the partition coefficients K_1^{∞} and K_2^{∞} respectively. The effects of a change in component partition coefficients merits further discussion.

From Equation 5.25 it can be seen that changes in the partition coefficients can have a number of effects. An increase in both the component partition coefficients will have a similar effect to a decrease in the mobile phase flow rate, which is to move the cut values towards the component preferentially travelling in the mobile phase. Conversely a decrease in both the partition coefficients will be equivalent to an increase in the mobile phase rate and, as a consequence, a shift in the "cut" value towards the component preferentially travelling with the liquid phase.

Perhaps the most significant effects will be as a result of a decrease in the partition coefficient of one component and an increase in the other. This can result in two possible effects. Firstly for the case specified by the inequality below,

$$(K_1^{\infty} + \beta_1) < \frac{L_m}{L_s} < \frac{L_m'}{L_s}(K_2^{\infty} - \beta_2) \qquad 5.27$$

which states that there is a narrowing of the separation limits which will further restrict the possibility of achieving separation. Secondly the reverse situation, specified by the following,

$$(K_1 - \beta_1) < \frac{L_m}{L_s} < \frac{L_m'}{L_s} < (K_2^{\infty} + \beta_2) \qquad 5.28$$

where, due to concentration effects, the separation limits have diverged. In this case, the use of high concentrations will create a greater range of possible separation conditions, and hence make the separation simpler.

5.2.3 The Effect of a Finite Separation Length

In common with other column separation processes the length available for separation is of prime importance in determining whether a successful separation will be achieved at a given set of flow conditions. In continuous chromatography if the "cut" partition coefficient, fixed by the machine operating conditions, approaches either of the limits of separation, defined by Equation 5.26, the probability of separation decreases. A situation develops which is analogous to the "pinch point" in distillation or

alternatively an "absorption factor" of unity in gas absorption. In both cases the driving force for mass transfer between the equilibrium and operating lines approaches zero. Therefore the number of theoretical stages required to achieve separation tends to infinity. A shift in the "cut", effected by the chromatograph, towards either of the separation limits will have a similar effect. A term, δ', must therefore be included in the inequality given in Equation 5.26 such that,

$$(K_1 + \delta'_1) < \frac{L_m}{L_s} < \frac{L'_m}{L_s} < (K_2 - \delta'_2) \qquad 5.29$$

The term δ' is a function of those parameters which influence the efficiency of a chromatographic column. For example, particle size, mobile phase flow rate, packing density, molecular weight and molecular diffusivities.

5.2.4 The Effect of a Discontinuous Mode of Operation

Unlike, for example, a distillation column the mechanics of the continuous chromatographic machine used in this research dictate that the feed enters at discrete intervals, equivalent to one pair of packed columns. This feature will be detrimental to the overall separation efficiency of the machine. Hence an additional factor s must therefore be included in Equation 5.29 so that.

$$(K_1 + \delta'_1 + s_1) < \frac{L_m}{L_s} < \frac{L'_m}{L_s} < (K_2 - \delta'_2 - s_2) \qquad 5.29$$

A similar equation can be developed for the purge section.

$$\frac{L_p}{L_s} > (K_2 + \delta_2' + s_2) \qquad 5.31$$

The parameter s will be a function of the length of the discontinuity, which will be determined by the length of the column between individual feed points, the eluent to feed ratio and the rotational speed of the tube bundle. Since the discontinuous nature of the process contributes to a decrease in the overall separating efficiency of the machine, s should ideallybe interelated with the parameter δ', discussed above.

Equations 5.30 and 5.31 provide a qualitative indication of the factors in continuous chromatography which will influence the process. The drawback in applying these equations is in elucidating, quantitatively, both the magnitude and the extent of any interaction of the various parameters governing the process.

The question of how the discontinuous mode of operation influences the fractionation of polymeric feedstock was, from the practical point of view, of considerable interest. A qualitative investigation was undertaken using the resultant velocity model discussed in Section 5.1.

5.2.4.1 The Influence of a Discontinuous Mode of Operation on Polymer Fractionation

Consider the hypothetical distribution, represented by Figure 5.4a, which consists of ten discrete components. This

distribution is fed into the chromatographic machine and the flow conditions set so that the prefeed and postfeed "cuts" effected by the machine coincide with the partition coefficients K_{CA} and K_{CB} respectively (Figure 5.4a). The continuous chromatograph has been diagrammatically represented in Figure 5.5a. Feed is pumped into column i for a fixed time period, called "the switch time". In the actual machine each tube pair is equivalent to one column represented in the diagram (Figure 5.5a). The switch time is equal to the time for one complete cycle of the tube bundle divided by the total number of tube pairs.

Over the switch time as the feed enters column i each component is subject to post-feed flow conditions. For components with partition coefficients less than K_{CB}, namely components 1-6 (Figure 5.4a), to preferentially move with the mobile phase their effective resultant velocities must be greater than zero. For separation to occur within the switch time these components will travel a distance greater than the column length, L. Figure 5.5b represents, in an idealised manner, the distance travelled by each component. Of particular importance is the fact that Figure 5.5b shows that at the end of the switch time, column i contains the complete range of feed components, though not necessarily through the whole column length.

At the end of the switch time the columns move counter-current to the mobile phase such that the feed now enters column i+1, column i having moved into the prefeed section (Figure 5.5b). Thus the components in column i are now subject to prefeed flow conditions and therefore those components with partition coefficients less than

FIGURE 5.4 Distribution for a Multicomponent Feed

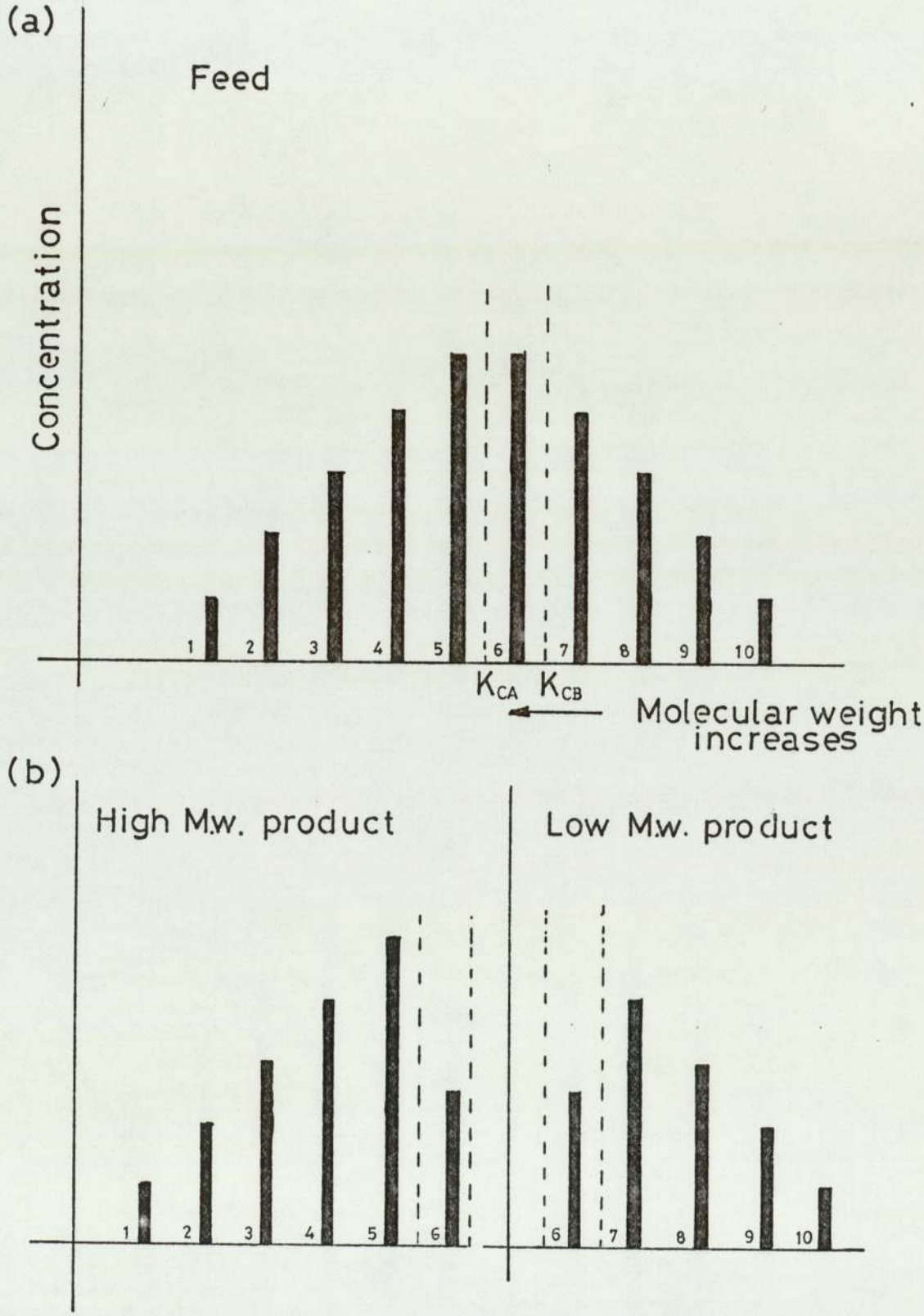

FIGURE 5.5 Diagram of Feed Point

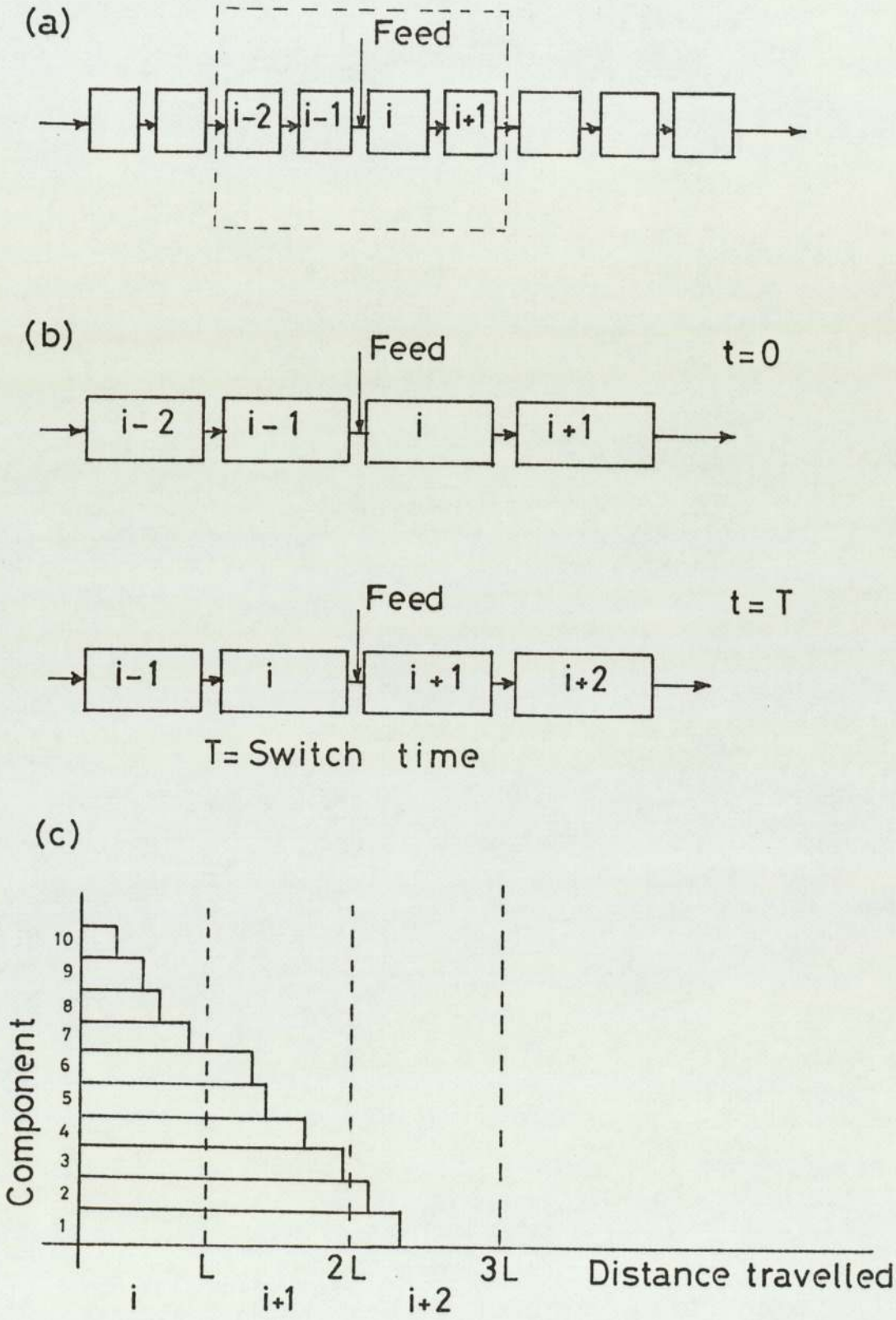

K_{CA}, components 1-5, will effectively travel with the mobile phase, components 6-10 preferentially moving in the direction of liquid phase travel. The situation has therefore developed where, at equilibrium, component 6 will be present in both products, Figure 5.4b. This overlap in the product distributions is a result of the two operating conditions in the machine. In practice the degree of overlap would be more significant due to the effects of component spreading. The example discussed above is very much an idealised picture but it serves to demonstrate the detrimental effect of a discontinuous mode of operation on the fractionation of a multi-component mixture.

Of particular interest from the point of view of one aspect of this research is the influence of the various operating parameters on the fractionation of a polymer. If a polymeric feed, represented by Figure 5.6a, is fractioned using the chromatographic machine there will be, for the reasons discussed above, a degree of overlap in the product molecular weight distributions. The extent of the overlap will be governed by the magnitude of the discontinuity of operation at the feedpoint and the overall efficiency of the fractionation process. If all these effects are included then we can expect a product distribution theoretically represented by Figure 5.6b.

In Section 5.2.2.it was discussed how the effects of concentration can be benificial to the separation of a two component mixture (Equation 5.27). Increased concentration effectively causing a greater freedom in the choice of operating conditions. The question arises as to whether the same can be said for polymer fractionation.

FIGURE 5.6 Feed and Possible Product Distributions

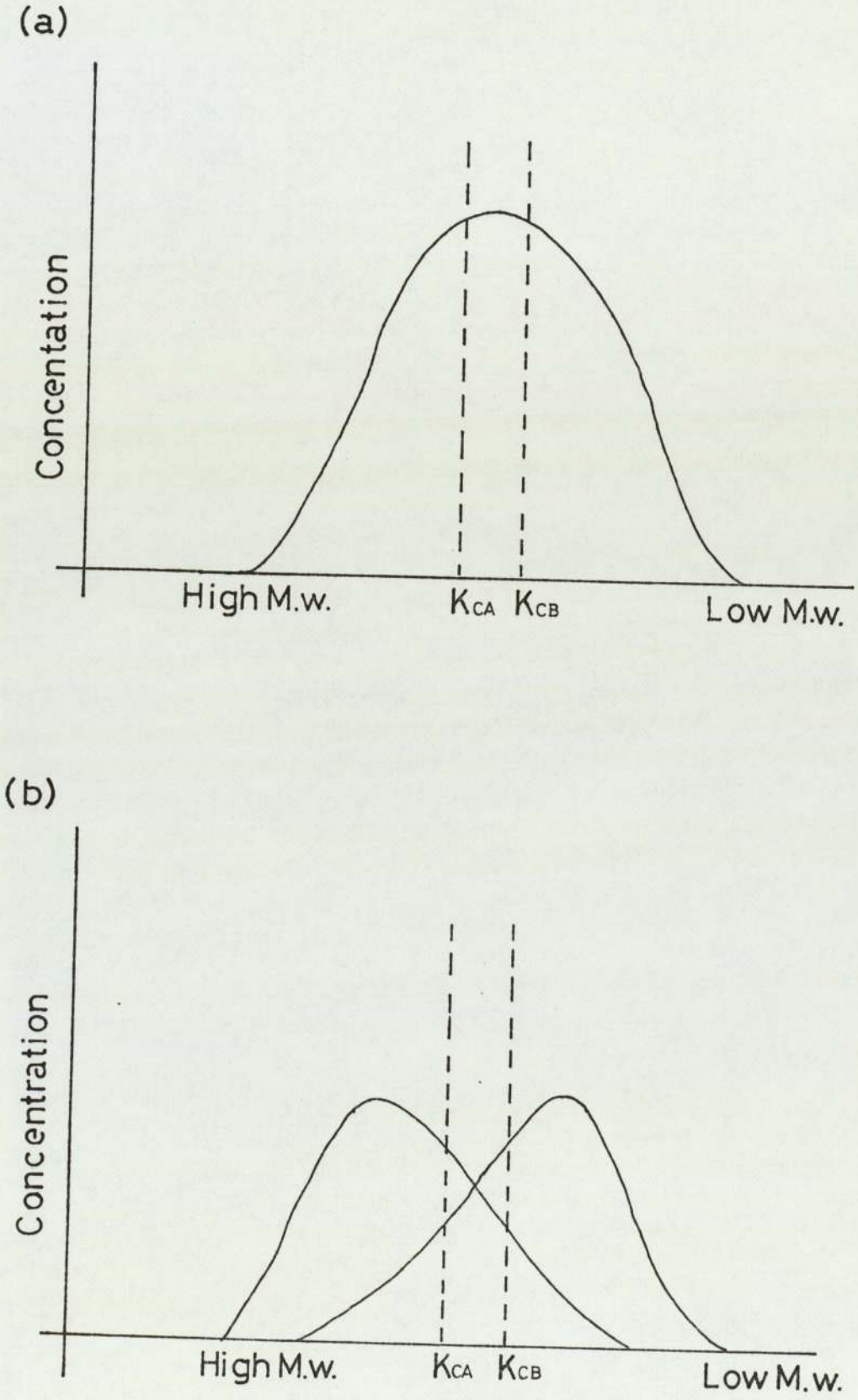

Experimental evidence[11,22,167,168,178,209] obtained on batch columns suggests that, at high concentrations, the partition coefficients of large molecules decrease and those of small molecules increase. What precise effect this has on the fractionation of a polymer by continuous chromatography merits experimental investigation.

CHAPTER 6

The Fractionation of Dextran by Continuous Gel Permeation Chromatography

6.1 INTRODUCTION

6.1.1 Industrial Background

Dextran is an anhydroglucose polymer, produced by the numerous strains of"Leuconostoc" and closely related bacteria in solutions containing sucrose[184]. Native dextran is soluble in water, resulting in very viscous solutions. Its molecular weight distribution is extremely wide, covering a range of molecular weights from hundreds of millions down to molecular weight of a few thousand. By a process of acid hydrolysis and repeated fractionation the chain length and molecular weight distribution of native dextran can be reduced.

Dextran fractions with well defined properties have found many applications in research work and in the medical field where a stable, chemically inert, water soluble and non-toxic colloid[184] is required. Medically, dextran is used in the treatment of anaemia, when complexed with iron, and as a blood volume expander and blood plasma substitute. For example, to prevent dehydration in cases of serious burns a solution of dextran is introduced into the blood stream. This produces an osmotic effect across the cell membranes and prevents water loss. However, if the dextran molecules are too small they are rapidly removed from the blood stream and have to be replaced. Only molecules having a molecular weight of the order of 70,000 are retained long enough to be of use. If the molecules are too large, a greater weight of dextran has to be used to obtain the same effect, osmotic pressure being dependent on the number of molecules present. This example serves to demonstrate the

need for narrow dextran molecular weight fractions. Maximum effect is achieved by using dextran with a narrow molecular weight distribution and the appropriate molecular weight average. The required mean molecular weights are 70,000 for blood plasma substitutes and 40,000 in the treatment of anaemia.

The pharmaceutical division of Fisons Ltd. (Holmes Chapel, England) are major produces of clinical dextran. Dextran with an acceptable molecular weight distribution and molecular weight average is produced using a process which involves three main stages, fermentation, acid hydrolysis and alcohol precipitation.

Essentially, native dextran from the fermentation stage is hydrolysed by hydrochloric acid which produces a wide molecular weight range. The hydrolysate then undergoes controlled alcohol precipitation which results in dextran fractions with acceptable characteristics. The alcohol, ethanol, is subsequently recovered by distillation. The need to improve dextran fractionation methods prompted Fisons Ltd. to financially assist the research of Professor P. E. Barker and co-workers in the development of continuous chromatography. Earlier work by Barker et al.[11,61] had established that dextran molecular weight distribution could be altered by continuous gel permeation chromatography. The problem therefore was to investigate the process and to determine what were the major factors influencing the fractionation process, and what were the limitations.

6.1.2 Research Objectives

The objectives of this part of the research were to investigate, on a laboratory scale, the use of continuous gel permeation chromatography to fractionate a dextran feedstock supplied by Fisons Ltd. In addition, it was proposed to demonstrate how the process can be used to improve molecular weight distributions and to provide information on the influence of operating conditions on the fractionation process.

6.2 METHODS AND MATERIALS

6.2.1 The Packing

The required characteristics of the chromatographic packing were that it should be:

(i) mechanically stable and chemically and biologically inert,

(ii) easily cleaned if contaminated,

(iii) incompressible under conditions of high flow,

(iv) a low resistance (high permeability) to fluid flow,

(v) compatible with aqueous solutions.

Table 4.1 and 4.3 (Section 4.3.1) list the majority of the commercially available gel permeation chromatographic media. These media can be divided into two chemical classes,

(i) Organic

(ii) Inorganic.

The organic packings consist of the xerogels[174] and xerogel-aerogel hybrids[174], most of which are either incompatable with water or, because they are gelatinous, compress under conditions of high liquid flow rate. This class of packing was therefore considered as being unsuitable.

The second class, the inorganic packings, are the aerogel[174] packings discussed in Section 4.3.1 and listed in Table 4.2. They are mainly made of glass or silica. An example of this type of packing are the porous silica beads discussed by De Vries et al.[159]. These are manufactured by Pechiney-Saint-Govain in France and marketed in the U.K. by Rhodia U.K. Ltd. (London) under the name of Spherosil, and by Waters Associates (Stockport) under the same of Porasil. This packing satisfied the criteria given above and was therefore chosen as the most suitable gel permeation chromatographic medium. Other packings like Bio-glass (porous glass) and EM-Gel OR (crushed silica) may have been equally well suited but factors such as cost and past experience[11] favoured the use of Porasil (Spherosil).

For analytical purposes Porasil is available in six different grades (see Table 6.1) and two different particle size ranges, 36-75μ and 75-125μ. Larger particle sizes are obtainable from Rhodia U.K. Ltd. (London).

6.2.2 The Eluent and Associated Equipment

Dextran is soluble in highly polar solvents such as water, dimethylformamide and dimethylsulphoxide. Since cost and simplicity were major factors considered when choosing the eluent, water was an obvious choice, being easily purified, readily available and easily handled and stored. Dextran readily dissolves in cold water producing highly viscous solutions.

Table 6.1 Porasil Characteristics

GRADE	SURFACE AREA m^2/gm	AVERAGE PORE DIAMETER Å	EXCLUDED MOL. WT. (BASED ON DEXTRAN)
A	480	100	60,000
B	200	100-200	250,000
C	50	200-400	400,000
D	25	400-800	1,000,000
E	4	800-1,500	1,500,000
F	1.5	>1,500	>2,000,000

Dextran, like other carbohydrates, is susceptible to biological degradation. Considerable care was therefore taken to prevent such degradation of the feedstock and stored products. The feed was supplied containing sodium azide (0.02% w/v) which was a recommended bacteriostat. However, during the course of the experimental programme it was found that sodium azide adversely affected the analytical technique. The preferred method was to store collected samples in a refrigerator at a temperature of between $0^{o}C$ and $2^{o}C$.

To ensure consistent pumping rates and to prevent dissolved gases, in the eluent, coming out of solution on the packing, the eluent was deaerated prior to use. The main deaerator consisted of a 20 litre aspirator of distilled water connected directly to the bottom of a 5 litre three necked flask contained in an electric Isomantle. The aspirator was fitted with a mariotte flask type of fitting to ensure a constant water level in the heating flask. Water was continuously boiled under reflux in the 5 litre flask and continuously withdrawn via a side arm and cooled in a closed system. The deaerated water was then piped through a filter

stick and into the purge and eluent pumps. The feed was deaerated using a smaller scale unit based on the design given in reference 213. Figure 6.1 gives a flow diagram of the chromatographic machine and the associated equipment.

6.2.3 The Analytical System

6.2.3.1 The Auto Analyser

A Techicon Auto Analyser system was used to perform automated analyses of liquid samples and streams. This consists of a modular flow-through system for the continuous analysis of solutions. A multi-channel peristattic pump (proportioning pump) gave flow rates of 0.015 to 3.90 cm^3 min^{-1} by the use of colour coded pumping tubes of various diameters. This enabled reagents to be mixed in widely varying proportions. Strong acids were pumped through acid-resisting tubing ("acidflex"). Mixing of solutions was achieved by joining the flow streams through 'T'-pieces and passing the combined flowstreams through a horizontal helical coil of glass tubing. These coils were jacketed to allow cooling with tap water where necessary. Reaction streams were heated to a constant temperature by passing them through coiled glass tubing immersed in a thermostatically controlled oil bath. The times of mixing, heating and cooling were controlled by changing the length of the coils with reference to the liquid flowrates. Back mixing in the tubing was minimised by introducing air bubbles into the flow streams. The liquid streams therefore consisted of equi-spaced slugs of liquid separated by air bubbles. These air bubbles were removed prior to the measurement of the absorption of the solution. The absorption was measured in a continuous flow cell of 1.5 cm path length and a

FIGURE 6.1 Line Diagram of Complete System

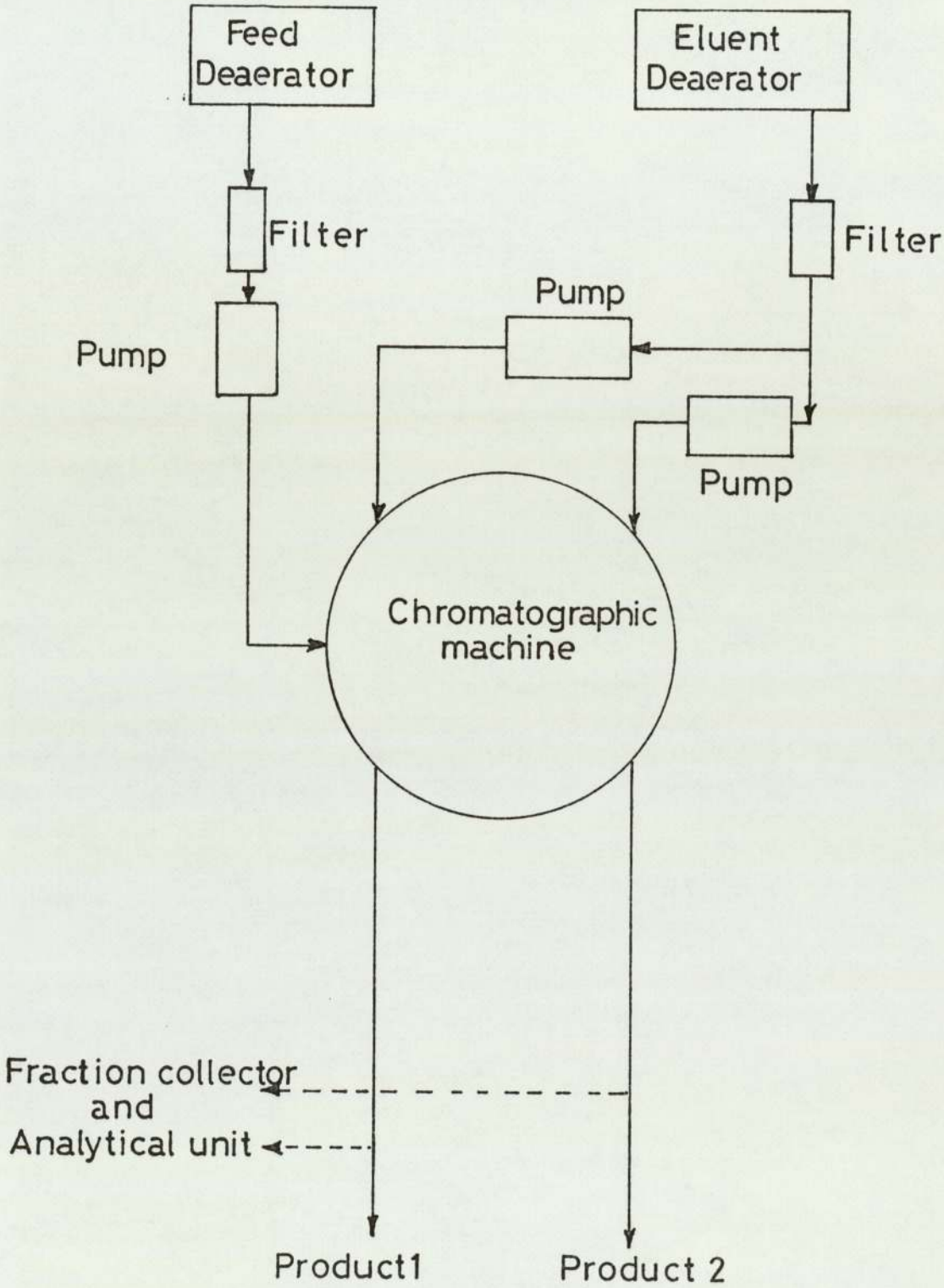

reference photocell gave an automatic zero balance on the recorder system. An interference filter of nominal wavelength was used and the results recorded by a triple point interrupted recorder. The response from the detector was a logarithmic function of concentration.

The assay used was the cysteine-sulphuric acid method developed by Dische et al.[210] and has previously been used with an Auto Analyser analytical system by Hatt[11]. In the automated assay a solution of the sample was mixed with air and the cysteine-sulphuric acid reagent. Details of the flow rates and reagent concentration are given in Appendix 3. After thorough mixing and cooling, the reaction stream was heated for 3 min at 98°C, cooled to ambient temperature and debubbled. The absorbance of the solution, developed as a result of producing a chromophore during the reaction, was measured at 420 nm. Figure 6.2 diagrammatically represents the automated cysteine-sulphuric acid assay.

The assay was calibrated using glucose solutions of known concentration. The glucose used was carefully dried under vacuum at 60°C to ensure that concentrations were based on the dry weight of glucose. The calibration curve, a plot of optical density versus concentration, is presented in Appendix 3. The response of the assay to a solution containing a known concentration of dextran can be obtained by multiplying the response of a glucose solution of the same concentration by the factor 162/180. This allows for the difference in weight of the hexose units in dextran and glucose. Alternatively the concentration of unknown dextran solutions could be calculated from its AutoAnalyser response, the response of a known glucose solution and the constant given above. An example of the calculation involved is given in Appendix 3.

FIGURE 6·2 Automated L-cysteine-sulphuric Acid Assay

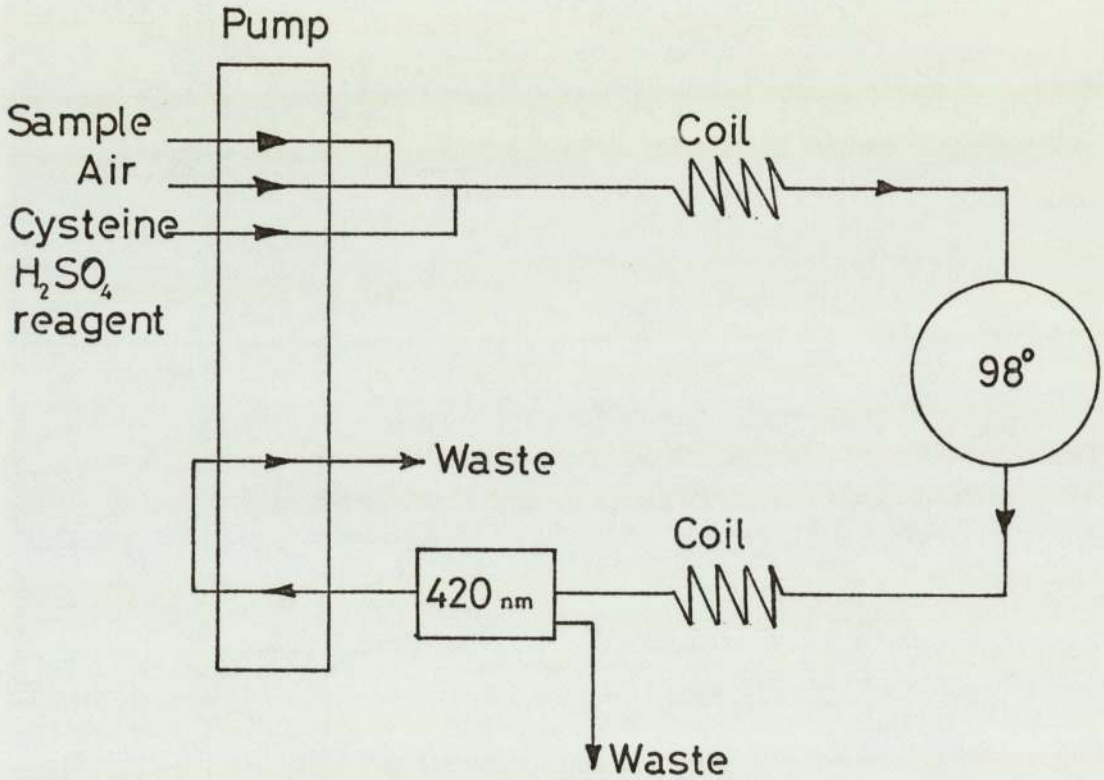

6.2.3.2 Analytical Columns and Column Calibration

Analytical Columns

The analytical columns were constructed of glass tubing surrounded by a water jacket. A Haake bath (Berlin-Lichterfelde W.G.) circulated water through the jacket and effectively controlled the temperature of the columns at 25°C throughout the research. Details of the column dimensions, the grades of Porasil employed, particle sizes and the eluent flow rates used are discussed in Section 6.3.

The columns were packed by the following procedure. A sample of Porasil was immersed in water and deaerated under vacuum. The slurry of beads was poured, via a funnel, into the top of a water-filled vertical column. A syringe attached to the column outlet permitted sufficient suction to be applied to initially pack the column. Deaerated, distilled water was then pumped through the column and the sides gently tapped until a stable packed bed had been achieved. Where necessary fresh packing was added. The packing was supported in the column by a small plug of glass wool fitted above a constriction formed at the base of the column. Figure 6.3 shows this constriction and the experimental arrangement used for sampling the liquid leaving the column.

Column Calibration

Dextran 'T' fractions (Pharmacia (U.K.) Ltd, London) were used to calibrate the analytical columns. These fractions had quite narrow molecular weight distributions and each fraction was supplied with a graph of its molecular weight distribution and data on its number and weight average molecular weights. Samples (25 μl)

FIGURE 6.3 Sampling Device at the Base of Analytical Columns

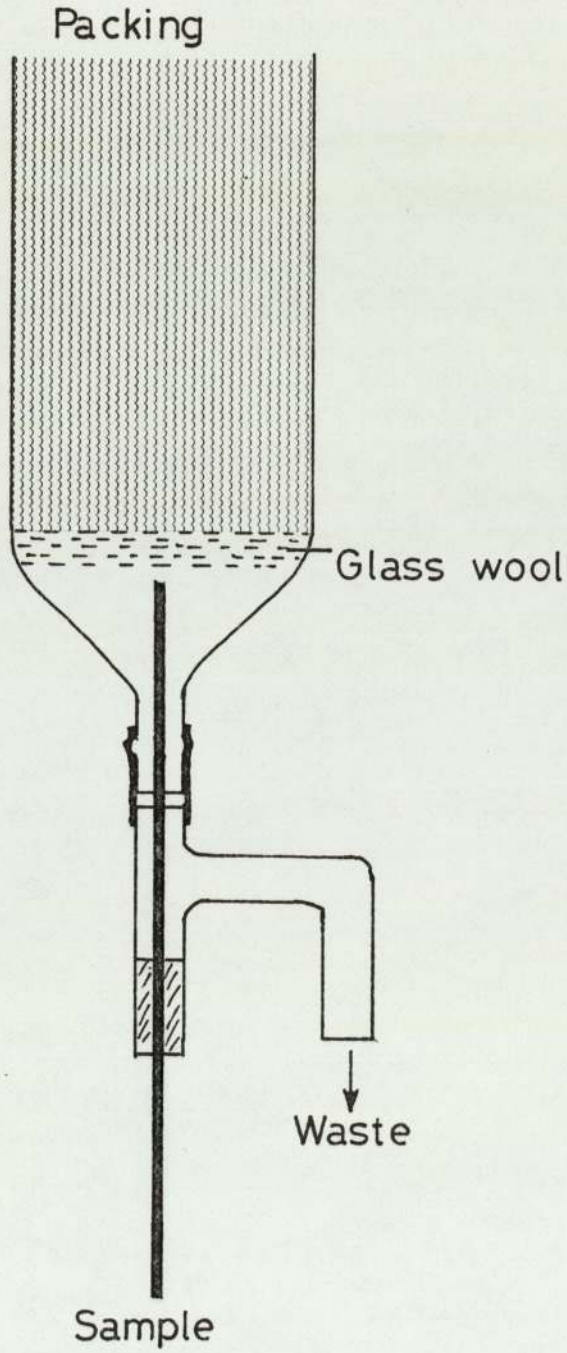

of dextran solutions with mean molecular weights ranging from 10,000 to 300,000 were eluted on the analytical columns. Samples of D-glucose and dextran 'T' 2000 ($\overline{M}w > 2 \times 10^6$) were eluted to obtain the total inclusion and total exclusion volumes of the column. The concentration of the calibration solutions was normally of the order of 2000 $\mu g\ cm^{-3}$. The samples were monitored using the automated cysteine-sulphuric assay.

Sample elution volumes were taken as the line represented by the median of the chromatogram[129]. This elution volume was taken to represent the molecular weight average ($\overline{M}w$), as determined by gel permeation chromatography. A value was assigned to this which corresponded to the molecular weight at 50% on the Pharmacia plot of cumulative weight for that sample. For many of the samples the peak values and the median elution volumes were the same. In the cases of D-glucose and dextran 'T' 2000 the peak maximum were used to obtain their elution volumes.

Graphs of retention factor, RF, versus the logarithm of mean molecular weight were plotted for each column. The term retention factor was used because it is a means by which samples analysed on the same packing but on different columns can be compared. The calibration plots for the three columns used in this research are included in Appendix 3. Throughout the research the column calibrations were periodically checked to ensure that they remained valid.

6.2.3.3 The Procedure used for Analysing Samples

The procedure used for analysing samples of unknown concentration and mean molecular weight was as follows. A standard solution of dried anhydrous glucose (40 $\mu g\ cm^{-3}$) was pumped through the calibrated Auto Analyser system and its response noted. This ensured that the assay reagents were still usable, and provided a standard. The sample, of unknown concentration, was then pumped through the system. From its response, and using the method discussed in Section 6.2.3.2, the concentration could be calculated. When necessary the samples were diluted or concentrated by known amounts. This made sure that the sample response remained on the linear portion of the assay calibration plot (Appendix 3). In addition it ensured that the chromatogram obtained, after column analysis, could be adequately treated.

Once the concentration of the sample was known a solution of approximately 2000 $\mu g\ cm^{-3}$ was prepared and a sample (normally 25 μl) loaded on to a column and eluted. The sample loading technique involved running the liquid on top of the packed bed down to the level of the bed, loading the sample with a calibrated micro-pipette on to the bed, running the sample into the bed followed by an equal volume of the eluent. The head of eluent was added, the recorder chart marked, the pumping line fitted and the sample eluted from the column.

The Auto Analyser peristaltic pump tubing has a lifetime of about 150-200 hours in use. The delivered flow rate varying in a gradual manner over this period. For this reason the flow rate of the eluent was measured by accurately weighing the eluate collected over a timed interval (normally 2-4 minutes). Measurements before and after

sample analysis established whether the flow rate remained constant over the eluting period. The delay time of the analytical system was regularly measured using a sample of glucose solution. The glucose solution was pumped through the AutoAnalyser and its residence time, or delay time, before detection measured with the constant speed chart recorder.

6.2.4 Data Treatment

Chromatograms from the Auto Analayser were a plot of optical density versus time. Optical density is a function of the dextran or glucose concentration in the eluate leaving the analytical column. Initially the median of the chromatogram was calculated manually. This was a tedious and time-consuming process. A computer program was therefore written which enabled the calculation of the elution volume of a sample more accurately. The program was written (Appendix 4) in BASIC-16 and was run on the departmental Honeywell 316 computer.

Essentially the heights, in terms of optical density, of the experimental chromatogram were read off at regular intervals from the beginning to the end of the chromatogram, Figure 6.4. A time interval of 1.25 minutes was found to be sufficiently accurate. From this data, the total area, the median of the peak and therefore its elution volume could be calculated. A modified quadrature technique was used to determine the total area of the peak. The computer program also converted the chromatogram into a cumulative form.

To enable the direct comparison of input and output molecular weight distributions to, and from, the continuous chromatograph, the computer program also had the facility to change the axes of the

FIGURE 6·4 Diagram Showing Data Measured on Experimental Chromatogram

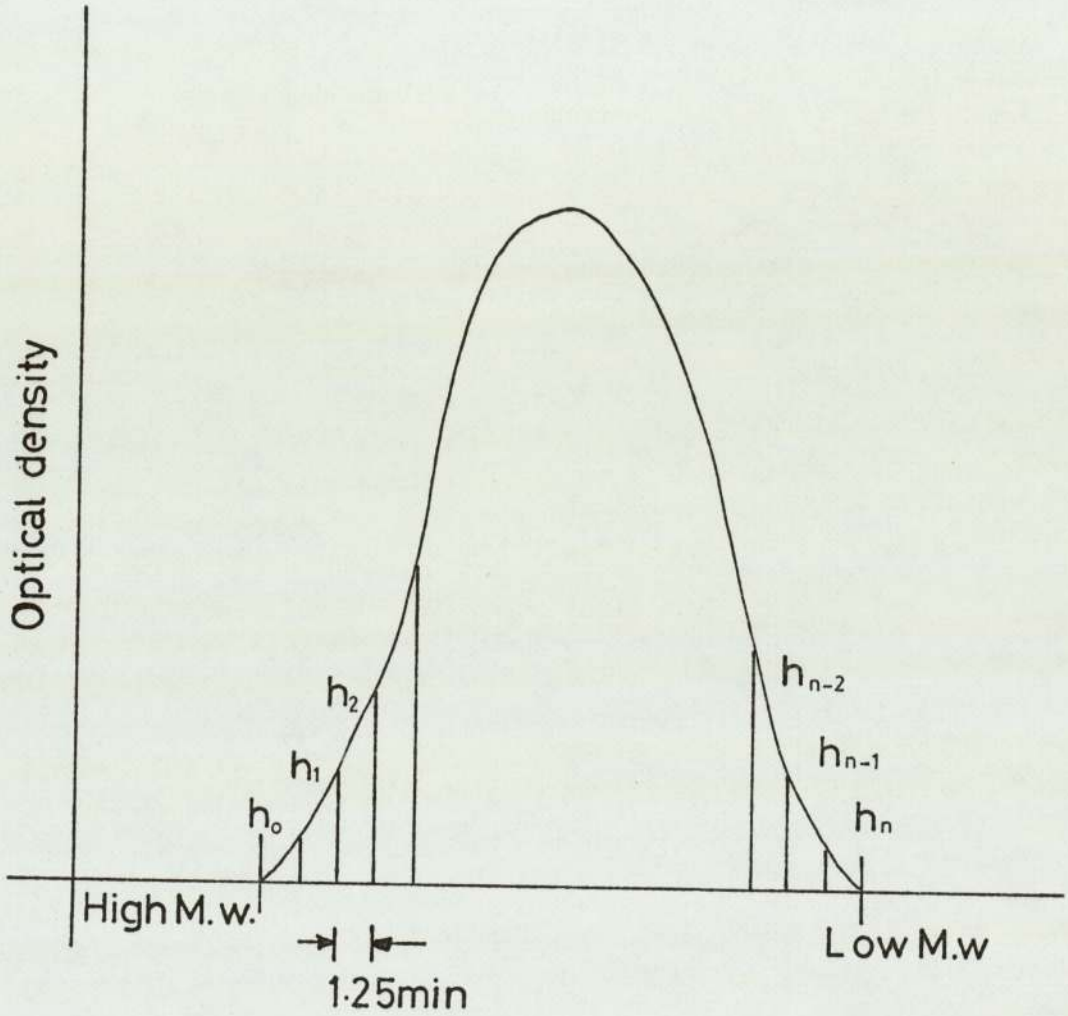

chromatogram. This initially involved normalising the chromatogram so that it was represented as concentration versus retention factor (elution volume/total column volume). Then, by making use of the sample volumetric input, or output, rate from, or to, the chromatographic machine the chromatogram can be represented in terms of a mass rate into, or out of, the machine. This technique provided an alternative method of representing the dextran mass balances. The limitation of the technique was the accuracy to which the heights of the chromatogram could be read.

Mass balances on both liquid and dextran were carried out at regular intervals during each experiment. This information was plotted as input and output rates versus time.

6.2.4 Experimental Errors

Experimental errors fall into two categories, firstly those induced by the measurement of the machine operating parameters and secondly analytical errors.

Errors in the analytical technique include those errors caused by the calibration technique, the measurement of analytical column flow rate and the inaccuracy of measuring trace heights from the chart recorder. The error that can be attributed to the calibration technique was estimated to be less than 1%. An error of the order of ±1% in the measurement of analytical column flow rates was expected. The major error in the analytical method was the accuracy to which the trace heights on the chart recorder could be read off, and also the measurement of elution times.

Both were estimated to be of the order ±2%. The errors involved in calculating sample concentration and elution volumes were therefore less than ±3% and ±3% respectively.

Fluctuation in the measurement of the combined eluent and purge flow rates into the chromatograph was ±0.03 cm^3 min^{-1}. This would introduce an error of ±1%. The feed pump was more sensitive and showed a greater variation in the measured delivery rate. The resulting error was estimated to be of the order of ±2%. A contributory factor to the errors in flow measurement was that due to the use of a stopwatch. The stopwatch was regularly checked against standard G.P.O. time signals and the error was calculated to be less than ±0.2%.

Measurement of the eluent and purge output flow rates were of the same order as that in the measurement of the input flow rates (±1%). A major source of fluctuations in eluent and purge output rates was the effect of leakage from the seal. This produced a maximum change in the eluent rate of ±8%, the change was normally of the order of ±1%.

The bundle speed used in this part of the research was measured as 0.0026 r.p.m. Variations in the measurement of the bundle speed was found to be less than ±1%. Neglecting the effects of leakage, dextran mass balances and theoretical "cut" calculations are expected to have an error of less than ±4% and ±3% respectively. Liquid mass balances were expected to have an error of ±2%.

6.3 Selection of Analytical Columns and Conditions

In Section 4.2.4 the significance of packing particle size and column diameter in relation to the operating efficiency of

batch gel permeation chromatographic columns was discussed. This discussion made reference to published work which in general concluded that column efficiency, as evaluated by height equivalent to a theoretical plate, improved as the column aspect ratio increased. Besides the advantage of improving column efficiency, careful selection of column diameter, particle size and analytical conditions significantly reduces the need to correct[206] chromatograms for the effects of peak dispersion. Experimental studies were therefore undertaken to determine the most suitable column, particle size and analytical conditions.

Part of this experimental program was carried out in conjunction with F. J. Ellison, a fellow research student in the Department. This was because the problems of obtaining satisfactory analytical columns were common to both of our research projects.

6.3.1 Column Dimensions and Particle Size

The theoretical treatment of chromatographic columns generally makes the assumption that a linear partition isotherm applies, which means that gaussian peak shapes result from impulse input functions. Column performance is usually described in terms of the number of theoretical plates[211], N, given by Equations 2.8 and 2.9. An alternative description of column performance is the rate of increase of the second moment per unit length of column (Equation 2.6). This rate, which has been discussed in Chapter 2 (Section 2.1.2.1), defines the height equivalent to a theoretical plate, H. From equations 2.6 and 2.7

$$H = \frac{L}{N} \qquad 6.1$$

$$N = \frac{(t_R')^2}{\sigma_t^2} \qquad 6.2$$

where t_R' = sample retention time (min)

σ_t^2 = time based second moment or variance of the sample peak.

A number of factors contribute to the total variance of a sample peak. In general, these include the contributions due to the spreading processes occurring within the column and the disturbances in the flow patterns in the flow lines,injection port and detector. A sample injection port was not used in this research and hence the contribution to the overall variance of the sample peak from this was assumed to be small. This assumption was thought to be reasonable because the sample loading technique adopted, described in Section 6.2.3.3, involved loading samples as a discrete solute band on the top of the column packing. Considerable care was taken so as not to disturb the initial plug shape of the solute.

Using the statistical rule, which states that contributing variances are additive, the total peak variance can be expressed as,

$$\sigma_t^2 = \sigma_c^2 + \sigma_e^2 \qquad 6.3$$

σ_c^2 = time based variance resulting from the g.p.c. column processes.

σ_e^2 = time based variance resulting from flow disturbance in the flow lines and the detector.

From Equation 6.3 it can be seen that by quantifying σ_e^2 the height equivalent to a theoretical plate, H, can be more accurately calculated by using σ_c^2 rather than the total peak variance, σ_t^2, hence H is given by,

$$H = L.\frac{\sigma_c^2}{(t_R')^2} \qquad 6.4$$

$$\therefore \quad \sigma_c^2 = H.\frac{(t_R')^2}{L} \qquad 6.5$$

Substituting for σ_c^2 in Equation 6.3 we obtain

$$\sigma_t^2 = \frac{(t_R')^2}{L} . H + \sigma_e^2 \qquad 6.6$$

Le Page et al.[158] have proposed that since σ_t^2 is a linear function of $(t'R)^2/L$ the intercept of a plot of σ_t^2 against $(t_R')^2/L$ can be used to obtain the extra column variance, σ_e^2.

Experiments were carried out eluting glucose samples on three columns (0.8 cm I.D., 60 cm, 90 cm and 120 cm in length) at three different flow rates (0.3 cm^3 min^{-1}, 0.6 cm^3 min^{-1} and 1.0 cm^3 min^{-1}). However it was found during these experiments that the disadvantage of the technique was that it relied on obtaining identical efficiencies for columns of varying lengths. Practically this is not easily achieved since packing uniformity must be obtained over the whole column length. An alternative method for quantifying extra column variance was therefore sought.

Ellison[22] proposed a method which involved injecting plugs of glucose solution into the sample line of the analytical unit and measuring the resulting plug shape at the detector. By calculating the variance of the input plug and the variance of the output plug, as measured by the detector, and applying the summation rule of variances the variance contributed by the Auto Analyser could be calculated from,

$$\sigma_e = \sigma_o^2 - \sigma_i^2 \qquad 6.7$$

σ_o^2 = time based output variance of glucose plug
σ_i^2 = time based input variance of glucose plug

The flow rates used in the Auto Analyser are essentially constant, therefore, the assumption can be made that the Auto Analyser variance is independent of column elution rate and is consequently independent of the shape of the input function to the Auto Analyzer. This technique was successfully used by Ellison[22] to quantify the contribution made by the analytical unit to the spreading of chromatogram peaks. Thus the efficiency, as expressed by H.E.T.P., of analytical columns could be accurately calculated using Equation 6.4.

In a study of the effects of packing particle size, distribution and column diameter, Ellison[22] showed that as column diameter, particle size and distribution were decreased column efficiency improved. In this study, glucose samples were eluted with distilled water on columns packed with Spherosil XOB075 the results obtained have been reproduced in Figure 6.5, plots 1-4. As a result of these experiments columns with internal diameters of 0.4 cm were chosen for use in this research. The author obtained a sample of

FIGURE 6·5 Plot of H.E.T.P. versus Flowrate

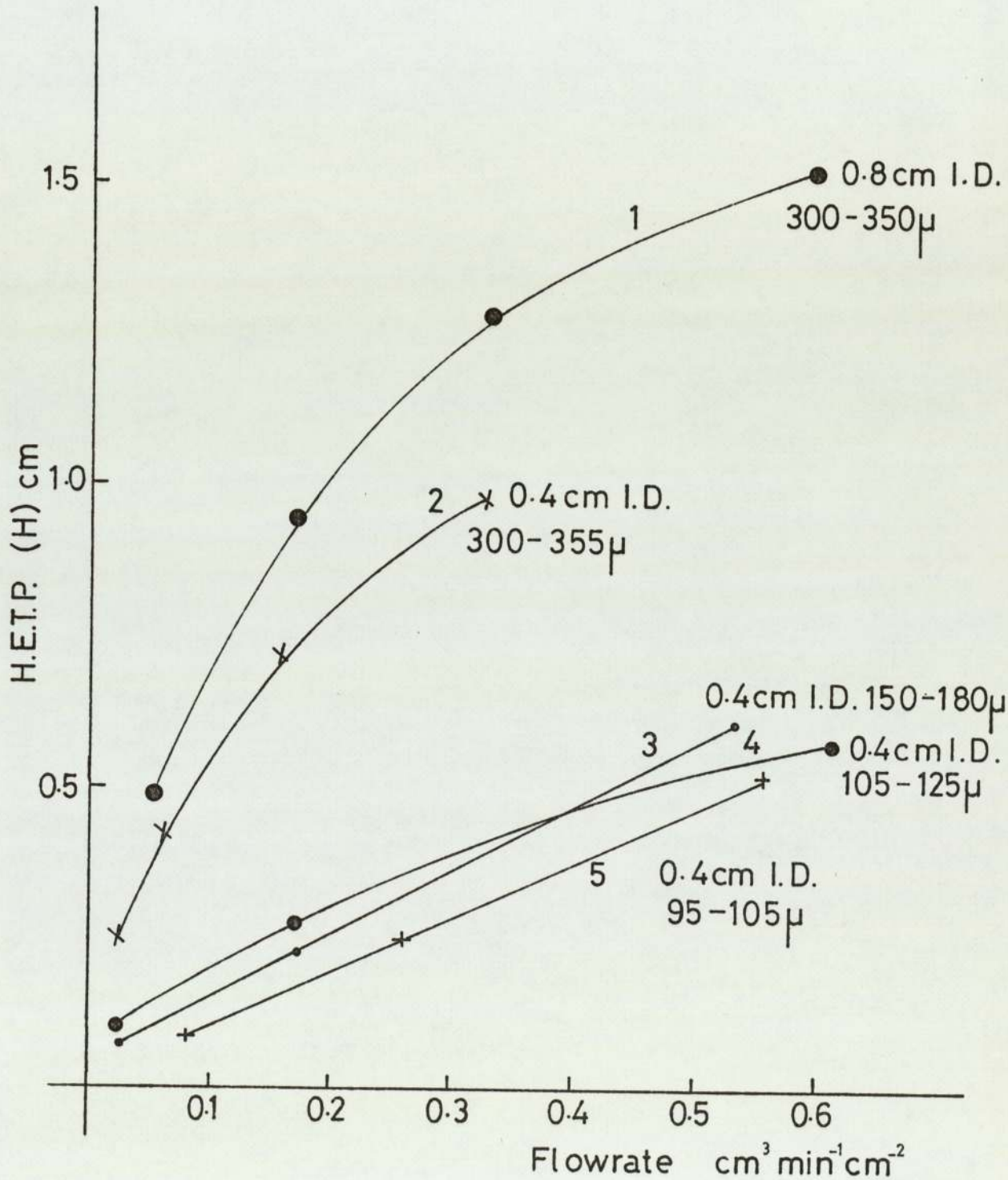

Porasil C (equivalent to Spherosil XOB075) and manually sieved out the particle size range 95 μm to 105 μm, which was packed into a 0.4 cm I.D. column. H.E.T.P. experiments were carried out eluting glucose with water, the results of which are given in Figure 6.5, plot 5. The improvement in efficiency by reducing the particle size range to 95-105 μm was marginal compared to the 105-125 μm and 150-180 μm ranges used by Ellison[22]. Therefore, a particle size range of 95 μm to 105 μm was selected for analytical purposes. The length of the analytical columns were arbitrarily chosen as 120 cm so that eluent rates of the order of 0.2 cm^3 min^{-1} (1.6 cm^3 min^{-1} cm^{-2}) resulted in analytical times of approximately one hour. Three columns were prepared and packed with Porasil B, C and D respectively. Particle size ranges and column dimensions were common to all three columns.

6.3.2 Analytical Flow Rates

As has been mentioned for general analytical purposes a nominal eluent rate of 0.2 cm^3 min^{-1} (1.6 cm^3 min^{-1} cm^{-2}) was chosen. This flow rate proved satisfactory for determining the mean molecular weight of unknown dextran samples but, because of the influences of column spreading, was not sufficiently accurate to give a true picture of sample molecular weight distributions. This was particularly relevant when product molecular weight distributions were compared with the original feed distribution. Since the packing used in the chromatographic machine was equivalent to Porasil C, the Porasil C column was used when this information was required.

The choice of a suitable eluent rate for accurate analysis was based on the following experimental work. Samples of Dextran T40 were eluted on the Porasil C column at three different rates (0.098 cm^3 min^{-1},

0.334 cm^3 min^{-1}, 0.723 cm^3 min^{-1}). For each of the chromatograms obtained, the exclusion and inclusion limits of the packing were marked. At flow rates of 0.334 cm^3 min^{-1} and 0.723 cm^3 min^{-1} the chromatogram of dextran T40 extended over the two limits, this indicated that band spreading processes were having a significant effect. However, at the lowest flow rate (0.098 cm^3 min^{-1}) it was found that only the high molecular weight end of the chromatogram extended over the totally excluded limit, (Figure 6.6). This chromatogram was converted to a cumulative distribution curve and compared with the cumulative distribution of dextran T40 as supplied by the manufacturer (Pharmacia Ltd., London). Close agreement was observed between these two curves, (Figure 6.7). There is a difference at the high molecular weight end which may have been as a result of a proportion of the dextran T40 chromatogram which was not fractionated. This part of the chromatogram corresponded to a retention factor equal to that of a totally excluded molecule, (Figure 6.6). Although there is no theoretical basis, it was concluded from these experiments that an eluent rate of nominally 0.1 cm^3 min^{-1} (0.8 cm^3 min^{-1} cm^{-2}) reduced the spreading to an acceptable level and was therefore suitable for the more accurate analysis of dextran samples. From Figure 6.5 it can be seen that at this flow rate the column had an H.E.T.P. of 0.08 cms (equivalent to 1250 plates/metre).

During these experiments it was observed that the elution volume of dextran T40 was dependent on the elution rate. Similar effects were also observed with glucose and dextran T500. This was in contradiction of the widely held opinion that sample elution volumes in gel permeation chromatography are independent of flow rate. Two possible causes were considered. Firstly, that there was a flow rate

FIGURE 6·6 Dextran T40 Chromatogram

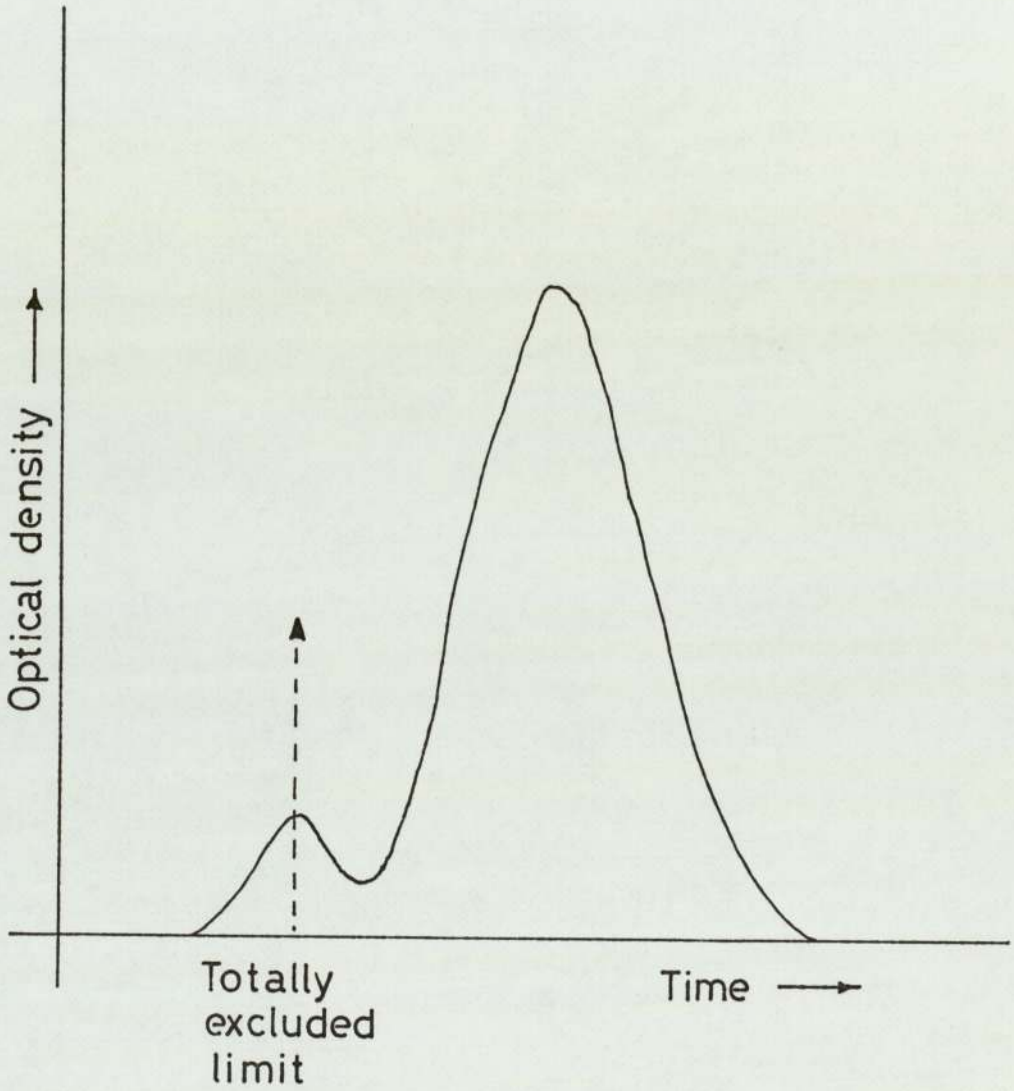

FIGURE 6·7 Comparison of Experimenetal and Pharmacia Dextran T40 Cumulative Plots

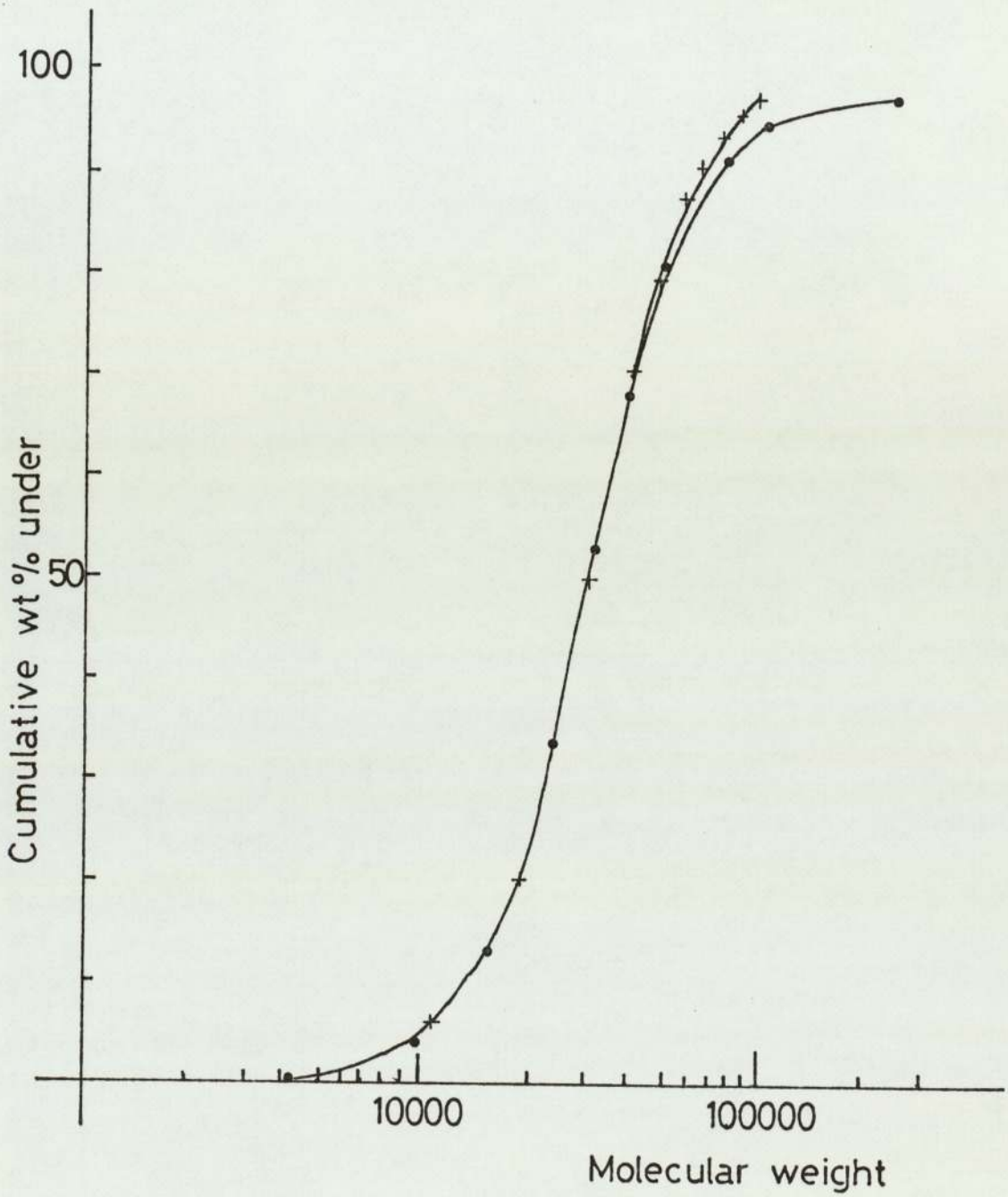

Experimental plot

Pharmacia plot

dependence of sample elution volumes on Spherosil and secondly there was a systematic error in analytical method. Holding[228] has subsequently shown the former not to be the case. Care was therefore taken to ensure that sample analysis was carried out at nominally the same flow rate as the column calibration flow rate. Consequently two calibration curves were used for the Porasil C column.

6.4 OPERATION OF THE CONTINUOUS CHROMATOGRAPH

6.4.1 Introduction

Experimental studies were carried out on the fractionation of dextran using the continuous chromatographic machine described in Chapter 3. The feed used in these studies was a "dextran 40 hydrolysate" supplied by Fisons Ltd. (Holmes Chapel) as a 13.9% w/v solution. The term "dextran 40 hydrolysate" is used to denote a dextran fraction with a nominal weight average molecular weight of 40,000. Due to the method of production the feed also contained small quantities of ethanol and sodium chloride. The molecular weight distribution of the 40 hydrolysate was estimated to be in the range 2000 to over 300,000[212] and its mean weight average molecular weight ($\overline{M}_W$) was experimentally determined as 32,000.

The mechanical problems associated with maintaining a satisfactory seal on the continuous chromatograph imposed limitations on the experimental program. Consequently dextran fractionation experiments were restricted to an investigation into the effects of feed concentration and to a lesser degree the effects of feed rate and bundle rotation speed. The objectives of the experimental program were to determine the influence of increased concentration on the "cut" effected by the machine, and to show that the original molecular weight distribution could be narrowed by cutting off both the high and low

molecular weight ends.

6.4.2 Preliminary Experiments

Before any of the structural alterations, described in Chapter 3, were made a number of preliminary experimental runs were carried out. The objective of these was to develop a suitable experimental procedure and to isolate any problems that might initially occur.

In the first of these experiments the undiluted dextran feedstock was pumped into the machine and fractionation achieved by altering the eluent rate until dextran was detectable in both product streams. At this stage detailed engineering drawings of the continuous chromatograph were obtained from Rank Hovis McDougall Ltd. This was so that the dead volume in the chromatograph could be accurately calculated and, as a result, the equation (Equation 5.10) for predicting "cut" values applied with greater precision. Graphs of predicted "cut" partition coefficients versus eluent rate for the tube bundle speeds used in this research are included in Appendix 5.

Two further experiments were then attempted at an elevated oven temperature (60°C) in the hope of obtaining a seal. It was subsequently found that increasing the temperature was detrimental to the successful operation of the seal. During these experiments the leakage was found to vary between 29% and 65%.

The packing used in these early experiments was Porasil D (80 μm - 125 μm), which was replaced with Spherosil XOB075 (200 μm-400 μm, particle size distribution analysis and pore size distribution analysis are given in Appendix 3) in the hope that by increasing the

particle size the resultant decrease in working pressure would help to reduce the leakage problem. In addition the importance of having optically flat sealing faces was established at this stage. Both faces were professionally lapped flat (Precision Lap Ltd., Camberley). After lapping the machine was reassembled and water pumped through the machine continuously over a two week period. It was observed that despite an initial leakage of 2.7% it gradually increased over the two weeks to greater than 30%. It was concluded that there were some basic structural weaknesses in the seal design. No further experimental work was undertaken until the sealing problem had been investigated.

After taking the necessary measures to improve the mechanical seal (discussed in Chapter 3) the seal faces were relapped and the machine reassembled. It soon became apparent that by reinforcing the bundle top face the problem with liquid leakage was significantly reduced. Liquid mass balances established that the leakage was less than 1%.

An experimental run was then undertaken, during which it was found that the feed pump failed to deliver a consistent flow rate, Figure 6.8. This was attributed to two factors, firstly air coming out of solutions in the pump piston chamber and secondly the failure of the non-return valves built into the pump. An experimental method was developed to improve the non-return valves, which is discussed in Appendix 1. A small scale deaerator, based on a design given in reference 213, was constructed and installed between the feed reservoir and the feed pump. Both remedies proved to be a satisfactory solution to the feed pumping problem.

FIGURE 6.8 Plot of Feed Flowrate versus Time Before the use of a Deaerator

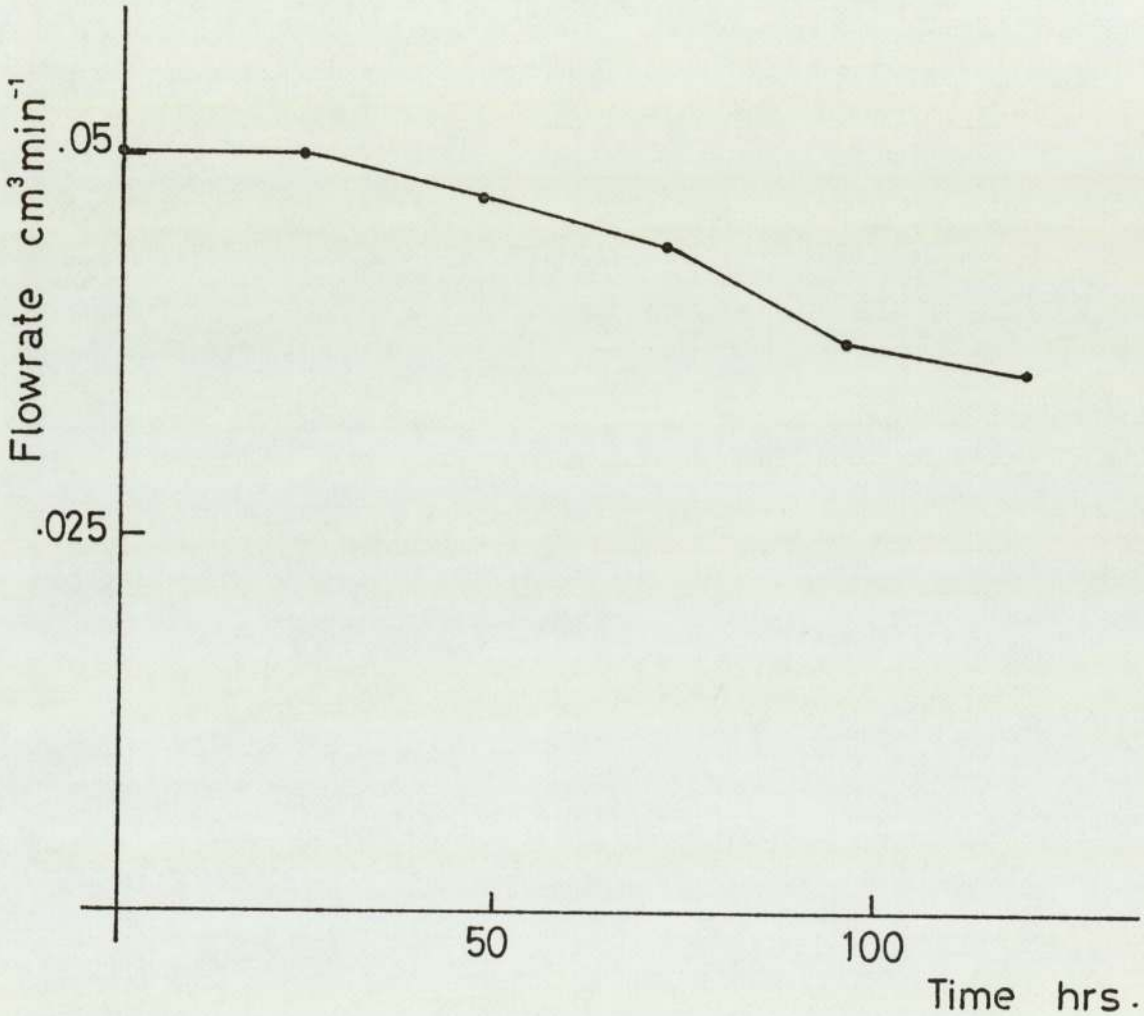

At this stage in the research project it proved necessary to move the continuous chromatograph to a new departmental building. Whether it was due to having to leave the equipment in an unheated building for a couple of weeks or because the equipment had inadvertently been damaged during the move is uncertain. However, on recommencing to pump water through the chromatographic machine the leakage had increased to 45%. Despite allowing the seal time to settle down no significant improvement in the leakage was observed. Both faces were then separated and relapped. Before relapping the opportunity was taken to have a second liquid lock installed into the machine (Figure 6.9). This had the following beneficial effects.

(i) It isolated the purge section which permitted higher purging rates to be used.

(ii) It improved the degree of flow control in the separating section.

(iii) It reduced the overall liquid back pressure exerted on the seal.

(iv) It made the operation of the machine more analogous to the semi-continuous chromatograph under construction by Ellison[22]. This unit was based on the design proposed by Barker and Deeble[69] and was to be applied to the larger scale fractionation of dextran.

Installing the second liquid lock involved cutting an additional notch into the cam operating the spring loaded valves and installing another input and output port on the static portion of the seal. A disadvantage of installing the second liquid lock was that it reduced the number of columns in the separating section of the machine from about 36 to 22.

FIGURE 6.9 The Addition of a Second Liquid Lock

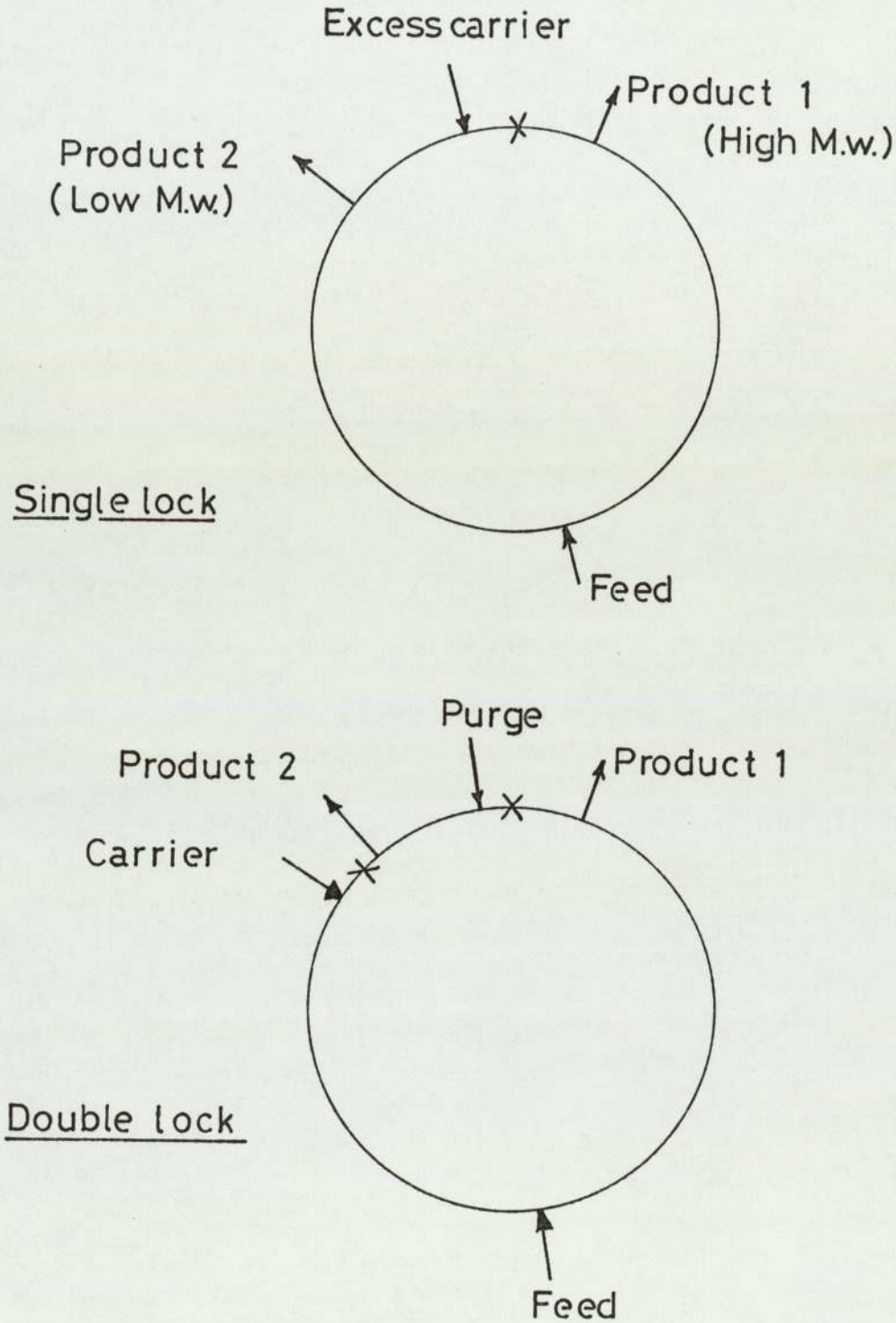

This was not considered to be a major disadvantage because of the reasons discussed above.

Once the faces had been relapped and the machine reassembled, leakage from the seal was found to be consistently less than 2%, which was considered to be acceptable. The continuous chromatograph was therefore operating satisfactorily. Thought was then given to the best experimental method. The factors considered were the required run time to achieve a pseudo-steady state and the sampling time to guarantee sufficient dextran for analysis. The latter was particularly important when using dilute operating conditions.

The length of the experiments was important because molecules with partition coefficients of the same order as the "cut" values effected by the machine will have separation factors that approach unity. Hence the theoretical time to achieve steady state would be very large. Run times of seven days (168 hrs) were chosen because it allowed sufficient time to show that equilibrium had been achieved and permitted the performance of the machine over long periods to be assessed. This was relevant from an industrial point of view. The comparatively slow eluent flow rates, approximately 1 cm^3 min^{-1}, restricted sample times to nominally 24 hour periods.

6.4.3 Dextran Fractionation Results

During the course of the experimental program the recurrent problem of leakage proved a major restriction on the number of experimental runs. In some cases experiments had to be

repeated several times before obtaining satisfactory operating conditions, this was inspite of the steps taken to reduce the leakage problem. In addition, during experiments that were carried out under dilute operating conditions it was established that sodium azide affected the assay, resulting in the necessity to repeat these experiments to obtain meaningful results.

All experiments were carried out at room temperature which varied between about 20°C and 25°C (daytime temperature). For comparison purposes this temperature range was not considered to be significant.

A complete record of the experimental results, including all analytical chromatogram data, is included in Appendix 6. Summaries of experimental operating conditions, theoretical "cut" values, product concentrations and mean molecular weights are given in Figure 6.10a to 6.16a. Liquid and dextran mass balances have been graphically presented in Figures 6.10b,c to 6.16b,c. Figure 6.17 is the normalised distribution of the feed used in Runs 1 to 6.

The first series of experiments, Runs 1 to 5, were designed to investigate the effect of increasing the feed concentration from 0.5% w/v to 20.8% w/v. In these experiments a nominal feed rate of 0.05 cm^3 min^{-1} was chosen for two reasons. Firstly, the feed pump was not capable of pumping, at a consistent rate, concentrated dextran solutions. Secondly this feed rate corresponded to an eluent to feed ratio of 20:1. This indicated that the change in the eluent rate from the prefeed section to the postfeed section was about 5%. It was assumed that at this eluent to feed ratio the effects of the discontinuity in the eluent rate at the feed point would be

Figure 6.10a Run 1 Results Summary

Feed concentration = 5680 μg cm^{-3}

Temperature, Pressure and Flow Rates

Time hr	Temp °C	Pressure mNm^{-2}	Eluent + purge input cm^3 min^{-1}	Feed input cm^3 min^{-1}	Purge output cm^3 min^{-1}	Eluent output cm^3 min^{-1}
0	21.5	103	2.870	0.050	2.035	1.108
24	22	103	2.950	0.050	2.038	1.100
48	22	103	2.920	0.050	1.943	1.106
72	22	90	2.910	0.050	2.021	1.099
144	21	110	2.950	0.050	1.962	1.086
168	21.5	103	2.920	0.050	2.018	1.103
192	21	117	2.950	0.050	1.956	1.113

Dextran Mass Balances

Sample Number + Time	Feed input rate μg min^{-1}	Low Molecular weight output μg min^{-1}	High Molecular weight output μg min^{-1}	Total output μg min^{-1}
1(24-48)	284	165	109	274
2(48-72)	284	167	138	305
3(72-144)	284	180	125	305
4(144-168)	284	177	123	300
5(168-192)	284	182	126	308
Average =	284	174	124	298

Figure 6.10a (Cont.)

Sample Concentrations

Sample	High M.W. $\mu g\ cm^{-3}$	Low M.W. $\mu g\ cm^{-3}$
1	99	81
2	125	86
3	114	89
4	114	90
5	114	90

Sample Mean Molecular Weights

Sample	High M.W.	Low M.W.
1	34000	10000
2	85000	16000
3	72000	11000
4	52000	12000
5	95000	9000

Theoretical "Cut" Positions (based on Porasil C)

Prefeed Retention factor	Postfeed Retention factor
0.537	0.562
0.537	0.565
0.537	0.562
0.537	0.565
0.537	0.562
0.537	0.565
0.542	0.57

FIGURE 6.10 Plots of Liquid and Dextran Mass Balances for Run 1

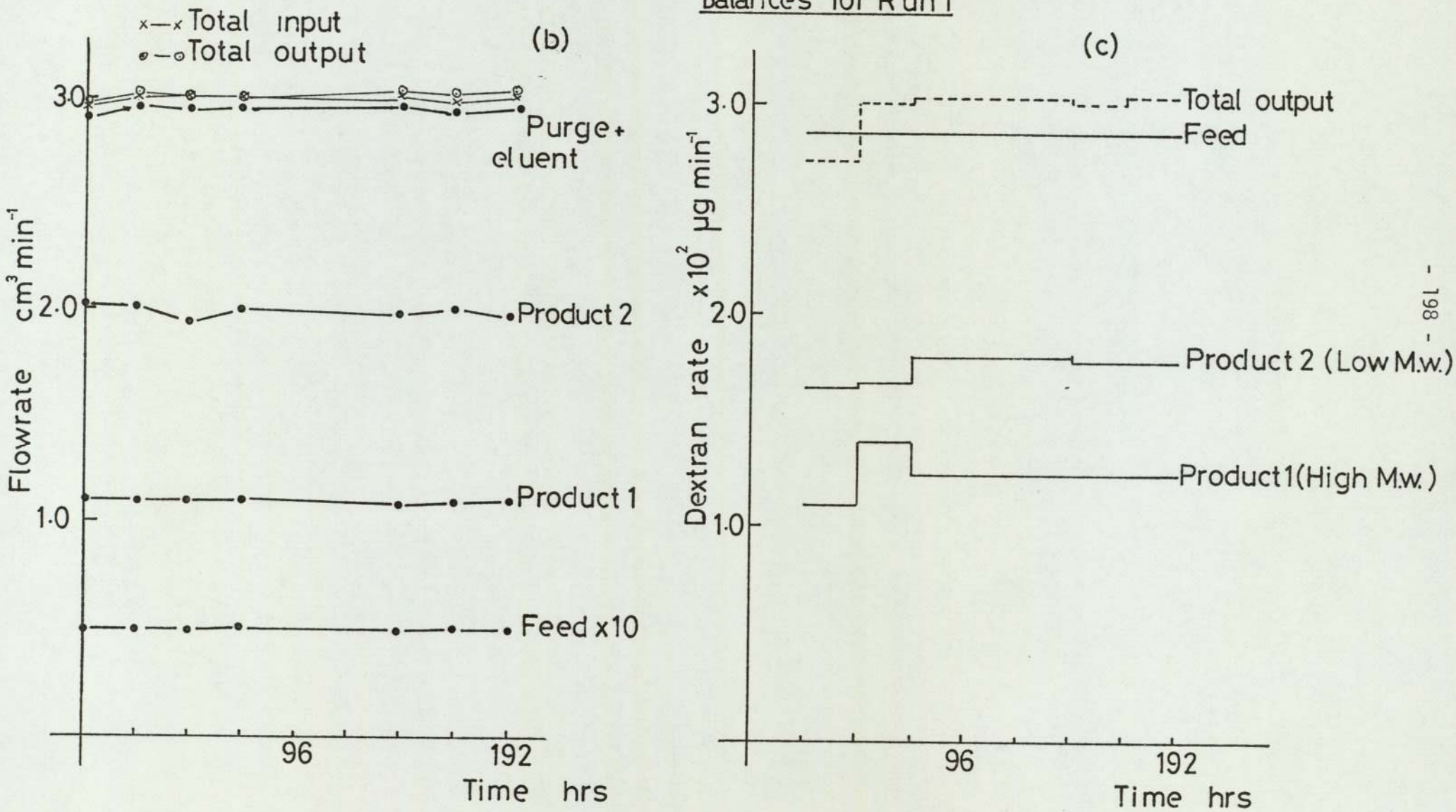

Figure 6.11a Run 2. Results Summary

Feed concentration = 46147 $\mu g\ cm^{-3}$

Temperature, Pressure and Flow rates

Time hr	Temp. °C	Pressure $KN\ m^{-2}$	Eluent + Purge $cm^3\ min^{-1}$	Feed input $cm^3\ min^{-1}$	Purge output $cm^3\ min^{-1}$	Eluent output $cm^3\ min^{-1}$
0	21.5	103	2.950	0.050	1.875	1.024
24	21.5	117	2.910	0.050	1.895	0.969
48	21.5	130	2.920	0.050	1.912	1.001
72	21.5	151	2.880	0.050	1.84	0.945
144	23.5	151	2.900	0.050	1.82	0.869
168	23	103	2.870	0.050	1.732	0.763
192	23	103	2.870	0.050	1.614	0.767

Dextran Mass Balances

Sample Number + Time	Feed input rate $\mu g\ min^{-1}$	Low Molecular weight output $\mu g\ min^{-1}$	High Molecular weight output $\mu g\ min^{-1}$	Total output $\mu g\ min^{-1}$
1(24-48)	2308	1207	374	1581
2(48-72)	2308	1139	358	1497
3(72-144)	2308	999	446	1445
4(144-168)	2308	777	351	1128
5(168-192)	2308	719	367	1085
Average	2308	968	379	1147

Figure 6.11a (Contd.)

Sample Concentrations

Sample	High M.W. $\mu g\ cm^{-3}$	Low M.W. $\mu g\ cm^{-3}$
1	380	634
2	367	610
3	495	546
4	431	434
5	480	430

Sample Mean Molecular Weights

Sample	High M.W.	Low M.W.
1	120000	16000
2	100000	15000
3	120000	16000
4	110000	25000
5	80000	25000

Theoretical "Cut" Positions (based on Porasil C)

Prefeed Retention factor	Postfeed Retention factor
0.495	0.505
0.48	0.495
0.485	0.5
0.48	0.49
0.46	0.48
.4	.4
.4	.4

FIGURE 6.11 Plots of Liquid and Dextran Mass Balances for Run 2

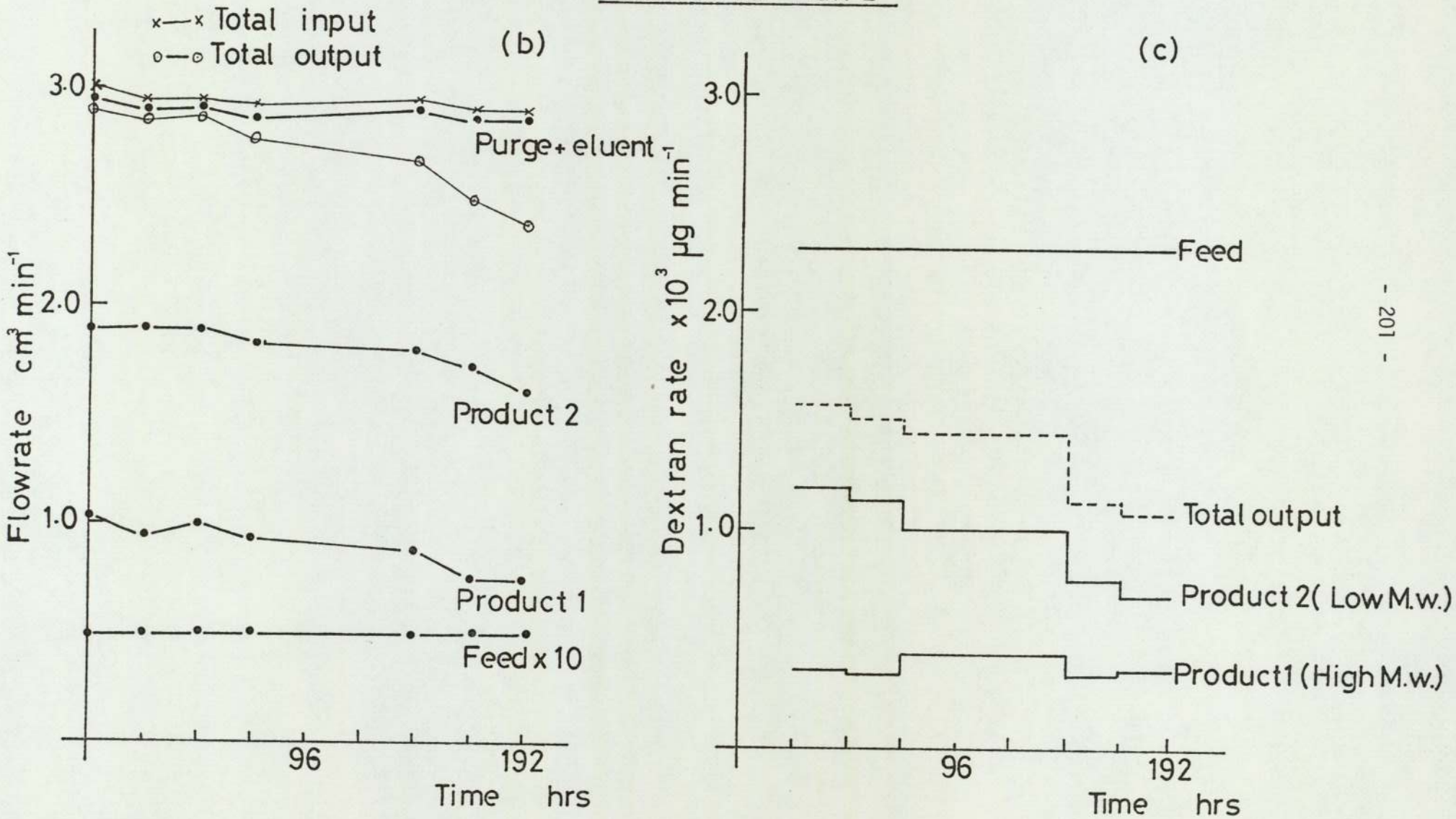

Figure 6.12a Run 3. Results Summary

Feed Concentration = 96828 $\mu g\ cm^{-3}$

Temperature, Pressure and Flow Rates

Time hrs	Temp. ^{o}C	Pressure $KN\ m^{-2}$	Eluent + purge $cm^3\ min^{-1}$	Feed input $cm^3 min^{-1}$	Purge output $cm^3 min^{-1}$	Eluent output $cm^3 min^{-1}$
0	20	103	2.960	0.050	1.967	1.059
24	20	103	2.960	0.050	1.994	1.056
48	20	103	2.950	0.050	1.942	1.063
72	20	103	2.950	0.050	1.884	1.046
96	20.4	103	2.960	0.045	2.045	1.038
168	20	103	2.950	0.042	1.968	1.065
192	20	103	2.950	0.045	1.952	1.04

Dextran Mass Balances

Sample Number + time	Feed input rate $\mu g\ min^{-1}$	Low Molecular weight output $\mu g\ min^{-1}$	High Molecular weight output $\mu g\ min^{-1}$	Total output $\mu g\ min^{-1}$
1(24-48)	4745	3461	1024	4485
2(48-72)	4841	3371	1104	4475
3(72- 96)	4551	3270	1068	4338
4(96 -168)	4066	4175	1060	5235
5(168-192)	4066	3015	1033	4048
Average =	4454	3458	1057	4516

Figure 6.12a (Contd.)

Sample Concentrations

Sample	High M.W. $\mu g\ cm^{-3}$	Low M.W. $\mu g\ cm^{-3}$
1	970	1736
2	1040	1736
3	1021	1736
4	1021	2042
5	970	1532

Sample Mean Molecular Weights

Sample	High M.W.	Low M.W.
1	100000	18000
2	120000	19000
3	120000	18000
4	140000	18000
5	130000	16000

Theoretical "Cut" Position (based on Porasil C)

Prefeed Retention factor	Postfeed Retention factor
0.52	0.537
0.52	0.537
0.528	0.545
0.52	0.537
0.513	0.53
0.528	0.545
0.52	0.537

FIGURE 6.12 Plots of Liquid and Dextran Mass Balances for Run 3

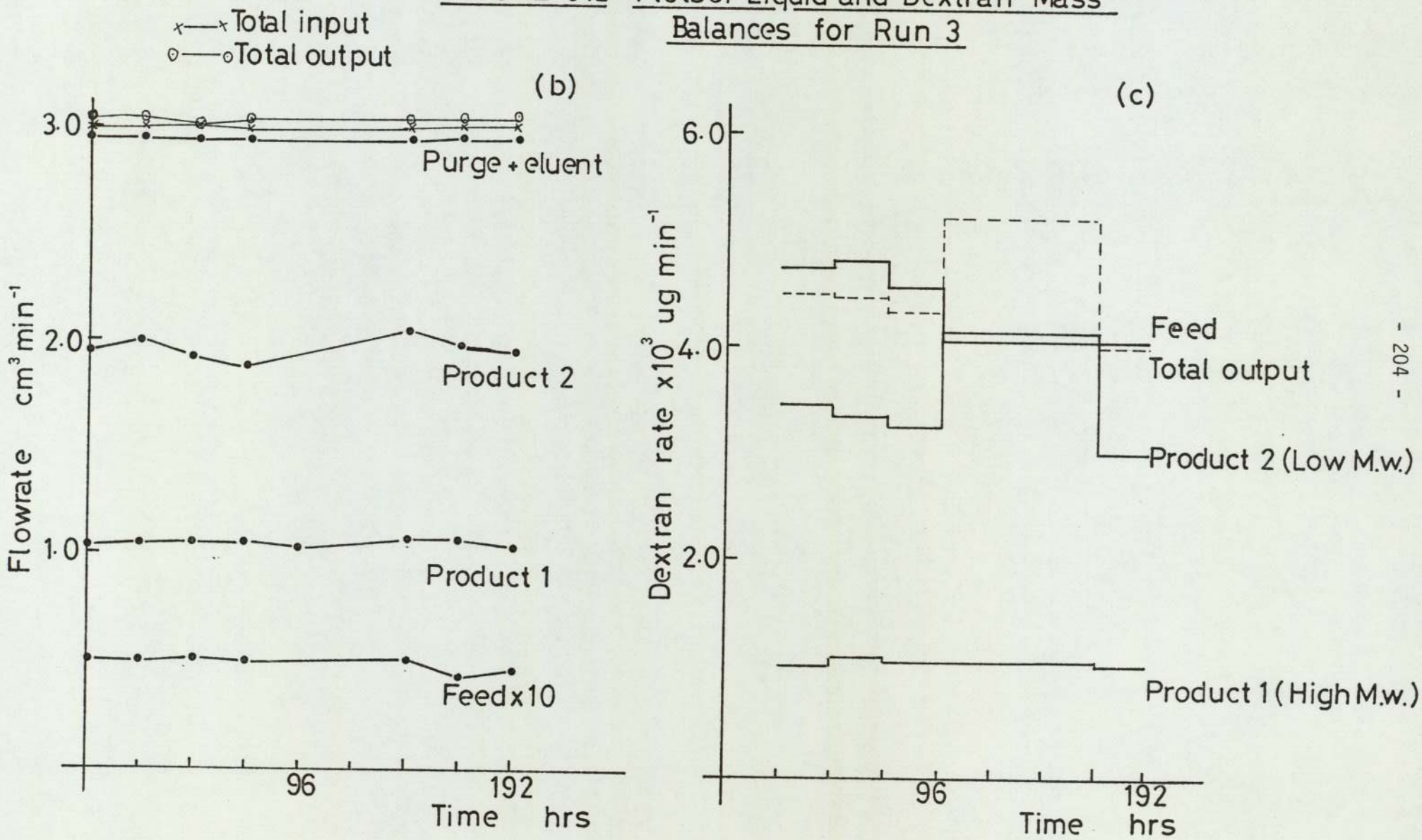

Figure 6.13a Run 4. Results Summary

Feed Concentration = 139154 $\mu g\ cm^{-3}$

Temperature, Pressure and Flow Rates

Time hrs.	Temp. ^oC	Pressure $KN\ m^{-2}$	Eluent + purge input $cm^3 min^{-1}$	Feed input $cm^3 min^{-1}$	Purge output $cm^3 min^{-1}$	Eluent output $cm^3 min^{-1}$
0	20	117	2.950	0.056	2.011	1.032
24	20	117	2.910	0.056	2.045	1.026
48	20.5	117	2.950	0.058	2.068	1.028
120	20	138	2.960	0.059	1.904	0.974
144	20.5	138	2.910	0.059	1.890	0.940
168	20	138	2.950	0.056	2.026	0.961
192	20	138	2.870	0.056	1.997	0.980

Dextran Mass Balance

Sample Number + time	Feed input rate $\mu g\ min^{-1}$	Low Molecular weight output $\mu g\ min^{-1}$	High Molecular weight output $\mu g\ min^{-1}$	Total output $\mu g\ min^{-1}$
1(24-48)	7793	6365	1171	7536
2(48-120)	8071	6783	893	8736
3(120-144)	8210	5718	872	6590
4(144-168)	8210	5142	837	5979
5(168-192)	7793	5851	916	6769
Average	8015	6184	937	7122

Figure 6.13a (Contd.)

Sample Concentrations

Sample	High M.W. $\mu g\ cm^{-3}$	Low M.W. $\mu g\ cm^{-3}$
1	1141	3112
2	870	3783
3	900	3003
4	890	2724
5	950	2891

Sample mean molecular weights

Sample	High M.W.	Low M.W.
1	140000	18000
2	160000	20000
3	170000	20000
4	170000	22000
5	200000	19000

Theoretical "Cut" Positions (based on Porasil C)

Prefeed Retention factor	Postfeed Retention factor
0.5	0.52
0.5	0.52
0.5	0.52
0.49	0.5
0.47	0.48
0.48	0.49
0.49	0.5

FIGURE 6.13 Plots of Liquid and Dextran Mass Balances for Run 4

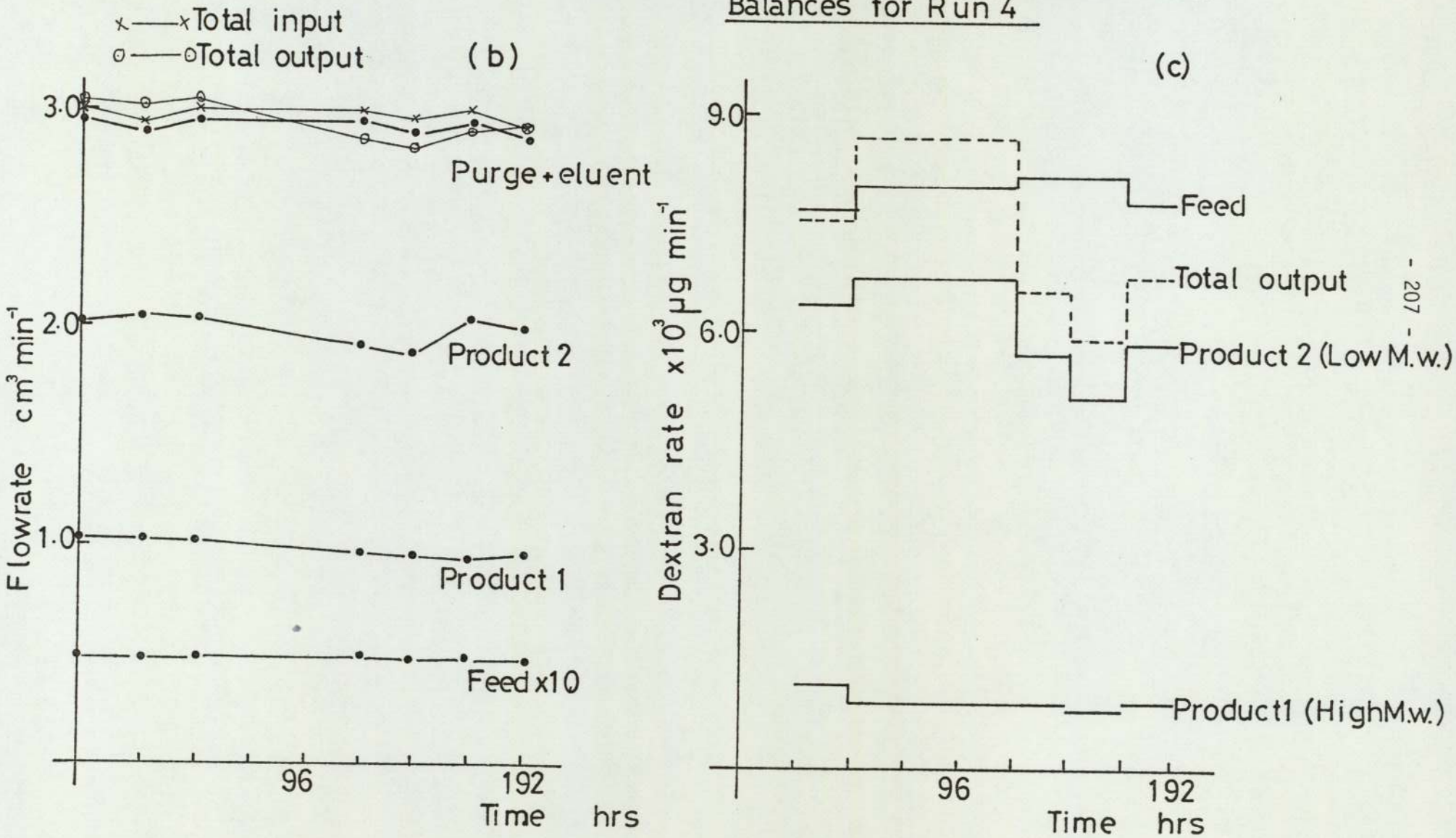

Figure 6.14a. Run 5. Results Summary

Feed concentration = 208590 $\mu g\ cm^{-3}$

Temperature, Pressure and Flow Rate

Time hrs.	Temp. ^oC	Pressure $KN\ M^{-2}$	Eluent + purge input $cm^3 min^{-1}$	Feed input $cm^3 min^{-1}$	Purge output $cm^3 min^{-1}$	Eluent output $cm^3 min^{-1}$
0	21	103	3.000	0.057	2.101	1.087
24	20.5	152	2.950	0.057	1.885	1.015
48	22.5	152	2.910	0.057	2.054	1.017
72	22	152	2.920	0.057	1.933	1.022
144	21	152	2.860	0.056	1.914	1.026
168	22	152	2.830	0.056	1.847	1.017
192	24	152	2.840	0.055	1.893	1.01

Dextran Mass Balance

Sample Number + time	Feed input rate $\mu g\ min^{-1}$	Low molecular weight output $\mu g\ min^{-1}$	High molecular weight output $\mu g\ min^{-1}$	Total output $\mu g\ min^{-1}$
1(24-48)	11890	9229	1104	10333
2(48-72)	11890	9187	1106	10293
3(72-144)	11785	11567	1236	12803
4(144-168)	11681	9832	1426	11258
5(168-192)	11472	9717	1414	11126
Average	11743	9905	1257	11162

Figure 6.14a (Contd.)

Sample Concentrations

Sample	High M.W. $\mu g\ cm^{-3}$	Low M.W. $\mu g\ cm^{-3}$
1	1088	4896
2	1088	4473
3	1209	5984
4	1390	5137
5	1390	5258

Sample Mean Molecular Weights

Sample	High M.W.	Low M.W.
1	195000	21000
2	190000	20000
3	195000	20000
4	195000	20000
5	200000	20000

Theoretical "Cut" Positions (based on Porasil C)

Prefeed Retention factor	Postfeed Retention factor
0.52	0.555
0.5	0.515
0.5	0.515
0.5	0.517
0.5	0.517
0.5	0.515
0.495	0.512

FIGURE 6.14 Plots of Liquid and Dextran Mass Balances for Run 5

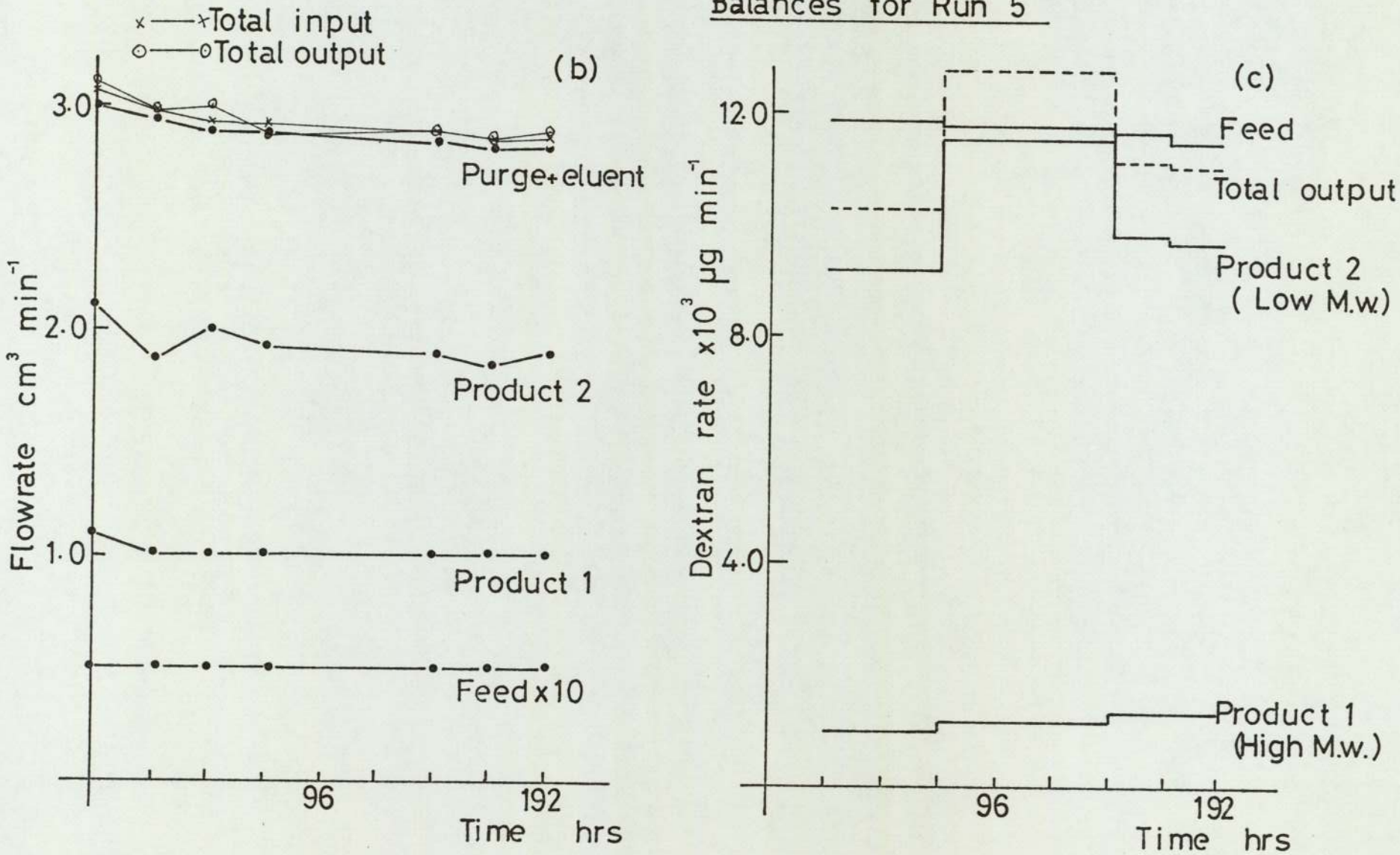

Figure 6.15a Run 6. Results Summary

Feed Concentration = 208590 $\mu g\ cm^{-3}$

Temperature, Pressure and Flow Rates

Time hrs.	Temp. ^oC	Pressure $KN\ M^{-2}$	Eluent + purge input $cm^3 min^{-1}$	Feed input $cm^3 min^{-1}$	Purge output $cm^3 min^{-1}$	Eluent output $cm^3 min^{-1}$
0	21	103	2.870	0.125	1.861	1.078
24	21	186	2.910	0.108	1.882	0.899
48	21	186	2.870	0.103	1.953	1.056
72	23	172	2.870	0.080	2.032	0.928
144	22	172	2.870	0.091	1.991	0.973
168	21.5	172	2.900	0.108	1.992	1.019

Dextran Mass Balance

Sample Number + time	Feed input rate $\mu g\ min^{-1}$	Low molecular weight output $\mu g\ min^{-1}$	High molecular weight output $\mu g\ min^{-1}$	Total output $\mu g\ min^{-1}$
1(24-48)	21902	19266	1331	20597
2(48-72)	18773	18604	1164	19768
3(72-144)	17730	20802	1023	21825
4(144-168)	20650	18684	1095	19779
Average	19764	19339	1153	20292

Figure 6.15a (Contd.)

Sample concentrations

Sample	High M.W. $\mu g\ cm^{-3}$	Low M.W. $\mu g\ cm^{-3}$
1	1480	10237
2	1102	9526
3	1102	10237
4	1125	9384

Sample Mean Molecular Weights

Sample	High M.W.	Low M.W.
1	215000	22000
2	265000	22000
3	250000	23000
4	190000	24000

Theoretical "Cut" Positions (based on Porasil C)

Prefeed Retention factor	Postfeed Retention factor
0.495	0.555
0.45	0.48
0.495	0.537
0.47	0.49
0.48	0.5
0.485	0.517

FIGURE 6.15 Plots of Liquid and Dextran Mass Balances for Run 6

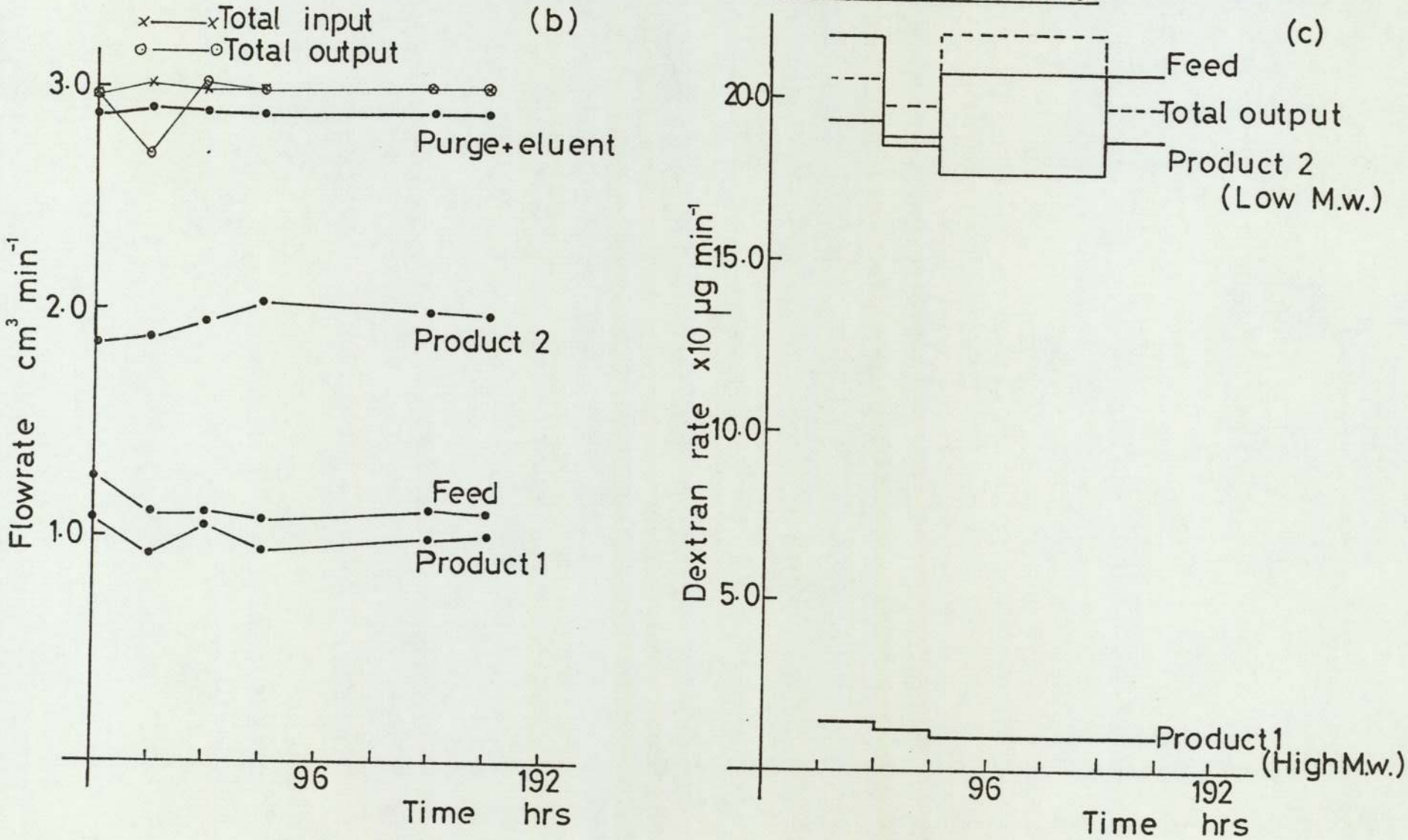

Figure 6.16a. Run 7. Results Summary

Feed Concentration = 25258 $\mu g\ cm^{-3}$

Temperature, Pressure and Flow Rate

Time hrs.	Temp. ^oC	Pressure $KN\ M^{-2}$	Eluent + purge input $cm^3 min^{-1}$	Feed input $cm^3 min^{-1}$	Purge output $cm^3 min^{-1}$	Eluent output $cm^3 min^{-1}$
0	23	103	2.990	0.053	2.023	1.129
24	23	103	3.070	0.050	2.015	1.121
48	23	103	3.080	0.050	1.937	1.127
120	21	120	3.090	0.050	1.944	1.137
144	21.5	120	3.140	0.050	1.982	1.137
168	23	103	2.910	0.050	1.965	1.01
192	23	103	3.010	0.050	2.018	1.001
216	23	103	2.960	0.044	2.012	1.009
240	23	103	2.960	0.050	2.021	1.011

Dextran Mass Balance

Sample Number + time	Feed input rate $\mu g\ min^{-1}$	Low molecular weight output $\mu g\ min^{-1}$	High molecular weight output $\mu g\ min^{-1}$	Total output $\mu g\ min^{-1}$
1(24-48)	1262	4.9	1254	1259
2(48-120)	1262	12.1	1236	1248
3(120-144)	1262	15.3	1268	1283
Average	1262	11	1252	1263
4(144-168)	1262	145	673	818
5(168-192)	1262	294	808	1102
6(192-216)	1187	220	892	1112
7(216-240)	1262	228	786	1014
Average	1243	222	789	1012

Figure 6.16a (Cont.)

Sample Concentrations

Sample	High M.W. $\mu g\ cm^{-3}$	Low M.W. $\mu g\ cm^{-3}$
1	1116	2.5
2	1092	6.2
3	1116	7.8
4	667	73
5	807	148
6	884	109
7	778	113

Sample Mean Molecular Weights

Sample	High M.W.	Low M.W.
1	30000	-
2	22000	8000
3	25000	4000
4	54000	<1000
5	42000	3000
6	44000	6000
7	38000	6000

Theoretical "Cut" Positions (based on Porasil C)

Prefeed Retention factor	Postfeed Retention factor
0.74	0.76
0.74	0.76
0.74	0.76
0.745	0.77
0.745	0.77
0.745	0.7
0.64	0.68
0.64	0.68
0.645	0.7

FIGURE 6.16 Plots of Liquid and Dextran Mass Balances for Run 7

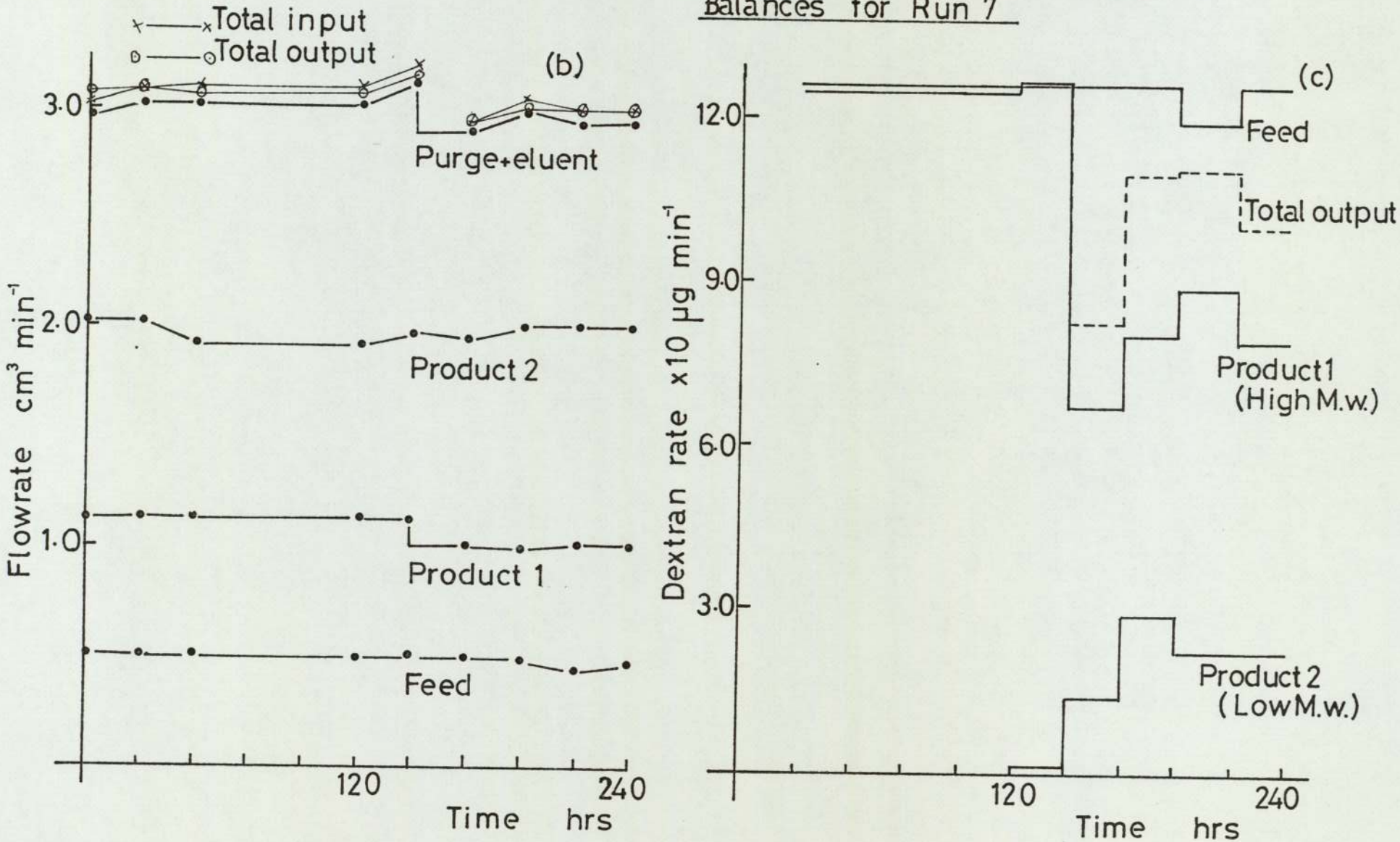

FIGURE 6.17 Feed Distribution — Based on Flow Conditions for Run 1

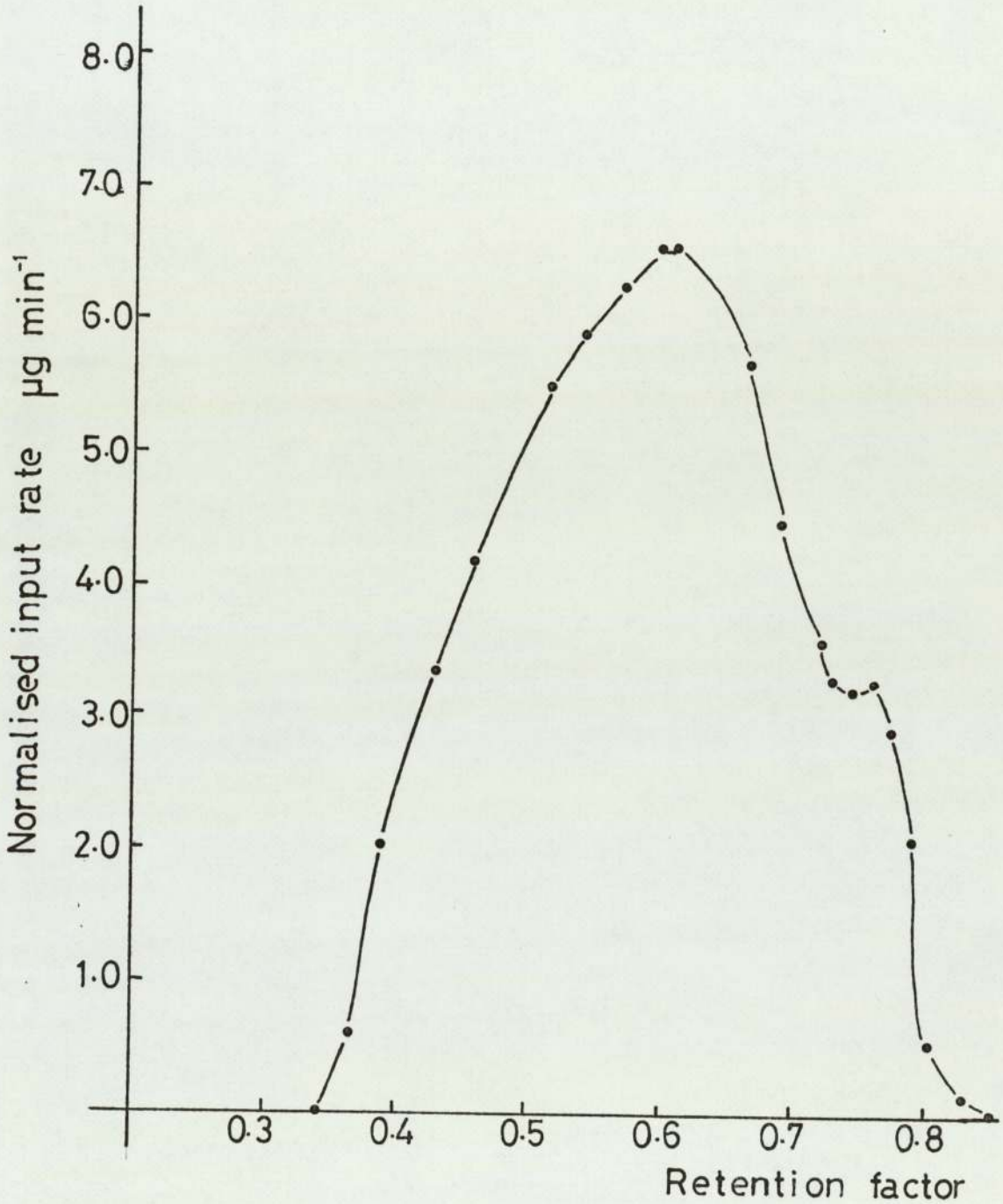

insignificant. Throughout these experiments the bundle speed was held constant at 0.0026 r.p.m. This bundle speed was equivalent to the liquid held in the pores of the packing moving at a rate of 0.663 $cm^3 min^{-1}$. The eluent rate was set at nominally 1.1 cm^3 min^{-1}. The purge rate was set at about 1.9 cm^3 min^{-1}. At this flow rate it ensured that no low molecular weight material was transferred from the purge section via the liquid lock to the high molecular weight product output port. The "cut" effected by the machine was always in excess of a partition coefficient of unity. Since, in gel permeation chromatography a molecule that completely permeates the packing has a partition coefficient of unity, all the material entering the purge section would theoretically be removed. In practice this was proved to be the case. Figures 6.10b to 6.16b show the variation in liquid flow rates during these experiments.

In Run 1 a 0.5% w/v dextran solution was pumped into the chromatograph at 0.05 cm^3 min^{-1}. Postfeed and prefeed eluent rates were initially 1.1 cm^3 min^{-1} and 1.05 cm^3 min^{-1} respectively. Throughout the experiment the flow conditions remained relatively stable, Figure 6.10b. Over the first 24 hours the product lines were attached to the fraction collector, which is described in Appendix 1. A fraction of each product was also continuously monitored over this period using the Auto Analyser. Figures 6.18 and 6.19 show the concentration output curves for both products (Figure 6.18) and the way in which concentration builds up with time (Figure 6.19). It is interesting to note that both products, from the machine, have an oscillatory pattern. This is in agreement with the discontinuous nature of the process and a similar observation

FIGURE 6.18 Product Output Curves at Equilibrium

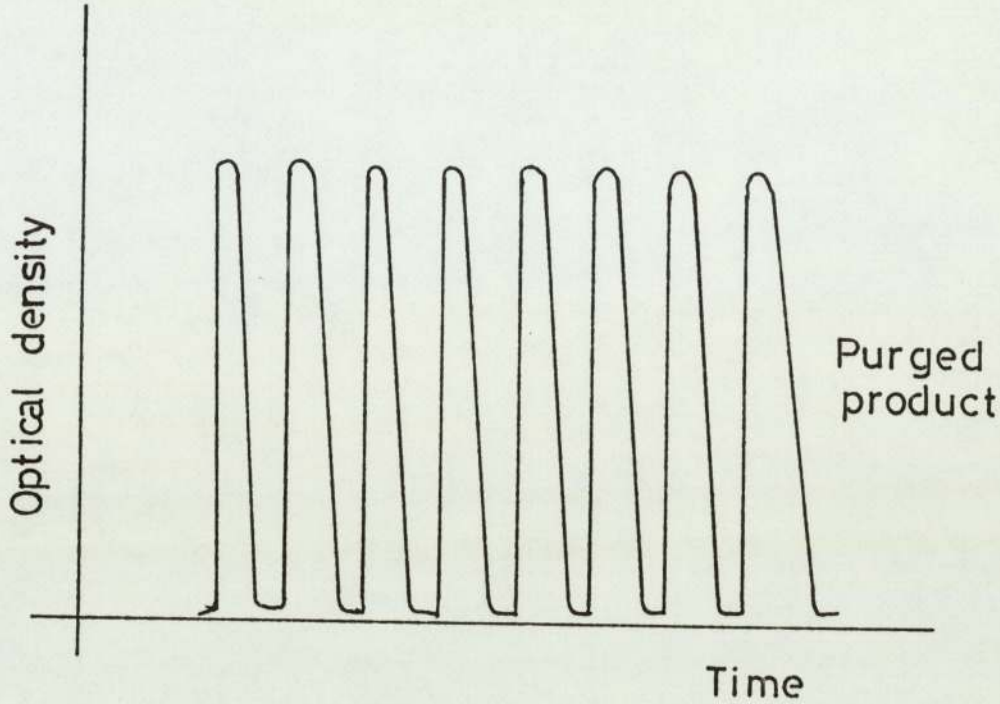

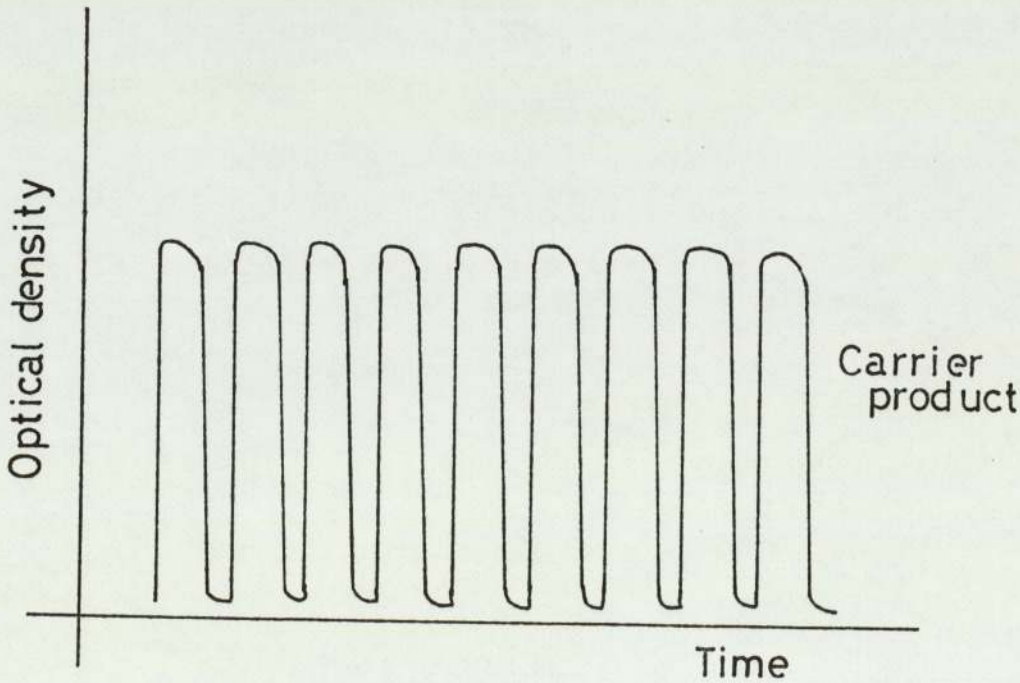

FIGURE 6.19 Product Concentration Build up with Time

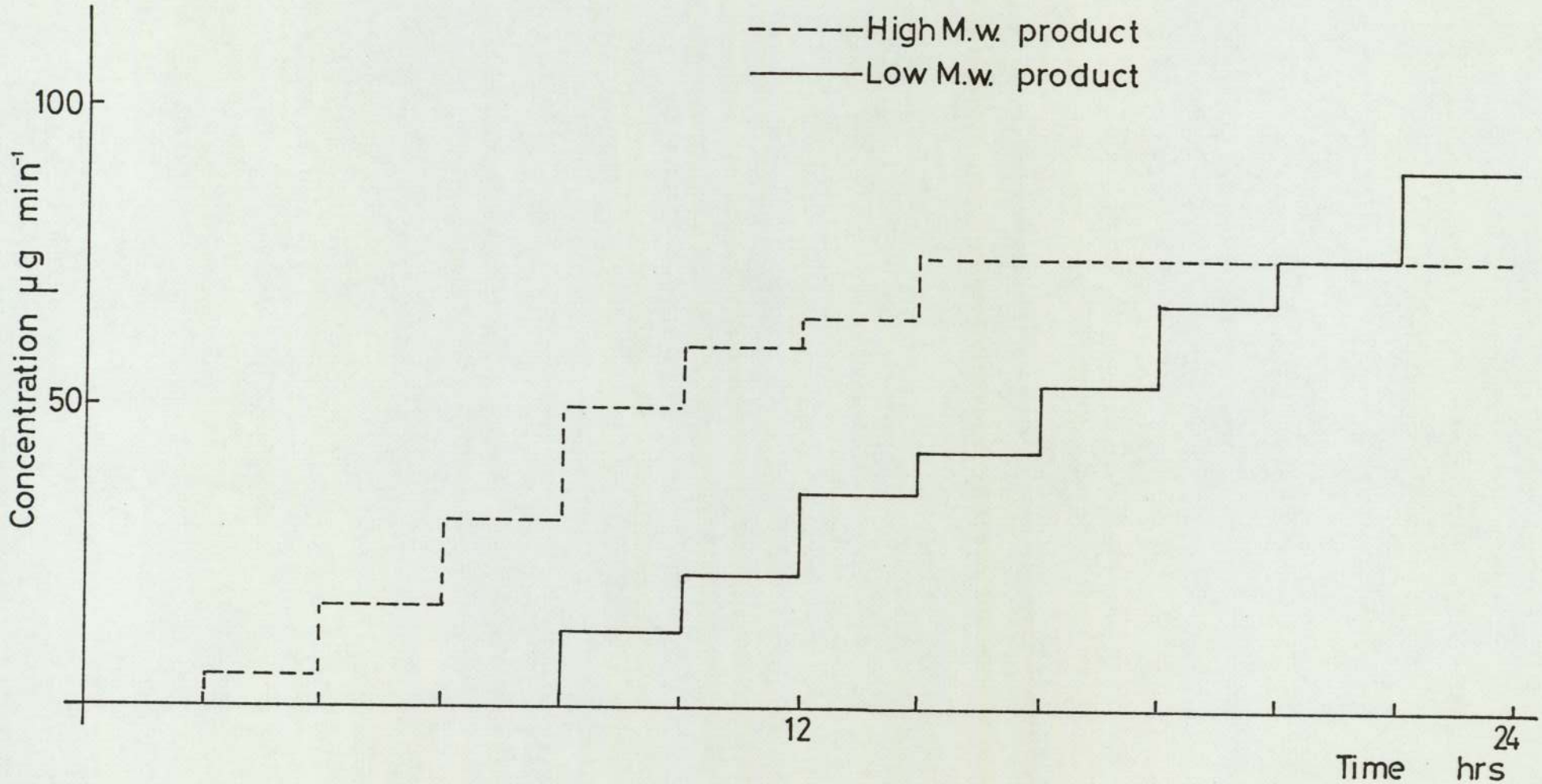

made by Deeble[9] in continuous gas-liquid chromatography.

The products collected by the fraction collector showed the build up of product molecular weight distribution with time, Figure 6.20. It can be seen how the highest and lowest molecular weights leave as products first. Then, as the experiment progressed, the product molecular weight distributions build up. The build up of the product distributions moving toward the predicted cut position, which agrees with the theory that molecules with partition coefficients of the same order as the "cut" position are the slowest moving components. The final product distributions are given in Figure 6.21. The prefeed and postfeed "cut" positions have been marked on this figure. Although the "cross over point" of the two product curves has no theoretical significance, it coincides with the theoretical "cut" values. This serves to demonstrate that the "cut" effected by the machine was in agreement with that theoretically predicted.

Dextran mass balances, Figure 6.10c, show that the total dextran output was comparatively stable after about 48 hours. The mean molecular weight of the products are presented in Figure 6.10a.

In Run 2 the feed concentration was increased by a factor of about 10 to 4.6%. The feedrate was kept constant at 0.05 $cm^3\ min^{-1}$. The post feed eluent rate steadily decreased, as a result of leakage, from 1.02 $cm^3\ min^{-1}$, at the start of the experiment, to 0.76 $cm^3\ min^{-1}$ at the end. Figure 6.11b graphically represents the liquid mass balances performed during this experiment. At the end of the experiment the leakage was measured and calculated to be about 20%. The decrease in eluent rate had a disasterous effect on the product

FIGURE 6·20 Product Distribution Build up with Time

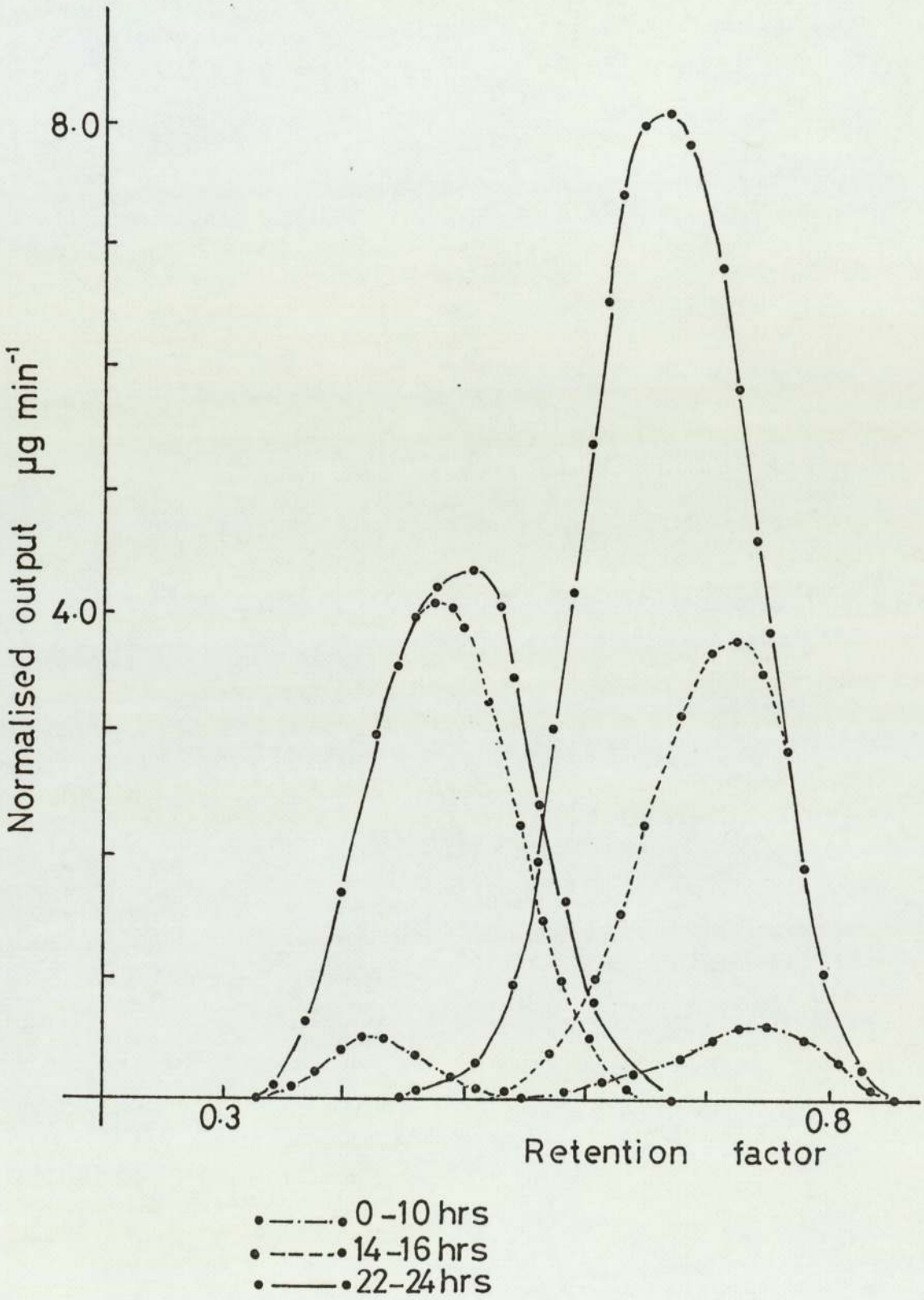

FIGURE 6·21 Run 1 Product Distributions

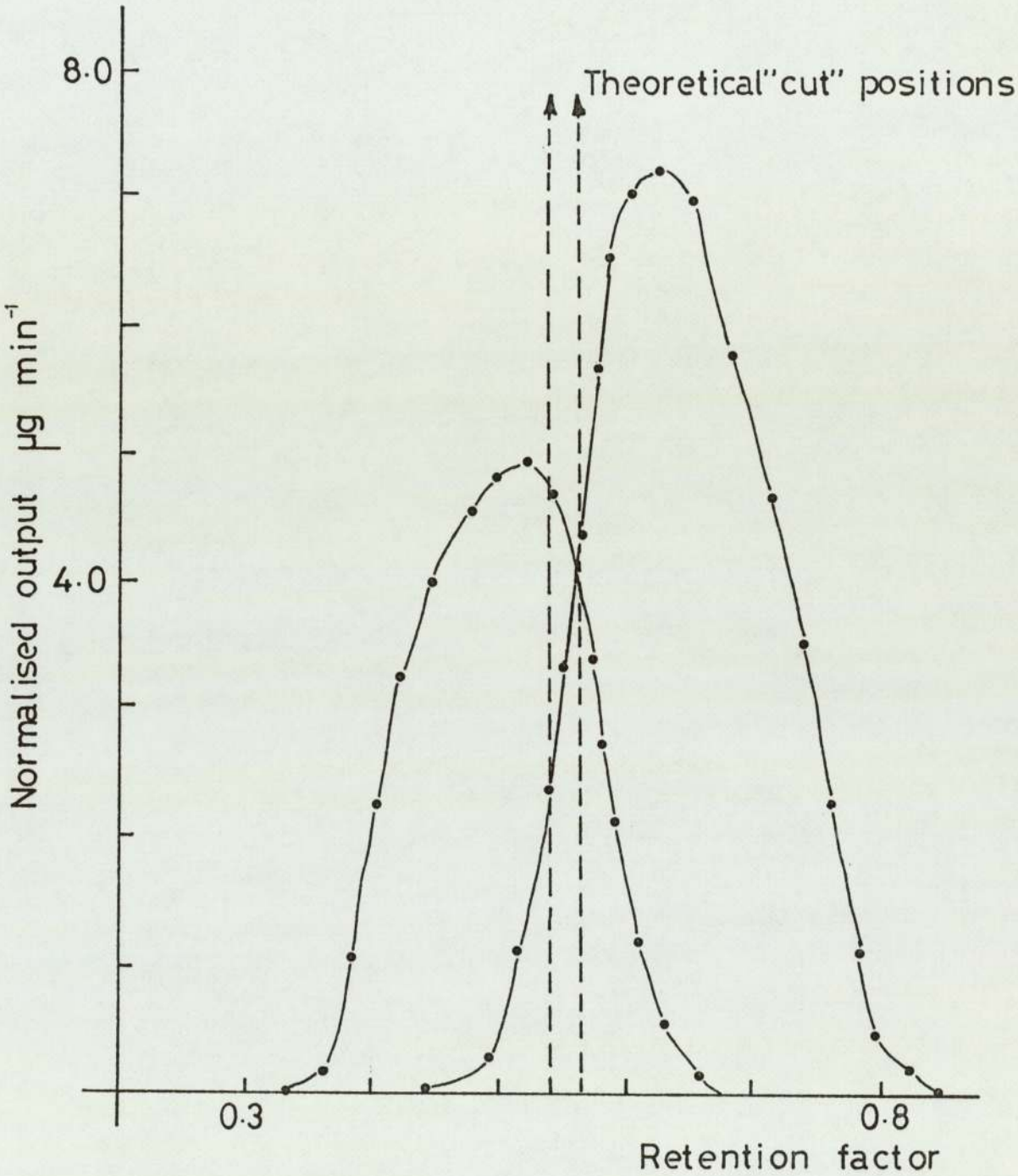

molecular weight distributions, Figure 6.22 is a typical example, and on the dextran mass balances, Figure 6.11c. A comparison of the summation of the product distributions, Figure 6.23a, with that of the original feed, Figure 6.23b, gives an indication as to the extent to which liquid leakage has adversely affected the fractionation process. The product samples used to illustrate this effect were taken during the period 48 hours to 72 hours. As would be expected the "dip" in the summation curve coincides with the theoretically predicted "cut" values. This is in agreement with the fact that molecules whose partition coefficients were of the same order as the "cuts" effected by the machine will migrate at the slowest rate.

In contrast to Run 2, Run 3 proved quite successful, both the eluent and purge rates remaining reasonably constant throughout the experiment, Figure 6.12b. The feed (9·7% w/v) was initially pumped at the same rate, 0.05 cm^3 min^{-1}, as in previous experiments. However, during the latter stages of the experiment this dropped to just over 0.04 cm^3 min^{-1}. Unlike a change in the eluent rate a change in the feed rate did not appear to affect the product mean molecular weights, (Figure 6.12a) nor their molecular weight distributions. Figure 6.24 gives a typical example of the analysis of both products. Once again the "cross over point" of the two distributions lies in between the theoretical "cut" positions. Unlike previous dextran mass balances, in this experiment there was an increase in the dextran output rate of the low molecular weight product over the time period 96 hrs to 168 hrs. A possible cause of this increase is discussed in Section 6.4.4.

FIGURE 6·22 Run 2 Product Distributions

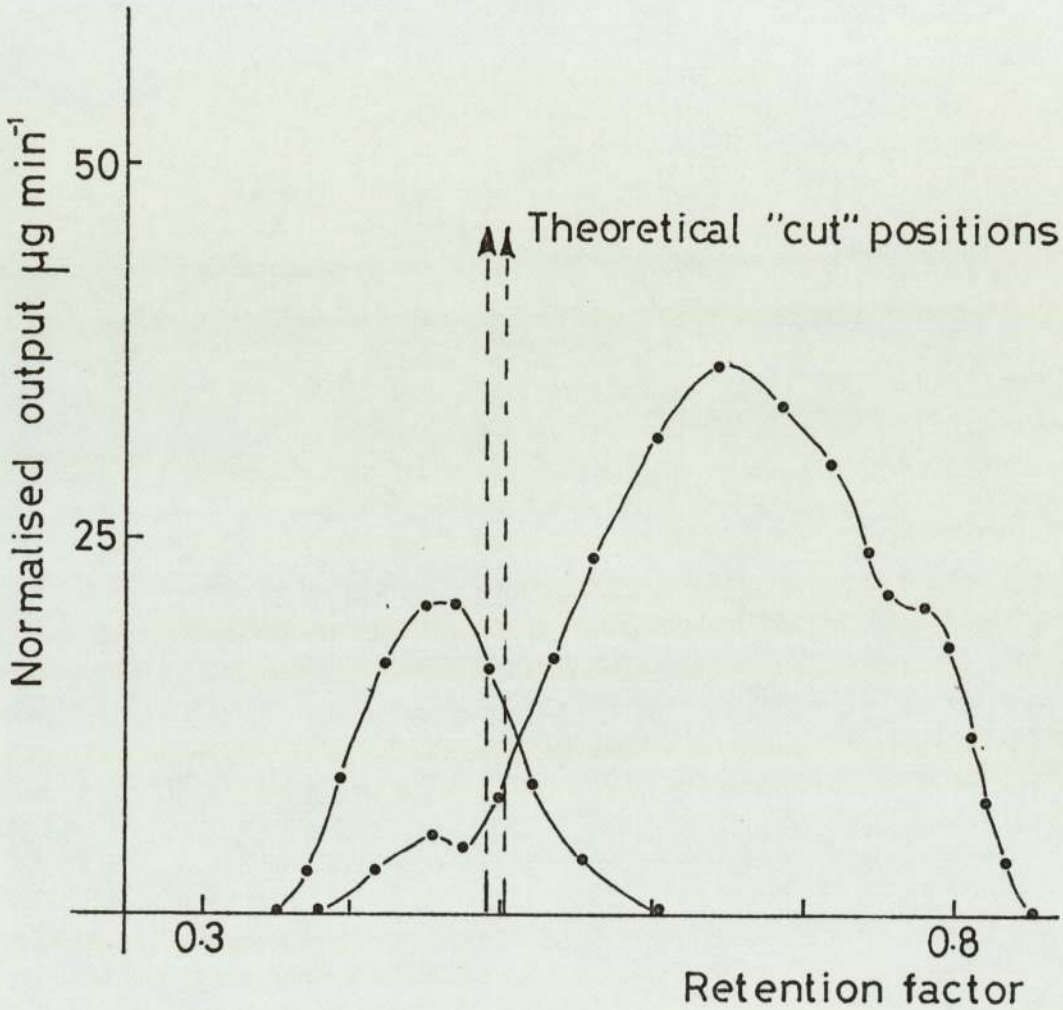

FIGURE 6.23 Feed and Product Curves for Run 2

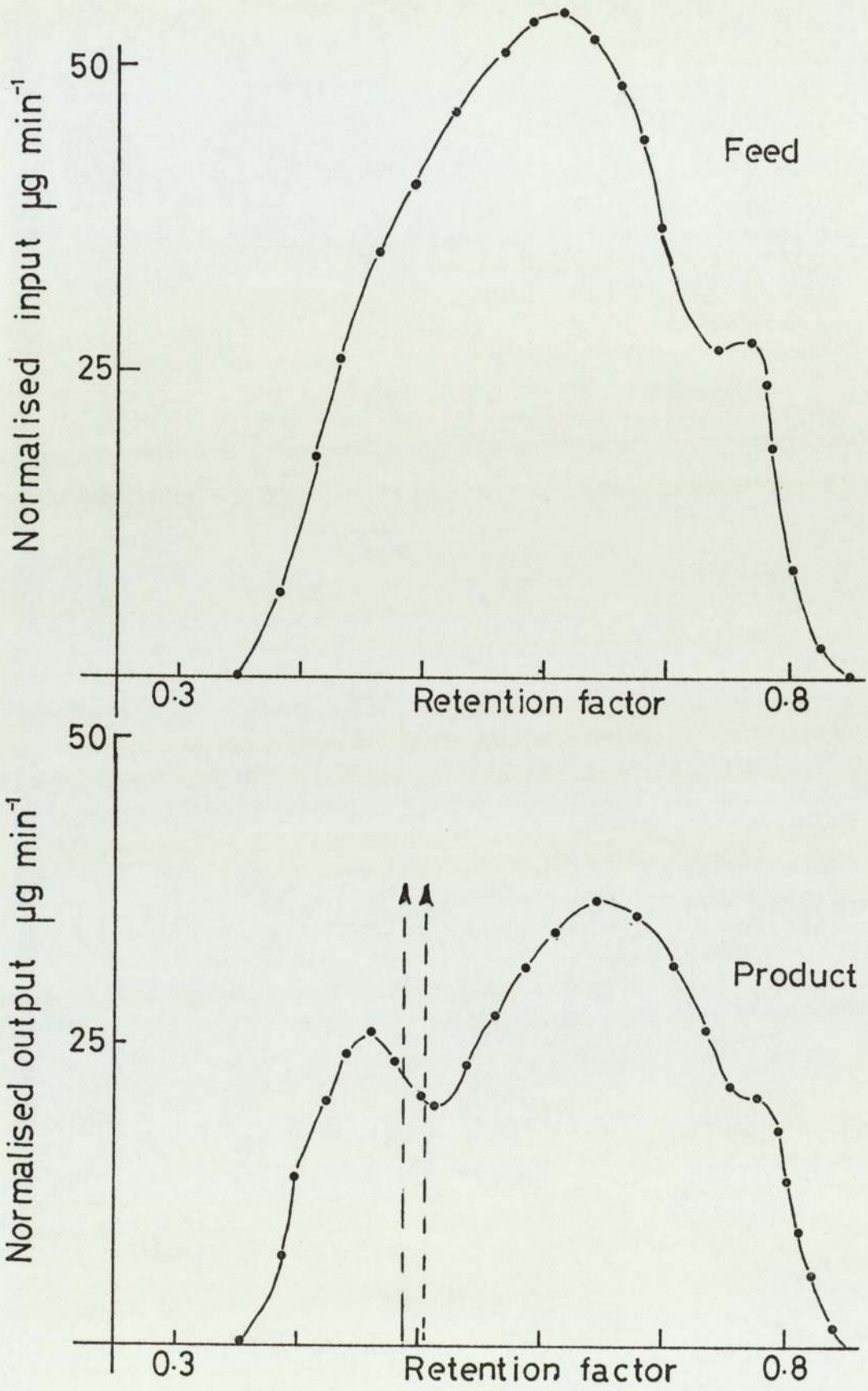

FIGURE 6.24 Run 3 Product Distributions

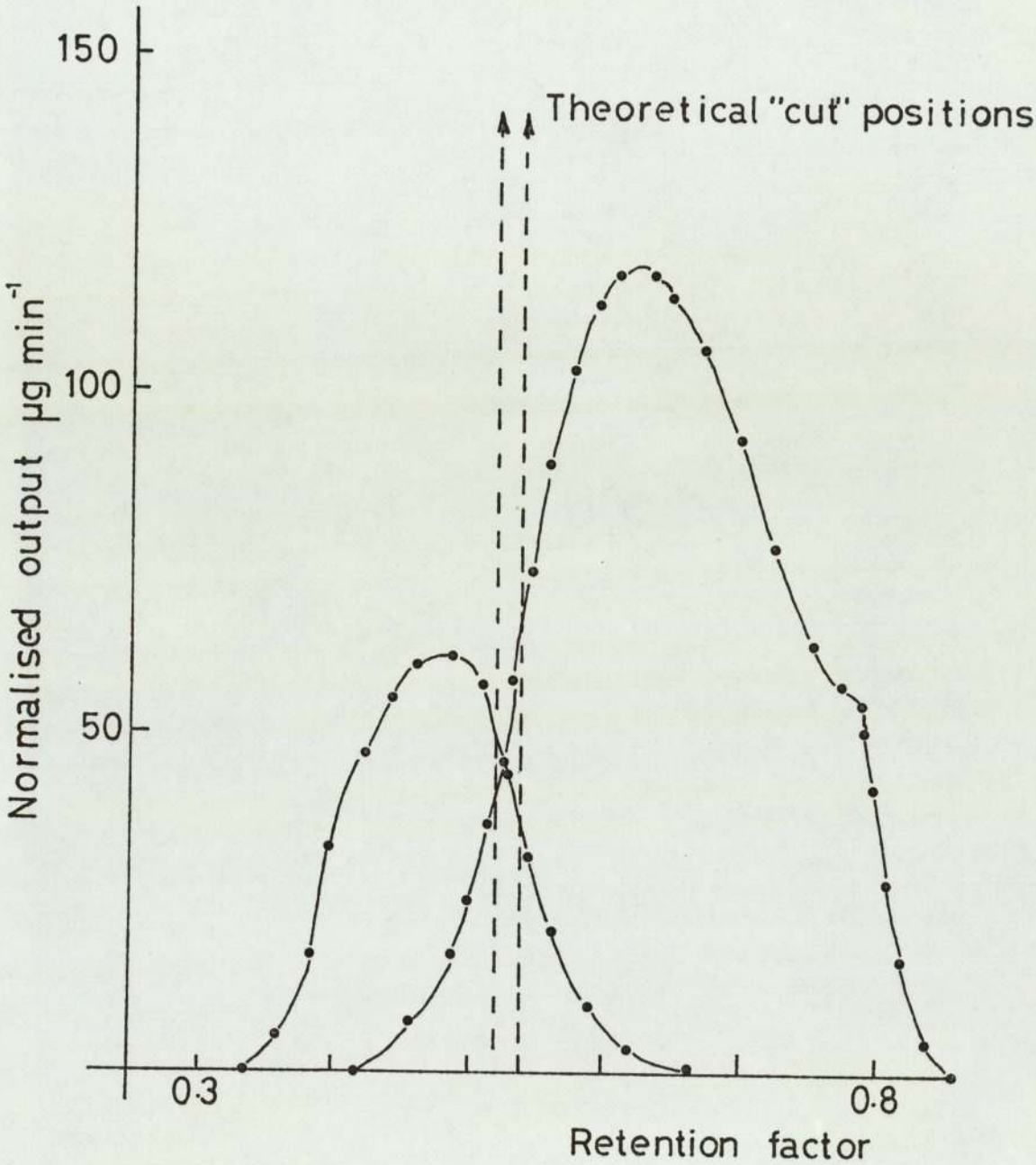

In the penultimate experiment, Run 4, the feed (13.9% w/v) was the undiluted dextran solution as supplied by Fisons Ltd. The feedrate was measured as 0.056 cm^3 min^{-1}, slightly higher than in the previous experiments. During the course of the run the eluent and purge rates decreased because of liquid leakage from the seal, Figure 6.13b. Effects on the product mean molecular weights, (Figure 6.13a), and molecular weight distribution were observed as a result. The dextran mass balances, Figure 6.13c, also reflects the effect of leakage. In addition, the increase in dextran output in the low molecular product, as was observed in Run 3,was also evident in this run.

Fortunately the flow conditions were stable in the early stages of the experiment which indicated that the fractionation achieved under these operating conditions could be determined, (Figure 6.25). A feature of this figure is that the "cross over point" of the two product distributions has moved to the high molecular weight side of the theoretically predicted "cut" position. This would indicate that increasing the feed concentration has influenced the fractionation process.

In an attempt to verify this concentration effect the feed concentration was increased to 20.8% w/v in Run 5. Setting the feed pump to deliver 0.05 cm^3 min^{-1} proved difficult because of the highly viscous nature of the feed. A consistent feed rate of 0.056 cm^3 min^{-1} was finally obtained. Other operating parameters were the same as in previous experiments. The flow rates did not vary, during the experiment, to an appreciable extent (Figure 6.14b).

FIGURE 6·25 Run 4 Product Distributions

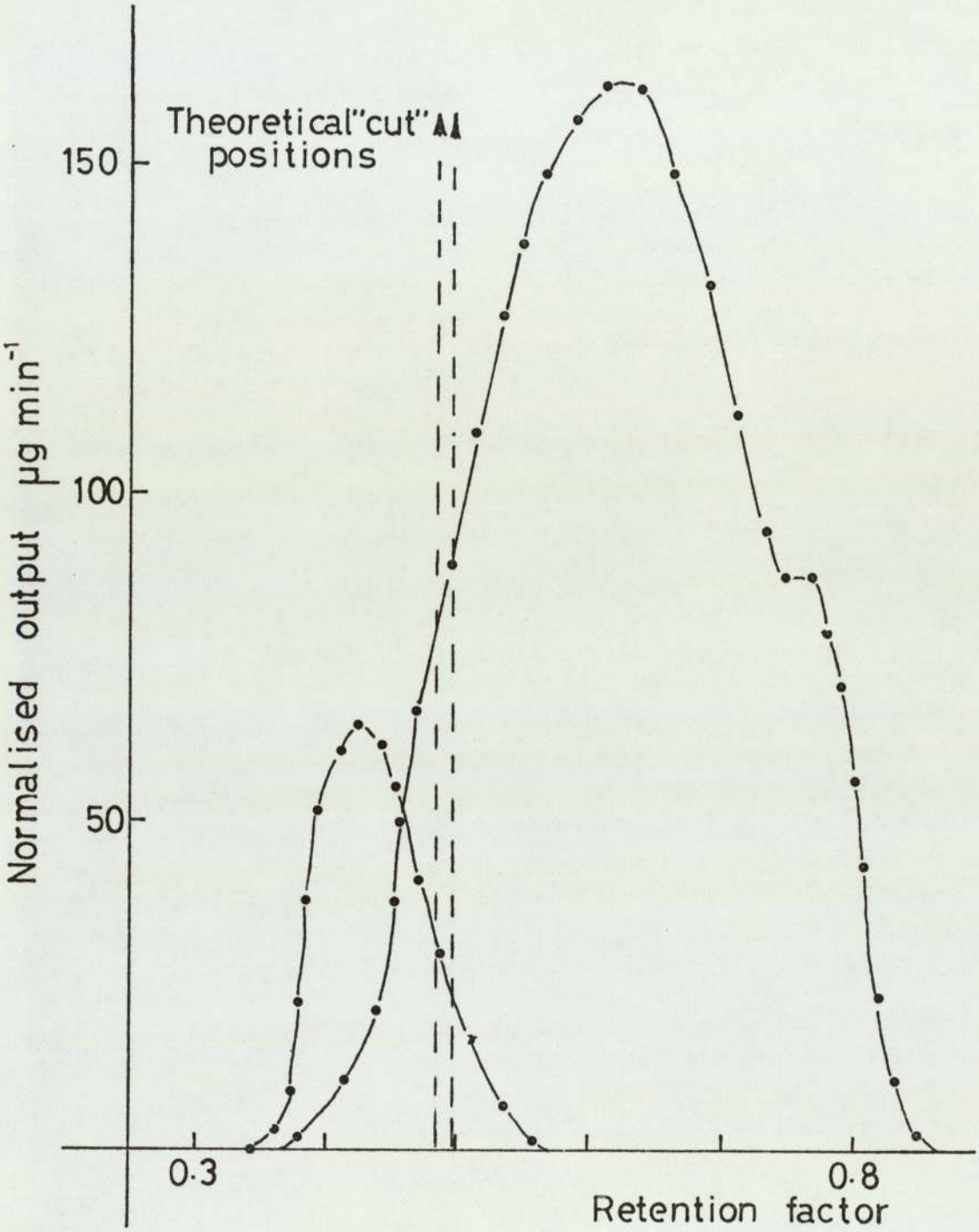

Analysis of the product samples showed that, (i) the mean molecular weights (Figure 6.14a) and (ii) the molecular weight distribution (Figures 6.26-6.30) remained unchanged after the first sampling period (24-48 hours). These results demonstrate how consistent, under constant operating conditions, the fractionation process is over long periods. Samples taken during 144 hours and 168 hours were analysed on the same packing to determine the fractionation achieved, this is presented in Figure 6.31. As in Run 4 the "cross over point" of the product distributions has shifted to the left of the theoretical "cut" positions. This observation confirms the conclusion drawn in Run 4 that increasing the feed concentration influences the fractionation process.

Increasing the overall operating concentration in the chromatograph does apparently increase the effective partition coefficients of molecules permeating the packing. It is probable that this increase is not a result of the molecules permeating the packing to a greater extent, but is caused by molecules in the mobile phase physically preventing them from diffusing out of the pores of the packing. Molecules in the mobile phase are in effect acting as a secondary gel permeation medium. This is in agreement with the concentration effects observed by Hellsing[168], Altgelt[209] and Hatt[11] on batch gel permeation chromatography columns.

The increase in the dextran output concentration observed in Run 3 was also evident in this experiment, (Figure 6.14c). In both these experiments the increase coincided with the sample collected over the weekend. A possible cause of these increases is discussed in Section 6.4.4.

FIGURE 6·26 High M.w. Product, Samples 1 and 2, Run 5

(Analysis on Porasil D)

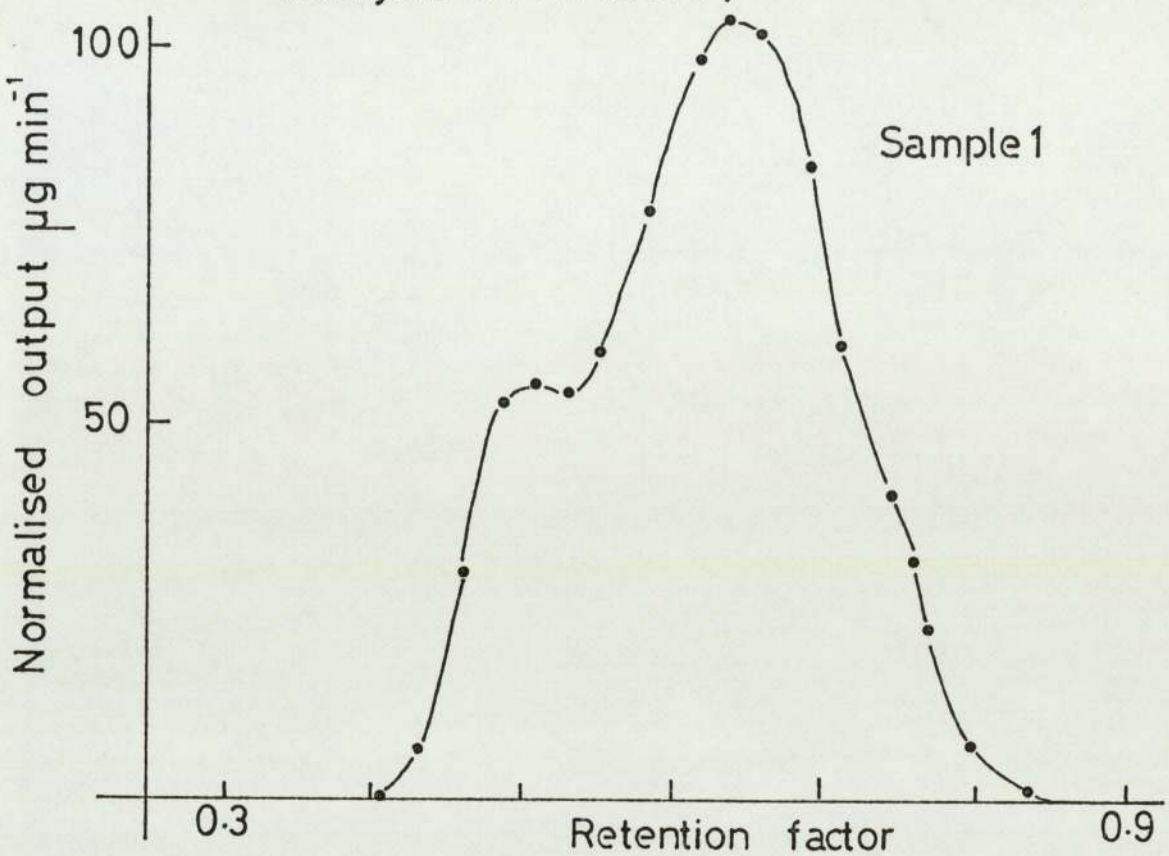

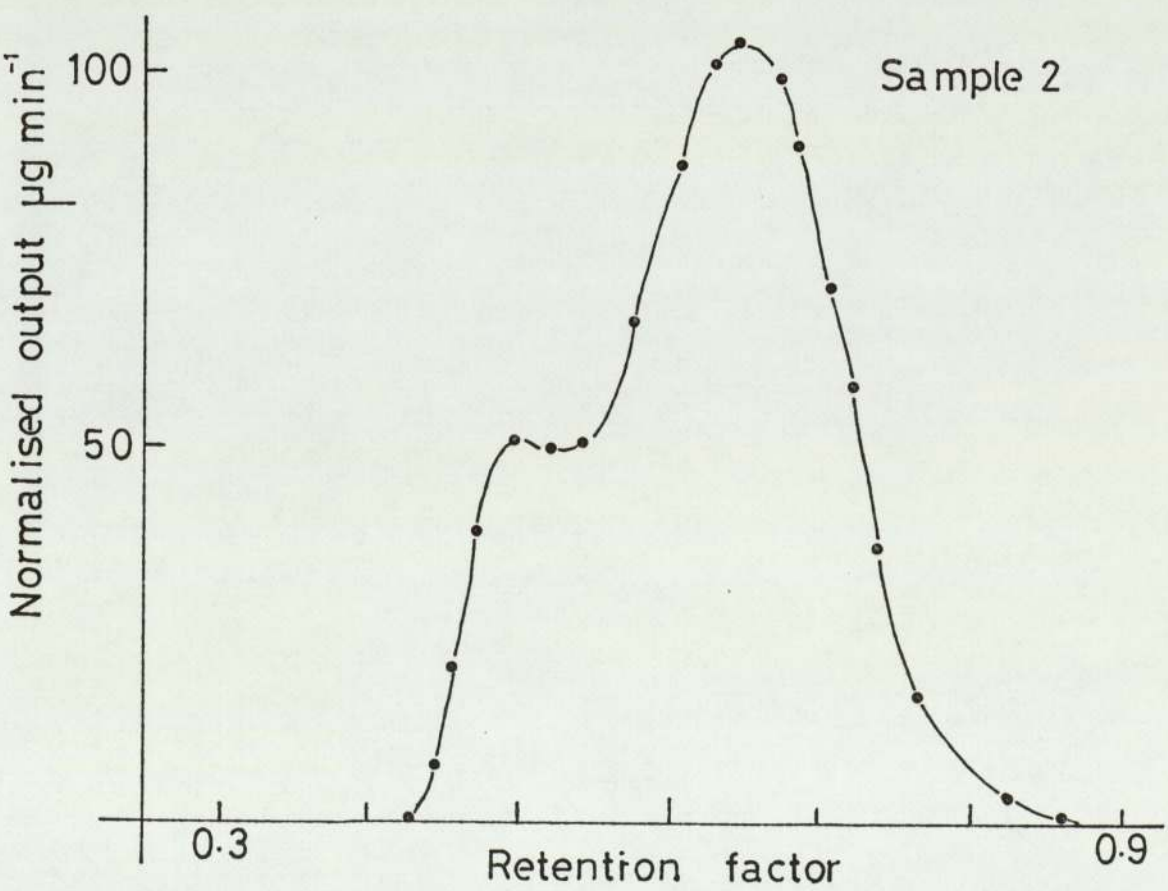

FIGURE 6·27 High M.w. Product, Samples 3and4, Run 5
(Analysis on Porasil D)

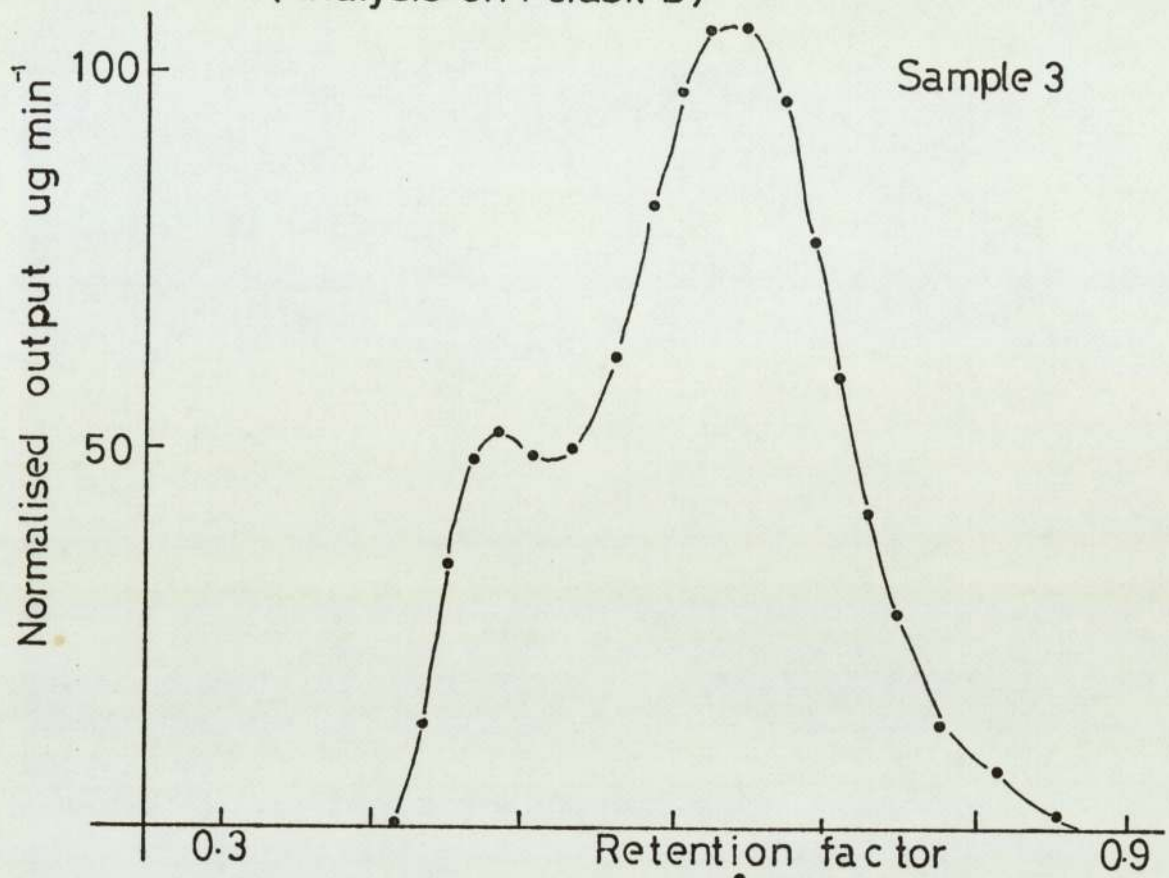

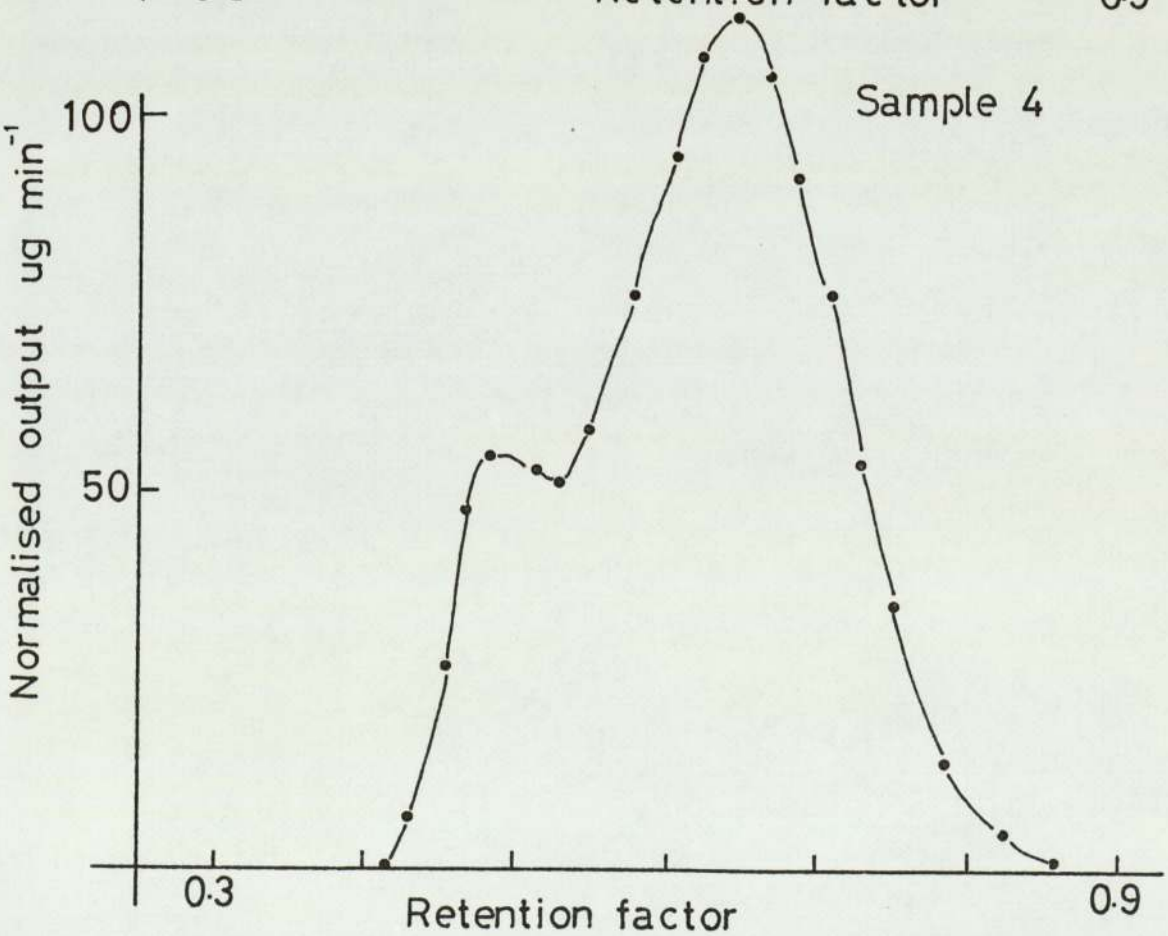

FIGURE 6·28 High M.w. Product, Sample 5; Low M.w. Product, Sample 1, Run 5

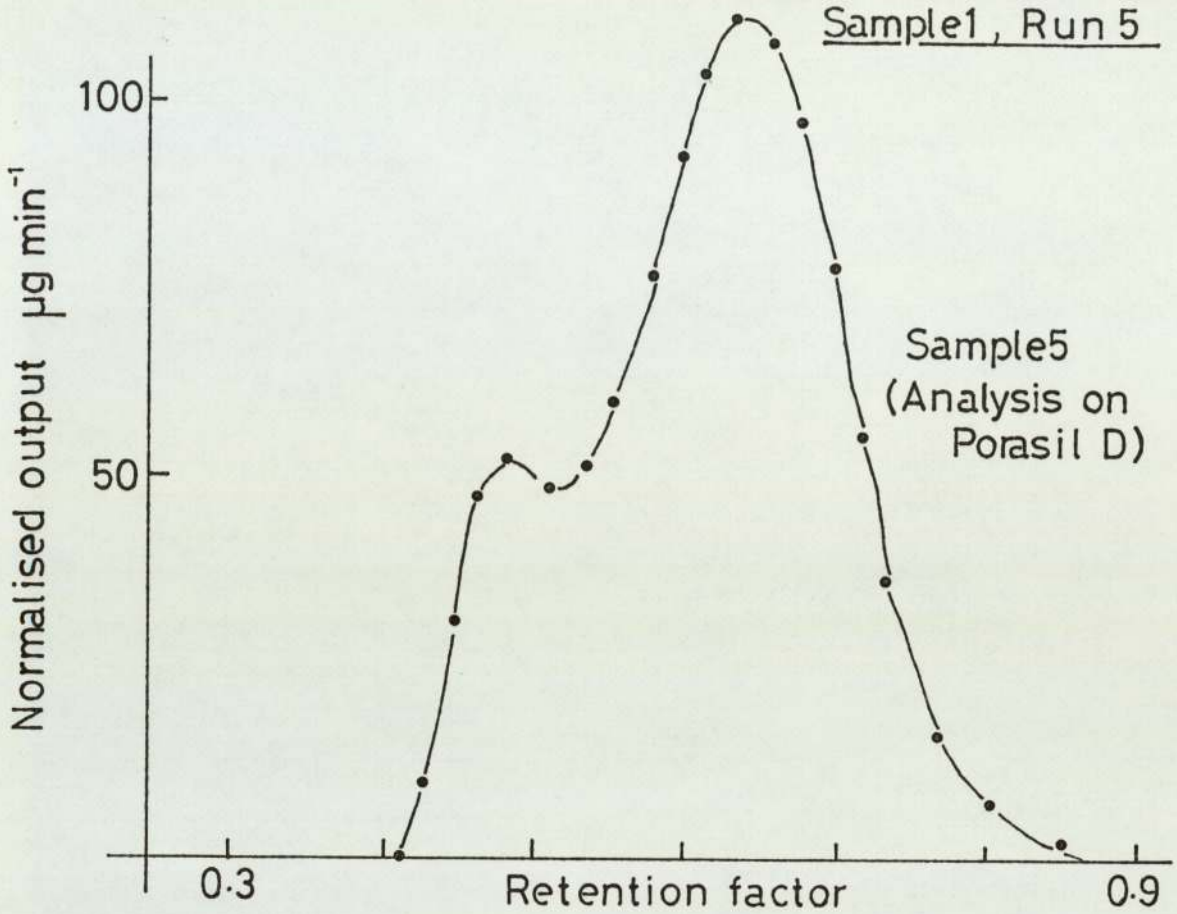

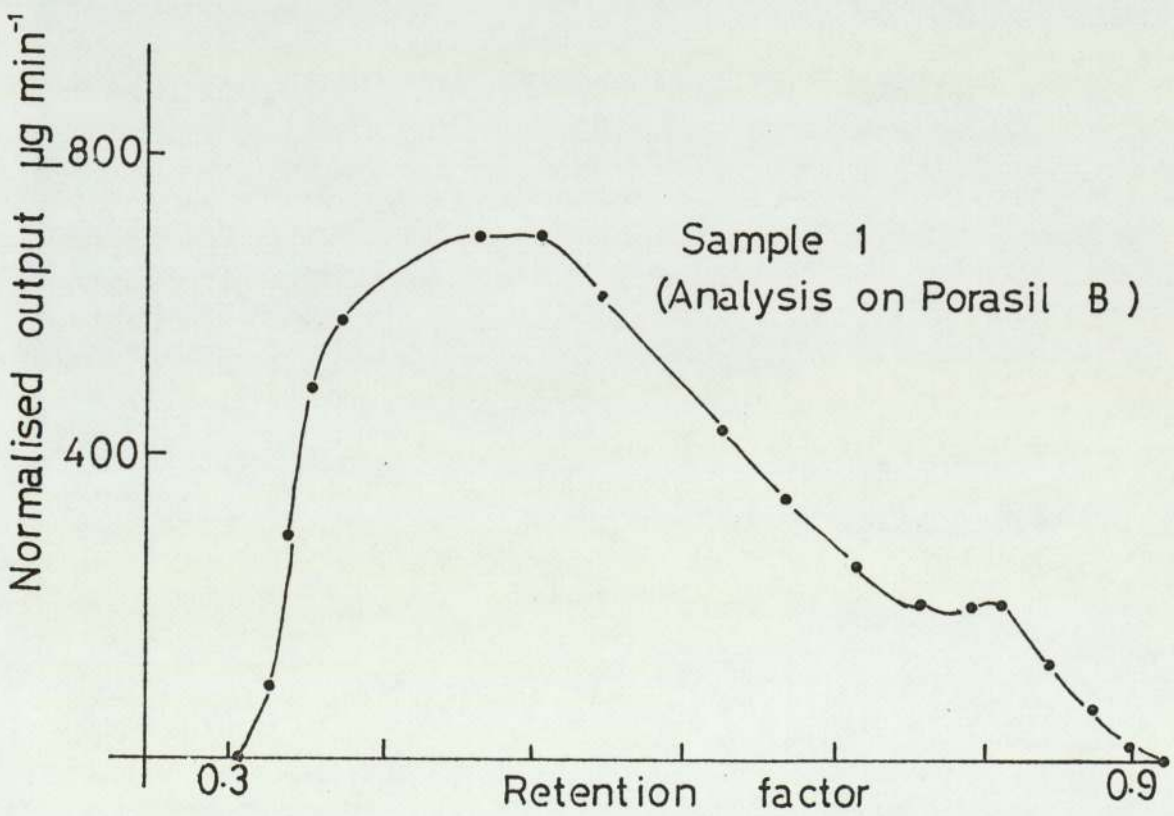

FIGURE 6·29 Low M.w. Product, Samples 2 and 3 Run 5
(Analysis on Porasil B)

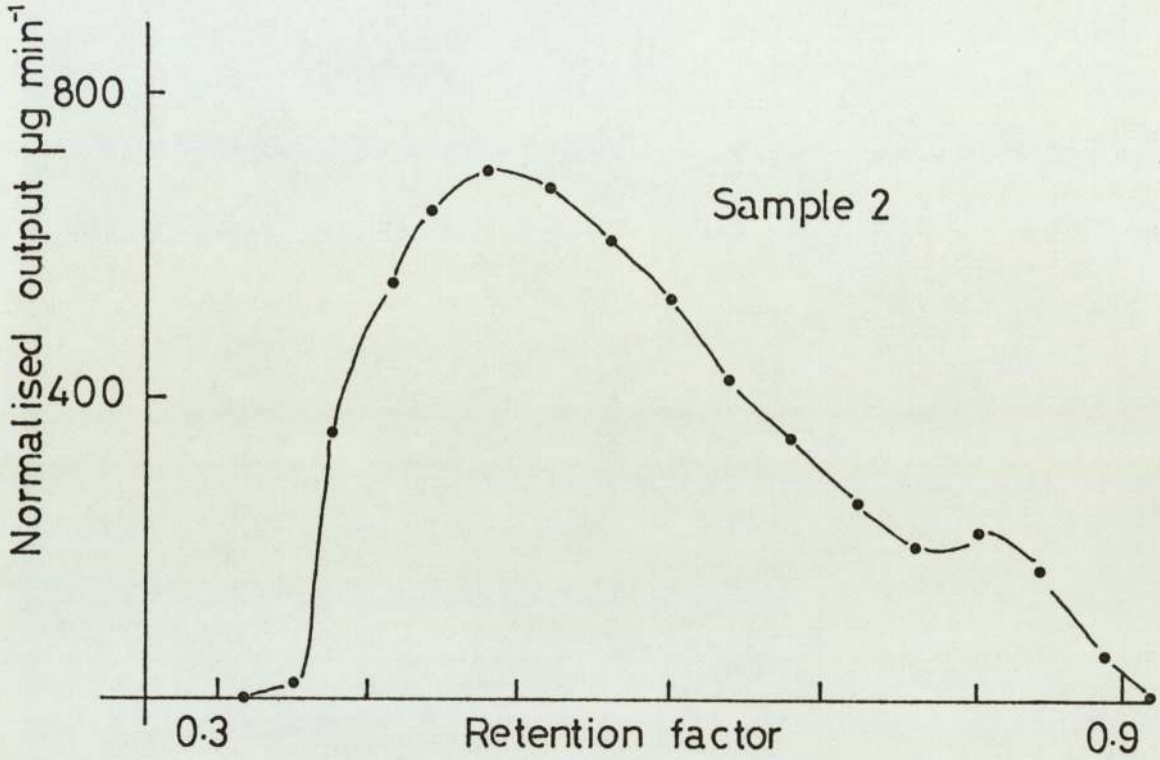

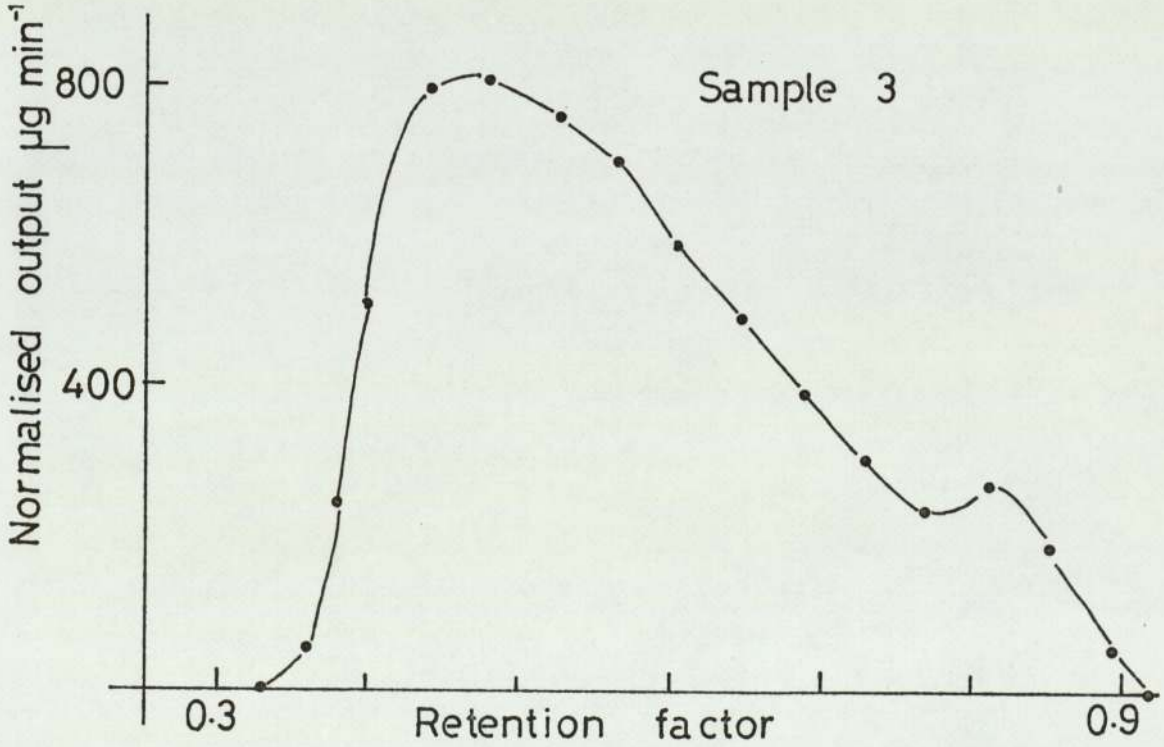

FIGURE 6·30 Low M.w. Product, Samples 4 and 5 Run 5
(Analysis on Porasil B)

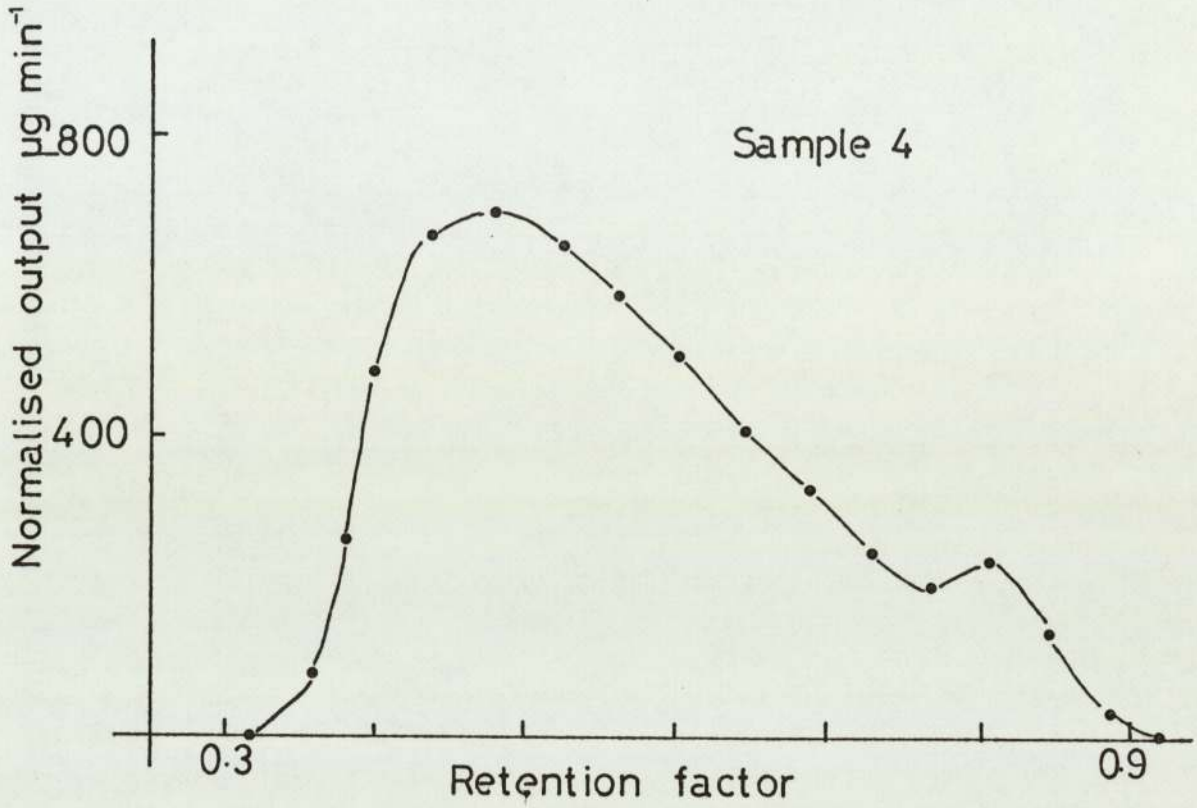

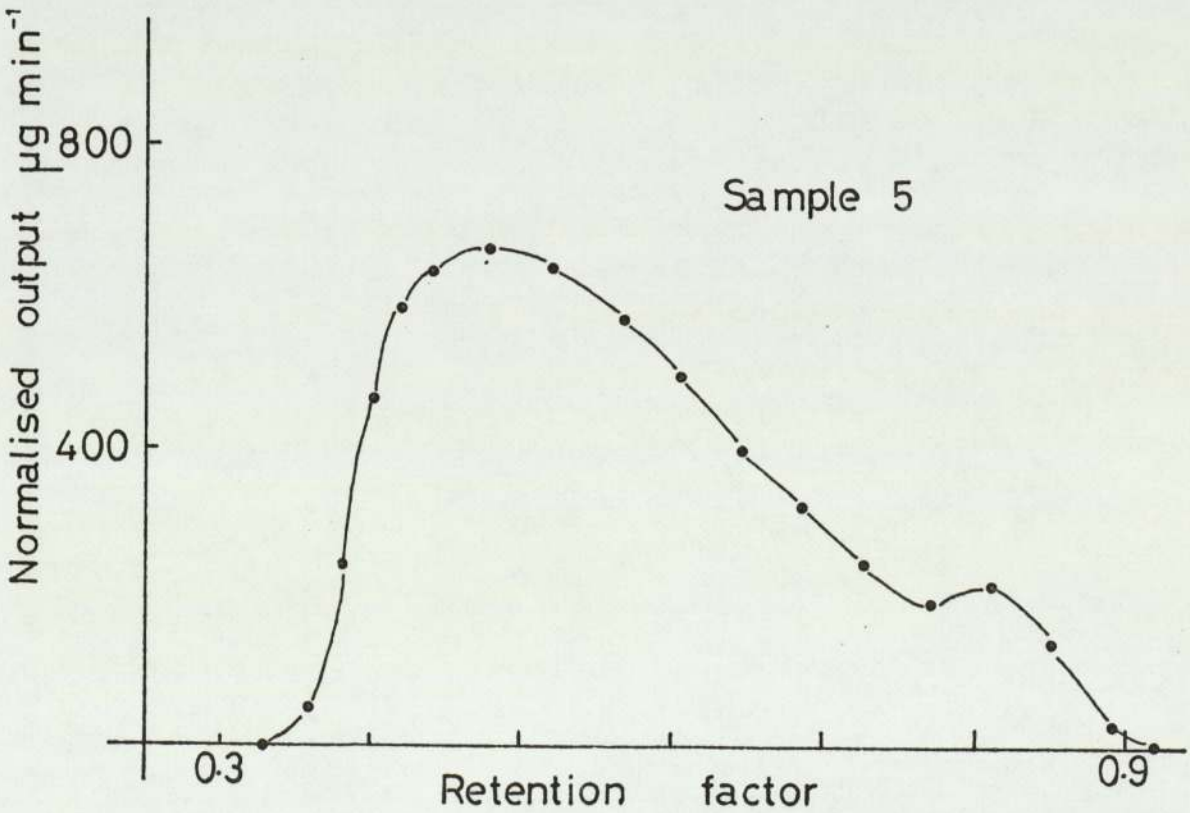

FIGURE 6.31 Product Distributions for Run 5

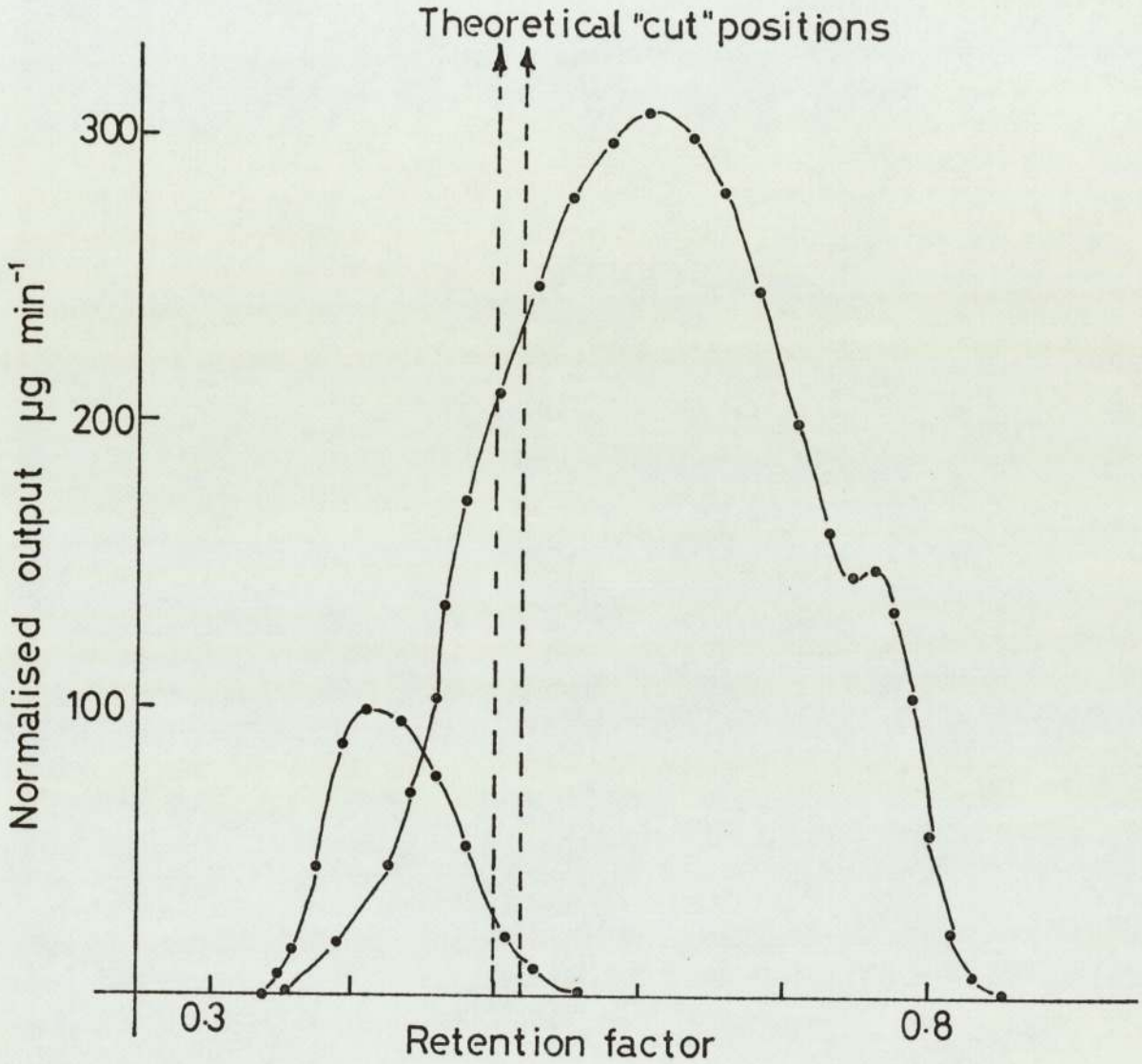

A consequence of the observed concentration effect is that fractionation could well be achieved at high dextran throughputs. This could be achieved by using high dextran concentrations and high feed rates. In Section 5.2.4.1 it was discussed how the two operating conditions used in the chromatograph would theoretically influence the fractionation process. The extent to which this effect occurs was worth experimental investigation, therefore experiments were undertaken to determine the effect of increasing the feed rate at high feed concentrations.

In Run 6 the feed concentration, eluent rate, purge rate and bundle speed were initially the same as those used in Run 5. The feed rate varied, over the duration of the experiment, from 0.125 cm^3 min^{-1} to 0.08 cm^3 min^{-1}. There was initially liquid leakage from the seal but this eventually stopped, and then flow conditions were relatively stable (Figure 6.15b).

Variations in the dextran mass balances (Figure 6.15c) are probably due to the changing feed rate. Product mean molecular weights and molecular weight distributions remained unchanged after 24 hours. A typical example of the separation achieved is presented in Figure 6.32. From this result it can be seen how only about 5% of the high molecular weight end of the feed distribution has been removed as the high molecular weight product.

Several attempts at increasing the feed rate proved unsuccessful. The increase in the back pressure, due to increased flow rate and liquid viscosity in the chromatograph, caused the mechanical seal to repeatedly fail. It was finally necessary to have both sealing faces professionally relapped to the required degree of

FIGURE 6·32 Product Distributions for Run 6

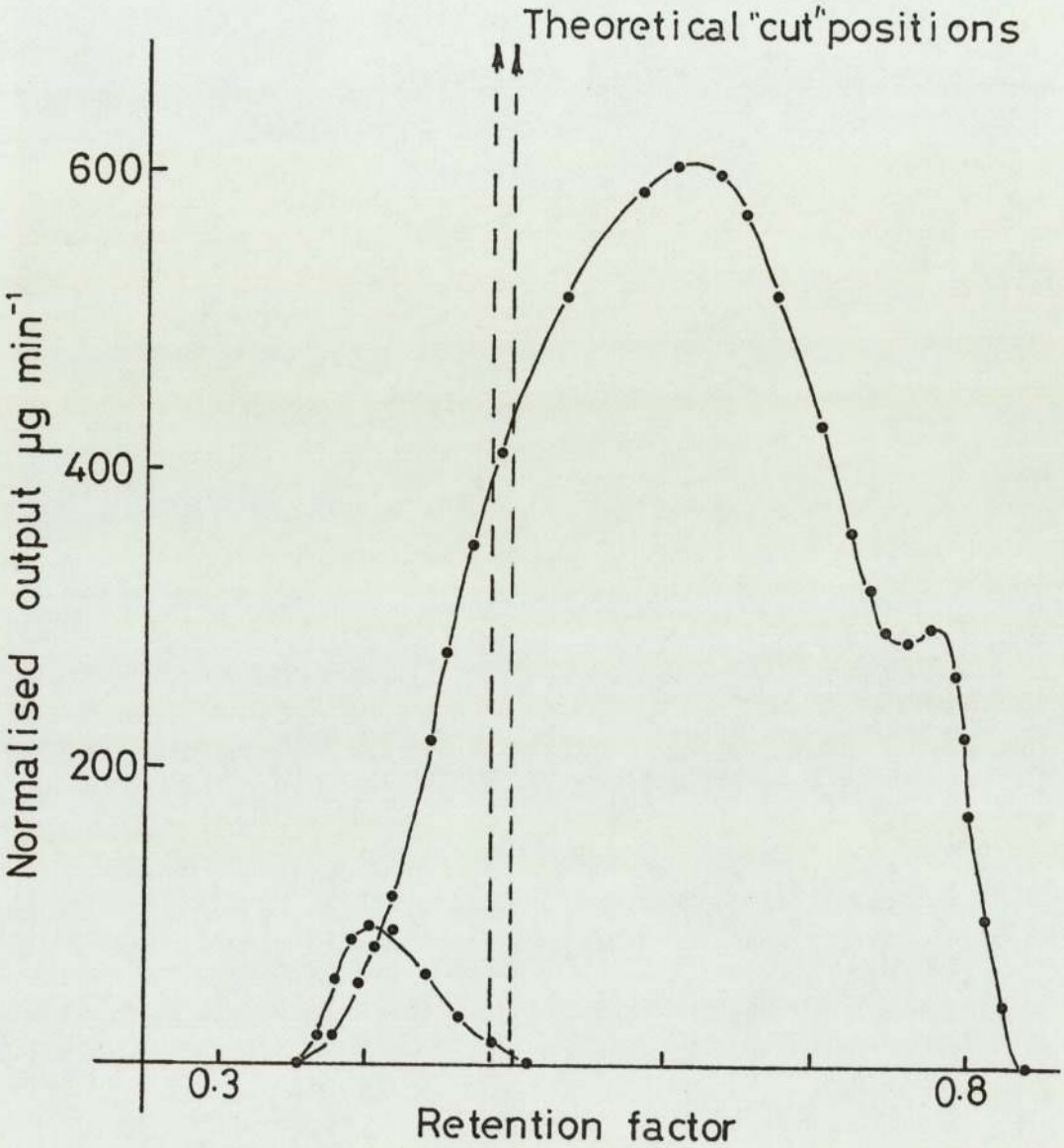

flatness before proceeding with the experimental programme. No further attempts were made to increase throughput.

Since one of the objectives of the research was to reduce the molecular weight distribution of the "40 hydrolysate" supplied by Fisons Ltd., a bulk sample of the low molecular weight product from Run 5 had been collected in order to remove the low molecular weight end of the distribution. The limitations on pressure drop implied that to achieve the required flow conditions it was necessary to alter the tube bundle speed from 0.0026 r.p.m. to 0.00207 r.p.m. This change in bundle speed was equivalent to altering the effective movement of the liquid held in the pores of the packing from a flow rate of 0.663 $cm^3\ min^{-1}$ to 0.526 $cm^3\ min^{-1}$.

The experiment to remove the low molecular end of the distribution, Run 7, was performed under comparatively dilute conditions. The possibility of concentration effects influencing the "cut" effected by the machine were therefore avoided. The feed concentration was measured as 2.5% w/v. In addition to the primary objective of this experiment it was proposed to show the effect of deliberately changing the eluent rate on the fractionation process. Flow rates were initially adjusted so that the "cut" positions coincided with the low molecular weight limit of the feed distribution (Figure 6.33). This part of the experiment continued for 144 hours. Samples collected over this period showed that as little as 1% of the dextran entering the chromatograph was removed as the low molecular weight product. Figure 6.34 gives a typical example of the separation achieved. It can be seen that under these flow conditions the feed molecular weight distribution has not been altered to any great extent.

FIGURE 6·33 Run 7 Feed Distribution

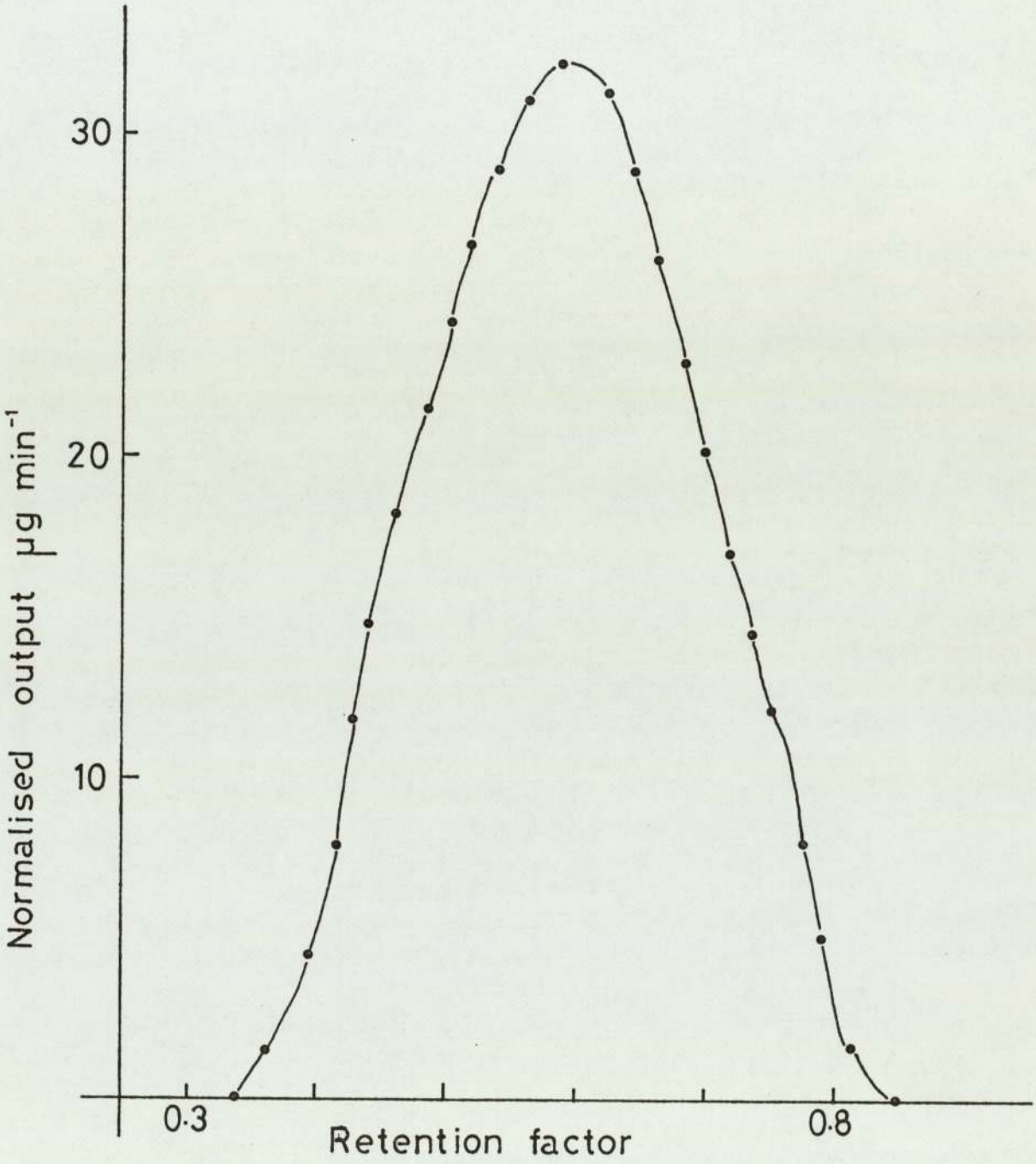

FIGURE 6.34 Product Distributions, Sample 3 Run 7.

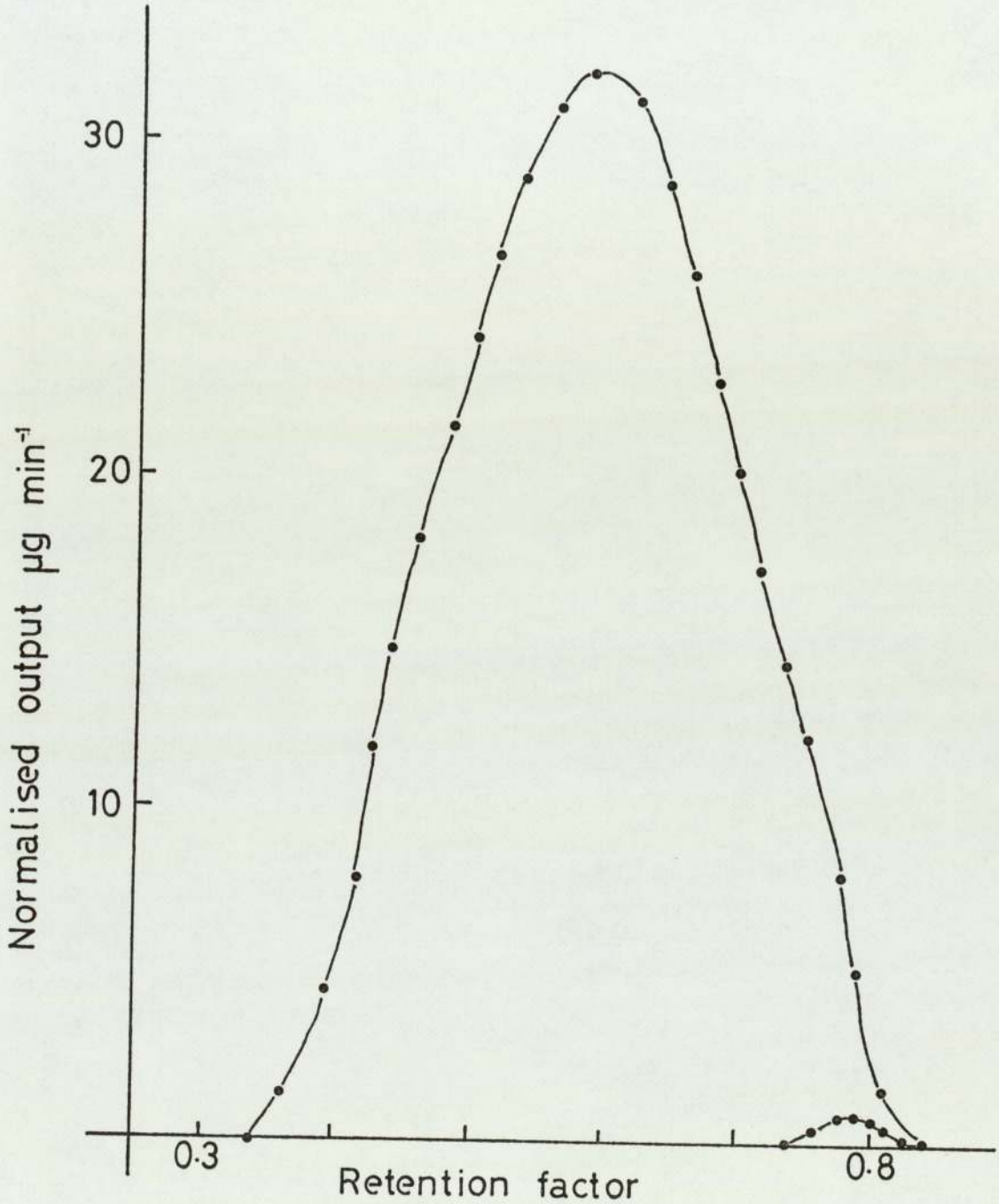

After the initial part of the experiment the eluent rate was changed from 1.13 $cm^3\ min^{-1}$ to 1.01 $cm^3\ min^{-1}$. This was equivalent to changing the prefeed "cut" position from a partition coefficient of 0.9 to 0.62 (retention factors of 0.78 and 0.68 respectively). The effect of this was reflected in the dextran mass balances, tabulated in Figure 6.16a and graphically presented in Figure 6.16c. The proportion of the feed distribution removed has been increased from 1% to about 20%. Figure 6.35 represents the fractionation achieved under these flow conditions. A feature of this result is the presence of a secondary peak at a retention factor of 0.48 (partition coefficient of 0.015). Since this peak is outside the range of retention factors occupied by the low molecular weight product distribution it was thought probable that it was due to a contaminating effect caused by the moving seal.

As has been discussed the mechanical seal relied, to some degree, on the presence of a liquid film between the two sealing faces. The counter current movement of the tube bundle would cause dextran held up in this film to move in the same direction as the bundle. This dextran could therefore have a contaminating effect on the products. Such an effect would explain the presence of a secondary peak in the low molecular weight product. By the same principle the high molecular weight product could also have been contaminated. However, since the sealing pressure is greatest at the high molecular weight product port the possibility of this occurring is reduced, because of the decrease in the thickness of the liquid film between the faces at this point.

FIGURE 6·35 Product Distributions, Sample 7 Run 7

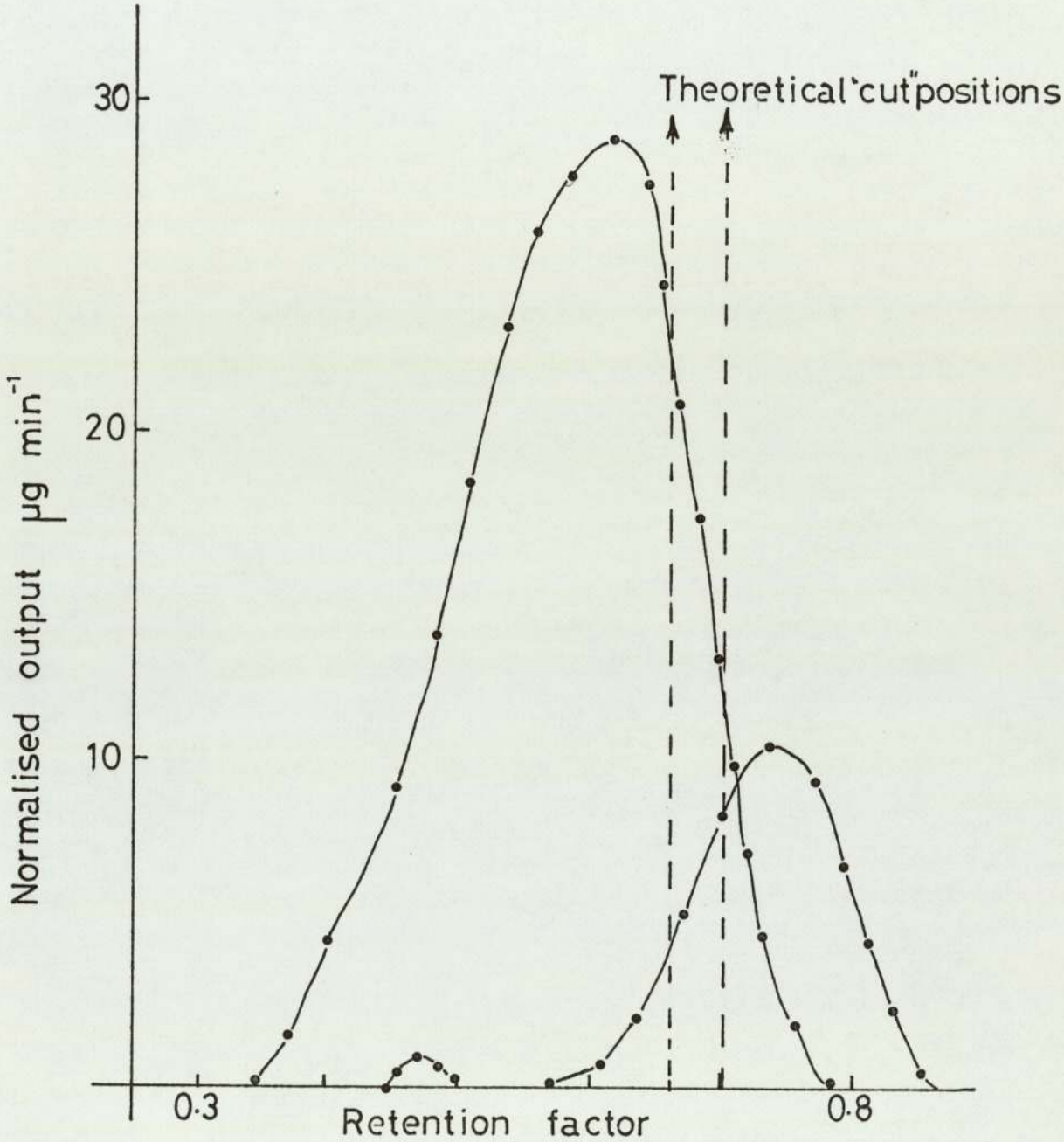

6.4.4 Conclusions

Despite the considerable care that was taken during all experiments to maintain a constant eluent output rate, it was found that during those experiments, numbered Runs 1-5, where flow conditions should ideally be the same, the eluent rate varied from a maximum of 1·1 cm^3 min^{-1} to 0.76 cm^3 min^{-1}. These variations were primarily due to liquid leakage from the seal and not pump failure. The onset of leakage followed no detectable pattern. For example, in Run 5 the flow rates varied very little despite a back pressure of 138-172 KN/m^2 (20-25 psig) compared with 69-86 KN/m^2 (10-12 psig) in Run 2, where the eluent output rate dropped from 1.02 cm^3 min^{-1} to 0.76 cm^3 min^{-1}. The temperature in both these experiments varied between 21.5^{o}C and 23°C which was well within the required temperature range. Such inconsistencies made interpretation of the experimental results difficult.

In Runs 1, 3 and 5 the variation in the eluent flow rate was small and well within experimental error. A comparison can therefore be made of the molecular weights of the products collected during these experiments. The mean molecular weight of the low molecular weight products increased from an average of 11,000 in Run 1 (feed conc. 0.56% w/v) to about 18000 in Run 3 (feed conc. 9.6% w/v) and finally to just over 20,000 in Run 5 (feed conc. 20.8% w/v). The corresponding increases in the high molecular weight products were 66,000 (Run 1), 125,000 (Run 3) and 195,000 (Run 5). These changes in the product mean molecular weights are in agreement with the observations made about a concentration effect causing a change in the "cut" effected by the chromatographic machine. The "cut" effectively shifting towards the high molecular weight end of the feed distribution.

A consequence of a change in the "cut" position will be that to maintain the cut position, and yet increase throughput by increasing the feed concentration, it will be necessary to increase the eluent rate. Precisely what effect this will have on the product molecular weight distributions is uncertain. However, since molecules of all sizes will be present in the mobile phase, any increase in the mobile phase velocity will promote the degree of overlap in the two product molecular weight distributions.

If high throughputs are to be achieved in continuous gel permeation chromatography then in addition to high feed concentrations it will be necessary to increase the feed rate. The purpose of Run 6 was to determine the effect of increasing feed rate on the process. It was shown that by increasing the feed rate at high feed concentration the degree of overlap in the product distributions increases. Such an effect, together with concentration effects might be expected to be detrimental but Ellison[22] has shown that, by increasing the eluent rate to counteract the effects of concentration, a dextran feed can be fractionated into two predominantly different molecular weight distributions at high feed concentrations (20% w/v) and an eluent to feed ratio of 1:1. Using equipment with a scale-up factor of 40 compared to the column cross sectional area of that used in this research, Ellison[22] has achieved throughputs of up to 2.8 tonnes per year.

A significant feature of Run 7 was the effect of changing the eluent rate. The resultant change in the "cut" position caused a change in the mean molecular weight of the low molecular weight product from <1000 to 5500, and a change from 22000 to 40000 in the

high molecular weight product. Although this change is only related to the molecular weight distribution of the feed, and the conditions used in this research it serves to demonstrate how a small change in the elution rate can influence the fractionation process. Run 7 also provided information about the adverse contaminating effect of using a moving mechanical seal, of the type used in the research, to produce the counter-current movement of the phases. Despite this, the main objective of establishing that continuous chromatography can be employed to reduce the molecular weight distribution of a polymeric feed was achieved. Figure 6.36 compares a cumulative plot of the original feed distribution with that of dextran T40 produced by ethanol precipitation and the product obtained after removing the high and low molecular weight ends of the original feed distribution.

In Section 6.44 it was mentioned that during runs 3,4,5 an increase in the concentration of the low molecular product was observed. It was thought probable that these increases were due to liquid loss from the seal brought on by temperature variations in the laboratory. In all three runs the increase occurred in the sample collected over the weekend period.

In common with other fractionation processes it is desirable to assess the effectiveness of the process. In a multicomponent systems, that consists of discrete components, expressing the percentage of each component in the products is one means of determining the effectiveness of a particular piece of process equipment. An alternative technique, commonly employed in chemical engineering, is to determine the equivalent number of ideal stages,

FIGURE 6.36 Cumulative Distributions

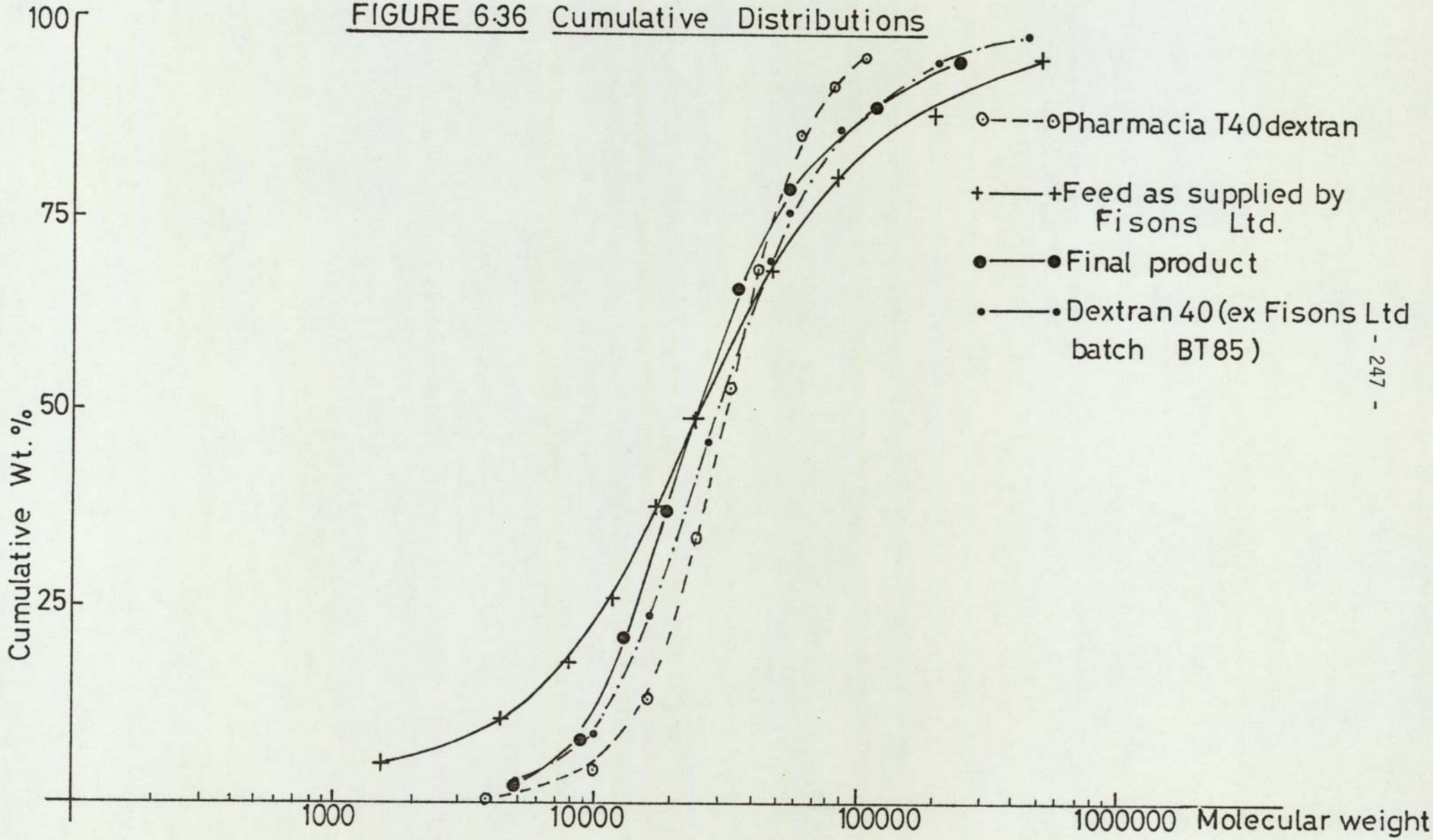

or "plates", required to bring about a specific degree of fractionation. Both these techniques cannot be applied to polymers because,

(i) both product streams contain the same material, the only difference is in their molecular weight distributions, and

(ii) the plate height is strongly dependent on the diffusion coefficient of the solute, which is of particular importance when fractionating polymers[158].

Therefore, from the above, the effectiveness, efficiency, of equipment used to continuously fractionate polymers is going to be dependent on the range of molecular sizes in the original feed. Consequently quantifying the efficiency of the process is a very complex problem.

However, since the objective of fractionating a polymer is to change its molecular weight distribution to within predefined limits, those operating parameters that effect the product require understanding before any attempt is made to quantify a particular fractionation. Two such factors, feed rate and concentration have been highlighted in the research, but the precise effect of other operating parameters on the fractionation process can best be determined by using a system which is not polymeric.

CHAPTER 7

Studies on the Continuous Separation of a Binary Mixture

7.1 INTRODUCTION

The use of the chromatographic machine to continuously fractionate a polymeric system had the disadvantage of using a feed with a molecular weight distribution. This feature complicated the investigation into the basic mechanisms governing the separation process. An obvious extension of the research was therefore to select and study the separation of a binary mixture. Each component of the binary should ideally have a single discrete molecular weight and with a well characterized chromatographic behaviour.

Since the chromatographic machine was already packed with Spherosil and any change in packing would be both an expensive and lengthy undertaking, it was decided to carry out the studies using the Spherosil packing. From the experimental information gained from the fractionation of dextran, the molecular weight range that could be separated on Spherosil XOB075 was evaluated as approximately 10,000 to 100,000, therefore the binary components would have to lie in this range. It was appreciated that these values were based on a calibration curve obtained for carbohydrate molecules, but it was assumed reasonable to use these molecular weights as a guide to selecting suitable binary components. In addition to the restrictions on molecular weight it was desirable that both components be soluble in aqueous solutions and that they should be obtainable in a pure state, in reasonable quantities (about 100-200 gms) and at a moderate cost. A naturally occurring mixture whose components were of a high value in a pure state would have been preferred from the point of stimulating industrial interest, but was not essential.

7.2 THE CHOICE OF BINARY COMPONENTS

A large number of chemicals can be separated or fractionated under suitable conditions by gel permeation chromatography, many examples of which are given in the text by Determann[13]. In many cases the chemicals used are incompatible with the aqueous conditions desired in this research.

A class of biochemicals that appeared suitable were proteins. These chemicals are water soluble and have high, but discrete molecular weights. In fact, gel permeation chromatography has become a well established technique for isolating proteins and also for determining their molecular weights. This technique usually involves a form of batch chromatography. The recovery of proteins from such columns are normally 100% but the separation is rarely so good as to leave no room for improvement[214]. Separations involving relatively large amounts of protein on batch columns can result in a decrease in column efficiency with the resultant loss of product purities and the quality of the separation. The use of continuous chromatography could be a means of increasing throughputs and product quality.

Since proteins satisfied the desirable features required of the binary mixture it was decided to investigate the range of proteins available. An examination of the catalogues, which list commercially available proteins, revealed the immense number of proteins that can readily be obtained. However, this did not give a clear indication of a suitable pair of proteins. In contrast, published literature proved more useful since several proteins have repeatedly been used in molecular weight determination studies[215-218]. Table 7.1 lists some of those proteins used. This table is by no means a comprehensive

Table 7.1

Protein/Enzyme	Molecular Weight	Reference
α-Chymotrypsinogen A	25,000	215
Pepsin	32,700	215
Alcohol dehydrogenase	80,000	-
Alkaline phosphotase	83,700	-
α-Amylase	45,000	223
Acid phosphotase	100,000	215
Cytochrome C	12,600	215
β-Lactoglobulin	35,000	216,223
Trypsin	23,500	-
Serum albumin bovine	69,000	215
Ovalbumin	45,000	215,223
α-Lactalbumin	16,000	216
Haemoglobin	64,500	215
Acetylcholine esterase	28,900	-
Ribonuclease	13,700	215

list of those proteins in the required molecular weight range, but represents those which were recommended or have been previously used for research purposes.

The quantities of proteins required for analytical or calibration purposes are small (<< 1 gm) and therefore, can economically be obtained. In this research comparatively large amounts were required. Consequently cost was a major consideration, and a factor which excluded the majority of the proteins listed in Table 7.1. The exceptions to this were pepsin, ovalbumin and bovine serum albumin (B.S.A.). These three proteins satisfied the criteria required of the binary mixture and had significant differences in their molecular weights. The final choice was pepsin and B.S.A., since ovalbumin[219] is susceptible to denaturation by shaking, when in solution. In addition, small amounts of insoluble denatured protein are often formed as a result of ordinary laboratory procedures when using ovalbumin at room temperatures.

Pepsin[220], a member of a class of proteins called enzymes, and bovine serum albumin[221,222] have molecular weights of 32,700 and 69,000 respectively. Both are soluble in an aqueous environment and can readily be obtained in a relatively pure form (> 96%). It is not proposed to discuss their individual biochemical and physiochemical properties since this is outside the scope of this research. Both pepsin and bovine serum albumin (fraction V) were purchased from Sigma (London) Ltd. and used without further purification.

The analytical procedure used in the dextran fractionation studies had proved to be an accurate but time-consuming technique. This, together with an increased work load on the Auto Analyser system, prompted the need for an alternative and faster method of analysis.

Miller et al.[223] have successfully shown that proteins can be dyed without significantly changing their chromatographic properties. It was therefore decided to dye each protein a different colour and then use a colorimetric technique for their analysis. This technique had the added advantage of providing a visual means of monitoring the progress of the separation experiments. The dyes used were Procion Blue MX-3G and Procion Red MX-2B and were obtained, free of charge, through the Academic Relations Department of Imperial Chemical Industries (Blakeley, Manchester).

7.3 THE ANALYSIS OF THE DYED PROTEINS

Analysis to determine the concentration of dyed protein solutions was carried out using a SP1800 U.V. Spectrophotometer (Pye Unicam, Cambridge, U.K.). The absorbance of solutions of dyed proteins were measured in matched 10 mm glass cells at frequencies of 520 nm for Procion Red and 610 nm for Procion Blue. Calibration of the spectrophotometer was performed using standard dyed protein solutions. The calibration curves obtained and the method used to calculate unknown component concentrations are given in Appendix 7.

During the development work, which is discussed in the following section (7.4), the spectrophotometer was used in the continuous mode with a 0.2 cm flow cell. The absorbance response was continually monitored with a variable speed chart recorder.

7.4 THE DEVELOPMENT OF THE EXPERIMENTAL METHODS

7.4.1 The Dyeing Technique

Aspinall and Miller[223,224] demonstrated that proteins could be dyed with the Procion series of triazine dyes and the coloured

products analysed by gel permeation chromatography. Procion dyes form covalent bonds with proteins[225] without greatly altering their molecular weight. An increase in molecular weight of the order of 3% has been measured[223,224].

Initially the dyeing technique was that commonly used for dyeing textiles[224]. Equal volumes of dye and protein solutions (1% w/v solution) are mixed and allowed to stand for 5 minutes. Sodium chloride (0.02 g cm^{-3}) is then added, dissolved and the mixture allowed to stand at ambient temperature for a further 30 minutes. Solid anhydrous sodium carbonate (0.001 g cm^{-3}) is then added to hydrolyse the excess dye, a reaction which is normally complete within one hour[226].

Both proteins, when dyed by this technique and analysed on a batch column, packed with Spherosil XOB075, gave chromatographs similar to that represented in Figure 7.1a. This figure shows two distinct peaks. The smaller peak is due to the protein and the larger is that due to excess dye. To avoid time-consuming preliminary separations with the chromatographic machine steps were undertaken to separate the excess dye from the dyed protein by a simple, non-chromatographic method. Attempts at reducing the amount of dye used in the reaction were only partially successful, reducing only the height of the dye peak rather than eliminating it.

A standard method of purifying[227] bovine serum albumin involves a crystallisation stage using ethanol. At ethanol concentrations in excess of 25% and at a temperature of -10°C bovine serum albumin crystallises out of solution. Since large amounts of methanol were more easily obtained, the precipitation of the dyed

FIGURE 7.1 Dyed Protein Chromatograms

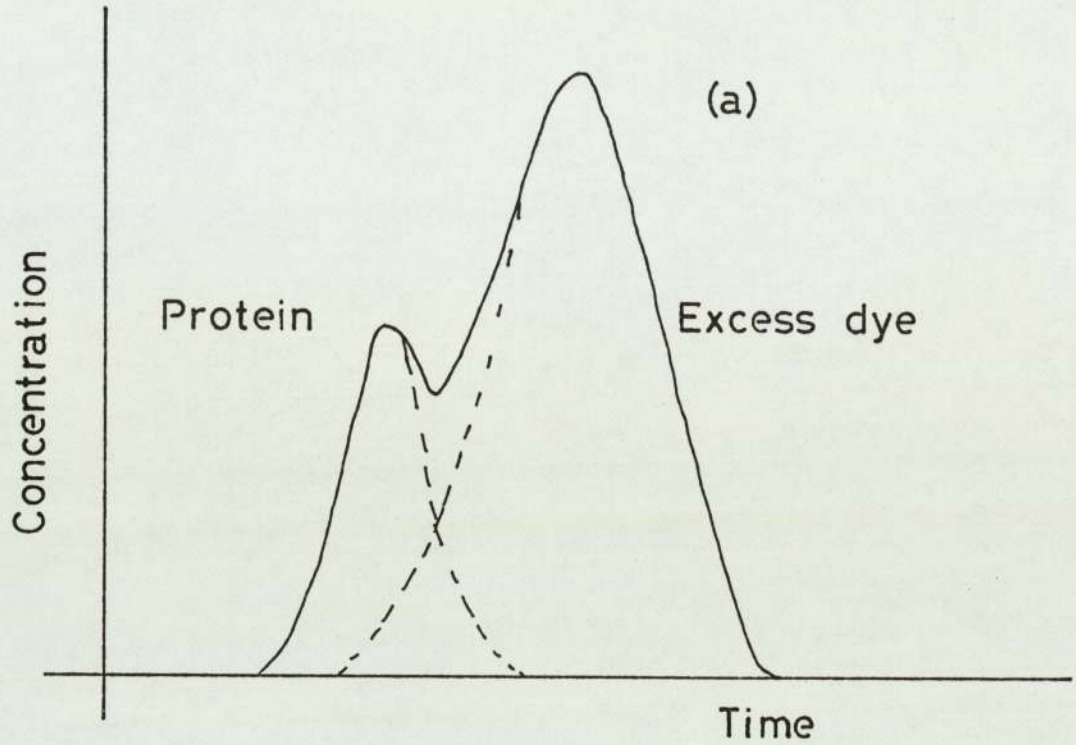

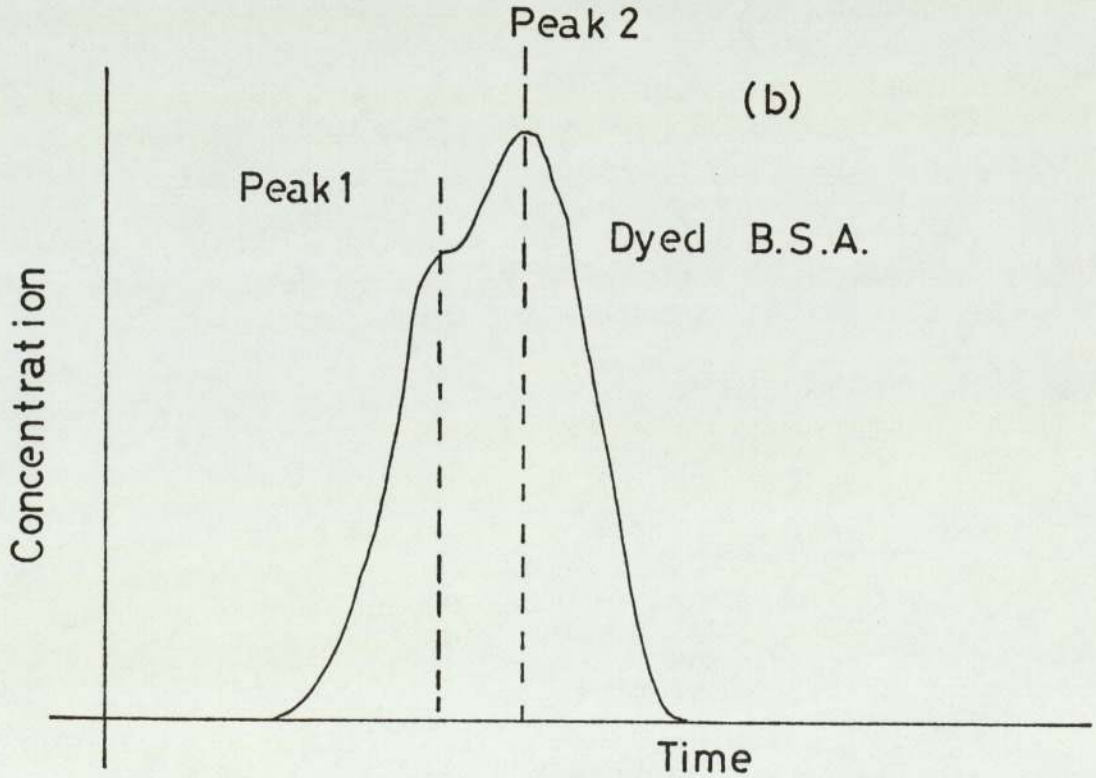

proteins was first attempted with methanol. Tests were initially carried out to confirm that the dyes were soluble in water-methanol mixtures. Both dyes were found to be partially soluble in pure methanol and readily dissolved in mixtures containing as little as 5% v/v water.

It was found that pouring the dyed protein mixture into methanol readily precipitated the bovine serum albumin at ambient temperature but it proved necessary to cool the dyed pepsin-methanol mixture to between 0-5°C to achieve the required results. Analysis of the redissolved dyed proteins established that precipitation with methanol effectively removed the excess dye. However, the amount of methanol required was 100 cm^3 per 50 mg of protein. This was acceptable for small scale investigations on batch columns but the chromatographic machine required an estimated 200 cm^3 of feed solution per experiment. Therefore, to make up a 1% protein solution of feed many litres of methanol would be required to precipitate the necessary dyed protein. Experiments were then undertaken to reduce the amount of methanol needed to precipitate the protein.

Initially, the protein and dye concentrations used were increased from 0.01 g cm^{-3} to 0.1 g cm^{-3}. Analysis of dyed B.S.A. gave a chromatogram (Figure 7.1b) which suggested that two components were present. It had previously been established that methanol precipiation removed the excess dye and it was therefore concluded that the change in the dyeing procedure had caused a change in the structure of bovine serum albumin. One of the properties of bovine serum albumin is that it has monomeric, dimeric and trimeric molecular forms[221]. Consequently, it was concluded that the increase in dye and protein concentrations used in the dyeing procedure could have caused the

formation of high molecular weight forms of bovine serum albumin. Similar effects were not observed with pepsin regardless of the dyeing procedure employed.

The following parameters were then investigated in order to develop a suitable dyeing procedure for bovine serum albumin;

(i) the ratio of dye to protein

(ii) the concentrations of dye and protein

(iii) sodium chloride concentration

(iv) pH

Table 7.2 summarises the experiments performed and the results obtained. In all these experiments analysis was performed on a column packed with Spherosil XOB030 (equivalent to Porasil D). The eluent was a Tris-HCl buffer pH 8. Before analysing any of the dyed bovine serum albumin samples a sample of undyed bovine serum albumin was analysed to obtain, for comparison purposes, its retention factor and peak shape. The final dyeing technique was developed as a result of this series of experiments.

The final method used for dyeing the proteins was as follows. Protein was dissolved in buffer (0.1M Tris-HCl) to give a concentration of 50 mg cm^{-3}, this solution was then mixed with an equal volume of the appropriate dye solution (25 mg dye cm^{-3}). The dyeing reaction was allowed to proceed for 30 minutes after which solid anhydrous sodium carbonate (0.01 gm per 50 mg of dye) was added, the mixture stirred, and then allowed to stand for a further 5 minutes. The solution was then poured into about ten times its volume of methanol. The methanol had been previously cooled to between $0^{o}C$ and $5^{o}C$. The precipitated dyed protein was filtered off and washed with methanol. Excess methanol was

Table 7.2 Summary of Dyeing Experiments

Expt. No.	Weight of Protein mg	Weight of dye mg	Protein solvent cm^3	Dye solvent cm^3	Sodium chloride g	Number of peaks	Retention factor
1 (Pure proteins)	200	0	Buffer 0.1M 2	0	0	1	0.64
2	200	200	Buffer 0.1M 2	Water 2	0.1	1	0.45
3	100	100	Buffer 0.1M 5	Water 5	0.04	1	0.57
4	100	100	Buffer 0.1M 10	Water 10	0.01	1	0.54
5	100	100	Buffer 0.1M 10	Water 10	0.05	1	0.45
6	100	100	Water 10	Water 10	0	1	0.55
7	100	100	Water 2	Water 2	0	1	0.46

Contd....

Table 7.2 Continued

Expt. No.	Weight of Protein mg	Weight of dye mg	Protein solvent cm^3	Dye solvent cm^3	Sodium chloride g	Number of peaks	Retention factor
8	100	100	Water 5	Water 5	0.04	1	0.511
9.	100	100	Buffer 0.1M 10	Water 10	0.02	1	0.58
10	100	100	Buffer 0.1M 10	Water 10	0.01	1	0.57
11	100	100	Buffer 0.1M 2	Water 2	0	1	0.5
12	100	50	Buffer 0.1M 2	Water 2	0	1	0.63
13	200	100	Buffer 0.1M 4	Water 4	0	1	0.64

removed by drawing air through the filtrate. The dyed protein was then redissolved in fresh buffer solution. Care had to be taken with the dyed bovine serum albumin to ensure that it was collected and redissolved as quickly as possible. This was because prolonged contact (in excess of half an hour) with methanol reduced its solubility.

By using the dyeing technique the two proteins could easily be distinguished and analysed. Chromatographic analysis indicated that both proteins were single components with significantly different partition coefficients on Spherosil XOB075. Details of the experimental method adopted to determine component partition coefficients is discussed in Section 7.4.2. The two dyed proteins provided a suitable, although synthetic, mixture for separation studies using the continuous chromatograph.

7.4.2 The Choice of Eluent

Beau et al.[138] have reported studies of the separation of horse serum and human blood serum on Porasil B. A 1% aqueous solution of triethylene glycol was used as the eluent so that adsorption was minimised. In view of the possibility of solute adsorption it was considered prudent to carry out a series of experiments to determine the most suitable eluent. There are forms of deactivated Porasil, Porasil X, available which alleviate the adsorption problem with the silica type of packing.

Three small columns (25 cm x 0.6 cm I.D.) were packed with clean, deaerated slurries of Spherosil XOB075 (200 μm-400 μm). The packing procedure was the same as that described in Section 6.2.3.2. Each of the columns was then used, in turn, for the following experiments.

One column was conditioned with a 1% triethylene glycol solution over two hours by pumping the solution through the column at a liquid flowrate of about 1 cm^3 min^{-1}. A solution of dyed bovine serum albumin (about 0.1% w/v) was then pumped through the column and the column output continuously monitored using the spectrophotometer. When the output response had reached a steady value the response of the input solution was measured. The results obtained are presented in Figure 7.2a. They indicate that the dyed protein solution eluting from the column at equilibrium gave an adsorption value, at the appropriate wavelengths that was equal to that of the input. The conclusion was drawn that the adsorption, on the chromatographic packing, of the dyed protein was not significant. On purging the column there was visual evidence, due to a pinkish tinge to the packing, that some protein had been irreversibly adsorbed.

In an attempt to eliminate the adsorption effect, the above experiment was repeated with a freshly packed column. The ionic content in the eluent was increased by making the 1% triethylene glycol solution 0.1Molar with respect to sodium chloride. The same experimental procedure was used as that described above. The results obtained are presented in Figure 7.2b. During the course of this experiment an increase in the colour intensity of the packing was observed. Purging with a 1% triethylene glycol solution failed to remove the adsorbed protein. It was concluded that an increase in the ionic strength had promoted the adsorption of the dyed protein. This was confirmed by the shape of the column output response curves (Figure 7.2b).

FIGURE 7.2 Dyed Protein Response Curves from Adsorption Experiments

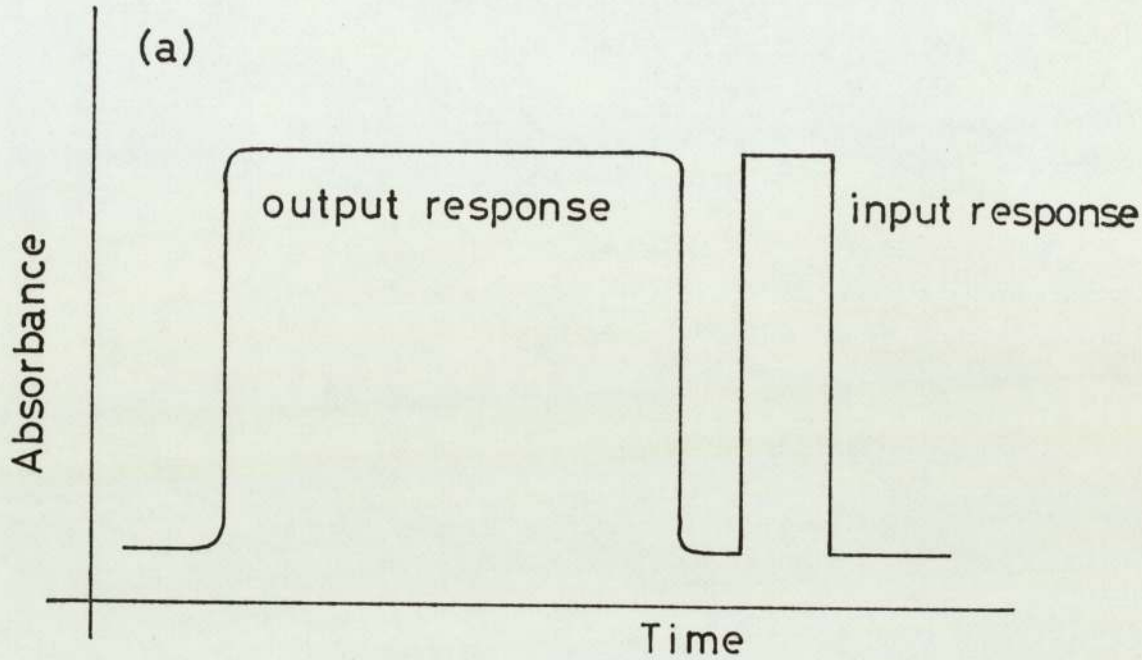

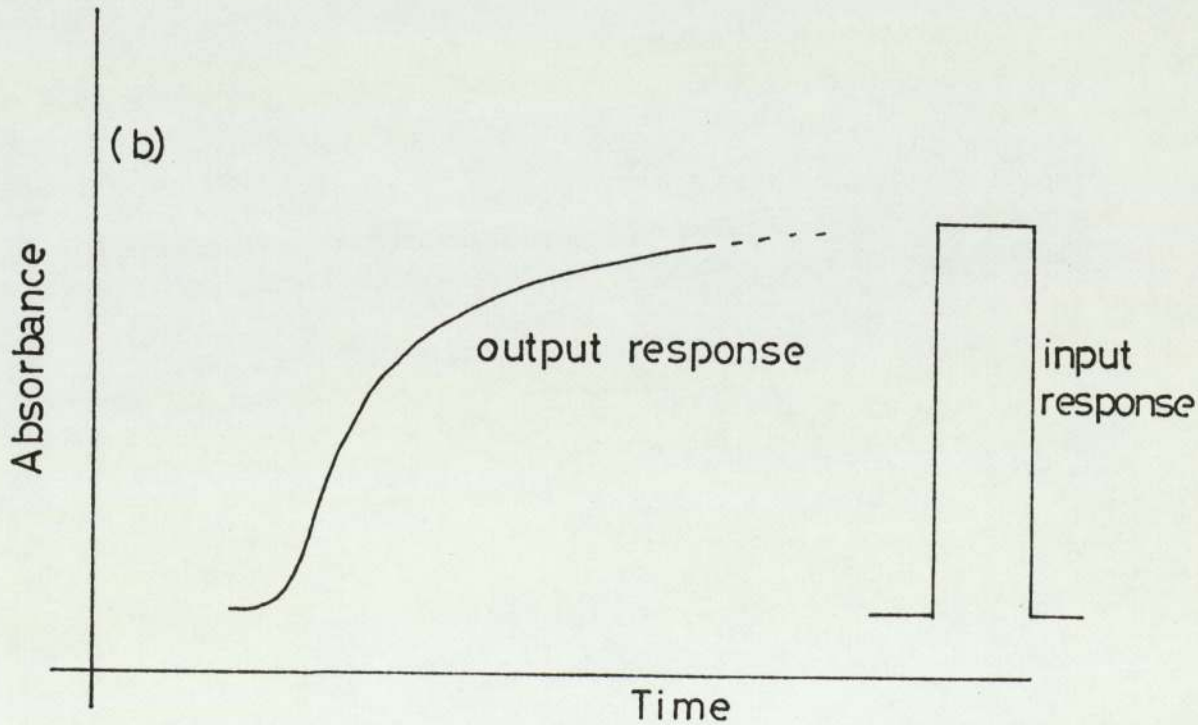

A final experiment was performed in which the third freshly packed column was used to confirm the results initially obtained. The concentration of dyed protein in the eluent, a 1% triethylene glycol solution, was increased to about 0.5% w/v and the results and conclusions were the same as described in the first experiment. In the first and the third experiments it had been observed that the glycol protein-eluent solution on initially exiting from the column gave a response equivalent to that of the input. This fact, despite the observed irreversibly adsorbed protein, led to the conclusion that the degree of adsorbtion was small and that the amount of dyed protein adsorbed was negligible. This conclusion was based on qualitative rather than quantitative evidence.

From the experiments described above a 1% triethylene glycol solution was initially chosen to be a suitable eluent. Experiments were then performed to determine the partition coefficients of the two dyed proteins. The amount of unused Spherosil XOB075 was small therefore a sample of contaminated packing was cleaned, with concentrated nitric acid, and thoroughly washed with distilled water before packing it into a 0.8 cm I.D. glass column to give a stable packed bed depth of 60 cms. A 1% triethyleneglycol solution was pumped through the column, to condition it, and freshly prepared sample of the two dyed proteins loaded separately on to the column and eluted. Both proteins were completely and irreversibly adsorbed on to the packing. This contradicted the earlier conclusions that triethylene glycol effectively suppressed adsorption. Since this adsorption effect had not been observed with the previously unused Spherosil employed in earlier experiments it was thought possible that washing the packing with nitric acid had in some way activated adsorption sites. If acidic

conditions had activated the sites, then it was possible that alkaline conditions would have the reverse effect.

Sodium hydroxide solution was added to the eluent, 1% triethylene glycol solution, to give a pH of 10. When this solution was pumped through the column the adsorbed protein was slowly removed. A 0.1M buffer (Tris-HCl, pH 8) proved to be faster and more effective. Once the adsorbed protein had been removed the column was reconditioned, by pumping eluent (1% w/v triethylene glycol) through it, and the dyed proteins reloaded and eluted. The calculated retention factor for each protein was equal to that of a totally excluded molecule. Solutions of Blue Dextran ($\overline{M}_W > 2 \times 10^6$) and acetylacetone (<1% w/v) were used to determine the retention factors of a totally excluded and included molecule.

A column of similar dimensions to that described above was prepared and packed with clean Spherosil XOB075. The column was then washed with buffer (0.1M Tris-HCl), then water and finally conditioned with the eluent (1% w/v triethylene glycol). Samples of the two dyed proteins were then eluted through the column and the retention factors calculated. In each case the retention factor corresponded to that of Blue Dextran, namely 0.42. Eluting the dyed proteins with distilled water produced the same result. A similar exclusion effect has subsequently been observed by Ellison[22] with dyed Dextran 'T' fractions and by Holding[228] with F.I.T.C. Dextran. Both these researchers eluted with distilled water on Spherosil. It was thought probable that this exclusion effect was a result of a property of the packing and that the eluent (1% w/v triethylene glycol) fails to suppress the effect. An alternative eluent was therefore sought.

In earlier experiments it had been shown how buffer solutions removed adsorbed dyed protein from the packing. Buffer solutions were therefore considered as possible eluents, and a series of experiments designed to investigate their suitability.

Buffer solutions at pH 5 (0.1M potassium hydrogen phthalate) and pH 7, 8 and 9 (0.1M tris (hydroxymethyl) aminomethane) were prepared and used to elute samples of the dyed proteins. At a pH of 5, and to a lesser degree at a pH of 7, both dyed proteins were completely adsorbed on to the packing. In contrast at a pH of 8 the adsorbed protein was removed and both protein samples eluted at substantially different retention factors. These were 0.54 for dyed bovine serum albumin and 0.67 for dyed Pepsin. Similar retention factors were experimentally determined with a buffered eluent at a pH of 9.

The incompatability of Spherosil, a porous silica matrix with a very large surface area (100 m^2/gm for XOB075)[229], with mildly alkaline eluents was a problem that required careful consideration. This was because any change in the pore size distribution and packing structure, due to silica dissolution, would adversely effect separating conditions both on batch columns and in the chromatographic machine. Enquiries were made of Waters Associates (Stockport, Cheshire)[230] and Rhodia U.K. Ltd. (London)[231] about this problem. The general opinion was that the silica type of packings were relatively stable at pH values less than 9, and that no significant effects should occur when using an eluent buffer at a pH of 8. The eluent chosen was therefore a 0.1 Molar solution of tris(hydroxymethyl) aminomethane. Sufficient concentrated hydrochloric acid was added to adjust the pH to 8.

The reagents used were of Analar or equivalent grade.

The partition coefficients of the dyed proteins were experimentally determined using a column (0.8 cm internal diameter) packed with Spherosil XOB075 (200 μm to 400 μm) to give a packed bed length of about 60 cms. Blue dextran and acetylacetone solution were used to determine the totally excluded and included volumes of the column. A peristaltic pump (Watson-Marlow, Cornwall) was used to pump the eluent. Equation 4.2 (Chapter 4) was used to calculate the partition coefficients. Numerically these were 0.28 for dyed bovine serum albumin and 0.58 for dyed pepsin, the accuracy of these values was estimated to be in the region of ±3%. The ratio of the component partition coefficients gave a separation factor of 2.07.

7.4.3 Preliminary Continuous Chromatograph Experiments

Prior to beginning any experimental separationsthe following maintenance was carried out on the continuous chromatograph. The seal faces were separated and carefully cleaned. Viton 'O' rings in the spring loaded valves were replaced and the ball races supporting the tube bundle checked and where necessary replaced. Hamilton G.T.S. valves (Field Instruments Ltd.) were screwed into four of the tube connecting blocks at the base of the tube bundle. These valves permitted sampling of the eluent during experiments. Unfortunately, circumstances prevented these sampling devices from ever being used.

When the maintenance had been completed the machine was reassembled and the seal faces allowed to run-in. Distilled water was pumped through the chromatograph over this period. Mass balances were periodically carried out until the leakage had dropped to less

than 2%. The eluting and purging fluid was then changed to the buffer solution (0.1M tris-HCl, pH 8) and the bundle packing conditioned overnight. The bundle speed had provisionally been set at 0.0026 r.p.m., the same speed as that used in the dextran studies.

After the conditioning period the eluent rate was altered to 1.04 cm^3 min^{-1} and a feed solution containing the dyed proteins (approximately 1% w/v) pumped into the bundle at a flow rate of 0.047 cm^3 min^{-1}. Flow conditions corresponded to "cut" partition coefficients of 0.34 and 0.404 in the prefeed and postfeed sections respectively. Both conditions were well within the theoretical separation limits of 0.28 and 0.58 fixed, under ideal conditions, by the component partition coefficients. Two hours after starting to feed protein solution into the machine there was visual evidence of excessive liquid loss from the inside and outside of the moving seal faces. Over this time the eluent back pressure was observed to gradually decrease from 103 KN/m^2 (15 p.s.i.g.) to 48 KN/m^2 (7 p.s.i.g.). A liquid mass balance revealed that the leakage had risen to over 10%. Purging the bundle with buffer followed by distilled water failed to restore the seal to a satisfactory operating condition. The precise cause of the rapid deterioration in the liquid seal posed a serious problem to the continuation of any further separation experiments.

It has been discussed in Chapter 4 how the satisfactory operation of moving seals rely, to some degree, on the maintenance of a lubricating boundary film between the sealing faces. The formation and maintenance of this film is dependent on the surface tension and, as a consequence, the wetting of the two sealing faces by the sealed fluid. However, since proteins have surfactant properties a rapid

drop in the surface tension of a liquid film between the sealing faces is to be expected. The drop in surface tension results in an increase in the wetting of the seal faces and subsequent seal failure. Surface tension measurements, using a Torsion Balance (White Electrical Instruments Ltd., Walsall), confirmed a drop in surface tension between distilled water and protein solutions. Table 7.3 lists the surface tension of distilled water, a 6% w/v dextran solution for comparison purposes, the protein feed solution, the buffer solution and a sample of the products. The table indicates that the surface tension dropped a minimum of 10% at the product ports and a maximum of 25% at feed point.

Table 7.3 Surface Tension Measurements

Fluid	Surface Tension Nm^{-1}
Distilled water	0.076
Buffer solution	0.074
6% Dextran solution	0.07
Product	0.067
Feed	0.057

The fact that purging the bundle with water had failed to restore satisfactory operating conditions it was decided to separate and examine the seal faces. Flecks of graphlon were found in several areas on both the stainless and graphlon faces. During the course of the dextran experiments a similar graphlon build up had

been observed. However, this had taken place over a period of several months rather than hours. It was thought probable that the increase in the wetting of the seal faces was responsible for the rapid build up of these graphlon flecks. This was because as the bundle face moves against the graphlon the edges of the troughs, machined into the stainless steel face, shave small amounts of graphlon from the static face. These slivers of graphlon then build up in localised areas and eventually cause separation of the seal faces. The particles of graphlon are kept in the liquid film by its increased wetting characteristics. These characteristics effectively prevent the particles from adhering to the faces, except where the film thickness is reduced as a result of a decrease in the liquid back pressure. Either film breakdown or seal face separation could individually or collectively result in the failure of the seal.

The problem therefore, was to reduce or if possible eliminate the surface tension and wetting effects. Since increasing the surface tension of a liquid is impossible, a practical solution was to reduce the wetting of the seal faces by the sealed fluid. This was effectively achieved by coating both faces with a thin layer of a hydrophobic material, in this case Silicon valve grease (Dow Corning). The use of silicon grease was only a partial solution to the problem because there was still the problem of a decrease in the surface tension of the liquid film between the faces. This could not be overcome without a major redesign of the equipment. However, there were a number of courses of action that could be taken to reduce the magnitude of the surface tension effect.

As a result of the pressure gradient around the sealing face the sealing load applied by the pneumatic rams varies around the seal.

This causes the thickness of the liquid film between the sealing faces to decrease from a maximum at the point of highest back pressure to a minimum at zero back pressure. Operating at lower eluent rates would reduce the difference between the two extremes in the film thickness. The bundle speed was therefore reduced in the hope that this would produce more favourable operating conditions. Despite the measures taken to obtain a satisfactory seal it was later found that they were only partially successful. At no stage in this part of the experimental program did the seal operate without some degree of leakage.

In Chapter 6 (Section 6.4.5) it was discussed how there was experimental evidence to suggest that temperature fluctuations in the laboratory adversely effected the running of the chromatographic machine. To avoid the possibility of this reoccurring a simple temperature control device was installed in the oven. The temperature control device that was a fixture of the oven was unable to control the temperature accurately below about 40°C. A Fisons Fi-monitor was therefore attached to a 60 watt electric light bulb and placed in the oven to act as a heater. The detector from the monitor was fixed to a sensitive mercury thermometer in the oven. A small box fan provided sufficient air circulation to ensure that the temperature was maintained in all experiments between 28°C and 29°C.

Before beginning a detailed experimental programme, two preliminary separations were carried out so as to develop a suitable experimental procedure. During these experiments it was established that the flow conditions remained comparatively stable for a nominal 24 hour period from the start of an experiment. The start up procedure developed was as follows; approximately two hours before

the scheduled start of the experiment, the seal faces were separated and carefully cleaned with acetone to remove any attached or loose graphlon. A thin layer of silicon grease was applied to each face, the seal reassembled and run-in for two hours before the start of the experiment. This procedure did not permit the optimum time for the faces to run-in, but it did allow the silicon grease to be most effective during the course of the experiment. Product samples were collected every two hours with the fraction collector, described in Appendix 1, and liquid mass balances carried out at regular intervals to check on the flow conditions. At the end of each experiment the eluent and feed pumps were stopped and the contents of pairs of tubes purged out and collected. The purge time was calculated from the bundle speed and the number of tube pairs. The purge samples were collected to provide information on component concentrations throughout the tube bundle.

The problem of liquid leakage was one which could not completely be overcome hence careful consideration was given to the objectives of this part of the research.

The limitation imposed by having to use a fixed bundle speed restricted the major objective to determining the influence of the eluent flow rate on the separation process. It was appreciated that, because of the leakage problem, these experiments could not be used to quantify the separation process, but it was hoped they would lead to a better qualitative understanding and in particular about the effects of the discontinuity in flow conditions at the feed point.

7.4.4 Data Treatment

The samples collected during each experiment were analysed,

using the spectrophotometer, and the component concentration calculated according to the method given in Appendix 7. Graphs of component outlet concentration versus time have been plotted.

Before plotting the concentration profile data, consideration was given to the best means of presentation. This was because a purged sample's concentration was a function of the tube purging time and purging rate. They therefore had to be normalised to take this into consideration. In addition, these concentrations had to be scaled to the liquid volume available, in a tube pair, to each component. The available tube volume was based on a components experimentally determined partition coefficient and the total tube volume. This technique makes the assumption that there is mobile and stationary, liquid, phase equilibrium, which, by the transient nature of the process, is not the case.

Normalised and scaled component concentration distributions should, ideally, be plotted in the form of a histogram because each concentration is representative of a mean value based on the available tube volume. Figure 7.3 is a typical example, it can be seen how this format confuses the interpretation. The data has therefore been plotted as point concentrations, each concentration corresponding to the mid point of a pair of tubes (Figure 7.4b).

7.4.5 Experimental Errors

Experimental errors fall into two categories, firstly those induced by the measurement of the machine operating parameters and secondly analytical errors.

FIGURE 7.3 Normalised Concentration Profile (Histogram form)

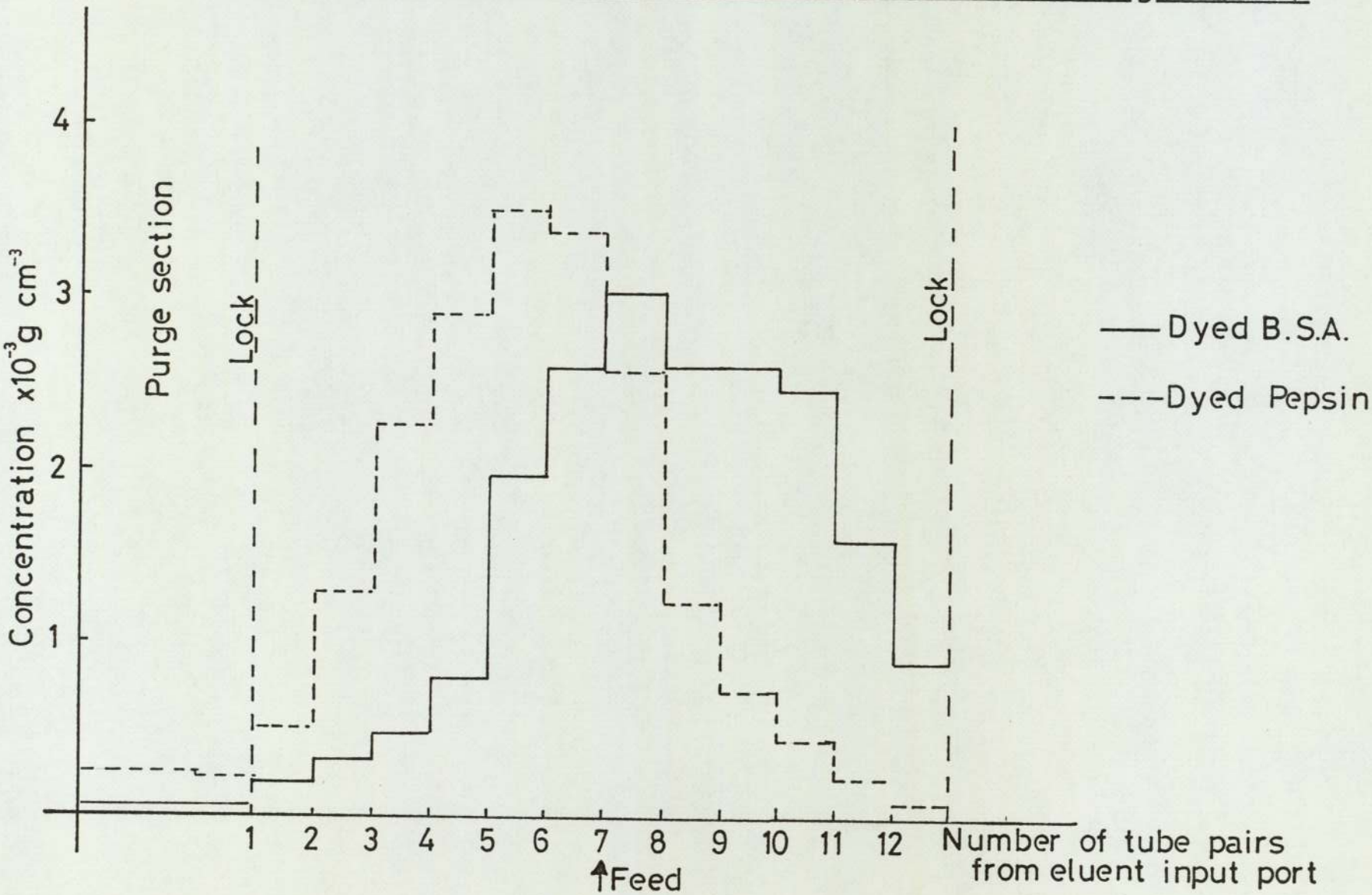

Errors in the analytical technique were attributed to the calibration procedure rather than the instrument used. The S.P. 1800 U.V. spectrophotometer is a highly accurate instrument and therefore errors in the readings obtained were assumed to be negligible. The calibration procedure involved the preparation of dyed protein solutions of known concentration. The error in preparing these solutions was small (<1%) however the main error was due to the method of determining the concentration of the base solution. This method involved drying a known volume and weight of dyed protein solution to a constant weight. An estimate of the error involved in this procedure was ±2%. Consequently the error in calculating sample concentrations was expected to be of the same order. This error could have been reduced to a negligible amount if the graphs had been based on sample optical density (O.D.) rather than concentration. The reason for this was that the spectrophotometer readings were in terms of optical density, which, up to a point, is a linear function of concentration (see calibration plot Appendix 7). The error attributed to the sample concentrations is due to the method of calibration rather than the method of analysis. However, the more conventional means of expressing the data was preferred.

The errors induced by the measurement of input and output flow rates to and from the chromatographic machine were expected to be of the same order as those defined in Section 6.4.2. Fluctuations in the eluent and purge output rates, due to leakage, produced a maximum change in the eluent rate of ±6%. Normally the change was less than ±3%. Variations in the purge output rate due to leakage were of the order of ±2%.

The bundle speed used in this part of the research was measured as 0.00207 r.p.m. (equivalent to a 8.3 hour cycle time). Variations in the measurement of the bundle speed was found to be less than ±1%.

The overall error in the sample concentrations therefore become ±2% and for the normalised concentration distribution, neglecting the effect of leakage the error becomes ±6%. This figure includes the error due to the partition coefficients. Finally mass balances and theoretical "cut" calculations are expected to have errors of ±5% and ±3% respectively.

7.5 BINARY SEPARATION STUDIES

7.5.1 Experimental Results

Summaries of the experimental operating conditions together with the normalised concentration profiles and product output curves are presented in Figures 7.4-7.9. A complete record of sample concentrations for each experiment has been included in Appendix 8.

The feed solution in all the experiments performed contained a nominal 1% w/v of each dyed protein. Run times were restricted to 24 hours, which was equivalent to about three revolutions of the tube bundle. The question as to whether a pseudo-equilibrium was established within the 24 hours is uncertain. As has been mentioned operating conditions became unstable after the initial 24 hours. The bundle speed was held constant in all experiments at 0.00207 r.p.m. and the eluent and feed rate varied. Table 7.4 lists the mean eluent rates in the prefeed and postfeed sections and the corresponding "cut" values they effect, in each experiment.

Table 7.4 Mean Eluent Rates and "Cut" Partition Coefficients

Run Number	Prefeed flow rate $cm^3\ min^{-1}$	Prefeed "cut" partition coefficient	Postfeed flow rate $cm^3\ min^{-1}$	Postfeed "cut" partition coefficient
1	0.867	0.47	0.917	0.56
2	0.786	0.34	0.836	0.42
3	0.678	0.12	0.728	0.22
4	0.688	0.14	0.738	0.24
5	0.69	0.15	0.84	0.44
6	0.87	0.49	1.02	0.77

Three experiments, Runs 1, 2 and 3, were carried out at a constant feed rate of 0.05 cm^3 min^{-1} and mean postfeed rates of 0.917 cm^3 min^{-1}, 0.836 cm^3 min^{-1} and 0.728 cm^3 min^{-1} respectively. The corresponding prefeed flow rates were 0.867 cm^3 min^{-1}, 0.786 cm^3 min^{-1} and 0.678 cm^3 min^{-1}. The "cut" values for each run are given in Table 7.4. In all the experiments, except Run 3, the cut values lay within the theoretical limits of separation imposed by the component partition coefficients.

In an attempt to experimentally determine the influence of a second component on component concentration profiles, an experiment, Run 4, was carried out using only one component (dyed bovine serum albumin) in the feed solution. The flow conditions were similar to those used in Run 3. These were a feedrate of 0.05 cm^3 min^{-1} and postfeed and prefeed eluent rates of 0.738 cm^3 min^{-1} and 0.688 cm^3 min^{-1}.

Two final experiments, Runs 5 and 6, were carried out with a feedrate of 0.15 cm^3 min^{-1}. This feed rate was chosen because it equals the maximum theoretical limits in elution rates, fixed by the component partition coefficients (Equation 5.21). Initially eluent rates were set such that, in each of the two experiments, only one of the flow conditions corresponded to a "cut" value which lay within the theoretical limits. The objective of this was to determine the influence of the postfeed and prefeed flow conditions on the separation process.

Unfortunately in all the experiments there was a considerable degree of liquid leakage from the mechanical seal, the consequences of which undoubtedly effected the stable operation of the chromatographic machine. No further experimental runs were therefore undertaken.

Figure 7.4a Binary Run 1 Results Summary

Feed concentration,

(i) dyed bovine serum albumin = 0.9×10^{-2} g cm^{-3}

(ii) dyed pepsin = 0.85×10^{-2} g cm^{-3}

Temperature, Pressure and Flow Rates

Time hrs.	Temp. ^{o}C	Pressure KN m^{-2}	Eluent + Purge input $cm^3 min^{-1}$	Feed input $cm^3 min^{-1}$	Purge output $cm^3 min^{-1}$	Eluent output $cm^3 min^{-1}$
0	28	96	2.88	0.05	1.904	0.961
5	28.5	96	2.88	0.05	1.949	0.926
16	28	96	2.87	0.05	1.920	0.847
18	28	103	2.88	0.05	1.835	0.905
24	28.5	103	2.87	0.05	1.835	0.936

Theoretical "cut" Partition Coefficients

	Prefeed cut partition coefficient	Postfeed cut partition coefficient
	0.56 0.5 0.35 0.46 0.52	0.68 0.59 0.45 0.54 0.61
Average	0.48	0.57

FIGURE 7.4 Binary Run 1 Concentration Profile

(b)

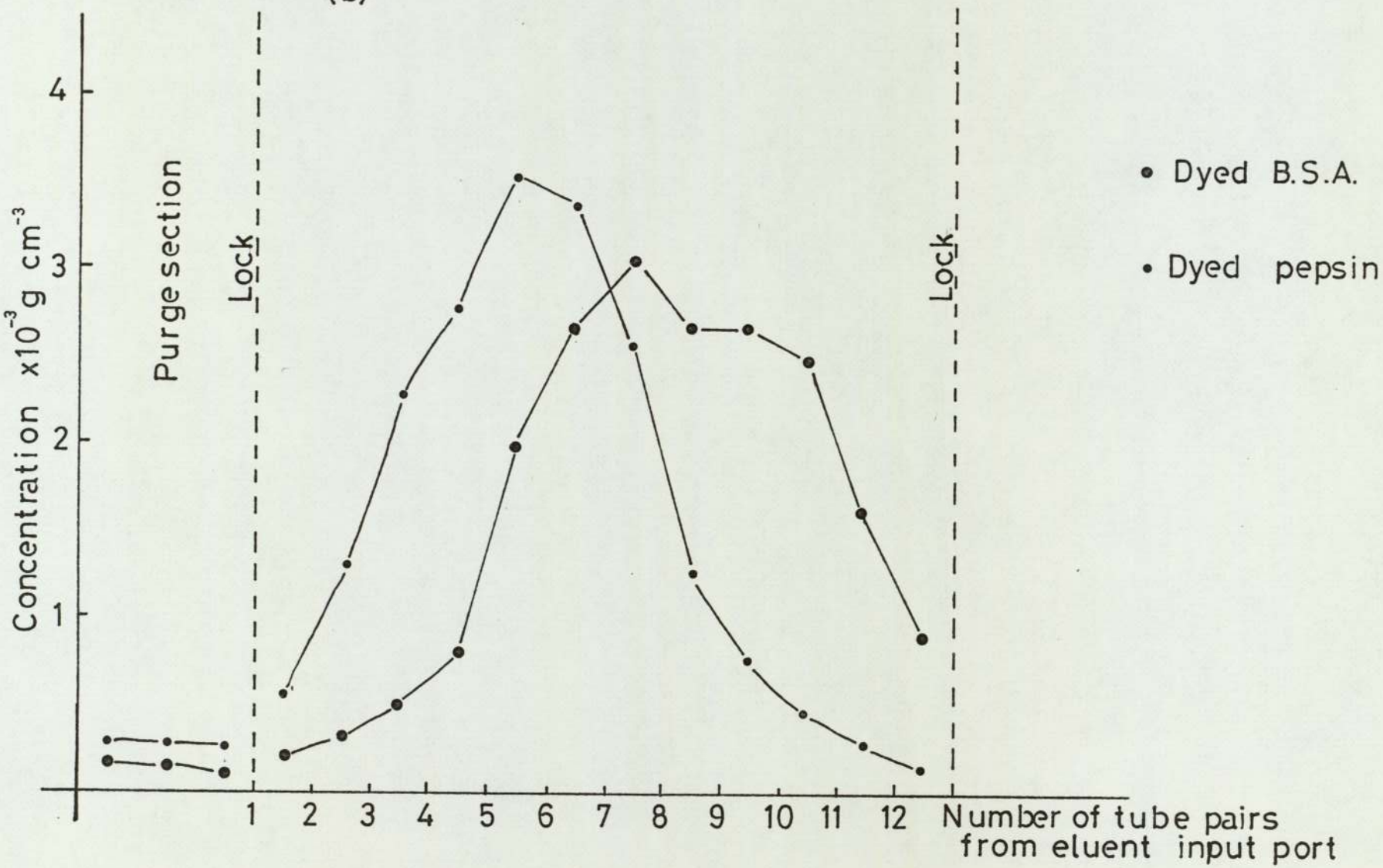

FIGURE 7.4 Product Output Concentrations for Run 1 (c)

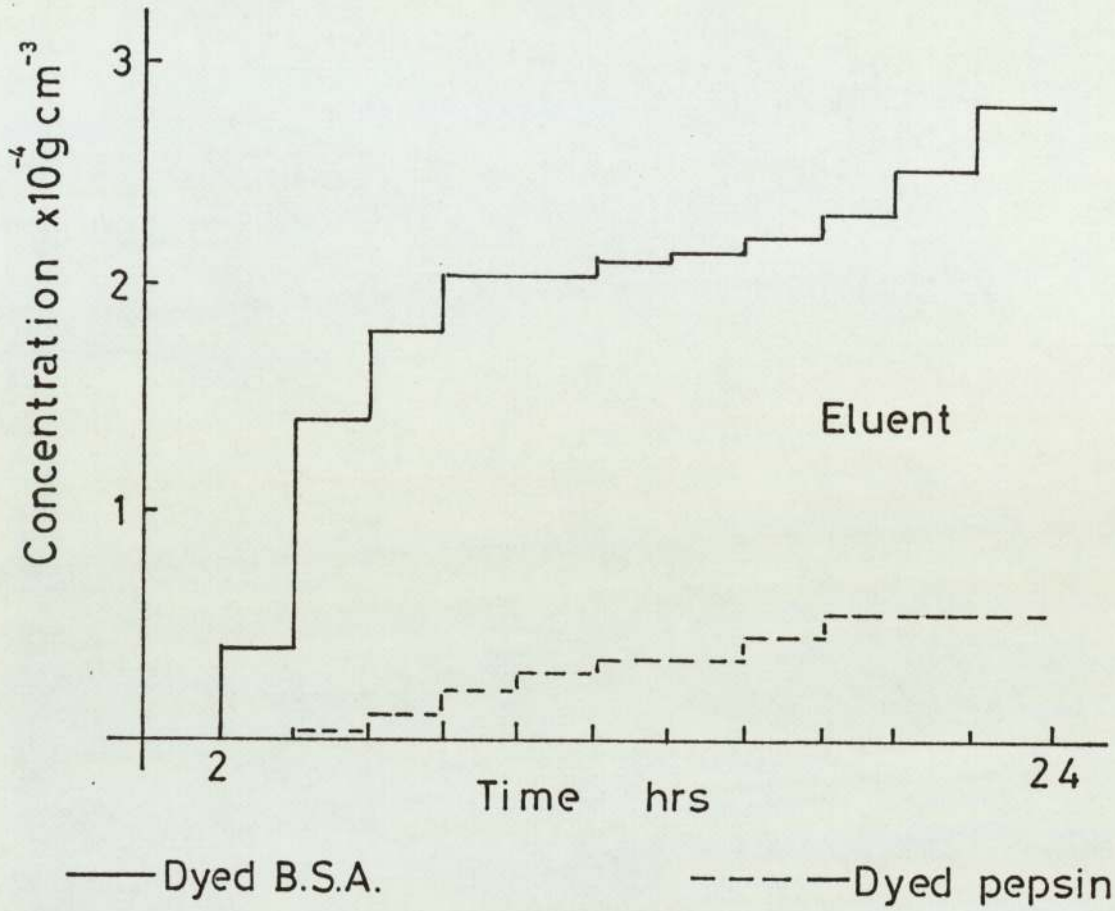

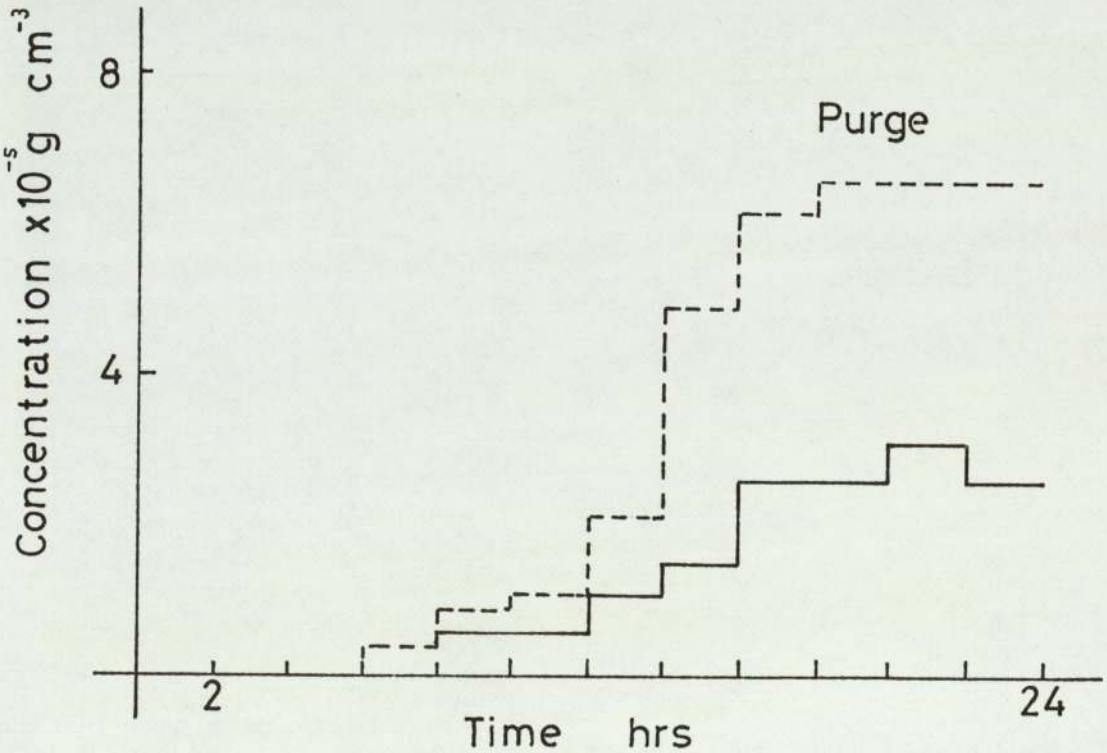

Figure 7.5a Binary Run 2 Results Summary

Feed concentrations,

(i) dyed bovine serum albumin = 0.88×10^{-2} g cm^{-3}

(ii) dyed pepsin = 0.85×10^{-2} g cm^{-3}

Temperature, Pressure and Flow Rates

Time hrs.	Temp. ^{o}C	Pressure KN m^{-2}	Eluent + purge input cm^3 min^{-1}	Feed input cm^3 min^{-1}	Purge output cm^3 min^{-1}	Eluent output cm^3 min^{-1}
0	28.5	90	2.73	0.05	1.881	0.863
16	29	90	2.77	0.05	1.889	0.831
18.5	29	83	2.72	0.05	1.838	0.832
20.5	29	83	2.73	0.05	1.832	0.814
22.5	29	83	2.76	0.05	1.874	0.829
24	29	83	2.76	0.05	1.818	0.845

Theoretical "Cut" Partition Coefficients

	Prefeed cut partition coefficients	Postfeed cut partition coefficients
	0.38 0.32 0.32 0.29 0.32 0.35	0.47 0.42 0.42 0.38 0.41 0.44
Average	0.33	0.42

FIGURE 7.5 Binary Run 2 Concentration Profile

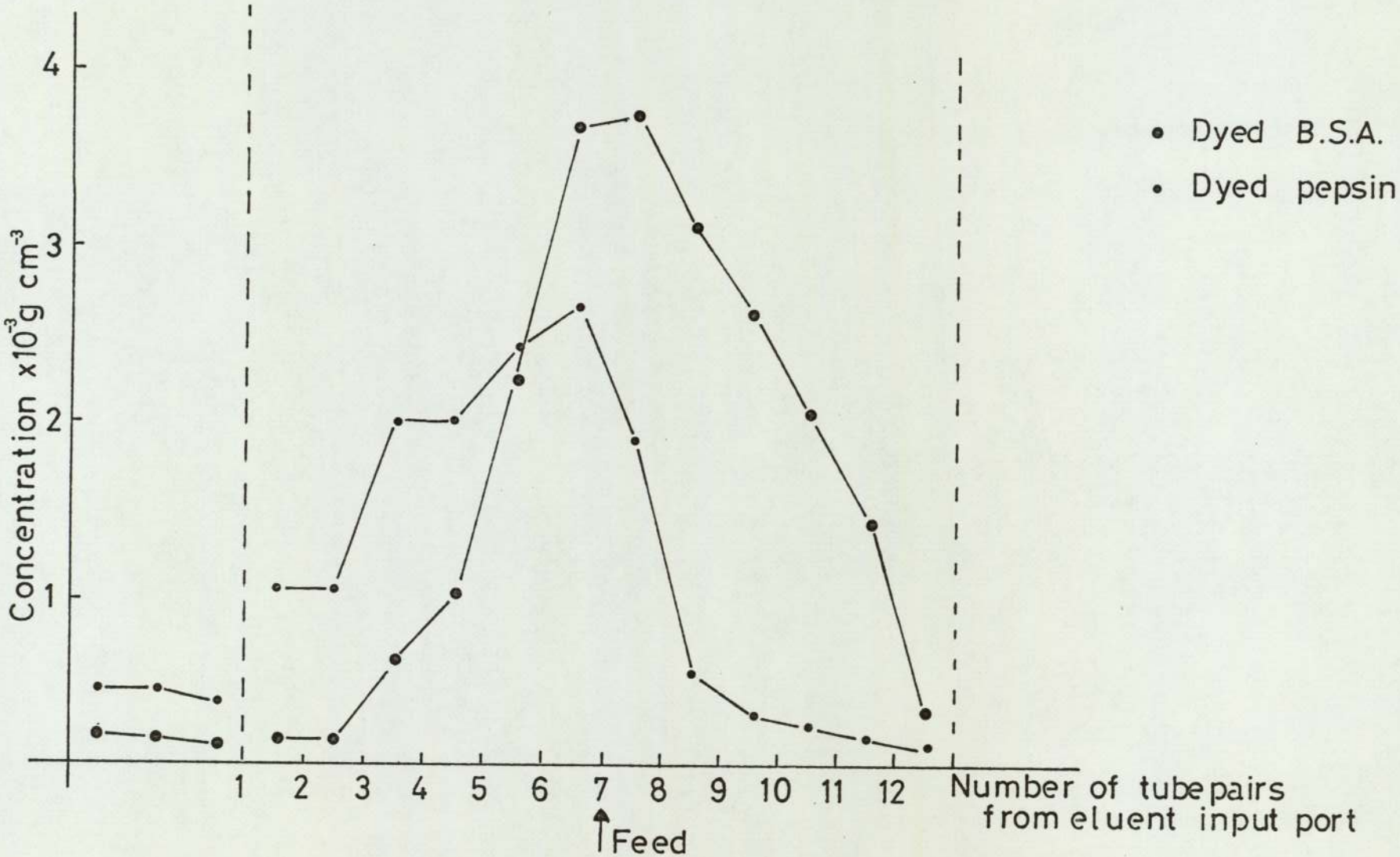

FIGURE 7.5 Product Output Concentrations for Run 2

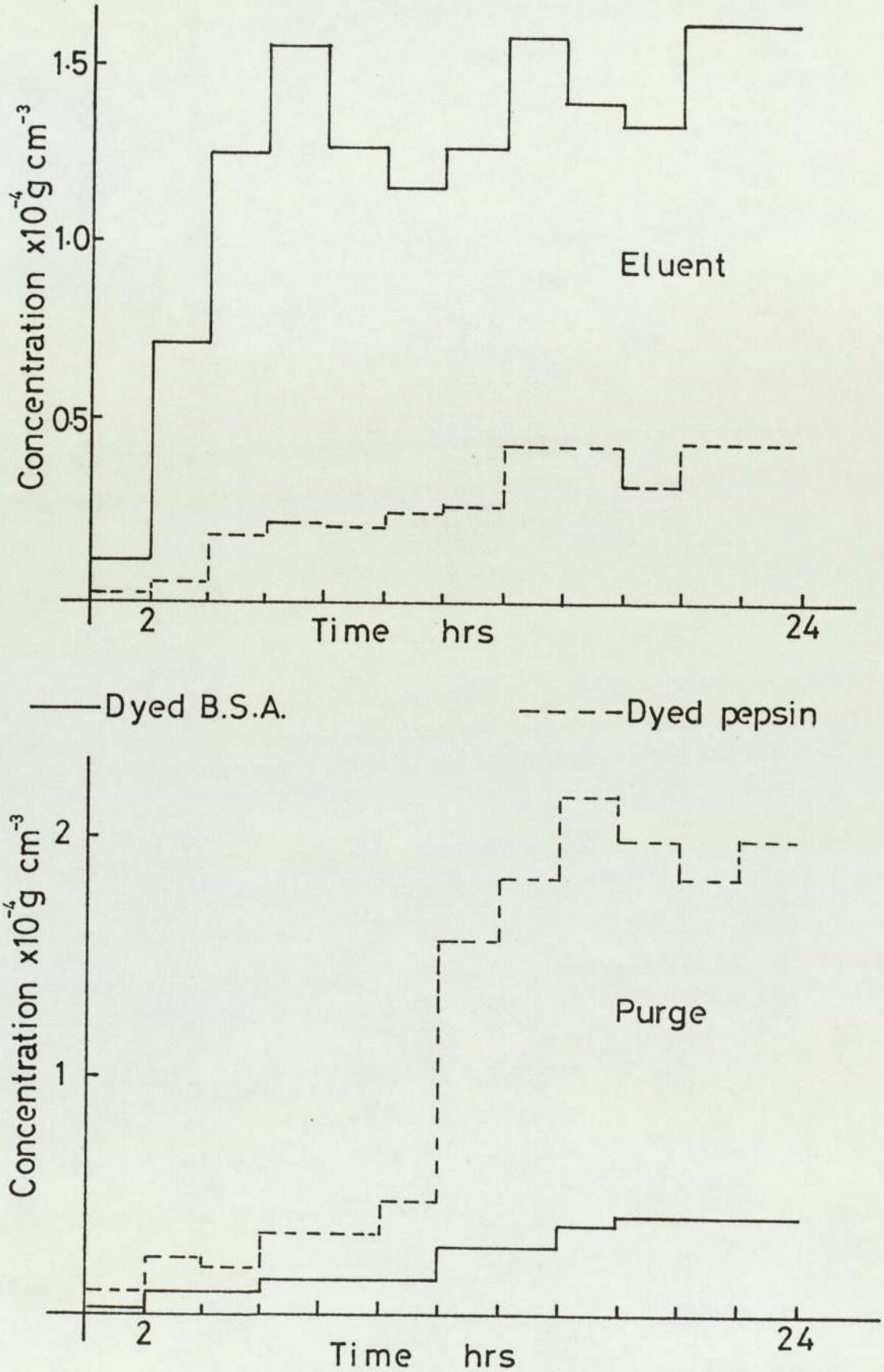

Figure 7.6a Binary Run 3 Results Summary

Feed concentrations,

(i) dyed bovine serum albumin = 1.03×10^{-2} g cm^{-3}

(ii) dyed pepsin = 0.84×10^{-2} g cm^{-3}

Temperature, Pressure and Flow Rates

Time hrs.	Temp. ^{o}C	Pressure KN m^{-2}	Eluent + Purge input cm^3 min^{-1}	Feed input cm^3 min^{-1}	Purge output $cm^3 min^{-1}$	Eluent output cm^3 min^{-1}
0	29	80	2.62	0.05	1.862	0.798
16	29	80	2.52	0.05	1.831	0.736
18	29	80	2.59	0.05	1.781	0.719
21	29	80	2.63	0.05	1.835	0.694
23	29	80	2.63	0.05	1.874	0.695

Theoretical "Cut" Partition Coefficients

	Prefeed cut partition coefficient	Postfeed cut partition coefficient
	0.26 0.14 0.09 0.05 0.05	0.35 0.23 0.2 0.16 0.16
Average	0.12	0.22

FIGURE 7.6 Binary Run 3 Concentration Profile

(b)

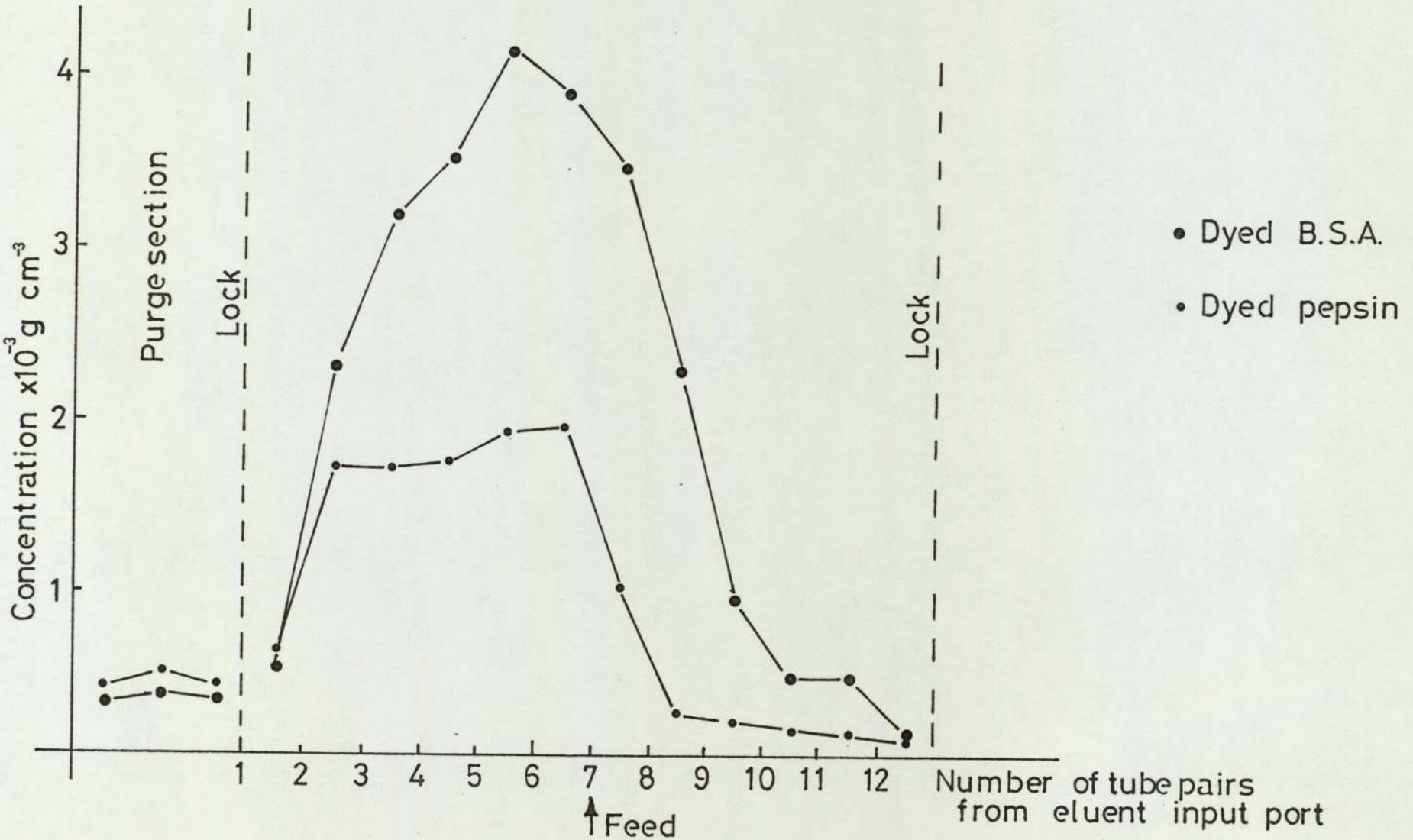

FIGURE 7.6 Product Output Concentrations for Run3
(c)

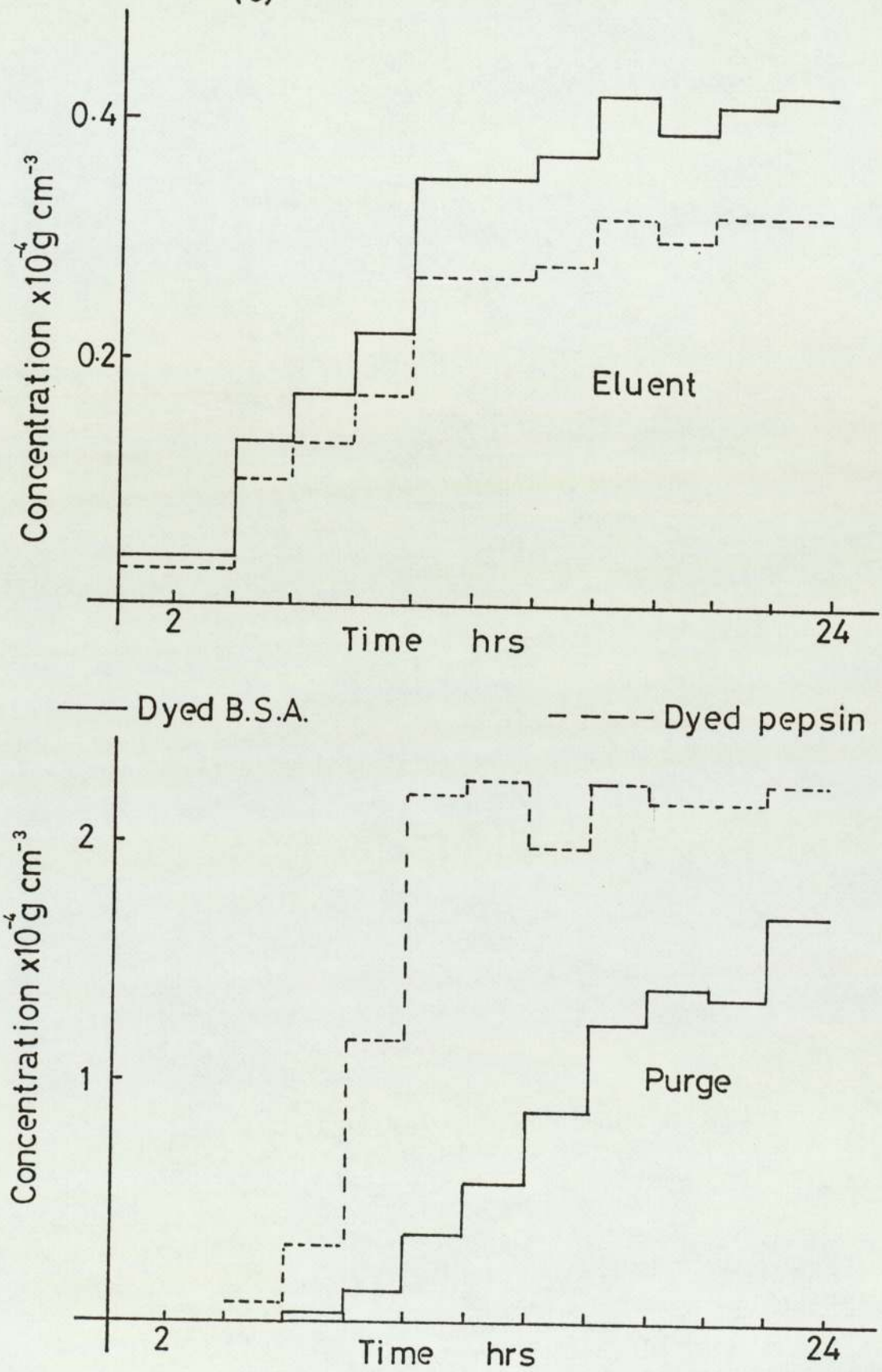

Figure 7.7a Binary Run 4 Results Summary

Feed concentration,

(i) dyed bovine serum albumin = 0.8×10^{-2} g cm^{-3}

Temperature, Pressure and Flow Rates

Time hrs.	Temp. ^{o}C	Pressure KN m^{-2}	Eluent + purge input cm^3 min^{-1}	Feed input cm^3 min^{-1}	Purge output cm^3 min^{-1}	Eluent output cm^3 min^{-1}
0	29	76	2.83	0.05	2.109	0.662
4	29	76	2.84	0.05	2.109	0.709
16	29	76	2.76	0.05	2.069	0.738
18	29	76	2.87	0.05	2.094	0.731
20	29	76	2.88	0.05	2.021	0.762
22	29	76	2.88	0.05	2.08	0.765
24	29	76	2.77	0.05	1.995	0.726

Theoretical "Cut" Partition Coefficients

	Prefeed cut partition coefficient	Postfeed cut partition coefficient
	0	0.09
	0.08	0.18
	0.14	0.24
	0.14	0.22
	0.18	0.28
	0.19	0.28
	0.12	0.22
Average	0.14	0.25

FIGURE 7·7 Run 4 Concentration Profile
(b)

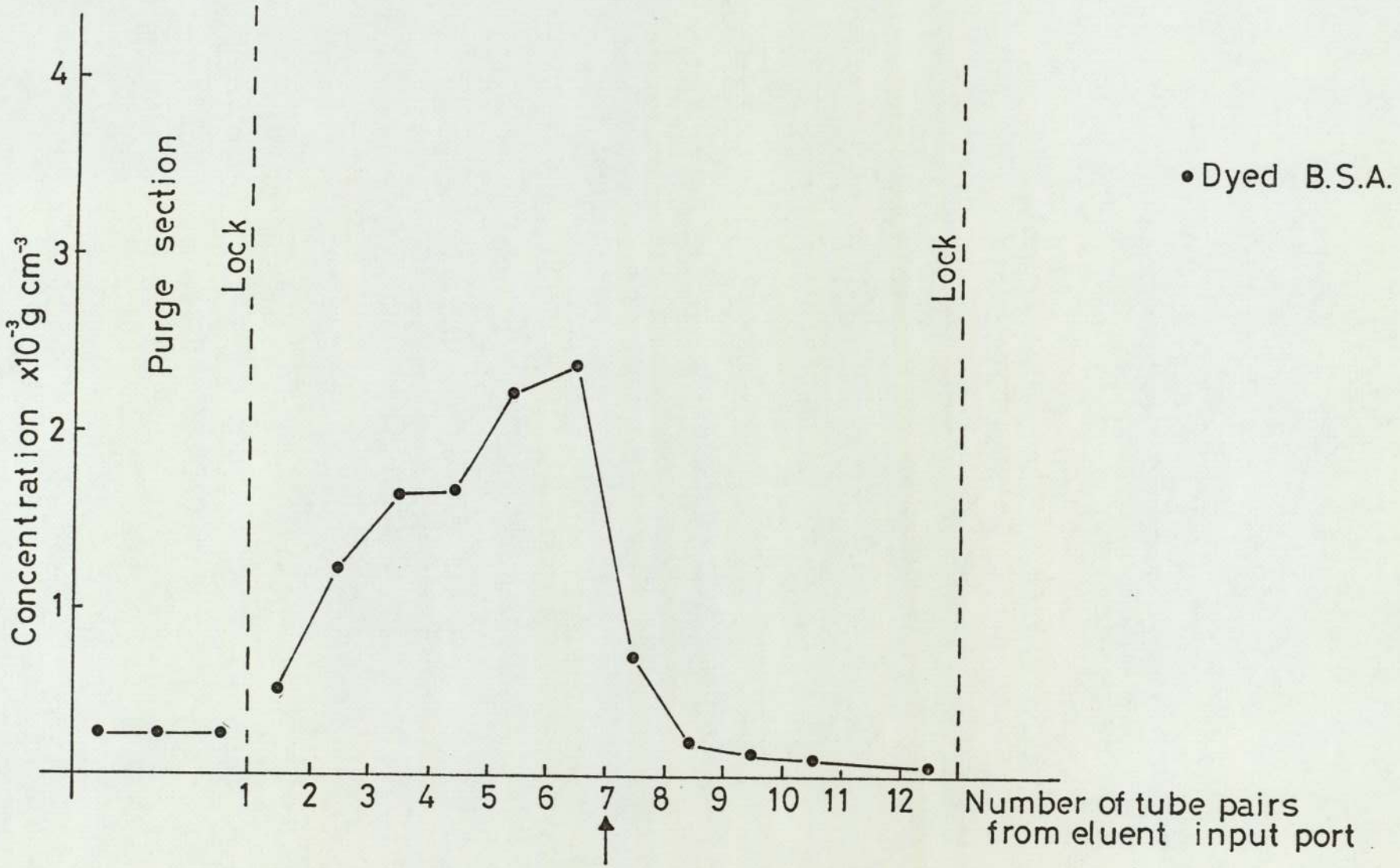

FIGURE 7.7 Product Output Concentrations for Run 4
(c)

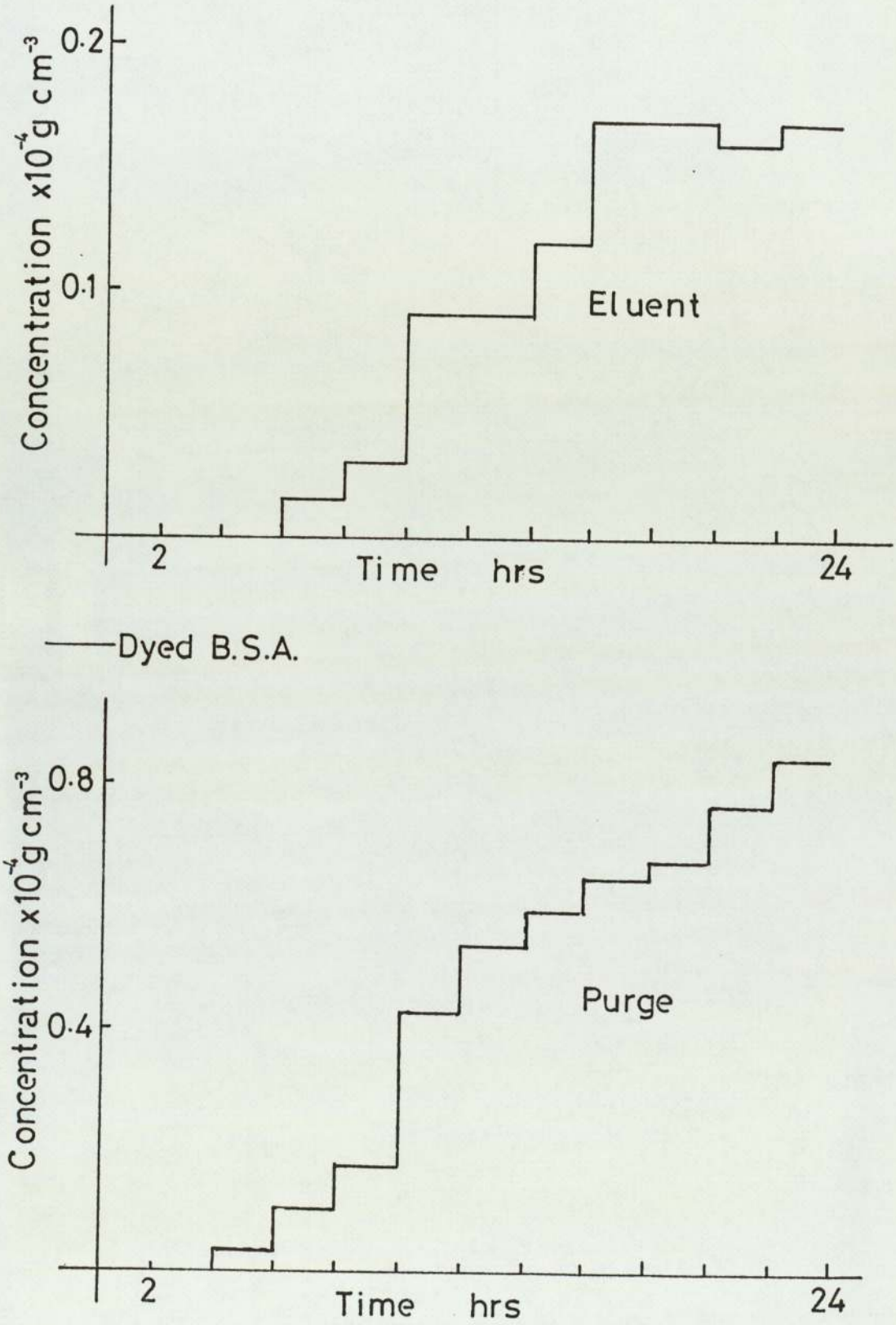

Figure 7.8a Binary Run 5 Results Summary

Feed concentration,

(i) dyed bovine serum albumin = 0.95×10^{-2} g cm^{-3}

(ii) dyed pepsin = 0.97×10^{-2} g cm^{-3}

Temperature, Pressure and Flow Rates

Time hrs.	Temp. ^{o}C	Pressure KN m^{-2}	Eluent + purge input cm^3 min^{-1}	Feed input cm^3 min^{-1}	Purge output cm^3 min^{-1}	Eluent output cm^3 min^{-1}
0	29	76	2.77	0.16	1.954	1.005
16	29	69	2.69	0.16	1.856	0.839
18	29	76	2.69	0.15	1.840	0.777
20	29	76	2.73	0.16	1.922	0.783
22	29	76	2.73	0.15	1.911	0.822

Theoretical "Cut" Partition Coefficients

	Prefeed cut partition coefficient	Postfeed cut partition coefficient
	0.44 0.13 0.03 0.04 0.11	0.74 0.43 0.31 0.32 0.4
Average	0.15	0.44

FIGURE 7.8 Binary Run 5 Concentration Profile
(b)

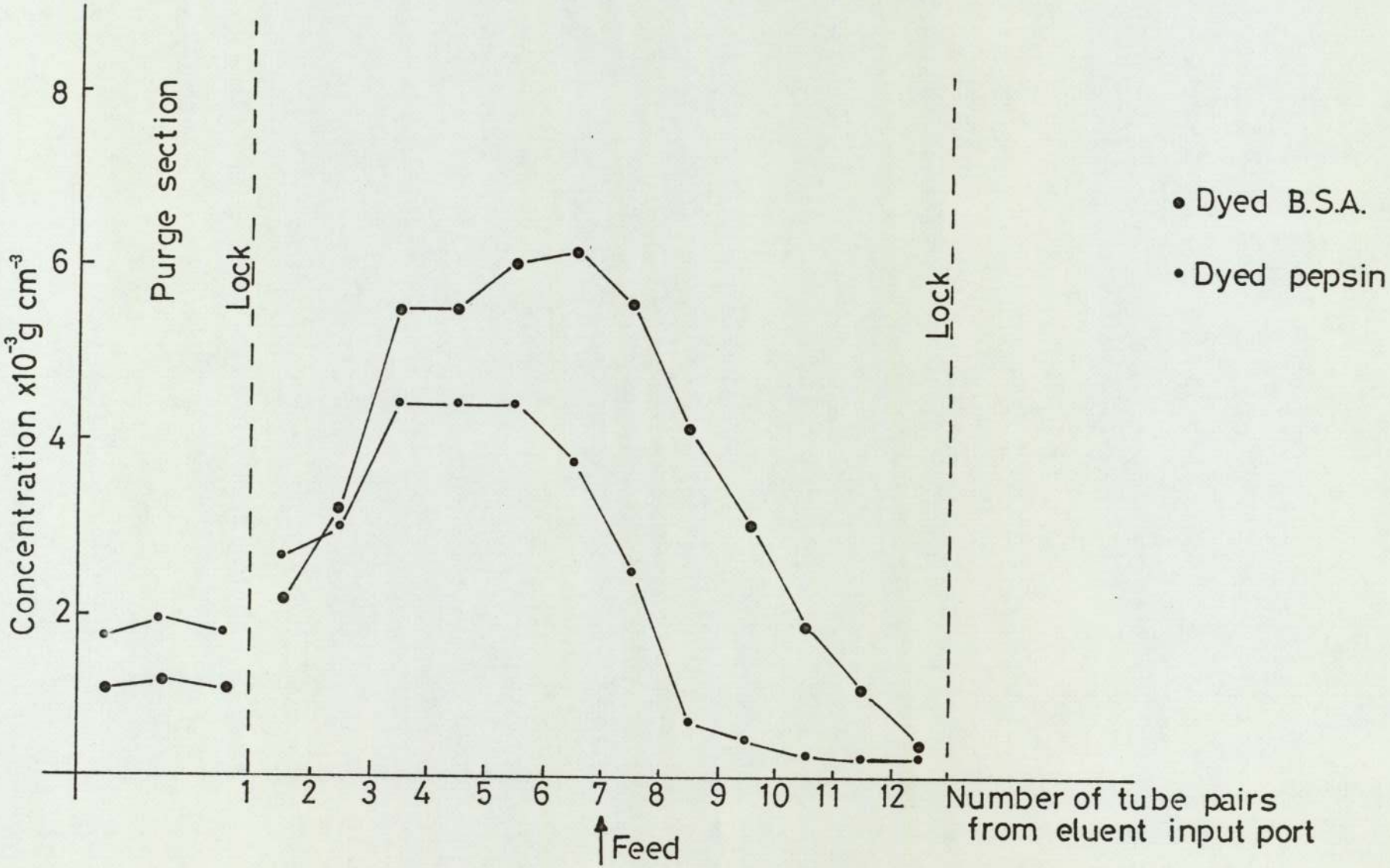

FIGURE 7.8 Product Output Concentrations for Run 5

(c)

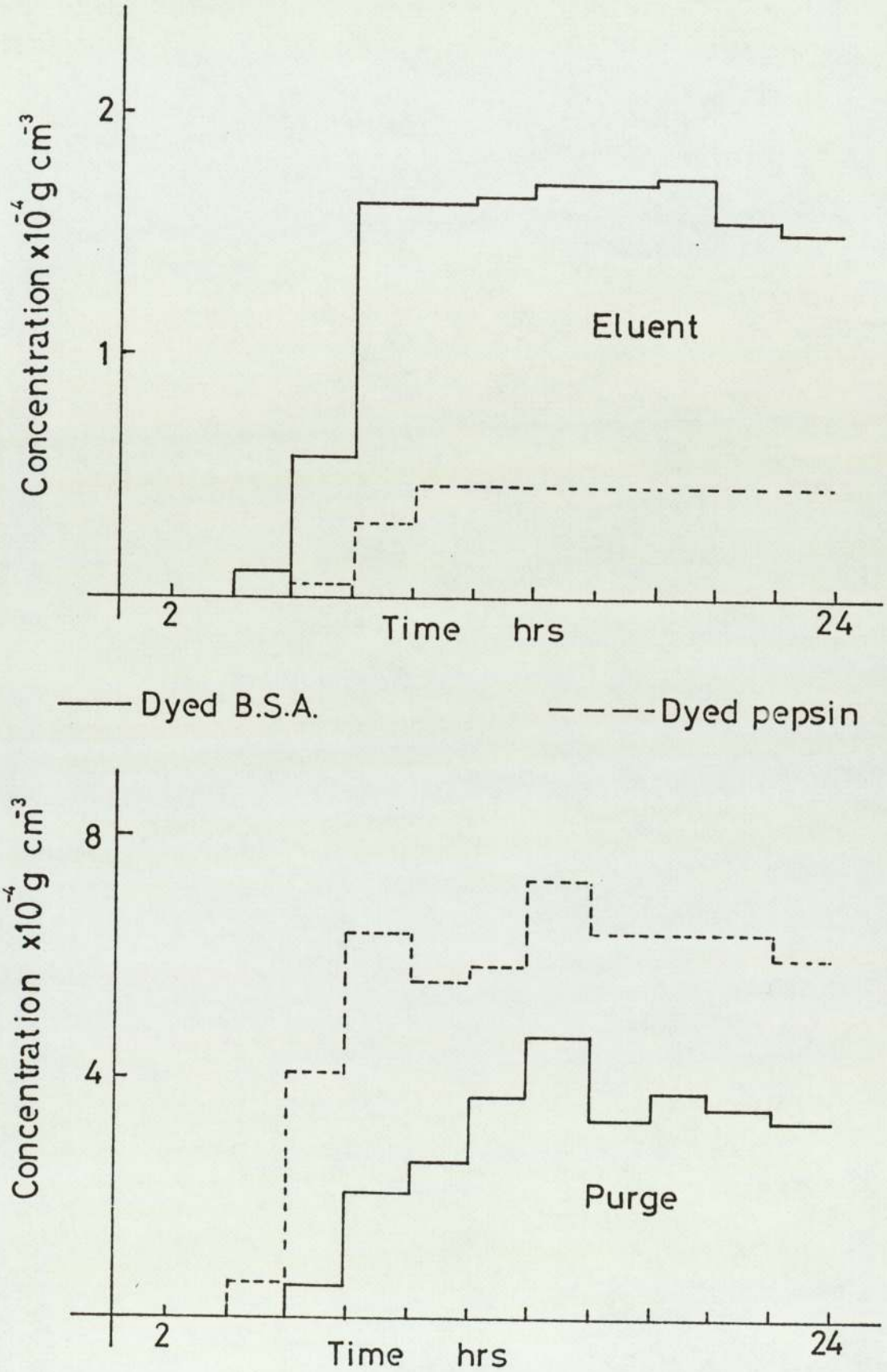

Figure 7.9a Binary Run 6 Results Summary

Feed concentrations,

(i) dyed bovine serum albumin = 0.93×10^{-2} g cm^{-3}

(ii) dyed pepsin = 0.94×10^{-2} g cm^{-3}

Temperature, Pressure and Flow Rates

Time hrs.	Temp. ^{o}C	Pressure KN m^{-2}	Eluent + purge input cm^3 min^{-1}	Feed input cm^3 min^{-1}	Purge output cm^3 min^{-1}	Eluent output cm^3 min^{-1}
0	29	117	3.08	0.15	2.044	0.989
16	29	117	3.09	0.15	2.094	1.014
18	29	117	3.09	0.15	2.103	1.009
20	29	117	3.09	0.15	1.958	1.069
22	29	117	3.04	0.15	1.958	1.040

Theoretical "Cut" Partition Coefficients

	Prefeed cut partition coefficient	Postfeed cut partition coefficient
	0.43 0.48 0.47 0.58 0.53	0.72 0.77 0.75 0.87 0.81
Average	0.5	0.79

FIGURE 7.9 Binary Run 6 Concentration Profile
(b)

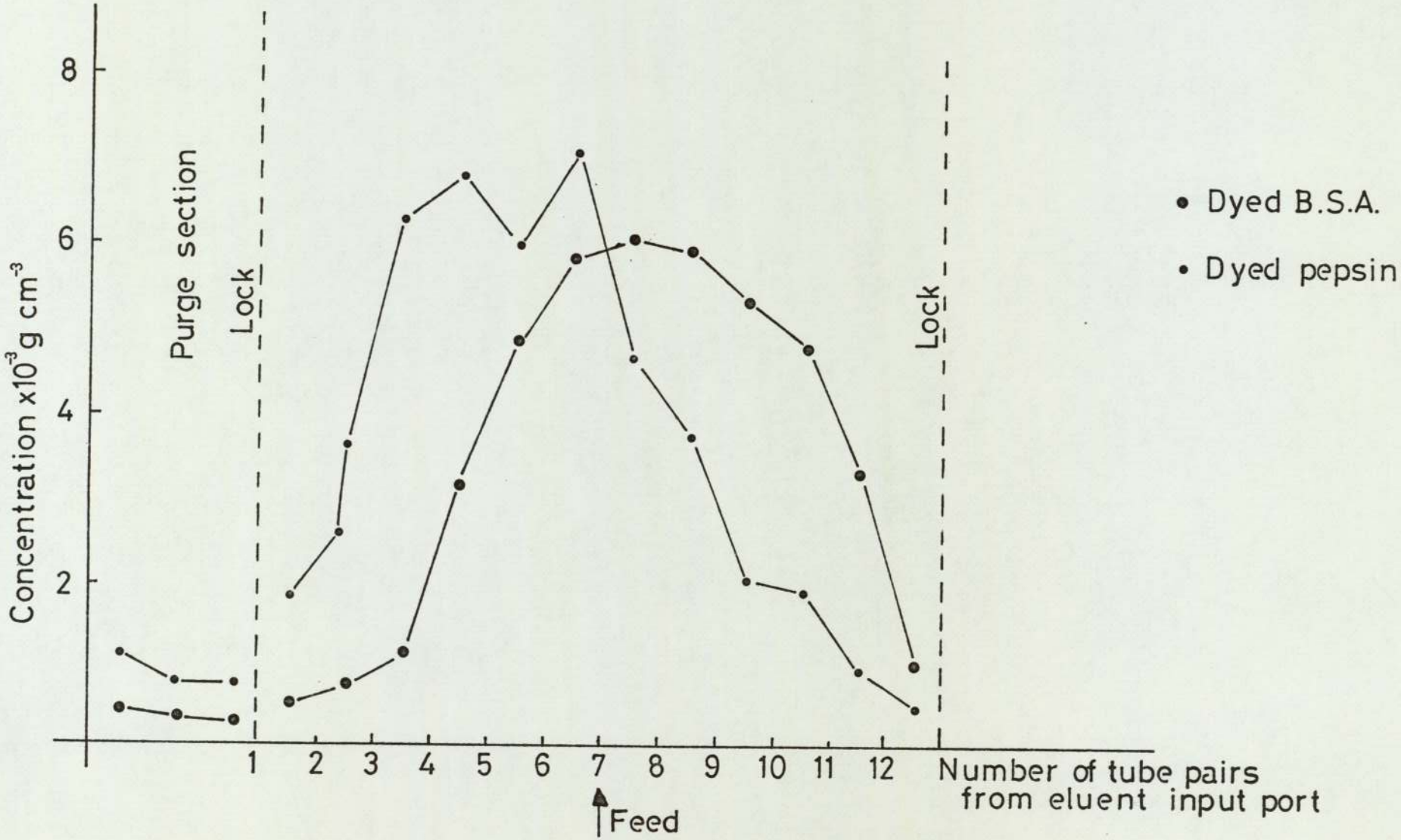

FIGURE 7.9 Product Output Concentrations for Run 6
(c)

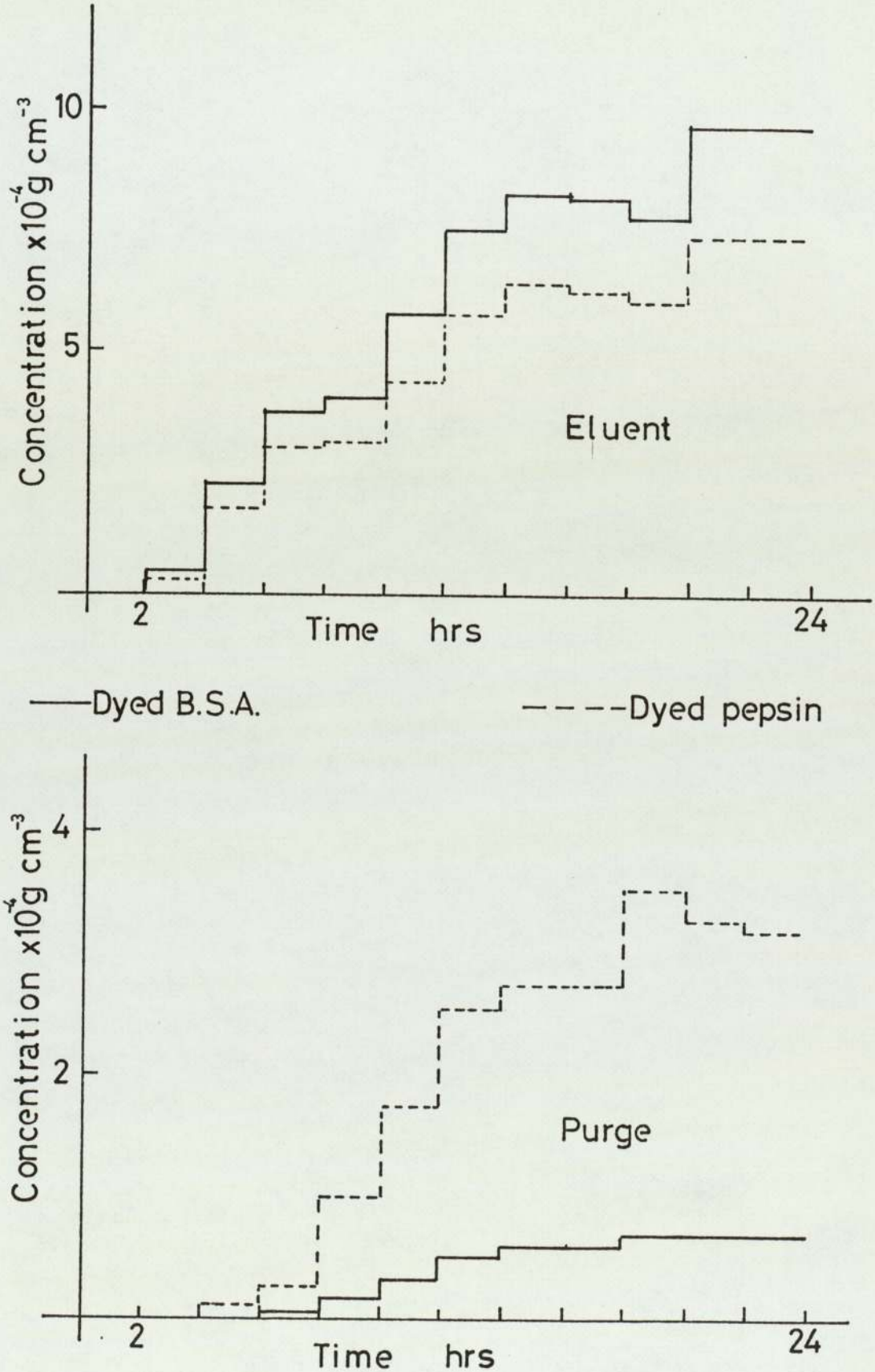

The information obtained from the completed experiments is discussed in the following section.

7.5.2 Discussion

The loss of liquid during each of the binary separation experiments prevented the use of product purities to interpret the degree of separation. Liquid leakage was observed in those areas of the seal where the back pressure was greatest, these were by the purge and eluent input ports, (Figure 7.10).

Component mass balances, established that the loss of dyed bovine serum albumin in all the experiments varied between 18% and 51%. For pepsin it varied between 8% and 57%. The mass balances were based on input and output liquid rates and the respective component concentrations at the end of each experiment. The failure of the mass balances can be put down to the following factors;

(i) liquid leakage from the seal,

(ii) changes in component hold up due to the varying flow conditions

(iii) adsorption of the components on to the packing.

An experiment similar to those described in Section 7.4.1 established that the adsorption of dyed protein onto the packing was not significant. A visual examination of a sample of the bundle packing at the end of the experimental runs confirmed that some dyed bovine serum albumin had been adsorbed. This was evident by the light pinkish tinge to the normally white Spherosil. Purging a sample of the packing with fresh buffer failed to remove this adsorbed material.

FIGURE 7.10 Diagram Showing Regions where Leakage was Visible.

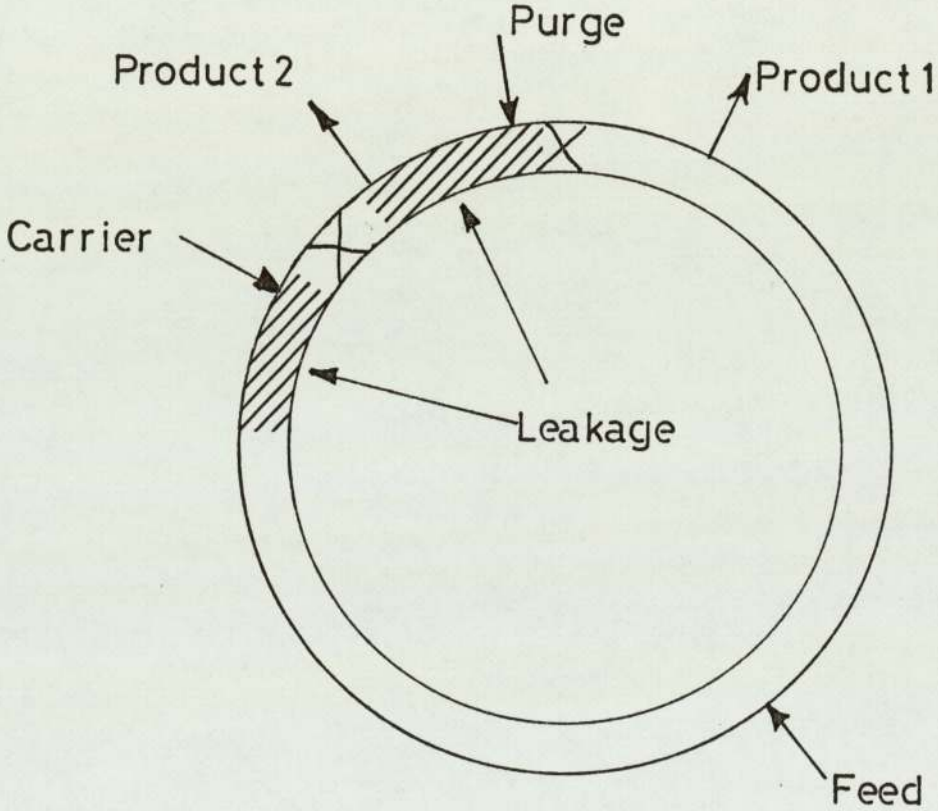

It was concluded that the adsorption of protein was not an effect which adversely influenced the separation process.

The second factor, the effect of changing flow conditions, may well have influenced the steady state operation of the machine but to what extent is uncertain. Plots of the product output concentrations, Figure 7.4c-7.9c indicate that, in the majority of experiments, a pseudo-equilibrium was achieved within 16-24 hours (equivalent to 2-3 cycles of the tube bundle). It should however be borne in mind that any effects due to changing equilibrium could well have been masked by liquid leakage and/or any concentration effects. With this in mind Run 4 had specifically been designed to investigate the influence of a second component and an increase in concentration. Figures 7.6b and 7.7b show the differences in the concentration profiles of dyed bovine serum albumin in Runs 3 and 4. The flow rates in these two runs were kept as similar as was practically possible. The feed in Run 4 contained one rather than two components, as in Run 3. Whether the differences in the concentration profiles are attributable to the presence of a second component in Run 3 cannot be stated with absolute certainty because of liquid leakage. However, the differences (Figures 7.6b and 7.7b) appear to be more significant than to be solely caused as a result of liquid loss.

From component and liquid mass balances taken towards the end of each experiment the dyed protein and liquid losses were calculated. Combining these two losses an estimate was made of the concentration of each component in the leaking liquid. From the component distribution plots, Figures 7.4b-7.9b, the region in which leakage occurred could then be determined. Table 7.5 summarises these results. It shows that in the majority of cases component loss occurred within the first

Table 7.5 Summary of Component Mass Balances

Run No.	Component	% loss	Concentration leakage $\times 10^{-3}$ g cm^{-3}	Tube number	Mean eluent rate cm^3 min^{-1}
1	B.S.A. Pepsin	34 57	0.9 1.6	3-4 2-3	0.867
2	B.S.A. Pepsin	51 20	1.1 0.6	3-4 1	0.786
3	B.S.A. Pepsin	27 8	1.1 0.4	1-2 1	0.678
4	B.S.A. -	18 -	0.7 -	1 -	0.688
5	B.S.A. Pepsin	33 8	2.4 0.6	1-2	0.69
6	B.S.A. Pepsin	13 38	0.7 2.4	1-2 1-2	0.87

three tube pairs of the prefeed section. Since this is the region of highest back pressure it is also the region where liquid leakage was most likely to occur.

It is interesting to note from Table 7.5 that in all the experiments, excluding Runs 1 and 6, the loss of protein decreases as the eluent rate decreases and the loss of bovine serum albumin is greater than that for pepsin. In Runs 1 and 6 the pepsin loss is greater than the dyed bovine serum albumin loss. This may be due to the higher eluent rate which would reduce the spreading of dyed bovine serum albumin into the prefeed section. The higher eluent rate would also increase the tendency of dyed pepsin to travel in the mobile phase. Hence any loss of liquid around the eluent input port could result in a greater loss of dyed pepsin compared to dyed bovine serum albumin.

Despite the influences of leakage a number of conclusions can be made from the binary separation studies. The concentration profiles of Run 1, 2 and 3 (Figures 7.4b-7.7b) show that as the eluent rate was decreases,

(i) the maximum concentration reached by the dyed bovine serum albumin increases and spreads further into the prefeed section,

(ii) the maximum pepsin concentration decreases.

The observed changes in the maximum concentration, reached by the two dyed proteins, was to be expected. A decrease in the eluent rate will have caused the following:

(i) A decrease in the rate that dyed bovine serum albumin travels in the direction of the mobile phase.

(ii) An increase in the rate of travel of dyed pepsin with the "stationary", or liquid phase.

These respective decreases and increases in the rate at which the components travel must change their residence times per unit volume of the column. Therefore, since the process is essentially continuous, there will be an increase in the hold up of dyed bovine serum albumin and a corresponding decrease in the hold up of dyed pepsin.

In Runs 5 and 6 the flow conditions were set such that only one of the "cut" values effected by the machine (Table 7.4) lay within the theoretical limits, imposed by the component partition coefficients. Figures 7.9b and 7.10b illustrate the concentration profiles obtained for these two experiments. No clear conclusions could be made as to which of the "cut" positions, if any, dominates the separation.

A feature of all the concentration profiles was the spreading of both components throughout the separation section of the machine. This, it was thought was primarily due to the inefficient operation of the chromatographic machine. Such factors as a large particle sized packing and the dead volume at the top and bottom of each tube would have contributed to this but the dominant factor is undoubtedly the leakage from the seal. Material losses of up to 57% would make any attempt at experimentally quantifying efficiency of little value.

CHAPTER 8

Computer Simulation Studies

8.1 SIMULATION OF THE CONTINUOUS CHROMATOGRAPHIC EQUIPMENT USED IN THIS STUDY

The mass transfer processes that operate in a chromatographic column are extremely complex. In essence all mathematical models attempt to define in a quantitative manner the rates of accumulation and depletion of a solute in a particular region in the column. The more complete the model the more complicated the equation involved. In single column co-current chromatography use has been made of the laws of conservation of mass to produce mass balance equations which, with suitable simplifications and boundary conditions, have been used to produce information about the concentration profiles within the column[16,233-236]. For this type of simple batch column chromatography the assumptions made make the equations involved accessible to mathematical treatment. Alternative procedures involving a statistical approach have been proposed by Sciance and Crosser[237] and by Charmichael[127]. Applying either the differential mass balance approach or the stochastic approach to continuous counter-current packed bed processes is a very complex task. Consequently, by necessity, the model described in the following text is an idealised picture of the processes occurring within the continuous chromatograph.

The primary objective of the model was to determine the idealised concentration profiles within the machine for a binary mixture. It was also proposed to use the computer simulation to obtain an insight into the theoretical effects of the chromatographic equipment operating parameters. The binary mixture used in the model was the dyed bovine serum albumin, dyed pepsin mixture used experimentally.

For simplicity the 44 tubes that make up the chromatograph are represented by 22 tube pairs. The total column length is divided into four sections;

(i) the separating section, 12 tube pairs,

(ii) the purge section, 3 tube pairs,

(iii) the liquid lock between the eluent input and the purge product output, 4 tube pairs,

(iv) the second liquid lock between the purge inlet port and the eluent output port, 3 tube pairs.

The number of columns involved at any one time are fixed by the position of the input and output ports, see Figure 8.1.

8.1.1. Theoretical Basis

The basis of the simulation is the equilibrium stage concept, or plate theory, discussed in Chapter 2. Using this method a chromatographic column is visualised as a series of ideal mixing stages. Each stage is defined as that volume element in which equilibration between the two phases occurs. The limitations of applying a discontinuous stage model to describe a continuous packed column are well appreciated[21]. The following assumptions have therefore been made.

(i) Component partition coefficients are independent of concentration and molecular interaction effects.

(ii) Equilibrium between the two phases is obtained instantaneously - i.e. thermodynamic equilibrium.

(iii) No account is taken of longitudinal dispersions and non-uniform velocity profile effects.

FIGURE 8.1 Positions of Sections in Rotating Chromatograph

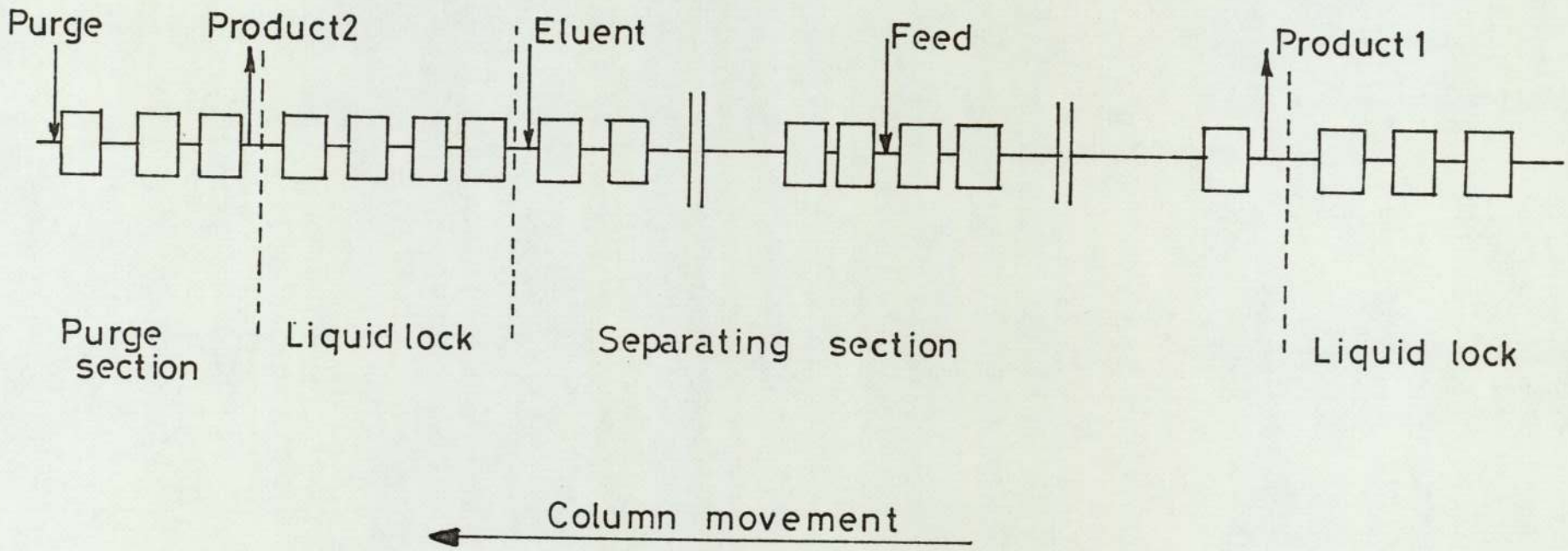

The equation defining the elution volume of a discrete solute in a gel permeation chromatographic column is given by,

$$V_e = V_o + V_i K_D \qquad 8.1$$

Applying this to one equilibrium stage of a chromatographic column, the liquid volume available to a specific component, V_T, will be the sum of the stage interstitial volume, V_m, and the available pore volume, $V_s.K_D$, i.e. $V_T = V_m + V_s.K_D$. If a solute is introduced into the mobile phase to give a concentration, C_o, then after equilibration with the liquid in the pores of the packing the mobile phase concentration, C', will be given by,

$$C' = \frac{C_o.V_m}{V_T} = \frac{C_o V_m}{V_m + V_s.K_D} \qquad 8.2$$

Since equilibrium between the two phases is assumed, Equation 8.2 also gives the solute concentration in the available pore volume.

Now consider part of a chromatographic column, Figure 8.2a, where at time t-Δt the mobile phase concentration in each stage is in equilibrium with the concentration in the available pore volume. Over the time Δt the mobile phase moves forward a distance equivalent to one stage, Figure 8.2b, and equilibration between the two phases takes place. At a time t the mobile phase moves forward again (Figure 8.2), and so on. The term Δt is the time spent by the mobile phase in each stage, and is calculated from,

$$\Delta t = \frac{V_m}{L_E} \qquad 8.3$$

L_E = mobile phase flow rate.

FIGURE 8.2 Diagram Showing the Model as Applied to a Section of Column

(a) $t-\Delta t$

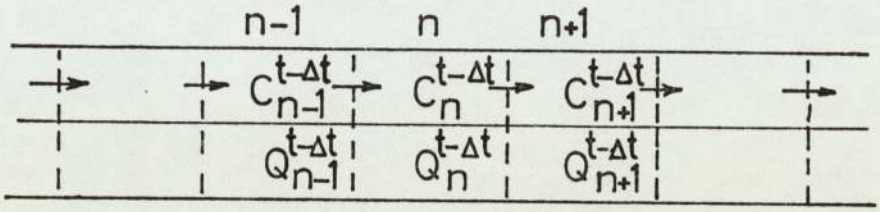

(b) $t-\Delta t+\Delta t$

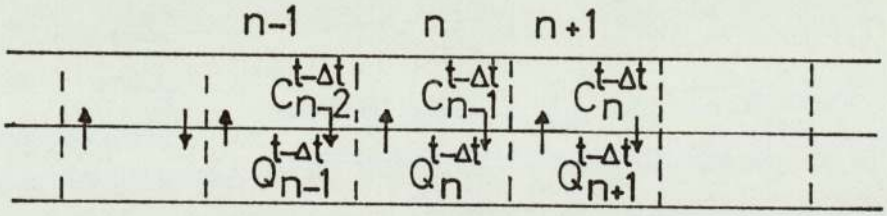

(c) t

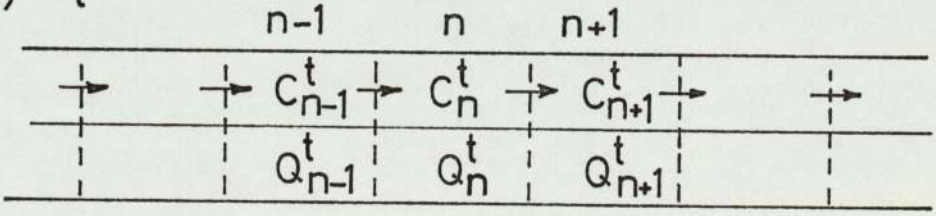

A mass balance on the nth stage over the time period $t-\Delta t$ to t gives,

$$C_n^t.V_m + Q_n^t V_s K_D = C_{n-1}^{t-\Delta t}.V_m + Q_n^{t-\Delta t}.V_s.K_D \qquad 8.4$$

Equilibrium between the two phases is assumed. Therefore $C_n^t = Q_n^t$ and $C_n^{t-\Delta t} = Q_n^{t-\Delta t}$. Hence Equation 8.4 becomes after rearranging

$$C_n^t = \{ \frac{C_{n-1}^{t-\Delta t}.V_m + C_n^{t-\Delta t}.V_s K_D}{V_m + V_s K_D} \} \qquad 8.5$$

For the ith component of a multicomponent system Equation 8.5 can be written as,

$$C_{n,i}^t = \{ \frac{C_{n-1,i}^{t-\Delta t}.V_m + C_{n,i}^{t-\Delta t}.V_s K_{D,i}}{V_m + V_s.K_{D,i}} \} \qquad 8.6$$

This equation provides a means of calculating the concentration of any component at any time, commencing from time zero, in every equilibrium stage of the column. The concentration profile of each component in the chromatograph can therefore be calculated.

8.1.2. Simulation of the Counter-Current Movement of the Packing

Over the time period equivalent to one switch time the chromatograph is assumed to operate in a manner similar to three interconnected batch columns. These are:

(i) the purge section,

(ii) the prefeed section,

(iii) the postfeed section.

The time spent by the tube pairs in the lock between the purge and prefeed section is taken into account by including a "dead" section into the model. In the "dead" section no fluid flow takes place. The switch time is the time that individual tube pairs are exposed to the input and output ports, and is calculated from the tube bundle cycle time and the total number of tube pairs in the chromatograph.

Each tube pair consists of a fixed number of equilibrium stages, N. Therefore, for each section of the machine there will be a fixed number of stages which is dependent on the number of tube pairs in the section. Over the period of the switch time the concentration of each component in each stage is calculated using Equation 8.6. At the end of the switch time the concentration profile is stepped backward by N stages. Thus the column and port functions are effectively kept stationary (Figure 8.3).

8.1.3 Program Layout

A detailed flow diagram of the program is given in Figure 8.4. The program listing is given in Appendix 9 and is written in FORTRAN IV. A disadvantage of the stage-to-stage calculation employed in this model is the large computation time that is required. For this reason the program had to be run on a C.D.C. 7600 at the University of Manchester Regional Computer Centre.

FIGURE 8.3 Diagram Showing Transfer of Concentration Profile

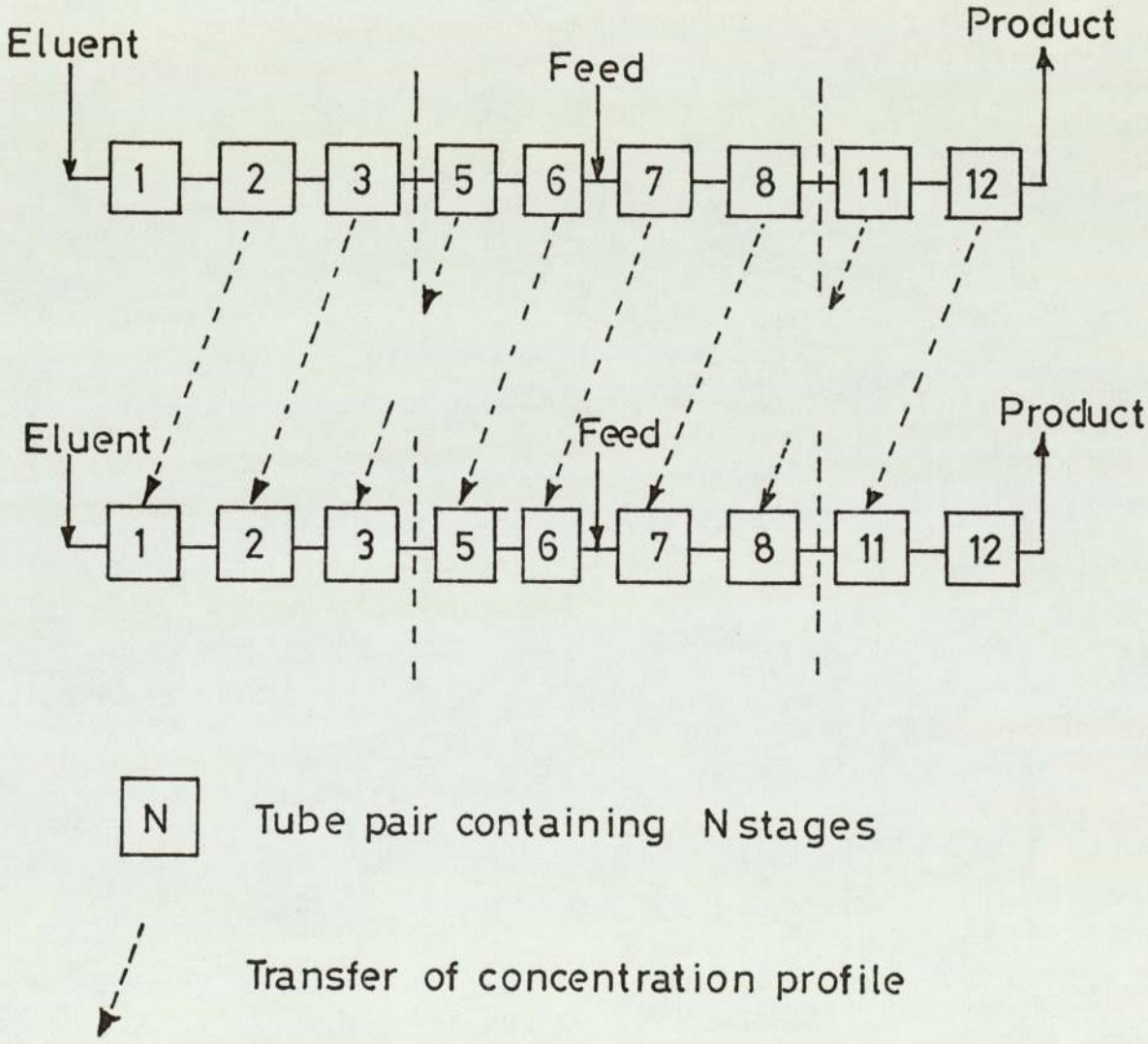

FIGURE 8.4 Flow Diagram of Continuous Chromatograph Simulation Program

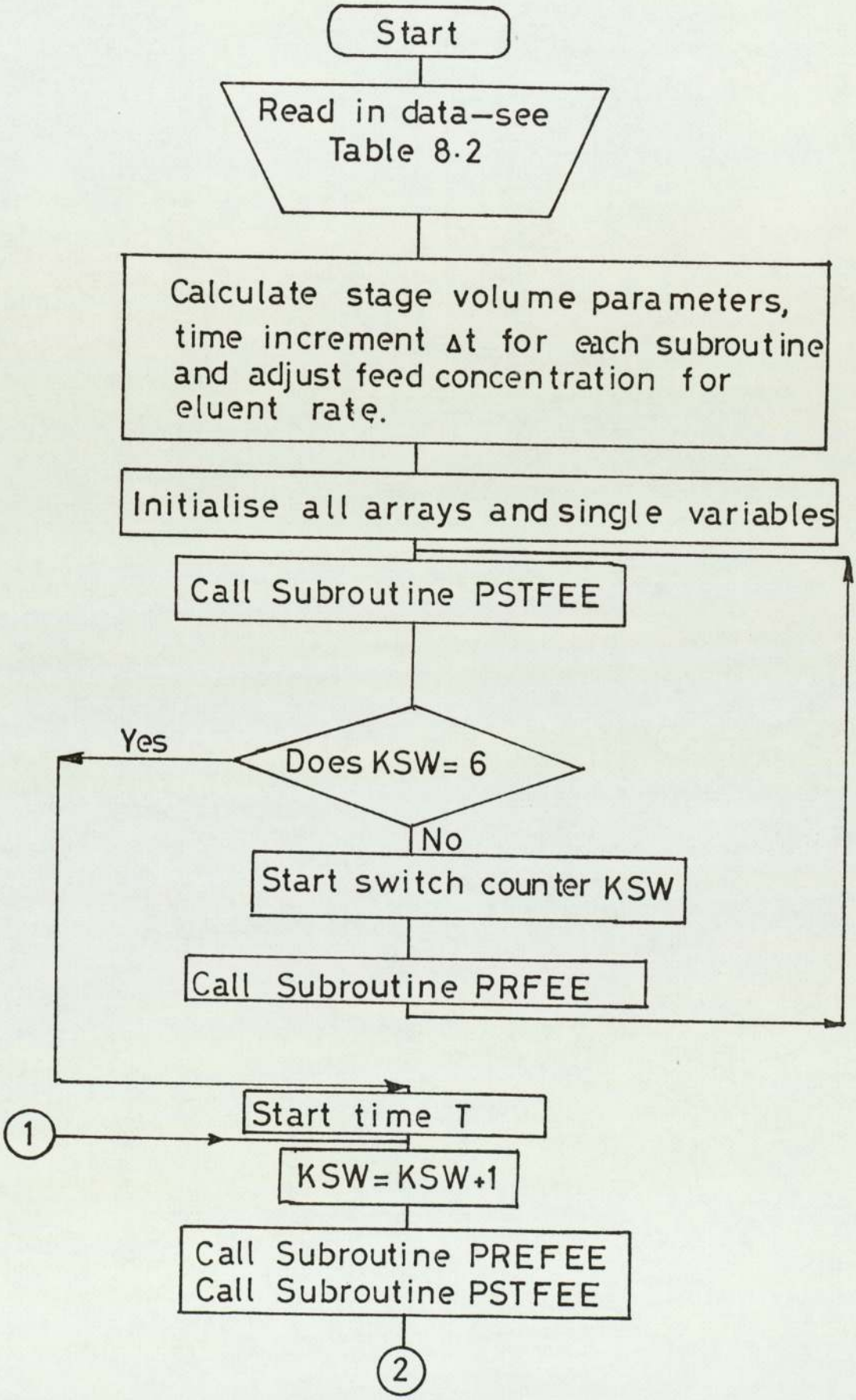

FIGURE 8.4 cont.

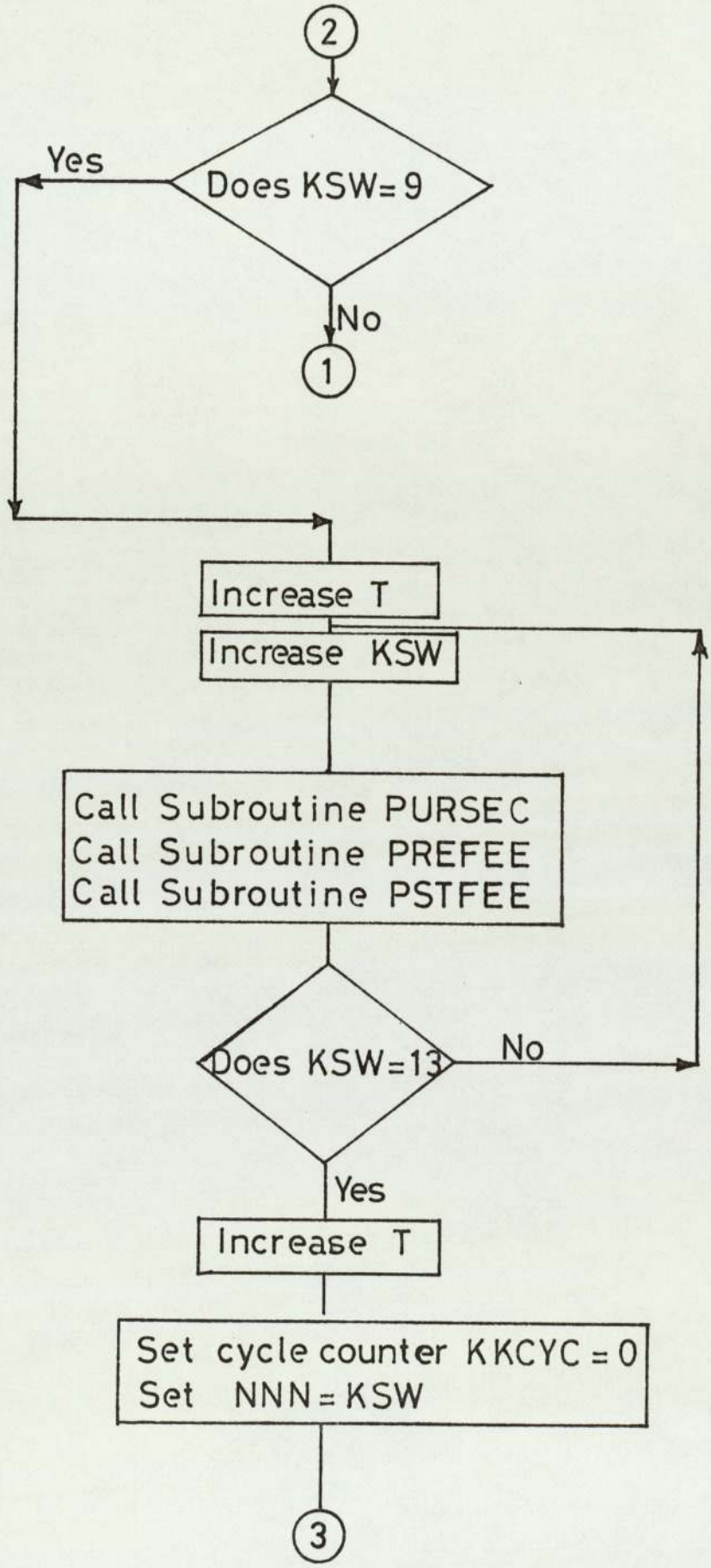

FIGURE 8·4 cont.

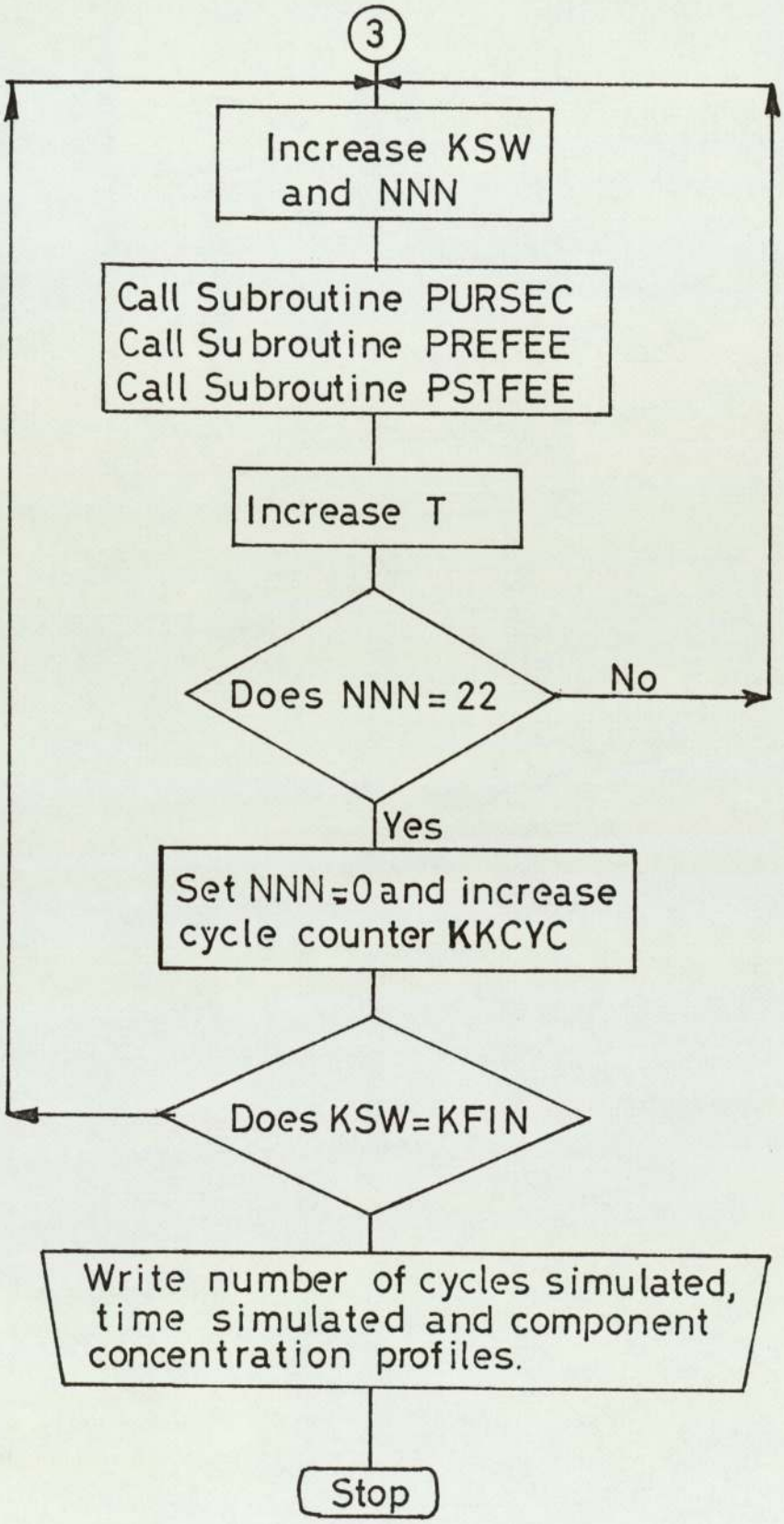

Normally the execution time was of the order of 20 seconds. In this time about 24 hours of the chromatograph operating time was simulated.

It has previously been discussed how the chromatograph was visualised as operating over one switch time in a manner similar to three batch columns. For each of these sections a Subroutine was written which simulated all the operations performed in that section. These routines have been named PURSEC, PREFEE and PSTFEE. PURSEC simulates the purge section, PREFEE simulates the prefeed and isolated section and finally PSTFEE simulates the feed point and the postfeed section. Variables such as the number of columns, number of components and the magnitude of the switch time are entered as arguments to the subroutines. Information on component concentrations in individual stages is entered via two dimensional COMMON blocks. Data input and output, preliminary calculations, machine start up and tests on the time and number of switches performed are carried out in the main program. Definitions of variable names are included in Table 8.1.

Since the magnitude of the time increment, Δt, is a function of both the eluent rate and the equilibrium stage mobile phase volume, V_m (Equation 8.3), the number of calculations performed in each of the subroutines over one switch varies. In the purge section this is of no consequence. However, in the transition from the prefeed to the postfeed section, (i.e. the feed point) this feature had to be taken into account, and was achieved by storing in a dummy array the mobile phase concentrations that are output from the prefeed section over one switch time.

Table 8.1 Definition of Major Variables in Computer Program

Variable Name	Definition
	(i) Dimensioned variables
PURC	Solute concentrations in mobile phase in purge section
PURE	Solute concentrations in liquid, "stationary" phase in purge section.
HISC	Solute concentration in mobile phase in the isolated section.
HISE	Solute concentration in liquid, "stationary", phase in the isolated section.
PRFC	Solute concentration in mobile phase in the prefeed section.
PRFE	Solute concentration in liquid, "stationary" phase in the prefeed section.
PSTC	Solute concentration in mobile phase in the postfeed section.
PSTE	Solute concentration in liquid, "stationary", phase in the postfeed section.
DUM, DUMM	Dummy arrays used for storing mobile phase solute concentrations at the feed point.
AKV	Component partition coefficients.

Table 8.1 (cont.)

	(ii) Single variables
FC	Component feed concentration. The same for all components.
SWT	Switch time - tube bundle cycle time divided by the total number of tube pairs.
PFL	Purge flow rate
PRFL	Prefeed flow rate
FFL	Feed flow rate
RFI	Retention factor of totally included component on tube bundle packing.
RFO	Retention factor of totally excluded component on tube bundle packing.
TCPUR	Number of columns in purge section
HISNC	Number of columns in the purge section
TCPF	Number of columns in prefeed section
TCPSF	Number columns in postfeed section
N	Number of equilibrium stages per tube pair
CV	Packed column volume per tube pair
DV	Total bundle dead volume
FCC	Adjusted feed concentration for the diluting effects of mobile phase flow rate.
DPUR	Δt for purge section
DPRF	Δt for prefeed section
DPSF	Δt for postfeed section
VI	Porous volume per equilibrium stage

Table 8.1 (cont)

VO	Interstitial volume per equilibrium stage
KFIN	Total number of switches to be simulated
KCYC	Total number of cycles to be simulated
XX	Number of equilibrium stage calculations performed in one switch time for postfeed section
X	Number of equilibrium stage calculations performed in one switch time for prefeed section
T	Total time simulated

The number of equilibrium stage concentrations in this array were then converted, using the feed rate and feed concentration, into the required number of stage concentrations for the postfeed section. Each of the converted concentrations in the dummy array was used in turn as the input to the first equilibrium stage of the postfeed section. This effectively simulated the feed point and also, in a simple way, treated the mixing effects which would result.

8.2 RESULTS

In all the computer simulation runs the binary system, dyed pepsin and dyed bovine serum albumin, was used. The experimentally determined partition coefficients of these two components have been used and, for the purposes of the model, they were assumed to be concentration independent. Feed concentrations of each component were kept equal in all simulations; the magnitude of the concentrations were, however, varied. Initially all simulations were limited to three cycles of the tube bundle, but for some experiments it was found necessary to increase this in order to obtain pseudo-steady state concentration profiles.

The simulation runs can be divided into the following series of experiments.

(i) The effect of the number of equilibrium stages.

(ii) Simulation of the binary experiments.

(iii) The effect of increasing the feed concentrations.

(iv) The effect of changing the tube bundle speed.

Fourteen runs were performed. A summary of the input data for each run is given in Table 8.2. One run, numbered Run 6, from Section (ii) was used as a standard, the effect of varying the parameters given in Sections (iii) and (iv) were then investigated.

The component concentration profiles were plotted after a specified number of cycles had been simulated. The profiles correspond to the situation that exists at the end of a switch time, i.e. the time immediately before the indexing back of the concentration profiles. All profiles are presented in Figures 8.5-8.18.

8.3 DISCUSSION OF THE RESULTS

8.3.1 The Effect of the Number of Equilibrium Stages (N)

As the number of equilibrium stages per tube pair was altered from 25 to 75, only a marginal change was observed in the component concentration profiles (Runs 1-4), Figures 8.5-8.8. This may well be true for the system studied where the separation factor was about 2, but as the separation becomes more difficult the importance of the number of equilibrium stages per column is expected to play a more important part.

From the point of view of the computer studies the greater the number of stages the more accurate the simulation is of a piece of continuous flow contact equipment. Unfortunately the program execution time is directly related to the number of equilibrium stages per tube pair. A compromise value was therefore sought between accuracy and execution time. A value of 60 plates per tube pair was chosen. This value corresponded to an unpacked stage volume of approximately 0.5 ml.

Table 8.2 Lists of Values of Computer Program Input Variables

(i) Variables common to all simulation runs.

Variable name	Value
TCPF	6
TCPSF	6
TCPUR	3
NC	2
HISNC	4
CV (cm^3)	28.5
DV (cm^3)	29.25
AKV(1)	0.28
AKV(2)	0.58
RFI	0.82
RFO	0.42
PFL (cm^3 min^{-1})	1.9

(ii) Variables that were altered in Simulation Runs.

RUN NO.	PRFL cm^3 min^{-1}	FFL cm^3 min^{-1}	SWT min	KCYC	N	FC g cm^{-3}
1	0.75	0.05	22.4	3	25	2
2	0.75	0.05	22.4	3	50	2
3	0.75	0.05	22.4	3	60	2
4	0.75	0.05	22.4	3	75	2
5	0.874	0.05	22.4	3	60	0.01
5	0.874	0.05	22.4	4	60	0.01
5	0.874	0.05	22.4	5	60	0.01
6	0.782	0.05	22.4	3	60	0.01
7	0.71	0.05	22.4	3	60	0.01
7	0.71	0.05	22.4	4	60	0.01
8	0.688	0.15	22.4	3	60	0.01
9	0.832	0.15	22.4	3	60	0.01
10	0.782	0.05	22.4	3	60	0.02
11	0.782	0.05	23.4	4	60	0.01
12	0.782	0.05	21.4	3	60	0.01
13	0.782	0.05	20.4	3	60	0.01
14	0.782	0.05	19.4	5	60	0.01

FIGURE 8·5 Computer Simulation Run 1

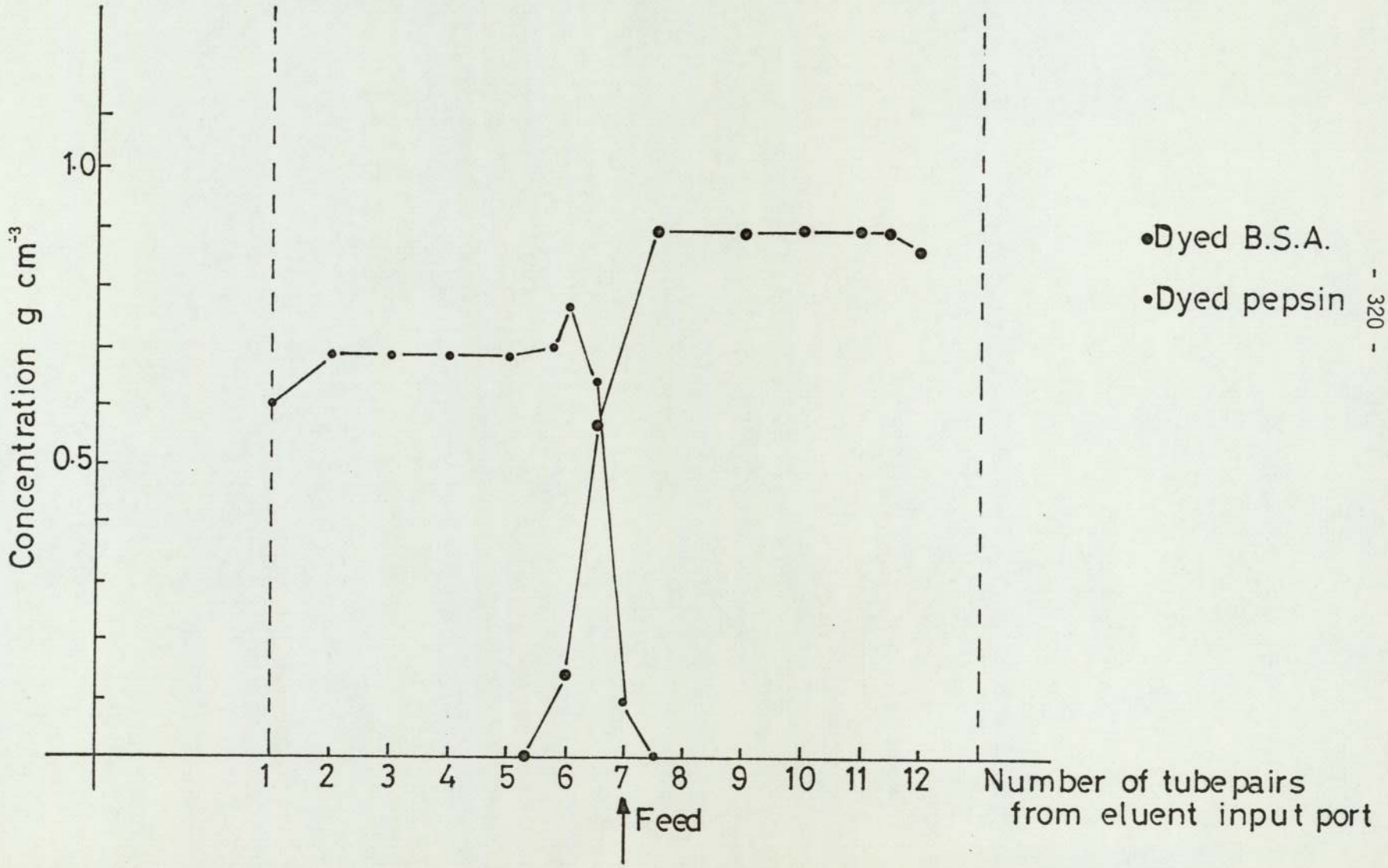

FIGURE 8·6 Computer Simulation Run 2

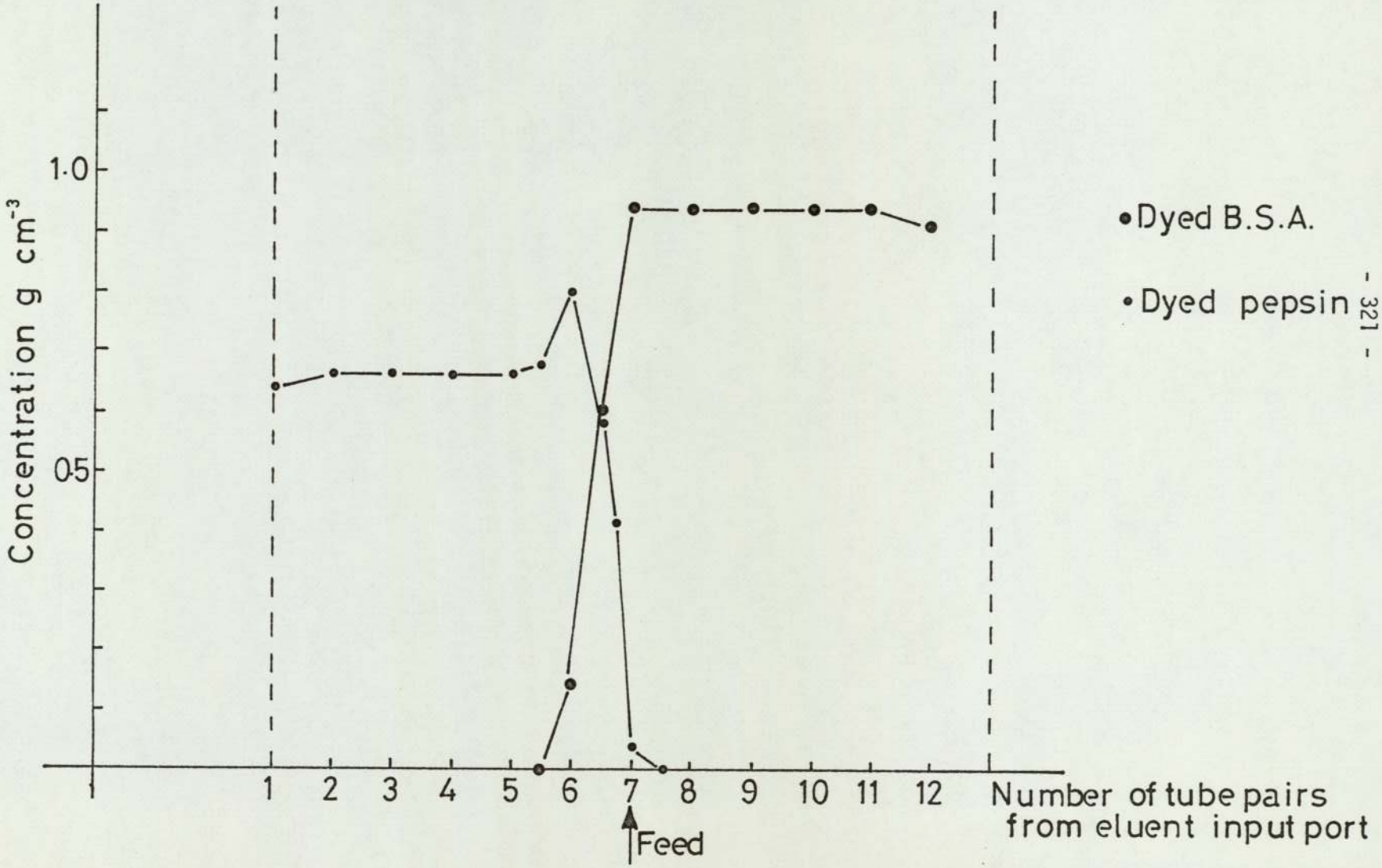

FIGURE 8.7 Computer Simulation Run 3

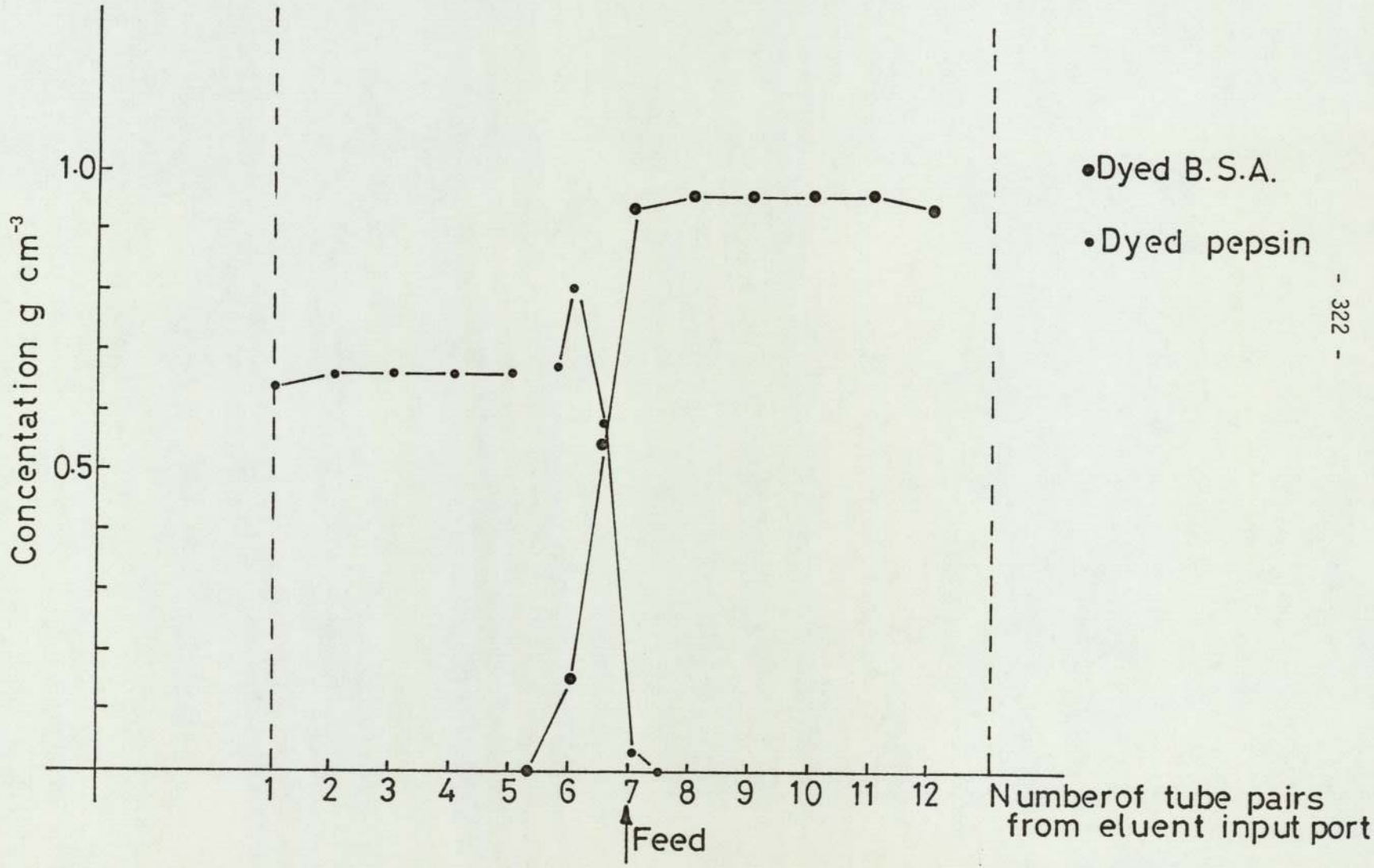

FIGURE 8·8 Computer Simulation Run 4

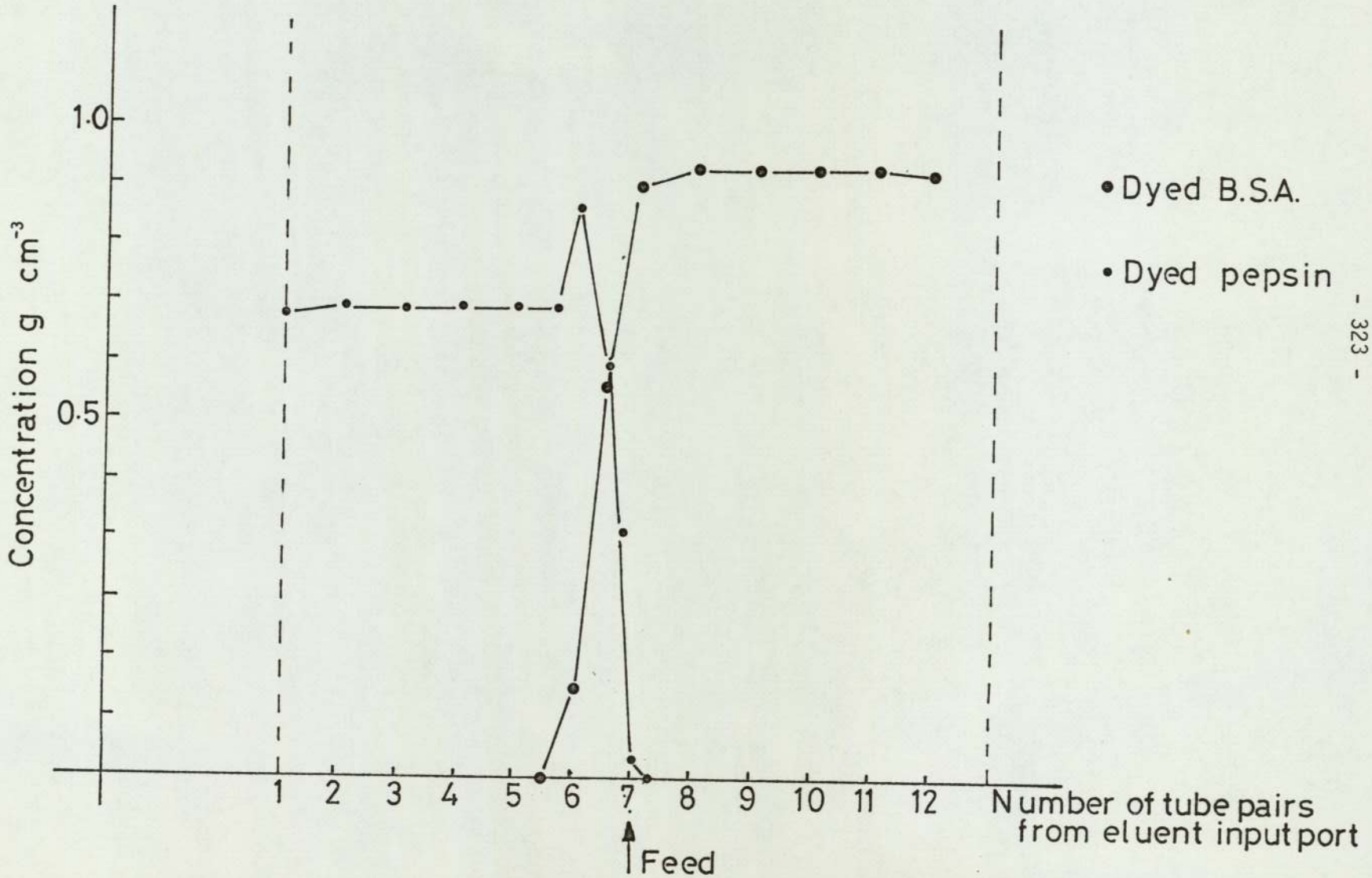

8.3.2 Simulation of the Binary Experiments

Runs 5-9 (Figures 8.9-8.13) were carried out to simulate, under ideal conditions, the experimental runs (Binary Runs 1-3, 5-6) described in Chapter 7. Eluent rates were chosen that corresponded to the mean "cut" partition coefficients in the experiments. No comparison can be made between the experimental and computer concentration profiles because of the adverse effects of liquid leakage in the experimental results. Despite this, some of the effects observed experimentally were confirmed by the model. In agreement with experimental observations, Runs 5-7 (Figures 8.9-8.11) showed that a decrease in the prefeed eluent rate from 0.874 $cm^3\ min^{-1}$ to 0.71 $cm^3\ min^{-1}$ caused an increase in the concentration reached by the dyed bovine serum albumin and a corresponding decrease in the concentration reached by dyed pepsin.

In practice it proved necessary to restrict experimental runs to a nominal 24 hour period, which had proved adequate time to reach pseudo-steady state. However, from the computer studies only in Run 6 (Figure 8.10) did 24 hours prove adequate. In Runs 5 and 7, 49.2 hours and 41 hours had to be simulated in order to achieve an acceptable equilibrium.

Two further experimental runs had been attempted with a feedrate of 0.15 $cm^3\ min^{-1}$. The simulation of these two runs gave component concentration profiles which are presented in Figures 8.12 and 8.13. In both runs only one of the two "cut" partition coefficients lay within the theoretical limits for separation. In Run 8 (Figure 8.12) the postfeed cut value lay between the two limits. Whereas in Run 9 (Figure 8.13) the prefeed cut value lay within the two limits. Component separation was not achieved in either of the simulations. This observation confirms the theory that both operating conditions

FIGURE 8.9 Computer Simulation Run 5

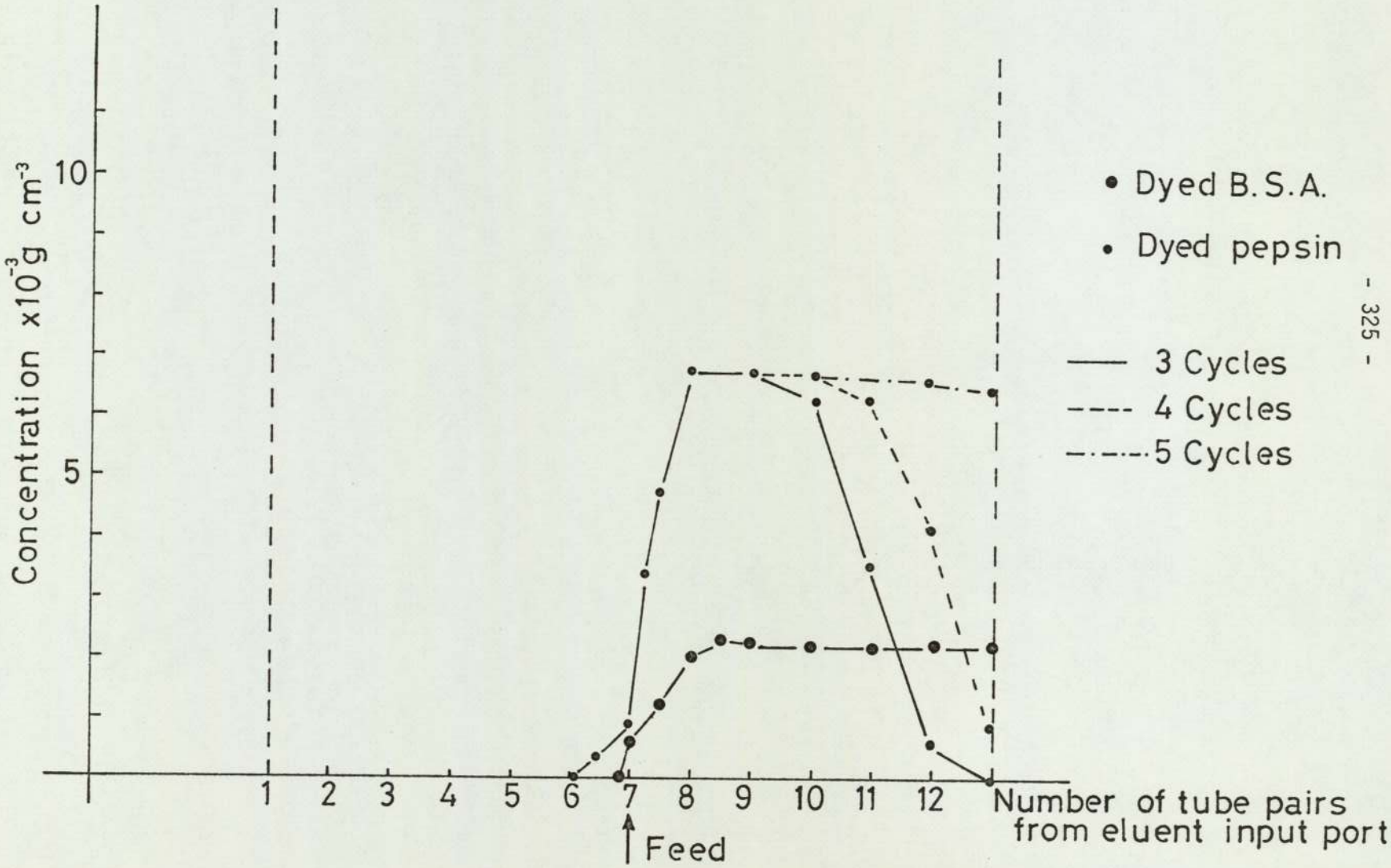

FIGURE 8·10 Computer Simulation Run 6

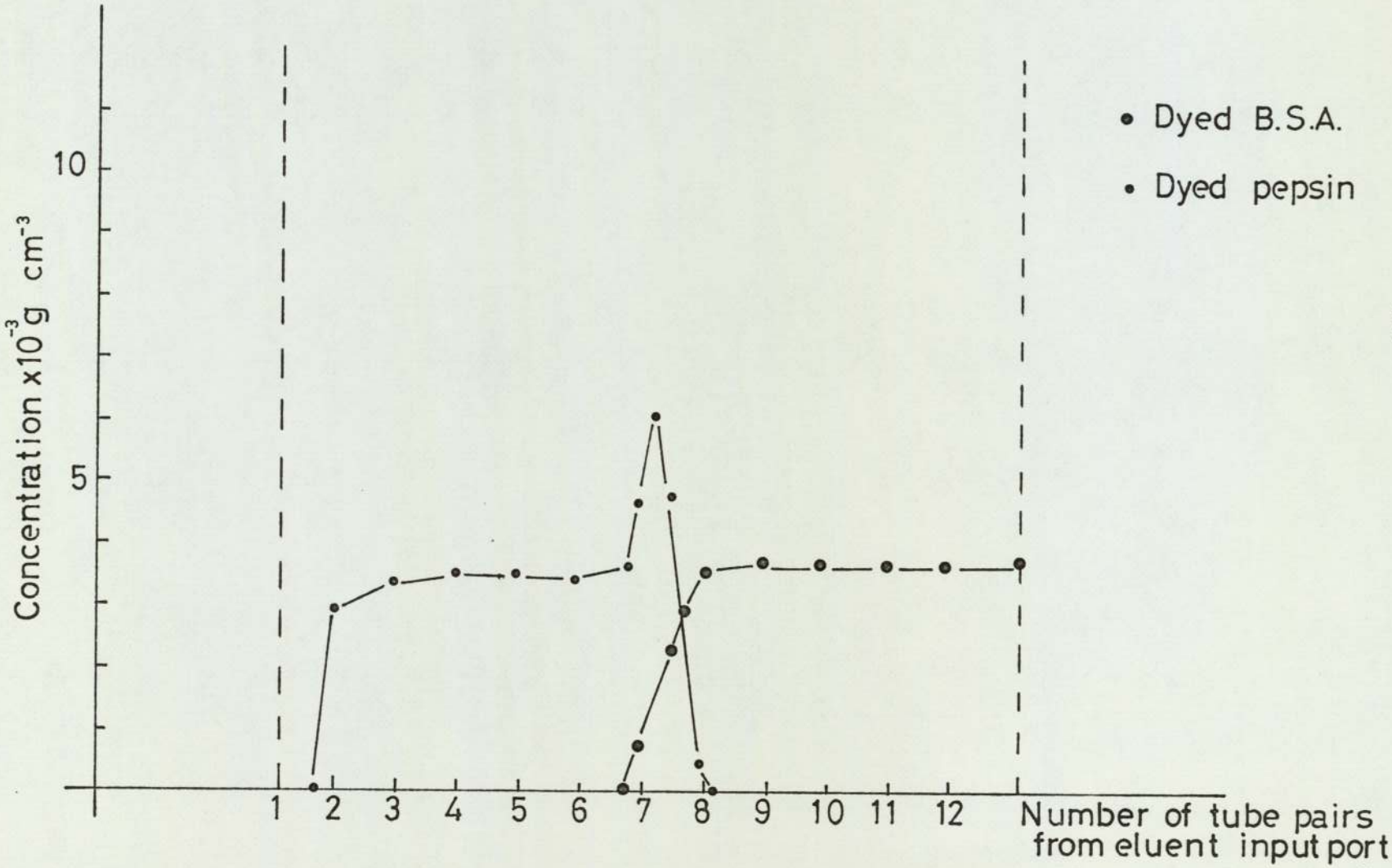

FIGURE 8.11 Computer Simulation Run 7

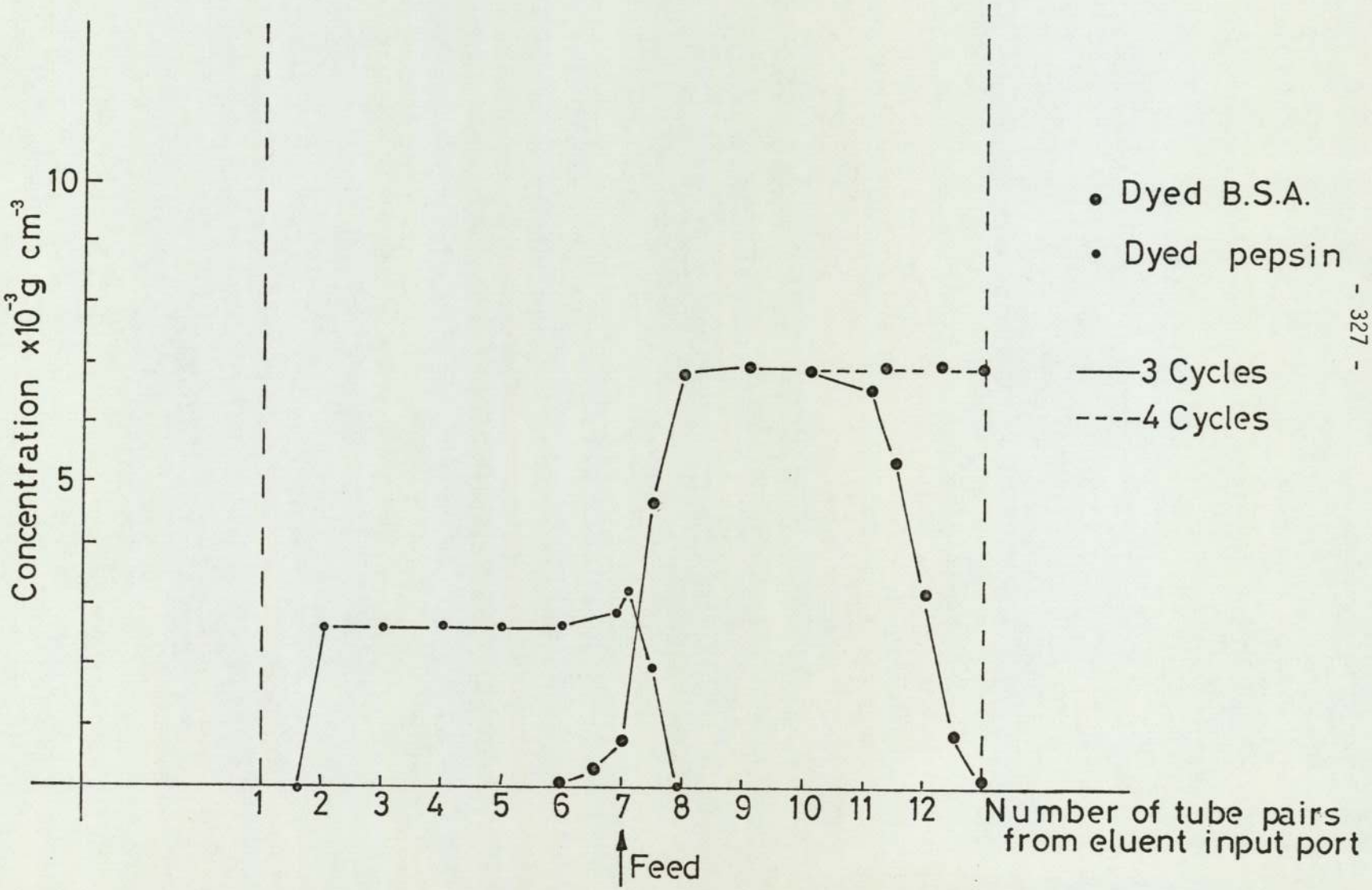

FIGURE 8.12 Computer Simulation Run 8

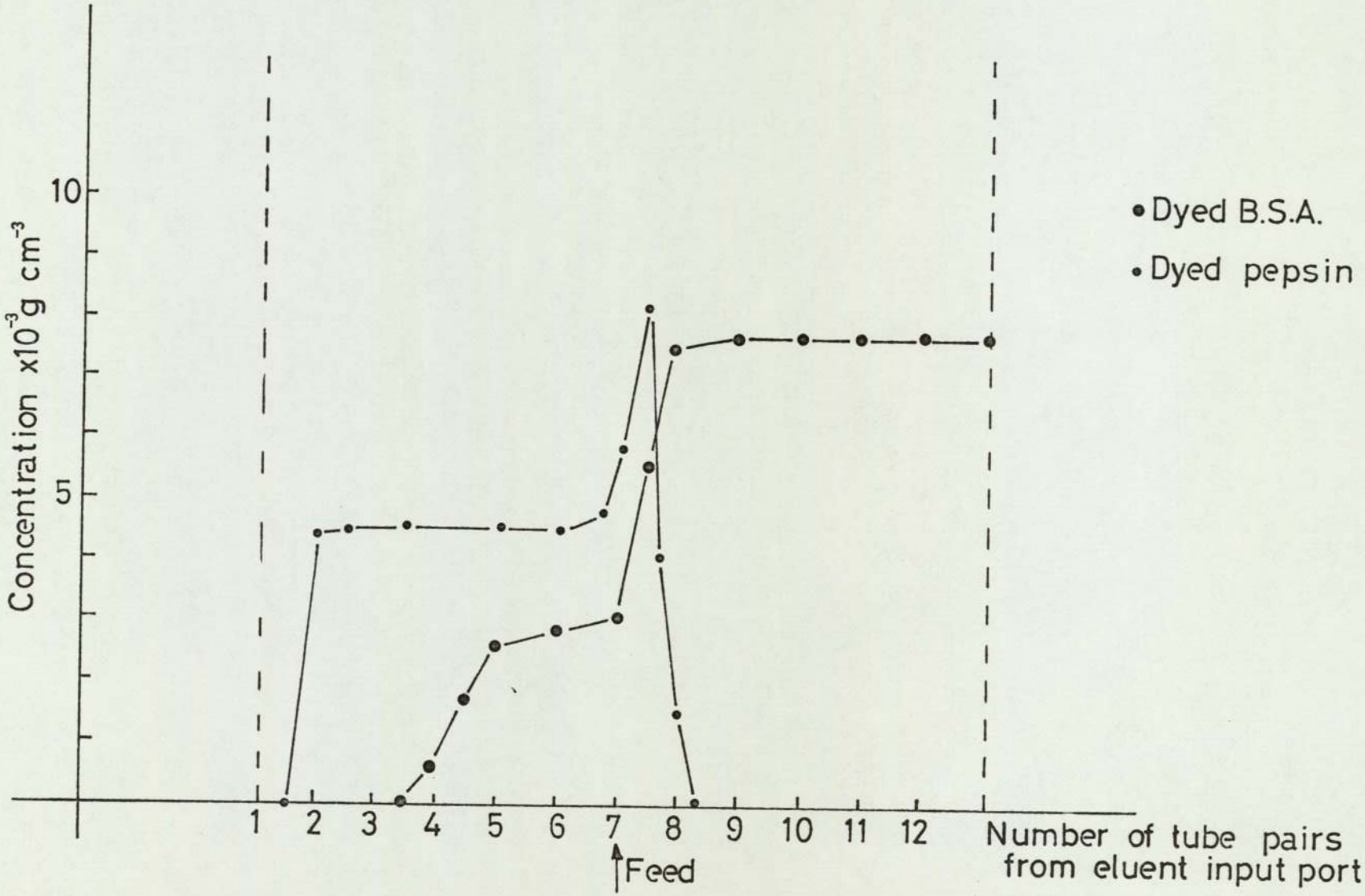

FIGURE 8.13 Computer Simulation Run 9

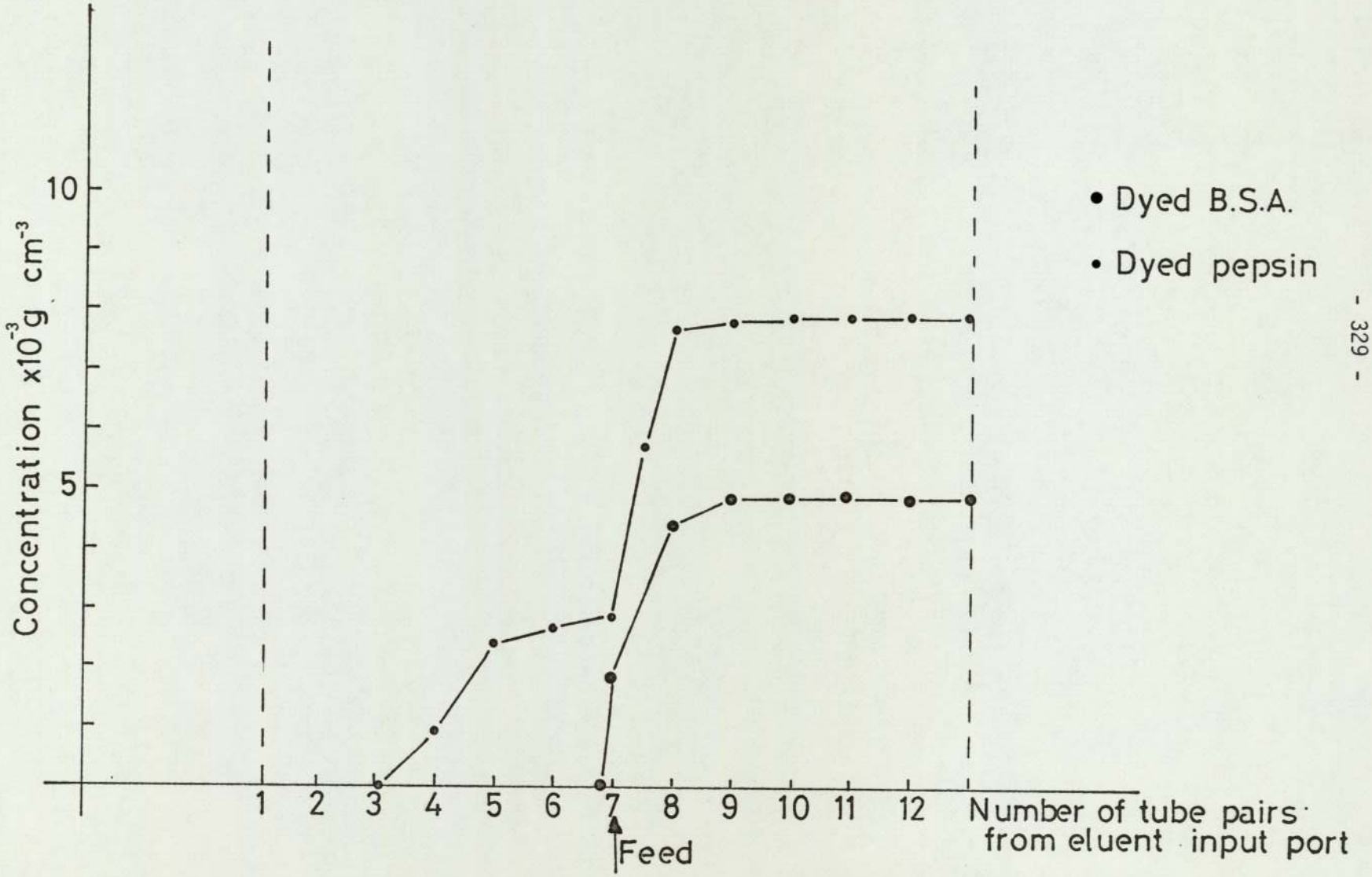

are important in the separation process. In addition to this it establishes that even under ideal conditions a high feed rate can influence the quality of separation achieved. It is interesting to note that the increase in dyed pepsin concentration around the feed point (Column 7) in Run 8 is significantly greater than in the previous runs, where the feed rate was considerably lower.

8.3.3 The Effect of an Increase in Feed Concentration

In Run 10 (Figure 8.14) the concentration of each component was increased from 0.01g cm^{-3} in Run 6, which is used as the standard, to 0.02g cm^{-3}. The effect on both component concentration profiles was to double the concentration level reached by the two components. Such an effect was to be expected in view of the assumption that the component partition coefficients are independent of concentration. In reality this would only be true under dilute conditions.

8.3.4 The Effect of Changing the Tube Bundle Speed

Altering the bundle speed is equivalent to changing the stationary phase flow rate, and should therefore have an effect similar to changing the eluent rate. In Runs 6, 11-14, the switch time was changed from 23.4 min to 19.4 min in 1 min intervals. The flow conditions were the same as those used in the standard, Run 6 (Figure 8.10). Figure 8.10 also represents the profile obtained with a switch time of 22.4 minutes.

In Run 11 (Figure 8.15) the postfeed and prefeed "cut" partition coefficients were calculated to be (Equation 5.10) 0.53 and 0.426 respectively. Figure 8.16 shows that separation of

FIGURE 8.14 Computer Simulation Run10

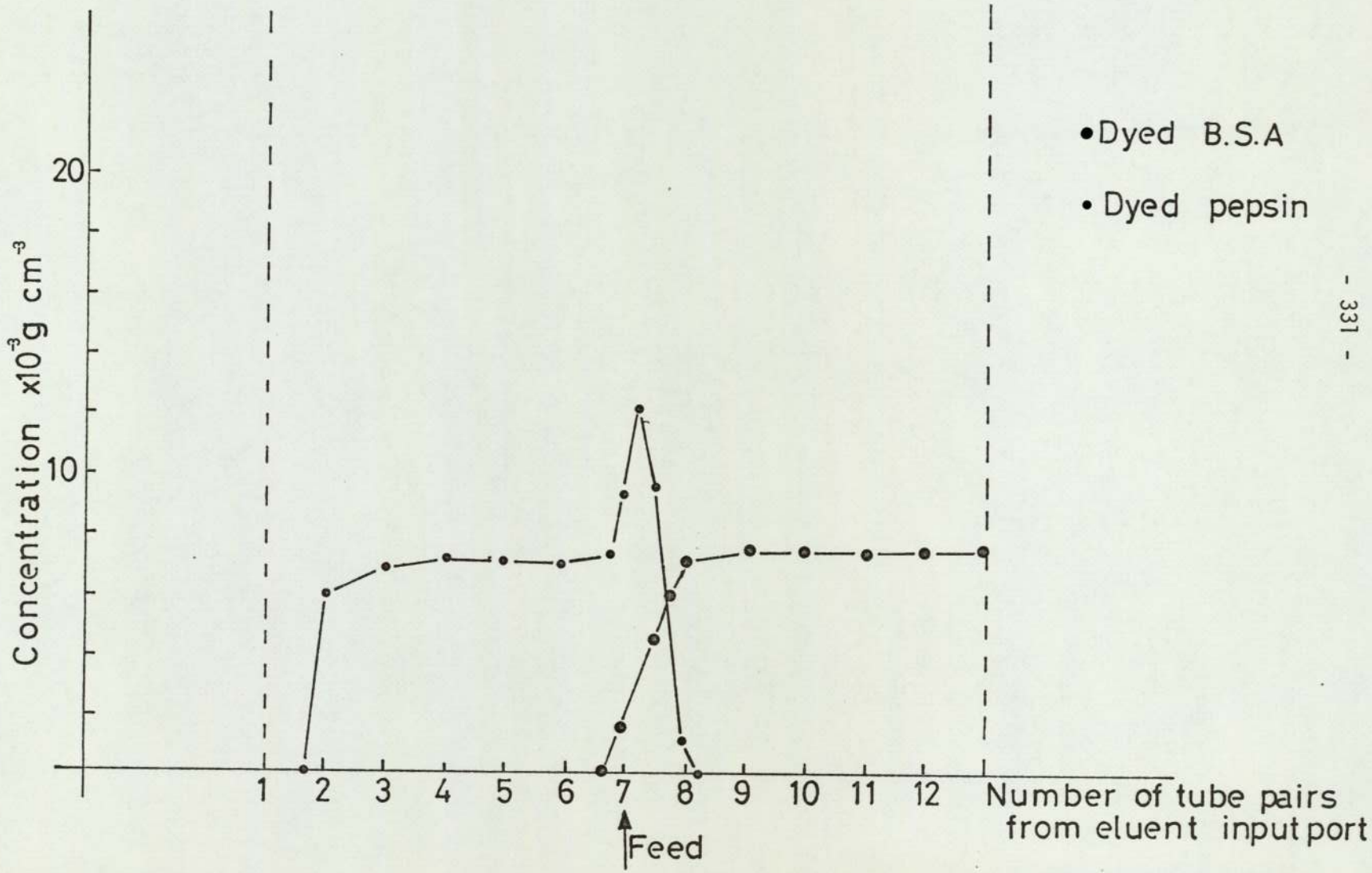

FIGURE 8.15 Computer Simulation Run 11

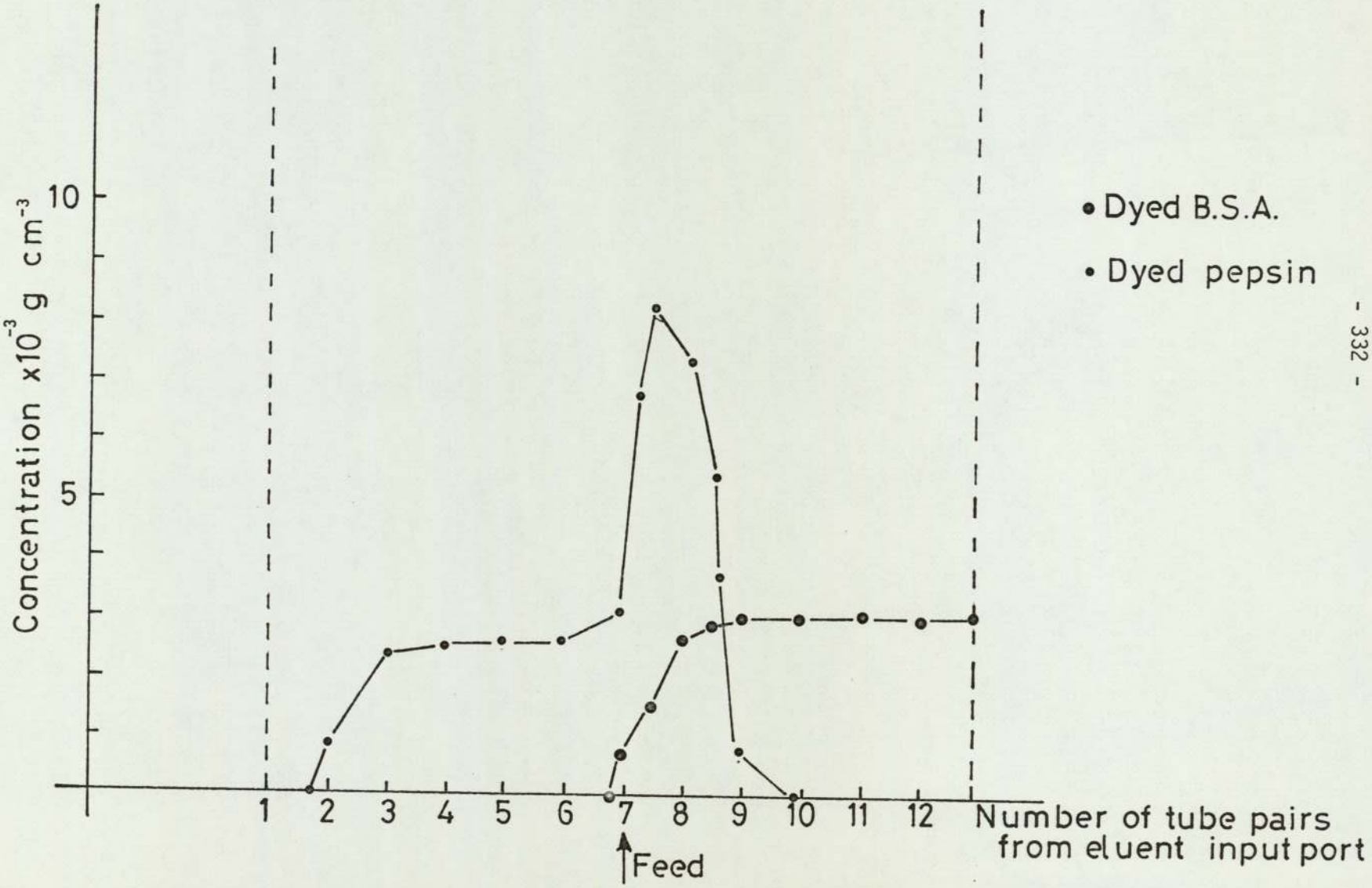

FIGURE 8·16 Computer Simulation Run12

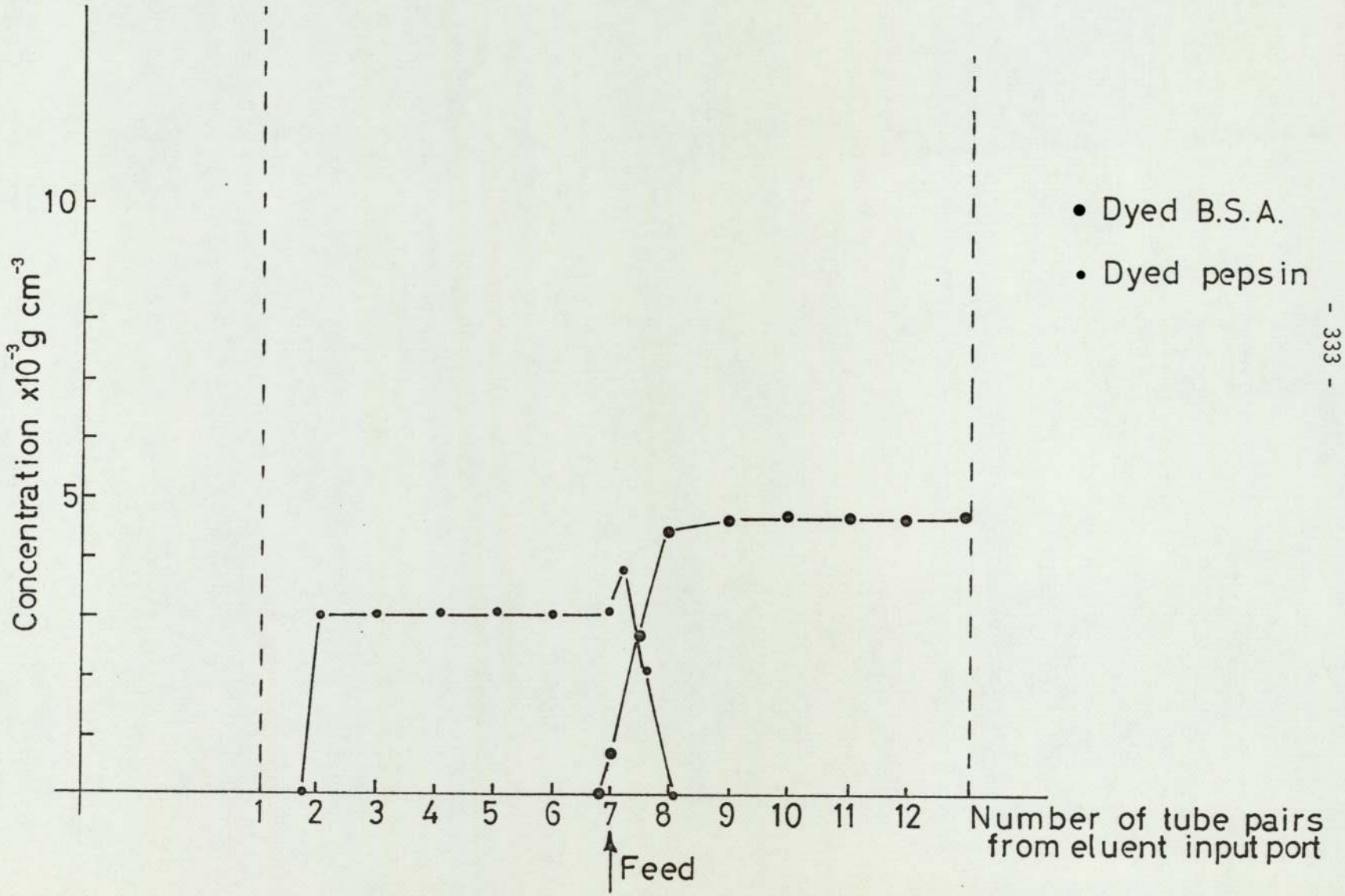

FIGURE 8.17 Computer Simulation Run13

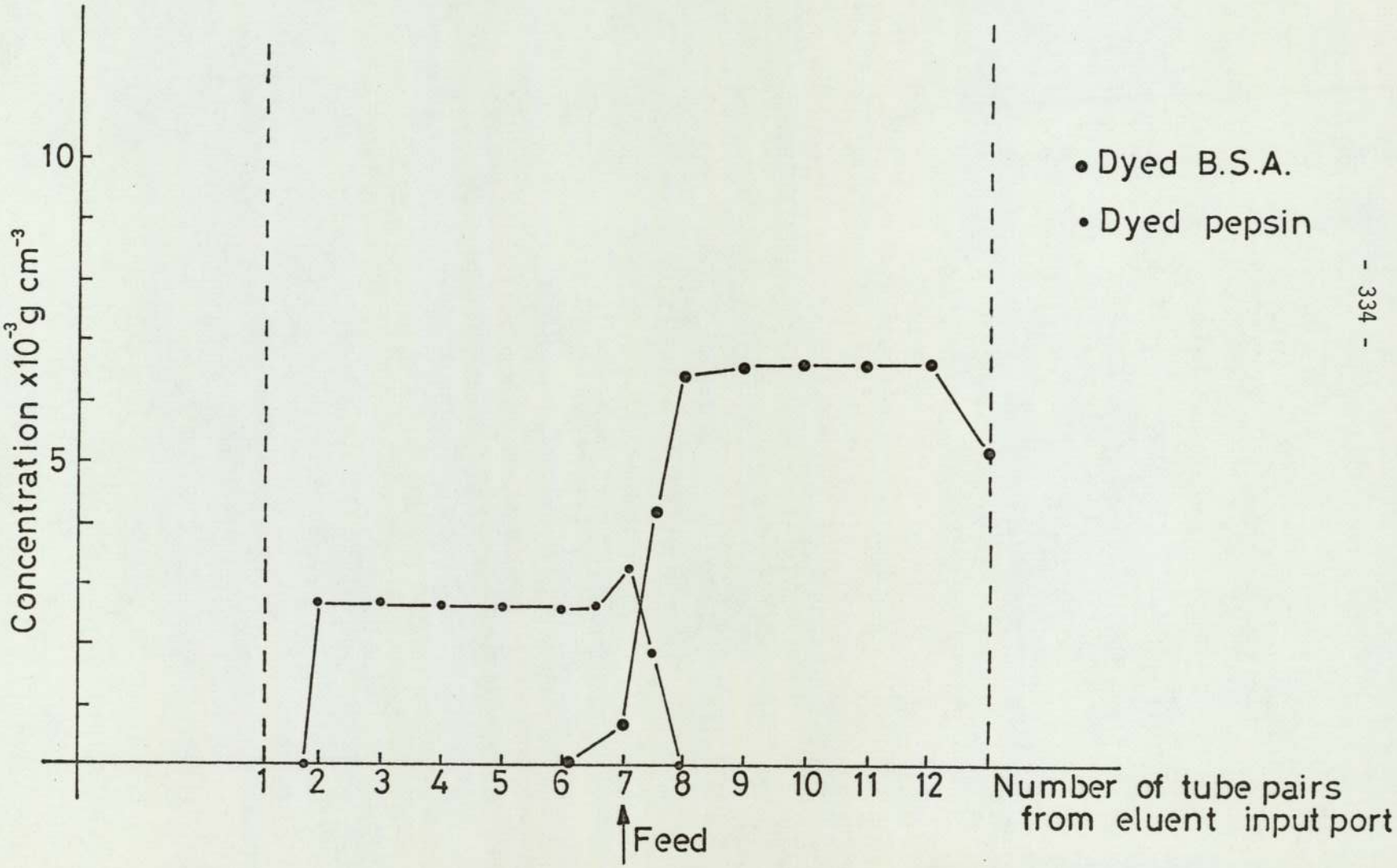

FIGURE 8·18 Computer Simulation Run 14

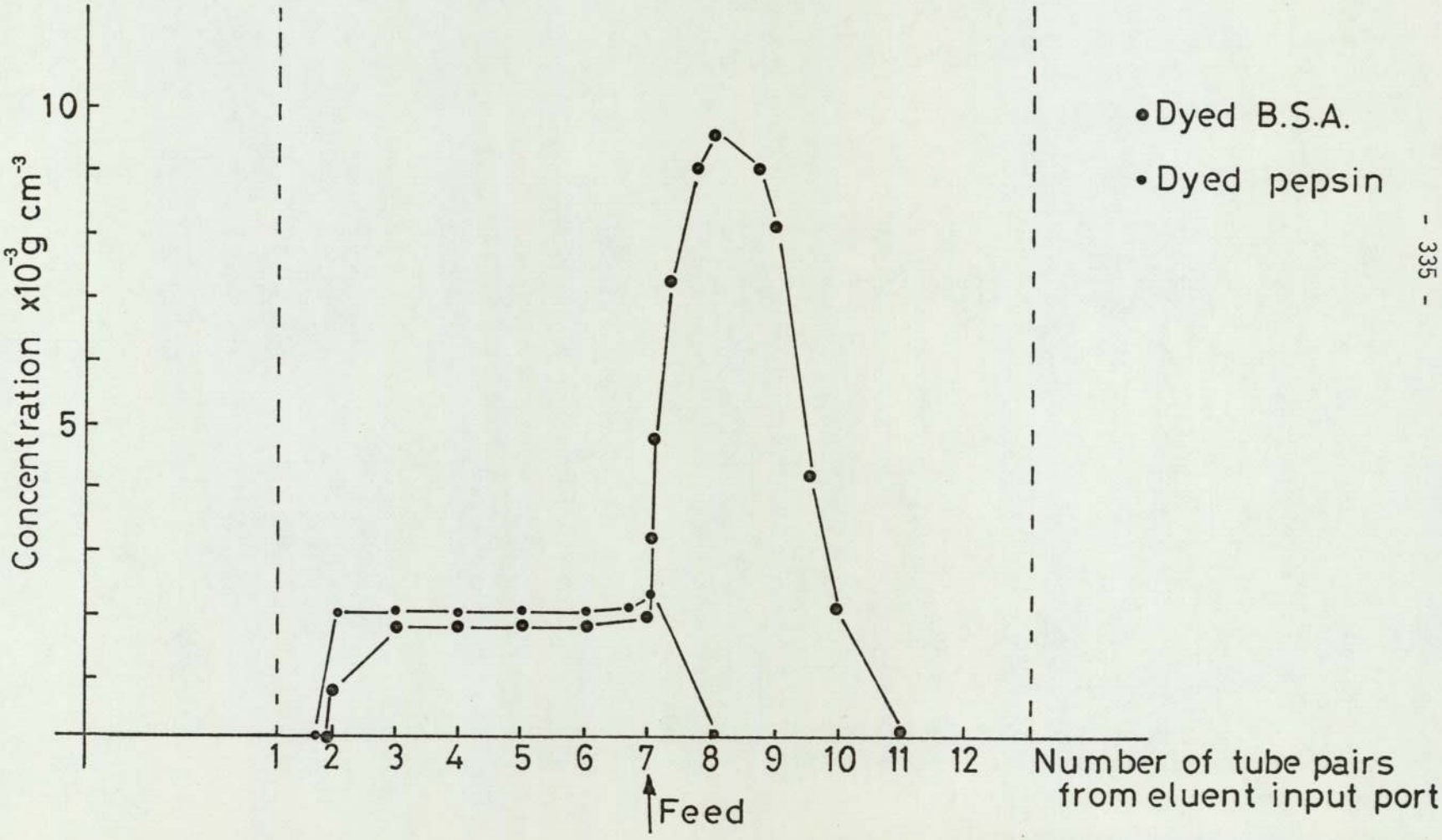

the two components has been achieved. A feature of this figure is the increase in the dyed pepsin concentration around the feed point (Column 7). This increase is due to the fact that the postfeed flow conditions correspond to a "cut" partition coefficient similar to that of dyed pepsin, with the result that there is a decrease in the migration rate of dyed pepsin in the postfeed section. As the switch time was decreased (Figures 8.10, 8.15-18), the effect of the flow conditions on the concentration of dyed pepsin at the feed point decreases. Conversely the concentration of dyed bovine serum albumin increases, until at a switch time of 19.4 min no separation is achieved. This was expected as the "cut" partition coefficients, 0.24 and 0.15 for postfeed and prefeed respectively, lie outside the theoretical limits for separation set by the component partition coefficients. The concentration profile for dyed bovine serum albumin obtained in Run 14 (Figure 8.18) has a shape similar to that predicted for dyed pepsin in Run 11 (Figure 8.15). The similarity is probably due to the fact that in both cases the operating conditions coincide with "cut" partition coefficients of the order of one or other of the theoretical operating limits.

In these five simulations it was observed that as the "cut" partition coefficients approach either of the limits of separation, the number of cycles required before a pseudo-steady state is achieved increases. Four cycles, 34.3 hours, in Run 11 and five cycles, 35.6 hours, in Run 14 compared to three cycles in Run 6 and 12, 24.6 hours and 23.5 hours respectively. This is in agreement with theory (Chapter 5) which stated that if the component partition coefficient is of the same order as the "cut" effected by the

continuous chromatograph then the rate at which that component moves, in the ideal case, approaches zero. Hence the time to achieve an accepted equilibrium increases.

8.3.5 Accuracy of the Simulation

It can be concluded that the model described represents an idealised picture of the actual process taking place within the chromatographic machine. The removal of the simplifying assumptions would result in a more realistic approach. Factors such as introducing the effects of a concentration dependent partition coefficient would greatly assist a theoretical study of the influence of concentration on the separation process.

In the model each tube pair was assigned an equal number of equilibrium stages, N. In reality this will not be the case, because the height equivalent to a theoretical plate, H, is a function of flow rate and component diffusion coefficients. Component diffusion coefficients are in turn a function of molecular size.

The simulation runs performed have, however, served to theoretically evaluate the influences of some of the key variables involved in the chromatographic process. These are the number of equilibrium stages, or theoretical plates, per tube pair, the eluent rate, the bundle speed and the feed rate. A major improvement to the model would be the introduction of concentration effects.

CHAPTER 9

Conclusions and Recommendations for Future Work

This research has shown that the principle of a continuous form of liquid-liquid chromatography can be applied, on a laboratory scale, to the continuous fractionation of dextran. Double fractionation of a dextran solution with a wide molecular weight distribution on Spherosil XOB075 (200 μm to 400 μm) in 0.8 cm diamter columns resulted in a dextran fraction with a molecular weight distribution comparable with that produced commercially by ethanol precipitation.

Experimental work established that the "cut" effected by the equipment was influenced by the feed concentration. Under constant flow conditions the "cut" effected by the equipment was shown to shift towards the high molecular weight end of the feed distribution as the feed concentration increased. Feed concentrations of between 0.5% w/v to 20.8% were used at feed rates of nominally 0.05 cm^3 min^{-1}.

Equipment operating conditions were dependent on the satisfactory operation of the mechanical seal. However, when conditions were stable the process was shown to produce products with consistent mean molecular weights and molecular weight distribution over periods up to 192 hours. A limitation on pressure drop restricted dextran throughput to a maximum of 1.14g hr^{-1}.

In agreement with the qualitative theory postulated in Chapter 5 the overlap in product molecular weight distribution is a property of the process. The degree of overlap is expected to be a function of process operating conditions.

Future work on dextran fractionation should include an investigation of the effects on the product molecular weight distribution of the following:

(i) Feed rate.

(ii) The use of high eluent rates and thus faster bundle speeds.

Other factors are the use of high feed concentration to increase throughput and the optimisation of fractionation length for a pre-defined cut position. Quantifying the effects of these parameters would assist in design procedures.

A binary mixture was used to investigate some of the effects of the various operating parameters. The limited number of runs performed with the dyed bovine serum albumin and dyed pepsin mixture could not be used to determine the effects of eluent rate on product purities because of liquid leakage from the seal. Component concentration profiles provided an indication ofthe effect of eluent rate on component concentrations within the equipment. A decrease in the eluent rate was shown to result in an increase in the concentration of the component preferentially travelling with the mobile phase and a decrease in the concentration of the component travelling with the packing. The separations achieved were undoubtedly influenced by the effects of leakage from the seal. This leakage was a result of a decrease in surface tension of the sealed fluid caused by the surfactant properties of the dyed protein mixture used.

Future work with binary mixtures could involve the use of alternative packings because of the incompatability of some solutes with the silica type of packing. Some of the rigid xerogel-aerogel hybrids listed in Table 4.3 might be more practical.

To enable the study of the individual factors affecting the performance of the continuous chromatographic unit a digital computer simulation has been developed. The simulation is based on a simple equilibrium stage model. Simulation studies of the dyed protein mixture separations have confirmed the observations made experimentally about component concentrations. Increasing the bundle speed was shown to have a similar effect to a decrease in the eluent rate. A pseudo-steady state condition was found, in the ideal case, to be dependent on the operating conditions. The nearer the "cut" effected by the machine to either of the component partition coefficients, the longer the time required for equilibrium to be reached. Component concentration profiles were shown, for the system studied, to be insensitive to the number of equilibrium stages assigned to each tube pair. In keeping with the simplifying assumptions made, the component concentrations were proportional, under constant flow conditions, to the feed concentration. A more realistic model would result if the effects of concentration were introduced.

Undoubtedly the major problem throughout the research was the moving seal which was an essential part of the chromatographic machine. The machine had initially been designed in such a way that stable operating conditions could not be achieved. An analysis of the problem established that the seal was structurally weak and, as a result, suffered from the adverse effects of localised distortion. This distortion caused seal face separation and resultant seal failure. Strengthening the tube bundle face proved to be a partial solution. However, the stable operation of the equipment remained very unpredictable. Both temperature fluctuation and the physical properties of the sealed medium were shown to influence the

satisfactory running of the seal. When stable operating conditions were obtained, the equipment operated without fault.

The development and application of continuous chromatography on an industrial scale will be controlled by the solution of the problem of scale up. An intrinsic part of this development will be, because of the high cost of chromatographic media, the use of small scale equipments. Equipment such as that used in this research has therefore an important role to play, providing the problems associated with the mechanical seal can be solved. Other problems connected with the design of such equipment are minor in comparison. A possible seal design is given in Figure 9.1.

The essential design features required are a single pressure loading device, possibly a hydraulic cylinder, which would apply pressure to a solid round metal spider (Figure 9.1). The spider would in turn apply pressure to a backing plate. The advantage of a single loading device is that pressure can be applied evenly over the whole of the sealed surface.

The backing plate should be of sufficient thickness so as to eliminate any distortion. The ring forming part of the seal should be set into the backing plate to prevent it deforming whilst under load. Graphlon was the material of construction used in this research. Because of the elasticity of this material there are problems associated with lapping it to the required degree of flatness. The use of a harder material with similar lubricating properties would alleviate this problem.

From the comparative success of adding a stiffening ring to the tube bundle face, it is proposed that in any new machine the tube bundle face be designed such that the forces acting upon it are

FIGURE 9.1 Possible Seal Design

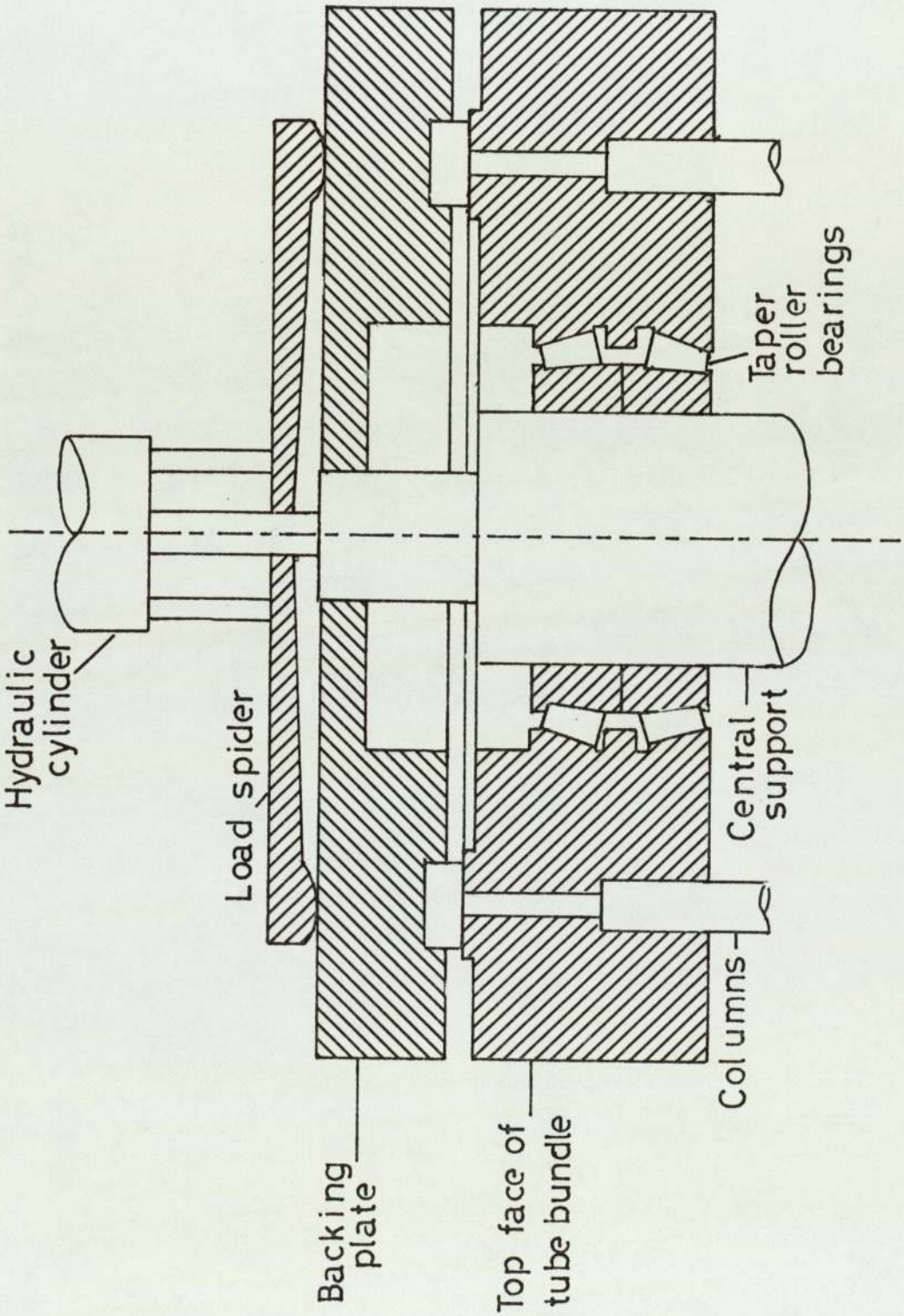

taken into account. This would reduce the possibility of unwanted distortion in the seal.

The problem of bearing failure could be reduced by mounting the bundle face on two large taper bearings. In doing this, the paths through which forces act causing distortion are kept to a minimum. All loads are therefore restricted to one region around the seal.

The tube bundle could be turned in a manner similar to that used in this research. It is however suggested that the drive be brought nearer to the frictional forces that have to be overcome. This could be accomplished by applying the drive to the top face of the tube bundle. There are two possible methods of driving the bundle. Firstly, a continuous method where the tube bundle is continuously rotated. The disadvantage of this method is that the seal is always in a state of dynamic stress. The second method, and probably the most suitable, is to keep the tube bundle static for a time equivalent to one switch time, at the end of which the bundle is indexed round the required distance.

Alternative future applications of continuous chromatography should be investigated. In particular, ion-exchange and the use of the process as a means of isolating and producing enzymes are attractive possibilities.

(i) Method for Improving the Operation of the D.C.L. pump, Head Size 1

The method developed to ensure that the feed pump, head size 1, operated satisfactorily during the course of the research is discussed below. The technique can equally well be applied to other head sizes rather than going to the expense of buying replacement parts.

In the positive displacement type of pump there are a pair of ball and seat valves on the inlet and outlet to the pumps piston chamber. These valves ensure that on the outward stroke the piston only draws liquid into the chamber from the input side. Conversely on the inward stroke liquid is forced out only through the output side. In pumps with head sizes 2 and 3 the throughput and pressure developed was sufficient to maintain a constant and unidirectional-rate of flow. However in the smaller pump, head size 1, this was not the case. Satisfactory operation relied on positive sealing of all the ball and seat valves, slight imperfections or scratches on the stainless steel ball or valve seat were sufficient to prevent satisfactory operation.

Initially the valve seats are examined under a microscope to check for evidence of pitting around the seat due to corrosion. Each seat is then ground, to remove imperfections, using a fine carborundum paste. The seat faces are then polished with a diamond paste to give a high degree surface shine. Periodic examination of the seat face is made to ensure that traces on the old seat of corrosion have been removed.

A simple cutting tool is then made (Figure 1A-1a) by mounting, using Araldite, one of the ball bearings used in the pump on the end of metal rod. The thickness of the rod is roughly that of the stainless steel ball. A glass cutter is then used to put a pair of vertical scratches on the ball. By carefully holding this

FIGURE 1A-1 Cutting Tool and Method

(a)

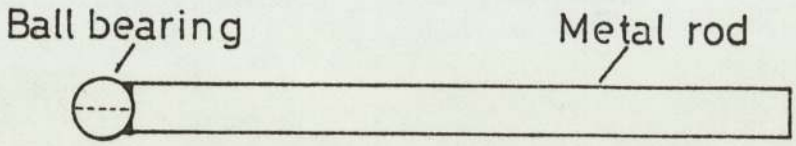

(b)

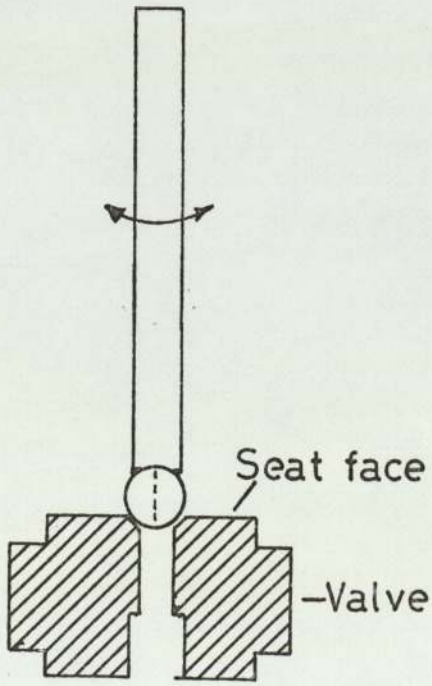

cutting tool in the required position (Figura 1A.1b) on the remade seat face, and gently rotating it a new seat for the metal ball can be made. Periodic examination under the microscope is made to check that the bevel on the ball seat is evenly formed.

Once this procedure has been carried out for all the valves the input and output sides of the pump are reassembled and used on a larger pump head, for example head size 3, for a 24 hour period, with an artificially applied back pressure of at least 344 KN/m^2 (50 p.s.i.g.). At the end of this period the input and output sides of the pump are reassembled on the smaller pump, head size 1.

Passing acetone followed by deaerated water through the pump head prior to use ensures that all traces of air are removed.

(ii) The Fraction Collector

A diagram of the fraction collector is given in Figure 1A.2. Basically it consisted of two 60 cm diameter, 2.5 mm thick, polypropylene discs. These discs were horizontally mounted on a central vertical shaft at a height of about 30 cm with a distance of 4 cm between them. The lower disc was held firmly by a nut screwed on to the central shaft. Four vertical rods mounted on its under surface and to a base plate ensured the rigidity of the equipment. Twenty four 5 cm diameter holes tapering to 2.5 cm were drilled through the outer circumference of the lower disc (Figure 1A.2). Sample bottles are placed under these holes.

The upper plastic disc was freely mounted, on two ball races, so that it could rotate. Two holes were drilled through the disc at each end of a line equal to the diameter. These holes were vertically above those drilled in the lower disc. The sample lines from the

FIGURE 1A-2 The Fraction Collector

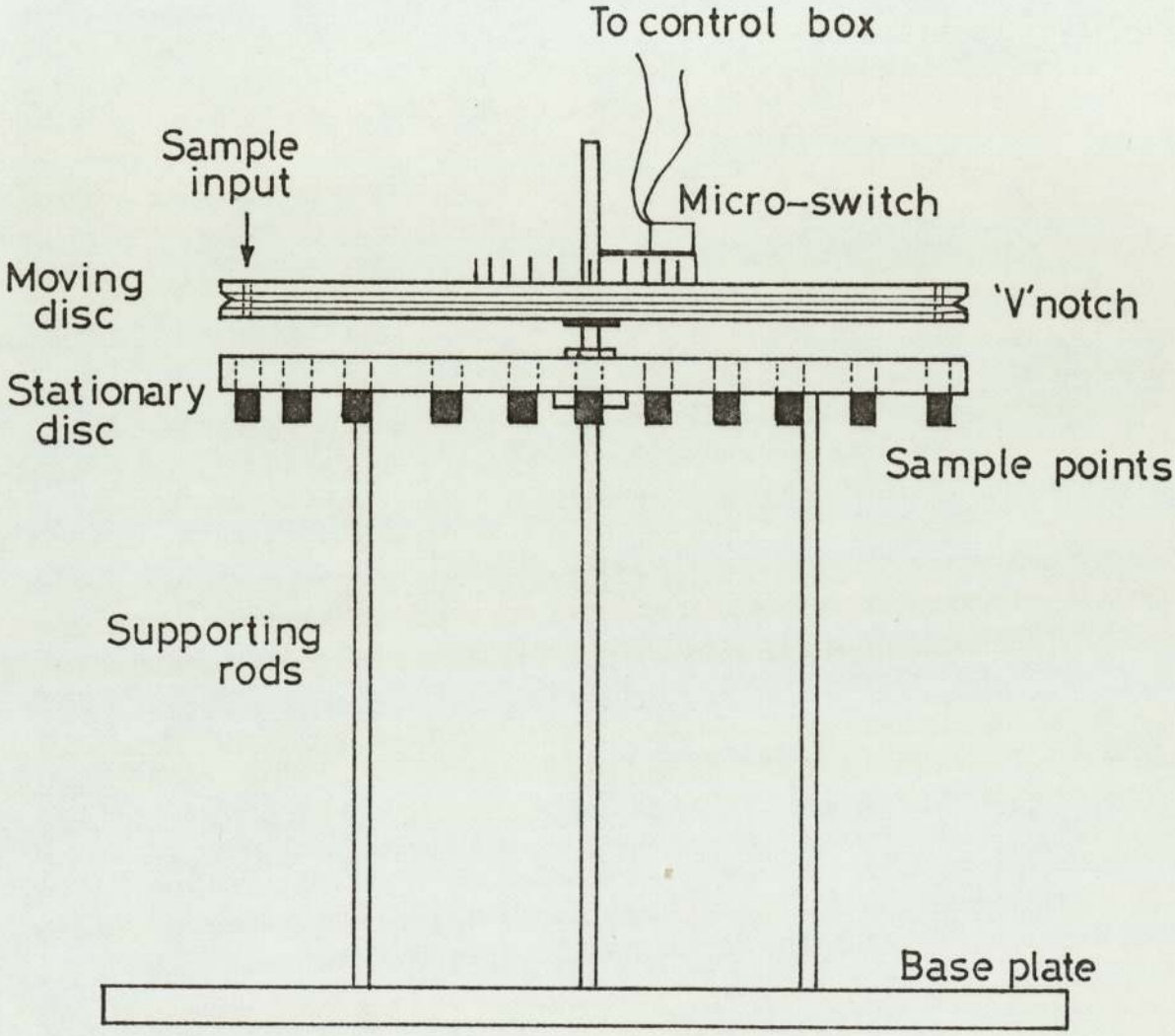

chromatographic machine were fixed into these holes. A 'V' notch machined into the edge of this disc permitted it to be driven by a 'V' belt attached to an electric motor.

A micro-switch, attached to the upper surface of the rotating disc, was connected to an electric drum timer, which controlled the sample times. The drum timer activated the electric motor which indexed round the sample points the required distance. The micro-switch, in turn, switched off the electric motor.

Copy of Report on Continuous Chromatograph

Original design:

1. Assuming a uniform clamping load F/unit radian and no supply pressure.

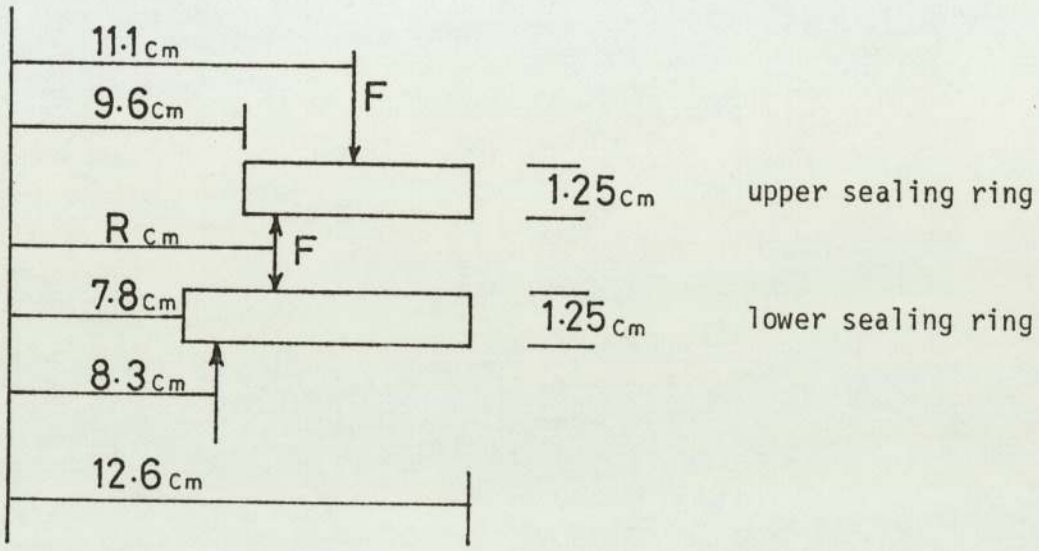

The load F on the upper sealing ring is assumed to act at the loading piston radius, the reaction at the lower face to act at the mid support cylinder radius.

The effective reaction between seal faces and seal ring acts at a radius R.

The couple/unit radian on the sealing ring is F(111-R).

The couple/unit radian on the seal face is F(R-83).

Now for an annular ring the rotation θ is given by:

$$\theta = \frac{12M}{Et^3 \ln (r_o/r_i)}$$

and since the two seal portions must rotate equally

$$\frac{111-R}{R-8.3} = \frac{\ln(12.6/9.6)}{\ln(12.6/7.8)}$$

Therefore R = 10.07 cms

If this radius were to be acceptable it should be within the central third of the seal. However the inner and outer seal radii are 9.9 cm and 124.5 cm respectively. Thus unless the seal face beds in sealing will be impossible.

2. Circumferential pressure variations

The fluid pressure varies circumferentially from 241 kN m^{-2} (35 p.s.i.g.) to 0 and this pressure acts at the radius opposing the daming load. At its peak value the sealed pressure will shift the reaction point further inwards and cause separation of the faces locally. Wear of the sealing ring will reduce this on time but probably not eliminate it due to circumferential variations in the sealed pressure.

Conclusions

It seems probable that distortions of the seal face are causing local separations of the seal faces at the point of highest sealed pressure. Wear of the sealing ring should reduce this in time but is unlikely to eliminate it. The only effective solution would be to significantly reduce the distortion.

Design

Owing to structural difficulties the only way to stiffen the existing design was to attach a rigid ring to the outside of the lower seal face. This was attached so as to eliminate local bending of this seal face at its outer edge.

APPENDIX 3

(i) Auto Analyser Flow Rates and Reagents

Reagents

L-cysteine hydrochloride (0.7g lit^{-1}) in Analar sulphuric acid (86% v/v).

Flow Rates

Sample	0.1 cm^3 min^{-1}
Air	0.32 cm^3 min^{-1}

Cysteine-sulphuric acid reagent 0.53 cm^3 min^{-1}.

(ii) Calculation of the Concentration of Dextran Sample

Glucose standard = $x \mu g\ cm^{-3}$

Response of glucose standard = y O.D.

Response of sample of unknown concentration = z O.D.

Concentration of sample = $w\ \mu g\ cm^{-3}$

$$w = \frac{x}{y} \times z \times \frac{162}{180}\ \mu g\ cm^{-3}$$

Numerical example

$x = 40\ \mu g\ cm^{-3}$, $y = 0.8$, $z = 0.45$

$$w = \frac{40}{0.8} \times 0.45 \times \frac{162}{180} = 20.25\ \mu g\ cm^{-3}.$$

FIGURE 3A-1 AutoAnanalyser Calibration Plot

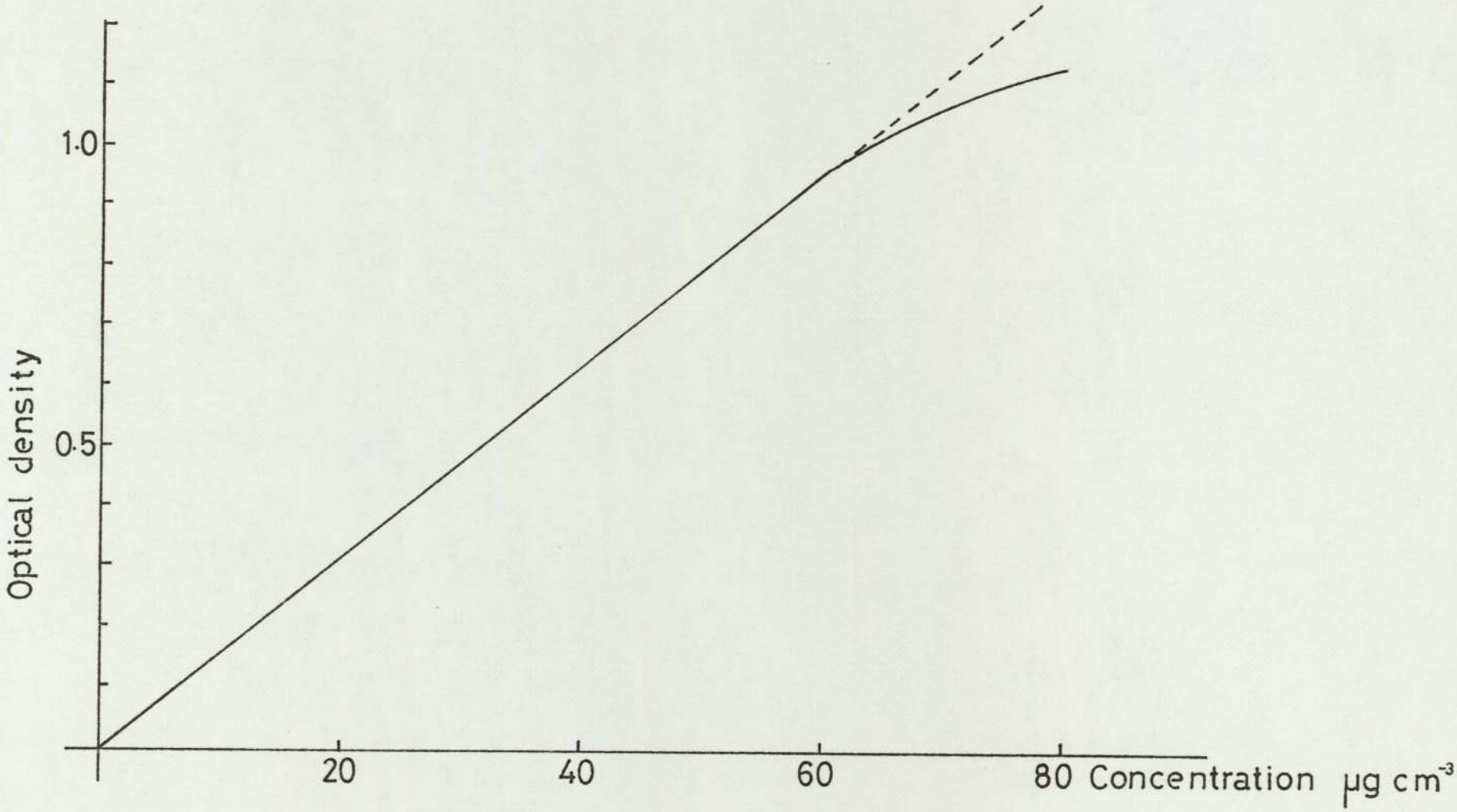

FIGURE 3A-2 Bundle Packing Particle Size Analysis

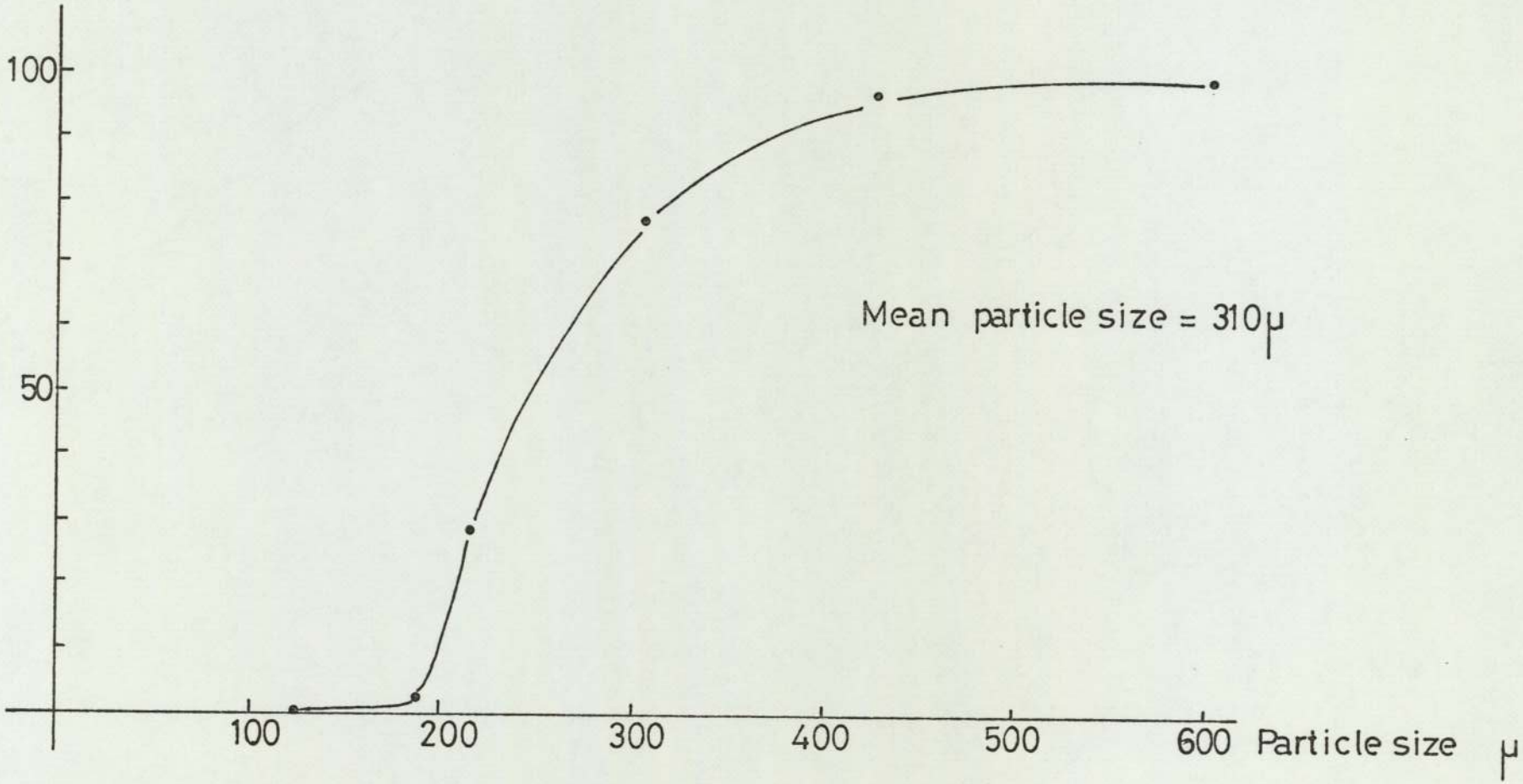

FIGURE 3A-3 Bundle Packing Pore Size Distribution

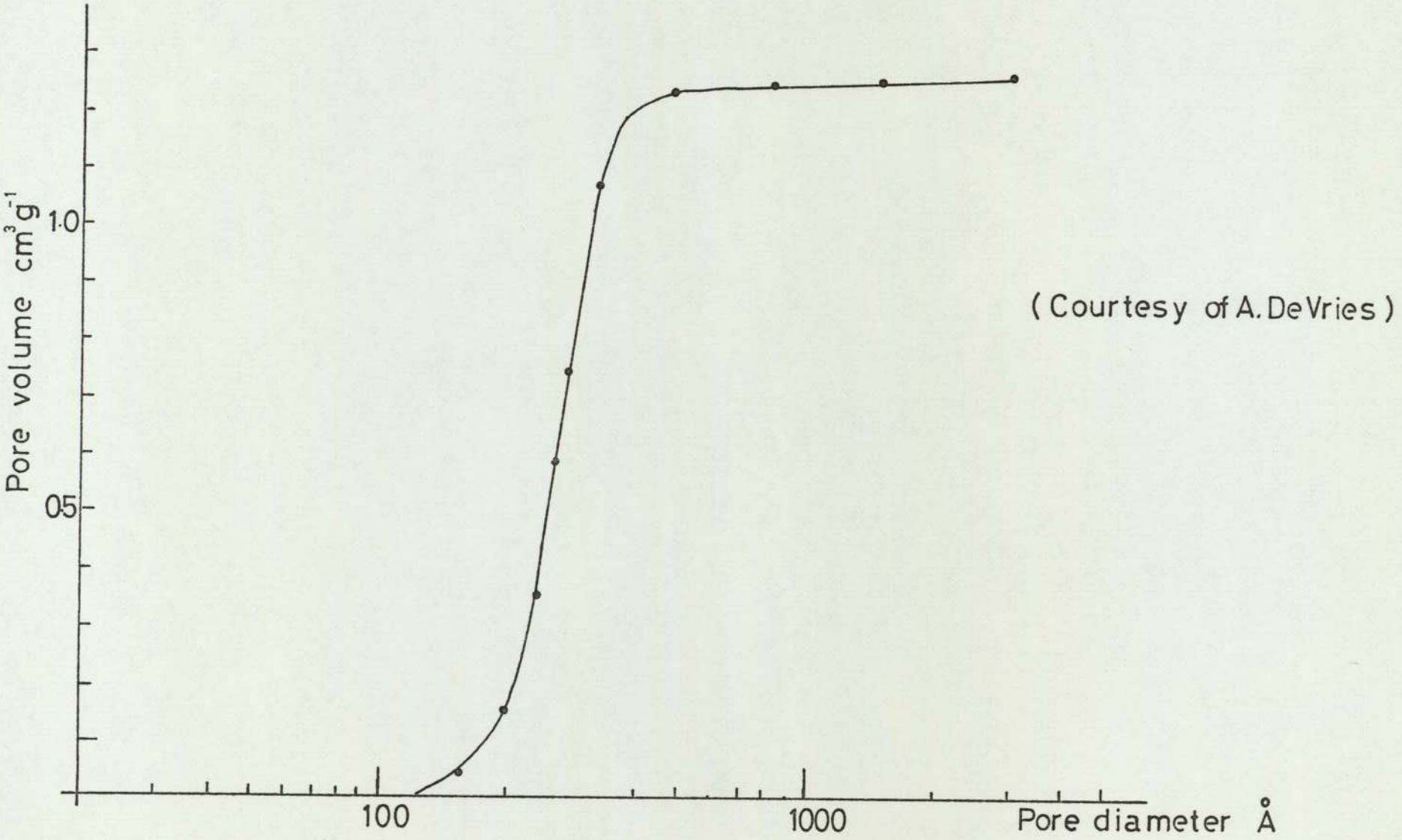

FIGURE 3A-4 Purge and Eluent Pump Calibrations

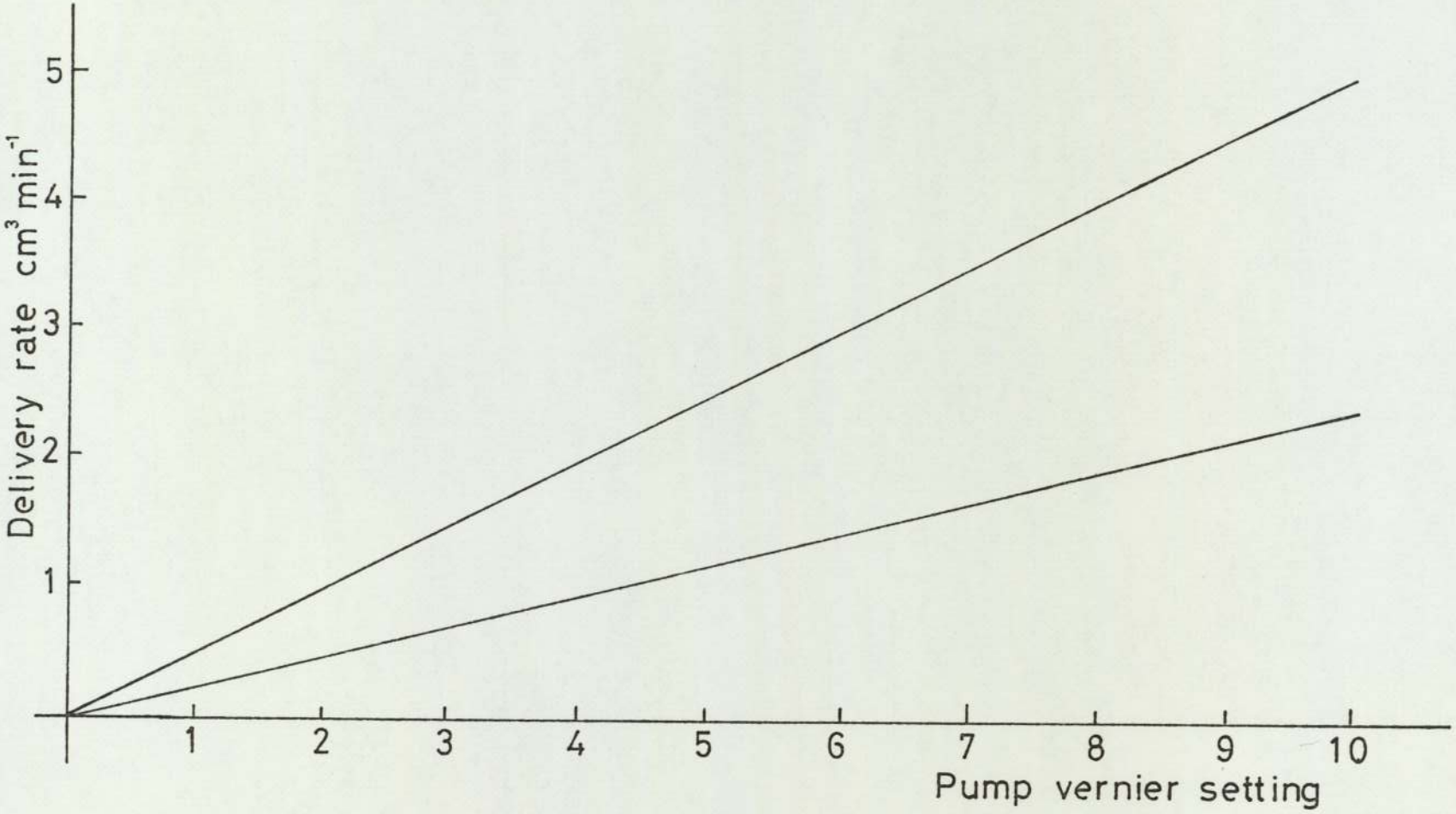

FIGURE 3A-5 Calibration for Bundle Packing

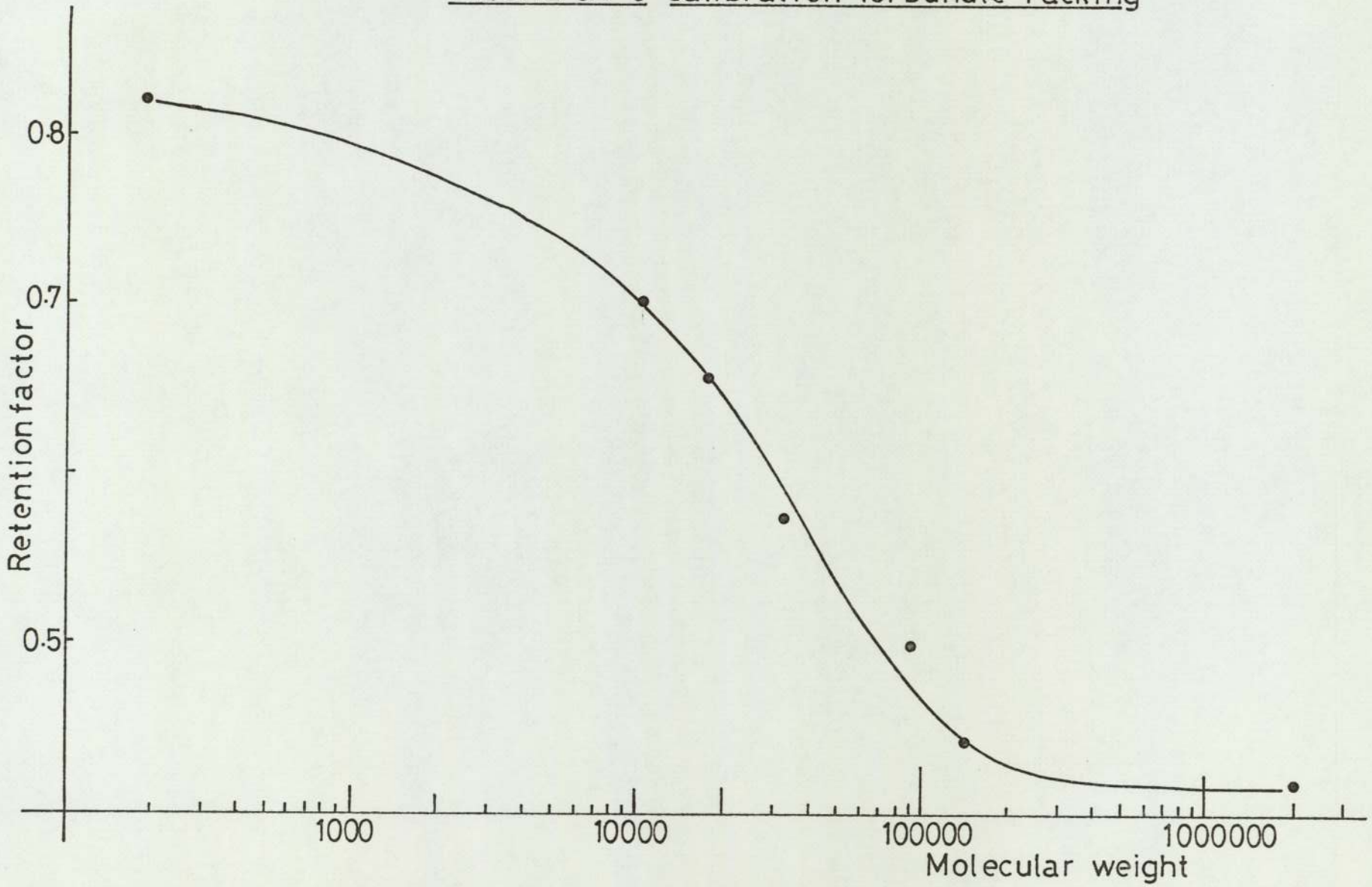

FIGURE 3A-6 Analytical Column Calibrations

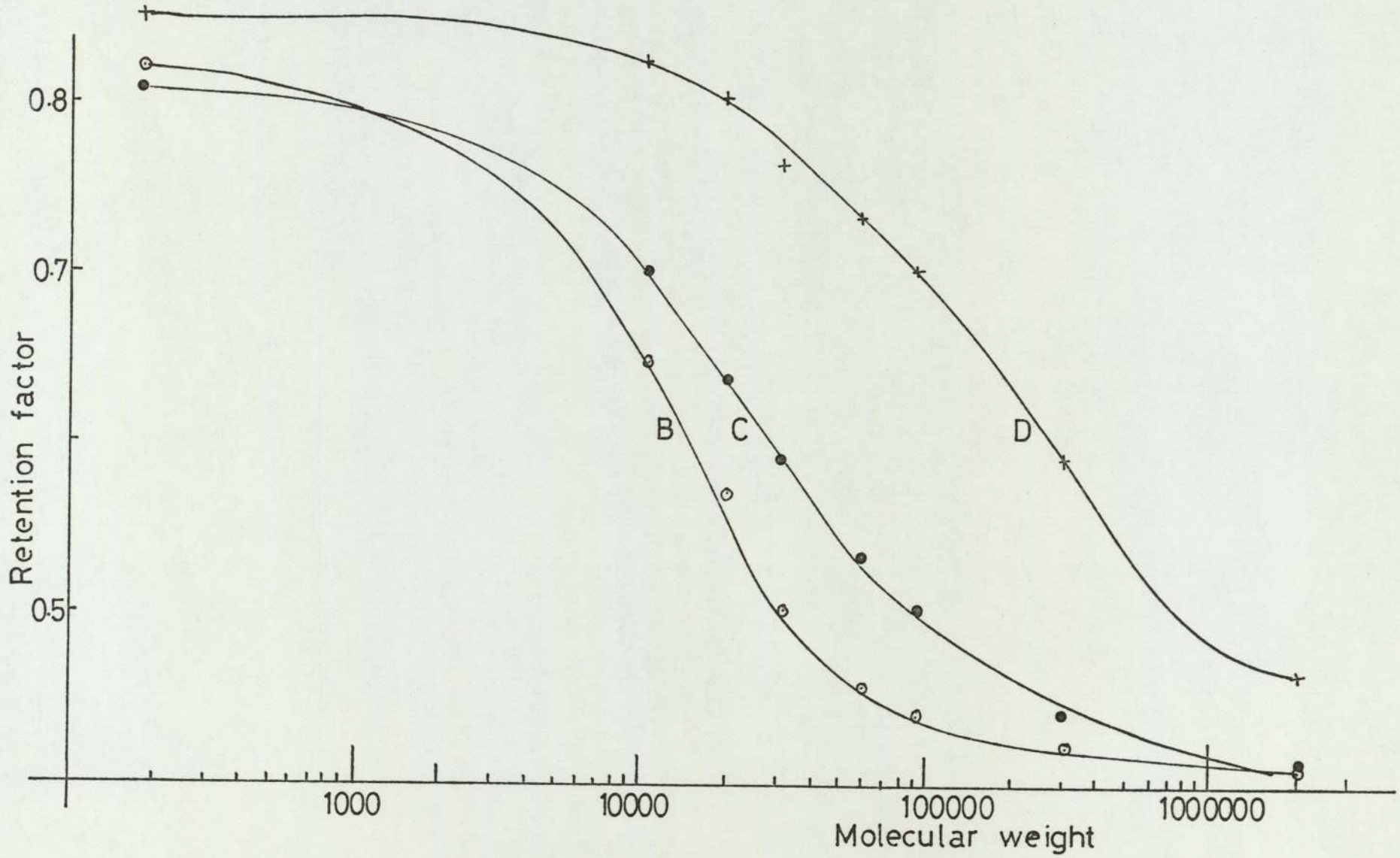

Chromatogram Treatment Program

```
10  DIM A(90),C(90),E(90),Q(90),M(90),U(90)
15  REM          NUMBER OF POINTS  N
16  REM          RUN NUMBER  R
17  REM         SAMPLE NUMBER S1
18  REM          PRODUCT NUMBER P
19  REM         INITIAL BASELINE B
20  REM          CHROMATOGRAM STARTING TIME T1
21  REM          FINAL BASE LINE B1
25  INPUT N,R,E1,S1,P,B,T1,B1
26  REM         GLUCOSE RESPONSE G1
27  REM           "       CONCENTRATION C1
28  REM         SAMPLE SIZE S2
29  REM          WASTE RATE W
30  REM         BUNDLE INPUT OR OUTPUT RATE X
31  REM          DILUTION OR CONCENTRATION FACTOR D2
32  REM         COLUMN VOLUME V
35  INPUT G1,C1,S2,X,D2,V
37  T=1.25
39  REM         STORE INITIAL BASELINE
42  D3=B
44  G=0
46  C(1)=0
47  C(N+1)=0
50  D1=(C1/G1)*(162/180)*(E1/S2)*D2
51  REM         PRINT D1
53  REM         INPUT G.P.C.DATA VIA ARRAY  A(I)
55  FOR J=1,N
56  INPUT A(J)
59  A(J)=A(J)-B
61  E(J)=T1*E1/V
63  IF B=B1 GOTO 67
65  B=B+((B1-D3)/N)
67  T1=T1+1.25
69  NEXT J
71  REM         CALCULATE PEAK AREAS
73  C(2)=(A(2)/2)*T
74  C(N)=(A(N-1)/2)*T
76  G=G+C(2)+C(N)+C(1)+C(N+1)
78  FOR J=3,N-1
79  IF A(J+1)=A(J) GOTO 85
80  IF A(J+1)<A(J) GOTO 83
81  C(J)=(A(J-1)*T)+(((A(J)-A(J-1))/2)*T)
82  GOTO 87
83  C(J)=(A(J)*T)+(((A(J-1)-A(J))/2)*T)
84  GOTO 87
85  C(J)=A(J)*T
87  G=G+C(J)
88  NEXT J
90  A1=G/2
```

Chromatogram Treatment Program (cont)

```
92   J=0
93   A2=0
95   J=J+1
97   A2=A2+C(J)
99   IF A2<A1 GOTO 95
101  REM            CALCULATE R.F. AT 50%
103  A2=A2-C(J)
105  Y=A1-A2
107  Y1=Y/C(J)
109  R6=E(J-1)+(Y1*(E(J)-E(J-1)))
110  PRINT TAB(8),"R.F. AT 50% =",R6
111  E8=(R6*V)/E1
112  E(N+1)=0
113  A(N+1)=0
114  PRINT TAB(8),"ELUTION TIME=",E8,"MIN"
116  M(1)=E(1)
117  M(N)=E(N-1)+((E(N)-E(N-1))/2)
118  FOR I=2,N-1
119  M(I)=E(I-1)+((E(I)-E(I-1))/2)
120  NEXT I
121  M(N+1)=E(N)
122  C(N+1)=0
125  PRINT TAB(8),"RUN NUMBER =",R
126  PRINT TAB(8),"SAMPLE NUMBER =",S1
127  PRINT TAB(8),"PRODUCT NUMBER =",P
128  PRINT
129  PRINT
130  PRINT TAB(15),"NORMALISED G.P.C. DATA"
131  PRINT TAB(2),"RETENTION",TAB(4),"DATA",TAB(6),"R.F",TAB(4),"MG/
132  PRINT TAB(2),"FACTOR",TAB(4),"POINTS",TAB(40),"INTO BUNDLE"
133  FOR J=1,N+1
134  Q(J)=C(J)*D1*X
135  PRINT E(J),TAB(6),A(J),TAB(4),M(J),TAB(6),Q(J)
136  NEXT J
137  K=G*D1
138  PRINT TAB(10),"SAMPLE CONCENTRATION","=",K,"MG/ML"
139  Z=K*X
140  PRINT TAB(8),"TOTAL RATE INTO OR OUT OF BUNDLE =",Z,"MG/MIN"
141  PRINT
142  PRINT
144  S8=0
145  REM            CALCULATE DATA FOR CUMULATIVE PLOT
146  PRINT TAB(10),"CUMULATIVE DATA"
147  FOR J=1,N
148  S8=S8+((C(J)*D1)/K)
149  U(J)=S8
150  PRINT TAB(10),U(J)
151  NEXT J
155  STOP
160  END
```

APPENDIX 5

FIGURE 5A-1 Theoretical Cut versus Eluent Rate

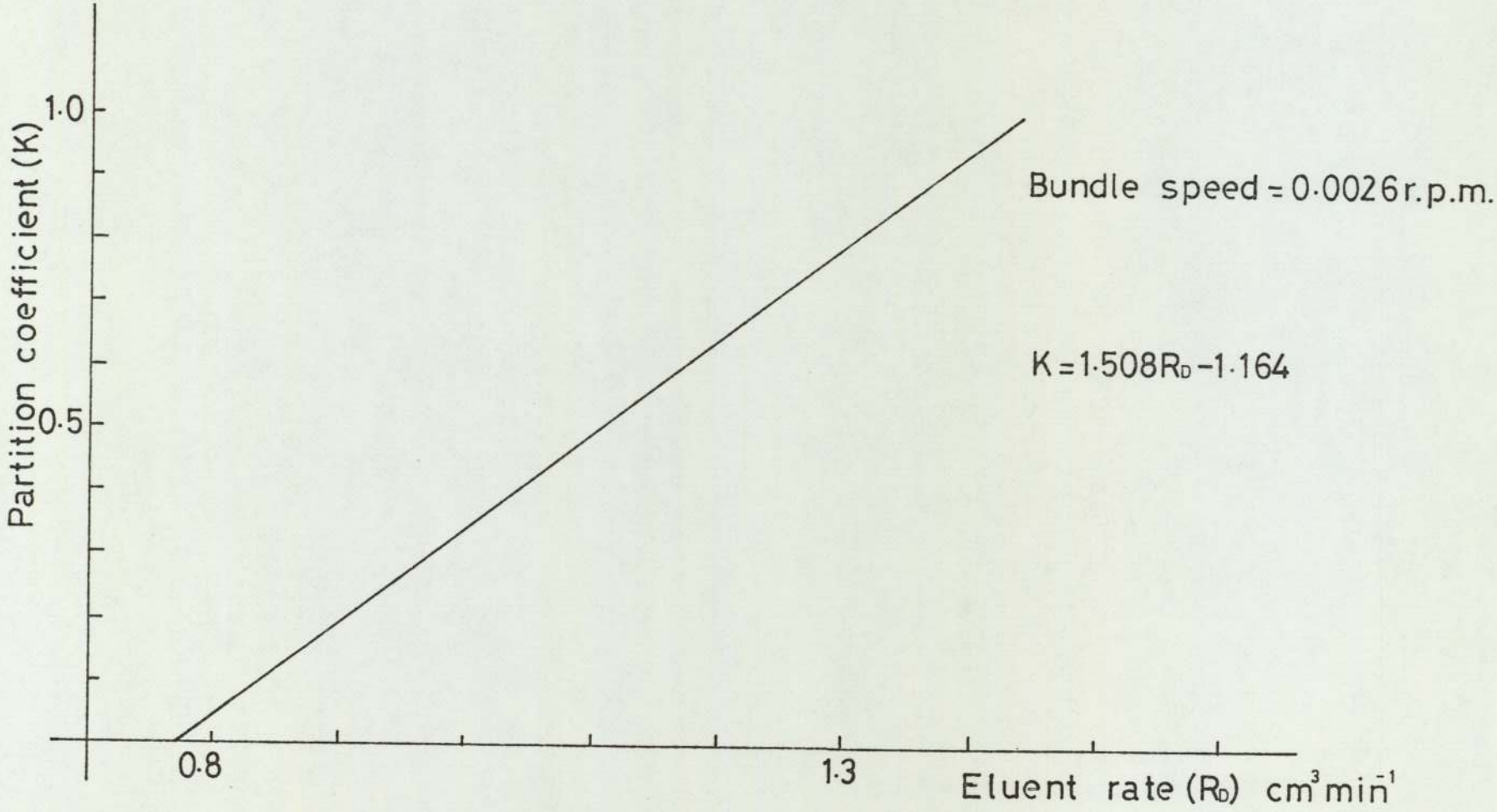

FIGURE 5A-2 Theoretical Cut versus Eluent Rate

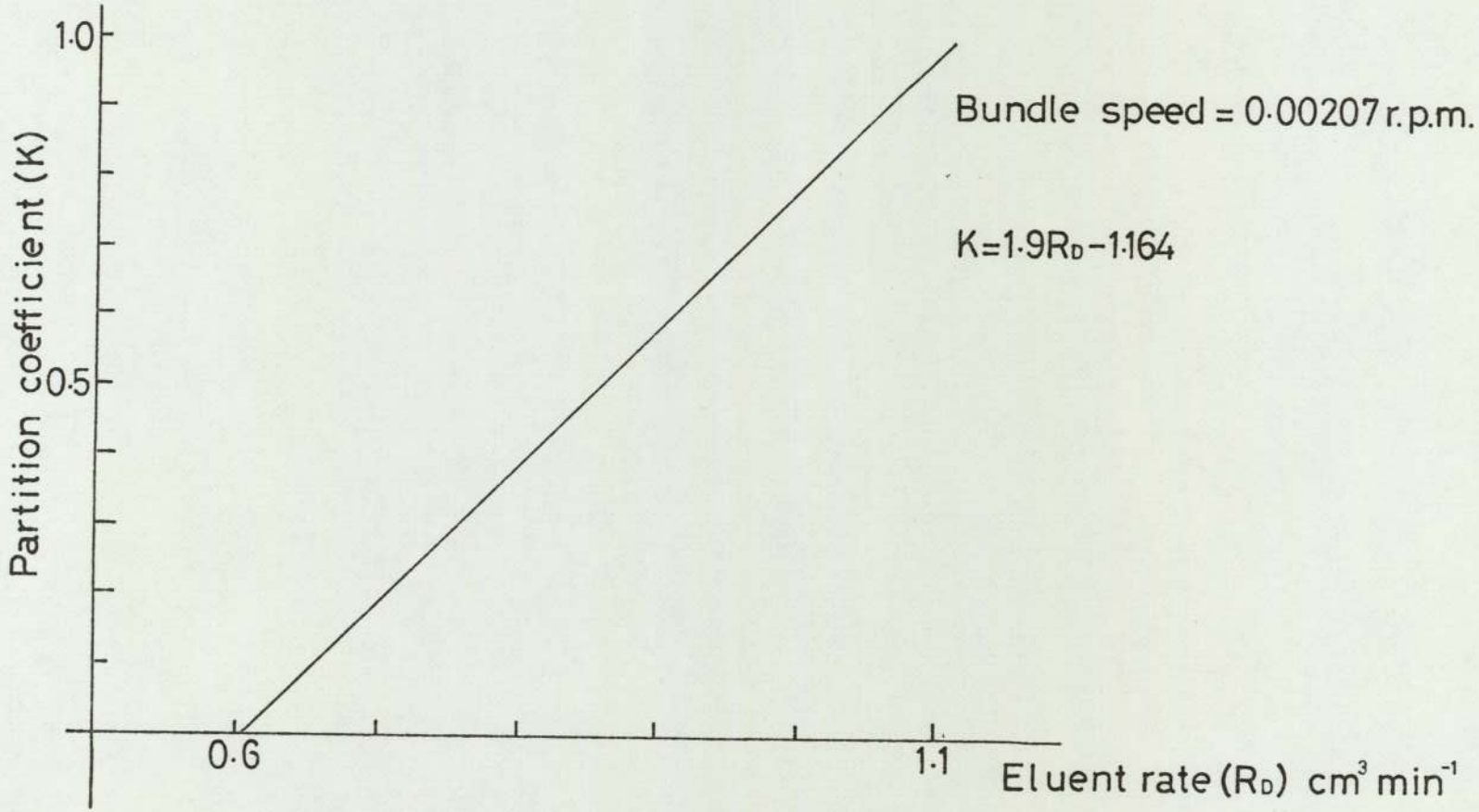

Analytical Data for Chromatograms

Conditions given below are for both products unless stated otherwise.

Figure Number	Eluent rate $cm^3\ min^{-1}$	Sample size cm^3	Standard Glucose conc. $g\ cm^{-3}$	Standard Glucose response O.D.	Dilution or concentration factor
17	0.0818	0.025	40	0.68	3.41
20					
0-10 hr					
High M.W.	0.09	0.05	40.26	0.78	0.052
Low M.W.	0.094	0.05	40.25	0.81	0.0035
14-16 hr					
High M.W.	0.09	0.025	40.26	0.78	0.052
Low M.W.	0.094	0.05	40.25	0.81	0.0344
22-24					
High M.W.	0.09	0.025	40.26	0.78	0.047
Low M.W.	0.09	0.025	40.25	0.81	0.042
22	0.082	0.025	40	0.712	1
24	0.835	0.025	40	0.685	1
25	0.082	0.025	40	0.68	1
26					
High M.W.	0.207	0.025	40	0.69	1
Low M.W.	0.235	0.025	40	0.78	1
27					
High M.W.	0.207	0.025	40	0.69	1
Low M.W.	0.235	0.025	40	0.78	1
28					
High M.W.	0.207	0.025	40	0.69	1
Low M.W.	0.235	0.025	40	0.78	1
29					
High M.W.	0.207	0.025	40	0.69	1
Low M.W.	0.235	0.025	40	0.78	1
30					
High M.W.	0.207	0.025	40	0.69	1
Low M.W.	0.235	0.025	40	0.78	1
31					
High M.W.	0.082	0.025	40	0.692	1
Low M.W.	0.082	0.025	40	0.692	2
32					
High M.W.	0.082	0.025	40	0.659	1
Low M.W.	0.082	0.025	40	0.659	5
33	0.083	0.025	40.8	0.695	5
34					
High M.W.	0.091	0.025	39.96	0.732	1
Low M.W.	0.091	0.025	40.26	0.732	0.0075
35					
High M.W.	0.091	0.025	39.96	0.745	1
Low M.W.	0.091	0.025	39.96	0.745	0.106

Feed Chromatogram Data Figures 6.17 and 6.33

Feed Runs 1-6 (based on concentration of 5614 g cm^{-3} and feed rate for Run 1)				Feed Run 7			
Raw chromatogram data		Normalised data		Raw chromatogram date		Normalised data	
Retention factor	Optical density	Retention factor	μg min^{-1}	Retention factor	Optical density	Retention factor	μg min^{-1}
0.342	0	0.342	0	0.326	0	0.326	0
0.355	0.005	0.352	0.102	0.340	0.005	0.337	0.609
0.369	0.018	0.365	0.58	0.355	0.012	0.351	1.27
0.382	0.038	0.379	1.05	0.369	0.017	0.365	1.94
0.396	0.059	0.393	2.03	0.384	0.027	0.380	3.16
0.410	0.077	0.406	2.29	0.398	0.043	0.295	4.76
0.423	0.092	0.420	2.80	0.412	0.063	0.409	7.22
0.437	0.101	0.433	3.36	0.427	0.093	0.423	10.31
0.451	0.110	0.447	3.88	0.441	0.133	0.438	15.25
0.464	0.125	0.461	4.16	0.456	0.143	0.452	17.22
0.478	0.133	0.474	4.45	0.470	0.157	0.466	19.06
0.491	0.142	0.488	4.76	0.485	0.180	0.481	21.89
0.505	0.152	0.501	5.14	0.499	0.197	0.495	23.87
0.519	0.164	0.515	5.47	0.513	0.212	0.510	25.71
0.532	0.175	0.529	5.71	0.527	0.227	0.524	27.86
0.546	0.181	0.543	5.91	0.542	0.240	0.538	29.27
0.559	0.188	0.556	6.10	0.557	0.252	0.553	30.93
0.573	0.193	0.570	6.27	0.571	0.257	0.567	31.66
0.587	0.199	0.583	6.45	0.585	0.26	0.582	32.14
0.600	0.204	0.597	6.55	0.600	0.259	0.596	32.31
0.614	0.207	0.610	6.57	0.614	0.254	0.611	31.80
0.627	0.206	0.624	6.45	0.629	0.248	0.625	30.98
0.641	0.202	0.638	6.29	0.643	0.231	0.639	29.30
0.655	0.011	0.651	6.04	0.657	0.211	0.654	27.05
0.668	0.010	0.665	5.69	0.672	0.196	0.668	24.63
0.682	0.009	0.678	5.11	0.686	0.181	0.683	22.76
0.696	0.008	0.692	4.53	0.701	0.156	0.697	20.02
0.709	0.007	0.706	4.07	0.715	0.136	0.711	17.34
0.723	0.006	0.719	3.59	0.729	0.121	0.726	15.59
0.736	0.006	0.733	3.33	0.744	0.108	0.740	13.78
0.75	0.006	0.747	3.24	0.758	0.091	0.755	11.85
0.764	0.005	0.761	3.28	0.773	0.071	0.769	9.36
0.777	0.005	0.774	2.93	0.787	0.045	0.783	6.25
0.791	0.003	0.788	2.11	0.802	0.020	0.798	3.14
0.804	0.001	0.801	1.06	0.816	0.01	0.812	1.57
0.818	0.0007	0.815	0.49	0.831	0.002	0.827	0.51
0.832	0.0002	0.828	0.16	0.838	0	0.838	0
0.845	0.0001	0.842	0.04				
0.852	0	0.852	0				

Dextran Run 1 Product Chromatogram Data (Figure 6.20)

0-10 hr samples

High molecular weight product				Low molecular weight product			
Raw chromatogram data		Normalised data		Raw chromatogram data		Normalised data	
Retention factor	Optical density	Retention factor	$\mu g\ min^{-1}$	Retention factor	Optical density	Retention factor	$\mu g\ min^{-1}$
0.326	0	0.326	0	0.328	0	0.328	0
0.341	0.004	0.337	0.016	0.344	0.006	0.341	0.003
0.356	0.039	0.352	0.161	0.360	0.009	0.356	0.006
0.371	0.104	0.367	0.502	0.376	0.014	0.372	0.009
0.386	0.194	0.382	1.00	0.391	0.019	0.387	0.012
0.401	0.303	0.397	1.63	0.407	0.028	0.403	0.019
0.416	0.393	0.412	2.22	0.423	0.038	0.419	0.026
0.431	0.438	0.427	2.57	0.439	0.052	0.434	0.037
0.446	0.461	0.442	2.72	0.454	0.062	0.451	0.044
0.461	0.465	0.457	2.76	0.470	0.074	0.466	0.052
0.476	0.412	0.472	2.55	0.486	0.095	0.482	0.065
0.491	0.352	0.487	2.25	0.502	0.100	0.497	0.073
0.506	0.282	0.502	1.80	0.517	0.091	0.513	0.07
0.521	0.221	0.517	1.14	0.533	0.087	0.529	0.065
0.536	0.156	0.532	1.04	0.549	0.092	0.544	0.067
0.551	0.101	0.547	0.69	0.564	0.104	0.560	0.074
0.566	0.061	0.562	0.44	0.580	0.116	0.576	0.083
0.581	0.031	0.577	0.24	0.595	0.145	0.591	0.101
0.596	0.016	0.592	0.120	0.611	0.175	0.607	0.126
0.611	0.007	0.607	0.053	0.627	0.235	0.623	0.162
0.626	0	0.626	0	0.643	0.305	0.639	0.218
				0.658	0.414	0.654	0.288
				0.672	0.504	0.670	0.358
				0.689	0.613	0.686	0.436
				0.705	0.723	0.701	0.521
				0.721	0.823	0.717	0.595
				0.737	0.863	0.733	0.631
				0.752	0.842	0.749	0.635
				0.768	0.782	0.764	0.594
				0.784	0.662	0.780	0.520
				0.799	0.512	0.796	0.412
				0.815	0.351	0.811	0.286
				0.831	0.216	0.827	0.184
				0.847	0.114	0.843	0.103
				0.862	0.05	0.858	0.05
				0.878	0	0.878	0

Dextran Run 1 Product Chromatogram Data (Fig. 6.20)

14-16 hour samples

High molecular weight product				Low molecular weight product			
Raw chromatogram data		Normalised data		Raw chromatogram data		Normalised data	
Retention factor	Optical density	Retention factor	μg min^{-1}	Retention factor	Optical density	Retention factor	μg min^{-1}
0.331	0	0.331	0	0.519	0	0.519	0
0.346	0.011	0.342	0.09	0.535	0.007	0.531	0.04
0.361	0.041	0.357	0.38	0.551	0.028	0.547	0.16
0.376	0.081	0.372	0.83	0.566	0.046	0.563	0.32
0.391	0.132	0.387	1.44	0.582	0.07	0.518	0.46
0.406	0.190	0.402	2.13	0.598	0.11	0.594	0.71
0.421	0.250	0.417	2.84	0.614	0.16	0.610	1.07
0.436	0.289	0.432	3.38	0.629	0.22	0.625	1.51
0.451	0.337	0.447	3.97	0.645	0.294	0.641	2.04
0.466	0.340	0.462	4.10	0.661	0.36	0.657	2.53
0.481	0.339	0.477	4.11	0.677	0.424	0.672	3.00
0.496	0.318	0.492	3.94	0.692	0.475	0.688	3.41
0.511	0.288	0.507	3.61	0.708	0.51	0.704	3.71
0.526	0.248	0.522	3.11	0.723	0.516	0.719	3.82
0.541	0.197	0.537	2.57	0.739	0.49	0.735	3.69
0.556	0.147	0.552	1.96	0.755	0.45	0.751	3.39
0.571	0.102	0.567	1.33	0.771	0.37	0.767	2.87
0.586	0.061	0.582	0.85	0.786	0.28	0.782	2.25
0.601	0.036	0.597	0.56	0.802	0.19	0.798	1.54
0.616	0.192	0.612	0.27	0.818	0.12	0.814	1.00
0.631	0.009	0.627	0.13	0.833	0.06	0.829	0.55
0.646	0.003	0.642	0.056	0.849	0.03	0.845	0.28
0.661	0.001	0.657	0.022	0.865	0.013	0.861	0.12
0.668	0	0.668	0	0.881	0	0.881	0

Dextran Run 1 Product Chromatogram Data (Figure 6.20)

22-24 hour sample

High molecular weight product				Low molecular weight product			
Raw chromatogram data		Normalised data		Raw chromatogram data		Normalised data	
Retention factor	Optical density	Retention factor	μg min^{-1}	Retention factor	Optical density	Retention factor	μg min^{-1}
0.329	0	0.329	0	0.452	0	0.452	0
0.344	0.006	0.339	0.04	0.467	0.006	0.463	0.09
0.358	0.03	0.354	0.25	0.481	0.008	0.478	0.14
0.373	0.07	0.369	0.65	0.496	0.013	0.492	0.21
0.388	0.11	0.385	1.09	0.511	0.02	0.507	0.32
0.403	0.176	0.399	1.72	0.526	0.035	0.522	0.57
0.418	0.24	0.415	2.48	0.541	0.064	0.537	1.02
0.433	0.29	0.429	3.02	0.555	0.1	0.552	1.64
0.448	0.35	0.444	3.59	0.570	0.15	0.566	2.50
0.464	0.37	0.459	4.02	0.585	0.212	0.581	3.56
0.478	0.39	0.475	4.19	0.599	0.28	0.596	4.82
0.493	0.404	0.489	4.36	0.615	0.35	0.611	6.04
0.508	0.4	0.505	4.41	0.629	0.4	0.625	7.09
0.523	0.38	0.519	4.22	0.644	0.44	0.641	7.86
0.538	0.34	0.535	3.87	0.659	0.451	0.655	8.19
0.554	0.28	0.549	3.21	0.674	0.445	0.670	8.13
0.568	0.215	0.565	2.59	0.688	0.43	0.685	7.91
0.583	0.16	0.579	1.85	0.703	0.38	0.699	7.18
0.598	0.1	0.595	1.25	0.718	0.34	0.714	6.36
0.628	0.03	0.624	0.42	0.732	0.28	0.729	5.36
0.643	0.018	0.639	0.22	0.747	0.23	0.744	4.36
0.658	0.008	0.655	0.09	0.762	0.175	0.758	3.41
0.673	0.003	0.669	0.05	0.777	0.12	0.773	2.45
0.681	0	0.681	0	0.791	0.07	0.788	1.54
				0.806	0.058	0.802	0.98
				0.821	0.017	0.817	0.38
				0.836	0.004	0.832	0.12
				0.851	0	0.851	0

Dextran Run 1 Product Chromatogram Data (Figure 6.21)

Sample 3 Analysis on Porasil 'C'

High molecular weight product				Low molecular weight product			
Raw chromatogram data		Normalised data		Raw chromatogram data		Normalised data	
Retention factor	Optical density	Retention factor	μg min^{-1}	Retention factor	Optical density	Retention factor	μg min^{-1}
0.338	0	0.338	0	0.504	0	0.504	0
0.352	0.005	0.348	0.06	0.518	0.002	0.515	0.03
0.366	0.031	0.362	0.45	0.532	0.007	0.529	0.12
0.379	0.064	0.376	1.12	0.546	0.012	0.543	0.22
0.393	0.104	0.390	1.83	0.560	0.024	0.556	0.43
0.407	0.142	0.404	2.60	0.574	0.047	0.571	0.83
0.421	0.173	0.418	3.24	0.588	0.078	0.584	1.43
0.435	0.203	0.432	3.83	0.602	0.138	0.59	2.44
0.449	0.206	0.445	4.03	0.616	0.188	0.612	3.57
0.463	0.216	0.459	0.76	0.629	0.253	0.626	4.85
0.477	0.233	0.473	4.48	0.643	0.293	0.640	5.82
0.491	0.245	0.487	4.73	0.658	0.343	0.651	6.74
0.505	0.256	0.501	4.95	0.672	0.351	0.668	7.17
0.518	0.261	0.515	5.08	0.685	0.352	0.682	7.27
0.532	0.255	0.529	4.99	0.699	0.340	0.695	7.04
0.546	0.242	0.543	4.81	0.713	0.322	0.709	6.73
0.560	0.207	0.557	4.17	0.727	0.300	0.724	6.36
0.574	0.167	0.571	3.42	0.741	0.269	0.738	5.67
0.588	0.124	0.584	2.66	0.755	0.241	0.751	5.13
0.602	0.084	0.598	1.83	0.768	0.211	0.765	4.51
0.616	0.051	0.612	1.15	0.782	0.183	0.779	3.93
0.629	0.028	0.626	0.66	0.796	0.146	0.793	3.19
0.643	0.016	0.640	0.35	0.810	0.123	0.807	2.66
0.657	0.008	0.654	0.19	0.824	0.094	0.821	2.08
0.615	0.005	0.668	0.11	0.838	0.068	0.835	1.46
0.685	0.003	0.681	0.07	0.852	0.031	0.849	0.79
0.699	0.001	0.695	0.03	0.866	0.012	0.863	0.34
.706	0	0.706	0	0.880	0.005	0.877	0.13
				0.894	0.001	0.89	0.05
				0.901	0	0.9	0

Dextran Run 2 Product Chromatogram Data (Figure 6.22)

Sample 2 Analysis on Porasil 'C'

High Molecular Weight Product				Low Molecular Weight Product			
Raw chromatogram data		Normalised data		Raw chromatogram data		Normalised data	
Retention factor	Optical density	Retention factor	μg min^{-1}	Retention factor	Optical density	Retention factor	μg min^{-1}
0.352	0	0.352	0	0.381	0	0.381	0
0.366	0.007	0.363	1.32	0.394	0.004	0.391	0.99
0.379	0.029	0.376	4.72	0.408	0.007	0.405	2.57
0.394	0.052	0.390	9.87	0.422	0.008	0.418	3.27
0.407	0.071	0.404	13.89	0.436	0.012	0.432	4.16
0.421	0.082	0.417	16.77	0.449	0.013	0.459	4.85
0.435	0.092	0.431	18.39	0.476	0.013	0.473	4.85
0.448	0.102	0.444	20.86	0.490	0.017	0.486	6.34
0.462	0.100	0.458	21.14	0.503	0.026	0.5	9.51
0.475	0.094	0.472	19.96	0.517	0.034	0.514	12.5
0.489	0.083	0.485	17.85	0.531	0.043	0.528	15.85
0.502	0.069	0.499	15.44	0.544	0.052	0.541	19.62
0.516	0.046	0.513	10.95	0.558	0.062	0.555	23.58
0.530	0.034	0.527	7.80	0.572	0.069	0.568	26.55
0.543	0.023	0.540	5.38	0.585	0.075	0.582	29.33
0.557	0.018	0.554	3.27	0.599	0.082	0.596	31.9
0.571	0.011	0.567	2.52	0.613	0.085	0.609	33.29
0.584	0.009	0.581	2.07	0.626	0.091	0.623	35.47
0.598	0.007	0.595	1.63	0.640	0.093	0.637	36.66
0.611	0.003	0.608	0.86	0.654	0.093	0.650	37.06
0.618	0.00	0.618	0	0.667	0.091	0.664	36.27
				0.681	0.088	0.678	35.08
				0.695	0.086	0.691	34.28
				0.708	0.082	0.705	32.89
				0.722	0.075	0.718	30.32
				0.736	0.067	0.732	27.54
				0.749	0.059	0.746	24.37
				0.763	0.055	0.76	21.99
				0.776	0.053	0.773	21.20
				0.79	0.049	0.787	20.01
				0.804	0.039	0.8	16.84
				0.817	0.019	0.814	9.51
				0.831	0.009	0.828	4.55
				0.845	0.001	0.841	0.99
				0.85	0	0.85	0

Dextran Run 3 Product Chromatogram Data (Figure 6.24)

Sample 2 Analysis on Porasil 'C'

High molecular weight product				Low molecular weight product			
Raw chromatogram data		Normalised data		Raw chromatogram data		Normalised data	
Retention factor	Optical density	Retention factor	μg min^{-1}	Retention factor	Optical density	Retention factor	μg min^{-1}
0.332	0	0.332	0	0.407	0	0.407	0
0.346	0.007	0.342	1.23	0.421	0.003	0.417	0.87
0.360	0.028	0.357	4.88	0.434	0.006	0.431	2.19
0.374	0.065	0.37	12.82	0.448	0.013	0.445	5.03
0.388	0.111	0.384	23.19	0.462	0.023	0.459	8.75
0.402	0.168	0.398	36.34	0.476	0.034	0.473	13.34
0.415	0.2	0.412	45.21	0.490	0.05	0.487	19.69
0.429	0.219	0.426	49.67	0.504	0.077	0.500	30.63
0.443	0.244	0.440	55.17	0.511	0.095	0.507	37.62
0.457	0.267	0.454	60.33	0.532	0.15	0.528	61.25
0.471	0.269	0.468	62.59	0.545	0.183	0.542	76.78
0.485	0.266	0.482	61.96	0.559	0.213	0.556	90.35
0.499	0.253	0.495	59.82	0.574	0.24	0.57	102.81
0.513	0.222	0.509	53.85	0.587	0.26	0.598	111.56
0.527	0.184	0.523	44.88	0.601	0.27	0.611	117.03
0.541	0.138	0.537	34.86	0.615	0.272	0.625	118.78
0.555	0.098	0.551	24.72	0.629	0.269	0.639	117.91
0.568	0.065	0.565	16.68	0.643	0.263	0.653	115.5
0.582	0.041	0.579	10.83	0.657	0.255	0.667	112.66
0.596	0.026	0.593	7.07	0.671	0.24	0.681	106.75
0.610	0.020	0.607	4.81	0.685	0.225	0.695	99.97
0.624	0.013	0.621	3.59	0.698	0.208	0.709	92.97
0.638	0.007	0.635	1.92	0.712	0.19	0.723	84.88
0.652	0.003	0.648	1.05	0.726	0.164	0.737	74.16
0.665	0.001	0.662	0.417	0.740	0.15	0.737	67.16
0.672	0	0.672	0	0.754	0.14	0.751	61.91
				0.768	0.135	0.765	59.50
				0.782	0.12	0.778	54.69
				0.796	0.087	0.792	42.22
				0.809	0.055	0.806	27.78
				0.823	0.02	0.820	12.03
				0.837	0.001	0.834	4.37
				0.851	0	0.851	0

Dextran Run 4 Product Chromatogram Data (Figure 6.25)

Sample 3 Analysis on Porasil 'C'

High molecular weight product				Low molecular weight product			
Raw chromatogram data		Normalised data		Raw chromatogram data		Normalised data	
Retention factor	Optical density	Retention factor	μg min^{-1}	Retention factor	Optical density	Retention factor	μg min^{-1}
0.338	0	0.338	0	0.356	0	0.356	0
0.352	0.014	0.348	2.11	0.369	0.006	0.366	1.85
0.366	0.057	0.362	9.48	0.383	0.011	0.38	4.12
0.379	0.36	0.376	24.77	0.397	0.018	0.393	7.0
0.393	0.239	0.389	45.11	0.410	0.027	0.407	10.31
0.407	0.289	0.403	58.81	0.424	0.039	0.421	14.84
0.420	0.314	0.417	65.14	0.437	0.063	0.434	23.29
0.434	0.318	0.431	67.14	0.45	0.103	0.448	37.51
0.447	0.282	0.444	61.24	0.465	0.158	0.461	61.42
0.461	0.241	0.458	53.54	0.478	0.179	0.475	71.32
0.478	0.177	0.471	39.63	0.492	0.213	0.489	84.10
0.488	0.124	0.485	28.77	0.506	0.243	0.502	96.88
0.502	0.089	0.489	19.81	0.519	0.276	0.516	110.28
0.516	0.059	0.512	13.80	0.533	0.305	0.529	123.27
0.529	0.036	0.529	8.96	0.546	0.333	0.543	134.40
0.543	0.019	0.539	4.74	0.56	0.351	0.556	143.06
0.556	0.007	0.553	2.00	0.574	0.368	0.571	150.27
0.570	0.002	0.567	0.737	0.587	0.38	0.584	155.22
0.577	0	0.577	0	0.601	0.391	0.597	160.37
				0.615	0.397	0.611	163.47
				0.628	0.4	0.625	164.7
				0.642	0.393	0.638	163.26
				0.655	0.378	0.652	157.69
				0.669	0.361	0.666	150.68
				0.682	0.337	0.679	141.20
				0.696	0.313	0.693	131.10
				0.710	0.28	0.707	118.11
				0.723	0.253	0.720	107.60
				0.737	0.223	0.734	94.61
				0.751	0.213	0.747	88.22
				0.765	0.215	0.761	88.4
				0.778	0.2	0.774	84.72
				0.792	0.163	0.788	71.32
				0.805	0.111	0.802	50.29
				0.819	0.046	0.815	24.53
				0.832	0.018	0.829	9.48
				0.846	0.006	0.842	3.09
				0.859	0	0.859	0

Dextran Run 5 Product Chromatogram Data (Figure 6.26)

Sample 1

High molecular weight product analysis on Porasil D				Low molecular weight product analysis on Porasil B			
Raw chromatogram data		Normalised data		Raw chromatogram data		Normalised data	
Retention factor	Optical density	Retention factor	μg min^{-1}	Retention factor	Optical density	Retention factor	μg min^{-1}
0.396	0	0.396	0	0.312	0	0.312	
0.432	0.008	0.423	2.74	0.354	0.016	0.343	9.19
0.468	0.081	0.459	29.87	0.395	0.401	0.384	289.22
0.505	0.101	0.495	54.26	0.436	0.556	0.426	570.78
0.541	0.11	0.532	58.37	0.477	0.685	0.467	698.01
0.577	0.139	0.568	70.97	0.581	0.656	0.508	680.64
0.613	0.18	0.605	93.18	0.559	0.591	0.549	616.76
0.649	0.19	0.641	104.68	0.6	0.496	0.590	527.34
0.686	0.151	0.677	89.34	0.641	0.402	0.631	433.32
0.722	0.09	0.713	56.18	0.683	0.313	0.672	339.29
0.758	0.075	0.749	37.27	0.724	0.246	0.714	266.74
0.795	0.018	0.785	11.78	0.765	0.186	0.755	200.38
0.831	0.009	0.822	5.48	0.806	0.208	0.796	202.35
0.867	0.001	0.858	0.822	0.847	0.161	0.837	190.08
0.885	0	0.885	0	0.888	0.036	0.878	59.78
				0.929	0.003	0.919	8.68
				0.971	0	0.971	0

Dextran Run 5 Product Chromatogram Data (Figure 6.27)

Sample 2

High molecular weight product Analysis on Porasil D				Low molecular weight product Analysis on Porasil B			
Raw chromatogram data		Normalised data		Raw chromatogram data		Normalised data	
Retention factor	Optical density	Retention factor	$\mu g\ min^{-1}$	Retention factor	Optical density	Retention factor	$\mu g\ min^{-1}$
0.426	0	0.426	0	0.344	0	0.344	0
0.462	0.057	0.453	20.80	0.364	0.048	0.354	26.73
0.499	0.093	0.489	50.65	0.405	0.444	0.395	349.77
0.535	0.091	0.526	49.47	0.447	0.604	0.437	644.95
0.571	0.117	0.562	59.82	0.488	0.629	0.477	703.43
0.607	0.165	0.598	83.89	0.529	0.594	0.518	675.58
0.644	0.191	0.634	103.31	0.570	0.529	0.559	605.96
0.680	0.165	0.671	96.08	0.611	0.449	0.601	525.20
0.716	0.099	0.707	64.42	0.652	0.359	0.642	422.17
0.753	0.045	0.744	32.76	0.693	0.294	0.683	346.98
0.789	0.018	0.780	11.81	0.734	0.219	0.724	261.77
0.825	0.006	0.816	4.58	0.776	0.176	0.765	206.07
0.861	0.002	0.852	1.75	0.817	0.206	0.806	221.67
0.879	0	0.879	0	0.858	0.12	0.847	173.77
				0.899	0.029	0.889	51.79
				0.94	0.009	0.93	12.81
				0.981	0.004	0.971	5.57
				1.0	0	1.0	0

Dextran Run 5 Product Chromatogram Data (Figure 6.28)

Sample 3

High molecular weight product Analysis on Porasil D				Low molecular weight product Analysis on Porasil B			
Raw chromatogram data		Normalised data		Raw chromatogram data		Normalised data	
Retention factor	Optical density	Retention factor	$\mu g\ min^{-1}$	Retention factor	Optical density	Retention factor	$\mu g\ min^{-1}$
0.415	0	0.415	0	0.329	0	0.329	0
0.451	0.065	0.442	23.44	0.370	0.11	0.359	59.76
0.487	0.096	0.478	53.23	0.411	0.629	0.401	512.69
0.523	0.088	0.514	49.09	0.452	0.764	0.442	790.53
0.559	0.113	0.551	57.36	0.494	0.764	0.483	806.25
0.596	0.163	0.587	82.19	0.534	0.714	0.524	764.31
0.632	0.197	0.623	105.08	0.575	0.649	0.565	698.79
0.668	0.18	0.659	103.15	0.617	0.539	0.606	591.32
0.704	0.12	0.695	74.47	0.658	0.444	0.648	489.09
0.741	0.06	0.732	39.99	0.699	0.354	0.689	394.74
0.777	0.025	0.768	16.82	0.741	0.274	0.730	308.24
0.813	0.013	0.805	8.27	0.781	0.224	0.771	240.09
0.85	0.005	0.841	3.58	0.822	0.269	0.812	268.93
0.886	0.002	0.877	1.65	0.804	0.141	0.854	193.96
0.904	0	0.904	0	0.905	0.034	0.894	51.37
				0.946	0.009	0.936	14.68
				0.987	0.006	0.977	7.33
				1.02	0	1.02	0

Dextran Run 5 Product Chromatogram Data (Figure 6.29)

Sample 4

High molecular weight product Analysis on Porasil D				High molecular weight product Analysis on Porasil B			
Raw chromatogram data		Normalised data		Raw chromatogram data		Normalised data	
Retention factor	Optical density	Retention factor	μg min^{-1}	Retention factor	Optical density	Retention factor	μg min^{-1}
8.400	0	0.400	0	0.329	0	0.329	0
0.436	0.023	0.427	7.20	0.370	0.14	0.359	81.47
0.472	0.1	0.464	49.03	0.411	0.557	0.401	482.09
0.509	0.095	0.50	54.29	0.452	0.657	0.442	663.72
0.545	0.105	0.536	55.12	0.494	0.668	0.483	692.78
0.581	0.15	0.572	76.18	0.534	0.617	0.524	655.93
0.618	0.2	0.608	103.88	0.576	0.537	0.566	578.09
0.654	0.203	0.645	114.13	0.617	0.452	0.607	497.66
0.690	0.16	0.681	96.96	0.658	0.367	0.648	401.66
0.727	0.085	0.717	57.62	0.699	0.292	0.689	327.97
0.763	0.04	0.753	27.70	0.740	0.217	0.730	244.42
0.799	0.017	0.790	11.91	0.781	0.194	0.771	202.90
0.835	0.008	0.826	5.26	0.822	0.222	0.812	227.81
0.871	0.005	0.863	3.32	0.864	0.095	0.854	135.96
0.908	0.003	0.899	1.94	0.905	0.017	0.894	28.02
0.944	0	0.944	0	0.946	0.005	0.936	7.78
				0.987	0	0.987	0

Dextran Run 5 Product Chromatogram Data (Figure 6.30)

Sample 5

High molecular weight product Analysis on Porasil D				Low molecular weight product Analysis on Porasil B			
Raw chromatogram data		Normalised data		Raw chromatogram data		Normalised data	
Retention factor	Optical density	Retention factor	$\mu g\ min^{-1}$	Retention factor	Optical density	Retention factor	$\mu g\ min^{-1}$
0.399	0	0.399	0	0.327	0	0.327	0
0.435	0.034	0.426	10.84	0.368	0.104	0.358	56.59
0.471	0.099	0.462	48.54	0.409	0.547	0.399	462.76
0.507	0.089	0.498	50.28	0.450	0.647	0.441	630.53
0.544	0.103	0.535	53.38	0.49	0.667	0.481	665.59
0.580	0.148	0.571	74.61	0.533	0.627	0.522	638.05
0.616	0.203	0.607	105.45	0.574	0.557	0.504	572.94
0.652	0.202	0.643	112.68	0.615	0.457	0.605	487.8
0.689	0.152	0.679	91.07	0.657	0.372	0.646	392.64
0.725	0.081	0.716	53.26	0.697	0.297	0.687	317.52
0.761	0.036	0.752	25.06	0.738	0.224	0.728	240.89
0.797	0.017	0.788	11.42	0.780	0.192	0.769	194.82
0.834	0.008	0.825	5.74	0.821	0.217	0.810	213.85
0.870	0.003	0.861	2.52	0.862	0.092	0.852	137.22
0.906	0	0.906	0	0.903	0.017	0.893	29.55
				0.944	0.005	0.934	7.01
				0.985	0.002	0.975	2.50
				1.0	0	1.0	0

Dextran Run 5 Product Chromatogram Data (Figure 6.31)

Sample 4 Analysis on Porasil 'C'

High molecular weight product				Low molecular weight product			
Raw chromatogram data		Normalised data		Raw chromatogram data		Normalised data	
Retention factor	Optical density	Retention factor	μg min^{-1}	Retention factor	Optical density	Retention factor	μg min^{-1}
0.337	0	0.337	0	0.340	0	0.340	0
0.351	0.016	0.347	2.21	0.354	0.004	0.350	2.44
0.364	0.107	0.361	16.38	0.368	0.009	0.305	6.52
0.378	0.256	0.375	47.41	0.382	0.015	0.378	11.41
0.392	0.386	0.388	79.03	0.395	0.024	0.392	17.93
0.405	0.450	0.402	96.97	0.409	0.034	0.405	24.86
0.419	0.468	0.416	101.57	0.422	0.05	0.419	37.50
0.433	0.454	0.429	100.59	0.436	0.076	0.432	55.43
0.446	0.414	0.443	93.25	0.449	0.13	0.446	92.12
0.460	0.333	0.457	77.93	0.463	0.177	0.460	135.74
0.474	0.263	0.470	61.96	0.471	0.205	0.474	161.00
0.487	0.178	0.484	44.67	0.491	0.235	0.487	185.46
0.501	0.112	0.498	28.47	0.504	0.267	0.501	210.74
0.515	0.069	0.511	17.31	0.518	0.293	0.515	232.34
0.528	0.046	0.525	11.29	0.532	0.315	0.528	253.13
0.542	0.024	0.538	6.37	0.545	0.332	0.541	267.80
0.555	0.014	0.552	3.53	0.559	0.346	0.555	279.62
0.569	0.007	0.566	1.89	0.572	0.363	0.569	291.85
0.583	0.004	0.579	1.01	0.586	0.375	0.582	303.67
0.596	0.001	0.593	0.46	0.599	0.38	0.596	308.56
0.604	0	0.604	0	0.613	0.38	0.610	310.19
				0.627	0.375	0.624	307.34
				0.641	0.36	0.637	297.56
				0.654	0.343	0.651	283.29
				0.668	0.32	0.665	266.6
				0.681	0.298	0.678	247.83
				0.695	0.27	0.692	225.41
				0.709	0.24	0.706	200.95
				0.722	0.21	0.719	176.49
				0.736	0.187	0.733	157.75
				0.750	0.18	0.747	147.56
				0.763	0.182	0.760	149.18
				0.777	0.165	0.774	135.74
				0.791	0.114	0.787	103.53
				0.805	0.05	0.801	55.03
				0.818	0.02	0.815	22.01
				0.832	0.005	0.826	6.11
				0.839	0	0.838	0

Dextran Run 6 Product Chromatogram Data (Figure 6.32)

Sample 3 Analysis on Porasil 'C'

High molecular weight product				Low molecular weight product			
Raw chromatogram data		Normalised data		Raw chromatogram data		Normalised data	
Retention factor	Optical density	Retention factor	$\mu g\ min^{-1}$	Retention factor	Optical density	Retention factor	$\mu g\ min^{-1}$
0.336	0	0.336	0	0.352	0	0.352	0
0.350	0.009	0.346	1.37	0.366	0.006	0.363	10.21
0.364	0.069	0.360	10.19	0.380	0.014	0.376	27.24
0.377	0.284	0.374	41.20	0.393	0.026	0.39	52.21
0.391	0.418	0.387	77.38	0.407	0.038	0.404	79.45
0.404	0.468	0.401	95.95	0.421	0.06	0.417	120.31
0.418	0.437	0.415	93.56	0.434	0.09	0.431	185.00
0.432	0.356	0.428	78.11	0.448	0.127	0.444	265.59
0.445	0.276	0.442	60.39	0.461	0.156	0.458	340.51
0.459	0.191	0.455	43.29	0.475	0.17	0.472	377.96
0.473	0.125	0.469	29.08	0.489	0.185	0.485	409.74
0.486	0.074	0.483	17.58	0.502	0.202	0.499	438.12
0.499	0.044	0.496	10.74	0.516	0.216	0.512	483.52
0.513	0.026	0.510	6.07	0.522	0.228	0.526	510.76
0.527	0.017	0.524	3.90	0.543	0.24	0.54	536.87
0.54	0.008	0.537	2.24	0.557	0.245	0.553	553.89
0.554	0.006	0.551	1.42	0.57	0.256	0.567	514.32
0.568	0.003	0.564	0.90	0.584	0.263	0.581	593.62
0.581	0.0002	0.578	0.15	0.598	0.266	0.594	601.56
		0.581	0	0.611	0.268	0.608	607.24
				0.625	0.268	0.629	609.51
				0.638	0.263	0.635	600.43
				0.652	0.253	0.649	582.27
				0.666	0.24	0.662	551.62
				0.679	0.22	0.676	515.3
				0.693	0.203	0.689	471.03
				0.706	0.18	0.703	447.2
				0.72	0.16	0.717	374.56
				0.734	0.143	0.731	335.97
				0.747	0.128	0.744	297.38
				0.761	0.13	0.758	290.57
				0.774	0.131	0.771	296.24
				0.788	0.11	0.785	266.73
				0.802	0.08	0.798	206.57
				0.815	0.03	0.812	97.61
				0.829	0.016	0.826	45.50
				0.843	0.006	0.839	18.16
				0.856	0	0.853	3.41
						0.856	0

Dextran Run 7 Product Chromatogram Data (Figure 6.34)

Sample 3 Analysis on Porasil 'C'

High molecular weight product				Low molecular weight product			
Raw chromatogram data		Normalised data		Raw chromatogram data		Normalised data	
Retention factor	Optical density	Retention factor	μg min^{-1}	Retention factor	Optical density	Retention factor	μg min^{-1}
0.345	0	0.345	0	0.345	0	0.345	0
0.361	0.005	0.557	1.23	0.361	0.002	0.357	0.004
0.375	0.01	0.372	2.58	0.376	0.004	0.372	0.006
0.391	0.014	0.387	3.29	0.391	0.007	0.387	0.011
0.406	0.023	0.402	5.27	0.406	0.009	0.402	0.015
0.426	0.031	0.417	7.26	0.426	0.012	0.417	0.02
0.436	0.051	0.432	11.28	0.436	0.018	0.432	0.028
0.451	0.063	0.447	16.07	0.451	0.016	0.447	0.027
0.466	0.067	0.462	16.78	0.466	0.012	0.462	0.023
0.481	0.076	0.477	18.76	0.481	0.01	0.477	0.018
0.496	0.088	0.492	21.64	0.496	0.009	0.492	0.014
0.511	0.101	0.509	24.64	0.511	0.008	0.509	0.013
0.526	0.111	0.523	27.65	0.526	0.008	0.523	0.014
0.542	0.119	0.538	29.63	0.542	0.009	0.538	0.019
0.557	0.126	0.553	31.74	0.557	0.012	0.553	0.022
0.571	0.134	0.568	33.47	0.571	0.014	0.568	0.027
0.586	0.137	0.583	34.82	0.586	0.016	0.583	0.030
0.601	0.139	0.598	35.41	0.601	0.018	0.598	0.033
0.616	0.141	0.613	35.86	0.616	0.020	0.613	0.036
0.632	0.141	0.628	36.06	0.632	0.022	0.628	0.038
0.647	0.138	0.643	35.51	0.647	0.022	0.643	0.037
0.662	0.129	0.658	33.67	0.662	0.022	0.658	0.037
0.677	0.121	0.673	31.70	0.677	0.022	0.673	0.037
0.692	0.109	0.688	28.47	0.692	0.023	0.688	0.038
0.707	0.097	0.703	25.36	0.707	0.025	0.703	0.040
0.722	0.078	0.718	21.36	0.722	0.033	0.718	0.052
0.737	0.069	0.733	18.26	0.737	0.062	0.733	0.090
0.752	0.054	0.748	14.64	0.752	0.112	0.748	0.16
0.767	0.043	0.763	11.66	0.767	0.192	0.763	0.28
0.782	0.033	0.778	9.06	0.782	0.242	0.778	0.38
0.797	0.023	0.794	6.46	0.797	0.254	0.794	0.42
0.812	0.014	0.809	3.99	0.812	0.221	0.809	0.38
0.827	0.007	0.824	2.41	0.829	0.114	0.824	0.24
0.842	0.002	0.839	0.96	0.842	0.056	0.839	0.11
0.850	0	0.850	0	0.858	0.018	0.854	0.04
				0.873	0.006	0.87	0.014
				0.888	0	0.888	0

Dextran Run 7 Product Chromatogram Data (Figure 6.35)

Sample 7 Analysis on Porasil 'C'

High molecular weight product				Low molecular weight product			
Raw chromatogram data		Normalised data		Raw chromatogram data		Normalised data	
Retention factor	Optical density	Retention factor	μg min^{-1}	Retention factor	Optical density	Retention factor	μg min^{-1}
0.353	0	0.353	0	0.461	0	0.461	0
0.361	0.004	0.337	0.436	0.476	0.024	0.472	0.75
0.384	0.012	0.380	2.16	0.491	0.012	0.487	0.72
0.399	0.015	0.395	3.36	0.507	0.004	0.502	0.258
0.414	0.024	0.410	5.11	0.521	0.002	0.518	0.117
0.429	0.031	0.426	6.41	0.537	0	0.533	0.023
0.445	0.037	0.441	7.94	0.552	0.002	0.548	0.070
0.46	0.046	0.456	9.69	0.567	0.003	0.564	0.129
0.475	0.058	0.471	12.21	0.583	0.006	0.578	0.234
0.490	0.068	0.486	14.74	0.598	0.011	0.594	0.469
0.506	0.084	0.501	17.71	0.613	0.02	0.609	0.797
0.521	0.094	0.517	20.57	0.628	0.034	0.624	1.43
0.536	0.105	0.532	22.87	0.643	0.059	0.639	2.48
0.551	0.114	0.547	24.84	0.659	0.09	0.655	3.84
0.566	0.121	0.562	26.59	0.674	0.127	0.670	5.55
0.581	0.126	0.578	27.78	0.689	0.166	0.685	7.34
0.596	0.129	0.593	28.64	0.704	0.194	0.700	8.77
0.612	0.131	0.608	29.16	0.719	0.219	0.715	9.92
0.627	0.126	0.623	28.47	0.735	0.224	0.731	10.46
0.642	0.117	0.638	26.55	0.749	0.22	0.745	10.39
0.657	0.132	0.653	27.18	0.765	0.204	0.761	9.80
0.672	0.087	0.669	20.49	0.780	0.74	0.776	8.63
0.688	0.067	0.684	16.01	0.794	0.144	0.791	7.10
0.703	0.047	0.699	11.54	0.810	0.094	0.806	5.11
0.718	0.317	0.714	7.95	0.825	0.063	0.822	3.21
0.734	0.019	0.729	4.92	0.841	0.032	0.837	1.89
0.748	0.010	0.745	2.66	0.356	0.01	0.852	0.703
0.764	0.005	0.760	1.64	0.871	0	0.871	0
0.779	0.002	0.775	0.61				
0.794	0	0.794	0				

Quantitative spectrophotometry[238] relies on the fact that the absorbance of a solution varies with its concentration. Beer's Law states that the absorbtive capacity of a solute in a solution is directly proportional to the concentration of the solute. It follows therefore, that the absorbance of a solution relative to the absorbance of the solvent, is proportional to the concentration. In addition, Lambert's law states that the absorbance of a sample is proportional to the length of its optical path. Therefore by combining both these laws we obtain the Beer-Lambert law. This law gives the absorbance of a solution to that of the solvent as,

$$A = \varepsilon . \ell . C_B$$

where ℓ is the path length in cm

C_B = solute concentration

ε = absorbtivity

This can be expressed as:

$$I = I_o 10^{-\varepsilon . \ell . C_B}$$

I_o = intensity of radiation incident on a sample

I = intensity of transmitted radiation.

Absorbance, A, is given by,

$$A = -\log_{10} \frac{I}{I_o} = -\log_{10} T$$

T = Transmittance.

Quantitative analysis is based on the Beer-Lambert Law. A single absorbing substance in a transparent medium can be estimated directly from a calibration graph of absorbance against concentration. The calibration graph is obtained for simple systems by using a series of standard samples. Calibration plots are also a means of checking the linearity of the spectrophotometer response with solute concentration.

Mixtures are analysed by making measurements at as many wavelengths as there are components and solving equations of the type:

$$A_1 = a_1'cx + a_1''cy + a''_1cz$$
$$A_2 = a_2'cx + a_2''cy + a_2''cz$$
$$A_3 = a_3'cx + a_3''cy + a''_3cz$$

where

A = the absorbance

a = absorbtivity

c = concentration

The absorbtivity of each component in a mixture is calculated from the gradient of a linear calibration plot for that component at each wavelength.

The calibration plots for each of the component used in this research, at wavelengths of 520 nm and 610 nm respectively, are included in this Appendix. From these calibration plots the absorbtivity of the two dyed protein, when in buffer solution, are calculated. Using these values the concentration of each dyed

protein when in a mixture of the two is given by:

$$cy = 2.257\ A_2 - 0.024\ A_1$$

$$cx = \frac{A_1 - 0.15\ cy}{0.9708}$$

cy,cx = concentrations ($x\ 10^{-3} g\ cm^{-3}$) of dyed pepsin and dyed bovine serum albumin respectively

A_1, A_2 = Absorbance of sample solution at 520 nm and 610 nm respectively.

Component absorbance are given bY;

$$Ay = A_2 - 0.01\ A_1$$

$$Ax = A_1 - 0.15\ A_2$$

Ay,Ax = absorbance of dyed pepsin and dyed bovine serum in sample solution.

FIGURE 7A-1 Calibration Plots for Dyed Pepsin

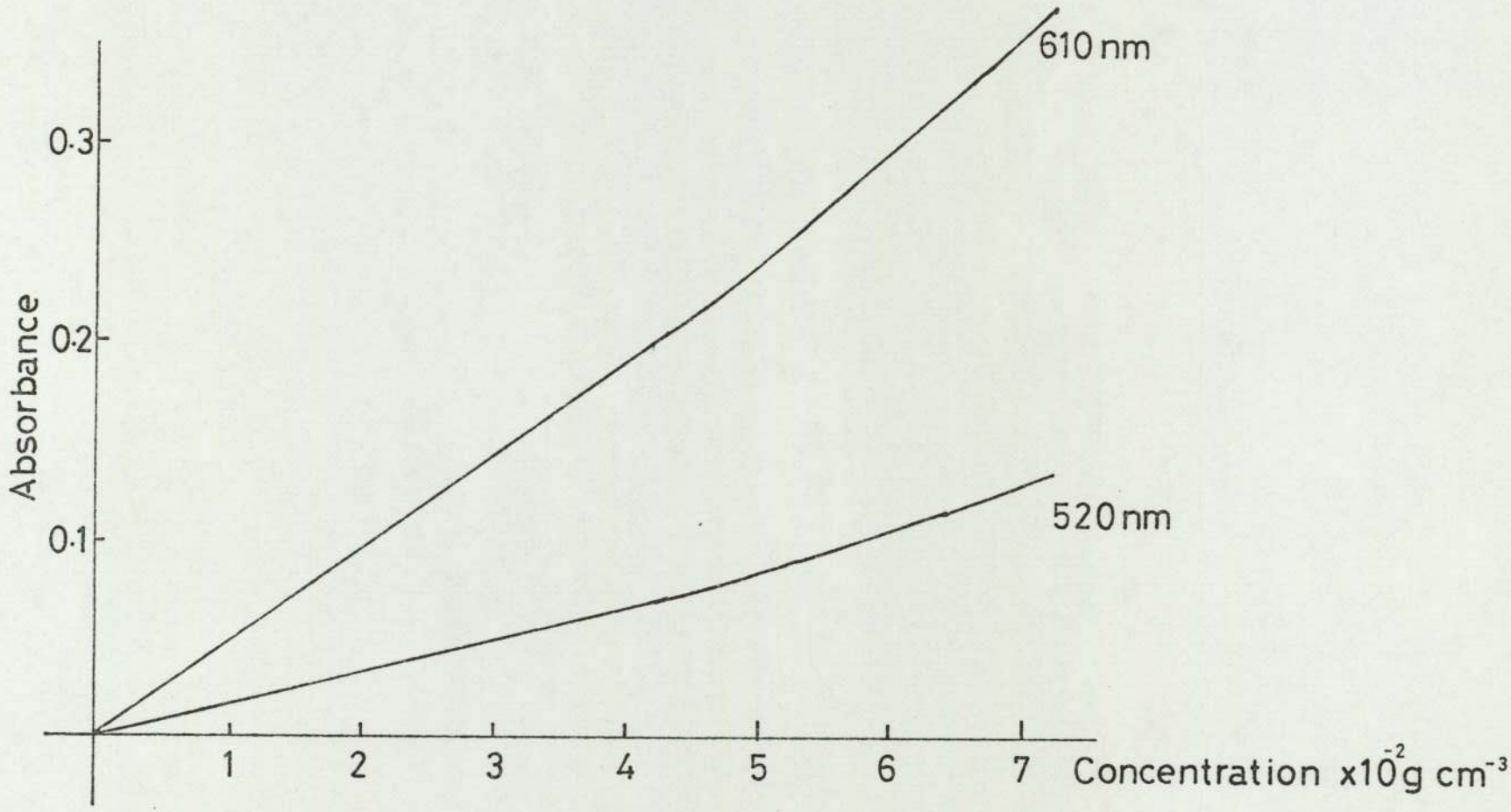

FIGURE 5A-2 Calibration Plot for Dyed B.S.A.

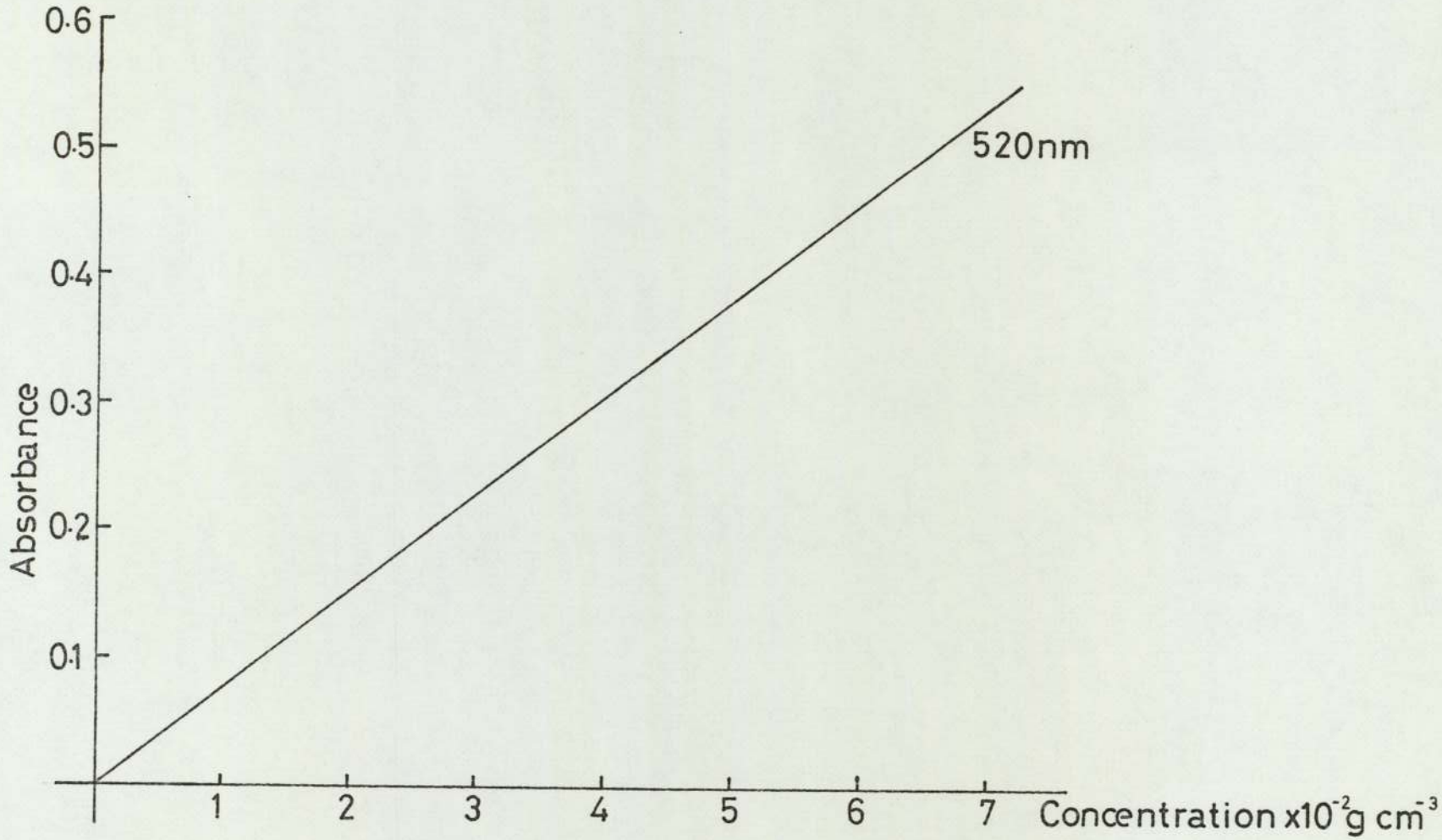

APPENDIX 8

Binary Run 1 Experimental Data

Product Output Concentrations

Purged product			Eluent product		
Time hrs.	Dyed Pepsin x 10^{-3}g cm^{-3}	Dyed Bovine serum albumin x 10^{-3}g cm^{-3}	Time hrs.	Dyed Bovine serum albumin x 10^{-3}g cm^{-3}	Dyed Pepsin x 10^{-3}g cm^{-3}
0.2	0	0	0-2	0	0
2-4	0	0	2-4	0.04	0
4-6	0	0	4-6	0.14	0.0043
6-8	0.004	0.0043	6-8	0.182	0.011
8-10	0.009	0.006	8-10	0.203	0.022
10-12	0.011	0.006	10-12	0.203	0.031
12-14	0.022	0.011	12-14	0.211	0.036
14-16	0.049	0.016	14-16	0.163	0.038
16-18	0.072	0.026	16-18	0.217	0.045
18-20	0.076	0.026	18-20	0.236	0.058
20-22	0.077	0.031	20-22	0.254	0.056
22-24	0.076	0.026	22-24	0.284	0.056

Concentration Profile Data

Tube pair number	Dyed Pepsin		Dyed bovine serum albumin	
	Initial concentration x 10^{-3}g cm^{-3}	Normalised concentration x 10^{-3}g cm^{-3}	Initial concentration x 10^{-3}g cm^{-3}	Normalised concentration x 10^{-3}g cm^{-3}
ISO 1	0.128	0.274	0.068	0.181
2	0.128	0.274	0.068	0.181
3	0.113	0.239	0.053	0.140
Sep 1	0.270	0.568	0.073	0.192
2	0.632	1.32	0.130	0.340
3	1.08	2.26	0.190	0.496
4	1.33	2.76	0.310	0.803
5	1.69	3.51	0.770	1.99
6	1.58	3.38	0.990	2.65
7	1.22	2.57	1.15	3.03
8	0.580	1.25	0.976	2.62
9	0.360	0.767	0.993	2.64
10	0.235	0.496	0.935	2.46
11	0.130	0.270	0.610	1.61
12	0.065	0.127	0.365	0.89

Binary Run 2 Experimental Data

Product Output Concentrations

Purged product			Eluent product		
Time hrs.	Dyed Pepsin $\times 10^{-3}$g cm^{-3}	Dyed Bovine serum albumin $\times 10^{-3}$g cm^{-3}	Time hrs.	Dyed Bovine serum albumin $\times 10^{-3}$g cm^{-3}	Dyed Pepsin $\times 10^{-3}$g cm^{-3}
0-2	0.011	0.0041	0-2	0.0125	0.0022
2-4	0.024	0.0108	2-4	0.0717	0.0044
4-6	0.0203	0.0103	4-6	0.125	0.018
6-8	0.036	0.016	6-8	0.156	0.022
8-10	0.036	0.016	8-10	0.127	0.021
10-12	0.058	0.017	10-12	0.115	0.025
12-14	0.158	0.031	12-14	0.127	0.027
14-16	0.185	0.032	14-16	0.159	0.036
16-18	0.22	0.04	16-18	0.140	0.036
18-20	0.2	0.042	18-20	0.134	0.0314
20-22	0.18	0.042	20-22	0.161	0.036
22-24	0.2	0.042	22-24	0.162	0.036

Concentration Profile Data

Tube pair number	Dyed Pepsin		Dyed bovine serum albumin	
	Initial concentration $\times 10^{-3}$g cm^{-3}	Normalised concentration $\times 10^{-3}$g cm^{-3}	Initial concentration $\times 10^{-3}$g cm^{-3}	Normalised concentration $\times 10^{-3}$g cm^{-3}
ISO 1	0.198	0.420	0.057	0.151
2	0.2	0.420	0.054	0.143
3	0.17	0.360	0.051	0.135
Sep 1	0.496	1.05	0.093	0.245
2	0.496	1.05	0.093	0.245
3	0.947	2.02	0.250	0.666
4	0.947	2.02	0.390	1.04
5	1.15	2.45	0.840	2.24
6	1.26	2.68	1.39	3.69
7	0.901	1.92	1.41	3.74
8	0.290	0.612	1.18	3.09
9	0.156	0.323	1.02	2.64
10	0.123	0.235	0.865	2.06
11	0.083	0.175	0.542	1.43
12	0.054	0.114	0.149	0.393

Binary Run 3 Experimental Data

Product Output Concentrations

Purged product			Eluent product		
Time hrs.	Dyed Pepsin $\times 10^{-3}$g cm^{-3}	Dyed Bovine serum albumin $\times 10^{-3}$g cm^{-3}	Time hrs.	Dyed Bovine serum albumin $\times 10^{-3}$g cm^{-3}	Dyed Pepsin $\times 10^{-3}$g cm^{-3}
0-2	0	0	0-2	0.0035	0.0027
2-4	0	0	2-4	0.003	0.0023
4-6	0.009	0	4-6	0.013	0.010
6-8	0.0338	0.0025	6-8	0.017	0.013
8-10	0.117	0.0136	8-10	0.022	0.017
10-12	0.221	0.038	10-12	0.035	0.027
12-14	0.225	0.057	12-14	0.035	0.027
14-16	0.199	0.088	14-16	0.037	0.028
16-18	0.225	0.127	16-18	0.042	0.032
18-20	0.217	0.139	18-20	0.039	0.03
20-22	0.217	0.136	20.22	0.041	0.032
22-24	0.225	0.171	22-24	0.042	0.032

Concentration Profile Data

Tube pair number	Dyed Pepsin		Dyed Bovine serum albumin	
	Initial concentration $\times 10^{-3}$g cm^{-3}	Normalised concentration $\times 10^{-3}$g cm^{-3}	Initial concentration $\times 10^{-3}$g cm^{-3}	Normalised concentration $\times 10^{-3}$g cm^{-3}
ISO 1	0.250	0.470	0.16	0.376
2	0.252	0.537	0.16	0.428
3	0.241	0.466	0.16	0.388
Sep 1	0.320	0.696	0.217	0.589
2	0.830	1.73	0.90	2.33
3	0.840	1.73	1.24	3.19
4	0.850	1.77	1.37	3.55
5	0.90	1.89	1.58	4.15
6	0.96	1.98	1.52	3.90
7	0.49	1.03	1.33	3.49
8	0.153	0.322	0.625	1.64
9	0.089	0.188	0.371	0.977
10	0.076	0.160	0.206	0.545
11	0.076	0.160	0.206	0.545
12	0.049	0.087	0.034	0.09

Binary Run 4 Experimental Data

(Single component - dyed bovine serum albumin)

Product Output Concentrations

Purged product		Eluent product	
Time hrs.	Dyed Bovine serum albumin $\times 10^{-3}$ g cm^{-3}	Time hrs.	Dyed Bovine serum albumin $\times 10^{-3}$ g cm^{-3}
0-2	0	0-2	0
2-4	0	2-4	0
4-6	0.003	4-6	0
6-8	0.011	6-8	0.0015
8-10	0.018	8-10	0.003
10-12	0.043	10-12	0.009
12-14	0.054	12-14	0.009
14-16	0.060	14-16	0.012
16-18	0.065	16-18	0.017
18-20	0.068	18-20	0.017
20-22	0.077	20-22	0.016
22-24	0.085	22-24	0.017

Concentration Profile Data

Tube pair number	Dyed Bovine serum albumin	
	Initial concentration $\times 10^{-3}$ g cm^{-3}	Normalised concentration $\times 10^{-3}$ g cm^{-3}
ISO 1	0.090	0.27
2	0.090	0.27
3	0.095	0.27
Sep 1	0.2	0.58
2	0.42	1.23
3	0.57	1.69
4	0.60	1.68
5	0.75	2.23
6	0.80	2.37
7	0.242	0.72
8	0.089	0.26
9	0.047	0.14
10	0.027	0.08
11	0.012	0.054
12	0.011	0.035

Binary Run 5 Experimental Data

Product Output Concentrations

Purged product			Eluent product		
Time hrs.	Dyed Pepsin $\times 10^{-3}$g cm^{-3}	Dyed Bovine serum albumin $\times 10^{-3}$g cm^{-3}	Time hrs.	Dyed Bovine serum albumin $\times 10^{-3}$g cm^{-3}	Dyed Pepsin $\times 10^{-3}$g cm^{-2}
0-2	0	0	0-2	0	0
2-4	0	0	2-4	0	0
4-6	0.063	0.0084	4-6	0.009	0
6-8	0.415	0.066	6-8	0.058	0.0045
8-10	0.654	0.216	8-10	0.187	0.031
10-12	0.564	0.259	10-12	0.185	0.045
12-14	0.586	0.372	12-14	0.191	0.045
14-16	0.732	0.474	14-16	0.196	0.045
16-18	0.643	0.335	16-18	0.197	0.049
18-20	0.643	0.375	18-20	0.198	0.045
20-22	0.645	0.353	20-22	0.18	0.045
22-24	0.598	0.331	22-24	0.175	0.045

Concentration Profile Data

Tube pair number	Dyed Pepsin		Dyed Bovine serum albumin	
	Initial concentration $\times 10^{-3}$g cm^{-3}	Normalised concentration $\times 10^{-3}$g cm^{-3}	Initial concentration $\times 10^{-3}$g cm^{-3}	Normalised concentration $\times 10^{-3}$g cm^{-3}
ISO 1	0.77	1.76	0.416	1.19
2	0.9	1.98	0.512	1.41
3	0.81	1.79	0.440	1.22
Sep 1	1.17	2.67	0.760	2.17
2	1.35	3.02	1.16	3.25
3	1.98	4.43	1.95	5.44
4	1.98	4.44	1.95	5.48
5	1.98	4.47	2.13	6.00
6	1.69	3.76	2.20	6.11
7	1.13	2.51	2.01	5.57
8	0.360	0.824	1.46	4.17
9	0.270	0.61	1.09	3.07
10	0.189	0.43	0.670	1.88
11	0.144	0.32	0.445	1.24
12	0.122	0.28	0.176	0.50

Binary Run 6 Experimental Data

Product Output Concentrations

Purged product			Eluent product		
Time hrs.	Dyed Pepsin $\times 10^{-3}$g cm^{-3}	Dyed Bovine serum albumin $\times 10^{-3}$g cm^{-3}	Time hrs.	Dyed Bovine serum albumin $\times 10^{-3}$g cm^{-3}	Dyed Pepsin $\times 10^{-3}$g cm^{-3}
0-2	0	0	0-2	0.005	0.004
2-4	0	0	2-4	0.035	0.027
4-6	0.009	0.003	4-6	0.233	0.180
6-8	0.023	0.006	6-8	0.380	0.295
8-10	0.101	0.017	8-10	0.410	0.318
10-12	0.176	0.031	10-12	0.580	0.447
12-14	0.257	0.051	12-14	0.750	0.580
14-16	0.275	0.058	14-16	0.825	0.640
16-18	0.275	0.061	16-18	0.812	0.629
18-20	0.356	0.68	18-20	0.775	0.6
20-22	0.329	0.073	20-22	0.960	0.745
22-24	0.321	0.070	22-24	0.960	0.745

Concentration Profile Data

Tube pair number	Dyed Pepsin		Dyed Bovine serum albumin	
	Initial concentration $\times 10^{-3}$g cm^{-3}	Normalised concentration $\times 10^{-3}$g cm^{-3}	Initial concentration $\times 10^{-3}$g cm^{-3}	Normalised concentration $\times 10^{-3}$g cm^{-3}
ISO 1	0.496	1.2	0.149	0.450
2	0.372	0.88	0.115	0.340
3	0.372	0.89	0.096	0.290
Sep 1	0.789	1.88	0.70	0.505
2	1.53	3.65	0.298	0.890
3	2.71	6.31	0.433	1.26
4	2.84	6.82	1.07	3.20
5	2.52	6.03	1.64	4.90
6	2.93	7.13	1.95	5.92
7	2.97	4.72	2.14	6.09
8	1.57	3.76	2.00	5.95
9	0.90	2.09	1.85	5.36
10	0.810	1.93	1.61	4.79
11	0.450	1.08	0.90	2.69
12	0.270	0.60	0.40	1.11

APPENDIX 9

```
      PROGRAM ANWCR1(INPUT,OUTPUT,TAPE1=INPUT,TAPE2=OUTPUT)
      COMMON PURC(2,700),PURE(2,700),PSTE(2,700),PSTC(2,700)
      COMMON PRFC(2,700),PRFE(2,700),HISC(2,700),AKV(5),DUM(2,700)
      COMMON HISE(2,700)
      COMMON FC,SWT,PFL,N,KSW,L
      COMMON KFIN
      READ(1,15)TCPF,TCPSF,TCPUR,NC,HISNC,CV,DV
      READ(1,25)(AKV(J),J=1,NC)
      READ(1,26)RFI,RFO

      READ(1,10)PFL,PRFL,FFL,SWT,KCYC,N,FC
      T=0.0
      KFIN=KCYC*22
      KSW=0
      VT=(CV+(DV/22.))/N
      VI=(RFI-RFO)*VT
      VO=RFO*VT
      DPSF=VO/(PRFL+FFL)
      DPRF=VO/PRFL
      DPUR=VO/PFL
      FCC=(FC*FFL)/(PRFL+FFL)
      DO 20 I=1,NC
      DO 30 J=1,700,2
      PSTC(I,J)=0.0
      PSTC(I,J+1)=0.0
      PSTE(I,J)=0.0
      PSTE(I,J+1)=0.0
      PRFC(I,J)=0.0
      PRFC(I,J+1)=0.0
      PRFE(I,J)=0.0
      PRFE(I,J+1)=0.0
      PURE(I,J)=0.0
      PURE(I,J+1)=0.0
      PURC(I,J)=0.0
      PURC(I,J+1)=0.0
      HISC(I,J)=0.0
      HISC(I,J+1)=0.0
      HISE(I,J)=0.0
      HISE(I,J+1)=0.0
      DUM(I,J)=FCC
      DUM(I,J+1)=FCC
   30 CONTINUE
   20 CONTINUE
      XX=SWT/DPSF
      X=SWT/DPRF
   66 CONTINUE
      CALL PSTFEE(TCPSF,NC,DPSF,VI,VO,XX,X)
      IF(KSW.EQ.6)GOTO 88
      KSW=KSW+1
      CALL PREFEE(TCPF,HISNC,NC,DPRF,VI,VO)
      GOTO 66
   88 CONTINUE
      T=T+(KSW*SWT)
  100 CONTINUE
      KSW=KSW+1
      CALL PREFEE(TCPF,HISNC,NC,DPRF,VI,VO)
      CALL PSTFEE(TCPSF,NC,DPSF,VI,VO,XX,X)
```

```
      IF(KSW.EQ.9) GOTO 99
      GOTO 100
   99 T=T+(3*SWT)
  101 KSW=KSW+1
      CALL PURSEC(TCPUR,NC,DPUR,VI,VO)
      CALL PREFEE(TCPF,HISNC,NC,DPRF,VI,VO)
      CALL PSTFEE(TCPSF,NC,DPSF,VI,VO,XX,X)
      IF(KSW.EQ.13) GOTO 102
      GOTO 101
  102 T=T+(4*SWT)
      NNN=KSW
      KKCYC=0
  108 KSW=KSW+1
      NNN=NNN+1
      CALL PURSEC(TCPUR,NC,DPUR,VI,VO)
      CALL PREFEE(TCPF,HISNC,NC,DPRF,VI,VO)
      CALL PSTFEE(TCPSF,NC,DPSF,VI,VO,XX,X)
      T=T+SWT
      IF(NNN.EQ.22) GOTO 110
      GOTO 108
  110 NNN=0
      KKCYC=KKCYC+1

      IF(KSW.EQ.KFIN) GOTO 888
      GOTO 108
  888 CONTINUE
      WRITE(2,199)
      WRITE(2,200)KKCYC,T
      ML=N*TCPSF
      MML=N*TCPF
      MMML=N*TCPUR
      NAP=10
      DO 222 I=1,NC
      DO 288 J=1,MML,2
      WRITE(2,444)(PRFE(I,J),PSTE(I,J),PURE(I,J))
  288 CONTINUE
  222 CONTINUE
  199 FORMAT(1H ,30X,23HCCR1  SIMULATION  STUDY)
 2000FORMAT(1H ,10X,17HNUMBER OF CYCLES=,2X,I6,2X,5HTIME=,2X,F10.5,7HMI
    1NUTES)
  201 FORMAT(10X,E16.8)
  400 FORMAT(1H ,20X,17HEND OF SIMULATION)
  444 FORMAT(20X,E16.8,10X,E16.8,10X,E16.8)
   10 FORMAT(4F10.5,2I6,F10.5)
   15 FORMAT(3F10.5,I6,3F10.5)
      WRITE(2,400)
      WRITE(2,401)
      WRITE(2,402)
      WRITE(2,408)
  408 FORMAT(1H1)
  401 FORMAT(40X,40H****************************************)
  402 FORMAT(50X,20H********************)
   25 FORMAT(F10.5)
   26 FORMAT(2F10.5)

      STOP
      END
```

```
      SUBROUTINE PURSEC(TCPUR,NC,DPUR,VI,VO)
      COMMON PURC(2,700),PURE(2,700),PSTE(2,700),PSTC(2,700)
      COMMON PREC(2,700),PREE(2,700),HISC(2,700),AKV(5),DUM(2,700)
      COMMON HISE(2,700)
      COMMON FC,SWT,PFL,N,KSW,L
      COMMON KFIN
      IF(KSW.GE.13) GOTO 20
      L=KSW-9
      GOTO 10
   20 L=4
   10 L=L*N
      DO 223 I=1,NC
      T=0.0
   44 CONTINUE
      DO 60 J=2,L
      IF(PURE(I,J-1).LT.1.E-09) GOTO 67
      GOTO 69
   67 PURE(I,J-1)=0.0
   69 PURC(I,J)=PURE(I,J-1)
   60 CONTINUE
      PURC(I,1)=0.0
      DO 30 J=1,L
      IF(PURE(I,J).LT.1.E-09.AND.PURC(I,J).LT.1.E-09) GOTO 901
      PURE(I,J)=((PURC(I,J)*VO)+(PURE(I,J)*AKV(I)*VI))/(VO+(VI*AKV(I)))
      GOTO 30
  901 PURE(I,J)=0.0
   30 CONTINUE
      T=T+DPUR
      IF(T.GT.SWT) GOTO 100
      GOTO44
  100 CONTINUE
      IF(KSW.LT.13) GOTO 223
      LAP=L-N+1
      DO 103 J=1,LAP
      PURE(I,J)=PURE(I,J+N)
      PURC(I,J)=PURE(I,J+N)
      PURE(I,J+N)=0.0
      PURC(I,J+N)=0.0
  103 CONTINUE
  223 CONTINUE
      RETURN
      END
```

```
      SUBROUTINE PREFEE(TCPF,HISNC,NC,DPRF,VI,VO)
      COMMON PURC(2,700),PURE(2,700),PSTE(2,700),PSTC(2,700)
      COMMON PRFC(2,700),PRFE(2,700),HISC(2,700),AKV(5),DUM(2,700)
      COMMON HISE(2,700)
      COMMON FC,SWT,PFL,N,KSW,L
      COMMON KFIN
      IF(KSW.LE.9) GOTO 77
      IF(KSW.LT.13) L=L+N
      KM=L-N+1
      DO 9 I=1,NC
      KL=1
      DO 8 J=KM,L
      PURC(I,J)=HISC(I,KL)
      PURE(I,J)=HISE(I,KL)
      KL=KL+1
    8 CONTINUE
    9 CONTINUE
   77 CONTINUE
      IF(KSW.GT.6)GOTO 20
      L=KSW
      GOTO 10
   20 L=6
   10 L=L*N
      DO 223 I=1,NC
      T=0.0
      M=1
   44 CONTINUE
      DUM(I,M)=PRFE(I,L)
      PRFC(I,1)=0.0
      DO 60 J=2,L
      IF(PRFE(I,J-1).LT.1.E-06) GOTO 67
      GOTO 69
   67 PRFE(I,J-1)=0.0
   69 PRFC(I,J)=PRFE(I,J-1)
   60 CONTINUE
      DO 30 J=1,L
      IF(PRFC(I,J).LT.1.E-06.AND.PRFE(I,J).LT.1.E-06) GOTO 901
      PRFE(I,J)=((PRFC(I,J)*VO)+(PRFE(I,J)*AKV(I)*VI))/(VO+(VI*AKV(I)))
      GOTO 30
  901 PRFE(I,J)=0.0
   30 CONTINUE
      M=M+1
      T=T+DPRF
      IF(T.GT.SWT) GOTO 100
      GOTO 44
  100 CONTINUE
      IF(KSW.EQ.KFIN) GOTO 33
      IF(KSW.LT.6) GOTO 223
      KLM=(HISNC*N)-N
      DO 99 J=1,KLM
      KM=J+N
      HISE(I,J)=HISE(I,KM)
      HISC(I,J)=HISC(I,KM)
   99 CONTINUE
      KLM=KLM+1
      DO 101 J=1,N
      HISE(I,KLM)=PRFE(I,J)
```

```
      HISC(I,KLM)=PRFE(I,J)
      KLM=KLM+1
  101 CONTINUE
      LA=L-N
      DO 103 J=1,LA
      PRFE(I,J)=PRFE(I,J+N)
      PRFC(I,J)=PRFE(I,J+N)
  103 CONTINUE
      LA=LA+1
      DO 104 J=LA,L
      PRFC(I,J)=0.0
      PRFE(I,J)=0.0
  104 CONTINUE
   33 CONTINUE
  223 CONTINUE
      RETURN
      END
```

```
      SUBROUTINE PSTFEE(TCPSF,NC,DPSF,VI,VO,XX,X)
      DIMENSION DUMM(2,700)
      COMMON PURC(2,700),PURE(2,700),PSTE(2,700),PSTC(2,700)
      COMMON PRFC(2,700),PRFE(2,700),HISC(2,700),AKV(5),DUM(2,700)
      COMMON HISE(2,700)
      COMMON FC,SWT,PFL,N,KSW,L
      COMMON KFIN
      L3=TCPSF*N
      IF(KSW.EQ.0) GOTO 125
      NNC=SWT/DPSF
      FRAC=X/XX
      DO 123 I=1,NC
      AAA=FRAC
      DUMM(I,1)=DUM(I,1)*FRAC+(1.0-FRAC)*FC
      K=2
  126 CONTINUE
      CCC=(1.-FRAC)+(1.-AAA)
      IF(CCC.GT.1.) GOTO 999
      BBB=(FRAC+AAA)-1.0
      DUMM(I,K)=(1.0-FRAC)*FC+(1.0-AAA)*DUM(I,K-1)+BBB*DUM(I,K)
      AAA=BBB
      IF(K.EQ.NNC) GOTO 124
      GOTO 989
  999 CONTINUE
      DDD=(1.-AAA)-(CCC-1.)
      DUMM(I,K)=(1.-FRAC)*FC+(DDD*DUM(I,K-1))
      K=K-1
      AAA=(1.-AAA)-DDD+1.
  989 CONTINUE
      K=K+1
      GOTO 126
  124 CONTINUE
  123 CONTINUE
  125 CONTINUE
      IF(KSW.GE.1) GOTO 902
      DO 127 I=1,NC
      DO 128 J=1,700,2
      DUMM(I,J)=DUM(I,J)
      DUMM(I,J+1)=DUM(I,J+1)
  128 CONTINUE
  127 CONTINUE
  902 CONTINUE
      DO 20 I=1,NC
      T=0.0
      M=1
   44 CONTINUE
      PSTC(I,1)=DUMM(I,M)
      DO 60 J=2,L3
      IF(PSTE(I,J-1).LT.1.E-06) GOTO 67
      GOTO 69
   67 PSTE(I,J-1)=0.0
   69 PSTC(I,J)=PSTE(I,J-1)
   60 CONTINUE
      DO 30 J=1,L3
      IF(PSTE(I,J).LT.1.E-06.AND.PSTC(I,J).LT.1.E-06) GOTO 901
      PSTE(I,J)=((PSTC(I,J)*VO)+(PSTE(I,J)*AKV(I)*VI))/(VO+(VI*AKV(I)))
      GOTO 30
```

```
901 PSTE(I,J)=0.0
 30 CONTINUE
    M=M+1
    T=T+DPSF
    IF(T.GT.SWT) GOTO 100
    GOTO 44
100 CONTINUE
    IF(KSW.EQ.KFIN) GOTO 33
    IF(KSW.LT.6) L=L+N
    IF(KSW.EQ.0) L=N
    DO 101 J=1,N
    KKK=L+J-N
    PREC(I,KKK)=PSTE(I,J)
    PREE(I,KKK)=PSTE(I,J)
101 CONTINUE
    JJ=N+1
    DO 109 J=JJ,L3
    JJJ=J-N
    PSTE(I,JJJ)=PSTE(I,J)
    PSTC(I,JJJ)=PSTE(I,J)
109 CONTINUE
    LAP=L3-N+1
    DO 118 J=LAP,L3
    PSTE(I,J)=0.0
    PSTC(I,J)=0.0
118 CONTINUE
 33 CONTINUE
 20 CONTINUE
    RETURN
    END
```

NOMENCLATURE

A, A_2'	=	Eddy diffusion term in the chromatographic theoretical plate expression
A'	=	$(1-\alpha)/\alpha$ where α is the fractional free cross section of the column
A''	=	Tube cross-sectional area
A_2	=	Cross sectional area equivalent to the pores of the packing
A_o	=	Available cross sectional area for fluid flow
a	=	Stokes radius
B	=	Longitudinal mobile phase diffusion term
C	=	Mass transfer term
C_s''	=	Mass transfer effects in stationary phase
C_{mi}	=	Mass transfer effects in mobile phase
C_m', C_s'	=	Resistance to mass transfer in the mobile and stationary phase respectively.
C_o	=	Initial mobile phase concentration
C'	=	Mobile phase concentration after equilibration
C_n^t	=	Mobile phase concentration on stage n at time t
$C_{n-1}^{t-\Delta t}$	=	Mobile phase concentration on stage n-1 at time $t-\Delta t$
C_m	=	Mobile phase solute concentration
C_s	=	Stationary phase solute concentration
D	=	Overall dispersion number
$\overline{D}_r$	=	Average radial diffusivity
D_p	=	Longitudinal dispersion coefficient
D_{ia}, D_m, D_1	=	Mobile phase diffusion coefficient
D_{is}, D_s, D_2	=	Stationary phase diffusion coefficient

d_p	=	Particle size
ε_a	=	Volume fraction occupied by the mobile phase
ε_β	=	Volume fraction occupied by the stationary phase
ε_s	=	Internal pore volume occupied by the stationary phase
ε_m	=	Interstitial volume fraction
F_1	=	Mass input rate of component 1
F_e	=	Feed flow rate
g	=	Geometric constant
H	=	Height equivalent to a theoretical plate (HE.T.P)
H_{md}	=	Mixing due to mobile phase
H_{mc}	=	Mixing due to stationary phase
H_{em}	=	Mass transfer effect in mobile phase
H_{es}	=	Mass transfer effect in stationary phase
h	=	Reduced plate height
h'	=	Velocity profile constant
K, K_2	=	Partition or distribution coefficient
K_1,K_2	=	Partition coefficient of components 1 and 2 at a finite concentration
K_1^∞, K_2^∞	=	Partition coefficients of components 1 and 2 at infinite dilution
K_c	=	"Cut" effected by machine, fixed by machine operating conditions.
K'	=	Eddy diffusion coefficient
K_1', K_2'	=	Proportionately constants
K_D	=	Fraction of total pore volume, V_i, that is available to a molecule, also defines partition coefficient in G.P.C.

K_{av} = Distribution factor

L = Total column length

L_E = Mobile phase flowrate, R_D

L_m = Relative mobile phase flowrate

L'_m = Relative mobile phase flowrate in postfeed section

L_s = Relative liquid, "stationary", phase flowrate

L_p = Relative purge flowrate.

L' = Concentration of rods

M = Molecular weight

M_{ex} = Smallest molecular weight that is excluded from gel.

$\bar{M}_n$ = Number average molecular weight

$\bar{M}_w$ = Weight average molecular weight

$\bar{M}_v$ = Viscosity average molecular weight

M_2 = Molecular weight of component i

N = Number of theoretical plates

n_i = Number of molecules with a molecular weight M_i

P = Capacity factor

Q = Volumetric flowrate

Q_n^t = Solute concentration in available pore volume on plate n at time t

$Q_n^{t-\Delta t}$ = Solute concentration in available pore volume on plate n at time t-Δt

R = Relative solute band migration rate

R' = Radius of a cylindrical channel

R_s = Solvent regain for gel

R''_c = Ratio of solute zone velocity to the mobile phase velocity

R"	=	Radius of spherical solute molecule
R_c	=	Column radius
R_o	=	Diameter of spherical partical
R_d	=	Diameter of impermeable core in particle
R_D	=	Mobile phase output rate
R.F.	=	Retention factor
	=	Sample elution volume/total packed bed volume
R.F. (excl)	=	Retention factor of totally excluded molecule
R.F. (incl)	=	Retention factor of totally included molecule
r	=	Radius of rods
r_2	=	Total bundle length/time for one cycle of tube bundle
S	=	Separation factor
S'	=	Reduced dispersion parameter
s	=	Correction to machine operating limits attributable to a discontinuous mode of operation
t_D	=	Dead time
t_R	=	Elution time
t'_R	=	Adjusted elution time
U	=	Interstitial mobile phase velocity
V_e	=	Elution volume
V_o	=	Column void volume
V_i	=	Pore volume
V_{e_o}	=	Elution volume of infinitely small sample
V_s	=	Sample volume
V_t	=	Total packed bed volume
V_2	=	Volume per unit of interphase area of stationary phase

V_{am}	=	Volume of gel matrix
V_{iace}	=	Accessible pore volume
V_T	=	Total liquid volume available to a component in a single equilibrium stage
V_m	=	Interstitial volume available in one stage
V_s	=	Total available pore volume in one equilibrium stage
v	=	Reduced velocity
v_m	=	Mobile phase velocity
v_s	=	Liquid phase velocity, r_2
v_α	=	Kinematic viscosity of the mobile phase
W	=	Peak width at the base
W'	=	Linear velocity of solvent flow
W_i	=	Geometric factor
W_1, W_2	=	Mass fraction of solute in the mobile and stationary phase respectively.
$\bar{W}_a$	=	Contribution from the apparatus
$\bar{W}_b$	=	Chromatogram base width
$\bar{W}_d$	=	Contribution from the diffusion spreading due to the hold up of molecules in the pores
$\bar{W}_m$	=	Contribution from the molecular size distribution
$\bar{W}_i$	=	Contribution from the interstitial volume within the column
$\bar{W}_s$	=	Contribution from sorption effects
X_1	=	Concentration of component 1 in liquid phase
Y_1	=	Concentration of component 1 in mobile phase
Z	=	Distance along a column of length L

Greek

α	=	That part of R_s not available to solute
	=	Mark Houwink constant
β_i	=	Change, due to concentration effects, in the partition coefficient of component i.
γ_s	=	Obstruction factor
$\phi, \gamma_m, \gamma_s'$	=	Tortuosity factors.
γ_i	=	Geometric factor
λ	=	Eddy-diffusion proportionality constant
λ_1, λ_2	=	Geometric factors
δ	=	Aspect ratio
δ'	=	Correction to machine operating limits attributable to a finite column length
ρ	=	Dimensionless parameter characterising maximising depth of penetration
σ_z^2	=	Length based second moment (variance)
σ_t^2	=	Time based second moment (variance) of sample peak
σ_c^2	=	Time based variance resulting from the G.P.C. column processes.
σ_e^2	=	Time based variance resulting from flow disturbances in the flow lines and the detector
σ_i^2	=	Time based input variance of glucose plug
σ_o^2	=	Time based output variance of glucose plug

REFERENCES

1. R. E. Treybal, "Mass Transfer Operations", 2nd Ed., International Stud. Edit., McGraw-Hill Kogakuska.

2. A. T. James and A. J. P. Martin, Biochem. J., 50, 679 (1952).

3. P. E. Barker and D. Critcher, Chem. Eng. Sci., 13, 82 (1960).

4. D. Critcher, Ph.D. Thesis, Univ. of Birmingham, 1963.

5. P. E. Barker and D. Lloyd, U.S. Patent 3338031.

6. D. Lloyd, Ph.D. Thesis, Univ. of Birmingham, 1963.

7. P. E. Barker and D. H. Huntington, J. Chromatog., 4, 59 (1966).

8. R. E. Deeble, Ph.D. Thesis, Univ. of Aston, 1974.

9. P. E. Barker, "Progress in Separation and Purification", Ed. Perry and Van Ross, 1971, J. Wiley and Sons Inc.

10. J. C. Janson, J. Agr. Food Chem., 19, 581 (1971).

11. B. W. Hatt, Ph.D. Thesis, Univ. of Birmingham, 1970.

12. J. C. Giddings, "Dynamics of Chromatography", Vol. I, 1965, Chromatographic Series, Arnold.

13. H. Determann, "Gel Chromatography", 1969, 2nd Edit., New York: Springer-Verlag.

14. K. H. Altgelt and L. Segal, "Gel Permeation Chromatography".

15. J. Bear, "Dynamics of Fluids in Porous Media", Environmental Science Series, American Elsevier, 1972.

16. J. J. Van Deemter, F. J. Zuiderweg and A. Klinkenberg, Chem. Eng. Sci., 5, 271 (1956).

17. J. N. Wilson, J. Amer. Chem. Soc., 62, 1583 (1940).

18. A. Klinkenberg and F. Sjenitzer, Chem. Eng. Sci., 5, 258 (1956).

19. A. J. Martin and R. L. M. Synge, Biochem. J., 35, 1358 (1941).

20. E. Grushka, E. R. Snyder and J. H. Knox, J. Chromatog. Sci., 13, 25 (1975).

21. E. Glueckauf, Trans. Farad. Soc., No. 385, 51, 34 (1955).

22. F. J. Ellison, unpublished work, Univ. of Aston in Birmingham.

23. J. M. Ryan and R. D. Timmings, Chem. Eng., May 19th, 170 (1969).

24. Anonymous, Chem. Eng. News, March 25th, 62 (1968).

25. U.S. Patent 3250058, May 10th, 1967.

26. L. Ek, Process Biochem., Sept, 25 (1968).

27. J. Brewer, Process Biochem., Sept, 39 (1971).

28. E. G. Samuelsson, P. Tibbling and S. Holm, Food Technol, 21, 121 (1967).

29. J. R. Condor, "Production Scale Chromatography", in "New Developments in Gas Chromatography", 137-186, Ed. H. Purnell, J. Wiley N.Y., 1973.

30. A. J. P. Martin, Discussions Farad. Soc., 7, 332 (1949).

31. J. C. Giddings, Anal. Chem., 34, 37 (1962).

32. D. Dinelli, M. Taramosso and S. Polezzo, U.S. Patent 3187486, 1965.

33. D. Dinelli, S. Polezzo and M. Taramosso, J. Chromatog., 7, 477 (1962).

34. S. Polezzo and M. Taramosso, J. Chromatog., 11, 19 (1963).

35. M. Taramosso and D. Dinelli, J. Gas Chromatog., 2, 150 (1964).

36. H. Svenson, Swedish Patent 133851, 1951.

37. H. Svenson, C. E. Agril, S. O. Dehlein and L. Hagdahl, Science Tools, 2, 17 (1955).

38. J. B. Fox, Jr., R. C. Calhown and W. J. Eglinton, J. Chromatog., 43, 48 (1969).

39. J. B. Fox, Jr., J. Chromatog., 43, 55 (1969).

40. R. A. Nicholas and J. B. Fox, Jr., J. Chromatog., 43, 61 (1969).

41. P. Dunhill and M. D. Lilly, Biotechnol. Bioeng. Symp., No. 3, 47 (1972).

42. L. C. Mosier, Cities Service Research and Development Co., U.S. Patent 3078647, 1963.

43. M. V. Sussman, K. N. Astill, R. Rombach, A. Cerullo and S. S. Chen, Ind. Eng. Chem. Fundam., 11, 181 (1967).

44. M. V. Sussman and R. N. S. Rathone, Chromatographia, No. 2, 8, 55 (1975).

45. E. J. Tuthill and J. Fedelman, U.S. Patent 3527350, 1970.

46. E. J. Tuthill, J. Chromatog. Sci., 8, 285 (1970).

47. R. H. Wilhelm, R. W. Rice and A. R. Bendelius, Ind. Eng. Chem. Fundam., 5, 141 (1966).

48. C. Berg, Chem. Eng. Progr., 47, 585 (1951).

49. H. Schultz, "Gas Chromatography", Ed. M. Van Swaay, Butterworths, London, 1963.

50. R. S. W. Scott, "Gas Chromatography", Ed. D. H. Deitz, Butterworths, London, 1958.

51. G. R. Fitch, M. E. Probert and P. F. Tiley, Chem. Soc., 4875 (1962).

52. D. W. Pritchard, M. E. Probert and P. F. Tiley, Chem. End. Sci., 26, 2063 (1971).

53. B. J. Bradley and P. F. Tiley, Chemistry and Industry, 18, 743 (1963).

54. R. F. Buhl and M. L. Yeagle, U.S. Patent 3264801, 1966.

55. U.S. Patent 2869672.

56. H. Pichler and H. Schultz, Brenstoff Chemie, 39, 48 (1958).

57. L. Luft, U.S. Patent 3016106, 1962.

58. D. Glasser, "Gas Chromatography 1966", Ed. A. B. Littlewood, Inst. of Petroleum, London, 19 (1967).

59. U.S. Patent 2893955.

60. P. E. Barker, "Progress in Separation and Purification", Ed. Perry and Van Ross, 1971, J. Wiley and Sons Inc.

61. P. E. Barker, S. A. Barker, B. W. Hatt and P. J. Sommers, Chem. Proc. Eng., No. 1, 52, 64 (1971).

62. P. E. Barker and Universal Fisher Eng. Co. Ltd., Crawley, Sussex, Brit. Patent 114596.

63. D. H. Huntington, Ph.D. Thesis, University of Birmingham, 1967.

64. P. E. Barker and Universal Fisher Engineering Co. Ltd., Brit. Pat. Appl. 33630/65, 43629/65, 5764/68, 44375/68.

65. P. E. Barker and S. Al-Madfai, J. Chromatog. Sci., 7, 425 (1969).

66. S. Al-Madfai, Ph.D. Thesis, Univ. of Birmingham, 1969.

67. L. Szepesy, Zs. Sebestyen, I. Feher and Z. Nagy, J. Chromatog., 108, 285 (1975).

68. Unidev information pamphlet on the "Sequential Separator", Unidev Ltd., Crawley, Sussex.

69. P. E. Barker and R. E. Deeble, Brit. Patent Appl. 27786/72 and U.S. Patent Appl. 368584.

70. D. M. Bell, unpublished work, Univ. of Aston in Birmingham.

71. G. Wilkes and P. F. Donley, J. Am. Soc. Lubric. Eng., August (1970).

72. S. C. W. Wilkinson, "Mechanical Seal Design", private communication.

73. D. McDonald, Process Eng., Jan. 66 (1974).

74. J. F. W. Galyer and C. R. Shotbolt, "Metrology for Engineers", Cassel, London.

75. C. Hooke, Department of Mechanical Engineering, University of Birmingham, private communication.

76. M. Adamson, Final year design problem, Mechanical Engineering Department, University of Aston in Birmingham, 1974.

77. A. Bush, as above.

78. H. Weil and T. I. Williams, Nature, Lond., 166, 1000 (1950).

79. M. Tswett, Trav. Soc. Nat. Varsovia., No. 6, 14 (1903).

80. A. J. P. Martin, Annu. Rev. Bio. Chem., 19, 517 (1950).

81. V. R. Deitz, Annal. N.Y. Acad. Sci., 49, 315 (1948).

82. J. Porath and P. F. Codin, Nature, 183, 1657 (1959).

83. J. C. Moore, J. Polym. Sci., A-2, 835 (1964).

84. G. H. Lathe and C. R. J. Ruthven, Biochem. J., 62, 665 (1956).

85. B. Lindquist and J. Storgårds, Nature, 175, 511 (1955).

86. R. M. Wheaton and W. C. Bauman, Anal. N.Y. Acad. Sci., 57, 159 (1953)

87. H. Deuel and H. Neukorm, Advan. Chem. Ser., 11, 51 (1954).

88. J. Claesson and S. Claesson, Phys. Rev. 73, 1221 (1948).

89. G. Weigner, J. Soc. Chem. Ind. (London), 50, 657 (1931).

90. K. H. Altgelt and J. C. Moore, "Polymer Fractionation", Ed. M. J. R. Cantow, Academic Press, N.Y. 1967.

91. A. Lambert, Br. Polym. J., 3, Jan, 13 (1971).

92. P. Andrews, "Molecular Sieve Chromatog., Nat. Inst. Research. Dairying, Shenfield, Reading.

93. A. R. Cooper, Chem. Brit., 9, 112 (1973).

94. R. F. Boyer, Technical Preprint 19530, 1969 (Waters Associates Ltd., Stockport).

95. M. J. R. Cantow, R. S. Porter and J. F. Johnson, Rev. Macromol. Chem., 1, 393 (1966).

96. W. Heitz and W. Kern, Agnew. Chem., 1, 527 (1970).

97. D. D. Bly, Science, 168, May, 527 (1970).

98. W. Heitz, Agnew. Chem. Internat. Edit., 9, 689 (1970).

99. L. Fischer, "Laboratory Techniques in Biochemistry and Molecular Biology", Ed. T. S. Work and F. Work, North Holland, 1969.

100. R. N. Kelley and F. W. Billmeyer, Separa. Sci., 5, 291 (1970).

101. T. C. Laurent and J. Killander, J. Chromatog., 14, 317 (1964).

102. B. J. Gelotte, J. Chromatog., 3, 330 (1960).

103. G. K. Ackers, Biochem., 3, No. 5, May, 723 (1964).

104. K. O. Pedersen, Biochem. Biophys. Suppl. 1, 157 (1962).

105. S. Hjerten and R. Mosbach, Anal. Biochem., 3, 109 (1962).

106. R. L. Steere and G. K. Ackers, Nature, 196, 475 (1962).

107. J. C. Giddings, E. Kucera, C. P. Russell and M. N. Meyer, J. Phys. Chem., 72, 4397 (1968).

108. P. Flodin, Thesis, University of Uppsala, 1962.

109. K. H. Altgelt, "Advances in Chromatography", Ed. J. C. Giddings and R. A. Keller, Dekker, N.Y., 1968.

110. R. L. Pecsok and D. Saunders, Separa. Sci., 1, 613 (1967).

111. W. W. Yau and C. P. Malone, J. Polym. Sci. B., 7, 663 (1967).

112. E. A. DiMarzio and C. M. Guttman, J. Polym. Sci. B., 7, 267 (1969).

113. J. Porath, Pure. Appl. Chem., 6, 233 (1963).

114. M. J. R. Cantow, R. S. Porter and J. F. Johnson, J. Polym. Sci. A-1, 5, 987 (1967).

115. E. A. DiMarzio and C. M. Guttman, Macromolecules, 3, No. 2, 131 (1970).

116. M. J. R. Cantow and J. F. Johnson, J. Polym. Sci. A-1, 5, 2835 (1967).

117. M. J. R. Cantow and J. F. Johnson, Polym., 8, 487 (1967).

118. E. F. Cassasa, J. Polym. Sci. B., 5, 773 (1967).

119. E. F. Cassasa, J. Polym. Sci. B., 6, 803 (1968).

120. E. F. Cassasa and Y. Tagami, Macromolecules, 2, 14 (1969).

121. L. Z. Vilenchic and B. G. Benlenki, J. Chromatog., 53, 13 (1971).

122. W. W. Yau, C. P. Malone and S. W. Fleming, J. Polym. Sci. B., 6, 803 (1968).

123. W. W. Yau, H. L. Suchan and C. P. Malone, J. Polym. Sci., A-2, 6, 1349 (1968).

124. W. W. Yau, C. P. Malone and H. L. Suchan, Separ. Sci., 5, 259 (1970).

125. J. J. Hermans, J. Polym. Sci. A-2, 6, 1217 (1968).

126. W. W. Yau, J. Polym. Sci. A-2, 7, 483 (1969).

127. J. B. Charmichael, Macromolecules, 1, 526 (1968).

128. F. H. Verhoff and N. D. Sylvester, J. Macromol. Sci. Chem. A-4, 979 (1970).

129. M. E. Van Kreveld and N. J. Van Den Hoed, J. Chromatog., 83, 111 (1973).

130. C. K. Cotton, C. N. Satterfield and C. J. Lai, A. I. Chem. E. J., 2, No. 2, 289 (1975).

131. E. F. Cassasa, J. Phys. Chem., 75, No. 26, 3929 (1971).

132. E. M. Renkin, J. Gen Physiol., 38, 225 (1955).

133. P. G. Squire, Arch. Biochem. Biophys., 107, 471 (1964).

134. G. K. Ackers, J. Biol. Chem., 242, 3237 (1967).

135. P. Andrews, Biochem. J., 91, 222 (1964).

136. B. Gelotte and J. Porath, "Chromatography", Ed. E. Heftmann, Rheinhold, New York, 1967.

137. A. G. Ogston, Trans. Farad. Soc., 54, 1754 (1958).

138. R. Beau, M. Le Page and A. J. De Vries, Appl. Polym. Symp., No. 8, 137 (1969).

139. W. Haller, J. Chromatog., 42, 676 (1968).

140. J. C. Giddings, Anal. Chem., 34, 1186 (1962).

141. J. C. Giddings, Anal. Chem., 35, 439 (1963).

142. J. C. Giddings, Anal. Chem., 35, 1338 (1963).

143. J. C. Giddings and K. L. Mallik, Anal. Chem., 38, No. 8, 997 (1968).

144. S. T. Sie and G. W. A. Rijnders, Anal. Chim. Acta., 38, 3 (1967).

145. G. I. Taylor, Proc. Roy. Soc., A219, 186 (1953); A223, 446 (1954); A225, 473 (1954).

146. R. Aris, Proc. Roy. Soc., A235, 67 (1956).

147. V. P. Dorweiller and R. W. Fahein, Am. Inst. Chem. Eng. J., 5, 139 (1959).

148. T. K. Perkins and O. Johnson, Soc. Petrol. Eng. J., 3, 70 (1963).

149. R. N. Kelley and F. N. Billmeyer Jr., Anal. Chem., 41, No. 7, 874 (1969).

150. R. N. Kelley and K. N. Billmeyer Jr., Anal. Chem., 42, No. 3, 399 (1970).

151. J. F. K. Huber and J. A. R. J. Hulsman, Anal. Chim. Acta, 38, 305 (1969).

152. J. F. K. Huber, J. Chromatog. Sci., 7, 85 (1969).

153. J. G. Hendrickson, J. Polym. Sci. A-2, 6, 1903 (1968).

154. H. Vink, J. Chromatog., 52, 205 (1970).

155. M. Kubin, J. Chromatog., 108, 1 (1975).

156. D. S. Horne, J. H. Knox and L. McKlaren, Separ. Sci., 5, 531 (1966).

157. J. H. Knox, Anal. Chem., 38, 253 (1966).

158. M. Le Page, R. Beau and A. J. De Vries, J. Polym. Sci., 21, 119 (1968).

159. A. J. De Vries, M. Le Page, R. Beau and C. L. Guillerman, Anal. Chem., 39, 935 (1967).

160. P. Flodin, J. Chromatog., 5, 103 (1961).

161. J. H. Knox and J. F. Parcher, Anal. Chem., K1, 1599 (1969).

162. A. R. Cooper and I. Kiss, Jr., Br. Polym. J., 5, 433 (1973).

163. W. V. Smith and G. A. Feldman, J. Polym. Sci. A-2, 7, 163 (1969).

164. F. A. Sliemers, K. A. Boni, D. F. Nenszer and G. P. Nance, "6th International Seminar on G.P.C.", Miami Beach, Florida, October, 1968.

165. A. R. Cooper and E. M. Barrall II, J. Appl. Polym. Sci., 17, 1253 (1973).

166. J. N. Little, J. L. Waters, K. J. Bombaugh and W. Paulir, J. Chromatog. Sci., 9, 341 (1971).

167. S. A. Barker, B. W. Hatt and P. J. Somers, Carbohydrate Research, 11, 355 (1969).

168. K. Hellsing, J. Chromatog., 36, 170 (1968).

169. G. K. Ackers and R. L. Steere, Biochim. Biophys. Acta, 59, 137 (1962).

170. A. C. Ouano, J. Macromol. Sci - Revs. Macromol. Chem., C9, No. 1, 123 (1973).

171. J. C. Moore, Separ. Sci., 5, 723 (1970).

172. A. Rubin, J. Polym. Sci. A-1, 9, 2587 (1971).

173. A. C. Ouano, J. Polym. Sci. A-1, 9, 2179 (1971).

174. R. Epton and C. Holliday, "An Introduction to Gel Permeation Chromatography", Koch-Light Laboratories Ltd., England.

175. L. A. Dark and R. J. Limpert, J. Chromatog. Sci., 11, 114 (1973).

176. W. J. Haller, Chem. Phys., 42, 686 (1965).

177. R. D. Conlon, Analyt. Chem., 41, 107A (1969).

178. L. E. Maley, J. Polym. Sci. C., 8, 253 (1965).

179. J. H. Ross and M. E. Carlo, J. Polym. Sci. C, 21, 143 (1968).

180. S. Terry and J. Rodrigiez, J. Polym. Sci. C, 21, 191 (1968).

181. K. P. Hupe and E. Bayer, J. Gas Chromatogr., 5, 197 (1967).

182. A. Karman, Anal. Chem., 38, 286 (1966).

183. S. G. Perry, Chem. Brit., 7, 366 (1971).

184. "Dextran", Pharmacia booklet, Pharmacia Fine Chemicals, Upsalla, Sweden.

185. J. Kucera, J. Chromatog., 19, 237 (1965).

186. O. Grubner, Anal. Chem., 43, 1934 (1971).

187. L. H. Tung, J. Appl. Polym. Sci., 10, 375 (1966).

188. W. N. Smith, J. Appl. Polym. Sci., 11, 639 (1967).

189. M. Hess and R. F. Kratz, J. Polym. Sci. A-2, 4, 731 (1966).

190. H. E. Pickett, M. J. R. Cantow and J. F. J. Johnson, J. Polym. Sci., 21, 67 (1968).

191. P. E. Pierce and J. E. Armonos, J. Polym. Sci. C, 21, 23 (1968).

192. S. T. E. Aldhouse and D. M. Stanford, "5th International G.P.C. Seminar," London May 1968.

193. H. Vink, Macromolec. Chem., 116, 241 (1968).

194. T. Provder and E. M. Rosen, Prepr. Div. Petrol Chem. Am. Chem. Soc., 15, A167 (1970).

195. E. M. Rosen and T. Provder, Prepr. Div. Petrol Chem. Am. Chem. Soc., 15, A192 (1970).

196. A. E. Hamielec and S. T. Balke, J. Appl. Polym. Sci., 13, 1381 (1969).

197. L. H. Tung, J. Appl. Polym. Sci., 13, 775 (1969).

198. L. H. Tung and J. R. Runyon, J. Appl. Polym. Sci., 13, 2397 (1969).

199. L. H. Tung, Prepr. Div. Petrol Am. Chem. Soc., 15, A4 (1970).

200. L. H. Tung, Div. Analyt. Chem. Am. Chem. Soc., paper 24 (1970).

201. T. Vladimiroff, J. Chromatog., 55, 175 (1971).

202. K. S. Chang and R. Y. Haung, J. Appl. Polym. Sci., 13, 1459 (1969).

203. K. S. Chang and R. Y. Haung, J. Appl. Polym. Sci., 16, 329 (1972).

204. A. E. Hamielec and W. H. Ray, J. Appl. Polym. Sci., 13, 1317 (1969).

205. J. H. Duerksen, Prepr. Div. Petrol Chem. Am. Chem. Soc., 15, A47 (1970).

206. A. J. De Vries, private communication.

207. P. E. Barker and D. H. Huntington, Dechema Monographien, 62, 153 (1968).

208. D. H. Huntington, Ph.D. Thesis, University of Birmingham, 1970.

209. K. H. Altgelt, A. C. S. Symposium on G.P.C., 159th Nat. Meet. Am. Chem. Soc. Houston, Texas, Feb., 1970.

210. Z. Dische, Methods in Carbohydrate Chem., 1, 513 (1962).

211. J. C. Sternberg, "Advances in Chromatography, 2, Ed. J. C. Giddings and R. A. Keller, E. Arnold, New York, 1966.

212. Fisons Ltd., Holmes Chapel, private communication.

213. Anal. Chem., 30, No. 7, 1193 (1958).

214. P. J. Andrews, Chromatog., 104, 454 (1975).

215. M. Alcira, Del. C. Battle, J. Chromatog., 28, 82 (1967).

216. P. Andrews, Nature, 196, 36 (1962).

217. J. Porath, Biochimica et Biophysica Acta, 39, 139 (1960).

218. N. Catsimpoulas and J. Kenney, J. Chromatog., 64, 77 (1972).

219. Newratt and Bailey, "The Proteins", 2, Part A.

220. J. S. Fruton and S. Simmonds, "General Biochemistry", Wiley, New York, London, 1958.

221. R. A. Phelps and F. W. Putman, "The Plasma Proteins", Ed. F. W. Putman, 1, Academic Press, New York, 1960.

222. Newratt and Bailey, "The Proteins", 2, Part B.

223. J. N. Mill er, O. Erinle, J. M. Roberts and C. Thirkettle, J. Chromatog., 105, 317 (1975).

224. P. T. Aspinall and J. N. Millner, Anal. Biochem., 53, 165 (1970).

225. J. Shore, J. Soc. Dye Colour, 84, 408 (1968).

226. Dr. Stead, I.C.I. Dyes Division, private communication.

227. E. J. Cohn, W. L. Hughes and J. H. Weare, J. Amer. Chem. Soc., 69, 1753 (1947).

228. Dr. S. Holding, University of Aston, private communication.

229. "Spherosil" literature, Rhodia (U.K.) Ltd.

230. Dr. Johnson, Waters Associates Ltd., private communication.

231. Mr. Barbour, Rhodia (U.K.) Ltd., private communication.

232. M. Rendell, Process Eng., April, 66 (1975).

233. H. Vink, Acta. Chem. Scand., No. 2, 18 (1964).

234. H. Vink, J. Chromatog., 15, 488 (1964).

235. H. Vink, J. Chromatog., 18, 25 (1965).

236. L. Lapidus and N. R. Amundson, J. Phys. Chem., 56, 984 (1952).

237. C. T. Sciance and O. K. Crosser, A. I. Ch. E. J., 12, No. 1, 100 (1956).

238. S.P. 1800 User manual, Pye Unicam, Cambridge.

239. A. C. Ouano and J. A. Biesenberger, J. Appl. Polym. Sci., 14, 471 (1970).